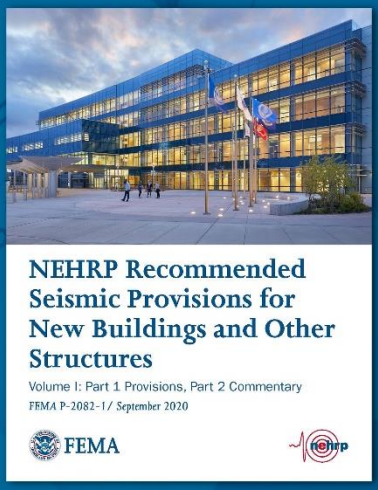

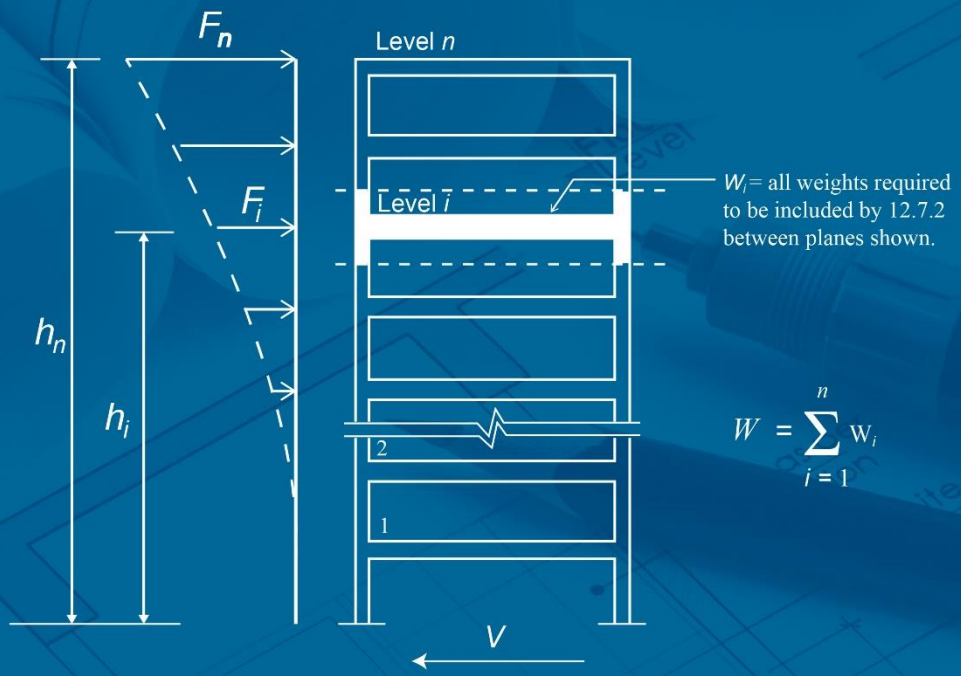

2020 NEHRP Recommended Seismic Provisions: Design Examples, Training Materials, and Design Flow Charts

FEMA P-2192-V1/November 2021

Volume I: Design Examples

FEMA nehrp

2020 NEHRP (National Earthquake Hazards Reduction Program) Recommended Seismic Provisions: Design Examples

Prepared for

Federal Emergency Management Agency

U.S. Department of Homeland Security

By

Building Seismic Safety Council

National Institute of Building Sciences

Washington, D.C.

The National Institute of Building Sciences (NIBS) brings together members of the building industry, labor and consumer interests, government representatives, and regulatory agencies to identify and resolve problems and potential problems around the built environment. NIBS is a nonprofit, non-governmental organization established by Congress in 1974.

The Building Seismic Safety Council (BSSC) was established in 1979 under the auspices of NIBS as a national platform for dealing with the complex regulatory, technical, social, and economic issues involved in developing and promulgating building earthquake hazard mitigation regulatory provisions that are national in scope. By bringing together in the BSSC all of the needed expertise and all relevant public and private interests, it was believed that issues related to the seismic safety of the built environment could be resolved and jurisdictional problems overcome through authoritative guidance and assistance backed by a broad consensus. BSSC's mission is to enhance public safety by providing a national forum that fosters coordination of and improvements in seismic planning, design, construction, and regulation in the building community.

This report was prepared under Contract HSFE60-15-D-0022 between the Federal Emergency Management Agency and the National Institute of Building Sciences.

This FEMA resource document can be obtained from the FEMA online library: https://www.fema.gov/emergency-managers/risk-management/building-science/earthquakes.

Foreword

The Federal Emergency Management Agency (FEMA) is required under the NEHRP Reauthorization Act (P.L. 115-307) "to use research results … support model codes that are cost effective and affordable in order to promote better practices within the design and construction industry and reduce losses from earthquakes." As one of the effective ways to fulfill this responsibility, FEMA supported the development of 2020 edition of the *NEHRP Recommended Provisions,* which successfully translated recent NEHRP and private sector research results into codifiable seismic design requirements, procedures, and guidelines. To help practicing engineers and relevant professionals to understand and implement these improved seismic provisions, FEMA has worked with the Building Seismic Safety Council (BSSC) of the National Institute of Building Sciences (NIBS) to develop the 2020 *NEHRP Recommended Provisions: Design Examples, Training Materials and Design Flow Charts*.

FEMA P-2192 is a three-volume series of educational materials for users of the 2020 *NEHRP Recommended Provisions* and the ASCE/SEI 7-22 standard. Volume 1 (FEMA P-2192-V1) includes eight chapters of design examples covering the major topics of change in the 2020 *NEHRP Recommend Provisions*. Volume 2 (FEMA P-2192-V2) provides a collection of training course presentations for the eight topics of design examples in Volume 1. Volume 3 (FEMA P-2192-V3) offers design flow charts for various parts of seismic design for buildings.

FEMA is thankful to the BSSC, the project technical lead, the project manager, contributing authors, and reviewers for significant efforts devoted in the development of the material. Their contribution and hard work provide invaluable guidance for users of the 2020 *NEHRP Recommended Provisions*, the ASCE/SEI 7-22 standard and 2024 edition of the national model building codes that are expected to adopt the new and related code changes. Together we will strive to increase seismic resilience in our communities.

Federal Emergency Management Agency

Preface and Acknowledgements

Since its creation in 1979, the National Earthquake Hazard Reduction Program (NEHRP) has provided a framework for efforts to reduce the risk caused by earthquakes. The Building Seismic Safety Council (BSSC) of the National Institute of Building Sciences is proud to have been selected by the Federal Emergency Management Agency (FEMA) to continue to play a role under NEHRP in improving the seismic resistance of the built environment. The BSSC is pleased to mark the delivery to FEMA of the 2020 *NEHRP Design Examples*, the companion document to the 2020 *NEHRP Recommended Seismic Provisions for New Buildings and Other Structures*.

The 2020 *NEHRP Design Examples* are developed to illustrate and explain some of the new changes of the 2020 *NEHRP Provisions*, ASCE/SEI 7-22 *Minimum Design Loads and Associate Criteria for Buildings and other Structures*, and the material design standards referenced therein in design applications. The *Design Examples* are developed primarily for design practitioners; however, college students learning about earthquake engineering and engineers studying for their licensing exam or designing in regions of moderate and high seismicity will find this document's explanation of earthquake engineering, the 2020 Provisions, and ASCE/SEI 7-22 seismic provisions helpful.

The BSSC is grateful to many individuals who make the 2020 edition of the design examples a reality.

Project Lead and Management		
Project Technical Lead	Bret Lizundia	
FEMA Project and Technical Oversight	Mai Tong and Robert Hanson	
BSSC Project Manager	Jiqiu (JQ) Yuan	
Chapter	**Author**	**Peer Reviewer**
Chapter 1, Introduction	Bret Lizundia	David Bonneville
Chapter 2, Sections 2.1-2.6 Fundamentals	James Harris	Bret Lizundia
Chapter 2, Section 2.7 Resilience-Based Design	David Bonowitz	James Harris
Chapter 3, Sections 3.1 Overview and 3.3 Multi-Period Response Spectra	Charlie Kircher	C.B. Crouse, Nicolas Luco and Sanaz Rezaeian
Chapter 3, Section 3.2 Update of Seismic Design Ground Motions	Nicolas Luco and Sanaz Rezaeian	C.B. Crouse

Project Lead and Management		
Chapter 3, Section 3.4 Other Changes to Ground Motion Provisions in ASCE/SEI 7-22	C.B. Crouse	Nicolas Luco and Sanaz Rezaeian
Chapter 4, Ductile Coupled Reinforced Concrete Shear Walls as a Distinct Seismic Force-Resisting System in ASCE/SEI 7-22	S. K. Ghosh and Prabuddha Dasgupta	Ian McFarlane
Chapter 5, Coupled Composite Plate Shear Walls/Concrete Filled (C-PSW/CF) as a Distinct Seismic Force-Resisting System in ASCE/SEI 7-22	Soheil Shafaei and Amit H. Varma	Ian McFarlane
Chapter 6, Three-Story Cross-Laminated Timber (CLT) Shear Wall	Philip Line and M. Omar Amini	Bret Lizundia
Chapter 7, Horizontal Diaphragm Design	Kelly Cobeen	Rafael Sabelli
Chapter 8, Nonstructural Components	Bret Lizundia and Jorge Moreno	John Gillengerten

In some cases, information in the *Design Examples* has been adapted from past editions, and the efforts of previous authors are gratefully acknowledged.

We are pleased to introduce the 2020 *NEHRP Provisions Design Examples* and hope you find it useful.

Charles J. Carter, SE, PE, PhD.
Chair, BSSC Board of Direction

Jiqiu (JQ) Yuan, PE, PhD
BSSC Executive Director

November 2021

Table of Contents

List of Figures

List of Tables

Chapter 1: Introduction

Bret Lizundia[1]

1.1 Overview

The 2020 *NEHRP Recommended Provisions: Design Examples* are written to illustrate and explain the applications of the 2020 *NEHRP Recommended Seismic Provisions for New Buildings and Other Structures* (FEMA, 2020a), *ASCE/SEI 7-22 Minimum Design Loads for Buildings and Other Structures* (ASCE, 2021), and the material design standards referenced therein and to provide explanations to help understand them. Designing structures to be resistant to a major earthquake is complex and daunting to someone unfamiliar with the philosophy and history of earthquake engineering. The target audience for the 2020 *Design Examples* is broad. Practicing engineers, college students learning about earthquake engineering, and engineers studying for their licensing exam should all find this document's explanation of earthquake engineering, the 2020 *Provisions*, and ASCE/SEI 7-22 seismic provisions helpful.

Major earthquakes are a rare occurrence, significantly rarer than other hazards, such as damaging wind and snowstorms, that must typically be considered in structural design. However, past experiences have shown that the destructive power of a major earthquake can be so great that its effect on the built environment cannot be underestimated. This presents a challenge since one cannot typically design a practical and economical structure to withstand a major earthquake elastically in the same manner traditionally done for other hazards.

Since elastic design is not an economically feasible option for most structures where major earthquakes can occur, the primary objective of building code requirements for ordinary buildings is to permit a structure to be damaged in such an event but remain safe. Unlike designing for strong winds, where the structural elements that resist lateral forces can be proportioned to elastically resist the pressures generated by the wind, in an earthquake, the seismic force-resisting elements must be proportioned to deform beyond their elastic range in a controlled manner. In addition to deforming beyond their elastic range, the seismic force-resisting system must be robust enough to provide sufficient stability so the building is not at risk of collapse. Furthermore, major falling hazards from architectural, mechanical, electrical, and plumbing (henceforth referred to as nonstructural) components that could kill or cause serious injury should be prevented.

While typical structures are designed to be robust enough to have a minimal risk of collapse and no significant nonstructural falling hazards in major earthquakes, there are other structures whose function or type of occupants warrants higher performance objectives. For example, hospitals, fire stations, and emergency operation centers need to be designed to maintain their function immediately after or returned to function shortly after the earthquake. Structures like schools and

[1] Bret Lizundia, S.E., Rutherford + Chekene

places where large numbers of people assemble have been deemed important enough to require a greater margin of safety against collapse than typical buildings. Structures housing hazardous materials need to be designed to protect against their escape. Additionally, earthquake resistant requirements and ruggedness testing are needed for the design and anchorage of architectural elements and mechanical, electrical, and plumbing systems to prevent loss of system function in essential facilities.

Current building standards, specifically ASCE/SEI 7 and the various material design standards published by the American Concrete Institute (ACI), the American Institute of Steel Construction (AISC), the American Iron and Steel Institute (AISI), the American Wood Council (AWC), and The Masonry Society (TMS) provide a means by which an engineer can achieve these design targets. These standards represent the most recent developments in earthquake resistant design.

The technical basis for most of the seismic provisions contained in ASCE/SEI 7 comes directly from the *NEHRP Recommended Seismic Provisions for New Buildings and Other Structures*. The stated intent of the *NEHRP Provisions* is to provide reasonable assurance of seismic performance that will:

1. Avoid serious injury and life loss due to
    a. Structural collapse
    b. Failure of nonstructural components or systems
    c. Release of hazardous materials
2. Preserve means of egress
3. Avoid loss of function in critical facilities, and
4. Reduce structural and nonstructural repair costs where practicable.

The *NEHRP Provisions* have explicit requirements to provide life safety for buildings and other structures through the design forces and detailing requirements. The current provisions have adopted a target risk of collapse of 1% over a 50-year period for a structure designed to the *Provisions.* The *Provisions* are intended to provide prevention of loss of function in critical facilities and to reduce repair costs in a more implicit manner through prescriptive requirements.

Having good building codes and design standards is only one action necessary to make a community's buildings resilient to a major earthquake. A community also needs engineers who can carry out designs in accordance with the requirements of the codes and standards and contractors who can construct the designs in accordance with properly prepared construction documents. The first item is what the *NEHRP Recommended Provisions: Design Examples* seeks to foster. The second item is typically addressed through quality assurance provisions found in building codes or recommended by the design professional.

The purpose of this introduction chapter is to offer general guidance for users of the design examples. The following sections are included.

- Section 1.2 provides a brief history of earthquake engineering.

- Section 1.3 gives a history of the *NEHRP Provisions* and its role in setting standards for earthquake resistant design. This is done to give the reader a perspective of the evolution of the *NEHRP Provisions* and some background for understanding the design examples.
- Section 1.4 summarizes key updates in the 2020 *NEHRP Provisions* and ASCE/SEI 7-22.
- Section 1.5 provides a history of the *NEHRP Design Examples* and how this 2020 version is intended to be used in conjunction with the 2015 version.
- Section 1.6 covers the organization of chapters and presentation approach used in the 2020 *Design Example*s. A brief summary of each chapter in the 2020 *NEHRP Design Example*s is provided.

1.2 Evolution of Earthquake Engineering

Prior to 1900, there was little consideration of earthquakes in the design of buildings. Major earthquakes were experienced in the United States, notably the 1755 Cape Ann Earthquake around Boston, the 1811 and 1812 New Madrid Earthquakes, the 1868 Hayward California Earthquake, and the 1886 Charleston Earthquake. However, none of these earthquakes led to substantial changes in the way buildings were constructed.

Many things changed with the Great 1906 San Francisco Earthquake. The earthquake and ensuing fire destroyed much of San Francisco and were responsible for approximately 3,000 deaths. To date, it is the deadliest earthquake the United States has ever experienced. While there was significant destruction to the built environment, there were some important lessons learned from those buildings that performed well and did not collapse. Most notable was the exemplary collapse resistance of steel framed buildings which consisted of riveted frames designed to resist wind forces and brick infill between frame columns, built in the Chicago style.

The recently formed San Francisco Section of the American Society of Civil Engineers (ASCE) studied the effects of the earthquake in great detail. An observation was that “a building designed with a proper system of bracing wind pressure at 30 lb per square foot will resist safely the stresses caused by a shock of the intensity of the recent earthquake” (ASCE, 1907). That one statement became the first U.S. guideline on how to provide an earthquake resistant design.

Earthquakes in Tokyo, Japan in 1923 and Santa Barbara, California in 1925 spurred major research efforts. Those efforts led to the development of the first seismic recording instruments, shake tables to investigate earthquake effects on buildings, and committees dedicated to creating code provisions for earthquake resistant design. Shortly after these earthquakes, the 1927 *Uniform Building Code* (UBC) was published (ICBO, 1927). It was the first model building code to hold provisions for earthquake resistant design, albeit in an appendix. In addition to that, a committee began working on what would become California’s first state-wide seismic code in 1939.

Another earthquake struck Long Beach, California in 1933. The most significant aspect of that earthquake was the damage done to school buildings. Fortunately, the earthquake occurred after

school hours, but it did cause concern over the vulnerabilities of these buildings. That concern led to the Field Act, which set forth standards and regulations for earthquake resistance of school buildings. This was the first instance of what has become a philosophy engrained in earthquake design standards: Requiring higher levels of safety and performance for certain buildings that society deems more important than a typical building. In addition to the Field Act, the Long Beach earthquake led to a ban on unreinforced masonry construction in California, which in later years was extended to all areas of moderate and high seismic risk.

Following the Long Beach Earthquake, there was significant activity both in Northern and Southern California, with the local Structural Engineers Associations of each region drafting seismic design provisions for Los Angeles in 1943 and San Francisco in 1948. Development of these codes were facilitated by observations from the 1940 El Centro Earthquake. Additionally, that earthquake was the first major earthquake where the strong ground motion shaking was recorded with an accelerograph.

A joint committee of the San Francisco Section of ASCE and the Structural Engineers Association of Northern California (SEAONC) began work on seismic design provisions which were published in 1951 as *Proceedings—Separate No. 66* (ASCE, 1951). *Separate 66,* as it is commonly referred to*,* was a landmark document which set forth earthquake design provisions which formed the basis of U.S. building codes for the next 40 years. Many concepts and recommendations put forth in *Separate 66*, such as a period dependent design spectrum, different design forces based on the ductility of a structure, and design provisions for architectural components, are still found in today's standards.

Following *Separate 66*, the Structural Engineers Association of California (SEAOC) formed a Seismology Committee, and in 1959 put forth the first edition of the *Recommended Lateral Force Requirements*, commonly referred to as the "The SEAOC Blue Book" (SEAOC, 1959). The Blue Book became the base document for updating and expanding the seismic design provisions of the UBC, the model code adopted by most western states, including California. SEAOC regularly updated the Blue Book from 1959 until 1999. Updates and new recommendations in each new edition of the Blue Book were incorporated into each subsequent edition of the UBC.

The 1964 Anchorage Earthquake and the 1971 San Fernando Earthquake both were notable events. Both earthquakes exposed significant issues with the way reinforced concrete structures would behave if not detailed for ductility. There were failures of large concrete buildings which had been designed to recent standards, and those buildings had to be torn down. To most engineers and the public, this was an unacceptable performance.

Following the 1971 San Fernando Earthquake, the National Science Foundation (NSF) gave the Applied Technology Council (ATC) a grant to develop more advanced earthquake design provisions. That project engaged over 200 distinguished experts in the field of earthquake engineering. The landmark report they produced in 1978, ATC 3-06, *Tentative Provisions for the Development of Seismic Regulations for Buildings* (ATC, 1978)*,* became the basis for the earthquake design

standards. The *NEHRP Provisions* trace back to ATC 3-06, as will be discussed in more detail in the following section.

There have been additional earthquakes since the 1971 San Fernando Earthquake which have had significant influence on seismic design. Table 1-1 provides a summary of major North American earthquakes and changes to the building codes that resulted from them through the 1997 UBC (ICBO, 1997). Of specific note are the 1985 Mexico City, 1989 Loma Prieta, and 1994 Northridge Earthquakes.

The 1985 Mexico City Earthquake was extremely devastating. Over 10,000 people were killed, and there was the equivalent of $3 to $4 billion of damage. The most significant aspect of this earthquake was ground shaking with a much longer period and larger amplitudes than would be expected from typical earthquakes. While the epicenter was located over 200 miles away from Mexico City, the unique geologic nature of Mexico City sited on an ancient lakebed of silt and clay caused long periods of ground shaking that lasted for an extended duration. This long period shaking was much more damaging to mid-rise and larger structures because these buildings were in resonance with the ground motions. In current design practice, site factors based on the underlying soil are used to modify the seismic hazard parameters to account for this effect.

The 1989 Loma Prieta Earthquake caused an estimated $6 billion in damage, although it was far less deadly than other major earthquakes throughout history. Only 63 people lost their lives, a testament to the over 40 years of awareness and consideration of earthquakes in the design of structures. Many of those deaths, 42, resulted from the collapse of the Cyprus Street Viaduct, a nonductile concrete elevated freeway. In this earthquake, the greatest damage occurred in Oakland, parts of Santa Cruz, and the Marina District in San Francisco, where the subsurface material was soft soil or poorly compacted fill. As with the Mexico City experience, this illustrated the importance of subsurface conditions on the amplification of earthquake shaking. The earthquake also highlighted the vulnerability of soft and weak story buildings. A considerable number of the collapsed buildings in the Marina District were wood framed apartment buildings with weak first stories because of the garage door openings. Those openings greatly reduced the wall area at the first story.

Five years later, the 1994 Northridge Earthquake struck California near Los Angeles. Fifty-seven people lost their lives, and the damage was estimated at around $20 billion. The high cost of damage repair emphasized the need for engineers to consider overall building performance, in addition to building collapse, and spurred the movement toward performance-based design. As with the 1989 Loma Prieta Earthquake, there was a disproportionate number of collapses of soft/weak first story wood framed apartment buildings.

Table 1-1. Recent North American Earthquakes and Subsequent Code Changes (from SEAOC, 2019)

Earthquake	UBC Edition	Enhancement
1971 San Fernando	1973	▪ Direct positive anchorage of masonry and concrete walls to diaphragms
	1976	▪ Seismic Zone 4, with increased base shear requirements ▪ Occupancy Importance Factor, *I*, for certain buildings ▪ Interconnection of individual column foundations ▪ Special inspection requirements
1979 Imperial Valley	1985	▪ Diaphragm continuity ties
1985 Mexico City	1988	▪ Requirements for columns supporting discontinuous walls ▪ Separation of buildings to avoid pounding ▪ Design of steel columns for maximum axial forces ▪ Restrictions for irregular structures ▪ Ductile detailing of perimeter frames
1987 Whittier Narrows	1991	▪ Revisions to site coefficients ▪ Revisions to spectral shape ▪ Increased wall anchorage forces for flexible diaphragm buildings
1989 Loma Prieta	1991	▪ Increased restrictions on chevron-braced frames ▪ Limitations on *b/t* ratios for braced frames
	1995	▪ Ductile detailing of piles
1994 Northridge	1997	▪ Restrictions on use of battered piles ▪ Requirements to consider liquefaction ▪ Near-fault zones and corresponding base shear requirements ▪ Revised base shear equations using 1/*T* spectral shape ▪ Redundancy requirements ▪ Design of collectors for overstrength ▪ Increase in wall anchorage requirements ▪ More realistic evaluation of design drift ▪ Steel moment connection verification by test

The most significant issue from the 1994 Northridge Earthquake was the unanticipated damage to steel moment frames. Steel moment frames had generally been thought of as the best seismic force-resisting system due in part to their performance in the 1906 San Francisco Earthquake. However, many moment frames experienced fractures of the weld that connected the beam flange to the column flange. This led to a multi-year, FEMA-funded problem-focused study to assess and improve the seismic performance of steel moment frames. It also led to penalties for having a lateral force-resisting system that does not have sufficient redundancy.

The profession is still learning from earthquakes. The 2010 Chile earthquake has led to updates in the design provisions for concrete wall structures, which have been incorporated into the ACI 318 standard referenced in the *NEHRP Provisions*. The 2011 Christchurch Earthquake spurned significant changes to the design of egress stairs in ASCE/SEI 7-16.

1.3 History and Role of the *NEHRP Provisions*

Following the completion of the ATC 3 project in 1978, there was desire to make the ATC 3-06 approach the basis for new regulatory provisions and to update them periodically. FEMA, as the lead agency of the NEHRP at the time, contracted with the then newly formed BSSC of the National Institute of Building Sciences (NIBS) to perform trial designs based on ATC 3-06 to exercise the proposed new provisions. The BSSC put together a group of experts consisting of consulting engineers, academics, representatives from various building industries and building officials. The result of that effort was the first (1985) edition of the *NEHRP Recommended Provisions for the Development of Seismic Regulations for New Buildings* (FEMA, 1986a,b). Figure 1-1 highlights seminal earthquake events, U.S. seismic regulations and code developments and the role of the *NEHRP Provisions*. Details on this development continue below.

From the publication of the first edition through the 2003 edition, the *NEHRP Provisions* were updated every three years (FEMA, 1988a,b; 1992a,b; 1995a,b; 1997a,b; 2001a,b; 2004a,b). Each update incorporated recent advances in earthquake engineering research and lessons learned from previous earthquakes. The intended purpose of the *Provisions* was to serve as a code resource document. While the SEAOC Blue Book continued to serve as the basis for the earthquake design provisions in the *Uniform Building Code,* the *BOCA National Building Code* (BOCA, 1993) and the *Standard Building Code* (SBCCI, 1994) both adopted the 1991 *NEHRP Provisions* in their 1993 and 1994 editions, respectively. The 1993 version of the ASCE/SEI 7 standard *Minimum Design Loads for Buildings and Other Structures* (ASCE, 1994), which had formerly been American National Standards Institute Standard A58.1, also utilized the 1991 *NEHRP Provisions* (FEMA, 1992a,b).

In the late 1990s, the three major code organizations, ICBO (publisher of the UBC), BOCA, and SBC decided to merge their three codes into one national model code. When doing so, they chose to incorporate the 1997 *NEHRP Provisions* as the technical basis for the seismic design requirements for the inaugural 2000 edition of the *International Building Code* (IBC) (ICC, 2000). Thus, the SEAOC Blue Book was no longer the base document for the UBC/IBC. The 1997 *NEHRP Provisions* proposed a number of major changes. Most significant was the switch from the older seismic maps of ATC 3-06 to new, uniform hazard spectral value maps produced by USGS in accordance with BSSC

Provisions Update Committee (PUC) Project 97. The 1998 edition of ASCE/SEI 7 (ASCE, 2000) was also based on the 1997 *NEHRP Provisions*.

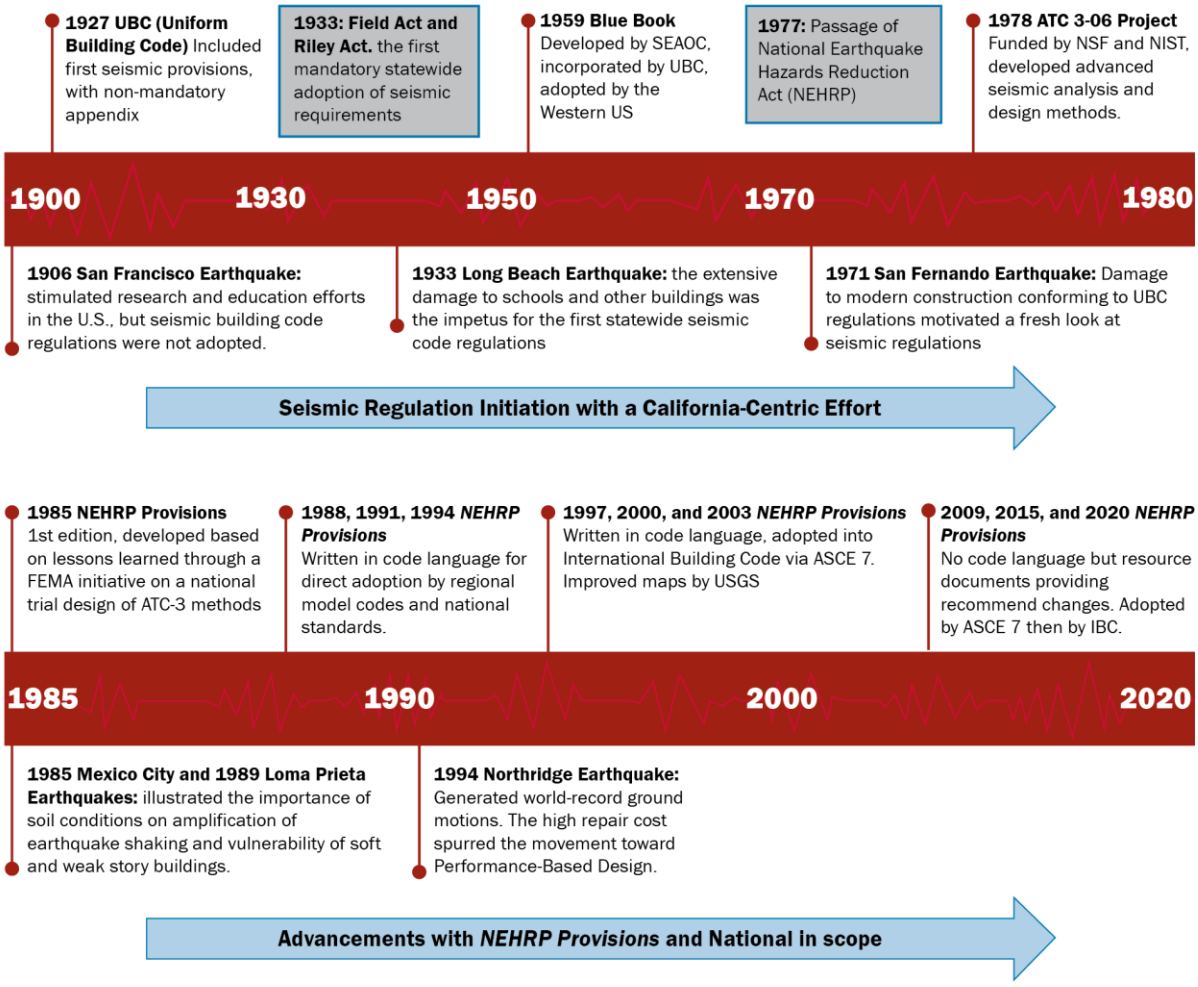

Figure 1-1. U.S. Seismic Code Development and the Role of the *NEHRP Provisions* (from FEMA, 2021c)

ASCE/SEI 7 continued to incorporate the 2000 and 2003 editions of the *Provisions* for its 2002 and 2005 editions, respectively (ASCE, 2003 and 2006). However, the 2000 IBC adopted the 1997 *NEHRP Provisions* by directly transferring the text from the provisions into the code. In the 2003 IBC (ICC, 2002), the provisions from the 2000 IBC were retained, and there was also language, for the first time, which pointed the user to ASCE/SEI 7-02 for seismic provisions instead of adopting the 2000 *NEHRP Provisions* directly. The 2006 IBC (ICC, 2006) explicitly referenced ASCE/SEI 7 for the earthquake design provisions, as did the 2009 and 2012 editions (ICC, 2009 and 2011).

With the shift in the IBC from directly incorporating the *NEHRP Provisions* for their earthquake design requirements to simply referencing the provisions in ASCE/SEI 7, the 2009 BSSC Provisions Update Committee decided to move the *2009 NEHRP Provisions* in a new direction. Instead of providing all the seismic design provisions within the *NEHRP Provisions*, which would be repeating the provisions

in ASCE/SEI 7, and then modifying them, the PUC chose to adopt ASCE/SEI 7-05 by reference and then provide recommendations to change it as necessary. Therefore, Part 1 of the *2009 NEHRP Provisions* contained major technical modifications to ASCE/SEI 7-05 which, along with other recommendations from the ASCE/SEI 7 Seismic Subcommittee, were the basis for proposed changes that were incorporated into ASCE/SEI 7-10 (ASCE, 2013) and included associated commentary on those changes. The PUC also developed a detailed commentary to the seismic provisions of ASCE/SEI 7-05, which became Part 2 of the *2009 NEHRP Provisions*.

In addition to Part 1 and Part 2 in the *2009 NEHRP Provisions*, a new section was introduced – Part 3. The intent of this new portion was to showcase new research and emerging methods, which the PUC did not feel were ready for adoption into national design standards but was important enough to be disseminated to the profession. This new three-part format marked a change in the *Provisions* from a code-language resource document to the key knowledge-based resource for improving the national seismic design standards and codes.

The 2015 *NEHRP Provisions* followed the same three-part format as the 2009 *NEHRP Provisions* (FEMA, 2009a,b). Part 1 provided recommended technical changes to ASCE/SEI 7-10 including Supplements 1 and 2. The changes in Part 1 of the 2015 *NEHRP Provisions* (FEMA, 2015a,b) were adopted, with some modifications, into ASCE/SEI 7-16. Part 2 contained an updated expanded commentary to ASCE/SEI 7-10, including commentary associated with the recommended technical changes from Part 1. In the 2015 *NEHRP Provisions*, several chapters in ASCE/SEI 7 were completely re-written, including those dealing with nonlinear response history analysis, seismic isolation, supplemental energy dissipation, and soil-structure interaction. In addition to the new chapters, significant changes were made to the seismic design parameters through new site factors and new requirements for when site specific spectra are required, updated linear analysis procedures, a new diaphragm design methodology, and a new procedure for designing structures on liquefiable soils.

Part 3 of the 2015 *NEHRP Provisions* contained five new resource papers. The resource papers from the 2009 *NEHRP Provisions* were evaluated by the 2015 NEHRP PUC. In some cases, the material from the 2009 resource papers formed the basis for Part 1 recommended technical changes in the 2015 *NEHRP Provisions*, such as ultimate strength design of foundations, nonlinear response history analysis, and the new diaphragm provisions. A number of papers were removed from Part 3 because the 2015 NEHRP PUC chose not to carry those papers forward. That decision was not necessarily intended to signify that the information contained in the papers was no longer valid, but that either new modifications to the 2015 *NEHRP Provisions* eliminated the need for the paper or the material in the paper need only be correlated with Part 1 changes in the 2015 *NEHRP Provisions* and relevant material standards.

The 2020 *NEHRP Provisions* also continued the Part 1, Part 2, and Part 3 organization. The 2020 *NEHRP Provisions* were sent to ASCE for consideration by the ASCE committee responsible for development of the next edition of ASCE/SEI 7, which will be ASCE/SEI 7-22. A summary of changes in the 2020 *NEHRP Provisions* and the seismic provisions of ASCE/SEI 7-22 is given in Section 1.4 of these 2020 *Design Examples*.

Today, someone needing to design a seismic-force resistant building in the U.S. would first go to the local building code, which has generally adopted the IBC with or without modifications by the local jurisdiction. For seismic design requirements, the building code typically points to relevant chapters of ASCE/SEI 7. Those chapters of ASCE/SEI 7 set forth the seismic hazard, design forces, and system detailing requirements. The seismic forces in ASCE/SEI 7 are dependent upon the type of detailing and specific requirements of the lateral force-resisting system elements. ASCE/SEI 7 then points to material specific requirements found in the material design standards published by ACI, AISC, AISI, AWC, and TMS for those detailing requirements. Within this structure, the *NEHRP Provisions* serves as a consensus evaluation of the design standards and a vehicle to transfer new knowledge to ASCE/SEI 7 and the material design standards. Figure 1-2 graphically illustrates the current approach.

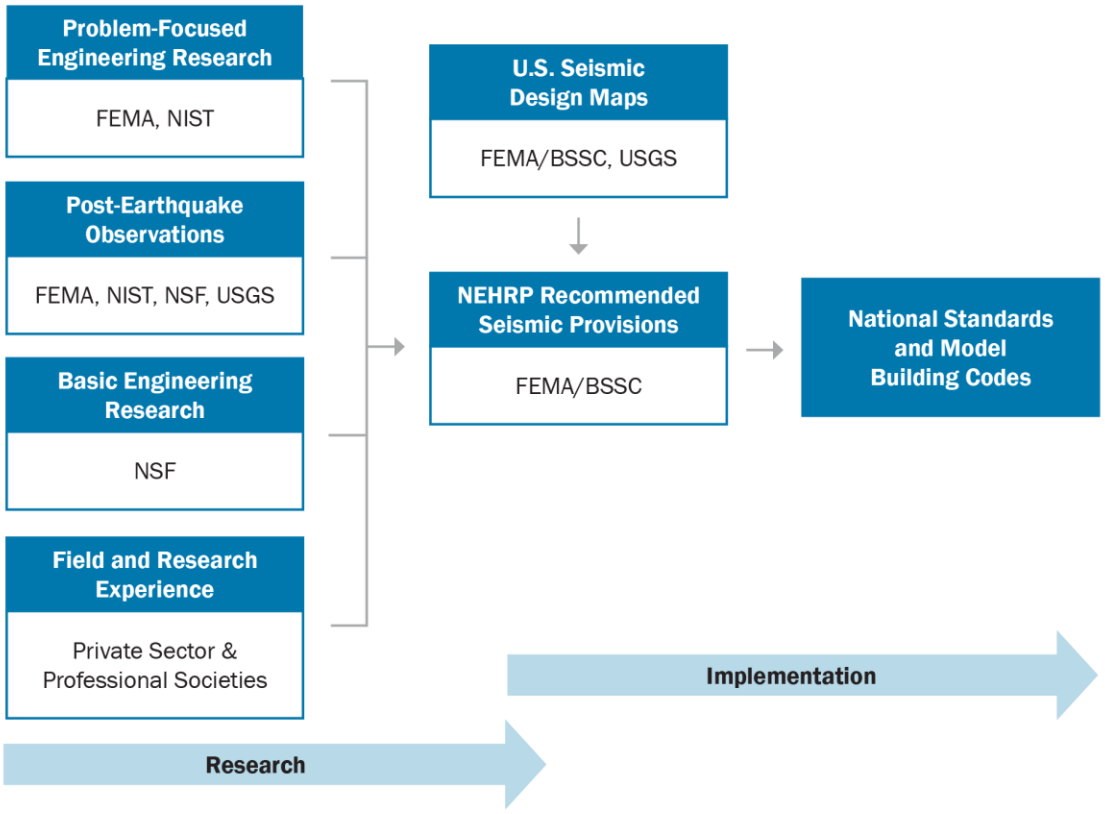

Notes: FEMA = Federal Emergency Management Agency; NIST = National Institute of Standards and Technology; USGS = U.S. Geological Survey; NSF = National Science Foundation; BSSC = Building Seismic Safety Council.

Figure 1-2. The *NEHRP Recommended Seismic Provisions* Serves as a Convergence of the Efforts Among the Four NEHRP Agencies and Private Sector and a Mechanism to Transfer Research Results for Improving Seismic Design Practice (from FEMA, 2021c)

1.4 Key Updates to the 2020 *NEHRP Provisions* and ASCE/SEI 7-22

This section summarizes key updates to the 2020 *NEHRP Provisions* and the associated ASCE/SEI 7-22 seismic provisions. These updates include:

- Earthquake design ground motions and spectral acceleration parameters
- Addition of three new shear wall seismic force-resisting systems
- Addition of provisions for diaphragm design
- Significant update of the nonstructural components chapter and the forces used for nonstructural design
- A relaxation in the requirements for modal response spectrum analysis and revisions in configuration irregularity requirements
- Revisions in displacement requirements
- Exceptions for buildings exceeding height limits
- Changes in the nonbuilding structures provisions
- Addition of quantitative reliability targets for essential facilities and individual members
- A Part 3 paper on how to apply the *NEHRP Provisions* for improved seismic resiliency
- A Part 3 paper on a new approach to seismic lateral earth pressures
- Soil-structure interaction provision definitions for different types of shear wave velocities were refined and clarified

This summary is drawn in part from Bonneville and Yuan (2019) and, in some cases, quoted directly. A detailed summary is provided in the "What is New in the 2020 *NEHRP Provisions*" section of the 2020 *NEHRP Provisions*. A total of 50 technical changes proposals were developed and deliberated, with 37 receiving consensus approval and incorporation into the 2020 *NEHRP Provisions.*

1.4.1 Earthquake Ground Motions and Spectral Acceleration Parameters

Earthquake Ground Motion Maps: The earthquake ground motion maps that underlie the 2020 *NEHRP Provisions* and ASCE/SEI 7-22 were developed in a cooperative manner between the USGS, which incorporates new earth science into the national seismic hazard model, and the BSSC PUC, through its Project 17 (BSSC, 2019) initiative which provides the engineering input on the parameters to be used in seismic design and analysis. After detailed study and consideration of various alternatives, the Project 17 Committee recommended that national seismic design value

maps continue to be developed on the basis developed by Project 07, as being ground motion that produces a 1% risk of collapse in 50 years for structures having 10% conditional probability of collapse given the occurrence of MCE_R shaking, except at those sites where such motion exceeds the deterministic lower limit. The deterministic lower limit was refined to be based on selection of scenario earthquakes through examination of hazard deaggregation. These recommendations were later approved by the PUC.

Multi-Point Spectra: Near the end of the 2015 *NEHRP Provisions* cycle, studies by Kircher (2015) showed that, for many sites, the two-parameter (S_S, S_1) spectrum used in combination with site factors (F_a and F_v) does not provide an accurate estimate of the spectral shape of ground motions, particularly at longer periods. This was shown to be the case for soft soil sites (Site Class D, E or F) affected by major active faults. It was determined that at such sites, peak spectral response values may be significantly underestimated using the conventional design spectrum (defined by S_S and S_1), and the spectrum instead should be determined based on response at other periods, suggesting the need for multi-period spectral values to be defined. This effect is significantly greater for a Site Class E site. Since there was not sufficient time for USGS to develop multi-period spectra in the 2015 cycle, the interim solution, included in ASCE/SEI 7-16 Section 11.4.8, was to require site-specific seismic studies for the design of structures on sites classified as Site Class D and E in areas of moderate and high seismic hazard unless conservative simplifying assumptions are made relative to design spectral values. In this cycle, the multi-period spectrum issue was addressed in a Project 17 work group, and that work was transferred to the PUC.

In the multi-period response spectrum (MPRS) approach, a database of MCE-level spectral acceleration values is provided by USGS for a geographic array of gridded data points for periods ranging from zero to 10 seconds for each site class. Consistent with current practice, Design Spectral Response values are taken as 2/3 of the MCE-level values. Spectral values for sites outside of the gridded values will be obtained by geographic interpolation. Since site class is integrated into the spectral values, the site coefficient tables are eliminated. This database replaces the maps of S_S and S_1 ground motion parameters that have been produced since the 1997 *NEHRP Provisions*. The amount of data required to represent the full spectral shape associated with the range of site classes and the full geographic grid makes it impractical to use maps to obtain spectral acceleration values. Maps remain in ASCE/SEI 7-22 Chapter 22 for select spectra acceleration parameters for select site classes.

Implementing the multi-period spectrum approach in the design requirements involves substantial changes to 2020 *NEHRP Provisions* and ASCE/SEI 7-22 Chapters 11 (Seismic Design Criteria), Chapter 20 (Site Classification Procedure for Seismic Design), Chapter 21 (Site-Specific Ground Motion Procedures for Seismic Design), and Chapter 22 (Seismic Ground Motion and Long-Period Transition Maps). The seismic design requirements for buildings in Chapter 12 (Seismic Design Requirements for Building Structures) and Chapter 15 (Nonbuilding Structures) are also affected. A summary by chapter follows.

- Chapter 11 Section 11.4.5 requires that the multi-period design response spectrum be used where a design response spectrum is required, except (1) if a site-specific ground motion

analysis is performed or (2) when values of the multi-period response spectrum are not available. In the latter case, a simplified two-period design response spectrum, representing the traditional design spectrum, is used. Web applications, based on USGS-derived data, provide the multi-period spectral values, as well as the S_{MS} and S_{M1} values to create S_{DS} and S_{D1} values (for the two-period spectrum) based on user-provided values of site location and site class.

In order to provide a better definition of the multi-period spectral shape on sites where it can vary significantly as a function of site class, intermediate site classes have been introduced. Site soil properties are now required to be classified as Site Class A, B, BC, C, CD, D, DE, E or F. The new BC (soft rock), CD (dense sand or very soft clay) and DE (loose sand or medium stiff clay) classes are introduced to provide the smoother transition between classes. The requirement to use the default site class (that producing highest spectral response accelerations) is maintained, and now incorporates the new Site Class CD, in addition to Site Classes C and D.

- Chapter 12 and Chapter 15 provisions continue to be framed in terms of design earthquake ground motions S_{DS} and S_{D1}, and only minor changes are required in the Equivalent Lateral Force Procedure.

- Chapter 20 (Site Classification Procedure for Seismic Design) provides revised definitions of site classes. The effort to add the three new site classes noted above led to a reassessment of the correlations between shear wave velocity, standard penetration resistance (blow count), and undrained shear strength, upon which the definitions in the site classifications table are based. The site classification procedure has been revised to define site class strictly in terms of shear wave velocity, which is considered more accurate. For sites at which shear wave velocity is not measured, or where it is not measured to a 100-foot depth, approximate generalized correlations between shear wave velocity and the other geotechnical parameters may be used to obtain an estimated shear wave velocity.

- Chapter 21 (Site Specific Ground Motion Procedures for Seismic Design) defines probabilistic and deterministic MCE ground motions and allows spectral response accelerations to be taken as the lesser of the two. As noted above, changes in USGS modeling procedures have resulted in the need to redefine the deterministic ground motion. Where the deterministic value was previously defined based on a single-magnitude characteristic earthquake on faults, it is now based on a scenario earthquake, which is determined from hazard deaggregation of the probabilistic ground motions at the site. In this procedure, the contribution of each active fault to the total hazard at a site is considered. Any fault that contributes less than 10% of the largest contributor at each period is ignored.

  ASCE/SEI 7-22 Section 21.4 defines the spectral response parameters S_{MS} and S_{M1} as 1.5 times the S_{DS} and S_{D1} values, which are defined as follows:

  - S_{DS} is taken as 90% of the maximum value of the spectral response accelerations between periods 0.2 and 5 seconds, inclusive.

- S_{D1}, for sites with values of $\overline{v_s}$ greater than 1,450 ft/sec, is taken as 90% of the maximum value of TS_a for periods ranging from 1 to 2 seconds. $\overline{v_s}$ (also known as $V_{S,30}$,) is the average shear wave velocity parameter derived from a measured shear wave profile from the ground surface to a depth of 30 meters or 100 feet

- S_{D1}, for sites with values of $\overline{v_s}$ less than or equal to 1,450 ft/sec, is taken as the maximum value of TS_a for periods ranging from 1 to 5 seconds, but not less than 100% of the value of S_a at 1.0 second.

The $\overline{v_s}$ value of 1,450 ft/sec corresponds to the upper end of Site Class CD (dense sand or very stiff clay). As noted above, the S_{MS} and S_{M1} values obtained from the USGS website are consistent with these definitions.

Chapter 3 of these 2020 *Design Examples* provides more details of the changes.

1.4.2 New Shear Wall Seismic Force-Resisting Systems

Three new shear wall systems were added to Table 12.2-1 in the 2020 *NEHRP Provisions* and in ASCE/SEI 7-22: one for reinforced concrete, one for composite structural steel and reinforced concrete, and one for wood.

The new reinforced concrete shear wall system is called a reinforced concrete ductile coupled wall, and the composite shear wall system is called a steel and concrete coupled composite plate shear wall. Both derive significant energy dissipation capacity through coupling beam yielding, with the resulting overall seismic behavior expected to be superior to the currently defined special shear wall systems, which do not specifically consider the configuration of internal wall elements. Both systems are considered particularly useful in mid-rise and high-rise construction, especially those utilizing a core wall system. In both cases, the research included FEMA P695 studies intended to justify design coefficients and factors representing greater ductility, proposing response modification coefficients, *R*, equal to 8. Both systems have unlimited height limits in Seismic Design Categories B and C and a height limitation of 160 feet in Seismic Design Categories D, E, and F. Interestingly, the reinforced concrete ductile coupled wall system has a minimum height limit of at least 60 feet "to ensure [an] adequate degree of coupling and significant energy dissipation [are] provided by the coupling beams" as the ASCE/SEI 7-22 Section C12.2.1 commentary notes.

Chapter 4 of these 2020 *Design Examples* provides a detailed design example for the reinforced concrete ductile coupled wall. Chapter 5 of these 2020 *Design Examples* provides a detailed design example for the steel and concrete coupled composite plate shear wall.

Cross-laminated timber (CLT) shear walls were also added as a new seismic force-resisting system. There are two variants of the system: one utilizing high aspect ratio shear walls having a height-to-length ratio of 4, with an *R*-factor of 4, and the other with height-to-length ratios between 2 and 4, with an *R*-factor of 3. In both cases, the height limit for all Seismic Design Categories is 65 feet. The aspect ratios were selected based on the availability of test results. A key to the ductility of the CLT

system is the top and bottom connection of panels, which consist of prescribed steel angles with bolts and nails.

Chapter 6 of this 2020 *Design Examples* provides CLT design examples.

1.4.3 Diaphragm Design

Alternative diaphragm design provisions were developed in the 2015 *NEHRP Provisions* cycle and adopted in ASCE/SEI 7-16. These provisions, offered as an alternative to the traditional diaphragm design requirements, acknowledged results of recent analytical studies and large-scale testing, which showed that actual forces imposed on diaphragms during strong ground shaking can be significantly higher than those predicted by traditional elastic design code requirements. The new provisions also acknowledged component testing results that show the ductility and capacity of most traditional systems generally exceed allowable values. In short, it was concluded that demands inherent in traditional requirements have been underestimated but have been assessed against unrealistically low elastic capacities. The alternative provisions provided a new equation to calculate demands along the height of the building, not simply based on forces that are a multiple of floor forces from the ELF procedure, and provided new diaphragm *R*-factors (R_S) for systems utilizing cast-in-place concrete, precast concrete, and wood sheathing. Diaphragm systems constructed of bare steel deck were omitted from the 2015 *NEHRP Provisions* due to a lack of available research at the time.

Diaphragm studies conducted in the 2015 *NEHRP Provisions* cycle also considered the specific performance of one-story rigid wall-flexible diaphragm (RWFD) buildings, that is, buildings for which response is dominated by dynamic response and inelastic action in the diaphragm. However, technical proposals did not evolve into code language. A Part 3 Resource Paper titled “One-Story Flexible Diaphragm Buildings with Stiff Vertical Elements” was published the 2015 *NEHRP Provisions*, based largely on FEMA P-1026, *Seismic Design of Rigid Wall-Flexible Diaphragm Buildings: An Alternate Procedure* (FEMA, 2015c).

Since the 2015 *NEHRP Provisions* cycle, significant research has been conducted on bare metal deck diaphragms through the Steel Diaphragm Innovation Initiative, a collaboration involving industry-sponsored academic research. Within this initiative, research by Schafer (2019) and others justified the inclusion of metal deck diaphragms in the alternative provisions discussed above and in the new set of provisions related to one-story RWFD buildings discussed below. The research covers metal deck performance from the standpoint of overall diaphragm behavior as well as the deck connectivity level, considering fasteners at deck seams and from deck to framing.

For the 2020 *NEHRP Provisions* and ASCE/SEI 7-22, specific provisions have been developed for one-story RWFD buildings, including a complete set of design requirements applicable to diaphragms utilizing both wood sheathing and bare metal deck and a simplified two-stage analysis, akin to the two-stage procedure allowed in the code for podium structures (rigid base and flexible upper levels) has been added. A key concept inherent in the bare steel deck provisions is that ductile steel deck diaphragm response only occurs when special detailing requirements are met, addressing deck to

deck and deck to framing connectivity. An interesting finding from the research is that steel deck that is mechanically fastened along deck section boundaries and to the underlying building frame performs well under high seismic demands if properly detailed. However, a steel deck that is welded, while having good strength and stiffness, is unable to develop the inelastic redistribution that is required in RWFD buildings. Diaphragm R_S factors have been provided for bare steel deck systems, for both the one-story RWFD case and for the alternative diaphragm provisions.

Chapter 7 of these 2020 *Design Examples* provides examples for all of the various diaphragm procedures in the 2020 *NEHRP Provisions* and in ASCE/SEI 7-22.

1.4.4 Nonstructural Components

Significant technical and organizational changes were made in Chapter 13 (Nonstructural Components) for the 2020 *NEHRP Provisions* and ASCE/SEI 7-22. The technical basis for much of the proposed change is derived from NIST Report NIST GCR 18-917-43, *Recommendations for Improved Seismic Performance of Nonstructural Components* (NIST, 2018). This resulted in a new nonstructural design equation for the horizontal force, F_p. It includes revisions to the amplification of accelerations up the height of the building, incorporation of the influence of the building seismic force-resisting system on nonstructural component response, and a more refined relationship between design levels and whether the component is likely to be in resonance with the building. It also requires that equipment support systems and platforms and distribution system supports be designed based on their dynamic response and ductility, rather than the properties of the components they support.

Chapter 8 of this 2020 *Design Examples* summarizes the development of the equations and applies them in a series of design examples.

1.4.5 Permitted Analytical Procedures and Configuration Irregularities

The FEMA P-2012 report, *Assessing Seismic Performance of Buildings with Configuration Irregularities: Calibrating Current Standards and Practice* (FEMA, 2018), provided useful information related to the effects of configurational irregularities on building seismic response and the effectiveness of the current provisions in improving performance. FEMA P695 (FEMA, 2009b) analysis was used to study the collapse margin ratio of buildings with mass and configuration irregularities. Among other findings, the studies showed that collapse performance was not substantially affected by either the magnitude of a mass irregularity or whether a building was designed using the Equivalent Lateral Force Procedure or Modal Response Spectrum Analysis (MRSA). Additional studies by PUC Issue Team 3 reached similar conclusions, which are documented in "Resource Paper 9 – Modal Response Spectrum Analysis Methods" of FEMA (2020b). Based on this, the mass irregularity was removed from Table 12.3-2 of the 2020 *NEHRP Provisions* and ASCE/SEI 7-22, and the requirements to use MRSA were removed in general. This resulted in the elimination of Table 12.6-1 Permitted Analytical Procedures from ASCE/SEI 7-22 and replacement in Section 12.6 with a sentence stating that any of the Chapter 12 analytical procedures are permitted

for any building, including Equivalent Lateral Force Procedure, Modal Response Spectrum Analysis, and Linear Response History Analysis.

In addition, with respect to torsion-related provisions, analyses for FEMA P-2012 showed that current design provisions are generally conservative, with the exception of buildings that rely heavily on lines of resistance orthogonal to the earthquake force for torsional resistance. Accordingly, the definitions for torsional irregularities were modified in Table 12.3-1 of the 2020 *NEHRP Provisions* and ASCE/SEI 7-22, and the associated provisions were revised to reduce unnecessary conservatism and requirements for building configurations that were not adequately addressed. In ASCE/SEI 7-16, buildings in Seismic Design Categories E and F were not permitted to have an extreme torsional irregularity; this restriction was removed in ASCE/SEI 7-22.

1.4.6 Displacement Requirements

The PUC considered the current requirements for story drift calculation and its application to protection against failure due to such actions as deformation compatibility and structural separation. An issue is whether design earthquake story drifts should be amplified by the structural system (ASCE/SEI 7 Table 12.2-1) *R*-factor rather than the C_d factor. This led to an effort to collect available information from nonlinear numerical studies and testing. It was determined that definitively answering this question required an effort that was beyond the scope of what could be achieved in the 2020 NEHRP cycle. However, several drift-related proposals were implemented in this cycle. The first, addressing the general C_d vs. *R* issue, is a Part 3 resource paper in the 2020 *NEHRP Provisions* that documents issues that arose in the studies undertaken and recommends steps that may be taken in the next NEHRP cycle or by separately funded research. Another proposal requires the amplification of design story drifts by the *R*-factor in the consideration of deformation compatibility in Section 12.12 of the 2020 *NEHRP Provisions* and ASCE/SEI 7-22. This was passed because it was judged to have significant safety-related implications and is similar to a stopgap provision instituted in ASCE/SEI 7-10 related to members spanning between structures. A third drift-related change, not directly related to the C_d vs. *R* issue, creates definitions needed for the provisions to include diaphragm deformation in displacements related to deformation compatibility, structural separation, and at supports of members spanning between structures. This impacts Sections 11.2, 11.3, 12.8.6, 12.12, and 13.3.2 of the 2020 *NEHRP Provisions* and ASCE/SEI 7-22.

1.4.7 Exceptions to Height Limitations

Table 12.2-1 of ASCE/SEI 7 defines the permitted seismic force-resisting systems and the height limitations for each system by Seismic Design Category. An exception was added to Section 12.2.1 in the 2020 *NEHRP Provisions* that allows buildings with lateral force-resisting systems conforming to the requirements of Table 12.2-1 to exceed the height limits prescribed in that table when the building is designed to the requirements of Chapter 16 for nonlinear response history analysis. It is based on the concept that the rules and acceptance criteria given in Chapter 16 provide adequate assurance of safety in such cases without the rigor associated with the FEMA P695 methodology. The exception does not apply to seismic force-resisting systems designated as not permitted for the Seismic Design Category in Table 12.2-1. The 2020 *NEHRP Provisions* Section 12.2.1 exception was

not adopted for ASCE/SEI 7-22. Language in ASCE/SEI 7-22 Section 12.2-1 remains the same as in ASCE/SEI 7-16 Section 12.2-1.

1.4.8 Nonbuilding Structures

Two changes were made in Chapter 15 (Nonbuilding Structures) in the 2020 *NEHRP Provisions* and ASCE/SEI 7-22. The first involves a modification of the coupled analysis provisions, affecting the analysis and design of a combined system, including a structure supporting a large nonbuilding structure or nonstructural component (thus also affecting Chapter 13 of the 2020 *NEHRP Provisions* and ASCE/SEI 7-22). The revision changes the ratio of secondary weight to total weight that triggers a combined analysis from 25% to 20%. The second change addresses the design of corrugated steel liquid storage tanks, which were not specifically addressed in previous versions of the *NEHRP Provisions*. The new provisions address Chapter 15 design requirements and materials specifications. The changes were considered initially by the Provisions Update Committee and then forwarded to ASCE for implementation directly into ASCE/SEI 7-22. As a result, they are not in the 2020 *NEHRP Provisions*, but are in ASCE/SEI 7-22. In addition, there was a general reorganization effort intended to clarify the scopes of Chapters 13 and 15.

1.4.9 Performance Intent and Seismic Resiliency

Section 1.1 of the 2020 *NEHRP Provisions* defines the performance intent of buildings that comply with the provisions. This was summarized in Section 1.1 of this chapter above. Two additions were made in the 2020 *NEHRP Provisions* to further define performance intent: one related to essential facility reliability targets and one related to individual member reliability targets.

Essential Facility Reliability Targets: It is generally assumed that structures designed to Risk Category IV requirements will retain their pre-earthquake function. Language was added to Commentary Section 2.1.5 of the 2020 *NEHRP Provisions* to set a target reliability in quantitative terms, suggesting a probability of loss of function of 10 percent or less for Risk Category IV structures subjected to design earthquake ground shaking.

Individual Member Reliability Targets: Language was added to Section 1.1.1 of the 2020 *NEHRP Provisions* to quantify the probability of failure of individual structural members in Risk Category II, III and IV structures subjected to design earthquake Level and MCE Level shaking. For design earthquake shaking, failure probabilities are set at 10% for a Risk Category II structure and 2.5% for a Risk Category IV structure. In MCE shaking, values are set at 25% for Risk Category II structures and 10% for Risk Category IV structures. These values are consistent with the target reliabilities inherent in Chapter 16 nonlinear response history analysis and in the general targets stated in ASCE/SEI 7-16 and ASCE/SEI 7-22 Chapter 1.

Seismic Resiliency: The PUC discussed functional (and economic) level performance in the 2015 *NEHRP Provisions* through a Part 3 resource paper. It provided hypothetical performance objectives at each Risk Category in terms of life safety, function, and economic risk using multiple ground motion intensities. In the 2020 *NEHRP Provisions*, a more comprehensive Part 3 resource paper was developed that addresses the relationship between future *NEHRP Provisions* and resilience-based

design. It recognizes the role to be played by building codes and standards in providing design criteria related to functional recovery time and discusses the possible transition of the *NEHRP Provisions* toward a standard that addresses functional recovery. It acknowledges that resilience involves not only safety but recovery of function, and therefore that the design standards would need to incorporate the element of time, which is not currently done.

Section 2.7 of these 2020 *Design Examples* discusses the use of the *NEHRP Provisions* for functional recovery and provides a conceptual example.

1.4.10 Seismic Lateral Earth Pressures

For structures assigned to Seismic Design Categories D, E and F, ASCE/SEI 7-22 Chapter 11 requires consideration of dynamic seismic earthquake pressures on basement and retaining walls, but the standard does not specify the methods for calculating these pressures. Conventional practice typically involves a pseudo-static acceleration applied to a mass of the retained soil assumed to be at a failure state. Recent research suggests that this classical approach is fundamentally flawed and generally results in an overestimation of earth pressures. A 2020 *NEHRP Provisions* Part 3 resource paper presents an alternative method to account for the physical mechanisms that produce seismic earth pressures. The procedures pertain to the seismic increment of earth pressure, as opposed to the pre-seismic (static) pressure. The seismic increment is additive to the static pressure. An example application of the procedure is provided in the resource paper.

1.4.11 Soil-Structure Interaction

Although it came too late for inclusion in the 2020 *NEHRP Provisions*, refinements were made in Chapter 19 of ASCE/SEI 7-22 in part due to issues that arose in the development of FEMA P-2091, *A Practical Guide to Soil-Structure Interaction* (FEMA, 2020c) regarding the definition of various terms such as the different types of shear wave velocities used in the equations to better reflect the intent.

1.5 The *NEHRP Design Examples*

Design examples were first prepared for the 1985 *NEHRP Provisions* (FEMA, 1986a,b) in FEMA 140, *Guide to Application of the NEHRP Recommended Provisions in Earthquake Resistant Building Design* (FEMA, 1995c). These design examples were based on real buildings. The intent was the same as it is now—to show engineers how to apply the *NEHRP Provisions*, the standards referenced by the *NEHRP Provisions,* and the concepts behind the *NEHRP Provisions*.

Because of the expanded role that the *NEHRP Provisions* were having as the basis for the seismic design requirements for the model codes and standards, it was felt that there should be an update and expansion of the original design examples. Following the publication of the 2003 *NEHRP Provisions* (FEMA, 2004a,b), FEMA commissioned a project to update and expand the design examples. This resulted in FEMA 451, *NEHRP Recommended Provisions: Design Examples* (FEMA, 2006). Many of the design problems drew heavily on the examples presented in FEMA 140 but were completely redesigned based on first the 2000 *NEHRP Provisions* and then the 2003 *NEHRP*

Provisions and the materials standards referenced therein. Other examples were created to reflect the myriad of structures now covered under the *NEHRP Provisions*.

With the 2009 update to the *NEHRP Provisions,* the *Design Examples* were revised, expanded, and published as FEMA 751 (FEMA, 2012). With the 2015 update to the *NEHRP Provisions*, the design examples in FEMA 751 were again updated to reflect the *2015 NEHRP Provisions* and the updated standards referenced therein and published as FEMA 1051 (design examples), FEMA P-1051A (training materials) and FEMA P-1051B (helpful flow charts) (FEMA, 2016a,b,c). Many of the design examples were the same as presented in FEMA 751, with only changes made due to changes in the provisions. There were also several new examples to illustrate new material or significant changes from Part 1 of the *2015 NEHRP Provisions.*

With the 2020 update to the *NEHRP Provisions*, because of the significance of some of the changes in the *Provisions*, a decision was made to concentrate this 2020 *Design Examples* on the significant new changes. Where changes were not made in the 2020 *NEHRP Provisions*, the 2015 *Design Examples* generally remain valid when using the 2020 *NEHRP Provisions* and the associated ASCE/SEI 7-22. Thus, the 2015 *Design Examples* and the 2020 *Design Examples* can be used in conjunction. It is important to recognize that there have been changes in the material standards referenced by the two 2015 and 2020 *NEHRP Provisions* that may have an impact on some details in the 2015 *Design Examples*. The flow charts have also been updated.

Table 1-2 provides a summary of the material that is in the 2015 *Design Examples* and 2020 *Design Examples* and what is applicable for the 2020 *NEHRP Provisions* and the associated ASCE/SEI 7-22.

Table 1-2. Using the 2015 and 2020 *NEHRP Design Examples*

Topic	2015 *Design Examples* and ASCE/SEI 7-16	2020 *Design Examples* and ASCE/SEI 7-22
Fundamentals	Chapter 2 – Summary of fundamentals of earthquake engineering	Chapter 2 – Summary of fundamentals of earthquake engineering, updated from 2015 *Design Examples.*
Seismic Resilience	Not covered in 2015 *Design Examples*. Use 2020 *Design Examples.*	Section 2.7 – Summarizes application of resilience design to the *NEHRP Provisions* and includes a CLT case study.
Earthquake Ground Motion	Chapter 3 – Provides basis for Risk Targeted design maps, discusses hazard assessment, site specific spectra, and ground motion selection and scaling. Selection and scaling discussion are still generally applicable with ASCE/SEI 7-22. Use 2020 *Design Examples* otherwise.	Chapter 3 – Summarizes basis for new design maps, addition of more site classes, major update from two-period spectra to multi-period spectra, and update on vertical ground motion.

Table 1-2: Using the 2015 and 2020 *NEHRP Design Examples* (Continued)

Topic	2015 *Design Examples* and ASCE/SEI 7-16	2020 *Design Examples* and ASCE/SEI 7-22
Linear Analysis	Chapter 4 – Design examples with equivalent lateral force procedure, modal response spectrum analysis, and new linear response history analysis. Applicable with ASCE/SEI 7-22.	Not covered in 2020 *Design Examples*. See Section 1.4 of this Chapter on relaxation of modal response spectrum analysis requirements.
Nonlinear Response History Analysis (NRHA)	Chapter 5 – Design example using NRHA for a tall reinforced concrete shear wall building. Applicable with ASCE/SEI 7-22.	Not covered in 2020 *Design Examples*.
Diaphragm Analysis	Chapter 6 – Design examples comparing traditional and new alternate methods. Use the 2020 *Design Examples*.	Chapter 7 – Design examples showing all diaphragm analysis methods including new methods introduced with the 2020 *NEHRP Provisions*. Diaphragm design for precast diaphragms has been moved out of ASCE/SEI 7-22 to ACI publications, and this is discussed.
Foundation and Liquefaction	Chapter 7 – Design examples for shallow and deep foundations and for foundations on liquefiable soil. Applicable with ASCE/SEI 7-22.	Not covered in 2020 *Design Examples*.
Soil-Structure Interaction (SSI)	Chapter 8 – Design example of a four-story reinforced concrete shear wall building with and without SSI. Applicable with ASCE/SEI 7-22.	No examples in 2020 *Design Examples*. See Section 1.4 of this Chapter for discussion on changes to SSI provisions in ASCE/SEI 7-22.
Structural Steel	Chapter 9 – Design examples for a high-bay warehouse with an ordinary concentric braced frame and an intermediate moment frame and for an office building with a special steel moment frame and a special concentric braced frame. Applicable with ASCE/SEI 7-22.	Not covered in 2020 *Design Examples*.
Reinforced Concrete	Chapter 10 – Design examples for an intermediate moment frame, a special moment frame, and special concrete shear walls. Applicable with ASCE/SEI 7-22.	Chapter 4 – Design example for a new reinforced concrete ductile coupled wall.

Table 1-2: Using the 2015 and 2020 *NEHRP Design Examples* (Continued)

Topic	2015 *Design Examples* and ASCE/SEI 7-16	2020 *Design Examples* and ASCE/SEI 7-22
Precast Concrete	Chapter 11 – Design examples for precast diaphragms, intermediate precast concrete shear walls, tilt-up concrete, and precast special moment frame. Applicable with ASCE/SEI 7-22.	Not covered in 2020 *Design Examples*.
Composite Steel and Concrete	Chapter 12 – Design example of composite partially restrained moment frame. Applicable with ASCE/SEI 7-22.	Chapter 5 – Design example for a new steel and concrete coupled composite plate shear walls.
Masonry	Chapter 13 – Design examples for two reinforced masonry bearing wall buildings. Applicable with ASCE/SEI 7-22.	Not covered in 2020 *Design Examples*.
Wood	Chapter 14 – Design examples for an apartment, wood roof diaphragm and roof-to-wall anchorage in a masonry building. Use the 2020 *Design Examples* for wood diaphragms.	Chapter 6 – Design example for new cross-laminated timber shear wall system.
Seismic Isolation	Chapter 15 – Design example of an essential facility with lead rubber bearings using the significantly revised isolation provisions. Applicable with ASCE/SEI 7-22.	Not covered in 2020 *Design Examples*.
Damping	Chapter 16 – Design example of fluid viscous dampers in a steel moment frame building. Applicable with ASCE/SEI 7-22.	Not covered in 2020 *Design Examples*.
Nonbuilding Structures	Chapter 17 – Design examples for pipe racks, industrial storage rack, power generating plant, pier, storage tanks, and tall vertical storage vessel. Applicable with ASCE/SEI 7-22.	No examples in 2020 *Design Examples*. See Section 1.4 for discussion on changes to nonbuilding structures in ASCE/SEI 7-22.
Nonstructural Components	Chapter 18 – Design examples for precast cladding, egress stair, roof fan anchorage, piping system, and elevated vessel. Use 2020 *Design Examples*.	Chapter 8 – Background on development of new design equations and other changes, plus design examples for precast cladding, egress stair, roof fan anchorage, piping system, and elevated vessel.

The 2015 and 2020 *Design Examples* not only cover the application of ASCE/SEI 7, the material design standards and the *NEHRP Provisions*, but they also illustrate the use of analysis methods and earthquake engineering knowledge and judgment in situations which would be encountered in real designs. The authors of the design examples are subject matter experts in the specific area covered by the chapter they authored. Furthermore, the companion 2020 *NEHRP Recommend Provisions: Training Materials* (FEMA, 2021a) and flow charts (FEMA, 2021b) provide greater background information and knowledge, which augment the design examples.

It is hoped that with the Part 2 Commentary in the 2020 *NEHRP Provisions*, the 2020 *Design Examples* and the 2020 *Training Materials*, an engineer will be able to understand not just how to use the *NEHRP Provisions*, but also the philosophical and technical basis behind the provisions. Through this understanding of the intent of the seismic design requirements found in ASCE/SEI 7, the material design standards and the *2020 NEHRP Provisions*, it is hoped that more engineers will find the application of those standards less daunting and thereby utilize the standards more effectively in creating innovative and safe designs.

1.6 Organization and Presentation of the 2020 *Design Examples*

1.6.1 Organization

Chapter 2 – Fundamentals presents a brief but thorough introduction to the fundamentals of earthquake engineering. While this section does not present any specific applications of the *Provisions,* it provides the reader with the essential philosophical background to what is contained within the *Provisions*. The concepts of idealizing a seismic dynamic load as an equivalent static load and providing ductility instead of pure elastic strength are explained. The chapter also includes a new section on how the *NEHRP Provisions* can be used for improved seismic resilience, such as functional recovery goals.

Chapter 3 – Earthquake Ground Motion explains the basis for determining seismic hazard parameters used for design in the 2020 *NEHRP Provisions* and ASCE/SEI 7-22. It discusses the basis of the updated earthquake ground motion maps, issues with traditional two-point spectra in past editions of the *NEHRP Provisions* and ASCE/SEI 7, additional site classes that have been added to better capture the influence of soil on ground motion amplitude and the response spectral shape, and the new multi-point spectra approach to better capture expected response. Examples are provided applying the new multi-point spectra. Vertical ground motion updates are also discussed.

Chapter 4 – Reinforced Ductile Coupled Shear Wall System discusses a new concrete shear wall seismic force-resisting system added to the 2020 *NEHRP Provisions* and ASCE/SEI 7-22 and provides a design example.

Chapter 5 – Coupled Composite Steel Plate Shear Walls covers a new composite shear wall seismic force-resisting system, called a coupled composite plate shear wall/concrete filled, added to the 2020 *NEHRP Provisions* and ASCE/SEI 7-22 and provides a design example.

Chapter 6 – Three-Story Cross-Laminated Timber (CLT) Shear Wall presents another new wood shear wall seismic force-resisting system that was added to the 2020 *NEHRP Provisions* and ASCE/SEI 7-22 and provides a design example.

Chapter 7 – Horizontal Diaphragm Analysis presents design examples of the determination of diaphragm design forces using the traditional diaphragm design force method in ASCE/SEI 7 and then new alternate diaphragm design methods. One alternate approach was added in the 2015 *NEHRP Provisions* and ASCE/SEI 7-16. Two other approaches were added in the 2020 *NEHRP Provisions* and ASCE/SEI 7-22. One is for one-story rigid walls, flexible diaphragm buildings. The second approach covers bare metal deck diaphragms with different design values for welded deck and mechanical fastened deck.

Chapter 8 – Nonstructural Components summarizes the significant changes that have been made to Chapter 13 of the 2020 *NEHRP Provisions* and ASCE/SEI 7-22. This includes a discussion on the development of new equations for design of nonstructural components and their anchorage, plus several design examples. The examples are of an architectural concrete wall panel, an egress stair, the supports for a large rooftop fan unit, the analysis and bracing of a piping system, and an elevated vessel. Requirements for demands from both inertial forces and drift-induced forces are covered.

1.6.2 Presentation

The 2020 *Design Examples* include several key features. Callout boxes in blue shading are used to highlight important issues, such as the following item.

Reference to ASCE/SEI 7-22

For ease of reader use, the 2020 *Design Examples* typically reference ASCE/SEI 7-22 sections and equations rather than the 2020 *NEHRP Provisions*. However, at the time of completion of writing the 2020 *Design Examples* in the summer of 2021, ASCE/SEI 7-22 had not been finalized or published. Publication was expected in December 2022. The June 17, 2021, draft of ASCE/SEI 7-22 issued for public comment was used as the reference document for ASCE/SEI 7-22. At that time, all major proposals from the ASCE committee responsible for the standard had been incorporated, but public review remained. This may lead to changes in the final published version of ASCE/SEI 7-22. As such, when that published version is available, the reader of this 2020 *Design Examples* should look at the sections in the published version where revisions from ASCE/SEI 7-16 are indicated to determine whether there are meaningful differences.

Callout boxes in green shading identify known differences between the 2020 *NEHRP Provisions* and the June public comment version of ASCE/SEI 7-22. The following box provides an example.

Changes Between the *NEHRP Provisions* and ASCE/SEI 7-22

Equation 13.3-6 in the 2020 *NEHRP Provisions* was modified for ASCE/SEI 7-22, by adding I_e into the denominator to better estimate the structure ductility.

In developing the 2020 *Design Examples*, several other strategies and conventions were adopted in the design example presentations. These include the following.

- Where there are a series of similar components that would be evaluated by the same calculation procedure, a worked-out example of the calculations is typically shown in detail only once. Summary tables then show the results for the other similar components.
- Significant figures are taken to a reasonable level for engineering presentation that is generally consistent within the example. Summary tables often are based on calculation spreadsheets that have more significant figures, so the final value of a calculation or compilations in tables that add values can have small roundoff differences.
- The focus is on key selected items in each example to keep the document size manageable. Not all necessary items that would need to be checked or designed are shown. In many cases, a list of these additional items is provided.
- Computer output is shown in some design examples. Neither FEMA, nor the authors and project participants, endorse any particular computer software program or vendor.
- To avoid confusion between a section in a standard and one within the 2020 *Design Examples*, a convention such as "Section 7.1 of these 2020 *Design Examples*" has been established.
- Terminology in the 2020 *Design Examples* is intended to match that given in ASCE/SEI 7-22, including capitalization.

1.7 References

ASCE (1907). *The Effects of the San Francisco Earthquake of April 18, 1906*, American Society of Civil Engineers, New York, NY.

ASCE (1951). *Proceedings—Separate No. 66*, American Society of Civil Engineers, Reston, VA.

ASCE (1994). *Minimum Design Loads for Buildings and Other Structures,* ANSI/ASCE 7-93, American Society of Civil Engineers, Reston, VA.

ASCE (2000). *Minimum Design Loads for Buildings and Other Structures,* ASCE 7-98, Structural Engineering Institute of the American Society of Civil Engineers, Reston, VA.

ASCE (2003). *Minimum Design Loads for Buildings and Other Structures,* SEI/ASCE 7-02, Second Edition, Structural Engineering Institute of the American Society of Civil Engineers, Reston, VA.

ASCE (2006). *Minimum Design Loads for Buildings and Other Structures, Including Supplement No. 1 and Errata,* ASCE/SEI 7-05, Structural Engineering Institute of the American Society of Civil Engineers, Reston, VA.

ASCE (2013). *Minimum Design Loads for Buildings and Other Structures, incorporating errata, Supplement 1, and expanded seismic commentary,* ASCE/SEI 7-10, Third Printing, Structural Engineering Institute of the American Society of Civil Engineers, Reston, VA.

ASCE (2017). *Minimum Design Loads and Associated Criteria for Buildings and Other Structures,* ASCE/SEI 7-16, Structural Engineering Institute of the American Society of Civil Engineers, Reston, VA.

ASCE (2021). ASCE 7-22: *Minimum Design Loads and Associated Criteria for Buildings and Other Structures,* public comment draft, Structural Engineering Institute of the American Society of Civil Engineers, Reston, VA, June 17.

ATC (1978). ATC 3-06: *Tentative Provisions for the Development of Seismic Regulations for Buildings,* Applied Technology Council Redwood City, California.

BOCA (1993). *The BOCA National Building Code*, 1993 Edition, Building Officials and Code Administrators International, Country Club Hills, IL.

Bonneville, D., and Yuan, J.Q. (2019). "The 2020 NEHRP Recommended Seismic Provisions, An Overview," *2019 SEAOC Convention Proceedings*, Structural Engineers of California, Sacramento, CA.

BSSC (2019). *BSSC Project 17 Final Report, Development of Next Generation of Seismic Design Values Maps for the 2020 NEHRP Provisions*, Building Seismic Safety Council, Washington, D.C.

FEMA (1986a). *NEHRP Recommended Provisions for Seismic Regulations for New Buildings and Other Structures*, Part 1: Provisions, FEMA 95 Report, 1985 Edition, prepared by the Building Seismic Safety Council for the Federal Emergency Management Agency, Washington, D.C., February.

FEMA (1986b). *NEHRP Recommended Provisions for Seismic Regulations for New Buildings and Other Structures*, Part 2: Commentary, FEMA 96 Report, 1985 Edition, prepared by the Building Seismic Safety Council for the Federal Emergency Management Agency, Washington, D.C., February.

FEMA (1988a). *NEHRP Recommended Provisions for Seismic Regulations for New Buildings and Other Structures*, Part 1: Provisions, FEMA 95 Report, 1988 Edition, prepared by the Building Seismic Safety Council for the Federal Emergency Management Agency, Washington, D.C., October.

FEMA (1988b). *NEHRP Recommended Provisions for Seismic Regulations for New Buildings and Other Structures*, Part 2: Commentary, FEMA 96 Report, 1988 Edition, prepared by the Building Seismic Safety Council for the Federal Emergency Management Agency, Washington, D.C., October.

FEMA (1992a). *NEHRP Recommended Provisions for Seismic Regulations for New Buildings and Other Structures*, Part 1: Provisions, FEMA 222 Report, 1992 Edition, prepared by the Building Seismic Safety Council for the Federal Emergency Management Agency, Washington, D.C., January.

FEMA (1992b). *NEHRP Recommended Provisions for Seismic Regulations for New Buildings and Other Structures*, Part 2: Commentary, FEMA 223 Report, 1992 Edition, prepared by the Building Seismic Safety Council for the Federal Emergency Management Agency, Washington, D.C., January.

FEMA (1995a). *NEHRP Recommended Provisions for Seismic Regulations for New Buildings and Other Structures*, *Part 1: Provisions*, FEMA 222A Report, 1994 Edition, prepared by the Building Seismic Safety Council for the Federal Emergency Management Agency, Washington, D.C., May.

FEMA (1995b). *NEHRP Recommended Provisions for Seismic Regulations for New Buildings and Other Structures*, *Part 2: Commentary*, FEMA 223A Report, 1994 Edition, prepared by the Building Seismic Safety Council for the Federal Emergency Management Agency, Washington, D.C., May.

FEMA (1995c). *Guide to Application of the NEHRP Recommended Provisions in Earthquake Resistant Building Design*, FEMA 140 Report, Federal Emergency Management Agency, Washington, D.C., September.

FEMA (1997a). *NEHRP Recommended Provisions for Seismic Regulations for New Buildings and Other Structures*, Part 1: Provisions, FEMA 302 Report, 1997 Edition, prepared by the Building Seismic Safety Council for the Federal Emergency Management Agency, Washington, D.C.

FEMA (1997b). *NEHRP Recommended Provisions for Seismic Regulations for New Buildings and Other Structures*, Part 2: Commentary, FEMA 303 Report, 1997 Edition, prepared by the Building Seismic Safety Council for the Federal Emergency Management Agency, Washington, D.C.

FEMA (2001a). *NEHRP Recommended Provisions for Seismic Regulations for New Buildings and Other Structures*, Part 1: Provisions, FEMA 368 Report, 2000 Edition, prepared by the Building Seismic Safety Council for the Federal Emergency Management Agency, Washington, D.C., March.

FEMA (2001b). *NEHRP Recommended Provisions for Seismic Regulations for New Buildings and Other Structures*, Part 2: Commentary, FEMA 369 Report, 2000 Edition, prepared by the Building Seismic Safety Council for the Federal Emergency Management Agency, Washington, D.C., March.

FEMA (2004a). *NEHRP Recommended Provisions for Seismic Regulations for New Buildings and Other Structures*, Part 1: Provisions, FEMA 450-1 Report, 2003 Edition, prepared by the Building Seismic Safety Council for the Federal Emergency Management Agency, Washington, D.C.

FEMA (2004b). *NEHRP Recommended Provisions for Seismic Regulations for New Buildings and Other Structures*, Part 2: Commentary, FEMA 450-2 Report, 2003 Edition, prepared by the Building Seismic Safety Council for the Federal Emergency Management Agency, Washington, D.C.

FEMA (2006). *NEHRP Recommended Provisions: Design Examples,* FEMA 451 Report, prepared by the Building Seismic Safety Council for the Federal Emergency Management Agency, Washington, D.C., August.

FEMA (2009a). *NEHRP Recommended Seismic Provisions for New Buildings and Other Structures*, , FEMA 750 Report, 2009 Edition, prepared by the Building Seismic Safety Council for the Federal Emergency Management Agency, Washington, D.C.

FEMA (2009b). *Quantification of Building Seismic Performance Factors,* FEMA P695 Report, prepared by the Applied Technology Council for the Federal Emergency Management Agency, Washington, D.C.

FEMA (2012). *2009 NEHRP Recommended Seismic Design Provisions: Design Examples,* FEMA 751 Report, prepared by the Building Seismic Safety Council for the Federal Emergency Management Agency, Washington, D.C.

FEMA (2015a). *NEHRP Recommended Seismic Provisions for New Buildings and Other Structures*, Volume I: Part 1 Provisions, Part 2 Commentary, FEMA P-1050-1 Report, 2015 Edition, prepared by the Building Seismic Safety Council for the Federal Emergency Management Agency, Washington, D.C., September.

FEMA (2015b). *NEHRP Recommended Seismic Provisions for New Buildings and Other Structures*, Volume II: Part 3 Resource Papers, FEMA P-1050-2 Report, 2015 Edition, prepared by the Applied Technology Council for the Building Seismic Safety Council, Washington, D.C., September.

FEMA (2015c). *Seismic Design of Rigid Wall-Flexible Diaphragm Buildings: An Alternate Procedure,* FEMA P-1026 Report, prepared by the Applied Technology Council for the Federal Emergency Management Agency, Washington, DC.

FEMA (2016a). 2015 *NEHRP Recommended Seismic Provisions: Design Examples,* FEMA P-1051 Report, prepared by the Building Seismic Safety Council for the Federal Emergency Management Agency, Washington, D.C., July.

FEMA (2016b). 2015 *NEHRP Recommended Seismic Provisions: Training and Educational Materials*, FEMA P-1052 Report, prepared by the Building Seismic Safety Council for the Federal Emergency Management Agency, Washington, D.C.

FEMA (2016c). 2015 *NEHRP Recommended Seismic Provisions: Design Examples Flow Charts*, FEMA P-1051B Report, prepared by the Building Seismic Safety Council for the Federal Emergency Management Agency, Washington, D.C.

FEMA (2018). *Assessing Seismic Performance of Buildings with Configuration Irregularities: Calibrating Current Standards and Practice,* FEMA P-2012 Report, prepared by the Applied Technology Council for the Federal Emergency Management Agency, Washington, D.C., December.

FEMA (2020a). *NEHRP Recommended Seismic Provisions for New Buildings and Other Structures*, Volume I: Part 1 Provisions, Part 2 Commentary, FEMA P-2082-1 Report, prepared by the Building Seismic Safety Council for the Federal Emergency Management Agency, Washington, D.C., September.

FEMA (2020b). *NEHRP Recommended Seismic Provisions for New Buildings and Other Structures*, Volume II: Part 3 Resource Papers, FEMA P-2082-2 Report, prepared by the Applied Technology Council for the Building Seismic Safety Council, Washington, D.C., September.

FEMA (2020c). *A Practical Guide to Soil-Structure Interaction*, FEMA P-2091 Report, prepared by the Applied Technology Council for the Federal Emergency Management Agency, Washington, D.C., December.

FEMA (2021a). 2020 *NEHRP Recommended Seismic Provisions: Design Examples, Training Materials*, *and Design Flow Charts, Volume II: Training Materials,* FEMA P-2192-V2 Report, prepared by the Building Seismic Safety Council for the Federal Emergency Management Agency, Washington, D.C.

FEMA (2021b). 2020 *NEHRP Recommended Seismic Provisions: Design Examples, Training Materials, and Design Flow Charts*, *Volume III: Design Flow Charts,* FEMA P-2192-V3 Report prepared by the Building Seismic Safety Council for the Federal Emergency Management Agency, Washington, D.C.

FEMA (2021c). *The Role of the NEHRP Recommended Seismic Provisions in the Development of Nationwide Seismic Building Code Regulations: A Thirty-Five-Year Retrospective*, FEMA P-2156 Report, prepared by the Building Seismic Safety Council for the Federal Emergency Management Agency, Washington, D.C., February.

ICBO (1927). *Uniform Building Code, 1927 Edition,* International Conference of Building Officials, Whittier, CA.

ICBO (1997). *Uniform Building Code, Volume 2, Structural Engineering Design Provisions, 1997 Edition,* International Conference of Building Officials, Whittier, CA.

ICC (2000). *International Building Code, 2000 Edition,* First Printing in March 2000, Thirteenth Printing in December 2005, *Thirteenth Printing,* International Code Council, Whittier, CA.

ICC (2002). *International Building Code, 2003 Edition,* First Printing in December 2002, Tenth Printing in November 2011, International Code Council, Whittier, CA, November.

ICC (2006). *International Building Code, 2006 Edition*, First Printing in January 2006, Eleventh Printing in March 2015, International Code Council, Whittier, CA.

ICC (2009). *International Building Code, 2009 Edition*, First Printing in February 2009, Thirteen Printing in June 2017, International Code Council, Whittier, CA.

ICC (2011). *International Building Code, 2012 Edition*, First Printing in May 2011, Thirteenth Printing in March 2019, International Code Council, Whittier, CA.

ICC (2014). *International Building Code, 2015 Edition*, First Printing in May 2014, Third Printing in October 2015, International Code Council, Whittier, CA.

ICC (2017). *International Building Code, 2018 Edition*, First Printing in October 2017, Fifth Printing in September 2020, International Code Council, Whittier, CA.

ICC (2020). *International Building Code, 2021 Edition*, First Printing in October 2020, International Code Council, Whittier, CA.

Kircher, C. (2015). "Investigation of an identified shortcoming in the seismic design procedures of ASCE 7-10 and development of improvements for ASCE 7-16," prepared for Building Seismic Safety Council, Washington, D.C.

NIST (2018). *Recommendations for Improved Seismic Performance of Nonstructural Components,* NIST GCR 18-917-43 Report, prepared by the Applied Technology Council for the National Institute of Standards and Technology, Gaithersburg, MD, September.

SBCCI (1994). *Standard Building Code*, 1994 Edition, Southern Building Code Congress International.

Schafer, B. (2019). *Research on the Seismic Performance of Rigid Wall Flexible Diaphragm Buildings with Bare Steel Deck Diaphragms*, CFSRC Report 2019-2, Cold-Formed Steel Research Consortium, January.

SEAOC (1959). *Recommended Lateral Force Requirements*, Seismology Committee, Structural Engineers Association of California, Sacramento, CA, July.

SEAOC (2019). *SEAOC Blue Book, Seismic Design Recommendations 2019,* Seismology Committee, Structural Engineers Association of California, Sacramento, CA.

Chapter 2: Fundamentals

James R. Harris[1] and David Bonowitz[2]

In introducing their classic text, *Fundamentals of Earthquake Engineering*, Newmark and Rosenblueth (1971) commented:

> In dealing with earthquakes, we must contend with appreciable probabilities that failure will occur in the near future. Otherwise, all the wealth of the world would prove insufficient to fill our needs: the most modest structures would be fortresses. We must also face uncertainty on a large scale, for it is our task to design engineering systems – about whose pertinent properties we know little – to resist future earthquakes and tidal waves – about whose characteristics we know even less. . . In a way, earthquake engineering is a cartoon. . . Earthquake effects on structures systematically bring out the mistakes made in design and construction, even the minutest mistakes.

Several points essential to an understanding of the theories and practices of earthquake-resistant design bear restating:

1. Ordinarily, a large earthquake produces the most severe loading that a building is expected to survive. The probability that *failure* will occur is very real and is greater than for other loading phenomena. Also, in the case of earthquakes, the definition of *failure* is altered to permit certain types of behavior and damage that are considered unacceptable in relation to the effects of other phenomena.
2. The levels of uncertainty are much greater than those encountered in the design of structures to resist other phenomena. This is in spite of the tremendous strides made since the Federal government began strongly supporting research in earthquake engineering and seismology following the 1964 Prince William Sound and 1971 San Fernando earthquakes. The high uncertainty applies both to knowledge of the loading function and to the resistance properties of the materials, members, and systems.
3. The details of construction are very important because flaws of no apparent consequence often will cause systematic and unacceptable damage simply because the earthquake loading is so severe and an extended range of behavior is permitted.

The remainder of this chapter is devoted to a very abbreviated discussion of fundamentals that reflect the concepts on which earthquake-resistant design are based. When appropriate, important aspects of the *NEHRP Recommended Seismic Provisions for New Buildings and Other Structures* are

[1] James Harris, P.E., Ph.D., J. R. Harris & Company, led the development of Sections 2.1 through 2.6.

[2] David Bonowitz, S.E., led the development of Section 2.7.

mentioned and reference is made to particularly relevant portions of that document or the standards that are incorporated by reference. The *2020 Provisions* (FEMA, 2020a) is composed of three parts: 1) "Provisions", 2) "Commentary" and 3) "Resource Papers on Special Topics in Seismic Design." Part 1 states the intent and then cites ASCE/SEI 7-16 *Minimum Design Loads for Buildings and Other Structures* (ASCE, 2017) as the primary reference. The remainder of Part 1 contains recommended changes to update ASCE/SEI 7-16; the recommended changes include commentary on each specific recommendation. All three parts are referred to herein as the *Provisions,* but where pertinent the specific part is referenced and ASCE/SEI 7-16 is referred to as the *Standard*. ASCE/SEI 7-16 itself refers to several other standards for the seismic design of structures composed of specific materials and those standards are essential elements to achieve the intent of the *Provisions*.

2.1 Earthquake Phenomena

According to the most widely held scientific belief, most earthquakes occur when two segments of the earth's crust suddenly move in relation to one another. The surface along which movement occurs is known as a fault. The sudden movement releases strain energy and causes seismic waves to propagate through the crust surrounding the fault. These waves cause the surface of the ground to shake violently, and it is this ground shaking that is the principal concern of structural engineering to resist earthquakes.

Earthquakes have many effects in addition to ground shaking. For various reasons, many of the other effects generally are not major considerations in the design of buildings and similar structures. For example, seismic sea waves or tsunamis can cause very forceful flood waves in coastal regions, and seiches (long-period sloshing) in lakes and inland seas can have similar effects along shorelines. These are outside the scope of the *Provisions*. The devasting tsunamis accompanying the 2004 Sumatra-Andaman and the 2010 Tohoku Earthquakes stimulated the development of methods to design structures to resist such hydrodynamic forces, and ASCE/SEI 7-16 includes a chapter devoted to that effect. Long-period sloshing of the liquid contents of tanks is addressed by the *Provisions*.

Abrupt ground displacements occur where a fault intersects the ground surface. (This commonly occurs in California earthquakes but did not occur in the historic Charleston, South Carolina earthquake or the very large New Madrid, Missouri, earthquakes of the nineteenth century.) Mass soil failures such as landslides, liquefaction, and gross settlement result from ground shaking on susceptible soil formations. Once again, design for such events is specialized, and it is common to locate structures so that mass soil failures and fault rupture are of no major consequence to their performance. Modifying soil properties to protect against liquefaction is one important exception; large portions of a few metropolitan areas with the potential for significant ground shaking are susceptible to liquefaction. Lifelines that cross faults require special design beyond the scope of the *Provisions*. The structural loads specified in the *Provisions* are based solely on ground shaking; they do not provide for ground failure. Resource Paper 12 ("Evaluation of Geologic Hazards and Determination of Seismic Lateral Earth Pressures") in Part 3 of the 2009 *Provisions* (FEMA, 2009) includes a description of current procedures for predicting seismic-induced slope instability,

liquefaction and surface fault rupture. Selected portions of that work are now included in the *Provisions*.

Nearly all large earthquakes are *tectonic* in origin. They are associated with movements of and strains in large segments of the earth's crust, called *plates*, and virtually all such earthquakes occur at or near the boundaries of these plates. This is the case with earthquakes in the far western portion of the United States, where two very large plates, the North American continent and the Pacific basin, come together. In the central and eastern United States, however, earthquakes are not associated with such a plate boundary, and their causes are not as completely understood. This factor, combined with the smaller amount of data about central and eastern earthquakes (because of their infrequency), means that the uncertainty associated with earthquake loadings is higher in the central and eastern portions of the nation than in the West. Even in the west, the uncertainty (when considered as a fraction of the predicted level) about the hazard level is probably greater in areas where the mapped hazard is low than in areas where the mapped hazard is high.

Two basic data sources are used in establishing the likelihood of earthquake ground shaking, or seismicity, at a given location. The first is the historical record of earthquake effects and the second is the geological record of earthquake effects. Given the infrequency of major earthquakes, there is no place in the United States where the historical record is long enough to be used as a reliable basis for earthquake prediction – certainly not as reliable as with other phenomena such as wind and snow. Even on the eastern seaboard, the historical record is too short to justify sole reliance on the historical record. Thus, the geological record is essential. Such data requires very careful interpretation, but they are used widely to improve knowledge of seismicity. Geological data have been developed for many locations as part of the nuclear power plant design process. Overall, there is more geological data available for the far western United States than for other regions of the country. Both sets of data have been taken into account in the *Provisions* seismic ground shaking maps. In recent years, data from earthquakes associated with pumping fluid into deep wells have also been considered in understanding the geologic procedures.

The amplitude of earthquake ground shaking diminishes with distance from the source, and the rate of attenuation is less for lower frequencies of motion than for higher frequencies. This effect is captured by the fact that the *Provisions* specify response acceleration parameters at 22 frequencies of vibration to define the hazard of seismic ground shaking for structures. They are based on a statistical analysis of the database of seismological information. The *Provisions* provide one additional parameter for definition of response to ground shaking, T_L. It defines an important transition point for long period (low frequency) behavior; it is not based upon as robust of an analysis as the other parameters.

The *Commentary* provides a more thorough discussion of the development of the maps, their probabilistic basis, the necessarily crude lumping of parameters and other related issues. Prior to its 1997 edition, the basis of the *Provisions* was to "minimize the hazard to life…" at the design earthquake motion, which was defined as having a 10 percent probability of being exceeded in a 50-year reference period (FEMA, 1995). As of the 1997 edition (FEMA, 1997), the basis became to avoid *structural collapse* at the maximum considered earthquake (MCE) ground motion, which is

defined as having a 2 percent probability of being exceeded in a 50-year reference period. In the 2009 edition of the *Provisions* the design basis was refined to target a 1% probability of structural collapse for ordinary buildings in a 50-year period. The MCE ground motion has been adjusted to deliver this level of risk combined with a 10% probability of collapse should the MCE ground motion occur. This new approach incorporates a fuller consideration of the nature of the seismic hazard at a location than was possible with the earlier definitions of ground shaking hazard, which were tied to a single level of probability of ground shaking occurrence.

The nature of the uncertainty in earthquake occurrence and in ground shaking amplitude combine to predict very high ground motions near faults that produce large earthquakes relatively frequently. Empirical evidence of building performance in past earthquakes indicates that design for such extreme motions is not necessary. Consequently, when the MCE concept was introduced, the *Provisions* included a semi-deterministic upper bound on the accelerations produced by the purely probabilistic method. The concept used was to combine the occurrence of a reasonable upper bound earthquake at the known fault location with a somewhat conservative estimate (mean plus one standard deviation) of the ground shaking at a site. The details of this method have evolved in subsequent editions of the *Provisions*, but the philosophical basis remains the same.

2.2 Structural Response to Ground Shaking

The first important difference between structural response to an earthquake and response to most other loadings is that the earthquake response is *dynamic*, not *static*. For most structures, even the response to wind is essentially static. Forces within the structure are due almost entirely to the pressure loading rather than the acceleration of the mass of the structure. But with earthquake ground shaking, the above ground portion of a structure is not subjected to any applied force. The stresses and strains within the superstructure are created entirely by its dynamic response to the movement of its base, the ground. Even though the most used design procedure resorts to the use of a concept called the equivalent static force for actual calculations, some knowledge of the theory of vibrations of structures is essential.

2.2.1 Response Spectra

Figure 2-1 shows accelerograms, records of the acceleration at one point along one axis, for several representative earthquakes. Note the erratic nature of the ground shaking and the different characteristics of the different accelerograms. Precise analysis of the elastic response of an ideal structure to such a pattern of ground motion is possible; however, it is not commonly done for ordinary structures. The increasing power and declining cost of computational aids are making such analyses more common, but, at this time, only a small minority of structures designed across the country are analyzed for specific response to a specific ground motion.

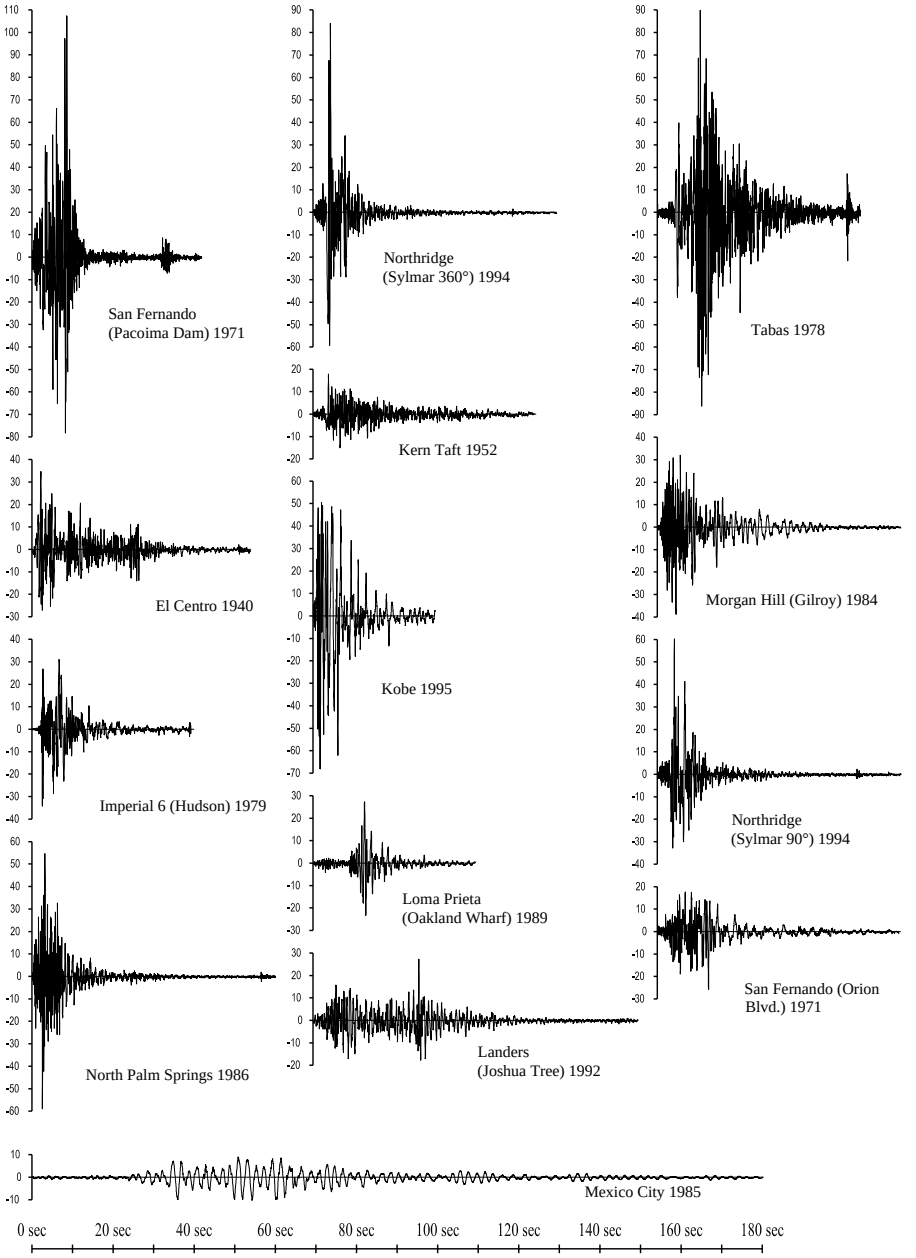

Figure 2-1. Earthquake Ground Acceleration in Epicentral Regions. Note: All accelerograms are plotted to the same scale for time and acceleration – the vertical axis is % gravity). Great earthquakes extend for much longer periods of time.)

Figure 2-2 shows further detail developed from an accelerogram. Part (a) shows the ground acceleration along with the ground velocity and ground displacement derived from it. Part (b) shows the acceleration, velocity, and displacement for the same event at the roof of the building located where the ground motion was recorded. Note that the peak values are larger in the diagrams of Figure 2-2(b) (the vertical scales are essentially the same). This increase in response of the structure at the roof level over the motion of the ground itself is known as dynamic amplification. It depends

very much on the vibrational characteristics of the structure and the characteristic frequencies of the ground shaking at the site.

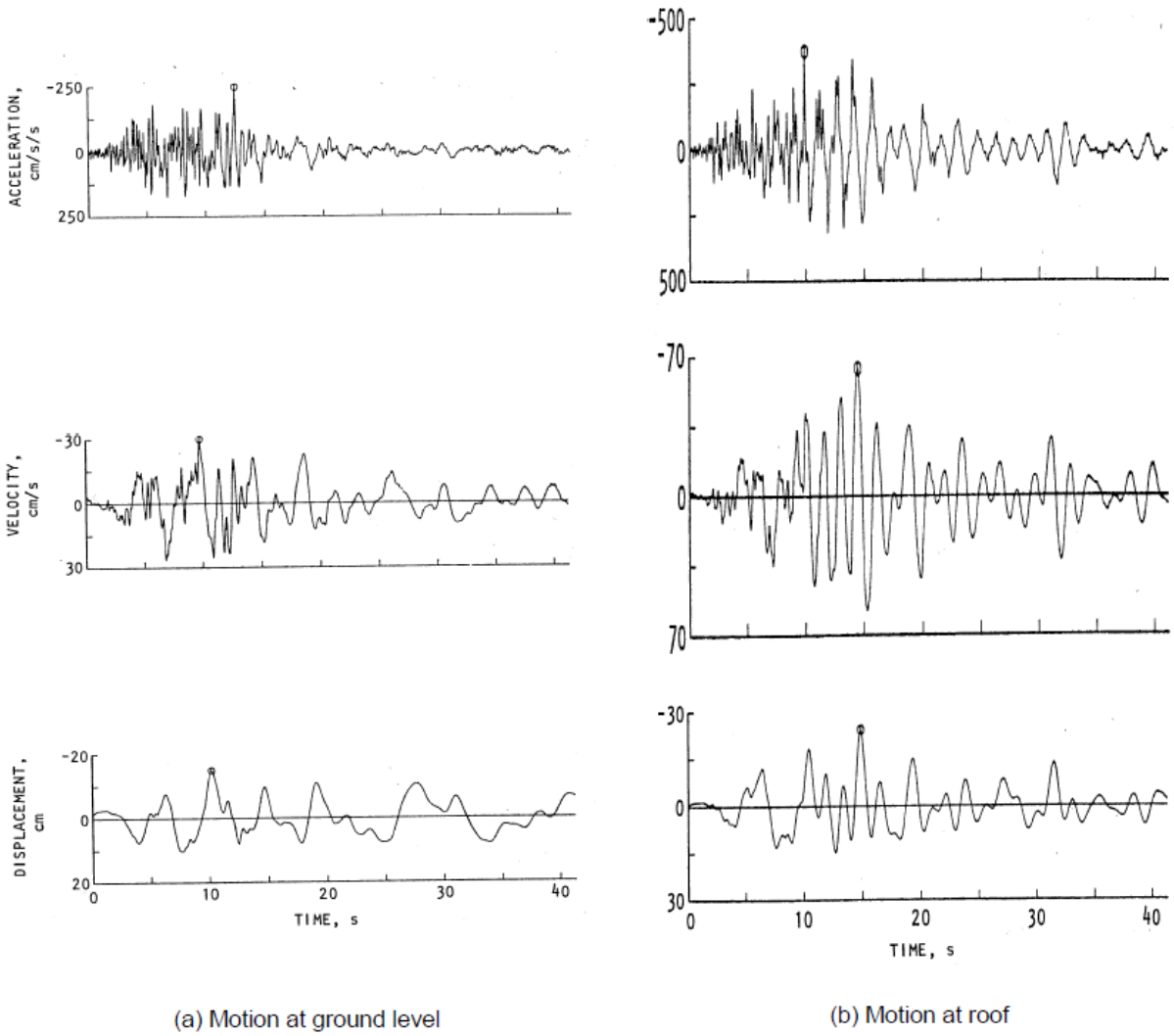

Figure 2-2. Holiday Inn Ground and Building Roof Motion During the M6.4 1971 San Fernando Earthquake: (a) North-South Ground Acceleration, Velocity and Displacement and (b) North-South Roof Acceleration, Velocity and Displacement (Housner and Jennings, 1982). The building was a seven-story, reinforced concrete frame, approximately five miles from the closest portion of the causative fault.

In design, the response of a specific structure to an earthquake is ordinarily estimated from a design response spectrum such as what is specified in the *Provisions*. The first step in creating a design response spectrum is to determine the maximum response of a given structure to a specific ground motion (see the maximum response points denoted by the circles in Figure 2-2b). The underlying theory is based entirely on the response of a single-degree-of-freedom oscillator, such as a simple one-story frame with the mass concentrated at the roof. The vibrational characteristics of such a

simple oscillator may be reduced to two: the natural period[1] and the amount of damping. By recalculating the record of response versus time to a specific ground motion for a wide range of natural periods and for each of a set of common amounts of damping, the family of response spectra for one ground motion may be determined. It is simply the plot of the maximum value of response for each combination of period and damping.

Figure 2-3 shows such a result for the ground motion of Figure 2-2(a) and illustrates that the erratic nature of ground shaking leads to a response that is very erratic in that a slight change in the natural period of vibration brings about a very large change in response. The figure also illustrates the significance of damping. Different earthquake ground motions lead to response spectra with peaks and valleys at different points with respect to the natural period. Thus, computing response spectra for several different ground motions and then averaging them, based on some normalization for different amplitudes of shaking, will lead to a smoother set of spectra. Such smoothed spectra are an important step in developing a design spectrum.

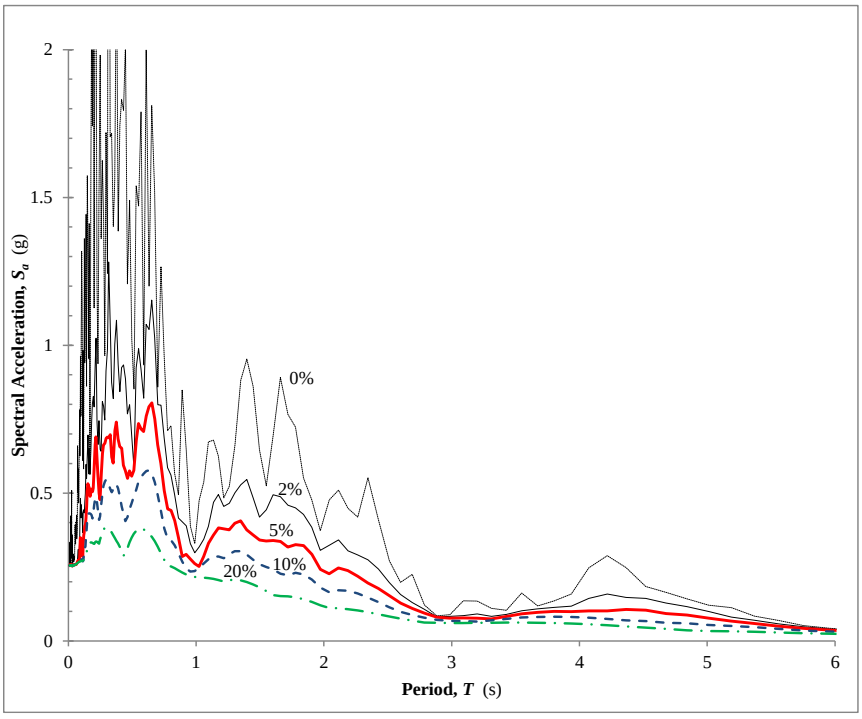

Figure 2-3. Response Spectrum of North-South Ground Acceleration (0%, 2%, 5%, 10%, 20% of Critical Damping) Recorded at the Holiday Inn, Approximately Five miles from the Causative Fault in the 1971 San Fernando Earthquake

[1] Much of the literature on dynamic response is written in terms of frequency rather than period. The cyclic frequency (cycles per second, or Hz) is the inverse of period. Mathematically it is often convenient to use the angular frequency expressed as radians per second rather than Hz. The conventional symbols used in earthquake engineering for these quantities are T for period (seconds per cycle), f for cyclic frequency (Hz) and ω for angular frequency (radians per second). The word frequency is often used with no modifier; be careful with the units.

Figure 2-4 is an example of an averaged spectrum. Note that acceleration, velocity, or displacement may be obtained from Figure 2-3 or 2-4 for a structure with a known period and damping.

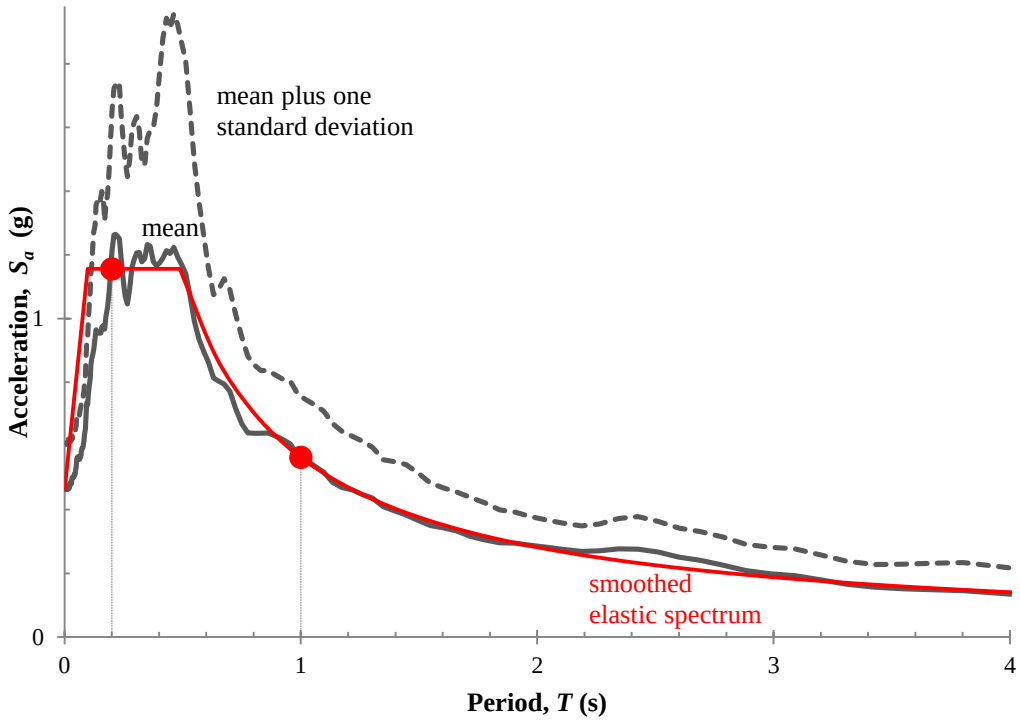

Figure 2-4. Averaged Spectrum. Note: In this case, the statistics are for seven ground motions representative of the de-aggregated hazard at a particular site.

Prior to the 1997 edition of the *Provisions*, the maps that characterized the ground shaking hazard were plotted in terms of peak ground acceleration (at period $T = 0$), and design response spectra were created using expressions that amplified (or de-amplified) the ground acceleration as a function of period and damping. With the introduction of the MCE maps in the 1997 edition, this procedure changed. Those maps presented spectral response accelerations at two periods of vibration, 0.2 and 1.0 second, and the design response spectrum was computed more directly, as implied by the smooth line in Figure 2-4. This has removed a portion of the uncertainty in predicting response accelerations.

The ground motions in the 2020 *Provisions* are given as spectral response accelerations at 22 periods from zero to 10 seconds. The shape of the spectrum varies from one location to another, but the two spectral ordinates for construction of the familiar spectral shape are also given for conventional analysis. Figure 2-5shows the two spectra for a location in Southern California.

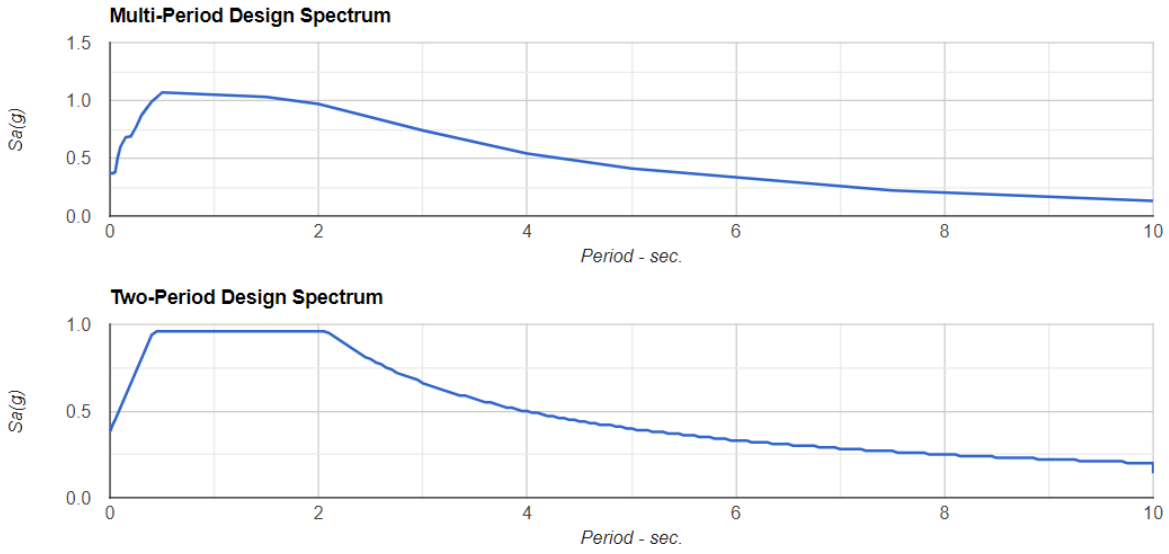

Figure 2-5. Comparison of the Multi-period Design Spectrum with the Two-period Spectrum from the 2020 *Provisions* for a Site in Southern California

Few structures are simple enough to vibrate as a single-degree-of-freedom system. The principles of dynamic modal analysis, however, allow a reasonable approximation of the maximum response of a multi-degree-of-freedom oscillator, such as a multistory building, if many specific conditions are met. The procedure involves dividing the total response into several natural modes, modeling each mode as an equivalent single-degree-of-freedom oscillator, determining the maximum response for each mode from a single-degree-of-freedom response spectrum and then estimating the maximum total response by statistically summing the responses of the individual modes. The *Provisions* does not require consideration of all possible modes of vibration for most buildings because the contribution of the higher modes (lower periods) to the total response is relatively minor.

The soil at a site has a significant effect on the characteristics of the ground motion and, therefore, on the structure's response. Especially at low amplitudes of motion and at longer periods of vibration, soft soils amplify the motion at the surface with respect to bedrock motions. This amplification is diminished somewhat, especially at shorter periods as the amplitude of basic ground motion increases due to yielding in the soil. The *Provisions* accounts for this effect by providing amplifiers that are to be applied to the spectral accelerations for various classes of soils. The site classes are based upon the velocity of a shear wave passing through the soil averaged over the top 100 feet (30 meters). The amount of amplification depends on both that average velocity and the amplitude of the motion in rock. Thus, very different design response spectra are specified depending on the type of soil(s) beneath the structure. The *Commentary* (Part 2) contains a thorough explanation of this feature.

2.2.2 Inelastic Response

The preceding discussion assumes elastic behavior of the structure. The principal extension beyond ordinary behavior referenced at the beginning of this chapter is that structures are permitted to strain beyond the elastic limit in responding to earthquake ground shaking. This is dramatically different from the case of design for other types of loads in which stresses, and therefore strains, are not permitted to approach the elastic limit. The reason is economic. Figure 2-3 shows a peak acceleration response of about 1.0 g (the acceleration due to gravity) for a structure with moderately low damping – for only a moderately large earthquake! Even structures that resist lateral forces well will have a static lateral strength of only 20 to 40 percent of gravity.

The dynamic nature of earthquake ground shaking means that a large portion of the shaking energy can be dissipated by inelastic deformations if the structure is ductile and some damage to the structure is accepted. Figure 2-6 will be used to illustrate the significant difference between wind and seismic effects. Figure 2-6 (a) would represent a cantilever beam if the load *W* were small and a column if *W* were large. Wind pressures create a force on the structure, which in turn produces a displacement. The force is the independent variable, and the displacement is the dependent result. Earthquake ground motion creates displacement between the base and the mass, which in turn produces an internal force. The displacement is the independent variable, and the force is the dependent result. Two graphs are plotted with the independent variables on the horizontal axis and the dependent response on the vertical axis. Thus, Part (b) of Figure 2-6 is characteristic of the response to forces such as wind pressure (or gravity weight), while Part (c) is characteristic of induced displacements such as earthquake ground shaking (or foundation settlement).

Note that the ultimate resistance (H_u) in a force-controlled system is marginally larger than the yield resistance (H_y), while the ultimate displacement (Δ_u) in a displacement-controlled system is much larger than the yield displacement (Δ_y). The point being made with the figures is that ductile structures have the ability to resist displacements much larger than those that first cause yield. Thus ductility is a much more important property when the demand is displacement than when the demand is force.

The degree to which a member or structure may deform beyond the elastic limit is usually referred to as ductility. Different materials and different arrangements of structural members lead to different ductilities. Response spectra may be calculated for oscillators with different levels of ductility. At the risk of gross oversimplification, the following conclusions may be drawn:

1. For structures with very long natural periods, the acceleration response is reduced by a factor equivalent to the ductility ratio (the ratio of maximum usable displacement to effective yield displacement – note that this is displacement and not strain).
2. For structures with very short natural periods, the acceleration response of the ductile structure is essentially the same as that of the elastic structure, but the displacement is increased.

3. For intermediate periods (which applies to nearly all buildings), the acceleration response is reduced, but the displacement response is generally about the same for the ductile structure as for the elastic structure strong enough to respond without yielding.

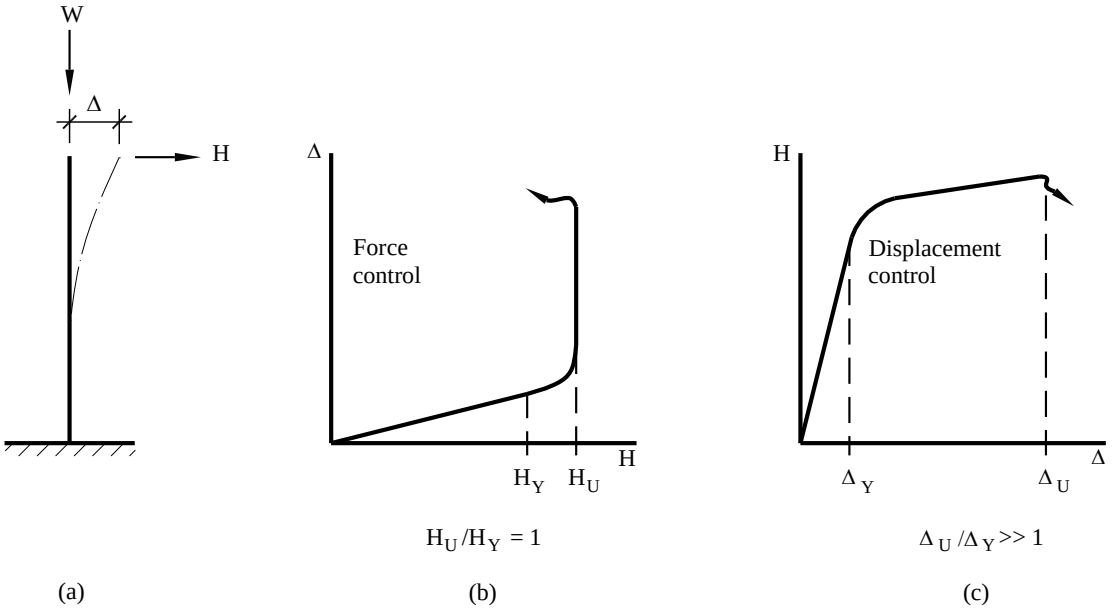

Figure 2-6. Force Controlled Resistance Versus Displacement Controlled Resistance (after Housner and Jennings 1982)

Note: In Part (b), the force H is the independent variable. As H is increased, the displacement increases until the yield point stress is reached. If H is given an additional increment (about 15 percent) a plastic hinge forms, giving large displacements. For this kind of system, the force producing the yield point stress is close to the force producing collapse. The ductility does not produce a large increase in load capacity, although in highly redundant structures the increase is more than illustrated for this very simple structure. In Part (c) the displacement is the independent variable. As the displacement is increased, the base moment increases until the yield point is reached. As the displacement increases still more, the resistance (H) increases only a small amount. For a highly ductile element, the displacement can be increased 10 to 20 times the yield point displacement before the system collapses under the weight W. (As W increases, this ductility is decreased dramatically.) During an earthquake, the oscillator is excited into vibrations by the ground motion and it behaves essentially as a displacement-controlled system and can survive displacements much beyond the yield point. This explains why ductile structures can survive ground shaking that produces displacements much greater than yield point displacement.

Inelastic response is quite complex. Earthquake ground motions involve a significant number of reversals and repetitions of the strains. Therefore, observation of the inelastic properties of a material, member, or system under a monotonically increasing load until failure can be very misleading. Cycling the deformation can cause degradation of strength, stiffness, or both. Systems that have a proven capacity to maintain a stable resistance to many cycles of inelastic deformation are allowed to exercise a greater portion of their ultimate ductility in designing for earthquake resistance. This property is often referred to as toughness, but this is not the same as the classic

definition used in mechanics of materials, which is the strain energy to failure under montonic loading.

Most structures are designed for seismic response using a linear elastic analysis with the strength of the structure limited by the strength at its critical location. Most structures possess enough complexity so that the peak strength of a ductile structure is not accurately captured by such an analysis. Figure 2-7 shows the load versus displacement relation for a simple frame. Yield must develop at four locations before the peak resistance is achieved. The margin from the first yield to the peak strength is referred to as overstrength, and it plays a significant role in resisting strong ground motion. Note that a few key design standards (for example, American Concrete Institute (ACI) 318 for the design of concrete structures) do allow for some redistribution of internal forces from the critical locations based upon ductility; however, the redistributions allowed therein are minor compared to what occurs in response to strong ground motion. Many types of structures, particularly buildings also possess additional overstrength from the resistance to lateral displacement provided by structural elements not deemed to be a part of the seismic-resisting system and by nonstructural elements, such as cladding.

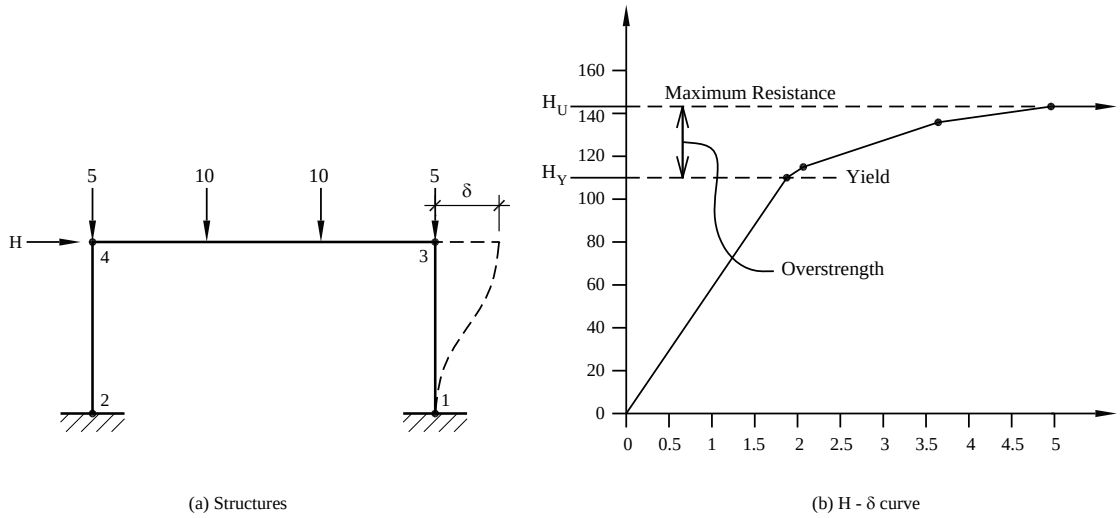

Figure 2-7. Initial Yield Load and Failure for a Ductile Portal Frame

Note: The margin from initial yield to failure (mechanism in this case) is known as overstrength.

To summarize, the characteristics important in determining a building's seismic response are natural period, damping, ductility, stability of resistance under repeated reversals of inelastic deformation and overstrength. The natural frequency is dependent on the mass and stiffness of the building. Using the *Provisions,* the designer calculates, or at least approximates, the natural period of vibration (the inverse of natural frequency). Damping, ductility, toughness and overstrength depend primarily on the type of building system but not the building's size or shape. Recent studies have shown that the total deformation capacity of the structure may be a more useful parameter than a ductility ratio to characterize a structure's resistance to collapse, but quantification of performance

based on that parameter is still a research topic. Three coefficients – R, C_d, and Ω_0 – are provided to encompass damping, ductility, stability of resistance and overstrength. R is intended to be a conservatively low estimate of the reduction of acceleration response in a ductile system from that for an elastic oscillator with a certain level of damping. It is used to compute a required strength. Computations of displacement based upon ground motion reduced by the factor R will underestimate the actual displacements. C_d is intended to be a reasonable mean for the amplification necessary to convert the elastic displacement response computed for the reduced ground motion to actual displacements. Ω_0 is intended to deliver a reasonably high estimate of the peak force that would develop in the structure. Sets of R, C_d, and Ω_0 are specified in the *Provisions* for the most common structural materials and systems.

2.2.3 Building Materials

The following brief comments about building materials and systems are included as general guidelines only, not for specific application.

2.2.3.1 WOOD

Timber structures nearly always resist earthquakes very well, even though wood is a brittle material as far as tension and flexure are concerned. It has some ductility in compression (generally monotonic), and its strength is significantly higher for brief loadings, such as in an earthquake, than for long term loads. Conventional timber structures (plywood, oriented strand board, or board sheathing on wood framing) possess much more ductility than the basic material primarily because the nails and other steel connection devices yield, and the wood compresses against the connector. These structures also possess a much higher degree of damping than the damping that is assumed in developing the basic design spectrum. Much of this damping is caused by slip at the connections. Light-framed wood construction also usually has significant overstrength from nonstructural sheathing material on walls and partitions. The increased strength, connection ductility, and high damping combine to give timber structures a large reduction from elastic response to design level. This large reduction should not be used if the strength of the structure is controlled by bending or tension of the gross timber cross sections. The large reduction in acceleration combined with the lightweight timber structures make them very efficient regarding earthquake ground shaking when they are properly connected. This is confirmed by their generally good performance in earthquakes. Capacities and design and detailing rules for wood elements of seismic force-resisting systems are now found in the *Special Design Provisions for Wind and Seismic* (AWC, 2020) supplement to the *National Design Specification for Wood Construction* (AWC, 2017).

2.2.3.2 STEEL

Steel is the most ductile of the common building materials. The moderate-to-large reduction from elastic response to design response allowed for steel structures is primarily a reflection of this ductility and the stability of the resistance of steel. Members subject to buckling (such as bracing) and connections subject to brittle fracture (such as partial penetration welds under tension) are much less ductile and are addressed in the *Provisions* in various ways. Defects, such as stress concentrations and flaws in welds, also affect earthquake resistance, as demonstrated in the

Northridge earthquake. The basic and applied research program that grew out of that experience has greatly increased knowledge of how to avoid low ductility details in steel construction. Capacities and design and detailing rules for seismic design of hot-rolled structural steel are found in the *Seismic Provisions for Structural Steel Building*s (AISC, 2016) and similar provisions for cold-formed steel are found in the *North American Standard for Seismic Design* (AISI, 2021).

2.2.3.3 REINFORCED CONCRETE

Reinforced concrete achieves ductility through careful limits on steel in tension and concrete in compression. Reinforced concrete beams with common proportions can possess ductility under monotonic loading even greater than common steel beams, in which local buckling is usually a limiting factor. Providing stability of the resistance to reversed inelastic strains, however, requires special detailing. Thus, there is a wide range of reduction factors from elastic response to design response depending on the detailing for stable and assured resistance. The 2020 *NEHRP Provisions Commentary* and the commentary with the ACI 318 standard *Building Code Requirements for Structural Concrete* (ACI, 2019) explain how to design to control premature shear failures in members and joints, buckling of compression bars, concrete compression failures (through confinement with transverse reinforcement), the sequence of plastification and other factors, which can lead to large reductions from the elastic response.

2.2.3.4 MASONRY

Masonry is a more complex material than those mentioned above, and less is known about its inelastic response characteristics. For certain types of members (such as pure cantilever shear walls), reinforced masonry behaves in a fashion similar to reinforced concrete. The nature of masonry construction, however, makes it difficult, if not impossible, to take some of the steps (e.g., confinement of compression members) used with reinforced concrete to increase ductility, and stability. Further, the discrete differences between mortar, grout and the masonry unit create additional failure phenomena. Thus, the response reduction factors for the design of reinforced masonry are not quite as large as those for reinforced concrete. Unreinforced masonry possesses little ductility or stability, except for rocking of masonry piers on a firm base and very little reduction from the elastic response is permitted. Capacities and design and detailing rules for seismic design of masonry elements are contained within The Masonry Society (TMS) 402 standard *Building Code Requirements for Masonry Structures*.

2.2.3.5 PRECAST CONCRETE

Precast concrete can behave quite similarly to reinforced concrete, but it also can behave quite differently. The connections between pieces of precast concrete commonly are not as strong as the members being connected. Clever arrangements of connections can create systems in which yielding under earthquake motions occurs away from the connections, in which case the similarity to reinforced concrete is very real. Some carefully detailed connections also can mimic the behavior of reinforced concrete. Many common connection schemes, however, will not do so. Successful performance of such systems requires that the connections perform in a ductile manner. This requires some extra effort in design, but it can deliver successful performance. As a point of

reference, the most common wood seismic-resisting systems perform well yet have connections (nails) that are significantly weaker than the connected elements (structural wood panels). Prior editions of the *Provisions* introduced advances in seismic design of precast system through important Part 3 papers. The advances have found their way into ASCE/SEI 7 and ACI 318. There are also supplemental ACI standards for specialized seismic force-resisting systems of precast concrete.

2.2.3.6 COMPOSITE STEEL AND CONCRETE

Reinforced concrete is a composite material. In the context of the *Provisions*, *composite* is a term reserved for structures with elements consisting of structural steel and reinforced concrete acting in a composite manner. These structures generally are an attempt to combine the most beneficial aspects of each material. Capacities and design and detailing rules are found in the *Seismic Provisions for Structural Steel Buildings* (AISC Standard 341).

2.2.4 Building Systems

Three basic lateral-load-resisting elements – walls, braced frames, and unbraced frames (moment resisting frames) – are used to build a classification of structural types in the *Provisions*. Unbraced frames generally are allowed greater reductions from elastic response than walls and braced frames. In part, this is because frames are more redundant, having several different locations with approximately the same stress levels and common beam-column joints frequently exhibit an ability to maintain a stable response through many cycles of reversed inelastic deformations. Systems using connection details that have not exhibited good ductility and toughness, such as unconfined concrete and the welded steel joint used before the Northridge earthquake, are penalized: the *R* factors permit less reduction from elastic response.

Connection details often make the development of ductility difficult in braced frames, and buckling of compression members also limits their inelastic response. The actual failure of steel bracing often occurs because local buckling associated with overall member buckling frequently leads to locally high strains that then lead to brittle fracture when the member subsequently approaches yield in tension. Eccentrically braced steel frames and new proportioning and detailing rules for concentrically braced frames have been developed to overcome these shortcomings. But the newer and more popular bracing system is the buckling-restrained braced frame. This new system has the advantages of a special steel concentrically braced frame, but with performance that is superior as brace buckling is controlled to preserve ductility. Design provisions appear in the *Seismic Provisions for Structural Steel Buildings* (AISC Standard 341).

Shear walls that do not bear gravity load are allowed a greater reduction than walls that are load bearing. Redundancy is one reason; another is that axial compression generally reduces the flexural ductility of concrete and masonry elements (although small amounts of axial compression usually improve the performance of materials weak in tension, such as masonry and concrete). The 2010 earthquake in Chile has led to improvements in understanding and design of reinforced concrete shear wall systems, because of the large number of significant concrete shear wall buildings

subjected to strong shaking in that earthquake. Systems that combine different types of elements are generally allowed greater reductions from elastic response because of redundancy.

Redundancy is frequently cited as a desirable attribute for seismic resistance. A quantitative measure of redundancy is included in the *Provisions* in an attempt to prevent the use of large reductions from elastic response in structures that actually possess very little redundancy. Only two values of the redundancy factor, ρ, are defined: 1.0 and 1.3. The penalty factor of 1.3 is placed upon systems that do not possess some elementary measures of redundancy based on explicit consideration of the consequence of failure of a single element of the seismic force-resisting system. A simple, deemed-to-comply exception is provided for certain structures.

2.2.5 Supplementary Elements Added to Improve Structural Performance

The *Standard* includes provisions for the design of two systems to significantly alter the response of the structure to ground shaking. Both have specialized rules for response analysis and design detailing.

Seismic isolation involves the placement of specialized bearings with low lateral stiffness and large lateral displacement capacity between the foundation and the superstructure. It is used to substantially increase the natural period of vibration and thereby decrease the acceleration response of the structures. (Recall the shape of the response spectrum in Figure 2-4; the acceleration response beyond a threshold period is roughly proportional to the inverse of the period). Seismic isolation is becoming increasingly common for structures in which superior performance is necessary, such as major hospitals and emergency response centers. Such structures are frequently designed with a stiff superstructure to control story drift, and isolation makes it feasible to design such structures for lower total lateral force. The design of such systems requires a conservative estimate of the likely deformation of the isolator. The early provisions for that factor were a precursor of the changes in ground motion mapping implemented in the 1997 *Provisions*.

Added damping involves the placement of specialized energy dissipation devices within stories of the structure. The devices can be similar to a large shock absorber, but other technologies are also available. Added damping is used to reduce the structural response, and the effectiveness of increased damping can be seen in Figure 2-3. It is possible to reach effective damping levels of 20 to 30 percent of critical damping, which can reduce response by factors of 2 or 3. The damping does not have to be added in all stories; in fact, it is common to add damping at the isolator level of seismically isolated buildings.

Isolation and damping elements require extra procedures for analysis of seismic response. Both also require considerations beyond common building construction to assure quality and durability.

2.3 Engineering Philosophy

The *Commentary*, under “Intent,” states:

> "The primary intent of the *NEHRP Recommended Seismic Provisions for New Buildings and Other Structures* is to prevent, for ordinary buildings and structures, serious injury and life loss caused by damage from earthquake ground shaking and ground failure. Most earthquake injuries and deaths are caused by structural collapse; therefore, the major thrust of the *Provisions* is to prevent collapse for very rare, intense ground motion, termed the risk-targeted maximum considered earthquake (MCE_R) motion. Additional objectives to preserve means of egress, maintain functionality of critical or essential facilities following major earthquakes, and to reduce damage costs, where practicable, are addressed as corollaries to the primary intent."

The *Provisions* states:

> "The degree to which these objectives can be achieved depends on a number of factors including structural framing type, building configuration, structural and nonstructural materials and details, and overall quality of design and construction. In addition, large uncertainties as to the intensity and duration of shaking and the possibility of unfavorable response of a small subset of buildings or other structures may prevent full realization of the intent."

At this point, it is worth recalling the criteria mentioned earlier in describing the risk-targeted ground motions used for design. The probability of structural collapse due to ground shaking is not zero. One percent in 50 years is a higher failure rate than is currently considered acceptable for buildings subject to other natural loads, such as wind and snow. The reason is as stated in the quote at the beginning of this chapter "…all the wealth of the world would prove insufficient…" Damage is to be expected when an earthquake equivalent to the design earthquake occurs. (The "design earthquake" is currently taken as two-thirds of the MCE ground motion). Some collapse is to be expected when and where ground motion equivalent to the MCE ground motion occurs.

The basic structural criteria are strength, stability, and distortion. The yield-level strength provided must be at least that required by the design spectrum (which is reduced from the elastic spectrum as described previously). Structural elements that cannot be expected to perform in a ductile manner are to have greater strength, which is achieved by applying the Ω_0 amplifier to the design spectral response. The stability criterion is imposed by amplifying the effects of lateral forces for the destabilizing effect of lateral translation of the gravity weight (the P-Delta effect). The distortion criterion is a limit on story drift and is calculated by amplifying the linear response to the (reduced) design spectrum by the factor C_d to account for inelastic behavior.

Yield-level strengths for steel and concrete structures are easily obtained from common design standards. The most common design standards for timber and masonry are based on allowable stress concepts that are not consistent with the basis of the reduced design spectrum. Although strength-based standards for both materials have been introduced in recent years, the engineering profession has not yet embraced these new methods. In the past, the *Provisions* stipulated adjustments to common reference standards for timber and masonry to arrive at a strength level equivalent to yield and compatible with the basis of the design spectrum. Most of these adjustments

were simple factors to be applied to conventional allowable stresses. With the deletion of these methods from the *Provisions*, other methods have been introduced into model building codes and the ASCE standard, *Minimum Design Loads for Buildings and Other Structures* to factor downward the seismic load effects based on the *Provisions* for use with allowable stress design methods.

The *Provisions* recognizes that the risk presented by a particular building is a combination of the seismic hazard at the site and the consequence of failure, due to any cause, of the building. Thus, a classification system is established based on the use and size of the building. This classification is called the Risk Category. A combined classification called the Seismic Design Category (SDC) incorporates both the seismic hazard and the Risk Category. The SDC is used throughout the *Provisions* for decisions regarding the application of various specific requirements. The design flow charts in FEMA P-2192-V3 (FEMA, 2021b) illustrate how these classifications are used to control the application of various portions of the *Provisions*.

2.4 Structural Analysis

The *Provisions* sets forth several procedures for determining the force effect of ground shaking. Analytical procedures are classified by two facets: linear versus nonlinear and dynamic versus equivalent static. The two most fully constrained and frequently used are both linear methods: an equivalent static force procedure and a dynamic modal response spectrum analysis procedure. A third linear method, a full history of dynamic response (previously referred to as a time-history analysis, now referred to as a response-history analysis), and a nonlinear method are also permitted, subject to certain limitations. These methods use real or synthetic ground motions as input, but require them to be scaled to the basic response spectrum at the site for the range of periods of interest for the structure in question. Nonlinear analyses are very sensitive to assumptions about structural behavior made in the analysis and to the ground motions used as input, and a peer review is required. A nonlinear static method, also known as a pushover analysis, has been described in prior editions of Part 3 of the *Provisions*, but it is not included in the *Standard*. The *Provisions* also reference ASCE 41, *Seismic Rehabilitation of Existing Buildings*, for the pushover method. The method is instructive for understanding the development of mechanisms, but there is professional disagreement over its utility for validating a structural design.

The two most common linear methods make use of the same design spectrums described previously. The reduction from the elastic spectrum to the design spectrum is accomplished by dividing the elastic spectrum by the coefficient *R*, which ranges from 1-1/4 to 8. Because the design computations are carried out with a design spectrum that is two-thirds the MCE spectrum that means the full reduction from elastic response ranges from 1.9 to 12. The specified elastic spectrum is based on a damping level at 5 percent of critical damping, and a part of the *R* factor accomplishes adjustments in the damping level. Ductility and overstrength make up the larger part of the reduction. The *Provisions* define the total effect of earthquake actions as a combination of the response to horizontal motions (or forces for the equivalent static force method) with response to vertical ground acceleration. The response to vertical ground motion is roughly estimated as a factor (positive or negative) on the dead load force effect. The resulting internal forces are combined with

the effects of gravity loads and then compared to the full strength of the members, reduced by a resistance factor, but not by a factor of safety.

With the equivalent static force procedure, the level of the design spectrum is set by determining the appropriate values of basic seismic acceleration, the appropriate soil profile type and the value for *R*. The particular acceleration for the building is determined from this spectrum by selecting a value for the natural period of vibration. Equations that require only the height and type of structural system are given to approximate the natural period for various building types. (The area and length of shear walls come into play with an optional set of equations.) Calculation of a period based on an analytical model of the structure is encouraged, but limits are placed on the results of such calculations. These limits prevent the use of a very flexible model in order to obtain a large period and correspondingly low acceleration. Once the overall response acceleration is found, the base shear is obtained by multiplying it by the total effective mass of the building, which is generally the total permanent load.

Once the total lateral force is determined, the equivalent static force procedure specifies how this force is to be distributed along the height of the building. This distribution is based on the results of dynamic studies of relatively uniform buildings and is intended to give an envelope of shear force at each level that is consistent with these studies. This set of forces will produce, particularly in tall buildings, an envelope of gross overturning moment that is larger than many dynamic studies indicate is necessary. In prior editions of the *Provisions*, dynamic analysis was encouraged, and the modal procedure was required for structures with large periods (essentially, this means tall structures) in the higher seismic design categories. Careful nonlinear response history analyses have shown that the reduced strength requirement previously provided for linear modal analysis is not justified, and the *Provisions* now require the same basic strength for both linear methods of analysis.

With one exception, the remainder of the equivalent static force analysis is basically a standard structural analysis. That exception accounts for uncertainties in the location of the center of mass, uncertainties in the strength and stiffness of the structural elements and rotational components in the basic ground shaking. This concept is referred to as horizontal torsion. The *Provisions* requires that the center of force be displaced from the calculated center of mass by an arbitrary amount in either direction (this torsion is referred to as accidental torsion). The twist produced by real and accidental torsion is then compared to a threshold, and if the threshold is exceeded, the accidental torsion must be amplified.

In many respects, the modal analysis procedure is very similar to the equivalent static force procedure. The primary difference is that the natural period and corresponding deflected shape must be known for several of the natural modes of vibration. These are calculated from a mathematical model of the structure. The procedure requires the inclusion of enough modes so that the dynamic response of the analytical model captures at least 90 percent of the mass in the structure that can vibrate. The base shear for each mode is determined from a design spectrum that is essentially the same as that for the static procedure. The distribution of displacements and accelerations (forces) and the resulting story shears, overturning moments and story drifts are determined for each mode directly from the procedure. Total values for subsequent analysis and design are determined by taking the square root of the sum of the squares for each mode. This summation gives a statistical

estimate of maximum response when the participation of the various modes is random. If two or more of the modes have very similar periods, more advanced techniques for summing the values are required; these procedures must account for coupling in the response of close modes. The sum of the absolute values for each mode is always conservative.

A lower limit to the base shear determined from the modal analysis procedure is specified based on the static procedure and the approximate periods specified in the static procedure. When this limit is violated, which is common, all results are scaled up in direct proportion. The consideration of horizontal torsion is the same as for the static procedure. Because the equivalent static forces are applied at each floor, the story shears and the overturning moments are separately obtained from the summing procedure, the results are not statically compatible (that is, the moment calculated from the summed floor forces will not match the moment from the summation of moments). Early recognition of this will avoid considerable problems in later analysis and checking.

For structures that are very uniform in a vertical sense, the two procedures give very similar results. The modal analysis method can be better for buildings having unequal story heights, stiffnesses, or masses. Both methods are based on purely elastic behavior, and, thus, neither will give a particularly accurate picture of behavior in an earthquake approaching the design event. Yielding of one component leads to redistribution of the forces within the structural system; while this may be very significant, none of the linear methods can account for it.

Both common methods require consideration of the stability of the building as a whole. The technique is based on elastic amplification of horizontal displacements created by the action of gravity on the displaced masses. A simple factor is calculated, and the amplification is provided for in designing member strengths when the amplification exceeds about 10 percent. The technique is referred to as the P-Delta analysis and is only an approximation of stability at inelastic response levels.

Recent editions of the *Provisions* have incorporated advances in nonlinear response history analysis methods. Such methods of analysis are not required, but they are permitted as an alternate to the linear methods of analysis to validate designs. When used for this purpose, it is possible to demonstrate that buildings will satisfy the intent of the *Provisions*, even though they may:

- Have innovative structural systems not otherwise covered by the *Provisions,*
- Have a conventional structural system, but do not satisfy some of the empirically-based limits, such as maximum height for a shear wall system,
- Require demonstration of damage control for vulnerable elements, such as a drift-sensitive cladding system.

When used for such, or similar, purposes the validation analyses must include prediction of response to a suite of ground motions scaled the emulate the MCE_R response spectrum. Acceptance criteria include limits on strains and deformations of ductile elements and strength of brittle elements. The selections and scaling of ground motions, the analytical modeling of nonlinear response, and the

acceptance criteria are all subject to peer review. This method of validation by prediction of performance using sophisticated analysis is often referred to as *performance-based earthquake engineering*, and has led to significant advances in practice, particularly for tall buildings.

2.5 Nonstructural Elements of Buildings

Severe ground shaking often results in considerable damage to the nonstructural elements of buildings. Damage to nonstructural elements can pose a hazard to life in and of itself, as in the case of heavy partitions or facades, or it can create a hazard if the nonstructural element ceases to function, as in the case of a fire suppression system. Some buildings, such as hospitals and fire stations, need to be functional immediately following an earthquake; therefore, many of their nonstructural elements must remain undamaged.

The *Provisions* treats damage to and from nonstructural elements in three ways. First, indirect protection is provided by an overall limit on structural distortion; the limits specified, however, may not offer enough protection to brittle elements that are rigidly bound by the structure. More restrictive limits are placed upon those Risk Categories for which better performance is desired given the occurrence of strong ground shaking. Second, many components must be anchored for an equivalent static force. Third, the explicit design of some elements (the elements themselves, not just their anchorage) to accommodate specific structural deformations or seismic forces is required.

The dynamic response of the structure provides the dynamic input to the nonstructural component. Some components are rigid with respect to the structure (light weights and small dimensions often lead to fundamental periods of vibration that are very short). Application of the response spectrum concept would indicate that the response history of motion of a building roof to which mechanical equipment is attached looks like a ground motion to the equipment. The response of the component is often amplified above the response of the supporting structure. Response spectra developed from the history of motion of a point on a structure undergoing ground shaking are called floor spectra and are useful in understanding the demands upon nonstructural components.

The *Provisions* simplify the concept greatly. The force for which components are checked depends on:

1. The component mass;
2. An estimate of component acceleration that depends on the structural response acceleration for short period structures, the relative height of the component within the structure and a crude approximation of the flexibility of the component or its anchorage;
3. The available ductility of the component or its anchorage; and
4. The function or importance of the component or the building.

Also included in the *Provisions* is a quantitative measure for the deformation imposed upon nonstructural components. The inertial force demands tend to control the seismic design for isolated or heavy components, whereas the imposed deformations are important for the seismic design for

elements that are continuous through multiple levels of a structure or across expansion joints between adjacent structures, such as cladding or piping.

2.6 Quality Assurance

Since strong ground shaking has tended to reveal hidden flaws or *weak links* in buildings, detailed requirements for assuring quality during construction are important. The actively implemented provisions for quality control are contained in the model building codes, such as the *International Building Code* (ICC, 2020) and the material design standards, such as *Seismic Provisions for Structural Steel Buildings*. Loads experienced during construction provide a significant test of the likely performance of ordinary buildings under gravity loads. Tragically, mistakes occasionally will pass this test only to cause failure later, but it is fairly rare. No comparable proof test exists for horizontal loads, and experience has shown that flaws in construction show up in a disappointingly large number of buildings as distress and failure due to earthquakes. This is coupled with the seismic design approach based on excursions into inelastic straining, which is not the case for response to other loads.

The quality assurance provisions require a systematic approach with an emphasis on documentation and communication. The designer who conceives the systems to resist the effects of earthquake forces must identify the elements that are critical for successful performance as well as specify the testing and inspection necessary to confirm that those elements are actually built to perform as intended. Minimum levels of testing and inspection are specified in the *Provisions* for various types of systems and components.

The quality assurance provisions also require that the contractor and building official be aware of the requirements specified by the designer. Furthermore, those individuals who carry out the necessary inspection and testing must be technically qualified and must communicate the results of their work to all concerned parties. In the final analysis, there is no substitute for a sound design, soundly executed.

2.7 Resilience-Based Design

2.7.1 Background

This example expands on ideas presented in Part 3, Resource Paper 1, “Resilience-based Design and the *NEHRP Provisions*” (FEMA, 2020b), referenced herein as Resource Paper 1. This example also references the “Three-Story Cross-Laminated Timber (CLT) Shear Wall” design example in Chapter 6.

In 2018, Congress made it part of NEHRP’s purpose to improve community resilience through the development of building codes and standards (Public Law 115-307, 2018). Earthquake resilience is broader than structural design; in fact, resilience is best understood as an attribute of organizations or social units, not of buildings. But seismic design of buildings can contribute to resilience by focusing on the building’s post-earthquake *functional recovery* time (EERI, 2019; FEMA-NIST, 2021).

The concept of functional recovery discussed in Resource Paper 1 was formalized in a 2021 FEMA-NIST report with two definitions, one for functional recovery as a performance state, and (consistent with principles of performance-based engineering) one for a design objective that links the performance level with a hazard level and a time-based metric (FEMA-NIST, 2021):[1]

> *Functional recovery is a post-earthquake performance state in which a building is maintained, or restored, to safely and adequately support the basic intended functions associated with the pre-earthquake use or occupancy*.
>
> *A functional recovery objective is functional recovery achieved within an acceptable time following a specified earthquake, where the acceptable time might differ for various building uses and occupancies*.

Thus, the resilience-based earthquake design of an individual building simply seeks to achieve functional recovery within a specified time after the event. Safety, which is the primary objective of the current *Provisions*, as well as the codes and standards that cite them, remains a floor on the design. Depending on the functional recovery objective, designing for functional recovery might or might not require changes or enhancements relative to the safety-based design.

Current codes and standards do not provide functional recovery design provisions, but the concept of functionality is not entirely new to the *Provisions*. *Provisions* Section 1.1.5 notes that functionality following the design earthquake is the presumed objective for buildings assigned to Risk Category IV, and the 2020 *Provisions* list eight characteristics of a functional building (discussed in Section 2.7.3.2). That said, two important differences between Risk Category IV provisions and functional recovery provisions are:

- The element of time. The Risk Category IV provisions expect essentially immediate functionality, just as they expect the building to be safe as soon as the earthquake shaking stops. By acknowledging that a building might need functional recovery after, say, three days or two weeks, functional recovery provisions can be less conservative than current Risk Category IV provisions.
- Consideration of externalities. As shown in Resource Paper 1 (Table 1), functional recovery provisions are likely to be more explicit than Risk Category IV provisions about conditions outside the building footprint, or even outside the scope of traditional design. For example, functional recovery provisions might include considerations of utility reliability or backup, hazards posed by

[1] The FEMA-NIST report covers both buildings and infrastructure systems. For clarity, the definitions shown here are edited to address only buildings. The FEMA-NIST report also defines *reoccupancy* and *reoccupancy objective* in a similar way. Reoccupancy is a more basic performance state that precedes functional recovery. Design for reoccupancy is outside the scope of this discussion, but FEMA (2018, Section 5.4.4) provides analytical findings for a selection of model multi-story buildings in terms of the probability of receiving an Unsafe (red) placard after a design earthquake. Except for steel braced frames, the probability is under 15 percent for a Risk Category II design and under two percent for a Risk Category IV design. Thus, for new code-designed buildings, the likelihood of immediate reoccupancy is, as expected, substantially higher than the likelihood of immediate functional recovery, discussed further in Section 2.7.2.2.

adjacent buildings, contents damage as it affects "basic intended functions," or recovery planning as a supplement to design. In this way, functional recovery provisions might be more comprehensive and conservative than current Risk Category IV provisions.

EERI (2019) described four sets of issues that will need to be addressed as a set of functional recovery design provisions are developed:

- Definitional. With reference to the FEMA-NIST definition of *functional recovery*, what are the "basic intended functions" of a given building's use or occupancy, and which physical components are necessary to maintain or restore them? As noted, *Provisions* Section 1.1.5 provides a tentative answer by listing eight characteristics of functionality (discussed in Section 2.7.3.2), and Resource Paper 1 (Table 1) suggests five categories for functional recovery design provisions: structural, nonstructural, recovery-critical contents, utility service, and reoccupancy and recovery planning.

- Policy. With reference to the FEMA-NIST definition of *functional recovery objective*, what is the "acceptable time" for functional recovery, given a building use or occupancy and a prescribed hazard level? Answering these policy questions amounts to selecting, or assigning, functional recovery objectives.

- Technical. Given a functional recovery objective, what design provisions will achieve it with appropriate reliability?

- Implementation. Should functional recovery design involve new regulations regarding project documentation, licensure, quality assurance, liability, insurance, or legal issues?

The implementation questions are beyond the scope of Section 2.7. Answers to the definitional questions would be embedded in the technical provisions. Therefore, the balance of this discussion will consider the policy question in Subsection 2.7.2 and the technical question in Subsections 2.7.3 and 2.7.4, considering two contexts: code-based functional recovery design and voluntary functional recovery design.

2.7.2 Functional Recovery Objective

Functional recovery design, like all performance-based design, requires an objective. As defined above, a functional recovery objective requires selection of both a design hazard level and an acceptable functional recovery time.

Building codes set objectives (often implicitly) based on a building's use and occupancy. For earthquake design, the use and occupancy determine the Risk Category and the Seismic Design Category, which in turn determine the design scope and criteria. As functional recovery provisions are developed for building codes, it is likely that they will also link a functional recovery objective to use and occupancy in some fashion.

Consider the CLT design example building from Chapter 6, shown in Figure 2-8. The example building is a six-unit townhouse that would typically be assigned to Risk Category II and Seismic Design Category D. As typical housing, the *International Building Code* (Section 310) would assign it to Occupancy Group R-2, and it would almost certainly have an occupant load under 50.

This discussion assumes R-2 occupancy. But a nearly identical three-story CLT structure could also be used as office suites (Group B) or as a mixed-use building. Considering just residential uses, the same structure with a few modifications might also be used as an assisted living facility (Group I-1) or a nursing home providing medical care (Group I-2). In a larger building, a Group I-2 facility might be assigned to Risk Category III. Beyond the building code's categories, many jurisdictions have policies and programs (supportive housing, rent subsidies, etc.) that might also use a three-story CLT structure. In all these cases, the tenants are vulnerable in the sense that they would likely have difficulty finding alternative housing if forced to relocate, even temporarily, after a damaging earthquake. So, the selection of an appropriate functional recovery objective should consider more than just the basic distinction between residential, institutional, business, or other occupancies. Section 2.7.2.3 discusses current thinking about appropriate functional recovery times for residential buildings.

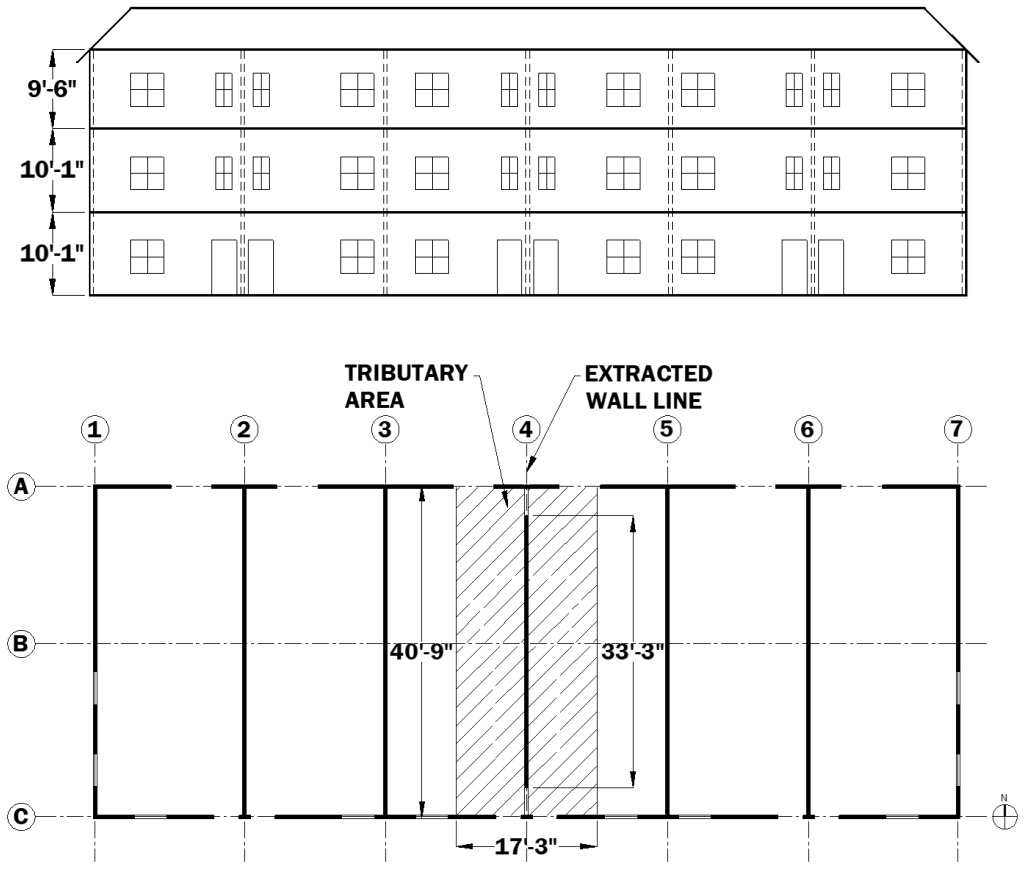

Figure 2-8. CLT Shear Wall Design Example Building. Top: Elevation. Bottom: Typical Floor Plan Showing Six Townhouse Units

2.7.2.1 HAZARD LEVEL

Both Resource Paper 1 and the FEMA-NIST report discuss possibilities for an appropriate design hazard level. Arguments can be made for selecting a site-specific hazard different from the hazard currently specified in the *Provisions*, or even a scenario event that better reflects the community resilience perspective.[1] As provisions for functional recovery are developed, an appropriate hazard will be selected through normal consensus processes for developing codes and standards. In the interim, both Resource Paper 1 and the FEMA-NIST report recognize the practicality and convenience of selecting the hazard level for a functional recovery objective to be on par with the *Provisions*' design earthquake. Selecting a much smaller hazard for functional recovery would not add anything to the *Provisions'* current safety-based objective; it would merely restate the assumption that a code-designed building will have less damage in a smaller earthquake and more damage in a larger one. Rather, a shift to functional recovery design should mean a heightened interest in functionality, as opposed to just safety, for a similarly rare event.

Therefore, for simplicity and clarity in the absence of a formal consensus, the hazard level selected for this discussion is identical to the *Provisions'* design earthquake.[2]

2.7.2.2 EXPECTED FUNCTIONAL RECOVERY TIME

Before considering a desired or acceptable functional recovery time, it is useful to consider the functional recovery time actually achieved by code-compliant Risk Category II designs. Only recently have analytical studies tried to quantify the recovery time of typical buildings. So far, the main finding is that functional recovery time is highly uncertain and can vary substantially between equally code-compliant systems.

- A FEMA-funded study estimated the repair times for five-story to 13-story code-designed office buildings with five different seismic force-resisting systems, for a range of hazard levels over a range of high seismicity sites (FEMA, 2018, Section 5.4). The repair times estimated by FEMA do not include "additional time required to identify, plan, and permit the work, arrange financing, or hire and mobilize contractors" (FEMA, 2018, Section 5.4.2); the time needed for these activities can often be shortened by advance planning, which Figure 2 of Resource Paper 1 refers to as "reoccupancy and recovery planning." That said, repair time is not the same as functional recovery time. The functional recovery time will be substantially shorter than the repair time if much of the repair can be done while the building is occupied and in use.
    - For the two concrete systems, the median repair time after a design earthquake is 17 to 21 days. For the three steel systems, it ranges from 15 to 81 days, with two braced frame systems having the longest repair times. For this discussion, if one assumes that half of the

[1] For further discussion, see Resource Paper 1, Section 2.2, and FEMA-NIST (2021), Chapter 2.

[2] The case studies listed in Table 2-1 of this design example further illustrate how some engineers (and their clients) have selected hazard levels for functional recovery objectives in the absence of a consensus standard.

repair time occurs after functional recovery is achieved,[1] the functional repair time may be taken as eight to 40 days (or, to avoid undue precision, one to six weeks).

- If designed with Risk Category IV criteria, as would be the case for an emergency operations center, the median repair times reduced to 12 to 15 days for the concrete systems, and 11 to 33 days for the steel systems.[2] Risk Category IV facilities tend to have more specialized nonstructural systems and contents, so an even greater portion of the estimated repair time is likely related to their sensitivity. A Risk Category II building designed with Risk Category IV criteria would not have those issues, so to adjust these findings for purposes of this discussion, if one assumes that two-thirds of the Risk Category IV repair time occurs after functional recovery is achieved, the functional repair time may be taken as four to 11 days, or one to two weeks. These median functional recovery times using Risk Category IV criteria for otherwise Risk Category II occupancies would seem to represent the best feasible functional recovery times in the absence of additional recovery planning.

- Haselton et al. (2021) used the same FEMA methodology to estimate functional recovery times for wood light-frame (not CLT) residential building types at a high seismicity site in Los Angeles. For a three- or four-story apartment building, the median functional recovery time was one to six months. The wide range indicates the uncertainty associated with estimates of functional recovery time, which are more complex than those associated with repair. (This study estimated functional recovery time directly, so no adjustment from repair time is needed.)

- Furley et al. (2021) estimated reoccupancy and functional recovery times for a two-story office building with CLT walls and supplemental damping devices (that is, different from the Chapter 6 example discussed here). For a spectral acceleration of 1.0 g, typical of a high seismicity area, the median functional recovery time was about 130 days, or four to five months. However, at least half that time was found to be caused by reoccupancy delays related to safety inspections, and beyond that, the actual repair time was driven by nonstructural damage related to the office occupancy and replacement lead times for the damping devices. In addition, the Furley et al. algorithm does not yet account for repairs made while the building is occupied. In a residential

[1] This assumption, and the "two-thirds" assumption below, is based entirely on judgment and is made only for purposes of this discussion. Current FEMA-funded work in progress might eventually identify reliable relationships between functional recovery time and full repair time. For now, the assumptions merely illustrate that the *Provisions* and the codes and standards that cite them do not yet provide consensus values.

[2] Even if the functional recovery times are substantially less than these full repair times, they would likely exceed the immediate functionality goal assumed by the *Provisions* for Risk Category IV facilities. Ultimately, field observations will determine whether the Risk Category IV design criteria or the FEMA P-58 methodology need adjustment. For now, the lesson from these Risk Category IV repair time estimates is that even in new facilities, damage that significantly affects functionality is a real possibility. Also noteworthy: Even when designed as Risk Category IV facilities, the two steel braced frame systems show longer repair times than the Risk Category II concrete systems.

building with a plain CLT system and prioritized reoccupancy, the functional recovery time might be substantially shorter.

Thus, for a broad range of newly designed multi-story buildings, one should expect a functional recovery time of at least a few weeks after a design earthquake, and perhaps a few months. An improved design based on current Risk Category IV provisions might reduce the functional recovery time to a few weeks.

That said, a CLT system like the example discussed here is different from any of the systems described above. While there are no studies yet specifically predicting repair time or functional recovery time of typical CLT buildings, there are reasons to think this new system will support faster functional recovery objectives. The system is assigned a relatively low *R*-factor, and any structural damage is expected to be limited to the ductile steel connectors that are relatively easy to replace, even with the units occupied (Line, 2021). Testing done to quantify the seismic performance factors and to justify the design provisions now in 2020 *Provisions* Section 14.5.2 and SDPWS-21 Appendix B showed "no observable damage in the connections … and no yielding recorded in the tie-down rods" in a design-level shake table test (van de Lindt et al., 2019a); nail withdrawal of only "a fraction of an inch" after cyclic loading to 2.5% drift (van de Lindt et al., 2021); and reliable nail withdrawal "as expected" when tested to failure (Amini et al., 2016). That said, the Haselton et al. (2021) and Furley et al. (2021) studies cited above also suggest that even with careful selection of the structural system, functional recovery time will be greatly influenced by nonstructural systems and by procedural factors outside the normal scope of building design.

2.7.2.3 DESIRED OR ACCEPTABLE FUNCTIONAL RECOVERY TIME

Assuming the R-2 occupancy, what is an acceptable functional recovery time? Again, model building codes and standards provide no policy consensus,[1] but a number of jurisdictions and institutions have produced relevant plans that might serve as useful touchstones, if not as policy precedents.

- Various "shelter-in-place" and "work-from-home" orders produced during the 2020 pandemic identified a wide range of community services as "essential." While not invoking Risk Category IV design or retrofit provisions, these orders recognized housing and many business types as necessary to community vitality and stability in ways that current building codes do not. They suggested a broader understanding of "substantial economic impact," "mass disruption of day-

[1] As discussed above, the 2020 *Provisions* imply essentially immediate functionality for buildings assigned to Risk Category IV. Section 2.1.5 of the 2020 *Provisions* notes, "The intent dictates a high probability of preventing loss of function, but does not explicitly state a reliability target. A desired target reliability for Risk Category IV buildings and nonbuilding structures is for there to be a 10% probability of loss of essential function given the Design Earthquake ground motion." For buildings *not* assigned to Risk Category IV, the *Provisions* provide neither an implied recovery time nor a reliability target. Also, the *Provisions* do not dictate which building uses should be assigned to Risk Category IV, stating in Section 1.1.5 that the designation of Risk Category IV uses "shall be left to the determination of the owner or operator of the facility, the governing building code, or the authority having jurisdiction."

to-day civilian life," and "substantial hazard to the community" – phrases used to assign risk categories in ASCE/SEI 7-22, Table 1.5-1).

- Resilience plans produced by West Coast jurisdictions, organizations, and the federal government have called for building code provisions to explicitly address functional recovery time. Some have focused on specific building uses, but none have yet stated specific functional recovery objectives. (OSSPAC, 2013; White House, 2016; San Francisco, 2016; Los Angeles, 2018)

- NIST (2016) calls for local resilience planners to assign different building uses to functional categories and recovery times. Specific assignments should be jurisdiction-specific, but in general, emergency housing, which includes nursing homes and housing for other vulnerable groups, should have "short term" recovery times of at most three days, and other housing should have intermediate recovery times of one to twelve weeks.

- The FEMA-NIST report (2021, Table B-1) offers conceptual functional recovery objectives that are generally consistent with NIST (2016). Housing is given as an example of a building use representing "daily necessities" that should have a target functional recovery time of "days to weeks."

- SPUR (2009) suggested a set of strawman recovery goals for San Francisco. Accounting for expected performance of the city's existing housing stock, it argued that to meet overall housing goals, new housing should be designed so that 85 percent should be usable within four hours of an M7.2 San Andreas event (somewhat smaller than the design earthquake for most of the city), 95 percent within 24 hours, and 100 percent within 30 days.

- For a new senior housing facility, San Francisco set a goal of functional recovery within one day of a 475-year event, intending to eliminate the need for any tenant relocation during repairs (Mar, 2021).

Many of these goals could prove difficult to achieve. They are listed here to indicate the thinking of organizations that have been especially active in the development of earthquake resilience and functional recovery concepts.

In summary, for the townhouse in the Chapter 6 CLT shear wall design example:

- Separate from any implied objective, a new code-designed multi-story residential building can expect to reach functional recovery within a few months after a design earthquake. If designed as a Risk Category IV facility, the expectation might be to achieve functional recovery within two weeks of a design earthquake. These expectations are based on a limited set of studies with concrete, steel, and wood light frame systems. Testing has suggested that the CLT shear wall system will have limited and highly controlled structural damage in a design earthquake, so the functional recovery time for a CLT building is likely to be shorter.

- If a functional recovery objective were specified based on current resilience-based policy suggestions and examples, it might call for functional recovery within at most 30 days of a design earthquake. Current Risk Category II design provisions might not satisfy this objective, but Risk Category IV provisions probably will.

- If the building might be used as housing for vulnerable tenants without resources to endure 30 days of relocation or limited functionality, the objective might instead call for functional recovery within one to three days of a design earthquake. Even current Risk Category IV design provisions might not satisfy this objective.

2.7.3 Code-based Functional Recovery Design Provisions

As discussed in Table 1 of Resource Paper 1, tentative design provisions to meet different functional recovery objectives might be developed by linking each design strategy already in the *Provisions* to the functional recovery times for which it is needed. Eventually, this mapping will be substantiated by research on the determinants of actual recovery; in the interim, it will be done through consensus processes, with reference to traditional test results.

2020 *Provisions* Section 2.1.5 notes that better performance, as intended for buildings assigned to Risk Category IV, can be achieved by "the increase in the importance factor and more stringent story drift limits, in combination with strict regulation of design, testing, and inspection." As discussed above, FEMA (2018) has shown that selection of the basic seismic force-resisting system (SFRS) can make a significant difference as well. Indeed, the FEMA study suggests that many common systems, as currently codified, cannot reliably achieve a functional recovery time less than a few days, even with Risk Category IV criteria. Nevertheless, the use of current Risk Category IV criteria will likely continue to be deemed sufficient, by consensus, for the design of any facility for which fast functional recovery is desired, though the current provisions might need to be supplemented with thorough quality assurance and recovery planning.

2.7.3.1 SEISMIC FORCE-RESISTING SYSTEM

A complete structural design would need to consider the SFRS, diaphragms, foundation, and other non-SFRS walls and framing. This discussion is limited to the CLT shear wall SFRS.

Section 14.5.2 of the 2020 *Provisions* includes design provisions for CLT seismic force-resisting systems. ASCE/SEI 7-22 includes CLT as a new seismic force-resisting system in Table 12.2-1. For CLT design provisions, ASCE/SEI 7-22 references the 2021 *Special Design Provisions for Wind and Seismic* (SDPWS) (AWC, 2020), a material standard referenced here as SDPWS-21. CLT shear wall design, as codified in SDPWS-21, is almost entirely prescriptive. It is based on capacity design principles that ensure yielding primarily in the prescribed steel connections between CLT wall panels, CLT diaphragms, and the foundation (Provisions Section C14.5.2.1 and SDPWS-21 Section C-B.1). Therefore, to the extent that yielding of connectors and fasteners can be limited (without changing the controlling mechanism), the SFRS effect on functional recovery time can be controlled.

Even as a prescriptive design, the new SDPWS-21 provisions for CLT suggest ways, in concept, that a CLT shear wall SFRS might be enhanced to reduce damage and functional recovery time. The discussion below is conceptual only; some elements of the system are specified to ensure a reliable failure of the nailed fasteners, so arbitrary changes to increase the strength or stiffness could affect the failure mode and the overall performance.

- Seismic importance factor, I_e (ASCE/SEI 7-22 Section 11.5.1). The Seismic Importance Factor is a function of the assigned Risk Category. Nothing in ASCE/SEI 7-22 or the SDPWS-21 prohibits CLT shear walls in Risk Category III or Risk Category IV buildings, so in concept, a Seismic Importance Factor greater than 1.0 could be used with the usual expectation of reducing damage, thereby shortening the structure's effect on functional recovery time. Or, recognizing that resilience and functional recovery are different from safety, recovery-based provisions might introduce a similar, but separate, recovery factor, I_r, to do the job. If the intent is to achieve the effect of using Risk Category IV criteria, however, merely increasing the Seismic Importance Factor is not enough, since Risk Category IV criteria also set tighter drift limits and require protection of more nonstructural components.

- Height limit (ASCE/SEI 7-22 Table 12.2-1). All else equal, a taller building might be prone to larger forces and deformations, more complicated dynamic response, more damage, and a longer functional recovery time, so a height limit might be a way to control performance. For CLT shear wall systems, however, ASCE/SEI 7-22 Table 12.2-1 sets the same height limit of 65 feet for every Risk Category, indicating that even Risk Category IV performance is achievable up to that height. If there is any benefit to a shorter building, the Chapter 6 design example should already realize it, since its 30-foot height is well under the limit.

- Response modification coefficient, *R* (ASCE/SEI 7-22 Table 12.2-1). For CLT systems with panel aspect ratios up to 4, including the Chapter 6 design example, the relatively low *R* value of 3 shows the intent of the 2020 *Provisions* and ASCE/SEI 7-22 to tightly limit even ductile damage. In more traditional systems, this low value might suggest unreliable or brittle performance. Here, it suggests low damage, which is a key to fast functional recovery. To limit damage even further, one might assign an even lower *R* value, but the same effect is more commonly achieved by assigning a Seismic Importance Factor (or recovery factor) greater than 1.0, as discussed above.

- Selection of CLT grade. Grade E1 CLT, as used in the Chapter 6 design example, is one of 14 CLT grades catalogued in the *Standard for Performance-Rated Cross-Laminated Timber (PRG 320)* (APA, 2020) material standard. The properties of the selected grade determine the strength and stiffness of the panel itself. In theory, these can determine the acceptability and expected damage of the design, so different CLT grades might yield different functional recovery times. As shown in the design example, however, the design of this three-story building is controlled by the system's strength, not its stiffness, and that strength is a function of the steel connectors, not the CLT panel (see design example Section 6.5). Therefore, selecting a different CLT grade would probably not affect the functional recovery time in this case.

- Classification of CLT walls (2020 *Provisions* Section 14.5.2.2 Items 2, 3, and 4 and SDPWS-21 Section B.2 Items 2, 3, and 4). 2020 *Provisions* Section 14.5.2 and SDPWS-21 Appendix B require the design to account for CLT walls or partitions that might not be needed for overall strength or stiffness and therefore are not considered part of the SFRS. This is to ensure deformation compatibility and to rule out irregularities (2020 *Provisions* Section C.14.5.2.2 and SDPWS-21 Section B.2). As long as these checks are satisfied, the presence of these walls adds unintended strength and stiffness, potentially reducing damage and functional recovery time. Non-SFRS walls would be difficult to require as part of a design strategy, however, so if additional strength or stiffness is needed, it would be more effective to increase requirements on the SFRS elements, perhaps with a Seismic Importance Factor (or recovery factor) greater than 1.0, as discussed above.

- Capacity of prescribed connectors (2020 *Provisions* Sections 14.5.2.3.2, 14.5.2.5, and 14.5.2.6 and SDPWS-21 Sections B.3.2, B.5, and B.6). The strength of a CLT shear wall system is largely a function of the prescribed strength of the prescribed angle connectors at the base of each panel in each story. When these connectors reach their strength in an earthquake, they yield in a controlled way; if the yielding (that is, ductile damage) is enough to require repair, even this reliable and beneficial response can add functional recovery time. In the Chapter 6 design example, system strength (as opposed to stiffness) appears to control the design, so damage in the design earthquake is expected. A lower *prescribed* capacity for the connectors will require more connectors to be installed for a higher *actual* capacity in the system, which will in turn reduce the expected damage, with a potential reduction in functional recovery time.

  As shown in design example Section 6.5.1, for a given panel length, four different parameters directly affect the system strength in a given story (represented by the unit shear capacity). Two of these parameters – the connector capacity of 2,605 pounds and the specific gravity factor, C_G – are derived from tests and are not subject to policy choices. (A different connector could be designed, but that would require new tests; a different wood species could be selected, but that would affect other aspects of the design.) Recovery-based code provisions could, however, adjust the resistance factor, currently prescribed as 0.5 in 2020 *Provisions* Section 14.5.2.6 and SDPWS-21 Section 4.1.1. While there is ample precedent in codes and standards for prescribing different design values for different objectives, in the present case the same effect could be achieved, more transparently, by using a Seismic Importance Factor (or recovery factor) greater than 1.0, as discussed above.

  - The modular nature of CLT shear wall design, together with considerations of symmetry and convenience, can sometimes provide additional capacity even without an intentional increase in design requirements. The unintended additional capacity is equivalent to an effective Seismic Importance Factor greater than 1.0. Design example Tables 6-4 and 6-5, however, show that for this example the effect is small, and the effective Seismic Importance Factor in the critical first story is just 1,371 plf capacity / 1,273 plf demand = 1.08.

  - Any change that would result in more prescribed connectors along the length of each CLT panel might eventually require connectors on both sides of the wall. Where there is not

enough length to stagger them, 2020 *Provisions* Section 14.5.2.3.1 and SDPWS-21 Section B.3.1 require a thicker CLT panel, which will have other effects on both the structural and architectural design.

- Deflection calculation and allowable deflection (2020 *Provisions* Section 14.5.2.4, SDPWS-21 Section B.4, and ASCE/SEI 7-22 Table 12.12-1). As noted above, the *Provisions* regard interstory drift as a key metric of performance overall, and high drift is widely understood as an indicator of damage. Tighter drift limits can be expected to reduce damage and shorten functional recovery time. For the CLT shear wall design example, ASCE/SEI 7-22 Table 12.12-1 sets the drift limit at 0.025 times the story height for this Risk Category II residential building because the three-story building is four stories or less and interior walls, partitions, ceilings and exterior wall systems are assumed to have been designed to accommodate story drifts. Design example Section 6.7 shows that the expected building drifts are only about one-third of this limit. Thus, setting tighter drift limits for certain functional recovery objectives would be rational, but at least in this case, even the Risk Category IV limit of 0.015 times the story height is already satisfied and probably would be even if a Seismic Importance Factor (or recovery factor) greater than 1.0 were applied.

- Hold-down deformation limit (2020 *Provisions* Section 14.5.2.3.4 Item 2 and SDPWS-21 Section B.3.4 Item 2). CLT shear walls are required to have hold-down devices to resist uplift and overturning. The provisions include a deformation limit of 0.185 inches, derived from criteria for conventional wood framing, intended "to avoid concentration of device elongation in one level" (2020 *Provisions* Section C14.5.2.3 and SDPWS-21 Section C-B.3). In concept, this limit could be tightened to further reduce the potential for disruptive repairs that might delay functional recovery. In design example Section 6.6.1, the estimated elongation is only half of the 0.185-in limit, suggesting that the potential benefit of a tighter limit (if deemed necessary) could be realized with no effect on many typical designs.

- Hold-down design force (2020 *Provisions* Section 14.5.2.3.4 Item 3 and SDPWS-21 Section B.3.4 Item 3). Separate from the deformation limit, the hold-down design force must be calculated assuming twice the unit shear capacity of the walls. Since the unit shear capacity is a function of the prescribed connectors, the hold-down design force will increase automatically if the required wall strength is increased as discussed above. Since the purpose of the factor is only to ensure development of the presumed yield mechanism in the connectors (2020 *Provisions* Section C14.5.2.3 and SDPWS-21 Section C-B.3), increasing this factor should have no effect on expected damage or expected functional recovery time.

- High aspect ratio panels (2020 *Provisions* Section 14.5.2.3.7 and ASCE/SEI 7-22 Table 12.2-1). In addition to the SFRS used in the Chapter 6 design example, the new provisions allow a CLT shear wall system with a panel aspect ratio of 4. For this system, ASCE/SEI 7-22 Table 12.2-1 allows a somewhat higher *R* value to reflect the higher displacement capacity of these walls (ASCE/SEI 7-22 Section C12.2-1). While equally safe, a similar building using this system would presumably experience higher drifts and more yielding in the prescribed connectors. Recovery-based design provisions might consider prohibiting the high aspect ratio CLT system for buildings with certain functional recovery objectives.

2.7.3.2 NONSTRUCTURAL SYSTEMS AND CONTENTS

Where structural damage is limited, a building's functional recovery time might be governed by the performance of its nonstructural systems or contents. These are outside the scope of the Chapter 6 design example, but a resilience-based design with a functional recovery objective must consider them.

Except for life safety systems (alarms, exit lighting, fire suppression, etc.) current safety-based design provisions for Risk Category II facilities typically do not seek functionality of nonstructural systems and do not address contents at all. Instead, they require bracing or anchorage only to prevent hazardous materials release and to hold the equipment in place to prevent falling hazards. As with the SFRS criteria, there are no consensus functional recovery design criteria for nonstructural systems and contents, but the *Provisions* do discuss general expectations associated with functionality in Risk Category IV facilities. In general, the design of nonstructural systems for buildings assigned to Risk Category IV must use an importance factor, I_p, of 1.5, must brace or anchor smaller components that are exempt for Risk Category II, must ensure backup utility services, and must consider the ruggedness of certain function-critical equipment. More details on nonstructural component performance objectives and provisions are provided in *Design Example* Chapter 8.

In addition to immediate reoccupancy (which depends on structural performance as well), 2020 *Provisions* Section 1.1.5 lists seven "qualitative characteristics" that define Risk Category IV performance with a design earthquake. The following notes consider these characteristics as they might apply to the Chapter 6 townhouse design example.

- Functionality of equipment serving "essential functions." For a non-Risk Category IV building, the "essential functions" are the "basic intended functions" referenced in the FEMA-NIST (2021) definition of functional recovery, given above. For a residential building, they are likely to be the same as those that commonly define habitability in local housing codes – light, ventilation, power, potable water, heat in winter, sanitation and cooking facilities, etc. In some buildings, or for some tenants, elevators and communications systems can be essential as well. These services are sometimes waived in the immediate aftermath of an earthquake, when basic shelter is the priority, and the duration of the waiver (a policy decision) can help define the functional recovery objective. Current Risk Category II provisions require no design at all for most piping, ducts, floor-mounted equipment, or small suspended equipment. Post-earthquake evaluation of a damaged building for habitability, including reduction in building systems and services, is discussed in detail in FEMA P-2055 (FEMA, 2019).

- No damage (or limited damage) to contents serving "essential functions." Contents generally include any components not constructed with the building but brought in by tenants. For a residential building, "essential" contents might include main kitchen appliances, but in many cases, these are assumed to be part of the building. Tall or suspended furnishings can sometimes pose earthquake risks, but these are not normally essential to the buildings "basic intended function" as housing. Current Risk Category II provisions do not include any design scope for contents.

- No damage to non-essential equipment and contents that would "compromise the essential functions." In a residential building, this category might be understood to include broken glass, fallen ceiling plaster, overturned contents, or other damage that cannot be removed or repaired within the acceptable functional recovery time.

- Building envelope "maintains integrity … to preserve essential functions." Current code provisions already cover potential damage to glazing, cladding, and roofing components as safety issues. For a residential building, post-earthquake assessment and repair of exterior components such as stucco can often be done from the exterior in ways that do not affect functional recovery.

- Nothing more than "minor leakage" in "piping carrying nontoxic substances." There is clearly a need for interpretation here, within the "definitional" issue area described in *Design Examples* Section 2.7.1

- "Toxic and Highly [sic] toxic substances are not released in a quantity harmful to occupants unless controlled through secondary containment." Again, functional recovery standards for the full range of building uses will need to parse this general goal. New residential buildings generally do not face risks from release of toxic or hazardous materials.

- "Egress is maintained." Basic safe egress is a prerequisite for reoccupancy, which precedes functional recovery. In a residential building, this objective can usually be met by limiting drifts in the structural design, limiting falling hazards along egress routes, and providing backup power for related mechanical and electrical components. Beyond basic egress, this category might also be understood to include functionality of secondary egress routes and accessibility required in all new construction. As with some habitability issues, strict compliance is sometimes waived in the immediate aftermath of an earthquake.

In considering these nonstructural systems and contents, it is useful to remember that part of the functional recovery objective is the acceptable time to restore function. Even essential equipment or contents damage is acceptable if it can be repaired within the acceptable time. Repair work that can be done while the building is serving its basic intended functions is also acceptable, as buildings routinely undergo planned maintenance, repairs, and alterations without a significant loss of use.

2.7.4 Voluntary Design for Functional Recovery

Resource Paper 1 discusses how the 2020 *Provisions'* current design criteria might be developed to serve functional recovery objectives. The previous section applied that idea, informally, to the new design provisions for CLT shear walls. Until that development occurs through consensus processes, engineers and their clients interested in functional recovery and resilience-based design will implement these concepts voluntarily, usually on a case-by-case basis.

For a project using CLT shear walls as its SFRS, voluntary implementation of resilience-based design can be done by considering the intent and expected outcome of 2020 *Provisions* Section 14.5.2 and SDPWS-21 Appendix B, as well as general performance expectations for structural systems,

nonstructural systems, and building contents, as illustrated in the previous section. As noted in Resource Paper 1, consideration should also be given to the availability of utility services and to the potential role of reoccupancy and recovery planning, distinct from building design. For the structural design, the engineer might choose to consult academic literature, including test results, for the proposed SFRS; for the CLT shear walls, several of these sources are listed in the References below or are cited by 2020 *Provisions* Section C14.5.2 and the SDPWS-21 Commentary to Appendix B. The engineer might also use a nonlinear analysis procedure to obtain a more complete understanding of likely damage patterns. Procedures and software provided in the FEMA P-58 series (see FEMA, 2018) might also be applied.

Table 2-1 lists nine recent projects in which engineers and developers voluntarily designed new buildings with organizational resilience or functional recovery objectives in mind. None of the listed projects uses CLT shear walls, and only one (Mar, 2021) is a residential building. The examples are offered here only as a resource for engineers interested in how some of their colleagues have implemented concepts of resilience-based design through functional recovery objectives.

Each of the projects had to satisfy appropriate local building codes (which probably referenced design criteria from a prior edition of the *Provisions*), and most ultimately included features not strictly required by those codes. In several cases, the developers or owners already had general performance objectives to supplement the implied objectives of the local building code. In some cases, the engineers and their clients developed objectives and criteria customized to the specific project. The costs of a resilience-based design were typically a concern, and multiple schemes were studied until affordable objectives and designs were selected. Voluntary implementation allows this flexible approach.

Table 2-1. Examples of Voluntary Design for Functional Recovery

Project	Building Use	Functional Recovery Objective or Expectation	Recovery-based Design Features or Criteria
181 Fremont (Almufti et al., 2016)	Office high-rise	Within weeks after design earthquake. (Also, immediate reoccupancy after design earthquake)	Reinforced concrete core, designed using ARUP's REDi criteria
Beaverton, Oregon schools (SEFT, 2015)	Public schools	Risk Category IV performance to serve as post-earthquake shelter	Risk Category IV criteria, backup generator
UCSF Mission Hall (Bade, 2014)	University offices	Operational performance after 84th percentile Hayward event	Enhanced Risk Category II criteria, concrete shear walls
Casa Adelante (Mar, 2021)	Senior housing	Within one day after 475-year event, no tenant relocation	Rocking walls, dampers
85 Bluxome (Moore, 2021)	Office mid-rise	Within "days to weeks" after "major earthquake"	Zero lot lines, SidePlate moment-resisting frame
UCSF Center for Vision Neuroscience (Berkowitz, 2021)	University research	Within 60 days after M7 San Andreas event	I_e = 1.25, 1.5% maximum drift
Oregon Treasury (Zimmerman, 2021)	Government offices	Within zero days after MCE_R	Base isolation, minimized nonstructural systems
Stanford Biomedical Innovations (Lizundia, 2021)	University research	Within 26 days after 475-year event	Modified Risk Category III criteria, element-specific R values, I_p = 1.5
Allenby Building (Westermeyer, 2021)	Government offices	Within zero days after 475-year event	Reduced drift limits, amplified demand, post-earthquake recovery plan

2.7.5 References

ACI (2019. *Building Code Requirements for Structural Concrete*, ACI 318-19, American Concrete Institute, Farmington Hills, MI.

AISI (2020). *North American Standard for Seismic Design of Cold-Formed Steel Structural Systems, ANSI/AISI S400-20*, American Iron and Steel Institute, Washington, DC.

AISC (2016). *Seismic Provisions for Structural Steel Buildings*, ANSI/AISC 341-16, American Institute of Steel Construction.

Almufti, I. et al. (2016). “The resilience-based design of 181 Fremont Tower,” *Structure*, June.

Amini, M. et al. (2016). “Determination of Seismic Performance Factors for CLT Shear Wall Systems,” World Conference on Timber Engineering, Vienna, August 22-25.

APA (2020). *Standard for Performance-Rated Cross-Laminated Timber*, ANSI/APA PRG 320-19, APA, 2020.

ASCE (2017). *Minimum Design Loads and Associated Criteria for Buildings and Other Structures*, ASCE/SEI 7-16, American Society of Civil Engineers, Reston, VA.

AWC (2017). *National Design Specification (NDS) for Wood Construction*, NDS-18, American Wood Council, Leesburg, VA, 2017

AWC (2020). *Special Design Provisions for Wind and Seismic (SDPWS)*, SDPWS-21, American Wood Council.

Bade, M. (2014). “Mission Bay Block 25 Building – An Exercise in Lean Target Value Design,” Presentation to the Lean Construction Institute, Finland, April 12.

Berkowitz, R. (2021). “UCSF Center for Vision Neuroscience,” 2021 EERI Annual Meeting, Session 3B, March 24.

EERI (2019). *Functional Recovery: A Conceptual Framework with Policy Options*, Earthquake Engineering Research Institute, Oakland, December 6.

FEMA (1995). *NEHRP Recommended Provisions for Seismic Regulations for New Buildings and Other Structures*, *Part 2: Commentary*, FEMA 223A Report, 1994 Edition, prepared by the Building Seismic Safety Council for the Federal Emergency Management Agency, Washington, D.C., May.

FEMA (1997). *NEHRP Recommended Provisions for Seismic Regulations for New Buildings and Other Structures*, Part 2: Commentary, FEMA 303 Report, 1997 Edition, prepared by the Building Seismic Safety Council for the Federal Emergency Management Agency, Washington, D.C.

FEMA (2009). “RP 12 – Evaluation of Geologic Hazards and Determination of Seismic Lateral Earth Pressures,” in Part 3, Resource Papers (PR) on Special Topics in Seismic Design, *NEHRP Recommended Seismic Provisions for New Buildings and Other Structures*, FEMA 750 Report, 2009 Edition, prepared by the Building Seismic Safety Council for the Federal Emergency Management Agency, Washington, D.C.

FEMA (2019). *Post-disaster Building Safety Evaluation Guidance – Report on the Current State of Practice, including Recommendations Related to Structural and Nonstructural Safety and Habitability*, FEMA P-2055, prepared by Applied Technology Council for Federal Emergency Management Agency, November.

FEMA (2018). *Seismic Performance Assessment of Buildings: Volume 5 – Expected Seismic Performance of Code-Conforming Buildings*, FEMA P-58-5, prepared by Applied Technology Council for Federal Emergency Management Agency, December.

FEMA (2020a). *NEHRP Recommended Seismic Provisions for New Buildings and Other Structures, Volume I: Part 1 Provisions and Part 2 Commentary*, 2020 Edition, FEMA P-2082-1, prepared by the Building Seismic Safety Council of the National Institute of Buildings Sciences for Federal Emergency Management Agency, September.

FEMA (2020b). *NEHRP Recommended Seismic Provisions for New Buildings and Other Structures, Volume II: Part 3 Resource Papers*, 2020 Edition, FEMA P-2082-2, prepared by the Building Seismic Safety Council of the National Institute of Buildings Sciences for Federal Emergency Management Agency, September.

FEMA (2021). 2020 *NEHRP Recommended Seismic Provisions: Design Examples, Training Materials, and Design Flow Charts*, *Volume 3: Design Flow Charts*, FEMA P-2192-V3 Report prepared by the Building Seismic Safety Council for the Federal Emergency Management Agency, Washington, D.C.

FEMA-NIST (2021). *Recommended Options for Improving the Built Environment for Post-Earthquake Reoccupancy and Functional Recovery Time*, FEMA P-2090 / NIST SP-1254, Federal Emergency Management Agency and National Institute of Standards and Technology, January.

Furley, J., van de Lindt, J., Pei, S., Wichman, S., Hasani, H., Berman, J., Ryan, K., Dolan, J., Zimmerman, R., and McDonnell, E., (2021). "Time to Functionality Fragilities for Performance Assessment of Buildings, *Journal of Structural Engineering*, American Society of Civil Engineers, Reston, VA., 147(12): 04021217.

Haselton, C., et al. (2021). "Post-Earthquake Reoccupancy and Functional Recovery Times for New Residential Buildings in California: What do Current Codes and Building Practices Provide?" Haselton Baker Risk Group, LLC, April 28.

ICC (2020). *International Building Code, 2021 Edition*, First Printing in October 2020, International Code Council, Whittier, CA.

Line, P. (2021). Personal correspondence to David Bonowitz based on first-hand and reported observations of test specimens, June 22.

Lizundia, B. (2021). "Resilient Design of the Stanford BRBF Biomedical Innovations Building," 2021 EERI Annual Meeting, Session 3B, March 24.

Los Angeles (2018). *Resilient Los Angeles*. City of Los Angeles, March.

Mar, D. (2021). "Making Resilience Affordable," 2021 EERI Annual Meeting, Session 3B, March 24.

Moore, M. (2021). "The Story of San Francisco's First USRC-Rated Building," 2021 EERI Annual Meeting, Session 3B, March 24.

NIST (2016). *Community Resilience Planning Guide for Buildings and Infrastructure Systems*, NIST Special Publication 1190, National Institute of Standards and Technology, May.

OSSPAC (2013). *The Oregon Resilience Plan: Reducing Risk and Improving Recovery for the Next Cascadia Earthquake and Tsunami*, Oregon Seismic Safety Policy Advisory Committee, February.

Public Law 115-307, (2018). “Earthquake Hazards Reduction Act of 1977,” as amended. Enacted December 11.

San Francisco (2016). *Resilient San Francisco: Stronger Today, Stronger Tomorrow*, City and County of San Francisco.

SEFT Consulting Group (2015). “Beaverton School District Resilience Planning for High School at South Cooper Mountain and Middle School at Timberland,” SEFT Consulting Group, July 10.

SPUR (2009). “The Resilient City, Part 1: Before the disaster,” in *Urbanist*, February.

van de Lindt, J., et al. (2019a). “Experimental seismic behavior of a two-story CLT platform building.” *Engineering Structures*, 183, pp. 408-422, January 15, https://doi.org/10.1016/j.engstruct.2018.12.079.

van de Lindt, J., et al. (2019b). “Quantification of Seismic Performance Factors for Cross-Laminated Timber Shear Walls,” June 12, https://drive.google.com/drive/folders/1W2GSdZ4ePMMvZIz7mDOUj6MKB1168e49.

van de Lindt, J., Rammer, D., Amini, M.O., Line, P., Pei, S., and Popovski, M. (2021). “Determination of Seismic Performance Factors for Cross-Laminated Timber Shear Wall System Based on the FEMA P695 Methodology,” General Technical Report FPL-GTR-281, Madison, WI: U.S. Department of Agriculture, Forest Service, Forest Products Laboratory (in press).

Westermeyer, J. (2021). “Resilient Design of an 11-Story Concrete Building,” 2021 EERI Annual Meeting, Session 3B, March 24.

White House (2016). “Executive Order 13717 of February 2, 2016: Establishing a Federal Earthquake Risk Management Standard,” *Federal Register*, v81, n24, February 5.

Zimmerman, R. (2021). “Resilient Design of a 2-story Seismically Base-Isolated Office Building in Salem, OR,” 2021 EERI Annual Meeting, Session 3B, March 24.

Chapter 3: Earthquake Ground Motions

Charlie Kircher[1], Nicolas Luco[2], Sanaz Rezaeian[2], and C.B. Crouse[3]

3.1 Overview

This chapter describes the earthquake ground motion requirements of the 2020 *NEHRP Provisions* (and ASCE/SEI 7-22) that have changed significantly from those of ASCE/SEI 7-16. Changes to the earthquake ground motion requirements of ASCE/SEI 7-16 are due to two primary factors: (1) incorporation of new values of earthquake ground motions based on the 2018 update of the National Seismic Hazard Model (NSHM) by the U.S. Geological Survey (USGS), and (2) re-defining the basic characterization of earthquake ground motions based on recommendations of the Project 17 committee. Project 17, a joint committee of BSSC volunteers and USGS representatives, formulated rules by which the next-generation seismic design value maps would be developed for the 2020 *NEHRP Provisions*, including the new multi-period response spectra (MPRS) described in Section 3.3. Other related changes to the ground motion requirements of ASCE/SEI 7-16 of significance include (1) an update of the values of peak ground accelerations (PGA) required for geotechnical investigation by ASCE/SEI 7-22 Section 11.8, (2) an update of the ratios of vertical to horizontal (V/H) components of response spectra for obtaining the vertical response spectrum per the requirements of ASCE/SEI 7-22 Section 11.9, and (3) the new site classes and definitions (ASCE/SEI 7-22 Chapter 20) based on shear wave velocity, and the approach for determining site class when a shear wave velocity measurement is not made but where geotechnical parameters, such as blow count or undrained shear strength, are used to estimate site shear wave velocity.

The 2018 update of the NSHM is described in Section 3.2, which also provides background on the process used by the USGS to develop seismic design maps from the 2018 NSHM and on the online tools to access values of the design ground motion parameters of the 2020 *NEHRP Provisions*. Examples are summarized for selected sites. The new multi-period response spectra (MPRS) recommended by Project 17 are described in Section 3.3, including example comparisons of the design response spectra of the 2020 *NEHRP Provisions* with those of ASCE/SEI 7-16 (and ASCE/SEI 7-10) for selected sites. Other significant changes to the ground motion requirements of the 2020 *NEHRP Provisions*, including (1) maximum considered earthquake geometric mean peak ground acceleration, (2) vertical ground motions, and (3) site class selection when shear wave velocity data are unavailable, are described with examples in Section 3.4.

[1] Charlie Kircher, P.E., Ph.D., Kircher & Associates, led the development of Sections 3.1 and 3.3.

[2] Nicolas Luco, Ph.D. and Sanaz Rezaeian, Ph.D., U.S. Geological Survey (USGS), led the development of Section 3.2.

[3] C.B. Crouse, P.E, Ph.D., led the development of Section 3.4.

Site-specific values of design parameters (and corresponding MPRS) are available online at a USGS web service, and at other related websites such as that of the Whole Building Design Guide (WBDG) of the BSSC for user-specified values of site location (latitude and longitude) and site class. The USGS web service can be accessed at https://doi.org/10.5066/F7NK3C76, and the WBDG web interface can be accessed at https://www.wbdg.org/additional-resources/tools/bssc2020nehrp.

3.2 Seismic Design Maps

Chapter 22 of ASCE/SEI 7-22 contains maps of risk-targeted maximum considered earthquake (MCE_R) spectral response accelerations, maximum considered earthquake geometric-mean (MCE_G) peak ground acceleration, and long-period transition period (T_L). The subsections below summarize (1) the development of MCE_R, MCE_G, and T_L maps; (2) the updates to these maps from ASCE/SEI 7-16 to the 2020 *NEHRP Provisions* and ASCE/SEI 7-22, including numerical examples; and (3) online access to values from the maps.

3.2.1 Development of MCE_R, MCE_G, and T_L Maps

For the conterminous United States, the MCE_R and MCE_G maps of the ASCE/SEI 7-22 were developed in accordance with its Chapter 21 site-specific ground motion procedures, using the 2018 National Seismic Hazard Model of the U.S. Geological Survey (USGS; Petersen et al., 2020). The MCE_R maps of S_{MS} and S_{M1} spectral response acceleration are per ASCE/SEI 7-22 Sections 21.2.1–21.2.3 and Sections 21.3–21.4, and the MCE_G map of PGA_M peak ground acceleration is per Section 21.5. These site-specific MCE_R and MCE_G procedures are summarized below in Sections 3.3.6 and 3.4.1, respectively, and are detailed in the ASCE/SEI 7-22 Chapter 21 commentary. The development of the MCE_R and MCE_G maps are detailed in the ASCE/SEI 7-22 Chapter 22 commentary, on pages 539–541. Both sets of maps are for the default site condition, which envelopes the MCE_R response spectra or MCE_G values for Site Classes C, CD, and D (e.g., see Figure 3-4 below), per the definition in ASCE/SEI 7-22 Section 11.4.2.1 and Section 3.3.4 below. For these and the other site classes summarized below in Section 3.3.5, corresponding MCE_R and MCE_G ground motions are accessible from the web tools summarized in Section 3.2.3 below.

For the states and territories outside of the conterminous United States, where the existing USGS seismic hazard models did not yet support direct development of MPRS, the MCE_R and MCE_G maps in ASCE/SEI 7-22 were developed using the FEMA P-2078 "Procedures for developing multi-period response spectra at non-conterminous United States sites" (Applied Technology Council, 2020). Via these procedures, the mapped S_{MS}, S_{M1}, and PGA_M values for the default site condition were approximated from Site Class BC values of S_S (at 0.2 seconds), S_1 (at 1 second), and PGA_M, as well as T_L. As detailed in the ASCE/SEI 7-22 Chapter 22 commentary (pages 539–541), these S_S, S_1, and PGA_M values were calculated in accordance with the site-specific ground motion procedures of ASCE/SEI 7-16 Chapter 21, using the existing USGS seismic hazard models for Alaska (Wesson et al., 2007), Hawaii (Klein et al., 2001), Puerto Rico and the U.S. Virgin Islands (Mueller et al., 2003), Guam and the Northern Mariana Islands (Mueller et al., 2012), and American Samoa (Petersen et al., 2012). It is expected that future USGS updates for these states and territories will enable direct

development of MPRS, just as the 2018 National Seismic Hazard Model has for the conterminous United States.

The T_L maps of ASCE/SEI 7-22 are the same as those originally introduced in the 2003 *NEHRP Provisions* (BSSC, 2004). Their development is detailed in Crouse et al. (2006) and consisted of two steps. First, a relationship between T_L and earthquake magnitude was established based on seismic source theory and response spectra from strong-motion accelerograms with reliable long-period content. Second, the modal magnitude was mapped from disaggregation of the USGS 2% probability of exceedance in 50-year ground motion hazard at a 2-second period (1 second for Hawaii), the longest period available at the time. The resulting T_L maps delimit the transition of the design response spectrum from a constant velocity ($1/T$) to constant displacement ($1/T^2$) shape.

3.2.2 Updates from ASCE/SEI 7-16 to ASCE/SEI 7-22

The MCE_R and MCE_G maps of ASCE/SEI 7-22 were updated from those in ASCE/SEI 7-16. The updates were based on (1) recommendations of the Project 17 collaboration between BSSC and the USGS (BSSC, 2019); (2) the 2018 update of the USGS National Seismic Hazard Model (NSHM) for the conterminous United States (Petersen et al., 2020); and (3) the FEMA P-2078 procedures described above in Section 3.2.1. Unlike the MCE_R and MCE_G maps of ASCE/SEI 7-16, which were for a reference site condition, the maps of ASCE/SEI 7-22 are for the default site condition, as mentioned above in Section 3.2.1.

The Project 17 recommendations are summarized in the ASCE/SEI 7-22 Chapter 22 commentary, on pages 524–525, and below in Sections 3.3.4–3.3.6. They include modifications to (1) site-class effects, (2) spectral periods defining the S_{MS} and S_{M1} ground-motion parameters, (3) deterministic caps on the otherwise probabilistic ground motions, and (4) maximum-direction scale factors. The updates in the 2018 USGS NSHM from the previous (2014) version are also summarized in the ASCE/SEI 7-22 Chapter 22 commentary, on pages 526–527. They include incorporation of (1) new NGA-East and other ground-motion models for the central and eastern United States, (2) deep sedimentary basin effects in the Los Angeles, Seattle, San Francisco, and Salt Lake City regions, (3) earthquakes that occurred in 2013 through 2017, and (4) updated weights for the western U.S. ground-motion models. Although the USGS seismic hazard models for the states and territories outside of the conterminous United States have not been updated with respect to what was used for ASCE/SEI 7-16, use of the FEMA P-2078 procedures resulted in updated MCE_R and MCE_G maps that approximately implement the Project 17 modifications listed above. The updated MCE_R maps for Alaska, Hawaii, Puerto Rico and the U.S. Virgin Islands, Guam and the Northern Mariana Islands, and American Samoa also included updates to the underlying S_S and S_1 values for consistency with the site-specific ground motion procedures of ASCE/SEI 7-22 Chapter 21. As mentioned above in Section 3.2.1, the FEMA P-2078 procedures for the states and territories outside of the conterminous United States approximate S_{MS}, S_{M1}, and PGA_M values for the default site condition from S_S, S_1, and PGA_M values for Site Class BC.

At locations in 34 high-risk (i.e., high-hazard and/or high-population) cities across the conterminous United States that were originally selected to examine ground-motion changes from ASCE/SEI 7-05

(ASCE, 2005) to the 2009 *NEHRP Provisions* (BSSC, 2009), the combined impacts of the Project 17 and 2018 NSHM modifications listed above are demonstrated in the ASCE/SEI 7-22 Chapter 22 commentary, on pages 527–538. From ASCE/SEI 7-16 to ASCE/SEI 7-22, the S_{MS}, S_{M1}, and PGA_M values for the default site condition changed by less than 15% at 31, 23, and 27 of the 34 locations, respectively. Most of the changes greater than 15% are decreases resulting from the Project 17 modification to site-class effects, i.e., the change from the site coefficients of ASCE/SEI 7-16 to direct use of 2018 NSHM values that more rigorously include site effects via the underlying ground-motion models (e.g., the aforementioned NGA-East models). At six locations in Hawaii, Alaska, Puerto Rico, and Guam, example S_{MS} and S_{M1} changes for the default site condition are presented in Chapter 7 of FEMA P-2078 (Table 7.3.1). All but two of these twelve changes from ASCE/SEI 7-16 to ASCE/SEI 7-22 are less than 15%. Other example changes to MCE_R and MCE_G ground motions from ASCE/SEI 7-16 to ASCE/SEI 7-22 and the 2020 *NEHRP Provisions*, whether inside or outside of the conterminous United States, can be seen by accessing the online tools summarized in the next subsection.

3.2.3 Online Access to Mapped and Other Ground-Motion Values

Values from the MCE_R, MCE_G, and T_L maps of ASCE/SEI 7-22, as well as values of MCE_R and MCE_G ground motions for the other-than-default site classes, can be obtained from the USGS Seismic Design Web Services, via https://doi.org/10.5066/F7NK3C76. Figure 3-1 shows a portion of the USGS webpage that lists the available web services, including those for ASCE/SEI 7-16 and earlier editions, and provides links to documentation for each. For the 2020 *NEHRP Provisions* and thereby ASCE/SEI 7-22, Figure 3-2 shows a portion of the documentation of the input (a.k.a. request) to the web service. Each web service is "run" by inputting into a web browser an address that includes the location (latitude and longitude) and site class of interest. An example of such a web address for the 2020 *NEHRP Provisions* is highlighted in Figure 3-3. Also shown there is a portion of the output (a.k.a., response) of the web service, which includes values of the mapped S_{MS} ("sms"), S_{M1} ("sm1"), PGA_M ("pgam"), and T_L ("tl") parameters. As noted in ASCE/SEI 7-22, the USGS Seismic Design Web Services spatially interpolate between the gridded data of the corresponding USGS Seismic Design Geodatabases. Step-by-step instructions for using the web services are provided via the aforementioned webpage, https://doi.org/10.5066/F7NK3C76.

In addition to the mapped MCE_R, MCE_G, and T_L parameters, the output of the USGS Seismic Design Web Services includes other parameters defined in Chapter 11 of ASCE/SEI 7-22. As shown in Figure 3-3, for example, the web service returns values of S_S ("ss"), S_1 ("s1"), and the Seismic Design Category ("sdc") for the Risk Category included in the web service input. Although not shown in Figure 3-3, the web service also returns the multi-period (22-period) MCE_R response spectrum for the location and site class of interest (under the label "multiPeriodMCErSpectrum"), as well as the underlying probabilistic and deterministic response spectra ("riskTargetedSpectrum" and "eightyFourthSpectrum," respectively), as defined in ASCE/SEI 7-22 Chapter 21. Likewise, the web service provides the probabilistic and deterministic values that underlie the MCE_G peak ground acceleration ("pgauh" and "pga84th," respectively). For convenience, the MCE_R and MCE_G deterministic lower limit values are also included in the output ("sadFloor" and "pgadFloor,"

respectively). Figure 3-4 shows the various MCE_R response spectra plotted for the same example location and site class as in Figure 3-3.

To provide a graphical user interface to the USGS web service for the 2020 *NEHRP Provisions* and thereby ASCE/SEI 7-22, the National Institute of Building Sciences (NIBS) developed the "BSSC Tool for 2020 NEHRP Provisions Seismic Design Map Values" as part of its Whole Building Design Guide (WBDG), at https://www.wbdg.org/additional-resources/tools/bssc2020nehrp. As stated there, this WBDG web interface directly extracts the seismic parameter values from the USGS web service. The WBDG interface is shown in Figure 3-5. An example of its output is provided in Figure 3-6, for the same location and site class as in Figure 3-3 and Figure 3-4. The outputted design spectral response accelerations, S_{DS} and S_{D1}, are simply two-thirds of the corresponding MCE_R values, S_{MS} and S_{M1}, per Section 11.4.4 of ASCE/SEI 7-22. Likewise, the multi-period design spectrum is two-thirds of the "multiPeriodMCErSpectrum" from the USGS web service, per ASCE/SEI 7-22 Section 21.3. For comparison with this multi-period spectrum, the output of the WBDG web interface also includes the two-period design spectrum defined in ASCE/SEI 7-22 Section 11.4.5.2 (based on just S_{DS}, S_{D1}, and T_L), again from the USGS web service. Lastly, the WBDG web interface returns the V_{S30} shear-wave velocity that corresponds to the user-selected site class, from Section 3.3.5 below and the metadata of the USGS web service. The similar "ASCE 7 Hazard Tool" graphical user interface to the USGS webs service for ASCE/SEI 7-22 is shown in Figure 3-7.

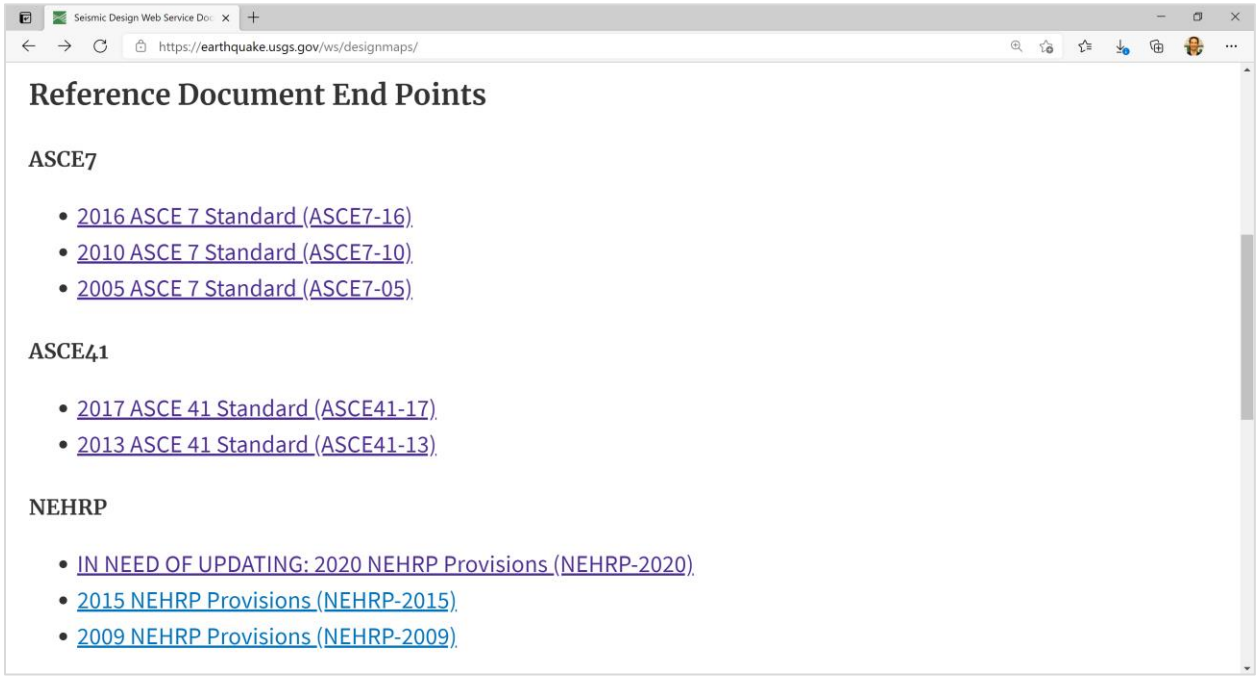

Figure 3-1. A Portion of the Entry Page for the USGS Seismic Design Web Services

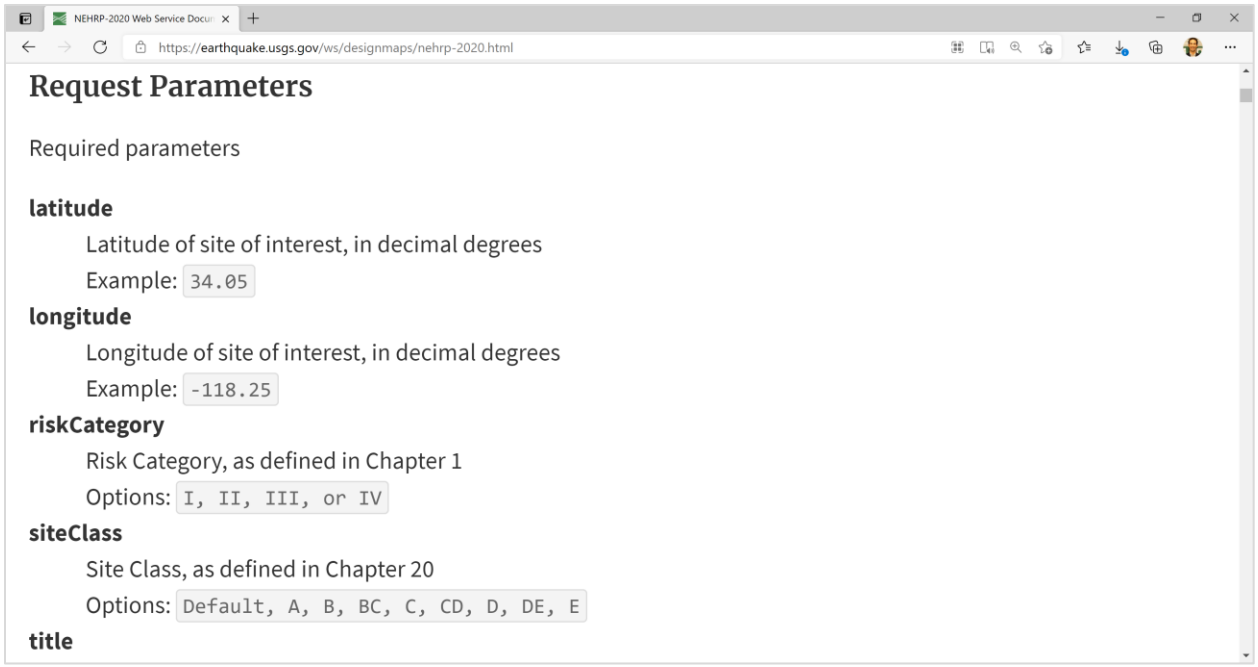

Figure 3-2. A Portion of the Documentation for the USGS Seismic Design Web Service for the 2020 *NEHRP Provisions* and Thereby ASCE/SEI 7-22

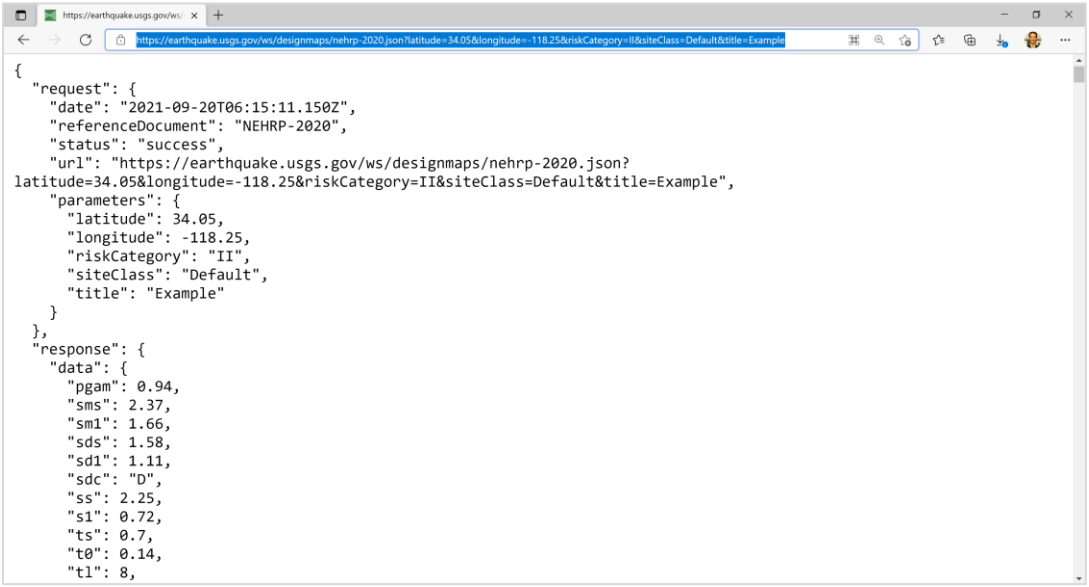

Figure 3-3. A portion of Example Output of the USGS Seismic Design Web Service for the 2020 *NEHRP Provisions* and Thereby ASCE/SEI 7-22

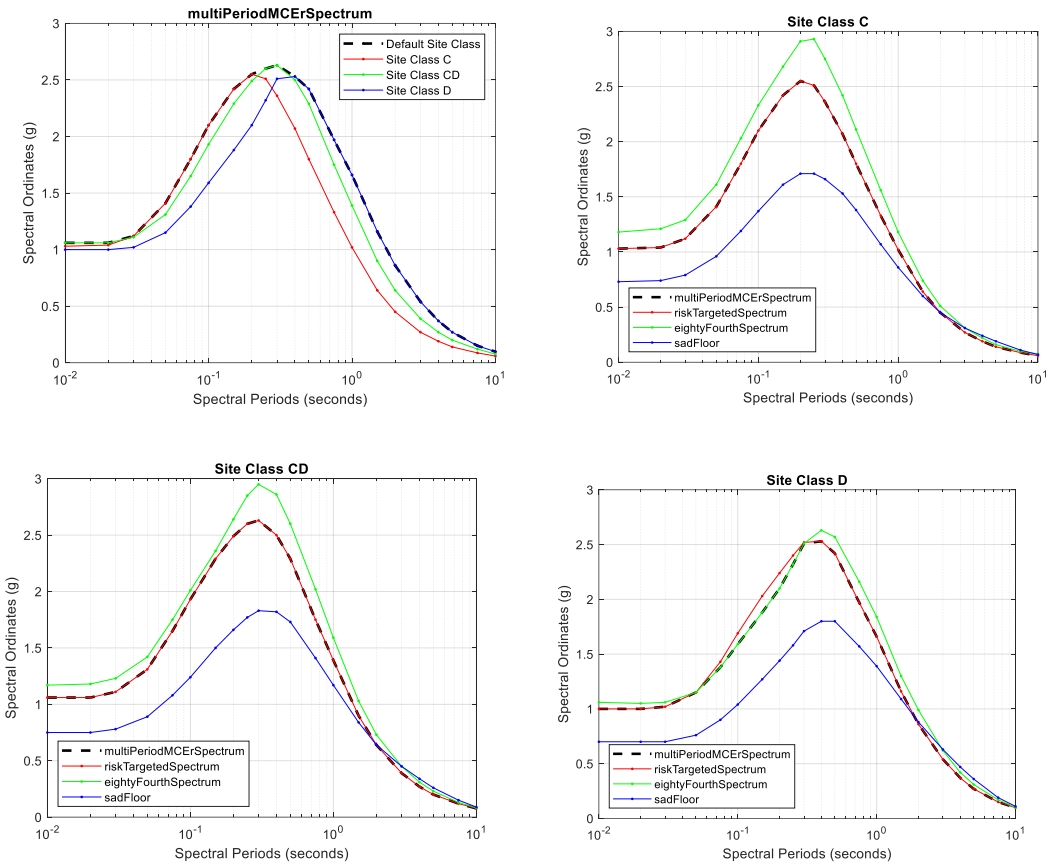

Figure 3-4. Plots of the MCE_R Response Spectra from the Remainder of Figure 3-3 Example Output of the USGS Seismic Design Web Service for the 2020 *NEHRP Provisions* and Thereby ASCE/SEI 7-22

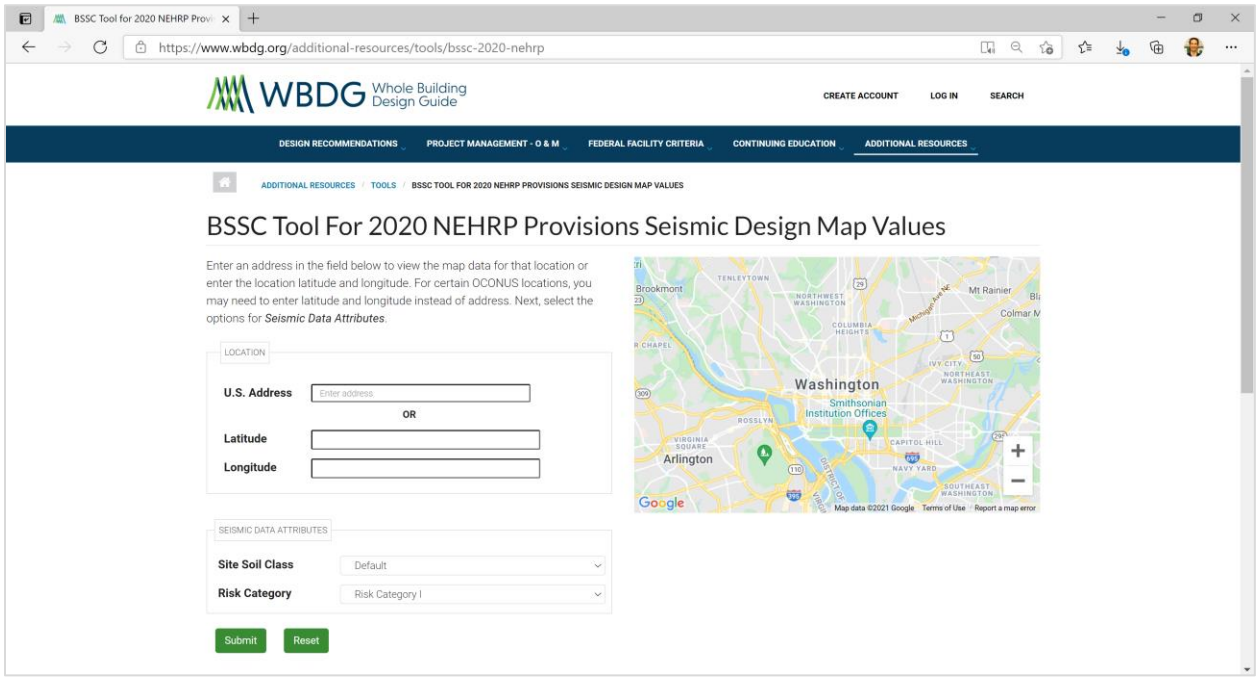

Figure 3-5. The WBDG Web Interface to the USGS Seismic Design Web Service for the 2020 *NEHRP Provisions* and Thereby ASCE/SEI 7-22

Figure 3-6. Example Output of the WBDG Web Interface to the USGS Seismic Design Web Service for the 2020 *NEHRP Provisions* and Thereby ASCE/SEI 7-22

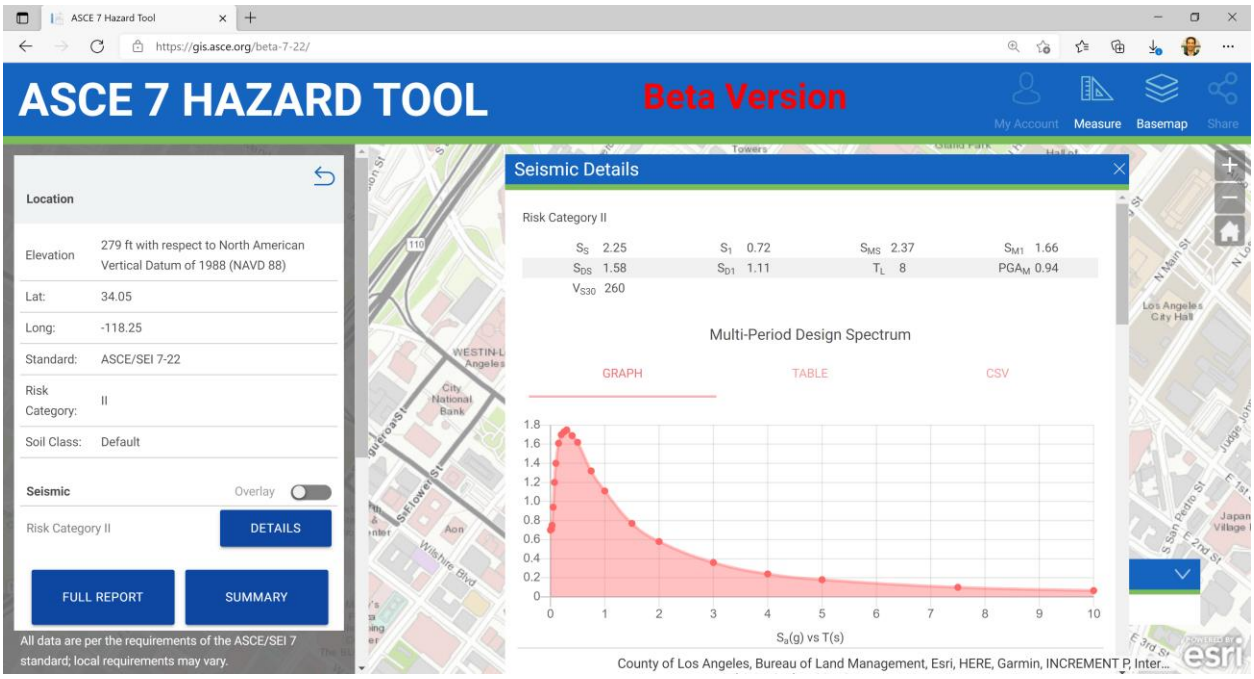

Figure 3-7. Example Output of the ASCE Web Interface to the USGS Seismic Design Web Service for the 2020 *NEHRP Provisions* and Thereby ASCE/SEI 7-22

3.3 Multi-Period Response Spectra

The MPRS represent a new framework for defining risk-targeted maximum considered earthquake (MCE_R) ground motions at 22 response periods (from 0 to 10 seconds) for the site class of interest. The MPRS affect the seismic design criteria of ASCE/SEI 7-22 Chapter 11, the site classification requirements of ASCE/SEI 7-22 Chapter 20, the site-specific ground motion procedures of ASCE/SEI 7-22 Chapter 21, and the seismic ground motion maps of Chapter 22. The changes to MCE_R ground motions (ASCE/SEI 7-22 Chapters 11 and 22) incorporate the 2018 update of the USGS NSHM described in Section 3.2. While the values of design ground motions have changed, the traditional design methods (e.g., equivalent lateral force procedure of Chapter 12) familiar to and commonly used by engineering practitioners for building design are not affected by the MPRS.

Defining earthquake design ground motions in terms of MPRS improves the accuracy of the frequency content of earthquake design ground motions and enhances the reliability of the seismic design parameters derived from these ground motions. These improvements make better use of the available earth science which has, in general, sufficiently advanced to reliably define spectral response for different site conditions over a broad range of periods. Three new site classes are added to better describe site effects. The MPRS eliminate the need for site-specific hazard analysis required by ASCE/SEI 7-16 for certain (soft soil) sites. The MPRS directly incorporate site amplification and other site (and source) dependent effects in the design parameters S_{DS} and S_{D1} (two-thirds of S_{MS} and S_{M1}), eliminating the need for site coefficients.

3.3.1 Background

During the closing months of the 2015 *NEHRP Provisions* cycle, a study (Kircher & Associates, 2015) was undertaken on behalf of the Provisions Update Committee (PUC) of the Building Seismic Safety Council (BSSC) to investigate the compatibility of the then-current Site Class coefficients, F_a and F_v, with the ground motion models (GMMs) used by USGS to produce the design maps. In the course of this study, it was discovered that the standard three-domain spectral shape defined by the short-period response spectral acceleration parameter, S_{DS}, the 1-second response spectral acceleration parameter, S_{D1}, and the long-period transition period, T_L, is not appropriate for soft soil sites (Site Class D or softer), in particular where ground motion hazard is dominated by large magnitude events. Specifically, on such sites, the standard spectral shape substantially underrepresents spectral response for moderately long period structures.

The 2015 NEHRP PUC initiated a proposal to specify spectral acceleration values over a range of periods, thus abandoning the present three-domain format, and therefore providing a better definition of likely ground motion demands. However, this proposal was ultimately not adopted due to both the complexity of implementing such a revision in the design procedure and time constraints. Instead, the PUC adopted a proposal prohibiting the general use of the three-parameter spectrum and instead required site-specific hazard determination for longer period structures on soft soil sites.

Subsequently, Project 17 was charged with formulating rules by which the next-generation seismic design value maps would be developed (BSSC, 2019). This effort included re-evaluating the use of multi-period response spectra (MPRS) as a replacement or supplement to the present three-domain (two-period) spectral definition, and consideration of how the basic design procedures embedded in ASCE/SEI 7-16 should be modified for compatibility with the multi-period response spectra. As a result, Project 17 developed (and unanimously approved) a comprehensive MPRS proposal, in four parts, for consideration by the 2020 NEHRP PUC. The four parts separately address MPRS-related changes to Chapters 11, 20, 21 and 22, respectively, and form the basis of the MPRS proposals adopted for the 2020 *NEHRP Provisions*. These revisions were subsequently incorporated into ASCE/SEI 7-22.

3.3.2 Design Parameters and Response Spectra of ASCE/SEI 7-16

Seismic design criteria are provided in Chapter 11 of ASCE/SEI 7-16 based on site class, where the determination of site class is defined in Chapter 20 of ASCE/SEI 7-16; site-specific earthquake ground motion procedures are described in Chapter 21 of ASCE/SEI 7-16; and mapped values of MCE_R ground motion parameters for reference site conditions (S_s and S_1) and the long-period transition period parameter (T_L) are defined in Chapter 22 of ASCE/SEI 7-16. The design values maps of Chapter 22 are difficult to read accurately, and users typically rely on a USGS website (or other web-based applications) to obtain values of seismic parameters for user-specified site location (latitude and longitude) and site conditions (site class).

Seismic design requirements are described in Chapter 12 of ASCE/SEI 7-16 using the seismic criteria of Chapter 11 (or Chapter 21). In particular, the applicability of permitted analytical procedures are described in ASCE/SEI 7-16 Section 12.6, which include the equivalent lateral force

(ELF) procedure of Section 12.8, the modal response spectrum analysis (MRSA) methods of Section 12.9 and the seismic response history procedures of Chapter 16. Section 11.4.4 of ASCE/SEI 7-16 provides equations for determining values of the MCE_R spectral response acceleration parameters at short periods (S_{MS}) and at 1.0 s period (S_{M1}) adjusted for site class effects. ASCE/SEI 7-16 Section 11.4.5 defines the design earthquake spectral acceleration parameter at short periods (S_{DS}) and at a period of 1.0 s (S_{D1}) as 2/3 of the parameters S_{MS} and S_{M1}, respectively. ASCE/SEI 7-16 Section 11.4.6 defines the frequency content of design ground motions using the generic response spectrum shape of ASCE/SEI 7-16 Figure 11.4-1.

An annotated copy of the ASCE/SEI 7-16 Figure 11.4-1 is shown in Figure 3-8 illustrating the three domains of constant acceleration (S_{DS}), constant velocity (S_{D1}/T), and constant displacement ($S_{D1}T_L/T^2$), the relationship of seismic design parameters S_{DS} and S_{D1} to the ELF seismic design coefficient, C_s, and the associated hypothetical site-specific multi-period design spectrum. The transition period, T_s, between the domain of constant acceleration and domain of constant velocity is defined by the ratio of the design spectral acceleration parameters, $T_s = S_{D1}/S_{DS}$. At periods less than $T = T_0 = 0.2T_S$, spectral response decreases from S_{DS} at $T = T_0$ to $0.4S_{DS}$ at $T = 0$ seconds. The parameters S_{DS} and S_{D1} are used in ASCE/SEI 7-16 Section 12.8 to determine seismic base shear of the ELF design procedure, and the design response spectrum of ASCE/SEI 7-16 Figure 11.4-1 is used in ASCE/SEI 7-16 Section 12.9 for MRSA. The value of the seismic design coefficient, C_s, of the ELF design procedure is the same at all periods from $T = 0$ seconds to $T = T_S$, ignoring the reduction in response at periods $T \le T_0$.

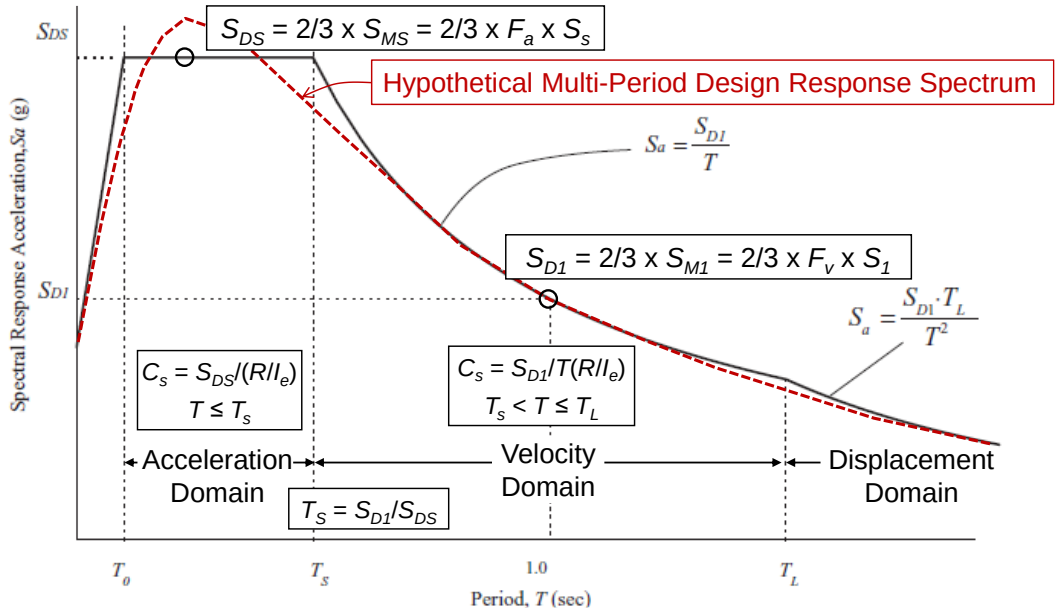

Figure 3-8. Design Response Spectrum (Annotated Copy of Figure 11.4-1, ASCE/SEI 7-16), Showing the Three Domains of Constant Acceleration, Velocity and Displacement and Associated Design Parameters, Anchored to a Hypothetical Multi-period Design Response Spectrum

The ELF procedure is permitted by ASCE/SEI 7-16 for design of all Seismic Design Category (SDC) B and C structures and for design of SDC D, E, and F structures of regular configuration that are less

than 160 feet in height, or which have a design period $T < 3.5\ T_S$, or which are less than 160 feet and do not have severe irregularity (Table 12.6-1). MRSA is permitted for all structures, regardless of configuration or design period, using the design response spectrum shape of ASCE/SEI 7-16 Figure 11.4-1 (shown in Figure 3-8), unless site-specific ground motion procedures are required to define response spectral accelerations (ASCE/SEI 7-16 Section 11.4.8). The vast majority of all buildings are designed for seismic loads using either the ELF procedure or MRSA methods and the design spectrum of ASCE/SEI 7-16 Figure 11.4-1.

3.3.3 Site-Specific Requirements of ASCE/SEI 7-16

Recognizing the potential for significant underestimation of seismic demand (Kircher & Associates, 2015) for certain (softer soil) sites controlled by larger magnitude events, the 2015 NEHRP PUC made substantial changes to Section 11.4.8 of ASCE/SEI 7-16 requiring site-specific hazard analysis of ASCE/SEI 7-16 Chapter 21 to be used for design of:

(1) Structures on Site Class E with values of S_S greater than or equal to 1.0 g, and
(2) Structures on Site Class D or Site Class E for values of S_1 greater than or equal to 0.2 g.

The site-specific requirements of ASCE/SEI 7-16 significantly impact the use of practical ELF (and MRSA) design methods, of particular importance for design of mid-period buildings at soil sites (Site Class D) where the value of S_1 is greater than or equal to 0.2 g. Areas of the conterminous United States where the value of S_1 is greater than or equal to 0.2 g are shown in Figure 3-9. Although these areas represent only about 10 percent of the conterminous United States, they represent over 90 percent of the seismic risk in terms of annualized economic loss (FEMA, 2017).

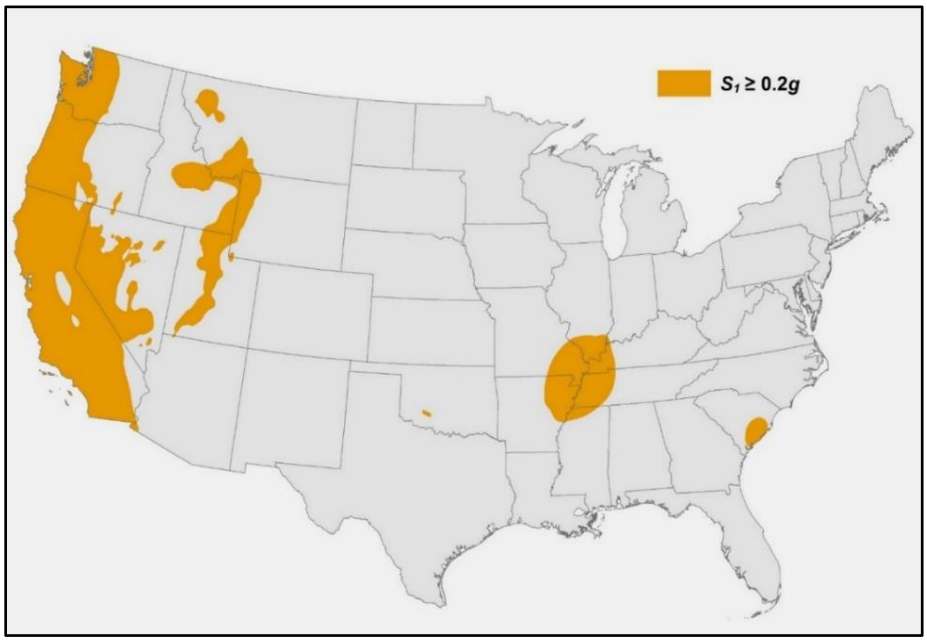

Figure 3-9. Map of the Conterminous United States Showing Areas Where the Value of S_1 is Greater Than or Equal to 0.2 g (K.S. Rukstales, USGS)

To minimize the impact of proposed changes on design practice, the site-specific requirements of Section 11.4.8 of ASCE/SEI 7-16 include exceptions permitting the use of reasonably conservative values of seismic design parameters in lieu of performing a site-specific ground motion analysis. In particular, ground motion analysis is not required for structures on Site Class D sites with S_1 greater than or equal to 0.2, where the value of the parameter S_{M1} (and S_{D1}) is increased by 50 percent. A 50 percent increase in S_{D1} essentially extends the domain of constant acceleration to a period of $T = 1.5T_s$ of ASCE/SEI 7-16 Figure 11.4-1 (shown in Figure 3-8). Considering other changes to site coefficients, the seismic design values of ASCE/SEI 7-16 are as much as 70 percent greater than those of ASCE/SEI 7-10 for mid-period buildings at Site Class D sites.

3.3.4 New Ground Motion Parameters of ASCE/SEI 7-22 Chapter 11

The new seismic design criteria of Chapter 11 of the 2020 *NEHRP Provisions* and ASCE/SEI 7-22 incorporate values of seismic design parameters, S_{MS} and S_{M1} (and S_{DS} and S_{D1}), derived from MPRS of the site of interest that include site amplification, spectrum shape, and other site (and source) effects. As noted earlier, users can obtain values of these and other ground motion data from a USGS web service for user-specific values of the location (i.e., latitude and longitude) and site conditions (i.e., site class) of the site of interest. Values of seismic design parameters S_{MS} and S_{M1} (and S_{DS} and S_{D1}), provided by the USGS web service, preclude the need to define earthquake ground motions for "reference site" conditions (Site Class BC) and site amplification factors for determining earthquake ground motions for other site conditions. Accordingly, Chapter 11 no longer has tables of site coefficients, F_a and F_v.

The definition of seismic design parameters, S_{DS} and S_{D1} (two-thirds of S_{MS} and S_{M1}), and their use in ASCE/SEI 7-22 Chapter 12 and other chapters of ASCE/SEI 7-22 to define seismic loads for ELF design, etc., remains the same as that of ASCE/SEI 7-16 (and prior editions of that standard). Thus, the traditional methods familiar to and commonly used by engineering practitioners for building design have not changed due to incorporation of MPRS in ASCE/SEI 7-22. An annotated copy of the traditional two-period design spectrum (Figure 11.4-1) of ASCE/SEI 7-22 is shown in Figure 3-10, illustrating the relationship of seismic design parameters S_{DS} and S_{D1} to the ELF seismic design coefficient, C_s, and the underlying site-specific multi-period design spectrum of the site of interest that is the basis of the values of S_{DS} and S_{D1}.

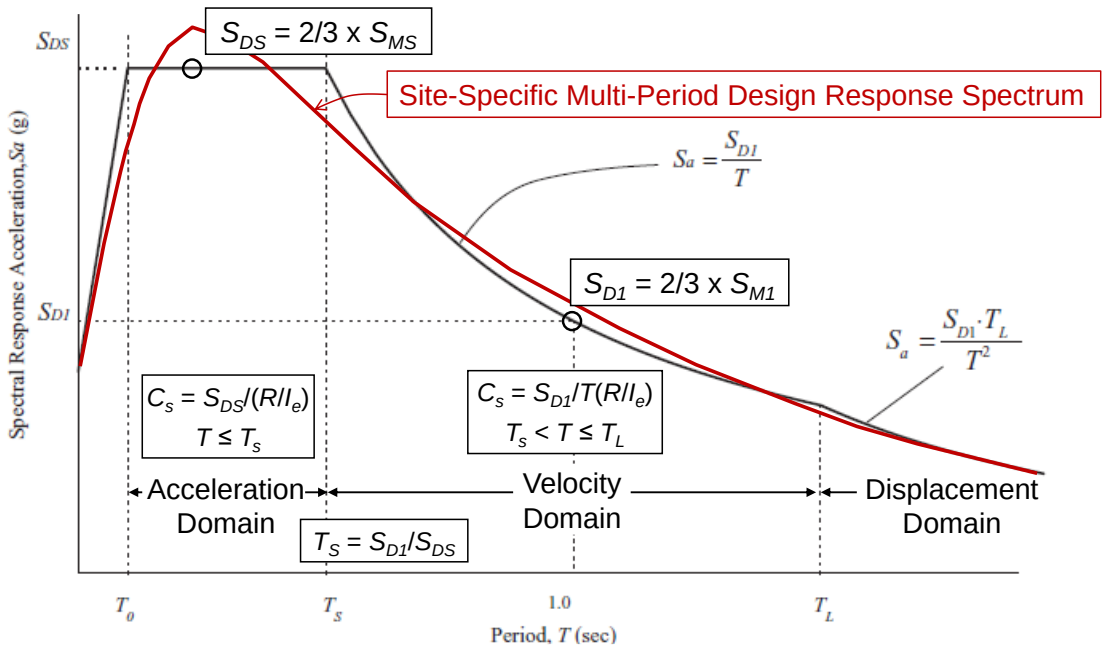

Figure 3-10. Two-period Design Response Spectrum (Annotated Copy of Figure 11.4-1, 2020 *NEHRP Provisions*) Showing the Three Domains of Constant Acceleration, Velocity and Displacement and Associated Design Parameters, and the Corresponding Multi-period Design Response Spectrum of the 2020 *NEHRP Provisions* and ASCE/SEI 7-22

New Multi-Period Response Spectra (MPRS) in ASCE/SEI 7-22 are Easy to Use

Though the introduction of MPRS required substantial changes in multiple chapters of ASCE/SEI 7-22 and revisions may initially appear overwhelming, the end result is that determination of design spectral acceleration parameters and design response spectra is actually easier than in previous editions of ASCE/SEI 7, and spectral values are more accurate. The definitions for S_{DS} and S_{D1} parameters used in equivalent lateral force (ELF) design do not change; ELF and modal response spectrum analysis (MRSA) methods themselves do not change; and the determination of design spectra acceleration parameters requires fewer steps.

A summary of the approach for ELF is as follows:

- Step 1: Identify the building location's latitude and longitude.
- Step 2: Select the site class (three new site classes have been added in ASCE/SEI 7-22 Chapter 20; see Section 3.3.5 in this chapter).
- Step 3: With the building location and site class, use the online tool to get the MPRS, S_{DS}, and S_{D1} directly (as covered in Section 3.2 of this chapter). F_a and F_v values are no longer needed to convert mapped values to design values. The final S_{DS} and S_{D1} values are derived from the site-specific MPRS and are directly provided by the tool.

- Step 4: Plug S_{DS} and S_{D1} into the Chapter 12 ELF equations just as done in previous editions of ASCE/SEI 7.

For MRSA, then there are two remaining steps:

- Step 5: With the building location and site class, use the online tool to get the MPRS directly (as covered in Section 3.2 of this chapter). The final site-specific design response spectrum is provided by the tool directly.
- Step 6: Scale the MRSA results to the ELF base shear as required by ASCE/SEI 7-22 Section 12.9, just as was required by ASCE/SEI 7-16.

Along with seismic design parameters, S_{MS} and S_{M1} (and S_{DS} and S_{D1}), users can obtain values of site-specific MPRS from a USGS web service for user-specified values of the site location (i.e., latitude and longitude) and site conditions (i.e., site class) of the site of interest. The multi-period design spectrum of the site of interest is preferred to the traditional two-period design spectrum, which is only permitted for design when MPRS are not available from the USGS web service. Sites where MPRS are not available include, for example, U.S. military installations located around the world. Site-specific MPRS provide a more refined description of the frequency content of the ground motions and thus are suitable for multi-mode response spectrum analysis and the selection and scaling of ground motion records for nonlinear response history analysis.

Values of seismic design parameters, S_{DS} and S_{D1} (and S_{MS} = 1.5 S_{DS} and S_{M1} = 1.5 S_{D1}), are based on the two-thirds of the MPRS of the site of interest in accordance with the requirements of Section 21.4 of ASCE/SEI 7-22. The requirements of Section 21.4 are illustrated in Figure 3-11 for a hypothetical high-seismicity site with soft soil (Site Class DE) site conditions ($\overline{v_s}$ = 600 ft/s). In this example, the value of S_{DS} is 1.03 g (i.e., 0.9 x 1.14 g) and the value of S_{D1} is 1.59 g (i.e., (3 s/1 s) x 0.9 x 0.59 g), with a corresponding transition period, T_S, of 1.54 seconds. The value of S_{D1} is defined by spectral acceleration at T = 3.0 seconds since the maximum value of S_a/T occurs at T = 3.0 seconds (and 90 percent of this value is greater than S_a at T = 1 second). The frequency content of the design spectrum (i.e., two-thirds of the MCE_R spectrum) of this example reflects the combined effects of site amplification and spectral shape, both of which contribute significantly to the enhanced frequency content at intermediate and longer periods for this soft soil site.

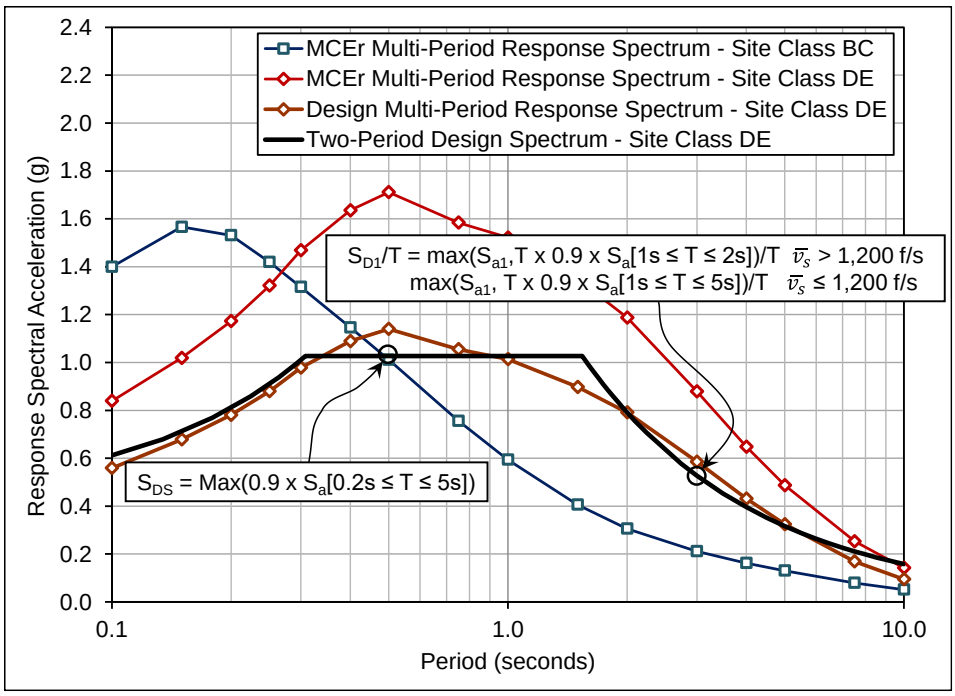

Figure 3-11. Example Derivation of Values of S_{DS} and S_{D1} from a Multi-period Site-Specific Design Spectrum of a Hypothetical High-seismicity Site with Soft Soil Site Class DE Site Conditions ($\bar{v}_s$ = 600 ft/s)

Spectral shape effects were not included in the site coefficients of ASCE/SEI 7-16, which necessitated ASCE/SEI 7-16 requiring site-specific ground motion analysis for softer soil sites. The MPRS of the ASCE/SEI 7-22 eliminate the need for such analyses, and site-specific analysis requirements of Chapter 11 of the ASCE/SEI 7-22 effectively revert back to those of ASCE/SEI 7-10 (e.g., site-specific analysis is only required for Site Class F sites with very poor soil conditions prone to potential failure under seismic loading). See Section 3.3.6 of this chapter for more information on site-specific analysis requirements.

Chapter 11 of ASCE/SEI 7-22 includes three new site classes (Site Class BC, CD and DE) to more accurately define the frequency content of earthquake ground motions, of particular importance to the characterization of ground motions of softer sites at longer periods of response. New site classes, including revised ranges of $\bar{v}_s$ values and related site classification criteria are defined in Chapter 20 of ASCE/SEI 7-22. Where soil properties are not known in sufficient detail to reliably determine the site class, "default" site conditions are now defined as the more critical spectral response of Site Class C, Site Class CD, and Site Class D at each response period (see also example in Section 3.4.3 of this chapter), unless, as noted in ASCE/SEI 7-22 Section 11.4.2.1, "the authority having jurisdiction determines, based on geotechnical data, that Site Class DE, E or F soils are present at the site." Default site conditions of ASCE/SEI 7-22 are consistent with those of ASCE/SEI 7-16, which effectively requires the more critical (i.e., greater ground motion) of Site Class C and D to be used for design.

3.3.5 New Site Classes of ASCE/SEI 7-22 Chapter 20

As noted in the previous section, the requirements of Chapter 20 of ASCE/SEI 7-22 define a more refined classification of site conditions that improve the accuracy of site amplification and corresponding values of seismic design parameters, particularly at longer response periods. Table 20.2-1 includes the three new site classes, Site Class BC, Site Class CD, and Site Class DE (for a total of eight site classes) and now defines each site class in terms of average shear wave velocity ($\overline{v_s}$) calculated in accordance with ASCE/SEI 7-22 Section 20.4.1. The lower-bound, upper-bound, , and center values of shear wave velocity of each of the eight site classes of Table 20.2.1 of ASCE/SEI 7-22; and the rounded, center-of-range values of shear wave velocity used by the USGS to develop site-specific MPRS ground motions are summarized in Table 3-1.

Table 3-1. Site Classes and Corresponding Lower-bound, Upper-bound, and Center Values of Average Shear Wave Velocity ($\overline{v_s}$) of Each of the Eight Site Classes of Table 20.2-1 of ASCE/SEI 7-22; and the Rounded, Center-of-range Values of Shear Wave Velocity Used by the USGS to Develop Site-specific MPRS Ground Motions

Site Class		Shear Wave Velocity, $\overline{v_s}$, (ft/s)			USGS[2] $\overline{v_s}$ (m/s)
Name	Description	Lower Bound[1]	Upper Bound[1]	Center	
A	Hard rock	5,000	--	--	1,500
B	Medium hard rock	3,000	5,000	3,536	1,080
BC	Soft rock	2,100	3,000	2,500	760
C	Very dense soil or hard clay	1,450	2,100	1,732	530
CD	Dense sand or very stiff clay	1,000	1,450	1,200	365
D	Medium dense sand or stiff clay	700	1,000	849	260
DE	Loose sand or medium stiff clay	500	700	600	185
E	Very loose sand or soft clay	--	500	--	150

1. Lower and upper bounds, per ASCE/SEI 7-22 Table 20.2-1.
2. Center-of-range (rounded) values used by USGS to develop MPRS.

A significant difference in the ASCE/SEI 7-22 definition of site class from that of Table 20.2-1 of ASCE/SEI 7-16 is the emphasis on average shear wave velocity and the importance of determining reliable values of $\overline{v_s}$. Whereas Table 20.2-1 of ASCE/SEI 7-16 and prior editions of ASCE/SEI 7 define site class in terms of standard penetration resistance or undrained shear strength, as well as average shear wave velocity, Table 20.2-1 of ASCE/SEI 7-22 now defines site class solely in terms of average shear wave velocity. For sites where a reliable value of the average shear wave velocity ($\overline{v_s}$) is not known (e.g., by a geotechnical investigation of the site), methods for determining a "conservative" value of the average shear wave velocity are described in the commentary of

ASCE/SEI 7-22 Chapter 20, which consider the inherent uncertainty associated with relating site class to standard penetration resistance or geotechnical data other than measured shear wave velocity (see Section 3.4.3 of this chapter).

3.3.6 New Site-Specific Analysis Requirements of ASCE/SEI 7-22 Chapter 21

The site-specific requirements of Chapter 21 of ASCE/SEI 7-22 are largely the same as those of ASCE/SEI 7-16 in terms of the definition of risk targeted MCE_R ground motions with notable exceptions described in the following paragraphs. Of particular significance: (1) MCE_R ground motions may now be based on (100 percent of) the MPRS at the site of interest in lieu of those determined by a traditional site-specific ground motion analysis, avoiding the often unwarranted cost of a site-specific analysis; (2) MCE_R ground motions determined by traditional site-specific ground motion analysis are not permitted to be taken as less than 80 percent of the MPRS of the site of interest (i.e., to provide a lower-bound safety net for ground motions developed by a site-specific analysis); and (3) the value of the seismic design parameter S_{D1} is now based on 90 percent, rather than 100 percent, of the site-specific design spectrum (i.e., two-thirds of the MPRS of the site of interest) at the period governing peak response in the velocity domain, but not less than 100 percent of site-specific design spectrum at a period of 1 second, as illustrated in Figure 3-11.

Other, more technical changes to the site-specific analysis requirements of Chapter 21 of ASCE/SEI 7-22 include (1) elimination of the approximate risk coefficient method (i.e., Method 1 in Section 21.2.1.1 of ASCE/SEI 7-16) for determining probabilistic (risk-targeted) MCE_R ground motions from uniform-hazard (2% in 50-year) ground motions, (2) revision of the period-dependent factors required for conversion of geometric mean (RotD50) ground motions to the maximum direction (RotD100) ground motions, and (3) revision of deterministic MCE_R ground motion requirements. Each of these changes to the requirements of Chapter 21 was used by the USGS to develop updated values of seismic design parameters and MPRS for Chapter 11 of ASCE/SEI 7-22 and the updated seismic design maps of Chapter 22 of ASCE/SEI 7-22.

The elimination of the approximate risk coefficient method does not affect the calculation of MPRS, which are determined by iterative integration, i.e., using the same requirements as those of Section 21.2.1.2 (Method 2) of ASCE/SEI 7-16. The revised factors used to convert geometric mean (RotD50) response to maximum direction (RotD100) response are based on the analyses of Shahi and Baker (2014). They tend to modestly increase short-period response and modestly decrease long-period response from those of ASCE/SEI 7-16 (see Resource Paper 4 of the 2015 *NEHRP Provisions*).

Changes to deterministic MCE_R ground motion requirements of Section 21.2.2 of ASCE/SEI 7-22 include (1) replacing “characteristic earthquakes” with “scenario earthquakes” in the definition of deterministic MCE_R ground motions, where the earthquake magnitude of scenario earthquakes is now determined by disaggregation of the probabilistic hazard at each period, (2) defining “active faults” in accordance with their hazard contributions from the disaggregations, and (3) replacing the lower limit on the deterministic MCE_R spectrum (e.g., Figure 21.2-1 of ASCE/SEI 7-16) with a new table of MPRS that define the lower limit deterministic MCE_R spectrum at all periods for the site class

of interest. The lower limit deterministic MCE_R spectrum effectively defines the spectral response boundary below which MCE_R ground motions are governed solely by probabilistic MCE_R ground motions (i.e., deterministic MCE_R ground motions are not required for design).

The first change to the definition of deterministic MCE_R ground motions was necessitated by the 2013 update to the Uniform California Earthquake Rupture Forecast, Version 3 (UCERF3) (Field et al., 2013), which eliminated the concept of "characteristic earthquakes" (see also ASCE/SEI 7-22 Chapter 21 commentary). In effect, the second change introduces a new definition of "active faults" that focuses on faults contributing significantly to the probabilistic ground motions; only those faults are considered in the calculation of deterministic MCE_R ground motions. Both issues were investigated by Project 17, and the related changes to Chapter 21 of ASCE/SEI 7-22 reflect recommendations of Project 17 to use probabilistically defined scenario earthquake ground motions constrained for consistency with the fundamental, 84th percentile definition of the deterministic MCE_R spectrum of Section 21.2.2 of ASCE/SEI 7-16.

The new definition of the lower limit on the deterministic MCE_R response spectrum replaces Figure 21.2-1 of ASCE/SEI 7-16 with the MPRS of Table 21.2-1 of ASCE/SEI 7-22. This change was necessitated by the elimination of the site coefficients (F_a and F_v) and the desire to update the two-domain spectrum of ASCE/SEI 7-16 with a more realistic multi-period characterization of the frequency content of lower-limit deterministic MCE_R ground motions. The MPRS of ASCE/SEI 7-22 Table 21.2-1 are plotted in Figure 3-12, illustrating the variation of the lower-limit deterministic MCE_R response spectrum with site class.

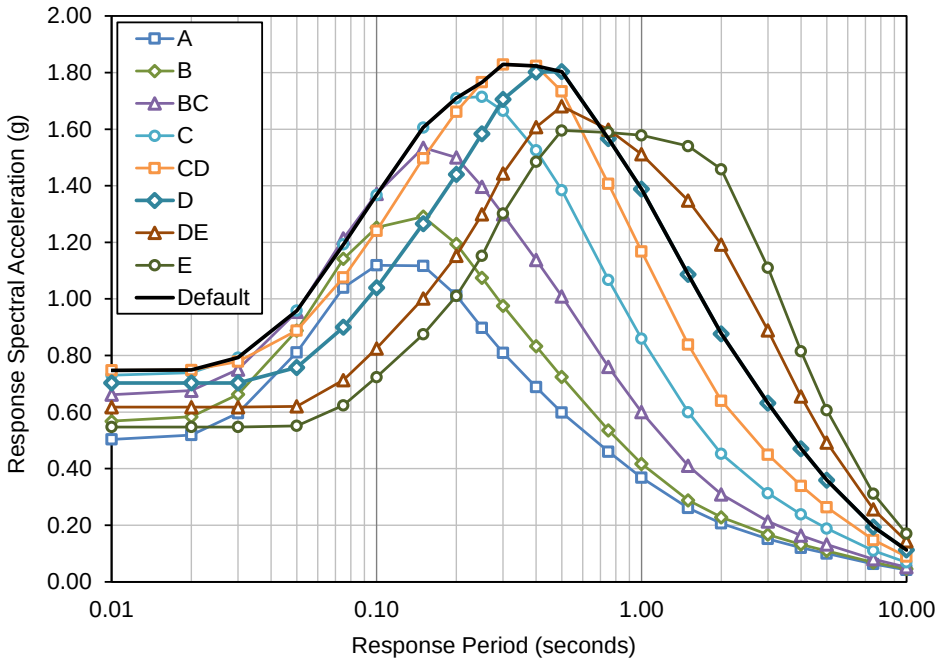

Figure 3-12. Plots of the Lower-limit Deterministic MCE_R Response Spectra of Table 21.2-1 of ASCE/SEI 7-22

The values of lower-limit deterministic MPRS of ASCE/SEI 7-22 Table 21.2-1 were developed as part of a broader study of MPRS (FEMA P-2078, 2020). These MPRS are based on an assumed magnitude M8.0 shallow crustal earthquake in the Western United States at a distance of about 12 km from the fault rupture. A magnitude M8.0 earthquake represents the approximate magnitude typically found by disaggregation of site hazard for sites near major fault systems (e.g., San Andreas Fault in the San Francisco Bay Area). A distance of 12 km from the site to fault rupture is the approximate distance at which a magnitude M8.0 earthquake generates a 0.2-second response of 1.5 g and a 1-second response of 0.6 g for Site Class BC site conditions. The deterministic lower limit MPRS of Table 21.2-1 of ASCE/SEI 7-22 are anchored to these values of 0.2-second and 1-second response for consistency with the deterministic lower limit on the MCE_R response spectrum of ASCE/SEI 7-16 (i.e., Figure 21.2-1 of ASCE/SEI 7-16). Note that Supplement 1 of ASCE/SEI 7-16 replaced Figure 21.2-1 with revised deterministic lower limit MCE_R criteria that represent an interim transition from the two-period spectrum of Figure 21.2-1 to the MPRS of Table 21.2-1 of ASCE/SEI 7-22.

Where a site-specific hazard analysis is performed, the lower limit deterministic MCE_R response spectra of ASCE/SEI 7-22 Table 21.2-1 (shown in Figure 3-12) provide a convenient means of screening out sites not requiring calculation of the deterministic MCE_R response spectrum (ASCE/SEI 7-22 Section 21.2.2). Where the probabilistic MCE_R response spectrum is less, at all periods of interest, than the lower limit deterministic MCE_R response spectrum of the site class of interest, the probabilistic MCE_R response spectrum governs site hazard, and the deterministic MCE_R response spectrum need not be calculated. An example map of the areas requiring calculation of deterministic MCE_R ground motions assuming default site conditions is shown in Figure 3-12. In these areas of strongest earthquake ground motions, the MCE_R response spectrum is defined by Section 21.2.3 of ASCE/SEI 7-22 as the lesser of deterministic MCE_R and probabilistic MCE_R ground motions, the same definition in ASCE/SEI 7-16. All other areas, i.e., the vast majority of sites in the conterminous United States, are governed solely by probabilistic MCE_R ground motions for default site conditions.

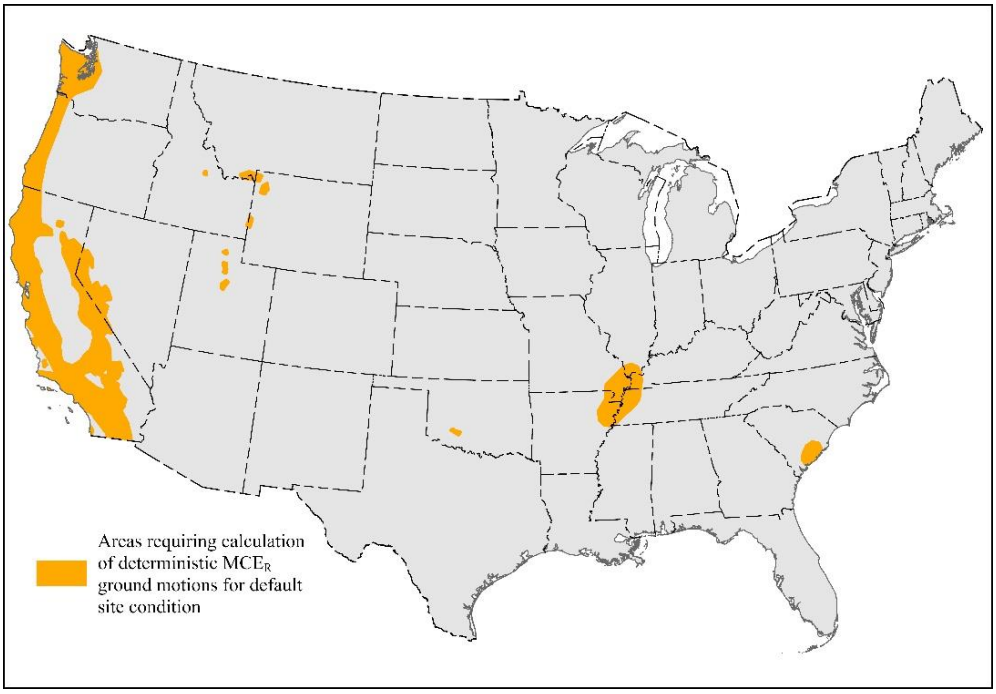

Figure 3-13. Example Map of the Conterminous United States Showing Areas Requiring Calculation of Deterministic MCE_R Ground Motions for Default Site Conditions (K.S. Rukstales, USGS)

3.3.7 Example Comparisons of Design Response Spectra

This section illustrates MPRS by example comparisons of multi-period design response spectra of ASCE/SEI 7-22 with the design response spectra of ASCE/SEI 7-16 and ASCE/SEI 7-10 for six sites: (1) two sites in the western United States (WUS sites) of the conterminous United States (CONUS), (2) two sites outside of the conterminous United States (OCONUS sites) and (3) two sites in the central and eastern United States (CEUS Sites). The four example WUS and CEUS sites of the CONUS and their geographical locations are taken from Table C22-1 of ASCE/SEI 7-22. The two OCONUS sites and their geographical locations are taken from Table 7.1-1 of FEMA P-2078 (2020).

Design response spectra of ASCE/SEI 7-16 and ASCE/SEI 7-10 are characterized by the so-called "two-period" design response spectrum shape shown in Figure 3-8 (Figure 11.4-1 of ASCE/SEI 7-16). The design response spectra of ASCE/SEI 7-22 are characterized by both multi-period design spectra and two-period design spectra, where two-period design spectra are based on the values S_{DS} and S_{D1} derived from the multi-period design spectrum of the site of interest (e.g., see Figure 3-11). Comparison of multi-period design spectra with two-period design spectra for the same site illustrates the improved characterization of the frequency content by the new MPRS of ASCE/SEI 7-22. In particular, note the correction of the under-estimation of mid-period ground motions of ASCE/SEI 7-10 for certain sites. Two-period design spectra of ASCE/SEI 7-22 facilitate direct comparison with the two-period design spectra of ASCE/SEI 7-10 and ASCE/SEI 7-16 (e.g., comparison of the values of S_{DS} and S_{D1} that define two-period design spectra). Recall, however, that

the two-period design spectra of ASCE/SEI 7-22 are not permitted for design unless multi-period design spectra are not available.

Design response spectra shown here assume hypothetical "default" site conditions. Default site conditions of ASCE/SEI 7-10 and ASCE/SEI 7-16 are the envelope response of Site Class C and D site conditions and, for ASCE/SEI 7-22, the envelope response of Site Class C, CD, and D site conditions. In all cases, response at longer periods is governed by Site Class D site conditions. The design response spectra of ASCE/SEI 7-16 shown in these figures incorporate the 50 percent increase at longer periods to represent design ground motions based on the exception of ASCE/SEI 7-16 Section 11.4.8 for Site Class D sites where site-specific analysis is not performed.

WUS Sites – Irvine (Southern California) and San Mateo (Northern California)

Example design response spectra (2/3 of MCE_R response spectra) are shown in Figures 3-14 for two WUS sites of the conterminous United States: (a) Irvine site (in southern California) and (b) San Mateo site (in northern California). The design response spectra of ASCE/SEI 7-22 are compared with those of ASCE/SEI 7-10 and ASCE/SEI 7-16. The following five design spectra are shown in each of these two figures:

(1) The two-period design spectrum (2PRS) of ASCE/SEI 7-10,

(2) The two-period design spectrum (2PRS) of ASCE/SEI 7-16,

(3) The two-period design spectrum (2PRS) of ASCE/SEI 7-22,

(4) The multi-period design spectrum (MPRS) of ASCE/SEI 7-22, and,

(5) The multi-period design spectrum derived from values of S_S, S_1, and T_L of ASCE/SEI 7-22 using the methods of FEMA P-2078.

The "derived" multi-period design response spectra of FEMA P-2078 are shown in these figures to illustrate their similarity to the corresponding multi-period design response spectra of ASCE/SEI 7-22. Derived multi-period design response spectra are not necessary for design at WUS (or CEUS) sites of the conterminous United States where MPRS are available and fully define MCE_R ground motions at all periods and site classes of interest.

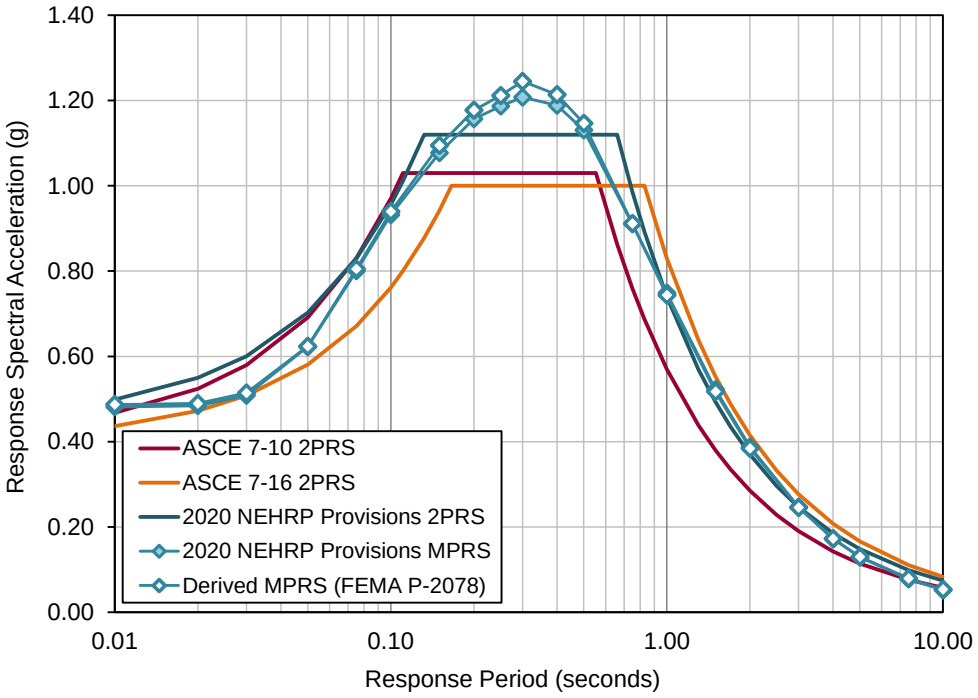

(a) Irvine (southern California) Site

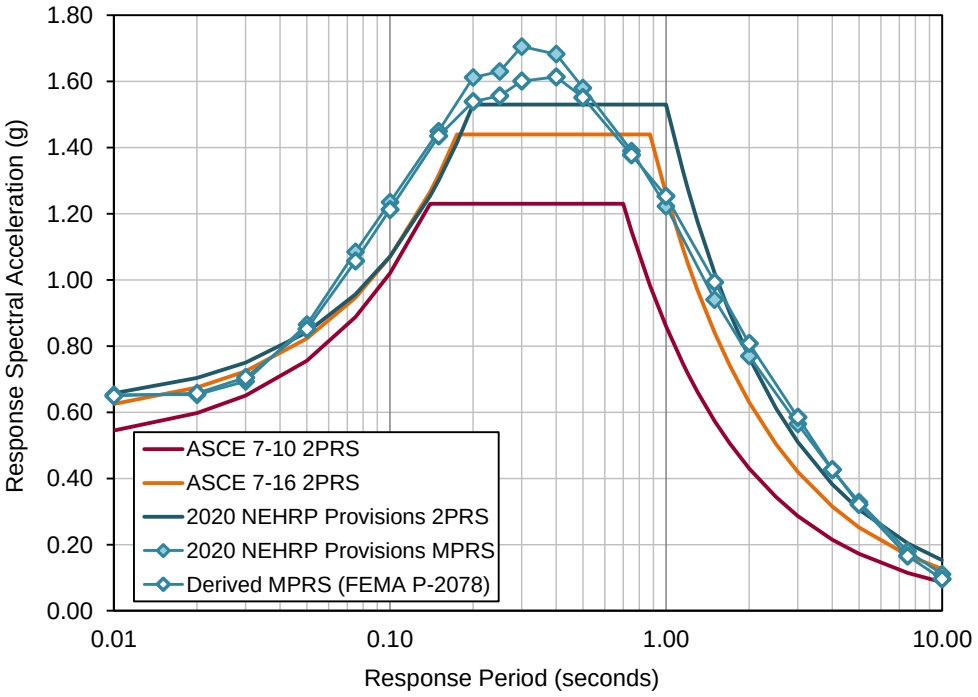

(b) San Mateo (northern California) Site

Figure 3-14. Comparison of Two-period Design Response Spectra (2PRS) of ASCE/SEI 7-10, ASCE/SEI 7-16, and the 2020 *NEHRP Provisions* (and ASCE/SEI 7-22), and the Multi-period Design Response Spectra of the 2020 *NEHRP Provisions* (and ASCE/SEI 7-22) and the Derived Multi-period Design Response Spectrum of FEMA P-2078 for the Irvine and San Mateo Sites Assuming "Default" Site Conditions

The design response spectra of the Irvine site are governed primarily by probabilistic MCE_R ground motions (e.g., Section 21.2.1 of ASCE/SEI 7-22), whereas the design response spectra of the San Mateo site are governed primarily by deterministic MCE_R ground motions (e.g., Section 21.2.2 of ASCE/SEI 7-22), in this case from an approximate M8.0 earthquake rupturing the nearby Peninsula Segment of the San Andreas Fault. The design response spectra of these two sites are typical of the range of ground motions in California areas of high seismicity. Other WUS sites of high seismicity include those in the Pacific Northwest (PNW) along the coastal areas of Oregon and Washington. Although sites in the PNW are influenced by subduction earthquakes, as well as shallow crustal earthquakes, the shape (frequency content) of their design response spectra is very similar to that of the California sites shown in Figures 3-13 and 3-14, with a possible exception being relatively strong ground motions at very long periods due to M9.0 earthquakes of the Cascadia Subduction Zone.

Comparison of the two-period design spectra of ASCE/SEI 7-10 with those of ASCE/SEI 7-16 illustrates the shortcomings discovered during the 2015 *NEHRP Provisions* cycle that led to the changes to the site-specific requirements of ASCE/SEI 7-16. The ground motions of ASCE/SEI 7-10 can substantially underrepresent ground motions for softer soil ("default") site conditions at longer periods. Comparison of the design spectra of ASCE/SEI 7-16 with those of ASCE/SEI 7-22 shows the mixed success of the 50 percent increase in seismic demand to correct the identified shortcomings. For the Irvine site, where hazard is governed by smaller magnitude (M7.0) earthquakes, the 50 percent increase in seismic demand of ASCE/SEI 7-16 is sufficient to match the two-period (and multi-period) design spectra of ASCE/SEI 7-22. For the San Mateo site, where ground motions are stronger and hazard is governed by very large magnitude (M8.0) earthquakes, the 50 percent increase in seismic demand of ASCE/SEI 7-16 is not sufficient to fully match the two-period (and multi-period) design spectra of ASCE/SEI 7-22 at longer response periods In this example, and at other softer soil sites where hazard is governed by large magnitude earthquakes, the design spectra of ASCE/SEI 7-22 better characterize the frequency content of the site-specific ground motions, which would otherwise be underrepresented by the two-period design spectrum of ASCE/SEI 7-16 at longer response periods.

As shown in Figures 3-14 and 3-15, multi-period design spectra derived from values of S_S, S_1, and T_L of ASCE/SEI 7-22 using the methods of FEMA P-2078 (so-called derived MPRS) closely match those of ASCE/SEI 7-22 for WUS sites and are therefore expected to reliably represent the frequency content of ground motions at sites outside of the conterminous United States (OCONUS sites) with comparable governing earthquake magnitudes, shaking levels, and site conditions. Derived MPRS are the basis for the multi-period design response spectra of the OCONUS sites, illustrated in the figures of the next section.

OCONUS Sites – Honolulu (Hawaii) and Anchorage (Alaska)

Example design response spectra (2/3 of MCE_R response spectra) are shown in Figures 3-15(a) and 15(b) for two OCONUS sites: (a) Honolulu (Hawaii) site and (b) Anchorage (Alaska) site. The design response spectra of ASCE/SEI 7-22 are compared with those of ASCE/SEI 7-10 and ASCE/SEI 7-16. The following four design spectra are shown in each of these two figures:

(1) The two-period design spectrum (2PRS) of ASCE/SEI 7-10,

(2) The two-period design spectrum (2PRS) of ASCE/SEI 7-16,

(3) The two-period design spectrum (2PRS) of ASCE/SEI 7-22, and

(4) The multi-period design spectrum (MPRS) of ASCE/SEI 7-22.

In these figures, the two-period and multi-period design response spectra of ASCE/SEI 7-22 are derived (by the USGS) from the values of S_S, S_1, and T_L using the methods of FEMA P-2078.

The two OCONUS sites represent a range of design ground motion levels, from rather modest shaking at the Honolulu site (i.e., PGA ≈ 0.2 g) to strong shaking at the Anchorage site (i.e., PGA ≈ 0.5 g). The Honolulu site on the island of Oahu is relatively far from active seismic sources, which are mainly near the Island of Hawaii. In contrast, the Anchorage site is relatively close to active seismic sources, including shallow crustal faults as well as the subduction source that caused the Great Alaskan Earthquake of 1964, the largest magnitude (M9.2) earthquake recorded in the United States.

Comparisons of design spectra of the two OCONUS sites show similar trends to those of the two WUS sites. This is expected since the methods of FEMA P-2078 used to derive the MPRS of OCONUS sites are based on spectral shape (frequency content) of WUS ground motion models. The two-period design spectrum of ASCE/SEI 7-22 is similar to that of ASCE/SEI 7-16 for the Anchorage site and somewhat less than that of ASCE/SEI 7-16 at longer periods for the Honolulu site, reflecting a modest conservatism in the 50 percent increase required by ASCE/SEI 7-16 at longer periods where ground motion levels are relatively low. The flatter shape at long periods of the multi-period design spectrum of the Anchorage, shown in Figure 3-15(b), reflects stronger shaking at longer periods expected for sites where ground motion hazard is governed by very large magnitude subduction earthquakes. For comparison, a similar flatter shape at long periods of the multi-period design spectrum of the San Mateo site is shown in Figure 3-14(b) for the San Mateo site, which is also governed by large magnitude (crustal) earthquakes.

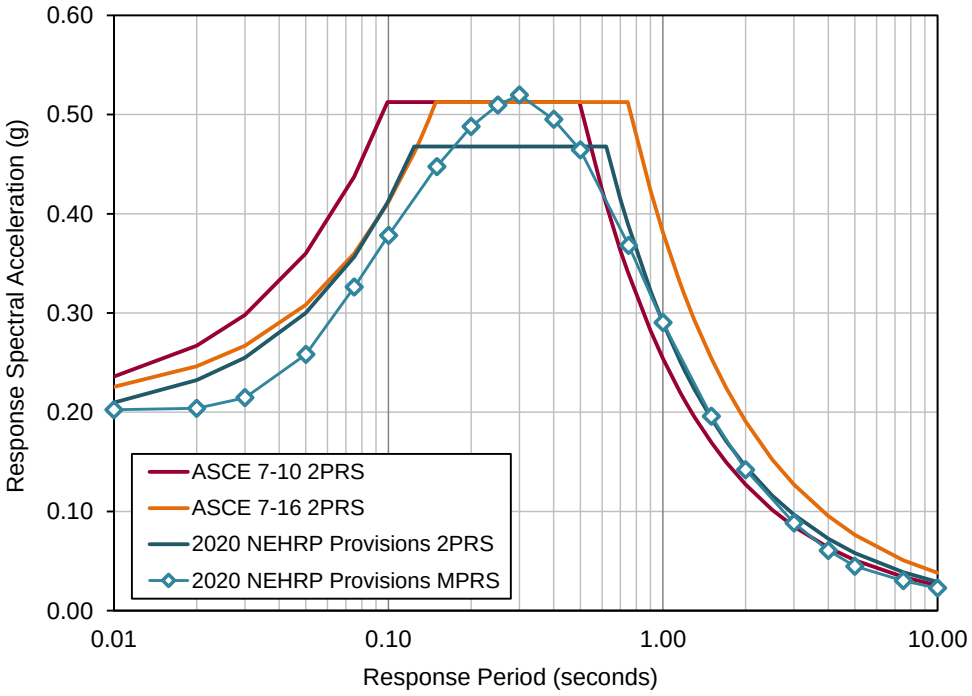

(a) Honolulu (Hawaii) Site

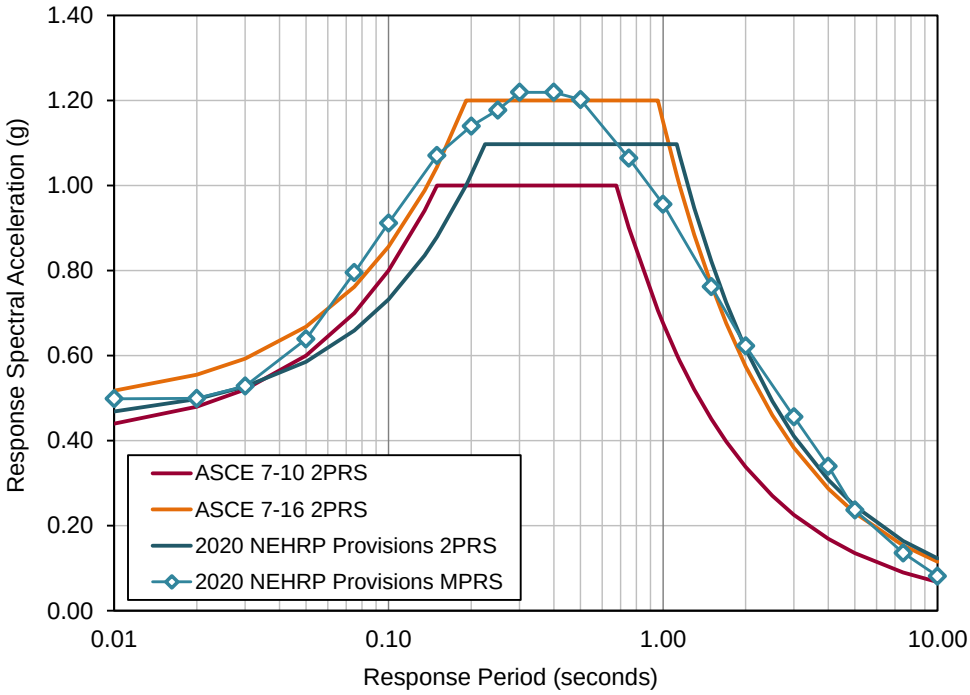

(b) Anchorage (Alaska) Site

Figure 3-15. Comparison of Two-Period Design Response Spectra (2PRS) of ASCE/SEI 7-10, ASCE/SEI 7-16, and the 2020 *NEHRP Provisions* (and ASCE/SEI 7-22) and the Multi-period Design Response Spectra of the 2020 *NEHRP Provisions* (and ASCE/SEI 7-22) for the Honolulu (Hawaii) and Anchorage (Alaska) Sites Assuming "Default" Site Conditions

CEUS Sites – St. Louis (Missouri) and Memphis (Tennessee)

Example design response spectra (2/3 of MCE_R response spectra) are shown in Figures 3-16(a) and 16(b) for two CEUS sites: (a) St. Louis (Missouri) site and (b) Memphis (Tennessee) site. The design response spectra of ASCE/SEI 7-22 are compared with those of ASCE/SEI 7-10 and ASCE/SEI 7-16. The following four design spectra are shown in each of these two figures:

(1) The two-period design spectrum (2PRS) of ASCE/SEI 7-10,

(2) The two-period design spectrum (2PRS) of ASCE/SEI 7-16,

(3) The two-period design spectrum (2PRS) of ASCE/SEI 7-22, and

(4) The multi-period design spectrum (MPRS) of ASCE/SEI 7-22.

The two CEUS sites represent design ground motion levels ranging from moderate shaking at the St. Louis site (i.e., PGA ≈ 0.25 g) to strong shaking at the Memphis site (i.e., PGA ≈ 0.5 g). Seismic hazard at both of these CEUS sites is governed by large magnitude (M7.7) earthquakes in the New Madrid Seismic Zone (NMSZ), but ground motions are stronger at the Memphis site due to closer proximity to the NMSZ. With the exception of sites near Charleston, South Carolina, design response spectra at other CEUS sites are generally less than those shown for the St. Louis and Memphis sites, although the shape (frequency content) is similar for all CEUS sites.

The shape (frequency content) of the multi-period design spectra of ASCE/SEI 7-22 for sites in the CEUS is fundamentally different and inconsistent with the two-period design response spectra of ASCE/SEI 7-16 (and ASCE/SEI 7/10), as shown in Figure 3-16(a) for the St. Louis site and in Figure 3-16(b) for the Memphis site. That is, the traditional three-domain design response spectrum of Figure 11.4-1 of ASCE/SEI 7-16 (and prior editions of ASCE 7), shown in Figure 3-16, misrepresents the frequency content of ground motions in the CEUS.

The remarkable consistency of the two-period design spectra of ASCE/SEI 7-22 (and the underlying values of S_{DS} and S_{D1}), shown in Figures 3-16(a) and 3-16(b), with those of ASCE/SEI 7-16 and ASCE/SEI 7-10 is due to the requirements of ASCE/SEI 7-22 Section 21.4, which ignore response spectral accelerations at periods less than 0.2 seconds when deriving values of the seismic design parameter, S_{DS}, from the corresponding site-specific (multi-period) design response spectrum (e.g., as illustrated in Figure 3-11). Ignoring response spectral acceleration at periods less than 0.2 seconds was a conscious decision by the 2020 *NEHRP Provisions* PUC to avoid over-design of structures which typically do not have fundamental periods less than about 0.2 seconds, recognizing that very short-period structures of low ductility could potentially be under-designed. The resulting values of S_{DS} can understate seismic demand on very short-period (high-frequency) subsystems and nonstructural components of structures in the CEUS by effectively ignoring the inherently strong high-frequency content of CEUS ground motions, as illustrated by the multi-period design spectra of ASCE/SEI 7-22 in Figure 3-16(a) and Figure 3-16(b).

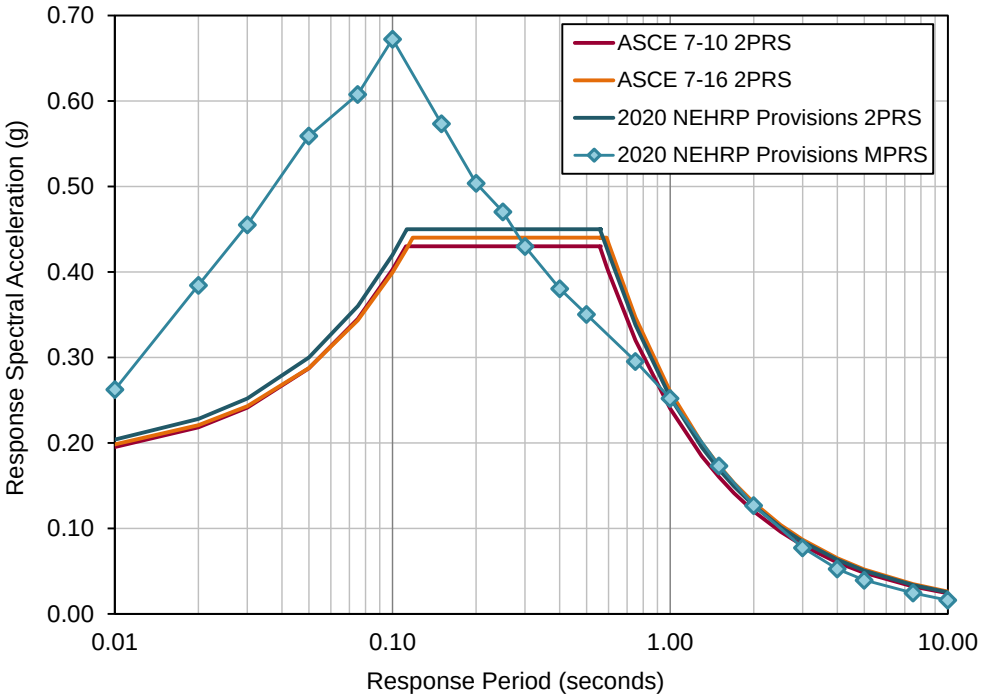

(a) St. Louis (Missouri) Site

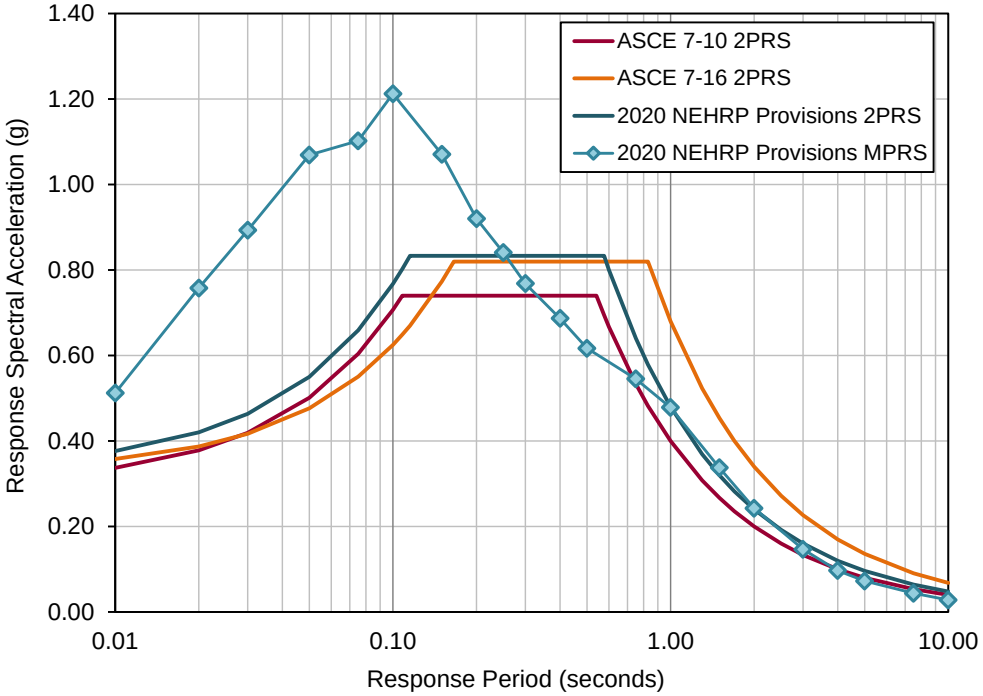

(b) Memphis (Tennessee) Site

Figure 3-16. Comparison of Two-period Design Response Spectra (2PRS) of ASCE/SEI 7-10, ASCE/SEI 7-16, and the 2020 *NEHRP Provisions* (and ASCE/SEI 7-22), and the Multi-period Design Response Spectra of the 2020 *NEHRP Provisions* for the St. Louis (Missouri) and Memphis (Tennessee) Sites Assuming "Default" Site Conditions

3.4 Other Changes to Ground Motion Provisions in ASCE/SEI 7-22

3.4.1 Maximum Considered Earthquake Geometric Mean (MCE_G) Peak Ground Acceleration (ASCE/SEI 7-22 Section 21.5)

The MCE_G peak ground acceleration is used for evaluations of soil liquefaction, seismically-induced permanent ground displacement, and strength loss, per ASCE/SEI 7-22 Section 11.8.3. In ASCE/SEI 7-16 Section 11.8.3, this acceleration was computed as the product of the mapped MCE_G peak ground acceleration, PGA, and a site coefficient, F_{PGA}, which accounted for the effects of the local soil or rock condition at a site.

The introduction of the MPRS into the ASCE/SEI 7-22 provisions eliminated the need for F_{PGA}, and it also necessitated revisions to ASCE/SEI 7-22 Sections 21.5.2 and 21.5.3. The provisions in ASCE/SEI 7-22 Section 21.5.2 are similar to those in Section 21.2.2 for the MPRS, with the deterministic lower limit value of PGA_G listed in the bottom row of ASCE/SEI 7-22 Table 21.2-1 for the site class determined in accordance with the site class requirements of ASCE/SEI 7-22 Section 11.4.2. This lower limit PGA_G replaces the 0.5 F_{PGA} lower limit in ASCE/SEI 7-16 Section 21.5.2. Like ASCE/SEI 7-22 Section 21.2.2, Section 21.5.2 also replaces "characteristic earthquakes" with "scenario earthquakes" determined from disaggregation for the probabilistic MCE_G peak ground acceleration and specifies that scenario earthquakes contributing less than 10% of the largest contributor to the seismic hazard shall be ignored in the calculation of the deterministic MCE_G peak ground acceleration. For example, if the fault that has the largest contribution for the probabilistic MCE_G peak ground acceleration (i.e., the geometric mean peak ground acceleration with a 2% probability of exceedance in a 50-year period per ASCE/SEI 7-22 Section 21.5.1) is Fault X (e.g., the Hayward Fault at an example San Jose, California site in the ASCE/SEI 7-22 Chapter 21 commentary), and this percentage contribution is *Y* (e.g., 50%), then all faults with a contribution less than 0.1*Y* (e.g., 5%) are ignored for the deterministic calculations (e.g., the Silver Creek Fault for the San Jose example).

The determination of the site-specific PGA_M per ASCE/SEI 7-22 Section 21.5.3 is similar to that in the same section of ASCE/SEI 7-16, except that the minimum value is taken as 80% of the PGA_M extracted from the USGS Seismic Design Geodatabase (https://doi.org/10.5066/F7NK3C76) for a given site and its site class.

3.4.2 Vertical Ground Motion for Seismic Design (ASCE/SEI 7-22 Section 11.9)

The provisions for the vertical component of ground motion in Section 11.9 in ASCE/SEI 7-16 are applied to both seismically active tectonic regions and stable continental regions of relatively low seismic hazard. However, Section 11.9.1 of ASCE/SEI 7-22 includes a separate provision for the stable region in the conterminous US east of 105° W longitude; this provision sets the vertical response spectrum equal to two-thirds (2/3) of the MCE_R response spectrum. The detailed

provisions in ASCE/SEI 7-22 Section 11.9.2 apply to the conterminous US west of this longitude, Alaska, Hawaii, and the US territories, all of which are considered active tectonic regions. Revisions to Section 11.9.2 appearing in ASCE/SEI 7-22 are described below.

The provisions were modified to account for (1) updated ground motion models for horizontal components and corresponding vertical-to-horizontal response spectral ratios (V/H), (2) the geometric mean definition of the H component in the V/H models and the maximum direction parameter used to compute the MCE_R response spectrum, (3) new site class definitions, and (4) vertical natural periods greater than 2.0 sec.

ASCE/SEI 7-22 Equations 11.9-1 through 11.9-4, which compute the vertical response spectral acceleration (S_{aMv}) in four period bands between 0 and 2.0 sec, were modified to reflect Item (1) and Item (2) in the preceding paragraph. Values of the vertical response spectral coefficient, C_v, appearing in these four equations, were modified to accommodate the new site class definitions. ASCE/SEI 7-22 Equation 11.9-5, which does not include C_v, was added to compute S_{aMv} for vertical periods greater than 2.0 sec; this equation corresponds to a V/H ratio of 0.5.

The S_{aMv} in Equation 11.9-1 through Equation 11.9-4 in ASCE/SEI 7-16 was expressed in terms of the S_{MS}, the short-period MCE_R response spectral acceleration parameter. In ASCE/SEI 7-22, this parameter was replaced by the ratio (S_{aM}/F_{md}), where F_{md} is the period-dependent factor that converts the geometric mean spectral ordinate (i.e., the geometric mean of the two horizontal components of spectral acceleration) to the maximum direction spectral ordinate (i.e., the maximum response spectral acceleration in the horizontal plane). ASCE/SEI 7-22 Equation 11.9-6 through Equation 11.9-8 compute F_{md} for three vertical period bands between 0 and 10 sec and are based on a smoothed version of the factors in Table 1 of Shahi and Baker (2014) that is specified in Section 21.2 of ASCE/SEI 7-22.

An example calculation illustrating the calculation of S_{aMv} from S_{aM} is presented in Table 3-2 for a site in Irvine, California. A plot of the resulting response spectra is shown in Figure 3-17.

Table 3-2. Example Calculation of S_{aMv} from S_{aM} for Site Class D Site in Irvine, CA. S_{MS} = 1.63 and C_v = 1.426 (interpolated value from ASCE/SEI 7-22 Table 11.9-1). F_{md} is from ASCE/SEI 7-22 Equations 11.9-6, 11.9-7, and 11.9-8

Period (seconds)	S_{aM} (g)	F_{md}	S_{aMv} (g)	ASCE/SEI 7-22 Equation # for S_{aMv}	Applicable Period Band for S_{aMv} Equation
0.00	0.708	1.20	0.547	11.9-1	$T_v \le 0.025$ sec [Note: 0.025 sec is not included in the standard 22 periods for S_{aM}; the S_{aM} = 0.722 was obtained by linear interpolation.]
0.01	0.713	1.20	0.550		
0.02	0.714	1.20	0.552		
0.025	0.722	1.20	0.558		
0.03	0.729	1.20	0.632	11.9-2	$0.025 < T_v \le 0.05$ sec
0.05	0.828	1.20	1.033		
0.075	1.037	1.20	1.294	11.9-3	$0.05 < T_v \le 0.10$ sec
0.10	1.238	1.20	1.544		
0.15	1.507	1.20	1.535	11.9-4	$0.10 < T_v \le 2.0$ sec
0.20	1.663	1.20	1.467		
0.25	1.758	1.203	1.383		
0.30	1.812	1.206	1.298		
0.40	1.783	1.213	1.101		
0.50	1.696	1.219	0.932		
0.75	1.366	1.234	0.605		
1.0	1.123	1.250	0.425		
1.5	0.784	1.253	0.242		
2.0	0.583	1.256	0.155		
3.0	0.370	1.261	0.147	11.9-5	$T_v > 2.0$ sec
4.0	0.258	1.267	0.102		
5.0	0.193	1.272	0.076		
7.5	0.116	1.286	0.045		
10	0.078	1.300	0.030		

In this example, the vertical response spectrum is greater than the horizontal response spectrum at short periods. This characteristic is common in high seismic regions at softer soil sites and is dictated by the value of C_v in ASCE/SEI 7-22 Table 11.9-1, where the value of C_v increases for larger values of S_{MS} and softer site classes.

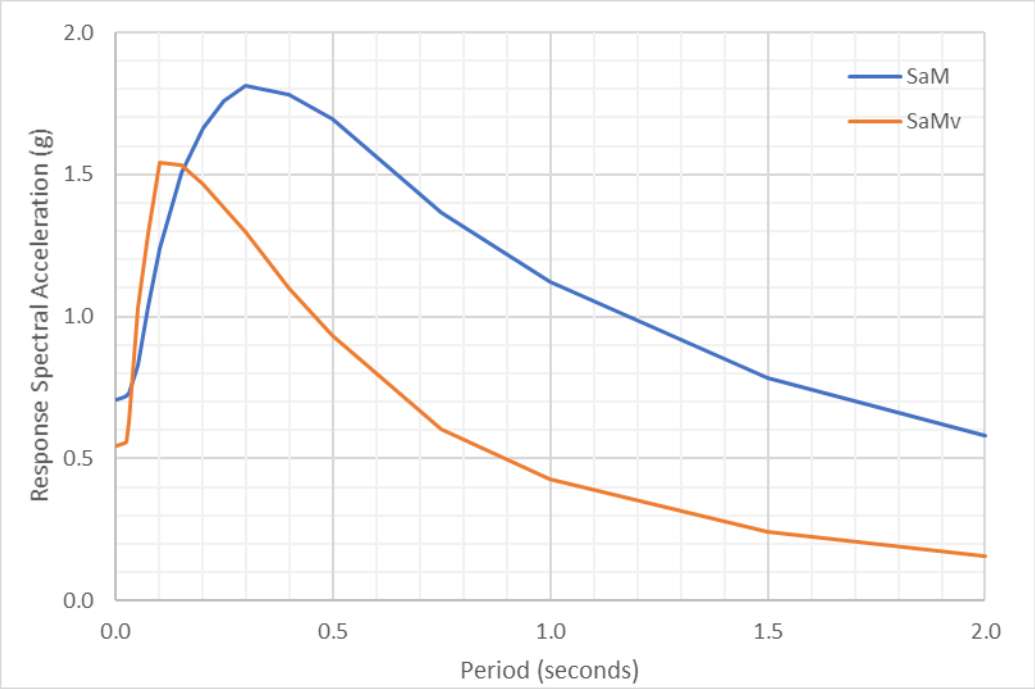

Figure 3-17. Horizontal (S_{aM}) and Vertical (S_{aMv}) MCE_R Response Spectra for Example Site in Irvine, CA (Site Class D)

3.4.3 Site Class When Shear Wave Velocity Data are Unavailable (ASCE/SEI 7-22 Section 20.3)

Unless a default site class is selected (see ASCE/SEI 7-22 Section 20.1 and Section 11.4.2.1), site class is determined from the average shear wave velocity ($\bar{v}_s$) in the upper 100 ft (30 m) at a site. When a shear wave velocity (V_s) survey is not performed to obtain the velocity, data required to compute $\bar{v}_s$, then one or more correlations between V_s and suitable geotechnical parameters must be used to compute a depth profile of V_s. Because of the uncertainty in these correlations, the value of $\bar{v}_s$ determined from the V_s profile must be multiplied by 1.3 and divided by 1.3. If the values of $\bar{v}_s$, 1.3 $\bar{v}_s$, and $\bar{v}_s/1.3$ result in different site classes, then the site class resulting in the larger value of S_{aM} shall be taken, and this determination shall be made at each spectral period. Detailed discussion on correlations is provided in the Commentary Section C20.3 of ASCE/SEI 7-22, which provides several references and general equations for correlations of V_s based on penetration resistance (e.g., SPT) and CPT data. [Note: Factors less than 1.3 can be used, provided they (1) were obtained from correlations derived for a specific local region, (2) show greater accuracy than global models, and (3) are approved by the local building official or Authority Having Jurisdiction.]

The following example illustrates the possible consequences when correlations are used to obtain $\bar{v}_s$. The same Irvine site used to construct the S_{aMv} values in Table 3-2 is selected. Assuming $\bar{v}_s$ of 850 ft/s (Site Class D) was estimated, then 1.3 $\bar{v}_s$ = 1,105 ft/s (Site Class CD) and $\bar{v}_s$ /1.3 = 654 ft/s (Site Class DE). The MPRS values of S_{aM} for each of these three site classes are presented in Table 3-3. The largest of the three S_{aM} values at each period is the final value.

Table 3-3. Example Calculation of S_{aM} for Irvine, CA Site when V_s Data are Not Available, and Correlation is Used to Estimate $\bar{v}_s$

Period (seconds)	S_{aM} (g) (Site Class D)	S_{aM} (g) (Site Class CD)	S_{aM} (g) (Site Class DE)	S_{aM} (g) (Final)
0.00	0.708	0.718	0.670	0.718
0.01	0.713	0.722	0.675	0.722
0.02	0.714	0.726	0.673	0.726
0.025[1]	**0.722**	**0.744**	**0.671**	**0.744**
0.03	0.729	0.763	0.668	0.763
0.05	0.828	0.904	0.736	0.904
0.075	1.037	1.142	0.927	1.142
0.10	1.238	1.346	1.122	1.346
0.15	1.507	1.608	1.344	1.608
0.20	1.663	1.736	1.511	1.736
0.25	1.758	1.781	1.671	1.781
0.30	1.812	1.779	1.770	1.812
0.40	1.783	1.663	1.810	1.810
0.50	1.696	1.515	1.779	1.779
0.75	1.366	1.162	1.508	1.508
1.0	1.123	0.912	1.313	1.313
1.5	0.784	0.594	1.004	1.004
2.0	0.583	0.426	0.795	0.795
3.0	0.370	0.267	0.517	0.517
4.0	0.258	0.188	0.356	0.356
5.0	0.193	0.143	0.263	0.263
7.5	0.116	0.089	0.153	0.153
10	0.078	0.061	0.099	0.099

[1]The 0.025-second period is not a period in the MPRS for horizontal components, but it is a period used to define two segments in the vertical component (ASCE/SEI 7-22 Equations 11.9-1 and 11.9-2).

Note that if a V_s survey was conducted at the site and a Site Class D was determined from the calculation of $\bar{v}_S$, then the S_{aM} would be between approximately 1 to 9% less than the final S_{aM} at short periods less than 0.3 sec, but it would be between 15 to 30% less for periods 1.0 sec and greater.

Also note in this example that if neither a V_s survey nor correlation is used to determine the $\bar{v}_S$ and hence the determination of the site class and S_{aM}, then the geotechnical engineer would be permitted to use the MCE_R spectral response accelerations from the most critical spectral response acceleration at each period of Site Class C, Site Class CD, and Site Class D (the default site conditions per ASCE/SEI 7-22 Section 11.4.2.1), unless the Authority Having Jurisdiction (AHJ) determines, based on geotechnical data, that Site Class DE, E, or F soils are present at the site. The AHJ, for example, may have geotechnical data from adjacent sites that the geotechnical consultant may not have for the site in question and thus may stipulate that these softer soils are present. Thus, if it can be demonstrated that the site does not fall into either Site Class DE, E, or F, then the default S_{aM} in this example would be between 15 to 30% less than the final S_{aM} in Table 3-3 for periods of 1.0 sec and greater, because the Site Class DE S_{aM} would be excluded from consideration.

3.5 References

ASCE (2005). "Minimum Design Loads for Buildings and Other Structures, ASCE/SEI 7-05," American Society of Civil Engineers, Structural Engineering Institute, Reston, VA.

Applied Technology Council (2020). "Procedures for developing multi-period response spectra at non-conterminous United States sites," FEMA P-2078 Report, Federal Emergency Management Agency.

BSSC (2004). "NEHRP Recommended Provisions for Seismic Regulations for New Buildings and Other Structures (FEMA 450), 2003 Edition," Building Seismic Safety Council, National Institute of Building Sciences, Washington, DC.

BSSC (2009). "NEHRP Recommended Seismic Provisions for New Buildings and Other Structures (FEMA P-750), 2009 Edition," Building Seismic Safety Council, National Institute of Building Sciences, Washington, DC.

BSSC (2019). "BSSC Project 17 final report: Development of next generation of seismic design value maps for the 2020 *NEHRP Provisions*," Building Seismic Safety Council, National Institute of Building Sciences, Washington, DC.

Crouse, C.B., Leyendecker, E.V., Somerville, P.G., Power, M., and Silva, W.J. (2006). "Development of seismic ground-motion criteria for the ASCE 7 standard," *Proceedings of the 8th U.S. National Conference on Earthquake Engineering*, San Francisco, CA.

FEMA (2017). "Hazus® Estimated Annualized Earthquake Losses for the United States," FEMA P-366, Federal Emergency Management Agency.

FEMA (2020). *Procedures for Developing Multi-Period Response Spectra at Non-Conterminous United States Sites*, FEMA P-2078, prepared by the Applied Technology Council for the Federal Emergency Management Agency.

Kircher & Associates (2015). "Investigation of an identified shortcoming in the seismic design procedures of ASCE 7-10 and development of recommended improvements for ASCE 7-16," prepared by Kircher & Associates for the Building Seismic Safety Council, National Institute of Building Sciences.

Klein, F.W. (2001). "Seismic Hazard in Hawaii: High Rate of Large Earthquakes and Probabilistic Ground-Motion Maps," *Bulletin of the Seismological Society of America*, 91(3):479.

Mueller, C.S., Frankel, A.D., Petersen, M.D., and Leyendecker, E.V. (2003). "Documentation for 2003 USGS Seismic Hazard Maps for Puerto Rico and the U.S. Virgin Islands," U.S. Geological Survey Open-File Report 03-379.

Mueller, C.S., Haller, K.M., Luco, N., Petersen, M.D., and Frankel, A.D. (2012). "Seismic hazard assessment for Guam and the Northern Mariana Islands," U.S. Geological Survey Open-File Report 2012–1015.

Petersen, M.D., Harmsen, S.C., Rukstales, K.S., Mueller, C.S., McNamara, D.E., Luco, N., & Walling, M. (2012). "Seismic hazard of American Samoa and neighboring South Pacific Islands—Methods, data, parameters, and results," U.S. Geological Survey Open-File Report 2012–1087.

Petersen, M.D., Shumway, A.M., Powers, P.M., Mueller, C.S., Moschetti, M.P., Frankel, A.D., Rezaeian, S., McNamara, D.E., Luco, N., Boyd, O.S., Rukstales, K.S., Jaiswal, K.S., Thompson, E.M., Hoover, S.M., Clayton, B.S., Field, E.H., & Zeng, Y. (2020). "The 2018 update of the US National Seismic Hazard Model: Overview of model and implications," *Earthquake Spectra*, 36(1), 5–41, Earthquake Engineering Research Institute, Oakland, CA.

Shahi, S.K., and Baker, J.W. (2014). "NGA-West2 models for ground motion directivity," *Earthquake Spectra*, v. 30, no. 3, p. 1285-1300.

Wesson, R.L., Boyd, O.S., Mueller, C.S., Bufe, C.G., Frankel, A.D., and Petersen, M.D. (2007). "Revision of time-Independent probabilistic seismic hazard maps for Alaska," U.S. Geological Survey Open-File Report 2007-1043.

Chapter 4: Reinforced Concrete Ductile Coupled Shear Wall System as a Distinct Seismic Force-Resisting System in ASCE/SEI 7-22

S.K. Ghosh[1] and Prabuddha Dasgupta[2]

A ductile coupled wall system of reinforced concrete is now defined in ACI 318-19 (ACI, 2019), and it is recognized as a distinct seismic force-resisting systems in ASCE/SEI 7-22 Table 12.2-1, Design Coefficients and Factors for Seismic Force-Resisting Systems. Three line items have been added to the table, featuring the ductile coupled wall system of reinforced concrete. The line items are under: A. Bearing Wall Systems, B. Building Frame Systems, and D. Dual Systems with Special Moment Frames. R = 8, C_d = 8, and Ω_0 = 2.5 are the design coefficients in all the line items. The height limits are the same as for corresponding uncoupled isolated wall systems. Several important changes made in ACI 318-19 for the design and detailing of special structural walls were implemented in the design of prototypes for the FEMA P695 study supporting the above values.

A few words about terminology may be in order here. "Reinforced Concrete Ductile Coupled Shear Wall System" is the terminology used in the title of this chapter. An effort has been made to use this terminology consistently throughout the chapter, except that "reinforced concrete" is typically dropped as being redundant or understood. The whole chapter, after all, is about a reinforced concrete system. There are, however, a few obstacles to attaining total consistency. The system discussed in this chapter is defined in ACI 318-19 Section 2.3 as follows: "structural wall, ductile coupled – a seismic-force-resisting-system complying with 18.10.9." Several aspects of this definition ought to be noted. First, "reinforced concrete" is not mentioned; it is understood. Second, shear walls are called structural walls in ACI 318-19. Third and most importantly, a wall, which is a structural member or element, is defined as a system; this is lax usage of terms. Finally, and this may not be important, "seismic-force-resisting-system" in the definition is "seismic force-resisting system" in ASCE/SEI 7-22 as well as in this chapter. In ASCE/SEI 7-22 Section 18.10.9 itself, the terminology used is Ductile Coupled Walls. Where ACI 318-19 is referenced directly, the terminology used here is Ductile Coupled Structural (Shear) Wall System. Where ACI 318-19 text is essentially reproduced (with or without quotation marks), terminology used by ACI Committee 318 is left alone. Finally, in ASCE/SEI 7-22 Table 12.2-1, the walls providing seismic force-resistance as part of the

[1] S.K Ghosh, Ph.D., S.K. Ghosh Associates
[2] Prabuddha Dasgupta, Ph.D., P.E., S.K. Ghosh Associates

structural system under discussion here are called Reinforced Concrete Walls. In portions of the table reproduced in this chapter, “shear” has not been inserted before “walls.”

In addition to the *2020 Provisions*, the following documents are either referred to directly or may serve as useful design aids.

Useful Design Aid Resources

ACI (2019). *Building Code Requirements for Structural Concrete,* ACI 318-19 and *Commentary*, ACI 318R-19, American Concrete Institute, Country Club Hills, MI.

ASCE (2017). *Minimum Design Loads and Associated Criteria for Buildings and Other Structures*, ASCE/SEI 7-16, American Society of Civil Engineers, Reston, VA.

CSA Group (2014). *Design of Concrete Structures*, A 23.3.14, Mississanga, Ontario, Canada.

FEMA (2009). *Quantification of Building Seismic Performance Factors*, FEMA P695, prepared by the Applied Technology Council for the Federal Emergency Management Agency, Washington, D.C., June.

Los Angeles Tall Buildings Structural Design Council (2017). *An Alternative Procedure for Seismic Analysis and Design of Tall Buildings Located in the Los Angeles Region,* 2017 Edition, Los Angeles, June.

Standards New Zealand (2006). *Concrete Structures Standard*, NZS 3101. 1&2: 2006, Wellington, New Zealand.

4.1 Introduction

Functional and often structural requirements make the use of shear walls desirable in many buildings. Functionally, shear walls are useful in buildings because they serve as partitions between spaces. Structurally, they make buildings laterally stiff, particularly when used interactively with moment frames, thereby helping to keep lateral deflections within tolerable limits. Often, such walls are pierced by numerous openings for windows, doors, and other purposes. Two or more walls separated by vertical rows of openings, with beams at every floor level between the vertically arranged openings, are referred to as coupled shear walls. When a coupled shear wall system is subject to lateral loads due to wind or earthquake forces, shear forces generated at the ends of the coupling beams accumulate into a tensile force in one of the coupled wall piers and into a compression force in the other wall pier. The couple, due to these tension and compression forces, resists a part of the overturning moment at the base of the wall system, with the remainder of the overturning moment being resisted by the wall piers themselves (Figure 4-1). The ratio of the overturning moment resisted by the tension-compression couple to the total overturning moment at the base of the coupled wall system is often referred to as the degree of coupling. The shorter and deeper the coupling beams, the higher the degree of coupling. When the degree of coupling is very low (25% or lower), the two wall piers tend to behave like isolated walls, and when the degree of

coupling is very high (75% or higher), the entire coupled wall system tends to behave like a shear wall with openings. It should be noted, however, that as inelastic displacements develop in the coupling beams, the degree of coupling tends to lose its significance.

A coupled shear wall system can be designed such that a considerable amount of earthquake energy is dissipated by shear yielding in coupling beams with low span-to-depth ratios or flexural yielding at the ends of coupling beams with higher span-to-depth ratios before flexural hinges form (typically) at the bases of the wall piers (assuming they are slender, with height-to-length ratios larger than or equal to two). Although such coupled wall systems are highly suitable as the seismic force-resisting systems of multistory buildings, they were not recognized as distinct entities in Table 12.2-1 of ASCE/SEI 7-16. Therefore, such systems needed to be designed using *R*-values that essentially ignore the considerable benefits of having the coupling beams, which can dissipate much of the energy generated by earthquake excitation. This chapter reports on a successful effort to address this situation.

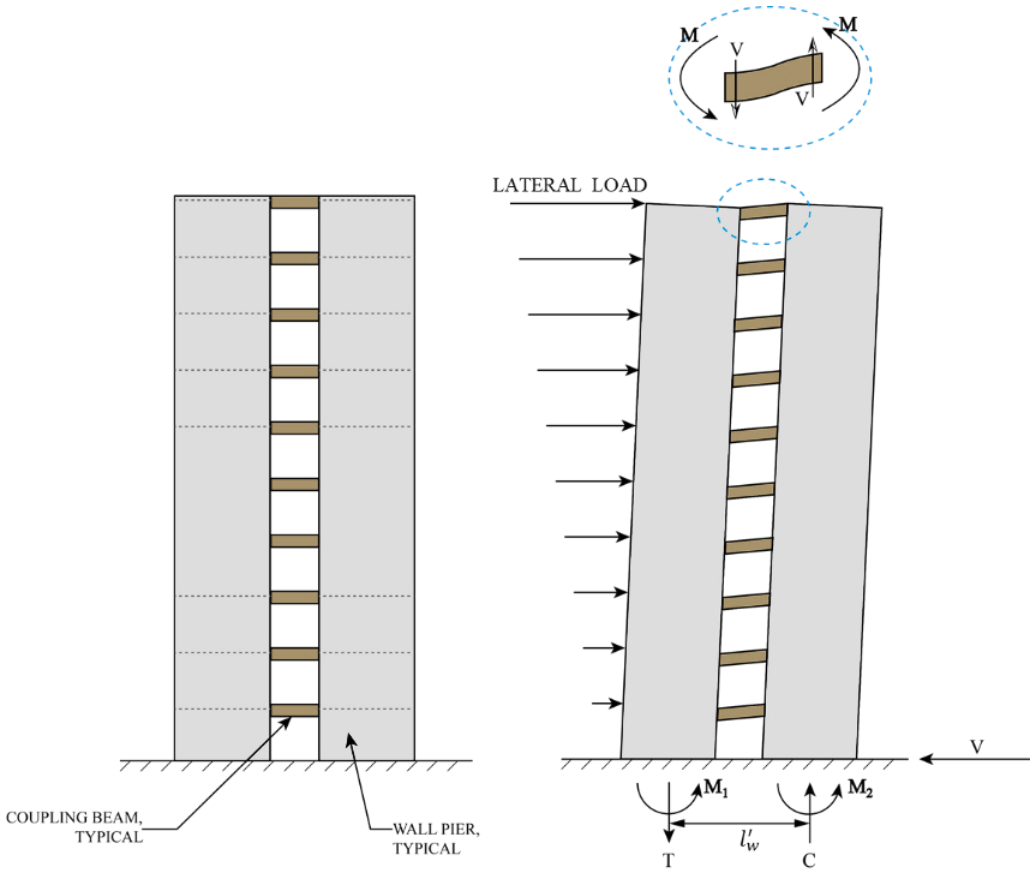

Figure 4-1. A Coupled Shear Wall System

4.2 Ductile Coupled Structural (Shear) Wall System of ACI 318-19

To quote from Bertero (1977), “Use of coupled walls in seismic-resistant design seems to have great potential. To realize this potential, it would be necessary to prove that it is possible to design and construct “ductile coupling girders” and “ductile walls” that can SUPPLY the required strength, stiffness, and stability and dissipate significant amounts of energy through stable hysteretic behavior of their critical regions.”

Thus, the discussion needs to focus not on just coupled walls but **ductile coupled walls** consisting of **ductile shear walls** and **ductile coupling beams**.

In the 2019 edition of ACI 318, a new system definition has been created to recognize the Ductile Coupled Structural (Shear) Wall (DCSW) system. The shear walls in such a system must be special structural walls in conformance with ACI 318-19 Section 18.10, including the proportioning requirements of Section 18.10.9, and the coupling beams must comply with the detailing requirements in ACI 318-19 Section 18.10.7.

The objective of the ductile coupled shear wall system is for the majority of energy dissipation to occur in the coupling beams. This is analogous to strong column weak beam behavior in moment frames. Studies were conducted at Magnusson Klemencic Associates (MKA) to identify system characteristics that lead to coupling beam energy dissipation of no less than 80% of total system energy dissipation under MCE ground motions. In these studies, nonlinear response history analyses were conducted using spectrally matched ground motion records on a variety of coupled shear wall archetypes. Archetypes ranged from 5 to 50 stories in height and considered a range of longitudinal reinforcement ratios in the coupling beams as well as the shear walls. Results of these analyses are presented in Figure 4-2. The x-axis represents the aspect ratio (clear span-to-total depth) of the coupling beams, with D designating a diagonally reinforced beam design and M designating a special moment frame beam design. For example, D4 is a diagonally reinforced coupling beam with an aspect ratio of 4 and M4 is a coupling beam detailed as a special moment frame beam with an aspect ratio of 4. The y-axis is the percentage of total system energy dissipation that occurs in the coupling beams alone. The resulting trend shows an energy “dome” with coupling beams dissipating the majority of system energy between aspect ratios of 2 and 5.

The primary characteristics of such a system were found to be governed by geometry. Squat walls were found to be too stiff to allow sufficient story drift for coupling beams to become inelastic. For this reason, shear walls in the Ductile Coupled Shear Wall (DCSW) system need to have a total height to length aspect ratio of no less than 2.0. Squat coupling beams were found to over-couple the seismic force-resisting system and lead to significant energy dissipation in the shear walls. As such, coupling beams in DCSW systems need to have clear span to total depth aspect ratio of no less than 2.0 in all cases. Very slender coupling beams, designated as having an aspect ratio greater than 5.0, are not stiff enough to contribute sufficient hysteretic energy dissipation and are allowed in no more than 10% of the levels of the building. Lastly, coupling beams conforming to these geometric constraints are required to be present at all levels in order to dissipate the intended amount of

energy. It has been clarified in ACI 318-19 that longitudinal reinforcement in coupling beams detailed as special moment frame beams and diagonal reinforcement in diagonally reinforced coupling beams must develop 1.25 times f_y of the reinforcement at each end. This last requirement is intended to preclude the use of fixed-pinned coupling beams that are the outcome where insufficient length exists to adequately develop the coupling beam reinforcement into the adjacent shear wall.

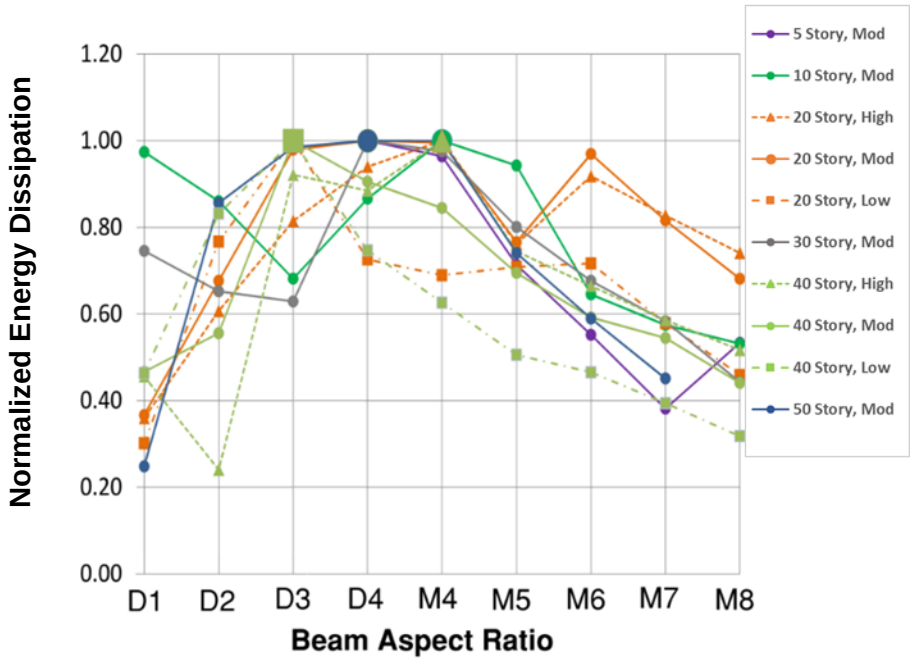

Figure 4-2. Energy Dissipation in Coupling Beams

Plotted along the y-axis of Figure 4-2 is energy dissipated by a coupling beam, normalized with respect to the energy dissipated by a coupling beam with an aspect ratio of 4 in a 40-story building. In Figure 4-2 legend, "High," "Mod(erate)," and "Low" refer to 100%, 75%, and 50%, respectively, of the amount of reinforcement needed to generate $V_n = 10\sqrt{f_c'}A_{cw}$ (see ACI 318-19 Equation 18.10.7.4). For coupling beams detailed as special moment frame beams, "High," "Mod," and "Low" mean 100%, 75%, and 50%, respectively, of the longitudinal reinforcement that would generate an M_{pr} for which $2M_{pr}/\ell_n = 10\sqrt{f_c'}A_{cw}$.

As noted earlier, the requirements of the Ductile Coupled Structural (shear) Wall system are in addition to those required for Special Structural (shear) Walls and Coupling Beams. The final language of the DCSW definition in ACI 318-19 reflects the input of ACI 318 Subcommittee H as well as BSSC PUC Issue Team (IT) 4 on Shear Walls.

Also as noted earlier, ACI 318-19 Section 2.3 – Terminology defines structural wall, ductile coupled as a seismic force-resisting-system complying with Section 18.10.9.

18.10.9 *Ductile coupled walls*

18.10.9.1 Ductile coupled walls shall satisfy the requirements of this section.

18.10.9.2 Individual walls shall satisfy $h_{wcs}/\ell_w \geq 2$ and the applicable provisions of 18.10 for special structural walls.

18.10.9.3 Coupling beams shall satisfy 18.10.7 and (a) through (c) in the direction considered.

(a) Coupling beams shall have $\ell_n/h \geq 2$ at all levels of the building.

(b) All coupling beams at a floor level shall have $\ell_n/h \leq 5$ in at least 90 percent of the levels of the building.

(c) The requirements of 18.10.2.5 shall be satisfied at both ends of all coupling beams.

4.3 Ductile Coupled Structural (Shear) Wall System in ASCE/SEI 7-22

Issue Team (IT) 4 of the Provisions Update Committee (PUC) of the Building Seismic Safety Council (BSSC) developed a proposal that led to the addition of three line items to ASCE/SEI 7-22 Table 12.2-1, Design Coefficients and Factors for Seismic Force-Resisting Systems, featuring the reinforced concrete ductile coupled shear wall system (Table 4-1). The line items are under: A. Bearing Wall Systems, B. Building Frame Systems, and D. Dual Systems with Special Moment Frames.

Table 4-1. Addition of Reinforced Concrete Ductile Coupled Walls to ASCE/SEI 7-16 Table 12.2-1

Seismic Force-Resisting System	ASCE/SEI 7 Section Where Detailing Requirements Are Specified	*R*	Ω_0	C_d	Structural System Limitations Including Structural Height, h_n (ft) Limits[d]				
					Seismic Design Category				
					B	C	D	E	F
A. BEARING WALL SYSTEMS									
1. Special reinforced concrete shear walls[g,h]	14.2	5	2½	5	NL	NL	160	160	100
2. Reinforced concrete ductile coupled walls	14.2	8	2½	8	NL	NL	160	160	100
3. Ordinary reinforced concrete shear walls[g]	14.2	4	2½	4	NL	NL	NP	NP	NP
…									

Table 4-1. Addition of Reinforced Concrete Ductile Coupled Walls to ASCE/SEI 7-16 Table 12.2-1 (Continued)

Seismic Force-Resisting System	ASCE/SEI 7 Section Where Detailing Requirements Are Specified	*R*	Ω_0	C_d	Structural System Limitations Including Structural Height, h_n (ft) Limits[d]				
					Seismic Design Category				
					B	C	D	E	F
B. BUILDING FRAME SYSTEMS									
4. Special reinforced concrete shear walls[g,h]	14.2	6	2½	5	NL	NL	160	160	100
5. Reinforced concrete ductile coupled walls	14.2	8	2½	8	NL	NL	160	160	100
6. Ordinary reinforced concrete shear walls[g]	14.2	5	2½	4½	NL	NL	NP	NP	NP
…									
D. DUAL SYSTEMS WITH SPECIAL MOMENT FRAMES…									
7. Special reinforced concrete shear walls[g,h]	14.2	7	2½	5½	NL	NL	NL	NL	NL
8. Reinforced concrete ductile coupled walls	14.2	8	2½	8	NL	NL	NL	NL	NL
9. Ordinary reinforced concrete shear walls[g]	14.2	6	2½	5	NL	NL	NP	NP	NP
…									

Based on a FEMA P695 study, $R = 8$, $C_d = 8$, and $\Omega_o = 2.5$ have been proposed in all the line items. The height limits are the same as for corresponding uncoupled isolated wall systems. It is possible to increase the 160-ft height limit to 240 ft for buildings without significant torsion because ASCE/SEI 7-22 Section 12.2.5.4 has been made applicable to these systems. A minimum height limit of 60 ft has been imposed on seismic force-resisting systems featuring the reinforced concrete ductile coupled walls because, in shorter buildings, there may not be enough coupling beams to absorb sufficient energy to merit an *R*-value of 8.

4.4 FEMA P695 Studies Involving Ductile Coupled Structural (Shear) Walls

The proposed response modification factors for seismic force-resisting systems featuring reinforced concrete ductile coupled shear walls were validated (Tauberg et al. 2019) using the FEMA P695 methodology (FEMA, 2009). A series of 37 ductile coupled shear wall buildings, as summarized in Table 4-2, were designed using a range of variables expected to influence the collapse margin ratio, with primary variables of building height (i.e., 6, 8, 12, 18, 24, and 30 stories), wall cross section (i.e., planar and flanged walls), coupling beam aspect ratio (ℓ_n/h) ranging from 2.0 to 5.0, and coupling beam reinforcement arrangement (i.e., diagonally and conventionally reinforced). The period domain in Table 4-2 is defined by the number of stories.

There have been four significant ACI 318-19 code changes, all adopted in the FEMA P695 study (Tauberg et al. 2019), to address the flexural-compression wall failure issue.

5. 18.10.3.1 (shear amplification) - would typically require design shear (required shear strength) V_u to be amplified by a factor of up to 3 (similar to New Zealand, Canada).
6. 18.10.6.4 - requires improved wall boundary and wall web detailing, i.e, overlapping hoops if the boundary zone dimensions exceed 2:1, crossties with 135-135 degree hooks on both ends, and 135-135 degree crossties on web vertical bars.
7. 18.10.6.2(b) (Check on mean top-of-wall drift capacity at 20% loss of lateral strength) - requires a low probability of lateral strength loss at MCE level hazard, and
8. 18.10.2.4 - Minimum wall boundary longitudinal reinforcement, to limit the potential of brittle tension failures for walls that are lightly-reinforced.

For details on these important changes, reference can be made to Ghosh, Taylor (2021a, 2021b).

The range of variables was chosen considering those used to define a Ductile Coupled Structural (Shear) Wall system in ACI 318-19. The resulting designs have the minimum wall area (length and thickness) required, which is governed by shear amplification and the requirement that walls sharing a common shear force not exceed a shear stress of $8\sqrt{f'_c}A_{cv}$. Typical floor plans and a wall elevation view are presented in Figure 4-3.

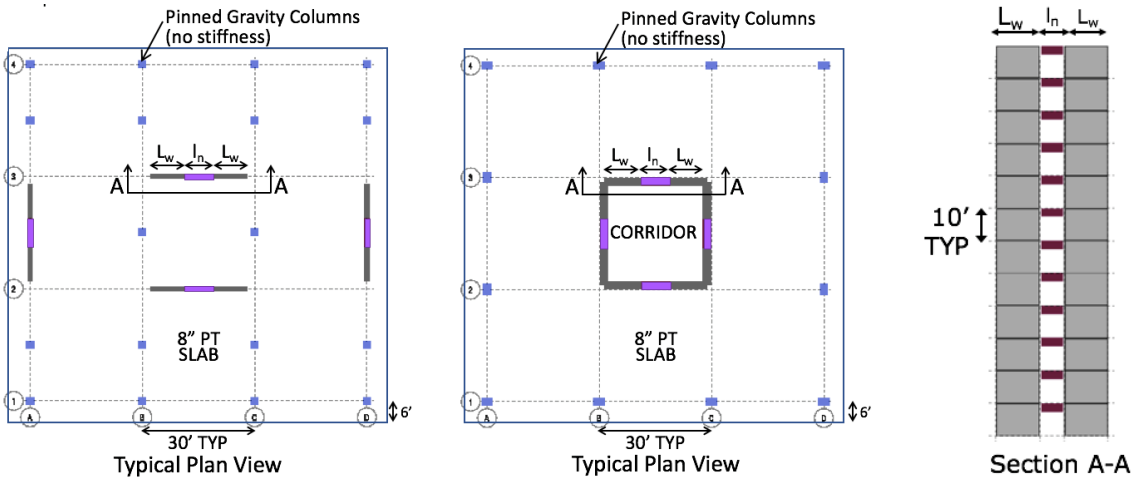

(a) Planar Walls (6, 8, 12 Story) (b) Flanged Walls (18, 24, 30 Story) (c) Elevation View

Figure 4-3. Archetype Floor Plans and Typical Wall Elevation View

Table 4-2. Coupled Wall Archetype Design Information

Performance Group Summary					
Group No.	**Grouping Criteria**				**Number of Archetypes**
	Basic Configuration	**Design Load Level**		**Period Domain**	
		Gravity	**Seismic**		
PG-1	Planar walls, diagonally reinforced coupling beams with ℓ_n/h = 2.0,2.4, 3.0, 3.3	Typical	SDC D_{max}	Short	9 (6, 8, 12 story)
PG-2	Planar walls, conventional reinforced coupling beams with ℓ_n/h = 3.3, 4.0, 5.0	Typical	SDC D_{max}	Short	7 (6, 8, 12 story)
PG-3	Flanged walls, diagonally reinforced coupling beams with ℓ_n/h = 2.0,2.4, 3.0, 3.3	Typical	SDC D_{max}	Short	4 (18 story)
PG-4				Long	8 (24 and 30 story)
PG-5	Flanged walls, conventional reinforced coupling beams with ℓ_n/h = 3.3, 4.0, 5.0	Typical	SDC D_{max}	Short	3 (18 story)
PG-6				Long	6 (24 and 30 story)

The designs were for Risk Category II structures with an importance factor I_e = 1.0. It incorporated provisions of ASCE/SEI 7-16 and ACI 318-19, as mentioned earlier, as well as the seismic design parameters specified in FEMA P695 (importance factor, redundancy factor, and site class and spectral values). The redundancy factor ρ was taken equal to 1.0 since the use of a larger value would increase seismic design forces (and strengths) and produce more conservative designs. The seismic spectral acceleration values used are summarized below for seismic hazard D_{max} as specified in FEMA P695.

S_S = 1.5g F_a = 1.0 S_{DS} = 1.00 g

S_1 = 0.6g F_v = 1.5 S_{D1} = 0.60g

Seismic design forces were determined using the Modal Response Spectrum Analysis (MRSA) method of ASCE/SEI 7, subject to scaling the base shear to 100% of the Equivalent Lateral Force base shear of ASCE/SEI 7-16 for a period $T = C_u T_a$. Modal damping ratio was assumed to be 5 percent, and the Complete Quadratic Combination (CQC) method was used to combine modal responses. The story heights were taken equal to 10 feet for all designs. Building stories, the fundamental period T_1, the design period $T = C_u T_a$, the design coefficient C_s, and the design base shear V are summarized in Table 4-3 for a subset of six of the 37 archetype designs in Table 4-2. In the archetype numbering, 6H, 8H, 12H, 18H, 24H, and 30H indicate total heights of 60, 80, 120, 180, 240, and 300 ft, respectively; DR indicates diagonally reinforced; and the last number, 2 or 3, indicates the clear span to total depth ratio of the coupling beams.

Table 4-3. Coupled Wall Archetype Design Information

Archetype	Total Height	T_1 (s)	$T = C_u T_a$ (s)	V (kips)	DOC	Wall Pier Dimensions	$P_{u,1}$[1] $/A_g f'_c$	$P_{u,2}$[2] $/A_g f'_c$	$P_{u,3}$[3] $/A_s f_y$
6H-DR-2 (planar wall)	60’	0.83	0.604	1,062 C_s = 0.124	0.60	l_w = 8.0’ $t_{w,L1\text{-}4}$ = 14” $t_{w,L5\text{-}6}$ = 10”	0.16	0.28	-0.31
8H-DR-3 (planar wall)	80’	1.27	0.749	1,201 C_s = 0.100	0.61	l_w = 8.5’ $t_{w,L1\text{-}4}$ = 14” $t_{w,L5}$ = 12” $t_{w,L6\text{-}8}$ = 10”	0.14	0.27	-0.27
12H-DR-3 (planar wall)	120’	2.14	1.015	1,360 C_s = 0.074	0.66	l_w = 9.25’ $t_{w,L1\text{-}4}$ = 16” $t_{w,L5\text{-}12}$ = 12”	0.13	0.30	-0.33
18H-DR-3 (flanged wall)	180’	3.14	1.376	1,489.5 C_s = 0.0545	0.66	l_w = 9.0’ $t_{w,L1\text{-}5}$ = 24” $t_{w,L6\text{-}8}$ = 20” $t_{w,L5\text{-}12}$ = 16”	0.13	0.19	-0.07
24H-DR-3 (flanged wall)	240’	3.39	1.707	1,654 C_s = 0.044	0.69	l_w = 10.0’ $t_{w,L1\text{-}18}$ = 24” $t_{w,L19\text{-}24}$ = 18”	0.17	0.23	-0.03
30H-DR-3 (flanged wall)	300’	3.62	2.018	2,112 C_s = 0.044	0.68	l_w = 11.25’ $t_{w,L1\text{-}10}$ = 30” $t_{w,L11\text{-}20}$ = 24” $t_{w,L21\text{-}30}$ = 18”	0.13	0.20	-0.06

[1] $P_{u,1}$ is the gravity axial stress under load combination 1.2D+1.6L.

[2] $P_{u,2}$ is the maximum axial stress under load combination (1.2+0.2S_{DS})D+0.5L+1.0E.

[3] $P_{u,3}$ is the minimum (net tensile) axial stress under load combination (0.9-0.2S_{DS})D+1.0E.

It should be noted that incorporating wall shear amplification in the design was necessary because preliminary analysis results using $R = C_d = 8$ and with walls designed in compliance with ACI 318-14

shear provisions did not meet the FEMA P695 acceptability criteria due to a high number of shear failures experienced during incremental dynamic analysis. The wall shear amplification requirement per the new code provision of ACI 318-19 amplifies the code level shear force (V_u) by a flexural overstrength factor (Ω_v) and a dynamic shear amplification factor (ω_v) that accounts for higher mode effects. The dynamic shear amplification factor (ω_v) depends on the number of stories (n_s). The overstrength factor (Ω_v) is the ratio of probable moment strength M_{pr} to code required strength M_u, which shall not be taken less than 1.5 per ACI 318-19. In this study, the ratio of M_{pr} to M_u was set equal to 1.5 for all designs so that the walls would not be overdesigned for shear strength and represent the governing case for collapse analysis.

Two-dimensional nonlinear models were created for each design using the structural analysis software Open Systems for Earthquake Engineering Simulation (OpenSees). Nonlinear static pushover (NSP) analyses were used to compute the system overstrength factor (Ω_0) and the period-based ductility (μ_T), while incremental dynamic analyses (IDA) were performed in accordance with FEMA P695 to assess collapse. Per FEMA P695, the period-based ductility (μ_T) is obtained by dividing the ultimate roof displacement (δ_u) by the effective yield displacement ($\delta_{y,eff}$). Effective yield displacement is defined by Eq. (5-3) in (Tauberg et al. 2019).

The dynamic analyses were conducted at Design Earthquake (DE) and Maximum Considered Earthquake (MCE) hazard levels, as well as at ground motion intensities representative of the collapse capacity of each design. For the IDAs, a set of twenty-two pairs of far-field horizontal ground motion records of FEMA P695 were used. The collapse capacity was determined by incrementally increasing the intensity of the 22 pairs of scaled far-field ground motions of FEMA P695 Appendix A until just less than half of the records caused collapse of the archetypical building as represented by the established failure modes of the model.

To assess collapse, three primary failure modes were considered to capture lateral strength loss and failure:

1. flexural failure (crushing of concrete, buckling of reinforcing bar, tensile fracture of longitudinal reinforcement) was assessed using a statistical drift capacity model developed based on an extensive database of wall tests,
2. shear failure (diagonal tension/compression) assessment was based on the relationship between wall shear force and tensile strain of wall longitudinal reinforcement, following Los Angeles Tall Buildings Seismic Design Council or LATBSDC (2017) recommendations, and
3. axial failure was estimated using a shear friction model.

It may be natural to wonder why axial failure is associated with shear friction. Explanation is provided in the following excerpt from (Tauberg et al., 2019). For references cited and the figure mentioned in the excerpt, refer to (Tauberg et al., 2019); the reference listings and the table are not reproduced here.

> "Wall axial failure is defined using the lateral drift capacity model proposed by Wallace et al. (2008) which defines the lateral drift capacity at axial failure using an assumed critical shear

crack angle and a shear friction model as shown in Figure 4.4. The initial model for the limit state of axial collapse is based on the column model proposed by Elwood and Moehle (2003, 2005), and modified for application to walls (Wallace et al., 2008). The model is based on equilibrium for an assumed shear friction relation, assuming the critical crack plane extends along the main diagonal of the wall pier (or over a single story). Axial failure results along the critical crack plane when the shear demand exceeds the shear friction capacity."

For the study, collapse was defined as being associated with either flexure or shear, meaning that the axial failure model did not govern because the lateral drift values at axial failure (generally greater than 5%) exceeded drifts at which flexural failure occurred; the axial failure model also has not been verified (although collapse of buildings with reinforced concrete walls has rarely been reported following strong earthquakes). Because amplified wall shear demands were used in design, shear failures were mostly suppressed, and flexure-related collapse was typically defined by the drift capacity model for most archetypes. Overall, the criteria used for collapse assessment in the study were conservative since the failure models predict the onset of strength loss (a 20% drop in lateral strength) and not necessarily collapse. The approach is conservative because loss of axial load carrying capacity typically does not occur until lateral strength drops to near zero. In some studies, axial failure has been assumed to occur at a specified roof drift ratio, which has been typically defined as 4 to 5% (NIST GCR-10-917-8), whereas, in this study, the conservative approach used to assess collapse resulted in drift ratios at failure that were typically about 3%.

Results from the incremental dynamic analyses are used to obtain the median collapse capacity intensity (S_{CT}) and the collapse margin ratio (CMR) for each archetype. The median collapse intensity (S_{CT}) is established by determining the 5%-damped spectral acceleration at which half of the ground motions cause the structure to collapse using the project failure criteria, i.e., with the drift capacity model or the shear failure model for this study. The collapse margin ratio is then computed to characterize the collapse safety of the archetype as the ratio of the median collapse spectral intensity S_{CT} to S_{MT}, where S_{MT} is the intensity of the Maximum Considered Earthquake (MCE) obtained from the response spectrum of MCE ground motions at the fundamental period (T) of the building.

$$\text{CMR} = S_{CT}/S_{MT}$$

$$\text{ACMR} = \text{SSF} \times \text{CMR}$$

The collapse margin ratio is adjusted by the period and ductility dependent spectral shape factors (SSFs) prescribed in FEMA P695 Section 7.2.2 in order to account for the effects of the frequency content (spectral shape) of the ground motion record set. For this study, the acceptable adjusted collapse margin ratios (ACMRs) were established as 1.96 and 1.56 for the 10% and 20% collapse probability scenarios, respectively. Once results from incremental dynamic analyses are obtained, each archetype is assessed for conformance with the FEMA P695 acceptability criteria by comparing its ACMR to the acceptable ACMR based on the system collapse uncertainty (β_{TOT}). For a given archetype, if the building ACMR is greater than the acceptable ACMR at 20% collapse probability ($ACMR_{20\%}$), then the archetype passes the performance criteria. The average of the ACMRs of the

archetypes in each performance group must also be compared to the acceptable ACMR at 10% collapse probability ($ACMR_{10\%}$) to assess whether the performance group as a whole passes the FEMA P695 performance criteria.

A summary of the analysis results for all archetypes is presented in Table 4-4. The results show that all 6-story to 30-story archetypes pass the FEMA P695 collapse acceptability criteria, thus validating the use of R = 8 for ductile coupled shear wall systems that are designed in conformance with ASCE/SEI 7-16 and ACI 318-19 provisions.

Table 4-4. Summary of Collapse Results for Ductile RC Coupled Wall Archetypes

Archetype ID	Pushover Results		IDA Results			Acceptability			
	Static Ω [a]	μ_T [b]	S_{MT} [c] [T]	S_{CT} [d] [T]	CMR [e]	SSF [f]	ACMR [g]	Accep. ACMR	Pass /Fail
6H-DR-2.0	2.28	7.54	1.49	2.68	1.80	1.35	2.42	1.56	Pass
8H-DR-2.0	2.11	5.43	1.20	1.90	1.58	1.29	2.04		Pass
8H-DR-2.4	2.09	6.06		1.95	1.62	1.32	2.13		Pass
8H-DR-3.0	2.25	5.26		1.95	1.62	1.29	2.08		Pass
8H-DR-3.3	2.12	5.60		1.95	1.62	1.30	2.10		Pass
Mean:	**2.17**	**5.98**				**Mean:**	**2.16**	**1.96**	**Pass**
6H-CR-5.0	1.73	7.97	1.49	2.55	1.71	1.36	2.32	1.56	Pass
8H-CR-3.3	1.63	8.03	1.20	1.85	1.54	1.38	2.23		Pass
8H-CR-4.0	1.59	7.93		1.85	1.54	1.38	2.29		Pass
8H-CR-5.0	1.45	7.57		1.85	1.54	1.37	2.22		Pass
Mean:	**1.60**	**7.87**				**Mean:**	**2.27**	**1.96**	**Pass**
12H-DR-2.0	1.36	6.65	0.89	1.33	1.50	1.41	2.12	1.56	Pass
12H-DR-2.4	1.40	6.07		1.33	1.50	1.39	2.08		Pass
12H-DR-3.0	1.54	5.50		1.39	1.57	1.36	2.14		Pass
12H-DR-3.3	1.59	6.15		1.39	1.57	1.39	2.18		Pass
Mean:	**1.47**	**6.09**				**Mean:**	**2.13**	**1.96**	**Pass**
12H-CR-3.3	1.35	8.06	0.89	1.22	1.38	1.46	2.01	1.56	Pass
12H-CR-4.0	1.36	7.76		1.29	1.46	1.46	2.13		Pass
12H-CR-5.0	1.31	7.71		1.29	1.46	1.46	2.12		Pass
Mean:	**1.34**	**7.84**				**Mean:**	**2.09**	**1.96**	**Pass**
18H-DR-2.0	2.06	6.24	0.65	0.97	1.48	1.49	2.21	1.56	Pass
18H-DR-2.4	2.01	5.35		0.97	1.48	1.44	2.14		Pass
18H-DR-3.0	1.98	5.11		1.02	1.55	1.43	2.21		Pass
18H-DR-3.3	2.04	4.40		1.02	1.55	1.38	2.15		Pass
Mean:	**2.02**	5.28				**Mean:**	**2.18**	**1.96**	**Pass**

Table 4-4. Summary of Collapse Results for Ductile RC Coupled Wall Archetypes (Continued)

Archetype ID	Pushover Results		IDA Results			Acceptability			
	Static Ω [a]	μ_T [b]	S_{MT} [c] [T]	S_{CT} [d] [T]	CMR [e]	SSF [f]	ACMR [g]	Accep. ACMR	Pass /Fail
18H-CR-3.3	1.59	6.09	0.65	0.91	1.39	1.48	2.06	1.56	Pass
18H-CR-4.0	1.58	5.85		0.97	1.48	1.47	2.18		Pass
18H-CR-5.0	1.65	5.42		0.97	1.48	1.44	2.14		Pass
Mean:	**1.61**	5.79				**Mean:**	**2.13**	**1.96**	**Pass**
24H-DR-2.0	1.63	11.94	0.53	0.76	1.443	1.61	2.32	1.56	Pass
24H-DR-2.4	1.65	9.70		0.76	1.443	1.61	2.32		Pass
24H-DR-3.0	1.80	7.10		0.77	1.455	1.57	2.28		Pass
24H-DR-3.3	1.83	7.07		0.77	1.455	1.57	2.28		Pass
Mean:	**1.73**	8.95				**Mean:**	**2.30**	**1.96**	**Pass**
24H-CR-3.3	1.390	10.04	0.53	0.75	1.43	1.61	2.30	1.56	Pass
24H-CR-4.0	1.391	9.40		0.75	1.43	1.61	2.30		Pass
24H-CR-5.0	1.513	8.16		0.76	1.44	1.61	2.32		Pass
Mean:	**1.43**	9.20				**Mean:**	**2.31**	**1.96**	**Pass**
30H-DR-2.0	1.21	14.61	0.45	0.79	1.77	1.61	2.85	1.56	Pass
30H-DR-2.4	1.25	13.66		0.79	1.77	1.61	2.85		Pass
30H-DR-3.0	1.43	10.30		0.82	1.84	1.61	2.96		Pass
30H-DR-3.3	1.62	8.32		0.82	1.84	1.61	2.96		Pass
Mean:	**1.38**	11.72				**Mean:**	**2.91**	**1.96**	**Pass**
30H-CR-3.3	1.24	14.44	0.45	0.76	1.70	1.61	2.74	1.56	Pass
30H-CR-4.0	1.29	10.13		0.76	1.70	1.61	2.74		Pass
30H-CR-5.0	1.44	10.03		0.75	1.68	1.61	2.71		Pass
Mean:	**1.32**	11.53				**Mean:**	**2.73**	**1.96**	**Pass**

Note:

a) Ω : Overstrength factor
b) μ_T : Period-based Ductility
c) S_{MT}: Intensity of the Maximum Considered Earthquake (MCE)
d) S_{CT}: Medial Collapse Capacity Intensity
e) CMR: Collapse Margin Ratio
f) SSF: Spectral Shape Factors
g) ACMR: Adjusted Collapse Margin Ratio

The C_d factor for the Reinforced Concrete Ductile Coupled Shear Wall System was assessed using the ratio of a median value of nonlinear inelastic roof drifts (δ) from 44 records at DE level shaking to

the design level drifts (δ_E/R). The design drifts in this study were obtained using a wall flexural effective stiffness $I_{eff} = 0.75I_g$ based on input from the advisory panel for the study for effective stiffness values commonly used in practice for RC coupled walls. This effective stiffness assumption results in lower design drifts than if, for example, $I_{eff} = 0.5I_g$ were used in design. However, since the archetypes have been designed for amplified shear demands and conform to the drift capacity check per the new provisions of ACI 318-19, the designs were not drift-governed, and the wall piers were thicker and stiffer than they would have been if designed per ACI 318-14. The maximum design drifts observed at the center of mass among any of the archetypes was less than 1.6% when using $I_{eff} = 0.75I_g$ and less than 2% when using $I_{eff} = 0.5I_g$ (per ACI 318-14, where this value is permitted to compute drifts).

Table 4-5 summarizes the drifts and resulting C_d values for a subset of archetypes. The computed C_d values for these archetypes result in a median value of C_d = 8.8 (coefficient of variation = 0.13). For the subset of archetypes listed in Table 4-5, adjusting the nonlinear response history analysis roof drift values for 5% damping results in a median value of C_d = 8.4. Therefore, a deflection amplification factor of C_d = *R* = 8 was proposed.

Table 4-5. Assessment of C_d Based on Drifts from a Subset of Archetypes

Archetype	Number of stories	h_n (ft)	Design $(\delta_E/R)/h_n$ (%)	Median RHA δ / h_n (%)	C_d $\delta / (\delta_E/R)$
30H-DR-3	30	300	0.145	1.14	**7.9**
18H-DR-3	18	180	0.111	1.22	**10.9**
12H-DR-3	12	120	0.161	1.58	**9.8**
8H-DR-3	8	80	0.127	1.14	**9.0**
6H-DR-2	6	60	0.109	0.94	**8.6**
6H-CR-5	6	60	0.130	1.05	**8.1**

As a result of this study, a system overstrength factor of $\Omega_0 = 2.5$ was proposed based on nonlinear static pushover analysis results indicating that mean overstrength values of the performance groups range from 1.3 and 2.2. The proposed response modification factor $R = 8$ was validated based on incremental dynamic analysis results indicating that mean Adjusted Collapse Margin Ratio values of the performance groups range from 2.09 to 2.91, corresponding to collapse probabilities of less than ten percent based on using a conservative definition of collapse as noted in the prior paragraph. The deflection amplification factor of $C_d = 8$ was proposed based on damping considerations, and the assessment of median roof drift responses from DE level shaking compared

to design roof drifts. A minimum height limit of 60 feet was recommended for the Ductile Coupled Shear Wall System with the proposed seismic response parameters to be adopted in ASCE/SEI 7; in shorter buildings, there may not be enough coupling beams to absorb sufficient energy to merit an *R*-value of 8. Overall, the results of this study suggested that an overstrength factor of $\Omega_0 = 2.5$, a response modification factor $R = 8$, and a deflection amplification factor of $C_d = 8$ are appropriate seismic design parameters for reinforced concrete Ductile Coupled Wall systems that are designed per ASCE/SEI 7-22 and ACI 318-19 provisions.

4.5 Design of a Special Reinforced Concrete Ductile Coupled Wall

4.5.1 Introduction

4.5.1.1 GENERAL

A 22-story reinforced concrete residential building is designed following the requirements of ASCE/SEI 7-22, and ACI 318-19. A computer rendering of the building framing is shown in Figure 4-4(a). The plan view of the building changes from one floor to another. A plan view of the second floor of the building is shown in Figure 4-4(b). Story elevations above the base and story heights can be seen in Table 4-6.

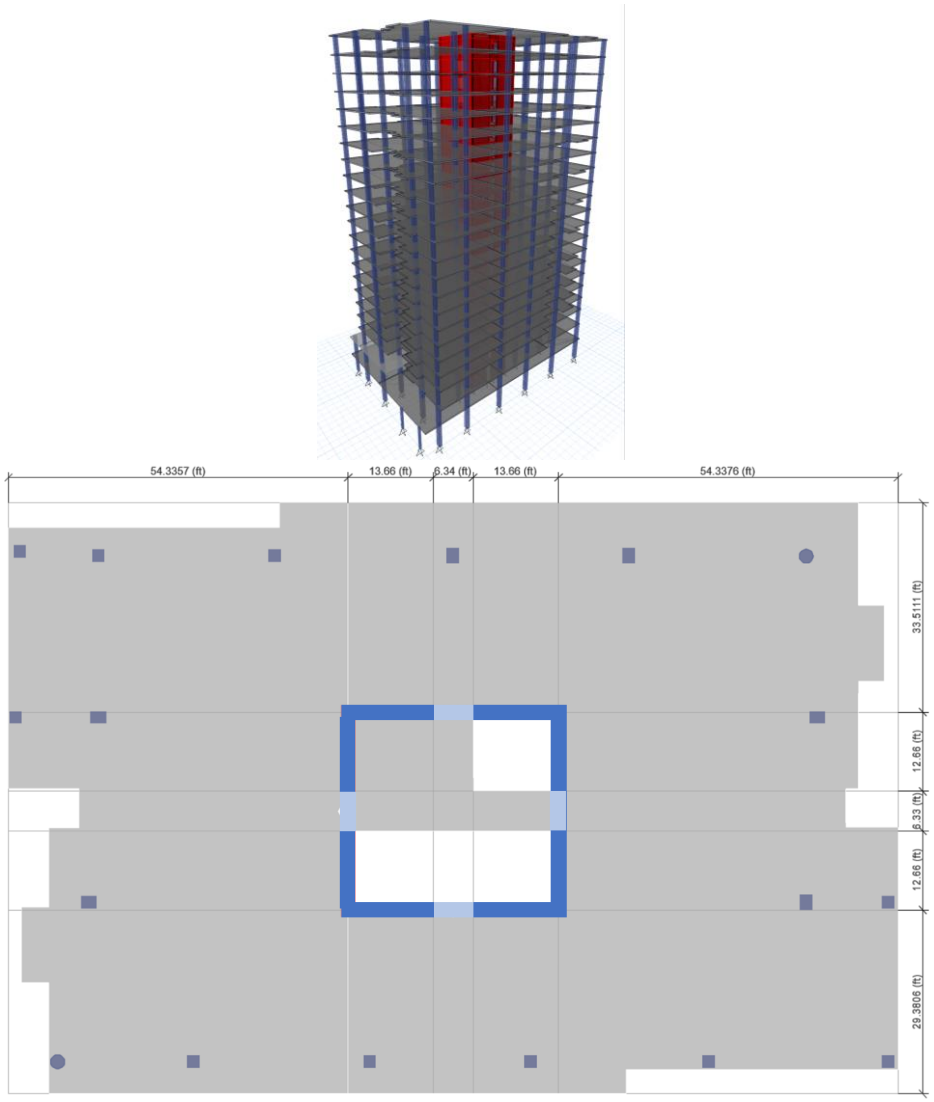

Figure 4-4. (a) A 3D View and (b) a Second-floor Plan View of the Example Building

The building consists of a flat plate-column gravity system with a central core, formed by four reinforced concrete coupled structural walls, which acts as the seismic force-resisting system. The structural walls are designed as Reinforced Concrete Ductile Coupled Structural (Shear) Walls. The advantage of this new system is a higher value of the response reduction factor, *R*, which is 8 for this system. Isolated or non-coupled special structural walls are assigned an *R*-value of 6 when designed as part of a building frame system and an *R*-value of 5 when designed as part of a bearing wall system. However, the higher *R*-value, and, consequently, a lower seismic base shear comes with some restrictions on the wall geometry as well as an added detailing requirement, as shown below:

- Individual walls need to satisfy $h_{wcs}/\ell_w \geq 2.0$, where h_{wcs} is the height of the entire structural wall above the critical section for flexural and axial loads, and ℓ_w is the wall length. In this example, h_{wcs} = 2,811 in. (234.25 ft) and ℓ_w = 164 in. (13.67 ft) along the x-axis of the building and 152

in. (12.67 ft) along the y-axis of the building. So, the minimum value of h_{wcs}/ℓ_w = 17.1 > 2.0. Thus, the building satisfies the first condition.

- Coupling beams need to satisfy $\ell_n/h \geq 2.0$ at all levels of the building, where ℓ_n is the length of the clear span of the beam, and h is the height of the beam. In this example, ℓ_n = 76 in. (6.33 ft) and h = 28 in. (2.33 ft). So, ℓ_n/h = 2.71 > 2.0. Thus, the coupling beams satisfy this condition.

- In at least 90 percent of the floors, all coupling beams need to have $\ell_n/h \leq 5.0$. In the example building, all coupling beams in all floor levels are of the same dimensions. So, this condition is also satisfied.

- The last condition requires the provisions related to development of the beam reinforcement to be in accordance with ACI 318 Section 18.10.2.5. This will be satisfied at the detailing stage of the beam.

So, the structural walls in the example building satisfy all the conditions to qualify to be designed as ductile coupled shear walls.

4.5.1.2 DESIGN CRITERIA

The member sizes for the structure are chosen as follows:

Shear walls: 26 in. thick

Slabs
2nd and 3rd floors: 8 in. thick
4th floor and higher: 7.5 in. thick

Gravity columns: Various sizes

Other relevant design data are as follows:

Material properties

- Concrete (used in structural walls and columns): f_c' = 8,000 psi (all stories)

- Concrete (used in slabs): f_c' = 6000 psi (floors)

- All members are constructed of normal weight concrete (w_c = 150 pcf)

- Reinforcement (used in all structural members): f_y = 60,000 psi

Service loads

- Superimposed dead load: 25 psf (includes superimposed dead load on the floor plus the weight of cladding distributed over the floor slab.)

- Floor live load: Based on the 40 psf live load prescribed in ASCE/SEI 7 Table 4.3-1 for residential buildings (private rooms and corridors serving them), a reduced live load of 20 psf is used in the example.

- Reduced roof live load: 20 psf

Seismic design data

Risk Category: II
Seismic importance factor, I_e = 1.0
Site Class: D

ASCE/SEI 7-22 requires structures in U.S. locations to be designed using multi-period spectra from the USGS Seismic Design Geodatabase. However, it is not the purpose of this design example to illustrate the use of multi-period spectra. See Chapter 3 of this guide for discussion of multi-period spectra. So, the example was done using the two-period design response spectrum of Section 11.4.5.2, using the following ground motion parameters.

The maximum considered earthquake spectral response acceleration:

At short periods, S_S = 1.65g, and
At 1-sec period, S_1 = 0.65g.

The maximum considered earthquake spectral response acceleration (site modified):

At short periods, S_{MS} = 1.65g, and
At 1-sec period, S_{M1} = 0.975g.

Design Spectral Response Acceleration Parameters (at 5% damping):

At short periods: S_{DS} = 2/3 S_{MS}/g = 2/3 × 1.65 = 1.10
At 1-sec period: S_{D1} = 2/3 S_{M1}/g = 2/3 × 0.975 = 0.65

Long-period transition period, T_L = 8 sec

Reinforced Concrete Ductile Coupled Structural (Shear) Walls … R = 8; C_d = 8.0, Ω_0 = 2.5 (ASCE/SEI Table 12.2-1)

Seismic Design Category: Based on both S_{DS} (ASCE/SEI Table 11.6-1) and S_{D1} (ASCE/SEI Table 11.6-2), the seismic design category (SDC) for the example building is D.

4.5.1.3 DESIGN BASIS

Although ASCE/SEI 7-22 permits the Equivalent Lateral Force procedure to be used in all situations, the modal response spectrum analysis (MRSA) procedure (ASCE/SEI Section 12.9.1) is used in this example. However, as part of the MRSA procedure, base shear is also determined using Equivalent

Lateral Force (ELF) procedure. This is because ASCE/SEI 7 requires that the base shear obtained from MRSA be scaled up to match the ELF base shear.

The building was modeled in ETABS 2016, and the total seismic weight was obtained from the program as 43,099 kips.

4.5.1.4 LOAD COMBINATIONS FOR DESIGN

The following load combinations are used in the strength design method for concrete.

a. $U = 1.4D$
b. $U = 1.2D + 1.6L$
c. $U = 1.2D + 0.5L + 1.0E$
d. $U = 0.9D + 1.0E$

where: D = dead load effect
L = live load effect
$E = \rho Q_E + 0.2S_{DS}D$ when the effects of gravity and seismic loads are additive
$E = \rho Q_E - 0.2S_{DS}D$ when the effects of gravity and seismic loads are counteractive
Q_E = the effect of horizontal seismic forces
ρ = redundancy factor (discussed below)

4.5.1.5 SYSTEM IRREGULARITY AND ACCIDENTAL TORSION

ASCE/SEI 7 requires consideration of accidental torsion in seismic analysis in a given direction when the structure has a horizontal irregularity Type 1a or 1b (torsional irregularity and extreme torsional irregularity, respectively) when subjected to seismic forces in the same direction. This was first investigated by performing preliminary analysis of the structure by applying the seismic forces separately along the x- and y-axes of the structure and by incorporating a load eccentricity equal to 5% of the floor width. Presence of torsional irregularity was determined by checking if the ratio of maximum to average story drift at any floor equals or exceeds 1.2.

It was found that, for seismic forces acting along the x-axis of the structure, no torsional eccentricity is present in the structure. Thus, for the final seismic analysis of the structure, no accidental eccentricity was considered.

For seismic forces acting along the y-axis of the structure, torsional irregularity was found to be present. As a result, a 5% accidental eccentricity, as described above, was included in the final analysis. Additionally, because the structure is assigned to SDC D, the accidental torsion was required to be amplified in the first four floor levels as the ratio of maximum to average story drift at those floors exceeded 1.2.

4.5.1.6 REDUNDANCY FACTOR, ρ

A check was made to see if the seismic force-resisting system of the structure can be considered redundant or not. A structure is considered redundant if removal of a shear wall or wall pier with a height-to-length ratio greater than 1.0 within any story would not result in more than a 33% reduction in story strength; nor would the resulting system have an extreme torsional irregularity (horizontal structural irregularity Type 1b).

In the example building, the height-to-length ratio of the shear walls in the first story is greater than one. There are four such walls of equal length in either direction. So, removal of one such wall would result in the reduction of the shear resistance of the building by approximately 25%.

After performing seismic analysis separately along the x- and y-axes of the building with the wall removed, it was seen that the maximum ratio of maximum to average story drift was 1.39, which is less than the 1.6 threshold for defining an extreme torsional irregularity in ASCE/SEI 7-22.

In view of the above, the seismic force-resisting system of the building can be considered redundant, and the value of ρ can be taken as 1.0.

4.5.1.7 ANALYSIS BY EQUIVALENT LATERAL FORCE PROCEDURE

Structural period calculation

Coefficient, C_t [ASCE/SEI Table 12.8-2]= 0.02

Coefficient, x [ASCE/SEI Table 12.8-2] x = 0.75

Structure height above base, h_n = 234.25 ft

Approximate period, $T_a = 0.02h_n^x = 0.02 \times 234.25^{0.75} = 1.2$ sec.

Fundamental period calculated by modal analysis in ETABS, T = 2.58 sec (along x-axis)

Fundamental period calculated by modal analysis in ETABS, T = 2.26 sec (along y-axis)

Calculated period is larger than the approximate period. However, the fundamental period cannot exceed C_uT_a.

For S_{D1} = 0.65, C_u = 1.4

$C_uT_a = 1.4 \times 1.2 = 1.68$ sec

Thus, T used in design = 1.68 sec < T_L (= 8 sec)

Base shear calculation

$V = C_SW$ (ASCE/SEI Eq. 12.8-1)

where:

$$C_S = \frac{S_{DS} I_e}{R} = \frac{1.10 \times 1.0}{8} = 0.138 \quad \text{(ASCE/SEI Eq. 12.8-2)}$$

$$\leq \frac{S_{D1} I_e}{RT} = \frac{0.65 \times 1.0}{8 \times 1.68} = 0.0485 \quad (\text{for } T \leq T_L) \quad \text{(ASCE/SEI Eq. 12.8-3)}$$

$$\geq 0.044 S_{DS} I_e = 0.044 \times 0.65 \times 1.0 = 0.029 \quad \text{(ASCE/SEI Eq. 12.8-5)}$$

$$\geq 0.01 \quad \text{(ASCE/SEI Eq. 12.8-5)}$$

$$\geq \frac{0.5 S_1 I_e}{R} = \frac{0.5 \times 0.65 \times 1.0}{8} = 0.041 \quad (\text{where } S_1 \geq 0.6\text{g}) \quad \text{(ASCE/SEI Eq. 12.8-6)}$$

Governing $C_S = 0.048$
Seismic weight, $W = 43{,}099$ kips
Base shear, $V = C_S W = 0.048 \times 43{,}099 = 2{,}090$ kips

4.5.1.8 MODAL RESPONSE SPECTRUM ANALYSIS

A three-dimensional analysis of the structure is performed using modal response spectrum analysis using ETABS (Version 2016) computer program. In the ETABS model, semi-rigid diaphragms are assigned at each level. Accidental torsion is addressed in the way described in Section 4.5.1.5 above.

According to ASCE/SEI Section 12.7.3, the mathematical model must consider cracked section properties. The stiffnesses of members used in the analyses are as follows:

For columns and shear walls, $I_{eff} = 0.7 I_g$
For coupling beams, $I_{eff} = 0.25 I_g$

For gravity columns, in order to minimize their contribution to the lateral stiffness of the structure, I_{eff} is taken as $0.1 I_g$. In addition, the columns are connected at the base by pinned connections. P-Δ effects were considered in the lateral analysis.

An adequate number of modes are considered in the modal analysis to incorporate 100% of the modal mass in each of x- and y-directions. Also, appropriate scale factors are applied to the base shears calculated in the x- and y-directions to amplify them to those calculated in the ELF procedure.

Floor forces and story drifts obtained from the MRSA are shown in Tables 4-6 and 4-7, respectively.

Table 4-6. Floor Forces from MRSA

Story	Elevation (ft)	Story height (ft)	X-Dir (kip)	Y-Dir (kip)
L23	234.25	10	195.346	195.346
L22	224.25	10	206.044	206.044
L21	214.25	10	192.838	192.838
L20	204.25	10	177.633	177.633
L19	194.25	10	165.042	165.042
L18	184.25	10	150.814	150.814
L17	174.25	10	138.882	138.882
L16	164.25	10	125.656	125.656
L15	154.25	10	114.433	114.433
L14	144.25	10	102.24	102.24
L13	134.25	10	91.783	91.783
L12	124.25	10	80.685	80.685
L11	114.25	10	71.058	71.058
L10	104.25	10	61.056	61.056
L09	94.25	10	52.344	52.344
L08	84.25	10	43.803	43.803
L07	74.25	10	35.838	35.838
L06	64.25	10	28.482	28.482
L05	54.25	10	21.771	21.771
L04	44.25	13	16.224	16.224
L03	31.25	15	12.95	12.95
L02	16.25	16.25	3.78	3.78

Table 4-7. Story Drifts from MRSA

Story	Story height (ft)	X-Direction				Y-Direction			
		δ_{xe} (in.)	C_d	δ_x (in.)	Relative Drift (%)	δ_{xe} (in.)	C_d	δ_x (in.)	Relative Drift (%)
L23	10	3.36	8	26.84	1.00	3.64	8	29.11	1.07
L22	10	3.21	8	25.65	1.02	3.48	8	27.83	1.09
L21	10	3.05	8	24.43	1.03	3.32	8	26.52	1.11
L20	10	2.90	8	23.18	1.05	3.15	8	25.19	1.13
L19	10	2.74	8	21.92	1.07	2.98	8	23.83	1.15
L18	10	2.58	8	20.64	1.08	2.81	8	22.45	1.17
L17	10	2.42	8	19.33	1.10	2.63	8	21.05	1.18
L16	10	2.25	8	18.02	1.10	2.45	8	19.63	1.19
L15	10	2.09	8	16.69	1.11	2.28	8	18.21	1.19
L14	10	1.92	8	15.36	1.11	2.10	8	16.77	1.20
L13	10	1.75	8	14.03	1.11	1.92	8	15.34	1.19
L12	10	1.59	8	12.70	1.10	1.74	8	13.91	1.19
L11	10	1.42	8	11.38	1.09	1.56	8	12.48	1.18
L10	10	1.26	8	10.07	1.08	1.38	8	11.06	1.17
L09	10	1.10	8	8.77	1.06	1.21	8	9.65	1.15
L08	10	0.94	8	7.50	1.04	1.03	8	8.27	1.13
L07	10	0.78	8	6.25	1.00	0.86	8	6.92	1.09
L06	10	0.63	8	5.06	0.95	0.70	8	5.60	1.04
L05	10	0.49	8	3.91	0.89	0.54	8	4.35	0.98
L04	13	0.36	8	2.85	0.80	0.40	8	3.18	0.87
L03	15	0.20	8	1.60	0.59	0.23	8	1.82	0.67
L02	16.25	0.07	8	0.55	0.28	0.08	8	0.62	0.32

4.5.1.9 STORY DRIFT LIMITATION

According to ASCE/SEI Section 12.12.1, the calculated relative story drift at any story must not exceed 2% (ASCE/SEI Table 12.12-1 for all other buildings in Risk Category I and II). As can be seen from Table 4-7, this is satisfied in all stories.

4.5.2 Design of Shear Walls

The design of one of the shear walls at the base of the structure is illustrated in this example. Similar procedures may be followed to design the shear wall at the other floor levels. The design of shear walls is performed in accordance with the provisions of ACI 318-19.

Each L-shaped segment of the shear wall core is designed as a flanged wall in each direction. (Figure 4-5). Per ASCE/SEI 7 Section 12.5.4, "any column or wall that forms part of two or more intersecting seismic force-resisting systems and is subjected to axial load due to seismic forces acting along either principal plan axis equaling or exceeding 20% of the axial design strength of the column or wall" needs to be designed considering the orthogonal combination of seismic forces along x- and y-axes of the structure in accordance with one of the procedures specified in ASCE/SEI 7 Section 12.5.3.1. The maximum axial compression on this flanged wall, when subjected to seismic forces along the x-axis, is 3,385 kips, and that when subjected to seismic forces along the y-axis is 3,586 kips. Both these values are less than 20% of the axial design strength of the wall, which is 29,547 kips (shown later). Thus, it is not required to consider orthogonal combinations of the seismic forces, and the wall is designed for the seismic forces along x- and y-axes separately.

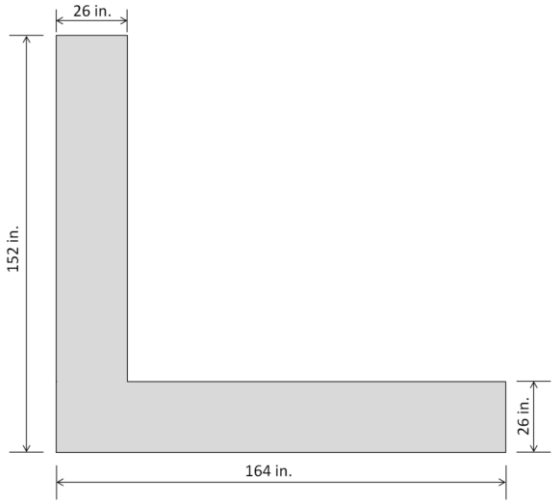

Figure 4-5. L-Shaped Wall Designed in the Example

4.5.2.1 DESIGN LOADS

Table 4-8 shows a summary of the axial force, shear force, and bending moment at the base of the example shear wall based on different load combinations. Seismic forces acting along the x-axis are considered in this design example. The design calculations for the seismic forces acting along the y-axis are similar and are not shown. However, Figure 4-7 shows the wall in its final configuration after considering seismic forces in both directions.

Table 4-8. Summary of Design Axial Force, Shear Force, and Bending Moment for Shear Wall between Floor 1 and Floor 2 When Subjected to Seismic Forces along x-Axis

	Load Combinations	Axial Force, P_u (kips)	Shear Force, V_u (kips)	Bending Moment, M_u (kip-ft)
1	$1.4D$	6,335	0	0
2	$1.2D+1.6L+0.5L_r$	6,071	0	0
3	$(1.2+0.2S_{DS})D+\rho Q_E+0.5L$	10,015	576	24,976
4	$(0.9D - 0.2S_{DS}D) + \rho Q_E$	6,460	573	24,585
5	$(0.9D - 0.2S_{DS}D) - \rho Q_E$	-378	573	24,585

4.5.2.2 DESIGN FOR SHEAR

Height of the shear wall, h_{wcs} = 2,811 in. (234.25 ft)
Length of the shear wall, ℓ_w = 164 in. (13.67 ft)
h_{wcs}/ℓ_w = 2,811/164 = 17.1

ACI 318-19 Section 18.10.2.2

At least two curtains of reinforcement shall be used if $V_u > 2A_{cv}\lambda\sqrt{f'_c}$ or $h_{wcs}/\ell_w \geq 2.0$. In this case,

For normal-weight concrete, $\lambda = 1$
$A_{cv} = \ell_w \times b_w = 164 \times 26 = 4{,}264$ in.2
$2A_{cv}\lambda\sqrt{f'_c} = 2 \times 4{,}264 \times 1 \times \sqrt{8000}/1000 = 763$ kips > 576 kips

However, $h_{wcs}/\ell_w = 17.1 > 2.0$.

So, at least two curtains of reinforcement are required.

ACI 318 Section 11.7.2.3 also stipulates that walls more than 10 in. thick, except single story basement walls and cantilever retaining walls, are to be provided with two layers of reinforcement.

ACI 318-19 Section 18.10.3.1

Design shear force, $V_e = \Omega_v\omega_v V_u \leq 3V_u$

For walls with $h_{wcs}/\ell_w > 1.5$, Ω_v is the greater of M_{pr}/M_u and 1.5. The probable moment strength M_{pr} is unknown at this stage. So, let us assume $\Omega_v = 1.5$ for now. This may very well prove to be unconservative. Once the flexural reinforcement has been provided, this will be verified or corrected, if necessary.

For walls with $h_{wcs}/\ell_w \geq 2.0$ and the number of stories above critical section, $n_s > 6$,

$\omega_v = 1.3 + n_s/30 \leq 1.8$

In this example, $n_s = 22$. n_s cannot be taken less than the quantity $0.007h_{wcs}$ (= 19.68), which is satisfied.

$\omega_v = 1.3 + 22/30 = 2.03 \Rightarrow \omega_v = 1.8$

So, an initial estimate of $\Omega_v\omega_v = 1.5 \times 1.8 = 2.7$. This will be verified once the correct value of Ω_v can be ascertained using M_{pr}.

$V_e = \Omega_v\omega_v V_u = 1.5 \times 1.8 \times 576 = 1{,}555$ kips

ACI 318-19 Section 18.10.4.4

Before starting to determine the required shear reinforcement, it is good to check if V_e exceeds the maximum shear strength allowed for this section. In that case, wall thickness may need to be increased.

The maximum nominal shear strength, V_n, allowed for a wall section is

$10A_{cv}\sqrt{f'_c} = 10 \times 4{,}264 \times \sqrt{8000}/1000 = 3{,}813$ kips

So, $\phi V_n = 0.75 \times 3{,}813 = 2{,}860$ kips > $V_e = 1{,}555$ kips

The provided wall section size is acceptable.

ACI 318-19 Section 18.10.4.1

For $h_w/\ell_w = 17.1 \geq 2.0$, $\alpha_c = 2$

For normal-weight concrete, $\lambda = 1$

$V_n = (\alpha_c\lambda\sqrt{f'_c} + \rho_t f_y) A_{cv} \geq V_e/\phi$ (ACI 318-19 Eq. 18.10.4.1)

ACI 318-19 Section 21.2.4.1 requires a ϕ of 0.6 to be used in the shear design of a member that resists earthquake forces and may fail in shear before it has a chance to fail in flexure. The shear walls in this example have a minimum h_w/ℓ_w ratio of 17.1, which makes them flexure-controlled, meaning that flexural failure will precede their failure in shear. Thus, the proper ϕ-value to use in their shear design is 0.75.

Required horizontal shear reinforcement ratio:

$$\rho_t = \left[\frac{V_e}{\varphi A_{cv}} - \alpha_c \lambda \sqrt{f'_c} \right] \Big/ f_y$$

$$= \left[\frac{1555 \times 1000}{0.75 \times 4264} - 2 \times 1.0 \times \sqrt{8000} \right] \Big/ 60000$$

$$= 0.0051$$

Two curtains of #7 horizontal shear reinforcement at a vertical spacing of 7 in. are adequate to resist this shear force. However, the 7" spacing is reduced to 5" in order to maintain uniformity with the reinforcement provided in the other leg of the shear wall to resist shear in y direction, leading to a provided ρ_t = 0.009. The 5" spacing also matches the vertical spacing of the transverse reinforcement provided in the special boundary element of the wall (shown later), which helps in the construction efficiency.

Per ACI 318-19 Section 18.10.2.1, the minimum ρ_t = 0.0025 and maximum reinforcement spacing = 18 in., both of which are satisfied.

ACI 318-19 Section 18.10.4.3

h_w/ℓ_w exceeds 2.0. Therefore, ρ_ℓ need not be larger than or equal to ρ_t.

ACI 318-19 Section 18.10.2.1

Longitudinal reinforcement ratio:

$\rho_\ell \geq 0.0025$ with a maximum spacing of 18 in.

Provided two curtains of #8 vertical reinforcement at 14 in. spacing (ρ_ℓ = 0.004). This will need to be increased at the end regions of the wall.

ACI 318-19 Section 18.10.2.4

In walls with $h_w/\ell_w \geq 2.0$ that are effectively continuous from the base of the structure to the top of the wall and are designed to have a single critical section for flexure and axial loads, the longitudinal reinforcement ratio within $0.15\ell_w$ of the ends of the wall needs to be at least $6\sqrt{f'_c} / f_y$. The end regions in an L-shaped wall where this needs to be provided are shown below in Figure 4-6. For the wall along the x-axis, the length of this region is 0.15×164 = 24.6 in. For the wall along the y-axis, the length of this region is 0.15×152 = 22.8 in. In the intersection area of the two legs of the wall, the end regions overlap and almost fully cover the intersection area, as shown in Figure 4-6 below.

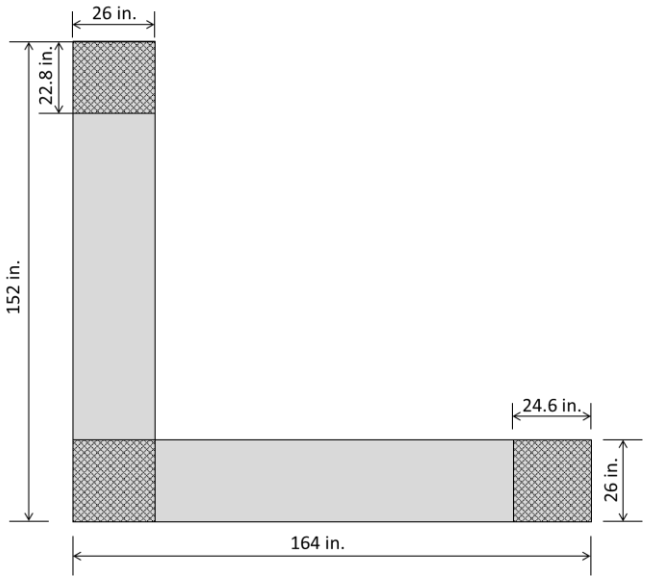

Figure 4-6. End Regions Requiring Vertical Reinforcement Per ACI 318-19 Section 18.10.2.4(a)

Nine #8 bars are provided in a 3×3 pattern in the wall intersection area.

$$\rho_\ell = 0.01 > 6\sqrt{f'_c}/f_y \ (= 0.009) \ \ldots\ldots\ldots\ldots \text{OK}$$

This needs to be satisfied at the other ends of the two legs of the wall. However, reinforcement provided there would be governed by special boundary element requirements, which is shown next.

4.5.2.3 BOUNDARY ELEMENTS OF SPECIAL REINFORCED CONCRETE SHEAR WALLS (ACI 318-19 SECTION 18.10.6)

ACI 318-19 Section 18.10.6.1

The need for special boundary elements at the edges of shear walls is to be evaluated in accordance with ACI 318-19 Section 18.10.6.2 (displacement-based approach) or ACI 318-19 Section 18.10.6.3 (stress-based approach). In this example, the displacement-based approach is used as the wall satisfies the three required conditions:

12. $h_{wcs}/\ell_w \geq 2.0$,
13. The wall is continuous from the base of the structure to the top of the wall, and
14. The wall has a single critical section for bending and axial loads.

ACI 318-19 Section 18.10.6.2(a): Displacement-based Approach

Compression zones are to be reinforced with special confinement reinforcement where:

$$\frac{1.5\delta_u}{h_{wcs}} \geq \frac{\ell_w}{600c} \text{ (ACI 318-19 Eq. 18.10.6.2a)}$$

In the expression above, δ_u is the design displacement, which is the total calculated lateral displacement expected for the design earthquake. For seismic forces along the x-axis of the structure, δ_u was determined from the ETABS analysis as 26.84 in (see Table 4-7).

In addition, *c* is the largest neutral axis depth of the wall cross-section calculated for the factored axial force and nominal moment strength consistent with the direction of the design displacement. This was determined using the computer program *spColumn* v7.00. Out of the two seismic load combinations considered, the axial compression P_u (= 10,015 kips) from the additive combination (1.2 *D* + 0.2 S_{DS} *D* + ρ Q_E + 0.5 *L*) had the highest nominal moment strength, M_n, associated with it. The corresponding depth of the neutral axis was found to be 95 in. when the non-flanged end of the wall is in compression. For this situation,

$$\frac{1.5\delta_u}{h_{wcs}}\left(=\frac{1.5\times 26.84}{2811}=0.0143\right) \geq \frac{\ell_w}{600c}\left(\frac{164}{600\times 95}=0.003\right)$$

Also, δ_u/h_{wcs} cannot be taken less than 0.005. In this example,

δ_u/h_{wcs} = 26.84/2,811 = 0.0095 > 0.005 .....OK

As a result, a special boundary element needs to be provided at the non-flanged end of the wall.

The same check was performed for the flanged end of the wall as well. However, when the flanged end of the wall is under compression, the neutral axis depth is small due to the presence of the flange, and as a result, the above check is not satisfied. So, a special boundary element is not necessary for the flanged end of the wall.

Special boundary element confinement is provided only at the non-flanged end of the wall, as shown below.

ACI 318-19 Section 18.10.6.2(b)(i): Height of special boundary element

The special boundary element reinforcement is to extend vertically from the critical section a distance not less than the larger of ℓ_w and $M_u/4V_u$.

ℓ_w = 164 in. (13.67 ft) ... governs

$$\frac{M_u}{4V_u}=\frac{24976}{4\times 576}=10.84 \text{ ft}$$

ACI 318-19 Section 18.10.6.2(b)(ii): Width of special boundary element

The width of boundary element, b (= 26 in.) $\geq \sqrt{0.025 c l_w} = \sqrt{0.025 \times 95 \times 164} = 19.3$ in.

Therefore, a more detailed check by ACI 318-19 Section 18.10.6.2(b)(iii) is not necessary.

.....OK

ACI 318-19 Section 18.10.6.4(a): Length of boundary element

Confined boundary element to extend horizontally from the extreme compression fiber a distance not less than the larger of $c - 0.1\ell_w$ and $c/2$.

$c - 0.1\ell_w = 95 - 0.1 \times 164 = 78.6$ in ≈ 80 in..... governs

$c/2 = 95/2 = 47.5$ in.

ACI 318-19 Section 18.10.6.4(b) and (c): Stability check for wall compression zone

Minimum width of the compression zone, b = 26 in., which is required to be at least $h_u/16$, where h_u is the laterally unsupported height (clear height) of the wall (ACI 318-19 Section 18.10.6.4(b)).

h_u = Story height – depth of coupling beam = 158 in.

$h_u/16 = 9.875$ in. < 26 in. .....OK

Also, for this wall, $h_{wcs}/\ell_w = 17.1 > 2.0$, and it is effectively continuous from the base of the structure to the top of the wall and designed to have a single critical section for flexure and axial loads. And $c/\ell_w = 95/164 = 0.58 > 3/8$. As a result, ACI 318-19 Section 18.10.6.4(c) requires the width of the flexural compression zone b over the length of 80 in. (calculated above) to be greater than or equal to 12 in. This is satisfied as the width of the wall is 26 in.

ACI 318-19 Section 18.10.6.4(a): Length of boundary element

Confined boundary element to extend horizontally from the extreme compression fiber a distance not less than the larger of $c - 0.1\ell_w$ and $c/2$.

$c - 0.1\ell_w = 95 - 0.1 \times 164 = 78.6$ in ≈ 80 in..... governs

$c/2 = 95/2 = 47.5$ in.

ACI 318-19 Section 18.10.6.4(b) and (c): Stability check for wall compression zone

Minimum width of the compression zone, b = 26 in., which is required to be at least $h_u/16$, where h_u is the laterally unsupported height (clear height) of the wall (ACI 318-19 Section 18.10.6.4(b)).

h_u = Story height – depth of coupling beam = 158 in.

$h_u/16 = 9.875$ in. < 26 in. .....OK

Also, for this wall, $h_{wcs}/\ell_w = 17.1 > 2.0$, and it is effectively continuous from the base of the structure to the top of the wall and designed to have a single critical section for flexure and axial loads. And $c/\ell_w = 95/164 = 0.58 > 3/8$. As a result, ACI 318-19 Section 18.10.6.4(c) requires the width of the flexural compression zone *b* over the length of 80 in. (calculated above) to be greater than or equal to 12 in. This is satisfied as the width of the wall is 26 in.

ACI 318-19 Section 18.10.6.4(d): Flanged section

It is required that in flanged sections, the boundary element is to include the effective flange width in compression. The boundary element is also required to extend into the web by at least 12 in.

In this example, the flanged side of the wall does not require a special boundary element. So, these requirements do not apply.

ACI 318-19 Section 18.10.6.4(g): Minimum area of transverse reinforcement

$$A_{sh}/sb_c = \text{Greater of } \begin{cases} 0.3\left(\dfrac{A_g}{A_{ch}} - 1\right)\dfrac{f'_c}{f_{yt}} \\ 0.09\dfrac{f'_c}{f_{yt}} \end{cases} \qquad \text{(ACI 318-19 Table 18.10.6.4(g))}$$

***Confinement perpendicular to the length of the wall*:** With a boundary element length of 80 in., width of 26 in. and 1.5 in. clear cover all around the boundary element:

$b_c = 80 - 2 \times 1.5 = 77$ in.

$A_g = 80 \times 26 = 2{,}080$ in.^{2}

$A_{ch} = (80 - 2 \times 1.5) \times (26 - 2 \times 1.5) = 1{,}771$ in.^{2}

$$A_{sh}/sb_c = \text{Greater of } \begin{cases} 0.3\left(\dfrac{2080}{1771} - 1\right)\dfrac{8}{60} \\ 0.09\dfrac{8}{60} \end{cases}$$

$= 0.012$

The vertical spacing of the transverse reinforcement, *s*, is needed to calculate the required A_{sh}. However, determination of *s* involves the horizontal spacing, h_x, of the laterally supported longitudinal bars, which, in turn, requires knowing A_{sh}. So, an iterative process is needed to ascertain an acceptable value of A_{sh} and its vertical spacing *s*.

Based on the ACI 318-19 Section 18.10.6.4(e) requirements, a vertical spacing of 6 in. would be acceptable, as shown later. However, in this example, a vertical spacing of 5 in. is provided to keep the required cross-sectional area of transverse reinforcement from being excessive, with s = 5 in., minimum required $A_{sh} = 0.012sb_c = 0.012 \times 5 \times 77 = 4.62$ in.^{2}

Provided 16 #5 bars in the form of hoops and cross-ties with a vertical spacing of 5 in.

A_{sh} provided = 16 × 0.31 = 4.96 in.^{2} > 4.62 in.^{2} ..... OK

***Confinement parallel to the length of the wall*:** With a wall width of 26 in. and 1.5 in. clear cover all around the boundary element, the width of the boundary element core for confinement along the length of the wall:

$b_c = 26 - 2 \times 1.5 = 23$ in.

$$A_{sh}/sb_c = \text{Greater of } \begin{cases} 0.3\left(\dfrac{2080}{1771} - 1\right)\dfrac{8}{60} \\ 0.09\dfrac{8}{60} \end{cases}$$

= 0.012

With s = 5 in., minimum required $A_{sh} = 0.012sb_c = 0.012 \times 5 \times 23 = 1.38$ in.^{2}

Provided 5 #5 bars in the form of a single hoop and two cross-ties with a vertical spacing of 5 in.

A_{sh} provided = 5 × 0.31 = 1.55 in.^{2} > 1.38 in.^{2} ..... OK

ACI 318-19 Section 18.10.6.4(f): Spacing limitation of transverse reinforcement

Transverse reinforcement is to be arranged such that the spacing h_x between laterally supported longitudinal bars around the perimeter of the boundary element does not exceed the lesser of

- 14 in. ....Governs
- Two-thirds of the boundary element thickness = 2/3 × 23 = 15.33 in. (for transverse reinforcement arranged perpendicular to the wall length)

So, maximum h_{sx} = 14 in.

For transverse reinforcement arranged perpendicular to the wall length, 16 #5 transverse bars are provided over a width of 80 in. Each of these transverse bars engages one #8 longitudinal bar at the perimeter of the boundary element. Assuming an approximately uniform spacing, the distance between laterally supported longitudinal bar at the perimeter:

$(80 - 2 \times 1.5 - 2 \times 0.625 - 1)/(16 - 1) = 4.98$ in. < 14 in. ....OK

For transverse reinforcement arranged parallel to the wall length, 5 #5 transverse bars are provided over a width of 26 in. Each of these transverse bars engages one #8 longitudinal bar at the perimeter of the boundary element. Assuming an approximately uniform spacing, the distance between laterally supported longitudinal bar at the perimeter:

$(26 - 2 \times 1.5 - 2 \times 0.625 - 1)/(5 - 1) = 5.18$ in. < 14 in. ....OK

Lateral support to the longitudinal bars is required to be provided by a seismic hook of a crosstie or corner of a hoop. The length of a hoop leg (measured as the outside dimension of the hoop leg) cannot exceed two times the boundary element core thickness ($2 \times 23 = 46$ in.), and adjacent hoops need to overlap (measured as the c/c distance of longitudinal bars enclosed by the overlapping hoops) at least the lesser of

- 6 in. .....Governs
- Two-thirds the boundary element thickness = $2/3 \times 26 = 17.33$ in.

To meet these requirements, three overlapping hoops with cross-ties are provided, as shown in Figure 4-7.

ACI 318-19 Section 18.10.6.4(e): Vertical spacing of transverse reinforcement

According to ACI 318-19 Section 18.7.5.3, as revised by ACI 318-19 Section 18.10.6.4(e), the transverse reinforcement is to be vertically spaced at a distance not exceeding

(a) One-third of the least dimension of the boundary element = 23/3 = 7.67 in.

(b) Six times the diameter of the smallest longitudinal reinforcement = $6 \times 1.0 = 6.0$ in. ..... Governs

(c) so, as defined by ACI 318-19 Eq. (18.7.5.3).

4 in. $\leq s_o = 4 + (14 - h_x)/3 \leq$ 6 in. (ACI 318-19 Eq. 18.7.5.3)

4 in. $\leq s_o = 4 + (14 - 5.18)/3 \leq$ 6 in.

4 in. $\leq s_o = 6.94$ in. $\leq$ 6 in. => $s_o = 6.0$ in.

The vertical spacing also cannot exceed the maximum value given in ACI 318-19 Table 18.10.6.5(b). For Grade 60 reinforcement within the height of the special boundary element, it is the lesser of

- Six times the diameter of the smallest longitudinal reinforcement = $6 \times 1.0 = 6$ in.
- 6 in.

The provided spacing of 5 in. satisfies both these limits.

ACI 318-19 Section 18.10.6.4(h): Concrete in floor system

Concrete within the thickness of the floor system at the special boundary element location is required to have a specified compressive strength of at least $0.7f'_c$. With the slab concrete strength of 6000 psi, this is satisfied.

ACI 318-19 Section 18.10.6.4(i and j)

The special boundary element confinement determined above is to be provided at the non-flanged end of the wall at the base of the shear walls. The confinement needs to extend vertically by at least 12.67 ft above the base (ACI 318-19 Section 18.10.6.2(b)). Below the base, the boundary element transverse reinforcement needs to extend at least 12 in.

ACI 318-19 Section 18.10.6.4(k)

Horizontal web reinforcement is required to be extended to within 6 in. of the wall end. It is also required to be anchored to develop f_y within the confined core of the boundary element.

All horizontal web rebars in the wall have clear cover and clear spacing more than d_b, and the bars are developed within the highly confined special boundary element of the wall. As a result, the provisions of ACI 318-19 Section 25.4.2.3 can be used for the development length calculation.

For No. 7 horizontal bars in the web,

$$\ell_d = \left(\frac{f_y \psi_t \psi_e \psi_s}{20\lambda\sqrt{f'_c}} \right) d_b \quad \text{(ACI 318 Table 25.4.2.3)}$$

$\lambda = 1.0$ for normalweight concrete

$\psi_t = 1.3$ (ACI 318-19 Table 25.4.2.5)

$\psi_e = 1.0$ (ACI 318-19 Table 25.4.2.5)

$\psi_g = 1.0$ (ACI 318-19 Table 25.4.2.5)

$$\ell_d = \left(\frac{60{,}000 \times 1.3 \times 1.0 \times 1.0}{20 \times 1.0 \times \sqrt{8000}} \right) \times 0.875 = 38.2 \text{ in.}$$

Length of confined core available within the boundary elements

$= 80 - 2\times1.5 = 77$ in. > 38.2 in. ..... OK

Length of boundary element available up to 6 in. from the outside surface

= 80 – 2×1.5 – 6 = 71 in. > 38.2 in. .....OK

Also, for horizontal web reinforcement: $A_v f_y/s = 2\times0.60\times60/5 = 14.4$ kips/in.

And for boundary element transverse reinforcement parallel to the web reinforcement:

$A_{sh} f_{yt}/s = 5\times0.31\times60/5 = 18.6$ kips/in. > $A_v f_y/s$

So, horizontal web reinforcement can be terminated in the boundary element without a standard hook at 6 in. from the end of the wall.

ACI 318-19 Section 18.10.6.5: Boundary confinement where special boundary element is not required

As mentioned before, when the flanged end of the shear wall is under compression, the depth of neutral axis, *c*, is small due to the presence of a large flange width, and ACI 318-19 Eq. (18.10.6.2a) is not satisfied. As a result, a special boundary element is not required to be provided in the wall flange. However, some minimum ties are still required, as shown below.

- In this example, $V_u \geq \lambda \sqrt{f'_c}\, A_{cv}$. So, the end of the horizontal web reinforcement that terminates at the edges of the wall flange is required to have a standard hook engaging the edge reinforcement. Alternatively, the edge reinforcement at the flange is required to be enclosed in U-stirrups having the same size and spacing as, and spliced to, the horizontal reinforcement. The first option is utilized for this example, as shown in Figure 4-7.

  Note: Four additional longitudinal bars are shown within the intersection region of the wall in order to anchor the horizontal web reinforcement.

- Confinement reinforcement needs to be provided in the flange where the longitudinal reinforcement ratio ρ_ℓ exceeds $400/f_y$. In this example

$400/f_y = 400/60{,}000 = 0.0067$

In the intersection region of the wall, 9 #8 longitudinal bars are provided within an area of 26 × 26 = 676 in.^{2}

$$\rho_\ell = 9 \times 0.79 / 676 = 0.0105 > 0.0067$$

So, in this region, transverse reinforcement needs to be arranged such that the spacing h_x of longitudinal bars laterally supported by the corner of a crosstie or hoop leg does not exceed 14 in. around the perimeter of the region. This is shown in Figure 4-7. The vertical spacing of this transverse reinforcement cannot exceed the maximum value given in ACI 318-19 Table 18.10.6.5(b). For Grade 60 reinforcement within the same height over which the special boundary element is provided (12.67 ft), it is the lesser of

- Six times the diameter of the smallest longitudinal reinforcement = 6 × 1.0 = 6.0 in.
- 6 in.

However, a vertical spacing of 5 in. is provided to match the spacing of the other transverse reinforcement for construction efficiency.

For Grade 60 reinforcement outside of the height over which the special boundary element is provided (13.67 ft), it is the lesser of

- 8 times the diameter of the smallest longitudinal reinforcement = 8 × 1.0 = 8.0 in.
- 8 in.

Outside of the intersection region, the flange is provided with 2 #8 longitudinal bars at 14 in. spacing => ρ_ℓ = 0.0043 < 0.0067. As a result, no transverse reinforcement is required in this portion of the flange. However, at the end of the flange, a special boundary element will need to be provided based on seismic forces along the y-axis of the structure. This will need to be done in the exact same way as described above. The calculations for the seismic forces acting along y-axis are not shown, but Figure 4-7 shows the wall in its final configuration after considering seismic forces in both directions.

In addition, for comparison purposes, Figure 4-8 is provided to illustrate what the final configuration of the wall would look like if Grade 80 reinforcement is used instead of Grade 60. While Grade 60 reinforcement has a much wider application in the United States, Grade 80 reinforcement has become popular in high seismic regions of the country. As can be seen from the two figures, use of Grade 80 steel leads to a considerable reduction in the amount of reinforcement in the wall. In addition to the smaller bar sizes, lesser congestion in the special boundary elements of the wall is especially noticeable. However, the vertical spacing of the transverse hoops and cross-ties in the special boundary elements remained the same (s = 5 in.) as that in the Grade 60 design. This is because the maximum value of that spacing is limited to 6 times the diameter of the smallest longitudinal bar. So, smaller bar sizes achieved by higher strength reinforcement ironically led to a tighter spacing compared to what would be necessary for confinement alone. The vertical spacing of the horizontal shear reinforcement is also smaller than what is required for resisting shear so that it matches the spacing of transverse reinforcement in the boundary elements for construction efficiency. Thus, some of the gains achieved by using Grade 80 reinforcement are negated by various other considerations.

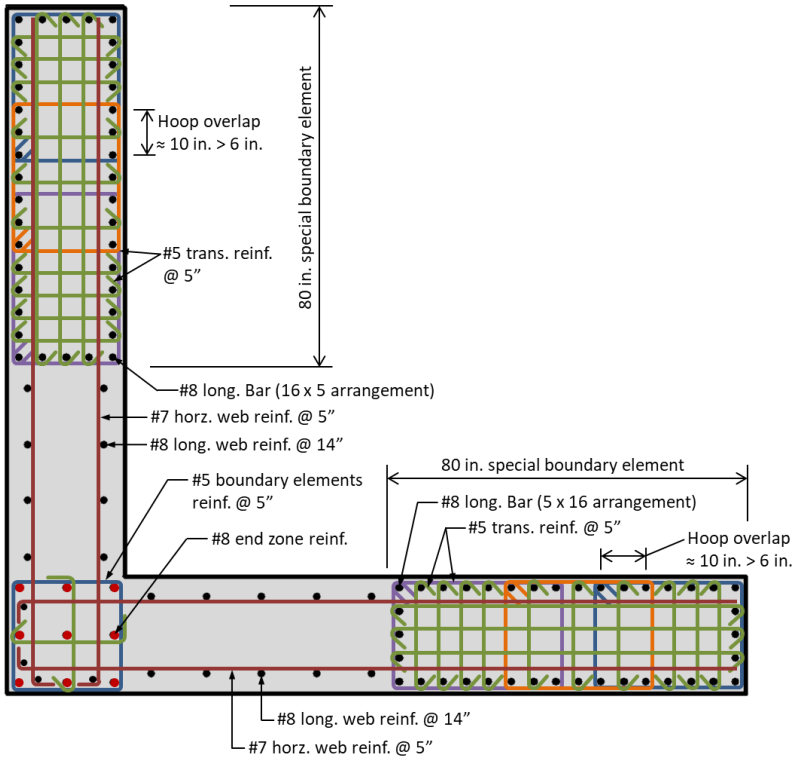

Figure 4-7. Reinforcement Details at the Critical Section of the Shear Wall Based on Seismic Forces Along x- and y-axes of the Building Using Grade 60 Reinforcement

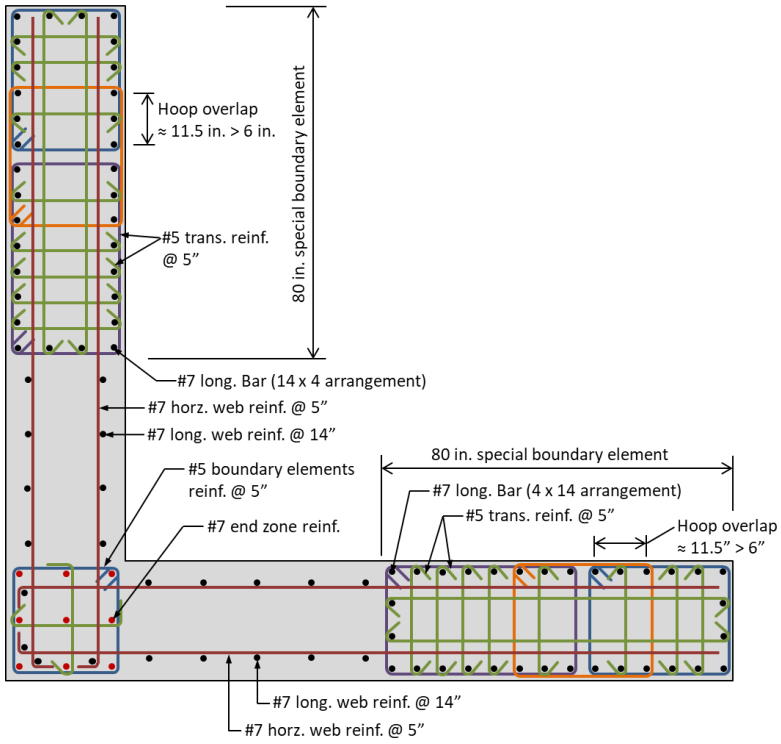

Figure 4-8. Reinforcement Details at the Critical Section of the Shear Wall Based on Seismic Forces Along x- and y-axes of the Building and Using Grade 80 Reinforcement

4.5.2.4 CHECK STRENGTH UNDER FLEXURE AND AXIAL LOADS (ACI 318-19 SECTION 18.10.5.1)

Shear walls and portions of such walls subject to combined flexural and axial loads are to be designed in accordance with ACI 318-19 Section 22.4. Boundary elements, as well as the wall web, are to be considered effective.

Figure 4-9 shows the P-M interaction diagram for the example shear wall. As can be seen, all the points representing required strength are within the design strength curve.

Also, probable moment strength M_{pr} of the final wall configuration, calculated for P_u = 10,015 kips (see Table 4-8) and using ϕ = 1.0 and $f_u = 1.25f_y$, was found to be 90,828 kip-ft. From Table 4-8, the corresponding M_u = 24,976 kip-ft. So the value Ω_v used for design shear can be recalculated as

$$M_{pr}/M_u = 90{,}828/24{,}976 = 3.64$$

This is larger than the initial value of 1.5 used before (Section 4.5.2.2 above). So, design shear V_e is recalculated as

$$V_e = \Omega_v \omega_v V_u = 3.64 \times 1.8 \times 576 = 3{,}774 \text{ kips}$$

However, V_e does not need to be taken greater than $3V_u$ (= 3 × 576 = 1,728 kips).

Thus, the design shear V_e = 1,728 kips. This is only 11% greater than what was initially estimated, and the provided reinforcement is adequate for this increase.

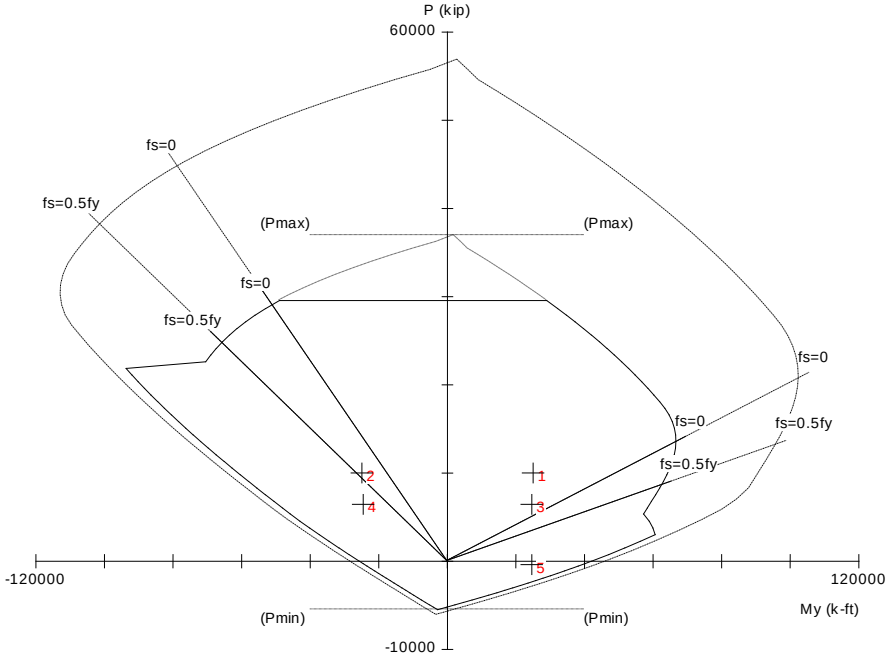

Figure 4-9. P-M Interaction Diagram for Seismic Forces Along x-axis

4.5.3 Design of Coupling Beam

A coupling beam oriented along the y-axis of the building at the second-floor level is selected for this example. The dimensions of the beam are given below:

Clear span of the beam, ℓ_n = 76 in. (6.33 ft)
Height of the beam, h = 28 in. (2.33 ft)
Width of the beam, b_w = 26 in. (2.17 ft)
ℓ_n/h = 76/28 = 2.7

Since the length to height ratio of this beam, 2.7, is less than 4 but greater than 2, per ACI 318-19 Section 18.10.7.3, this beam can be designed as a deep coupling beam using two intersecting groups of diagonally placed bars, or as a special moment frame flexural member in accordance with the ACI 318-19 Sections 18.6.3 through 18.6.5. The second option is adopted for this example.

4.5.3.1 DESIGN LOADS

The forces on this beam due to gravity loads are minimal. So, the design shear and moment are determined from the seismic forces alone. The governing forces on this beam come when the seismic forces are acting along the y-axis of the building. Those forces are shown below.

V_u = ±154 kips

M_u = ±488 kip-ft

4.5.3.2 DESIGN FOR FLEXURE

ACI 318-19 Section 18.6.3.1: Limits on flexural reinforcement

The minimum area of flexural reinforcement required for both top and bottom faces of the beam is shown below. Assuming a 1.5 in. clear cover, No. 8 bars (1 in. dia.) as longitudinal reinforcement and No. 4 bars (0.625 in. dia.) as transverse reinforcement:

Effective depth, d = 28 – 1.5 – 0.5 – 0.5 = 25.5 in.

$$A_{s,min} \geq \frac{3\sqrt{f_c'}}{f_y} b_w d = \frac{3\sqrt{8000}}{60{,}000} \times 26 \times 25.5 \quad = 2.97 \text{ in.}^2$$

...(ACI 318-19 Section 9.6.1.2(a))

$$\geq \frac{200}{f_y} b_w d = \frac{200}{60{,}000} \times 26 \times 25.5 \quad = 2.21 \text{ in.}^2$$

...(ACI 318-19 Section 9.6.1.2(b))

Also, for Grade 60 steel, the maximum area of flexural reinforcement required for both top and bottom faces of the beam is

$A_{s,max} = 0.025 b_w d = 0.025 \times 26 \times 25.5 = 16.58$ in.^{2} (ACI 318-19 Section 18.6.3.1)

Also, at least two bars should be continuous at both top and bottom (ACI 318-19 Section 18.6.3.1).

Provided flexural reinforcement and flexural strength

Try the following reinforcement:

6-#8 bars at the bottom => $A_s = 4.74$ in.^{2}
6-#8 bars at the top => $A_s = 4.74$ in.^{2}

Using *spColumn* software, the positive and negative design moment strengths (i.e., ϕM_n^+ and ϕM_n^-) at all locations of the beam were found to be

$\phi M_n = 526$ ft-kips > 488 kip-ft ..... O.K.

The same reinforcement is continued through the length of the beam. For a beam with a length of 6.33 ft, it is not worth cutting off some of the bars near midspan.

ACI 318-19 Section 18.6.3.2

At the joint face, the positive moment strength must be at least half the negative moment strength. Since the top and bottom reinforcement are the same, this is automatically satisfied.

Additionally, both the negative and the positive moment strength at any section along member length must be at least one-fourth the maximum moment strength provided at the face of either joint. Since no bar is being cut off near midspan, this requirement is also satisfied.

ACI 318 Section 18.10.9.3

In a ductile coupled shear wall, the longitudinal reinforcement needs to be developed at both ends of the beam in accordance with ACI 318-19 Section 18.10.2.5. Item (a) of that section requires that for coupling beams reinforced like a special moment frame beam, the development length of longitudinal reinforcement must be 1.25 times the values calculated for f_y in tension.

All longitudinal rebars in the beam have clear cover and clear spacing more than d_b, and the bars are developed within the highly confined special boundary element of the adjacent walls. As a result, the provisions of ACI 318-19 Section 25.4.2.3 can be used for the development length calculation.

$$\ell_d = \left(\frac{1.25 f_y \psi_t \psi_e \psi_s}{20 \lambda \sqrt{f_c'}} \right) d_b$$

$\lambda = 1.0$ for normalweight concrete
$\psi_t = 1.3$ (ACI 318-19 Table 25.4.2.5)
$\psi_e = 1.0$ (ACI 318-19 Table 25.4.2.5)

ψ_g = 1.0 (ACI 318-19 Table 25.4.2.5)

$$\ell_d = \left(\frac{1.25 \times 60{,}000 \times 1.3 \times 1.0 \times 1.0}{20 \times 1.0 \times \sqrt{8000}} \right) \times 1.0 \approx 55 \text{ in.}$$

Thus, all longitudinal rebars need to be extended into the wall web by a distance of 55 in.

4.5.3.3 MINIMUM TRANSVERSE REINFORCEMENT REQUIREMENTS

ACI 318-19 Section 18.6.4.1

End regions of the beam would exhibit cyclic inelastic response when the structure is subjected to the design seismic ground motion. As a result, confinement reinforcement is required to be provided in the coupling beam over a length of two times the total depth,

$2h$ = 2 × 28 = 56 in. from both support faces.

The first hoop is to be placed no more than 2 in. from support.

The hoop spacing must not exceed:

- $d/4$ = 25.5/4 = 6.375 in.
- 6 in.
- For Grade 60 reinforcement - six times the diameter of the smallest primary flexural reinforcing bar = 6 × 1.0 = 6 in.

Since this hoop spacing needs to be provided within 56 in. from both supports, and the total length of the coupling beam is 76 in., #4 confinement hoops are provided at 6 in. spacing over the whole length of the beam starting from 2 in. from each wall face.

4.5.3.4 DESIGN FOR SHEAR

ACI 318 Section 18.6.5.1

$V_e = \frac{M_{pr}^- + M_{pr}^+}{\ell_n}$ (gravity load effects are small on this beam, and are neglected for simplicity)

For calculating the probable flexural strength at the joint faces, the tensile stress in steel should be taken as $1.25f_y$, and the strength reduction factor ϕ is to be taken as 1.0.

With 6-#8 bars at top and bottom:

M_{pr}^+ and M_{pr}^- = 724 kip-ft

As a result,

$$V_e = \frac{M_{pr}^- + M_{pr}^+}{\ell_n} = \frac{2 \times 724}{6.33} = 229 \text{ kips}$$

ACI 318-19 Section 18.10.4.5

Before starting to determine the required shear reinforcement, it is good to check if V_e exceeds the maximum shear strength allowed for this section.

The maximum nominal shear strength, V_n, allowed for a coupling beam section is

$$10A_{cv}\sqrt{f_c'} = 10 \times 26 \times 28 \times \sqrt{8000}/1000 = 651 \text{ kips}$$

So, $\phi V_n = 0.75 \times 651 = 488$ kips > V_e

The provided coupling beam section size is acceptable.

ACI 318-19 Section 18.6.5.2

Transverse reinforcement over a beam length of 56 in. from both supports (as determined in from ACI 318-19 Section 18.6.4.1) to resist shear V_e must be determined assuming $V_c = 0$ if both the following two conditions are met:

(i) Earthquake-induced shear force $\geq 0.5V_e$
In this example, 100% of the beam shear is earthquake-induced. (Satisfied)

(ii) $P_u = 0$ kip $\leq 0.05 A_g f_c' = 0.05 \times 34 \times 24 \times 4 = 163.2$ kips (Satisfied)

Since both conditions are met, $V_c = 0$.

The shear reinforcement can be determined as follows:

$$V_s = \frac{V_e}{\varphi} - V_c$$

$$= 229/0.75 - 0 = 305 \text{ kips}$$

Required spacing of six-legged #4 stirrups,

$$s = \frac{A_v f_{yt} d}{V_s} = \frac{6 \times 0.2 \times 60 \times 25.50}{305} = 6.0 \text{ in.}$$

Provided s = 6.0 in. ....OK

Also, the shear force carried by web reinforcement, V_s, cannot exceed $8\sqrt{f_c'}\, b_w d$ (ACI 318-19 Section 22.5.1.2)

$$8\sqrt{f_c'}\, b_w d = 8 \times \sqrt{8000} \times 26 \times 25.5/1000 = 474 \text{ kips} > V_s \text{ (= 305 kips) ....OK}$$

The arrangement of beam reinforcement can be seen in Figure 4-10.

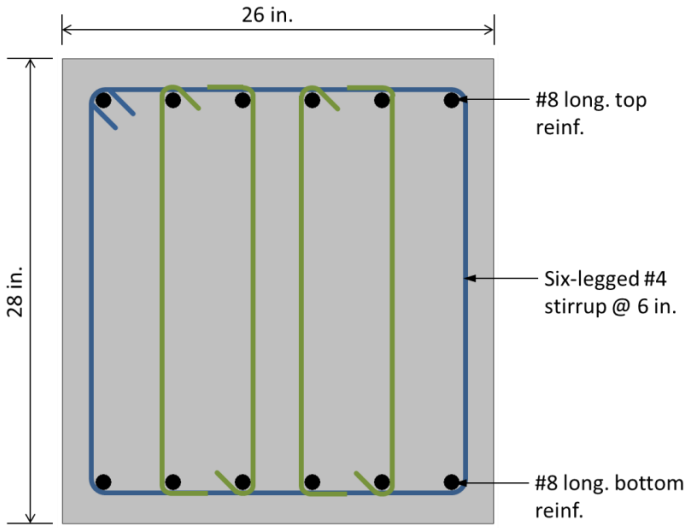

Figure 4-10. Reinforcement in a Coupling Beam at the Second Floor Level Along the y-axis of the Building

4.6 Acknowledgements

The authors are grateful to Negin Tauberg for her valuable help with Section 4.4. Much gratitude is due to Joe Ferzli and Jason Thome of Cary Kopczynski and Company, Seattle, for their great help with the design example. Bodhi Sunder Rudra of S. K. Ghosh Associates LLC is acknowledged for his outstanding help in preparing this manuscript.

4.7 References

See the "Useful Design Aid Resources" in Section 4.1 above for additional references.

Bertero, V.V., (1977). "Seismic Behavior of R/C Wall Structural Systems," Proceedings, Workshop on Earthquake-Resistant Reinforced Concrete Building Construction, University of California, Berkeley, July, pp. 323-330.

NIST (2010). *Evaluation of the FEMA P-695 Methodology for Quantification of Building Seismic Performance Factors*, Report NIST GCR-10-917-8, prepared by the NEHRP Consultants Joint Venture for the National Institute of Standards and Technology, November 15, 268 pp.

Tauberg N., Kolozvari K., Wallace J.W., (2019). *Ductile Reinforced Concrete Coupled Walls: FEMA P695 Study*, Final Report, July, 106 pp.

Chapter 5: Coupled Composite Plate Shear Walls / Concrete Filled (C-PSW/CFs) as a Distinct Seismic Force-Resisting System in ASCE/SEI 7-22

Soheil Shafaei[1] and Amit H. Varma[1]

Composite Plate Shear Wall / Concrete Filled (C-PSW/CF), also known as the SpeedCore system, is an efficient seismic force-resisting system for buildings, which was already addressed in ASCE/SEI 7-16. Coupled C-PSW/CF are more ductile and have more redundancy than uncoupled composite plate shear walls, but ASCE/SEI 7-16 did not assign them seismic design coefficients in Table 12.2-1. A FEMA P695 study was conducted to substantiate the design coefficients that should be used for such coupled C-PSW/CF structures. Adding this as a separate category in Table 12.2-1 was important because modern high-rise buildings often have elevator core wall systems; many of these core walls could utilize the coupled C-PSW/CF systems. Two line items featuring this system are now added to ASCE/SEI 7-22 Table 12.2-1 under Building Frame Systems and Dual Systems with Special Moment Frames. R = 8, C_d = 5.5, and Ω_0 = 2.5 are the design coefficients in both line items. The height limits are the same as for corresponding uncoupled isolated wall systems.

A definition for the coupled C-PSW/SF system and design and detailing requirements for it are so far not given in ANSI/AISC 341-16 (AISC, 2016a) or ANSI/AISC 360-16 (AISC, 2016b). A new Section 14.3.5 in ASCE/SEI 7-22 (ASCE, 2021) includes specific provisions for the definition and application of this coupled C-PSW/CF system, including details on the design philosophy and limits on applicability. It is anticipated that the provisions in Section 14.3.5 will ultimately end up distributed in ANSI/AISC 341-22 (AISC, 2022a) and AISC 360-22 (AISC, 2022b). Rather than construct the requirements in Section 14.3.5 to modify the applicable sections of ANSI/AISC 360-22 and ANSI/AISC 341-22, it is presented as a completely new comprehensive section in ASCE/SEI 7-22 for clarity.

This chapter outlines the above developments and presents a detailed design example illustrating the coupled C-PSW/CF seismic force-resisting system.

[1] Soheil Shafaei, Ph.D., and Amit H. Varma, Ph.D., Purdue University

5.1 Introduction

Functional and often structural requirements make the use of shear walls desirable in many buildings. Functionally, shear walls are useful in buildings because they serve as partitions between spaces. Structurally, they make buildings laterally stiff, thereby helping to keep lateral deflections within acceptable limits. Often, such walls are pierced by numerous openings for windows, doors, and other purposes. Two or more walls separated by vertical rows of openings, with beams at every floor level between the vertically arranged openings, are referred to as coupled shear walls. When a coupled shear wall system is subject to lateral loads due to wind or earthquake forces, shear forces generated at the ends of the coupling beams accumulate into a tensile force in one of the coupled wall piers and into a compression force in the other wall pier. The couple, due to these tension and compression forces, resists a part of the overturning moment at the base of the wall system, with the remainder of the overturning moment being resisted by the wall piers themselves (Figure 5-1). The ratio of the overturning moment resisted by the tension-compression couple to the total overturning moment at the base of the coupled wall system is often referred to as the degree of coupling. The shorter and deeper the coupling beams, the higher the degree of coupling. When the degree of coupling is very low, the two wall piers tend to behave like isolated walls, and when the degree of coupling is very high, the entire coupled wall system tends to behave like a shear wall with openings. It should be noted, however, that as and when inelastic displacements develop in the coupling beams, the degree of coupling tends to lose its significance.

A coupled shear wall system can be designed such that a considerable amount of earthquake energy is dissipated by flexural yielding in coupling beams before flexural hinge formations (typically) at the bases of the wall piers. Coupling beams are required to have length-to-depth ratios between three and five. Wall piers are required to have height-to-length ratios larger than or equal to four. Although such coupled wall systems are highly suitable as the seismic force-resisting systems of multistory buildings, they are not recognized as distinct entities in Table 12.2-1 of ASCE/SEI 7-16. Therefore, such systems need to be designed using *R*-values that essentially ignore the considerable benefits of having the coupling beams, which can dissipate much of the energy generated by earthquake excitation. This chapter reports on a successful effort to remedy this situation.

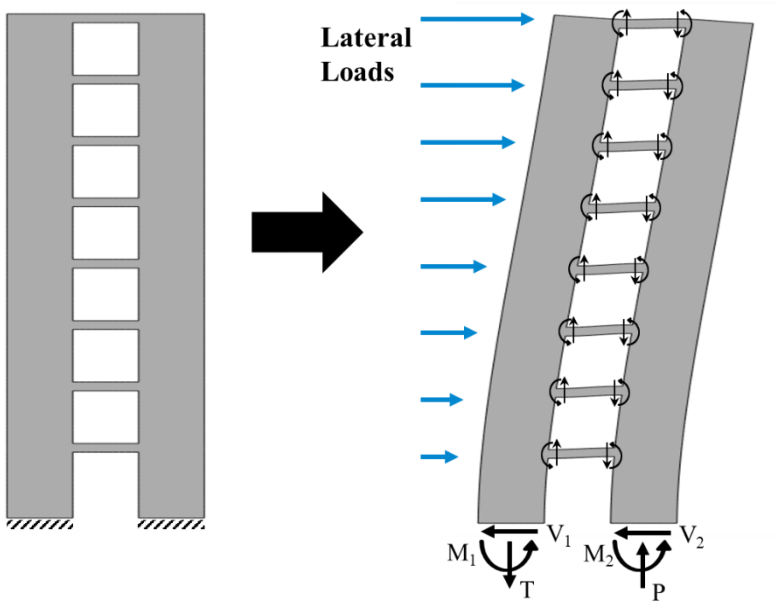

Figure 5-1. A Coupled C-PSW/CF Subjected to Lateral Loads

5.2 Coupled Composite Plate Shear Wall / Concrete Filled (C-PSW/CF) Systems

C-PSW/CFs are an alternative to conventional reinforced concrete (RC) shear walls and core wall structures in building structures. Similar to RC walls, composite walls provide the stiffness, strength, and deformation capacity needed to serve as the primary lateral force-resisting system. C-PSW/CFs may be used as the elevator core structure or as individual shear walls in building structures. Two versions are possible: uncoupled and coupled. In a given building structure, it is possible to have coupled system in one direction and uncoupled system in the orthogonal direction.

The coupled C-PSW/CF system consists of: (i) composite C-PSW/CFs and (ii) composite coupling beams. Both the composite walls and composite coupling beams consist of a concrete core sandwiched between two steel plates that serve as the primary reinforcement, completely replacing conventional rebars. Figure 5-2(a) shows a typical C-PSW/CF with its components. Tie bars connect the two steel plates together and provide stability during transportation and construction activities. After concrete casting, the tie bars become embedded in the concrete infill and provide composite action between the steel and concrete. The coupling beams are built-up steel box sections with concrete infill. Figure 5-2(b) shows a composite coupling beam. Similar to the composite walls, the built-up steel section provides primary reinforcement to the coupling beam. The empty steel modules, including both the walls and the coupling beam components, are typically fabricated in the shop, transported to the site, erected, and filled with concrete. The composite walls can be planar, C-shaped, or I-shaped, following the typical geometric configurations of conventional concrete core walls.

It is important to note that there are no additional reinforcing bars needed in either the C-PSW/CFs or the composite coupling beams. The empty steel modules are filled with plain concrete, which is usually self-compacting concrete (SCC). There are no temperature and shrinkage concerns related to strength. The effects of concrete cracking due to locked-in shrinkage strain are included in the stiffness equations. The steel plates provide all the reinforcement needed to resist forces. The steel modules, including the plates, tie bars, and shear studs (if used), are pre-fabricated in the shop and shipped to the field for assembly and erection. The modular steelwork serves as formwork for the concrete infill and falsework for construction activities. Generally, the steel parts come without painting, but after assembly, they might be painted or fireproofed, if needed (Anvari et al. 2020). Commercial interest in the coupled C-PSW/CF system is motivated by these potential advantages of modularity, construction schedule, and overall project economy. In addition, another benefit of using C-PSW/CFs is that they are thinner than corresponding reinforced concrete shear walls, providing more available floor area.

The composite walls are required to have height-to-length (h_w/L_w) ratio greater than or equal to 4.0. This requirement is specified to ensure that the walls are flexure critical, i.e., flexural yielding and failure governs behavior rather than shear failure. Calculations can also be performed to show that the wall is flexure critical, i.e., plastic hinges (with expected flexural capacity) form at the base of the walls before shear failure occurs. The shortest archetype structure that was evaluated using the FEMA P695 approach for this system was three stories with two 45 feet tall composite walls with 10-foot length (Bruneau et al. 2019), corresponding to a height-to-length ratio equal to 4.5 for each wall.

The composite coupling beams are also required to be flexure critical, i.e., flexural yielding and failure governs behavior rather than shear failure. Calculations can be performed to show that the composite beam is flexure critical, i.e., plastic hinges (with expected flexural capacity) form at the ends of the beams before shear failure occurs. For at least 90% of the stories of the building, composite coupling beams are also required to have clear length-to-section depth ratios greater than or equal to 3.0 and less than or equal to 5.0, i.e, $3.0 \leq L/d \leq 5.0$. This requirement is specified based on the range of parameters included in the FEMA P695 studies conducted to establish the seismic factor (*R* etc.) for the system.

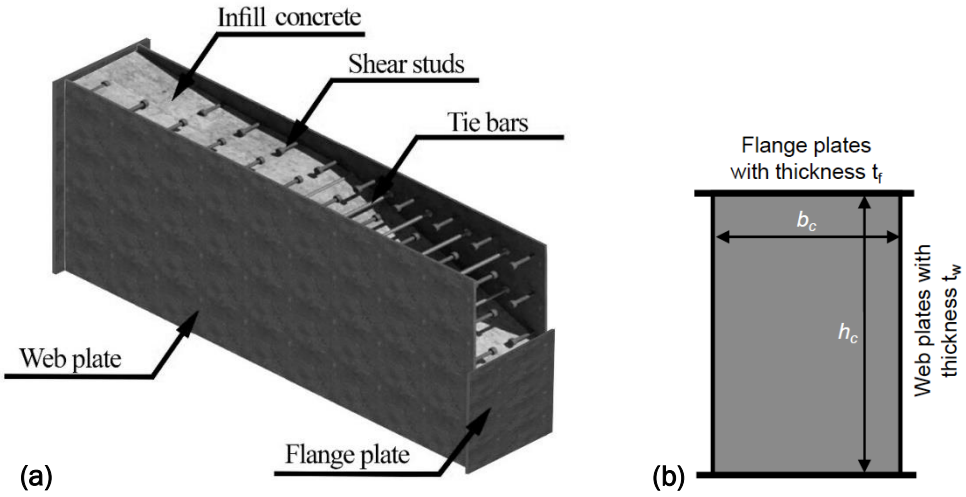

Figure 5-2. Components of: (a) C-PSW/CF (Shafaei et al. 2021b), and (b) Composite Coupling Beam

5.3 Coupled C-PSW/CF System in ASCE/SEI 7-22

Issue Team (IT) 4 of the Provisions Update Committee (PUC) of the Building Seismic Safety Council (BSSC) developed a proposal that led to the addition of two line items to ASCE/SEI 7-22 Table 12.2-1, Design Coefficients and Factors for Seismic Force-Resisting Systems, featuring the steel and concrete coupled composite plate shear walls (Table 5-1). The line items will be under: B. Building Frame Systems, and D. Dual Systems with Special Moment Frames.

Note: The coupled C-PSW/CF system is called “Steel and concrete coupled composite plate shear walls” in ASCE/SEI 7-22; however, “Coupled Composite plate shear walls / concrete filled” (coupled C-PSW/CF) name is used for this coupled system in ANSI/AISC 341-22 and AISC Design Guide 37.

Table 5-1. Addition of Coupled C-PSW/CF to ASCE/SEI 7-22 Table 12.2-1

Seismic Force-Resisting System	ASCE/SEI 7-22 Section Where Detailing Requirements Are Specified				Structural System Limitations Including Structural Height, (ft) Limits[d]				
					Seismic Design Category				
					B	C	D[e]	E[e]	F[f]
…									
B. BUILDING FRAME SYSTEMS									
…									
26. Steel special plate shear walls	14.1	7	2	6	NL	NL	160	160	100
27. Steel and concrete coupled composite plate shear walls	14.3	8	2½	5½	NL	NL	160	160	100
…									
D. DUAL SYSTEMS WITH SPECIAL MOMENT FRAMES CAPABLE OF RESISTING AT LEAST 25% OF PRESCRIBED SEISMIC FORCES									
…									
13. Steel special plate shear walls	14.1	8			NL	NL	NL	NL	NL
14. Steel and concrete coupled composite plate shear walls	14.3	8	2½	5½	NL	NL	NL	NL	NL

Based on a FEMA P695 study, R = 8, C_d = 8, and Ω_o = 2.5 have been adapted in all the line items. The height limits are the same as for corresponding uncoupled isolated wall systems, eccentrically braced frames, steel special concentrically braced frames, steel buckling-restrained braced frames, and steel special plate shear walls. It will be possible to increase the 160-ft height limit to 240 ft for buildings without significant torsion because ASCE/SEI 7-22 Section 12.2.5.4 has been made applicable to these systems.

ASCE/SEI 7-22 Section 14.3.5 includes detailed requirements for the coupled C-PSW/CF system and its components, including the composite walls, composite coupling beams, and various connections, splices etc. These include:

1. A detailed discussion of the scope of coupled C-PSW/CF system along with dimensional constraints and geometric requirements.

   (a) For example, the wall height-to-length (h_w/L_w) ratio is required to be greater than 4 to achieve flexure critical behavior.

   (b) The composite coupling beam clear length-to-section depth ratios are limited to values between 3.0 and 5.0 for at least 90% of the stories along the structure height to achieve flexure critical behavior.

2. The basis of design is that the coupled C-PSW/CF system, designed in accordance with the requirements of ASCE/SEI 7-22, provides significant inelastic deformation capacity through flexural plastic hinging in the composite coupling beams and through flexural yielding at the bases of the composite walls, as shown in Figure 5-3. Figure 5-3(b) shows typical milestones of the pushover behavior of a coupled C-PSW/CF including (a) flexural yielding of coupling beams (Point A), (b) formation of plastic hinges in coupling beams and flexural yielding of C-PSW/CF (Point B), (c) formation of plastic hinges in C-PSW/CFs at the base and fracture initiation in coupling beams (Point C), and (d) fracture initiation in C-PSW/CFs (Point D).

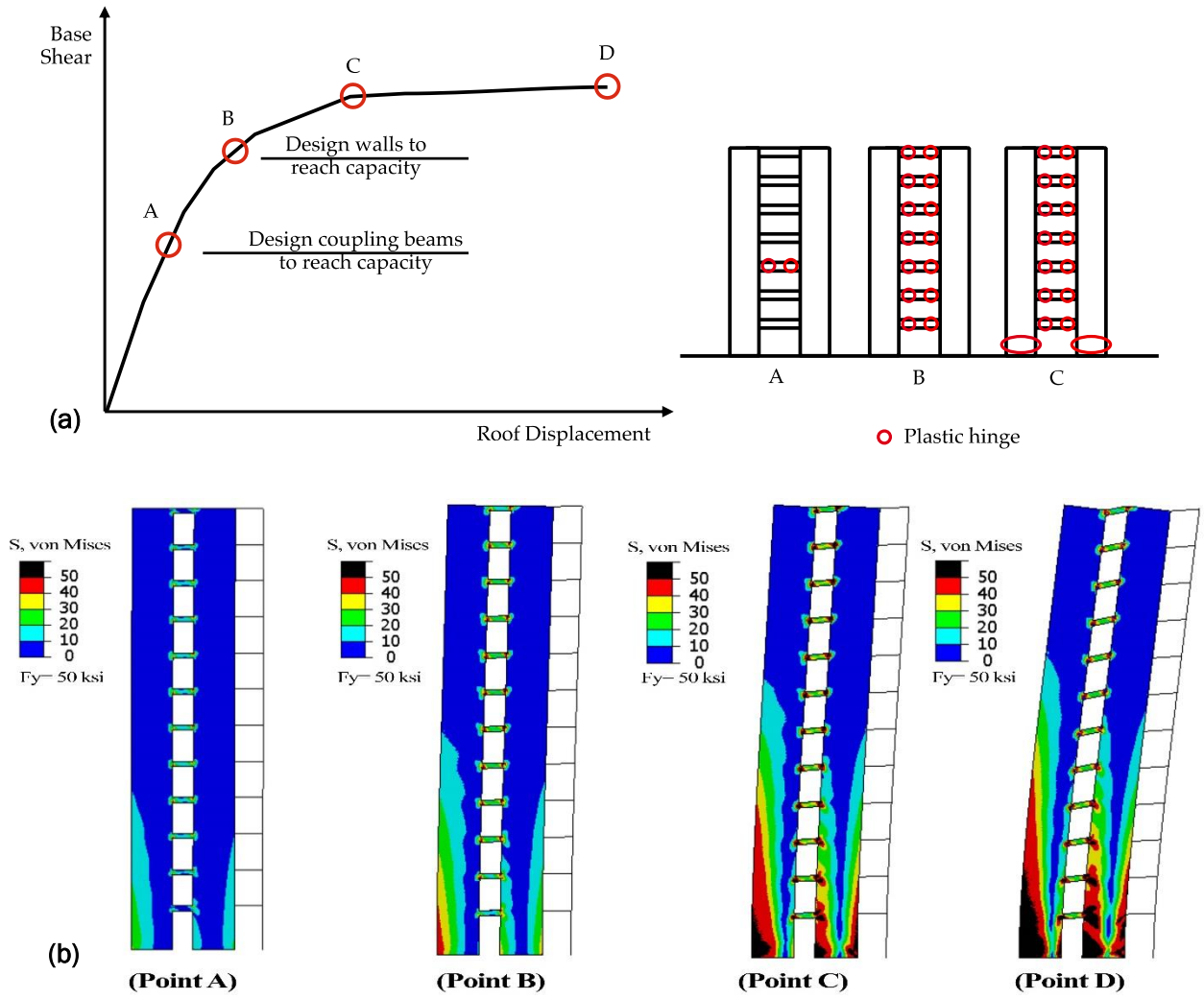

Figure 5-3. (a) Desired Pushover Response of Designed Coupled C-PSW/CFs (AISC Design Guide 37) (b) A Typical Pushover Response of Coupled C-PSW/CF using 2D Finite Element Modeling (Shafaei et al. 2022)

3. For conducting elastic analysis, the stiffnesses of composite walls and coupling beams can be estimated by section analysis accounting for the effects of concrete cracking or be based on recommendations provided in the ASCE/SEI 7-22 commentary or AISC 360-22.

4. The coupling beams are sized for code-level seismic forces and intended to yield before flexural yielding of C-PSW/CFs at the base, as shown in Figure 5-3 (Point A). The required strengths for the C-PSW/CFs are determined using the capacity-limited seismic load effect, which is marked as "Point B" in Figure 5-3. In other words, the C-PSW/CFs are designed for amplified seismic forces corresponding to the formation of the plastic hinges in all coupling beams along the height of wall, as shown in Figure 5-3 (Point B).

5. The required shear strengths for the composite walls are amplified by a factor of 4 to account for higher mode effects, overstrength in the walls resulting from expected material properties and strain hardening. For reinforced concrete walls, this amplification factor is about 2-3 (ACI 318-19 Section 18.10), but a conservative value of 4 was used for composite walls in the absence of better information and in recognition of their inherent (significant) composite shear strength.

6. Design and detailing requirements for composite walls are specified, including minimum and maximum area of steel, plate slenderness requirement resulting in maximum spacing of ties and/or shear studs, and tie spacing requirements based on considerations of empty module behavior during construction and concrete casting.

7. Design and detailing requirements for composite coupling beams are specified, including minimum and maximum area of steel, flange and web slenderness requirements, and flexure critical requirements.

8. Equations for calculating the design strength of composite walls in tension, compression, shear, and flexure are specified in ANSI/AISC 341-22. The design strength of composite walls subjected to combined axial force and flexure can be calculated using methods specified in ANSI/AISC 341-22 Chapter H8, Section 6d.

9. Equations for calculating the shear strength of composite coupling beams are specified, and the flexural strength is calculated using methods in ANSI/AISC 341-22 Chapter H8, Section 7.

10. Requirements for the coupling beam-to-wall connections are specified. These include requirements for developing the expected flexural and shear strength at the coupling beam ends and provide a rotation capacity of 0.030 rad. before flexural strength decreases to 80% of the flexural plastic strength of the coupling beam.

11. Requirements for composite wall-to-foundation connections are specified. These include the required strengths for the composite wall-to-foundation connections based on the capacity-limited seismic load effect.

12. Requirements for protected zones in the composite walls and coupling beam are specified, and requirements for demand critical welds in various splices and connections are specified.

5.4 FEMA P695 Studies Involving Coupled C-PSW/CFs

The FEMA P695 studies conducted on coupled C-PSW/CFs are summarized in Kizilarslan et al. (2021a). Since the coupled C-PSW/CF system is relatively new, this FEMA P695 study was performed using two different sets of nonlinear hysteretic models (Kizilarslan et al. 2021b) using OpenSees software: (i) distributed plasticity fiber models (Model 1) for both the composite walls and coupling beams, and (ii) distributed plasticity fiber models (Model 2) for the composite walls but concentrated plasticity models for the coupling beams. Both sets of models were calibrated extensively against experimental results, as detailed in Bruneau et al. (2019). Distributed plasticity fiber models were developed using effective stress-strain curves proposed by Shafaei et al. 2021a, which were developed based on detailed 3D finite element models of tested C-PSW/CF specimens. Both sets of models implicitly account for various limit states and failure modes, including steel

yielding, local buckling, cyclic hysteresis, low-cycle fatigue and fracture, and concrete tension cracking, compression inelasticity and crushing, effects of confinement, and cyclic hysteretic crack opening-closing behavior with damage (Shafaei et al. 2021a).

The archetype structures focused on low-rise to mid-rise buildings (8-22 stories). The design space is divided into performance groups for the FEMA P695 study. The performance groups are differentiated based on basic configuration, design load level, and structure period. Two structural configurations under two seismic load levels were evaluated. These correspond to four performance groups (PG) with 16 archetypes designed and analyzed. The structure height governed the wall configuration of the archetypes as shown in Table 5-2. Three different coupling beam clear length-to-section depth ratios (L/d = 3, 4, and 5) were considered. The resulting details of the archetype structures are provided in Kizilarslan et al. (2021a) and not repeated here.

Table 5-2. Archetype Performance Group Summary Table

Case	Basic Configuration	Seismic Design Category (SDC)	No. Stories	*L*/*d*	Performance Group
PG-1A	Type I (Planar)	D_{max} (S_{DS}=1.0*g* and S_{D1}=0.6*g*)	8	3	1
PG-1B				4	1
PG-1C				5	1
PG-2B	Type I (Planar)	D_{min} (S_{DS}=0.5*g* and S_{D1}=0.2*g*)	8	4	2
PG-1D	Type I (Planar)	D_{max} (S_{DS}=1.0*g* and S_{D1}=0.6*g*)	12	3	1
PG-1E				4	1
PG-1F				5	1
PG-2E	Type I (Planar)	D_{min} (S_{DS}=0.5*g* and S_{D1}=0.2*g*)	12	4	2
PG-3A	Type II (C-shaped)	D_{max} (S_{DS}=1.0*g* and S_{D1}=0.6*g*)	18	3	3
PG-3B				4	3
PG-3C				5	3
PG-4B	Type II (C-shaped)	D_{min} (S_{DS}=0.5*g* and S_{D1}=0.2*g*)	18	4	4
PG-3D	Type II (C-shaped)	D_{max} (S_{DS}=1.0*g* and S_{D1}=0.6*g*)	22	3	3
PG-3E				4	3
PG-3F				5	3
PG-4E	Type II (C-shaped)	D_{min} (S_{DS}=0.5*g* and S_{D1}=0.2*g*)	22	4	4

Both the nonlinear hysteretic modeling approaches were used independently to conduct a detailed evaluation of the archetype structures in accordance with the FEMA P695 methodology.

1. Nonlinear pushover analyses were conducted to estimate the overstrength and period-based ductility for all archetypes.
2. Incremental dynamic analyses (IDA) were conducted by gradually scaling up ground motions from low to high magnitude until collapse. The default 44 far-field ground motions specified by FEMA

P695 were considered and scaled appropriately for the archetype structures such that the median spectral acceleration of the 44 ground motions matched that at the design basis earthquake and maximum considered earthquake spectral acceleration levels.

3. For the coupled C-PSW/CF system, collapse was defined conservatively at 5% drift ratio. The archetype structure had much more reserve capacity, but at the recommendation of the provisions update committee and the recognition that extensive nonstructural damage could occur, 5% drift ratio was used conservatively to define collapse of the coupled C-PSW/CF system.
4. The results from the IDA were used to estimate the collapse margin ratio (CMR) values as the ratio of the median collapse spectral acceleration $\hat{S}_{CT}$ to the median spectral acceleration S_{MT} for all the archetypes. The CMR values were adjusted to consider the frequency content of the selected ground motions records and calculate the adjusted collapse margin ratios (ACMR).
5. FEMA P695 specifies $ACMR_{20\%}$ and $ACMR_{10\%}$ (acceptable adjusted collapse margin ratio for 20% and 10% collapse probability under MCE ground motions) as the acceptable threshold values to evaluate the performance of individual archetypes and average performance of several archetypes in a performance group. These threshold values depend on the total system collapse uncertainty, which is a composite of uncertainty factors associated with ground motions, design requirements, test data, and nonlinear modeling. Using the values for "good" rating given in FEMA P695, the $ACMR_{20\%}$and $ACMR_{10\%}$ are 1.96 and 1.56, respectively.
6. Results from the two independent FEMA P695 investigations are reported in Table 5-3. All the individual 8-, 12-, 18- and 22-story archetypes passed the $ACMR_{20\%}$ threshold (1.96) with a significant margin. Additionally, the average of the ACMR values in a performance group also passed the $ACMR_{10\%}$ threshold (1.56) with a significant margin. Even if values given for "poor" rating given in FEMA P695 were used, the ACMR values for the individual archetypes and the performance groups would still exceed the recalculated $ACMR_{20\%}$ and $ACMR_{10\%}$ thresholds.
7. Nonlinear Model 2 has a lower rotation capacity in the coupling beam-to-wall connections than Nonlinear Model 1. The coupling beam ends in Nonlinear Model 2 were modeled using concentrated plastic hinges that used envelopes of cyclic moment-rotation behavior that were marginally passing the connection rotation requirements (Kizilarslan et al. 2021).

Table 5-3. Summary of FEMA P695 Results for Archetypes by Performance Group

Perf. Group	Case	No. Stories	Nonlinear Model 1					Nonlinear Model 2				
			Pushover		IDA			Pushover		IDA		
			Ω_o	μ_T	CMR	ACMR	ACMR Avg.	Ω_o	μ_T	CMR	ACMR	ACMR Avg.
1	PG-1A	8	2.22	7.03	3.70	4.63	4.27	2.1	10.0	2.57	3.24	3.87
	PG-1B		2.14	7.84	3.03	3.82		2.0	12.0	2.44	3.10	
	PG-1C		1.96	8.50	2.77	3.55		2.1	12.7	2.61	3.35	
	PG-1D	12	2.33	5.89	3.10	4.05		2.3	7.5	3.57	4.68	
	PG-1E		2.33	6.54	3.78	4.95		2.3	10.3	3.44	4.51	
	PG-1F		2.15	6.88	3.50	4.62		2.1	11.3	3.31	4.37	
2	PG-2B	8	2.05	10.68	3.91	4.73	5.22	1.7	10.8	5.11	6.18	6.70
	PG-2E	12	2.13	7.86	4.72	5.71		2.3	7.7	5.48	7.21	
3	PG-3A	18	2.19	6.92	4.13	5.45	6.58	2.0	4.1	2.21	2.95	2.60
	PG-3B		2.38	8.14	3.84	5.07		2.1	4.9	1.85	2.45	
	PG-3C		2.23	9.85	3.60	4.75		2.0	5.6	1.79	2.14	
	PG-3D	22	2.55	5.29	4.94	6.52		2.1	3.5	2.11	2.78	
	PG-3E		2.31	5.94	6.65	8.78		2.0	4.6	1.98	2.64	
	PG-3F		2.38	7.90	6.74	8.90		2.2	4.9	2.01	2.64	
4	PG-4B	18	2.22	10.21	7.43	8.99	8.49	2.3	4.8	3.55	4.24	4.24
	PG-4E	22	1.89	6.47	6.60	7.99		2.6	3.4	3.73	4.24	

Results from the FEMA P695 evaluations of the 3-22 story archetypes indicate that the initial *R*-factor of 8 used to design is adequate. The system overstrength factor is quite close to 2.5. Additionally, the C_d factor was assessed using the ratio of a median value of nonlinear inelastic drift ratios at design-basis shaking (δ_{in}) to the design level drifts (δ_e) from equivalent lateral force analysis. The stiffness values for estimating δ_e were based on the recommendations included in ASCE/SEI 7-22 Section 14.3.5 and in AISC 360-22. The C_d factor of 5.5 was deemed to be adequate for design.

5.5 Design of Coupled C-PSW/CF System

5.5.1 Overview

This example illustrates a seismic design of an 18-story office building using a coupled C-PSW/CF system according to ASCE/SEI 7-22. The steps followed in this design are in accordance with the design procedure presented in the 2020 *Provisions* (2020) and AISC Design Guide 37 (AISC, 2021). The 18-story office building is designed for typical design loads, floor geometry, and high seismic design loads.

In addition to the *2020 Provisions* and ASCE/SEI 7-22, the following documents are either referred to directly or may serve as useful design aids.

Useful Design Aid Resources

AISC (2016a). *Seismic Provisions for Structural Steel Buildings*, ANSI/AISC 341-16, American Institute of Steel Construction.

AISC (2016b). *Prequalified Connections for Special and Intermediate Steel Moment Frames for Seismic Applications*, ANSI/AISC 358-16, American Institute of Steel Construction.

AISC (2016c). *Specification for Structural Steel Buildings*, ANSI/AISC 360-16, American Institute of Steel Construction.

AISC (2017). *Steel Construction Manual, 15th Edition*, American Institute of Steel Construction.

AISC (2021), *Design of Composite Plate Shear Walls / Concrete Filled (C-PSW/CF)*, AISC Design Guide 37, American Institute of Steel Construction.

AISC (2022a). *Seismic Provisions for Structural Steel Buildings*, ANSI/AISC 341-22, Committee on Specifications, American Institute of Steel Construction, Chicago, Illinois [under development].

AISC (2022b). *Specification for Structural Steel Buildings*, ANSI/AISC 360-22, Committee on Specifications, American Institute of Steel Construction, Chicago, Illinois, [under development].

Broberg, M., Shafaei, S., Kizilarslan, E., Seo, J., Varma, A. H., Bruneau, M. and Klemencic, R. (2022). "Capacity Design of Coupled Composite Plate Shear Walls – Concrete Filled (CC-CPSW/CF)," *Journal of Structural Engineering*, ASCE, Accepted.

Bruneau., M., Varma, A.H., Kizilarslan, E., Broberg, M., Shafaei, S., Seo, J. (2019). "*R*-Factors for Coupled Composite Plate Shear Walls—Concrete Filled (Coupled-C-PSW/CF)," *Final Project Report, Charles Pankow Foundation*, CPF #06-16, McLean, Virginia, 419 p.

Kizilarslan, E., Broberg, M., Shafaei, S., Varma, A.H., Bruneau., M., (2021a). "Seismic Design Coefficients and Factors for Coupled Composite Plate Shear Walls, Concrete Filled (Coupled-C-PSW/CF)," *Engineering Structures*, 244, 112766. https://doi.org/10.1016/j.engstruct.2021.112766

Kizilarslan, E., Broberg, M., Shafaei, S., Varma, A. H., & Bruneau, M. (2021b). "Non-linear analysis models for Composite Plate Shear Walls-Concrete Filled (C-PSW/CF)," *Journal of Constructional Steel Research*, 184, 106803. https://doi.org/10.1016/j.jcsr.2021.106803

Shafaei, S., Varma, A. H., Broberg, M., and Klemencic, R. (2021a). "Modeling the Cyclic Behavior of Composite Plate Shear Walls/Concrete Filled (C-PSW/CF)," *Journal of Constructional Steel Research*, 184, 106810. https://doi.org/10.1016/j.jcsr.2021.106810

Shafaei, S., Varma, A.H., M., Seo, J., and Klemencic, R. (2021b). "Cyclic Lateral Loading Behavior of Composite Plate Shear Walls / Concrete Filled (C-PSW/CF)," *Journal of Structural Engineering*, 147(10), 04021145. https://doi.org/10.1061/(ASCE)ST.1943-541X.0003091.

5.5.2 Building Description

Figure 5-4 shows the floor plan of the office building with 120 ft length and 100 ft width (a total of 12,000 square feet of area per floor). Coupled L-shaped Composite Plate Shear Walls / Concrete Filled (C-PSW/CFs) are used to resist seismic loads in north-south and east-west directions. Steel gravity frames are placed around the coupled C-PSW/CFs, and elevators and stairs are located inside the core walls, as shown in Figure 5-4. The composite metal deck floor is also used for the floor system design of the gravity frames, which is a typical gravity system associated with a C-PSW/CF. This example presents the seismic design of coupled C-PSW/CF in an east-west direction.

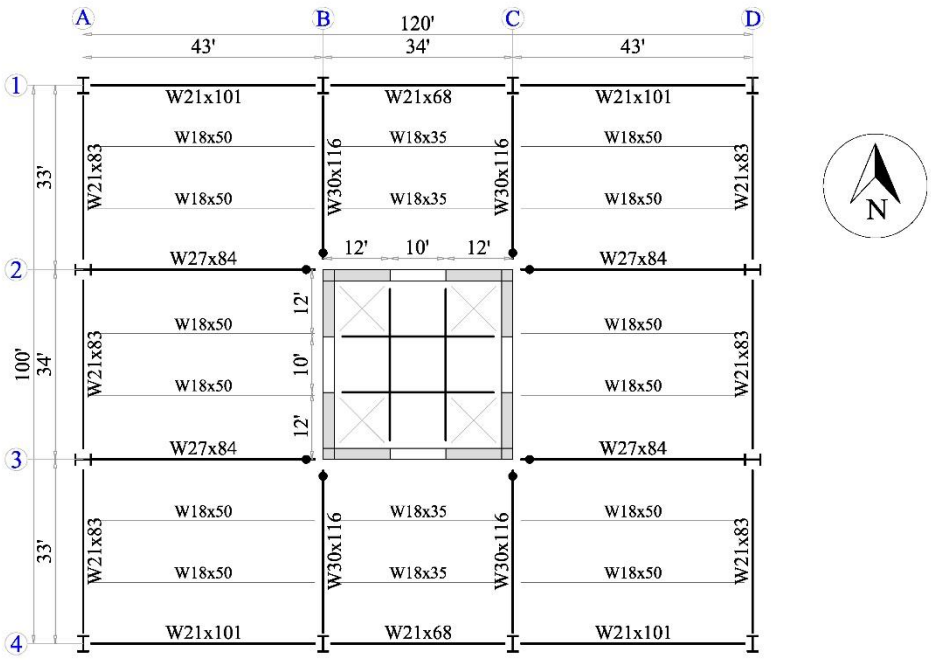

Figure 5-4. Typical Plan of 18-story Building Using a Coupled C-PSW/CF System

Figure 5-5 shows the section view of the coupled C-PSW/CF with perimeter steel gravity frames (Grid 3). The first story height is 17 feet, and the typical story height is 13 feet. Lengths of each L-shaped

wall and coupling beam are 12 and 10 feet, respectively, which result in a total length of 34 feet for core system.

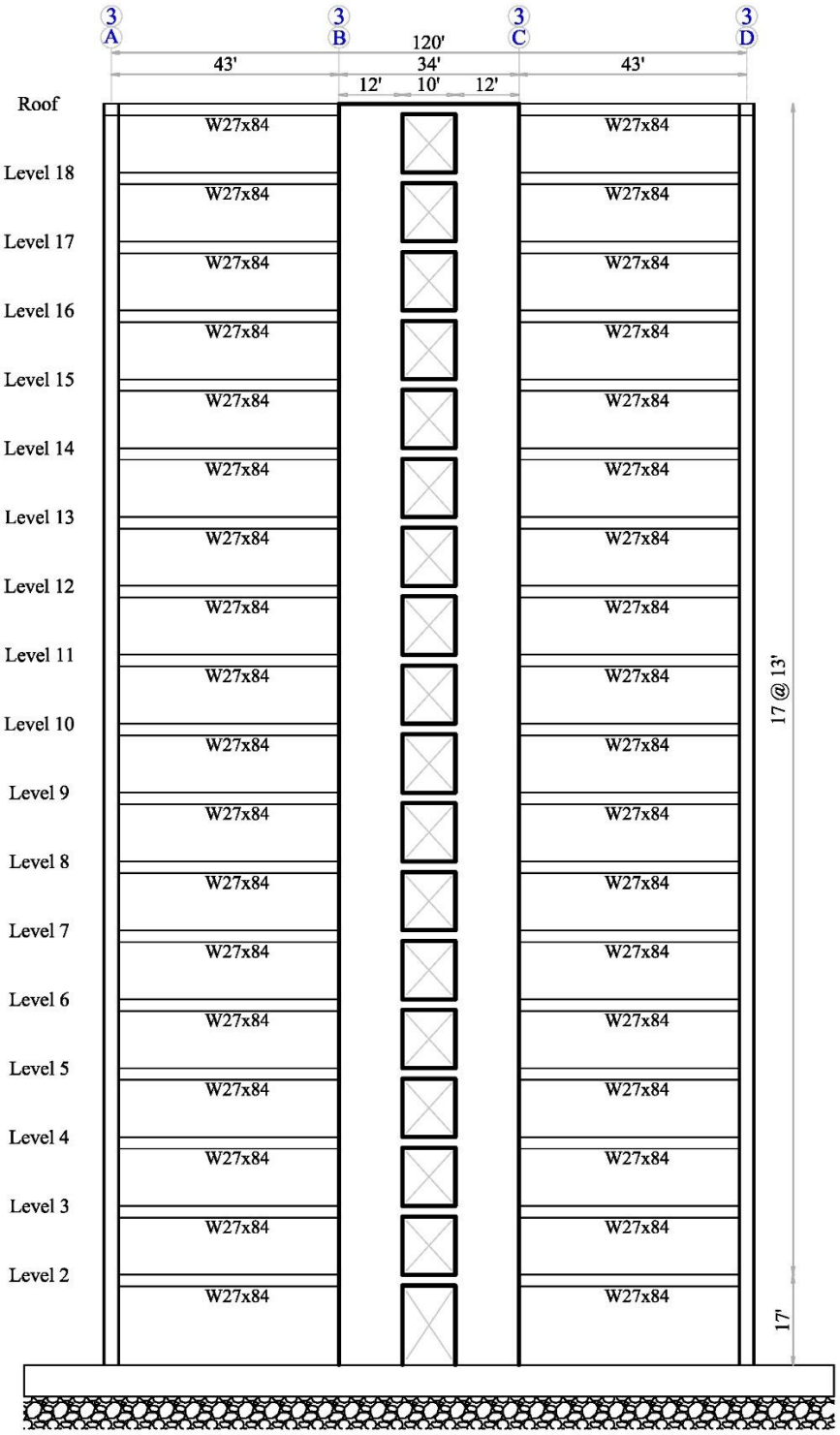

Figure 5-5. Section View of Coupled C-PSW/CF and Steel Gravity Frames on Gridline 3

5.5.3 General Information of the Considered Building

5.5.3.1 MATERIAL PROPERTIES

ASTM A572 Grade 50 steel (steel plates), ASTM A992 Grade 50 steel (wide flange sections), and self-compacting concrete (SCC) are used in the design of this 18-story building. SCC has a flowability from 19 in. to 30 in., which is measured by a slump flow test. SCC is typically used for the construction of the C-PSW/CF system, as it has a good segregation resistance and does not require vibration. The material properties are as follows:

Steel

F_y = 50 ksi
F_u = 65 ksi
E_s = 29,000 ksi
G_s = 11,500 ksi
R_y = 1.1 (ANSI/AISC 341-16 Table A3.1)

Concrete

f'_c = 6 ksi
E_c = 4,500 ksi
G_c = 1,770 ksi
R_c = 1.5 (ANSI/AISC 341-16 H5-5)

5.5.3.2 LOADS

In addition to the self-weight of structure (gravity frames and core walls), the following loads are considered:

Floor live load = 50 psf (reducible)

Partition = 15 psf

Superimposed dead load (ceiling and floor finish) = 15 psf

Curtain wall = 15 psf (wall surface area)

5.5.3.3 LOAD COMBINATIONS

For the considered structure, load combinations provided in Chapter 2 of ASCE/SEI 7-22 are considered.

$1.4D$
$1.2D + 1.6L$ (or $0.5L_r$)
$1.2D + 0.5L \pm 1.0E$
$0.9D \pm 1.0E$

5.5.3.4 BUILDING SEISMIC WEIGHT

A 3D computer model of the building was developed using the ETABS software program, as shown in Figure 5-6, for the design of steel gravity frames. Based on the preliminary design of gravity frames, as shown in Figure 5-4, the self-weight of structure is calculated. Building seismic weight is calculated as follows.

First Story

Gravity frames (columns, beams, girders, composite slab, etc.) and C-PSW/CFs	= 1,276 kips
Superimposed dead load	= 180 kips
Curtain wall	= 99 kips
Total weight	= **1,555 kips**

Typical Story

Gravity frames (columns, beams, girders, composite slab, etc.) and C-PSW/CFs	= 1,174 kips
Superimposed dead load	= 180 kips
Curtain wall	= 86 kips
Total weight	= **1,440 kips**

Roof

Gravity frames (columns, beams, girders, composite slab, etc.) and C-PSW/CFs	= 999 kips
Superimposed dead load	= 180 kips
Curtain wall, including parapet	= 54 kips
Total weight	= **1,263 kips**

Total seismic weight of the building is 25,855 kips.

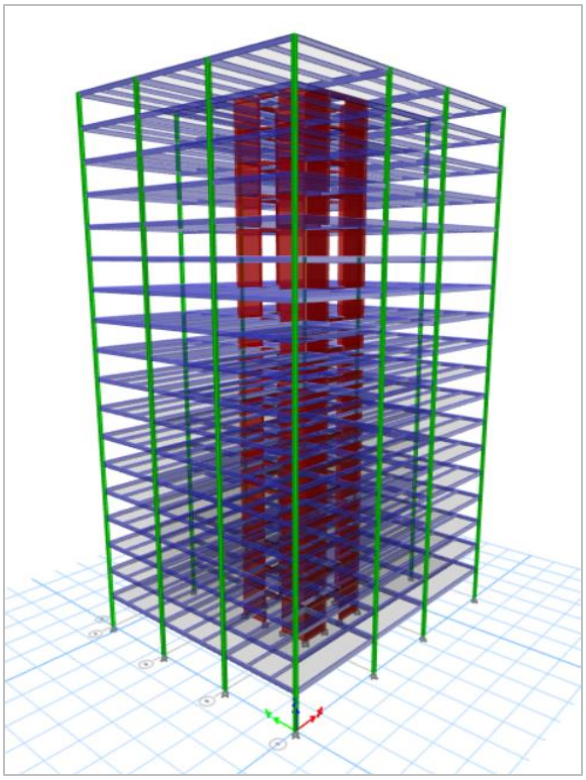

Figure 5-6. 3D View of ETABS Model Used for Designing Steel Gravity Frames

5.5.3.5 SEISMIC DESIGN PARAMETERS

The seismic design parameters of this example are as follows:

S_{DS} = 1.101g
S_{D1} = 0.650g
Site Class D
Seismic Importance Factor, I_e = 1.0 (Risk Category II)
Seismic Design Category D

Coupled C-PSW/CFs are used in both directions to resist seismic loads, as shown in Figure 5-4. The seismic redundancy factor (ρ) is 1.0 (ASCE/SEI 7-22 Section 12.3.4.2). In accordance with the 2020 Edition of the *NEHRP Recommended Seismic Provisions* and upcoming ASCE/SEI 7-22, the proposed response modification factor (R), deflection amplification factor (C_d), and over-strength factor (Ω_o) for a coupled C-PSW/CF are following:

R = 8
Ω_0 = 2.5
C_d = 5.5
ρ = 1

In seismic design, ASCE/SEI 7-22 requires considering the accidental torsion in each direction when the building has a horizontal irregularity. In this design example, no accidental torsion and eccentricity are present in the structure; therefore, the seismic design of the coupled C-PSW/CF was performed without including accidental eccentricity.

5.5.3.6 SEISMIC FORCES

The period of the structure is calculated according to Section 12.8.2 of ASCE 7 standard. The approximate fundamental period of the structure is calculated as 1.21 seconds, shown below, using the "all other structural systems" category:

$T_a = C_t \boldsymbol{h_n^x}$ = (0.020) (238 ft)$^{0.75}$ = 1.21 seconds (ASCE/SEI 7-22 Eq. 12.8-7)

The approximate fundamental period is generally lower in a detailed computational model; therefore, an upper limit on the period recommended by ASCE/SEI 7-22 is required:

C_u = 1.4 (ASCE/SEI 7-22 Table 12.8-1)

$T = C_u T_a$ = (1.4) (1.21) = 1.70 seconds

The period of the structure is also estimated using a detailed 3D computer model developed in ETABS software program. The computed period of 3D ETABS model is 1.87 seconds, which is higher than the upper limit. Therefore, the period of the structure is considered to be the upper limit, C_uT_a=1.70 seconds, for the calculation of seismic forces.

There are no irregularities along the height of the structure, and the building floor plan is symmetric. In this example, the Equivalent Lateral Forces (ELF) procedure was used to calculate the seismic loads. The design base shear of the building is calculated using ASCE/SEI 7-22 Equation 12.8-1, where *W* is the total seismic weight calculated in Section 5.5.3.4 0. The calculations of ELF for the considered building are illustrated as follows:

$V = C_s W$ (ASCE/SEI 7-22 Eq. 12.8-1)

Seismic response coefficient, C_s, is estimated according to ASCE/SEI 7-22 Section 12.8.1.1.

$$C_S = \frac{S_{DS}}{R/I_e} = \frac{1.101}{8/1} = 0.138$$ (ASCE/SEI 7-22 Eq. 12.8-2)

$$C_{S,Max} = \frac{S_{D1}}{T(R/I_e)} = \frac{0.65}{1.7(8/1)} = 0.048$$ (ASCE/SEI 7-22 Eq. 12.8-3)

$$C_{S,Min} = 0.44\, S_{DS}\, I_e = (0.44)(1.101)(1) = 0.048$$ (ASCE/SEI 7-22 Eq. 12.8-5)

$$C_{S,Max} = \frac{0.5\, S_1}{(R/I_e)} = \frac{(0.5)(0.650)}{(8/1)} = 0.041$$ (ASCE/SEI 7-22 Eq. 12.8-6)

The seismic response coefficient that governs is 0.048 from Eq. 12.8-3, and this matches the minimum value from Eq. 12.8-5, and the design base shear is calculated to be 1.238 kips.

$V = C_s W = (0.048)\ (25{,}844) = 1{,}238$ kips

ASCE/SEI 7-22 Equations 12.8-11 and 12.8-12 are used for the vertical distribution of seismic forces, as shown below, where k is determined to be 1.6 using linear interpolation in accordance with ASCE/SEI 7-22 Section 12.8.3.

$$F_X = C_{VX} V \qquad \text{(ASCE/SEI 7-22 Eq. 12.8-11)}$$

$$C_{VX} = \frac{W_X h_x^k}{\sum_{i=1}^{n} W_i h_i^k} \qquad \text{(ASCE/SEI 7-22 Eq. 12.8-12)}$$

$$k = 1.6 \qquad \text{(ASCE/SEI 7-22 Section 12.8.3)}$$

$$OTM = \sum_{i=1}^{n} F_i h_i$$

Lateral seismic forces, shears and overturning moment (OTM) are shown in Table 5-4. The overturning moment (OTM) of the building is computed 217217 kip-ft.

Table 5-4. Vertical Distribution of Seismic Forces

Level	Elevation (ft.)	Weight (kips)	Wh^k (kip-ft)	C_{vx}	F_x (kips)	V_x (kips)	OTM (kip-ft)
Roof	238	1,263	7,941,532	0.118	146.2	146.2	34,788
Level 18	225	1,440	8,276,512	0.123	152.3	298.5	34,275
Level 17	212	1,440	7,525,512	0.112	138.5	437	29,364
Level 16	199	1,440	6,801,579	0.101	125.2	562.2	24,912
Level 15	186	1,440	6,105,409	0.091	112.4	674.6	20,901
Level 14	173	1,440	5,437,767	0.081	100.1	774.7	17,315
Level 13	160	1,440	4,799,497	0.071	88.3	863	14,134
Level 12	147	1,440	4,191,536	0.062	77.1	940.1	11,341
Level 11	134	1,440	3,614,936	0.054	66.5	1,006.7	8,916
Leve 10	121	1,440	3,070,888	0.046	56.5	1,063.2	6,839
Level 9	108	1,440	2,560,756	0.038	47.1	1,110.3	5,090
Level 8	95	1,440	2,086,130	0.031	38.4	1,148.7	3,648
Level 7	82	1,440	1,648,895	0.025	30.3	1,179.1	2,489
Level 6	69	1,440	1,251,340	0.019	23	1,202.1	1,589
Level 5	56	1,440	896,334	0.013	16.5	1,218.6	924
Level 4	43	1,440	587,639	0.009	10.8	1,229.4	465
Level 3	30	1,440	330,535	0.005	6.1	1,235.5	183
Level 2	17	1,555	144,016	0.002	2.7	1,238.2	45
SUM	-	25,855	67,270,814	1	**1,238**		**217,217**

5.5.4 Structural Analysis (Seismic Design)

5.5.4.1 C-PSW/CFS AND COUPLING BEAM SECTION

Sizes of L-shaped C-PSW/CFs and coupling beams are selected based on the initial estimates of lateral loads. C-PSW/CFs and coupling beam sizes are optimized through iteration. Figure 5-7 shows selected core wall cross section dimensions. In this example, the selected sizes for L-shaped C-

PSW/CFs and rectangular composite coupling beams are acceptable designed dimensions; therefore, the following sections illustrate the limit state checks.

L-shape C-PSW/CFs have length (L_w) of 12 feet and wall thicknesses (t_{sc}) of 16 in. Steel plate (t_p) and concrete (t_c) thicknesses are ½ in., and 15 in., respectively. Composite coupling beam width (b_{CB}) and height (h_{CB}) are 16 and 24 in., respectively. Coupling beam flange ($t_{CB,f}$) and web ($t_{CB,w}$) plate thicknesses are ½ and ⅜ in., respectively.

L-shape C-PSW/CFs

L_w = 12 ft
t_{sc} = 16 in.
t_p = ½ in.

Coupling beams

L_{CB} = 10 ft
b_{CB} = 16 in.
h_{CB} = 24 in.
$t_{CB.f}$ = ½ in.
$t_{CB.w}$ = ⅜ in.

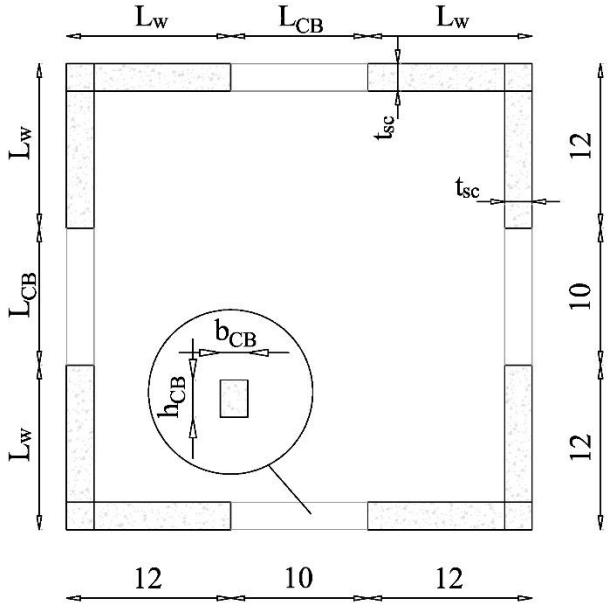

Figure 5-7. Core Walls Plan Section Dimensions

5.5.4.2 NUMERICAL MODELING OF COUPLED C-PSW/CF

For seismic design, a 2D computer model of the coupled C-PSW/CF was developed using a commercial software program (SAP2000) to determine the interstory drift and shear force demands in coupling beams. Coupling beams and L-shaped C-PSW/CFs were modeled using beam elements. When the coupled C-PSW/CF, shown in Figure 5-8, is subjected to lateral seismic loads, two walls are in tension, and the other two walls are in compression due to the coupling action. In this example, the two compression or tension walls are considered one wall (beam element) in computer modeling and the limit state checks. Additionally, in the 2D computer model, flexural, axial, and shear stiffnesses of coupling beam are doubled to model the two beams.

Effective flexural, axial, and shear stiffnesses of C-PSW/CFs and coupling beams were used in the computational model. Effective flexural, axial, and shear stiffnesses of coupling beams were calculated according to ANSI/AISC 360-16. Effective flexural, axial, and shear stiffnesses of C-PSW/CF are calculated per AISC Design Guide 37 (AISC, 2021) as follows:

$EI_{eff} = E_s I_s + 0.35 E_c I_c$
$EA_{eff} = E_s A_s + 0.45 E_c A_c$
$GA_{v.eff} = G_s A_{s.wall} + G_c A_c$

Figure 5-8 shows a 2D computer model of the coupled C-PSW/CF which is subjected to seismic loads calculated in the previous section. Additionally, based on a tributary area force distribution, axial dead and live loads on L-shaped C-PSW/CFs (tension or compression walls) are calculated and defined in the 2D computer model. Axial dead and live loads per wall pair for each story are as follows:

$A_{Tti} = 2291.5$ ft^2 (Tributary area of tension or compression walls)
$F_{Tri.DL} = 275$ kips (Axial dead load)
$F_{Tri.LL} = 115$ kips (Axial live load)

In the 2D computer model, the effective distance (L_{eff}) between centers of areas (elastic centroids) of L-shaped C-PSW/CFs are considered. The effective distance is calculated of 323.8 in. As shown in Figure 5-8, rigid links are considered at the ends of coupling beams to simulate the effect of wall length. Effective flexural, axial, and shear stiffnesses of L-shaped C-PSW/CFs and coupling beams are calculated as follows:

$L_{eff} = 324$ in.
$EI_{eff} = 6.17 \times 10^{10}$ kip-in^2
$EA_{eff} = 3.35 \times 10^{7}$ kips
$GA_{v.eff} = 1.11 \times 10^{7}$ kips
$0.64\ EI_{eff.CB} = 5.92 \times 10^{7}$ kip-in^2
$0.8\ EA_{eff.CB} = 2.03 \times 10^{6}$ kips
$GA_{v.eff.CB} = 8.32 \times 10^{5}$ kips

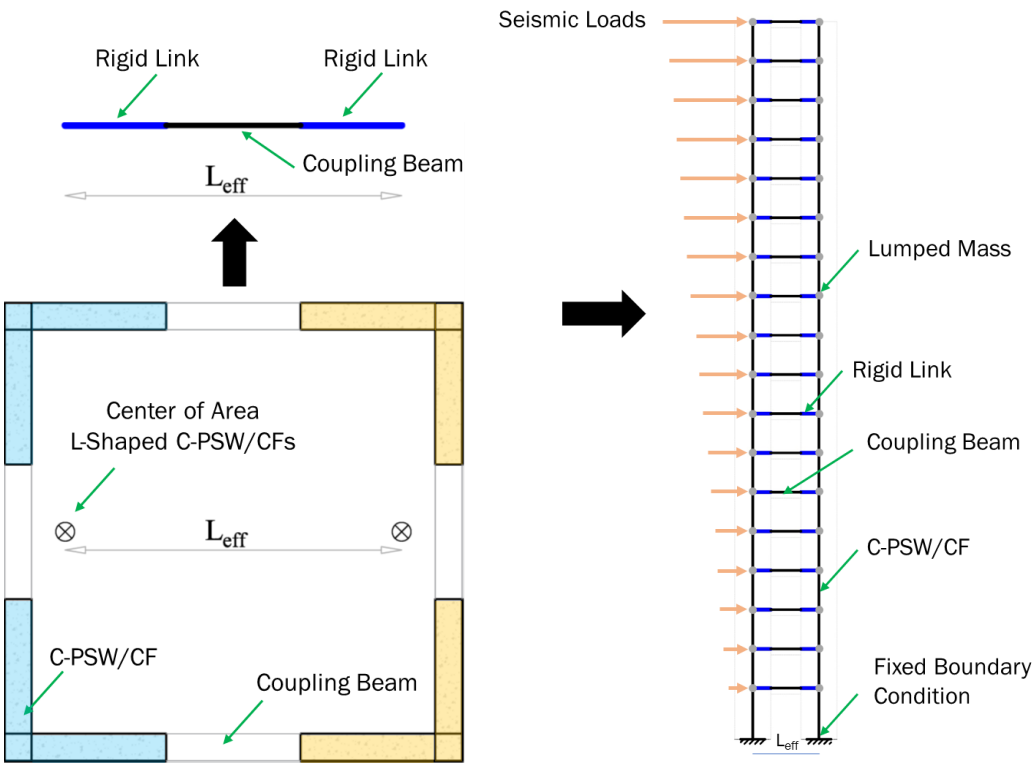

Figure 5-8. 2D Computer Modeling of Coupled C-PSW/CF Used in Seismic Design

Linear elastic analysis was performed to determine the lateral deflection and coupling beam shear force demands. Table 5-5 presents story displacement, amplified displacement, interstory drift, and coupling beam force shear demands. Amplified displacement is calculated by multiplying story displacement value by the deflection amplification factor, C_d = 5.5. Interstory drift is calculated using the amplified displacement. In this design example, the maximum design interstory drift is limited to 2% in accordance with ASCE/SEI 7-22 Table 12.12-1 as this is Risk Category II building, taller than four stories, and does not have a masonry seismic force-resisting system. From the structural analysis of the 2D model, the maximum interstory of the structure is 1.65%, which is lower than the maximum design interstory drift limit. Figure 5-9 shows deformation shape, lateral displacement, and interstory drift of the coupled C-PSW/CF. The deformed shape of the coupled C-PSW/CF shows the behavior of system is not similar to uncoupled C-PSE/CFs. In the uncoupled system, lateral forces are resisted by the flexural deformation of wall at the base; however, in the coupled system, lateral forces are resisted by both flexural deformation of individual walls at the base and coupling action. The colors in Figure 5-9a are associated with lateral displacements and correlate with the lateral displacement in Figure 5-9b.

Table 5-5. Vertical Distribution of Seismic Forces

Level	Story Elevation (ft.)	Displacement (in.)	Amplified Displacement (in.)	Interstory Drift (%)	Coupling Beam Shear Force Demand (kips)
Roof	238	6.95	38.24	1.32	89.2
Level 18	225	6.59	36.26	1.38	97.1
Level 17	212	6.22	34.20	1.44	110.2
Level 16	199	5.83	32.05	1.51	126.0
Level 15	186	5.42	29.80	1.56	129.4
Level 14	173	4.99	27.45	1.61	159.9
Level 13	160	4.55	25.01	1.64	176.0
Level 12	147	4.09	22.50	1.65	190.6
Level 11	134	3.63	19.94	1.65	203.1
Level 10	121	3.16	17.36	1.63	213.1
Level 9	108	2.69	14.79	1.57	220.1
Level 8	95	2.23	12.25	1.49	223.5
Level 7	82	1.78	9.81	1.38	222.4
Level 6	69	1.36	7.47	1.22	216.0
Level 5	56	0.97	5.33	1.02	202.8
Level 4	43	0.62	3.42	0.75	180.9
Level 3	30	0.33	1.83	0.33	147.5
Level 2	17	0.12	0.67	0.00	98.7
Average					167

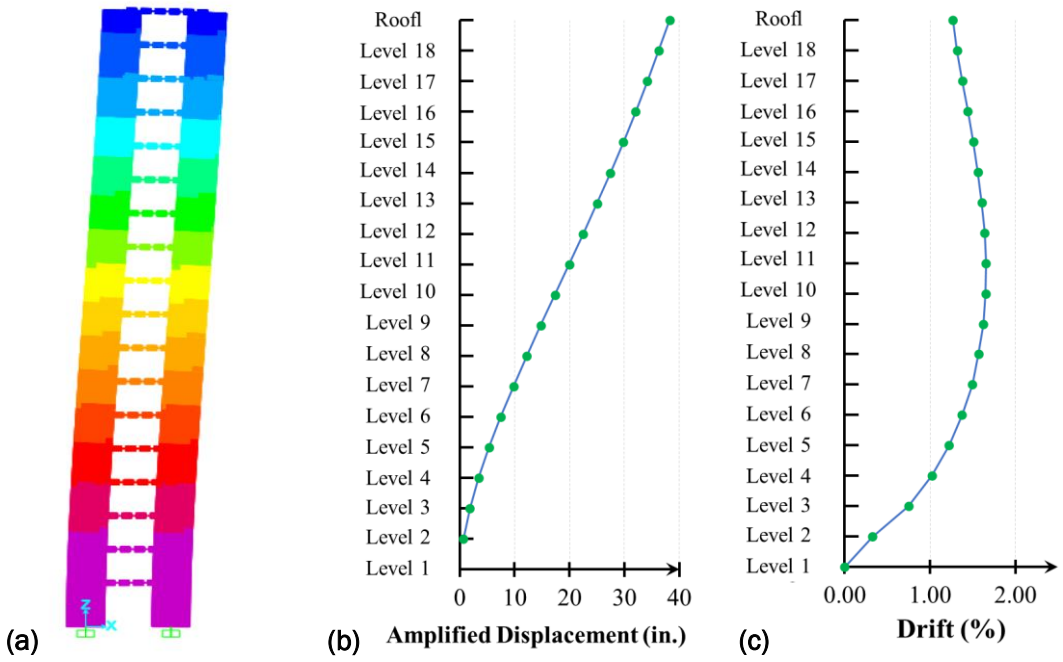

Figure 5-9. Coupled C-PSW/CF: (a) Deformation Shape from Computer Model, (b) Amplified Lateral Displacement, and (c) Interstory Drift

From the structural analysis of 2D model, the average and maximum required shear strengths ($V_{r.CB}$ and $V_{max.CB}$) for coupling beams are calculated. The average required shear strength is used to size the coupling beams. Structural designers can choose to use the average or maximum required shear strengths (AISC Design Guide 37). Since a portion of the OTM will be resisted by the coupling action and the remainder by the individual walls, the result of this choice is the relative proportioning of wall and coupling beam elements. Since the system is designed to ensure plasticity spreads along the height of the structure, either method is acceptable. The average and maximum required shear strengths for coupling beam are 167 and 223.5 kips, respectively. The average and maximum required flexural strengths ($M_{U.CB}$ and $M_{max.CB}$) for coupling beams are calculated at 835 and 1,117 kip-ft, respectively.

$$V_{\mathrm{r.CB}} = 167 \text{ kips}$$

$$V_{\mathrm{U.CB}} = V_{\mathrm{Max.CB}} = 223.5 \text{ kips}$$

$$M_{\mathrm{r.CB}} = \frac{V_{r.CB}\, L_{\mathrm{CB}}}{2} = 835 \text{ kip-ft}$$

$$M_{\mathrm{Max.CB}} = M_{\mathrm{U.CB}} = \frac{\mathrm{V_{Max.CB}\, L_{CB}}}{2} = 1{,}117 \text{ kip-ft}$$

5.5.5 Design of Coupling Beams

Coupling beams are sized to meet the average required shear strength and provide adequate stiffness to meet the inter-story drift limit. This section presents design checks for coupling beams.

5.5.5.1 FLEXURE-CRITICAL COUPLING BEAMS

Coupling beams of the coupled C-PSW/CF system are designed to be a flexure critical member in accordance with ANSI/AISC 341-22 Section H8.5c. In this example, composite coupling beams of coupled L-shaped C-PSW/CFs are proportioned to be flexure critical members by controlling shear strength (AISC Design Guide 37), as shown below.

$$V_{\text{n.Exp.CB}} \geq \frac{2.4\, M_{\text{P.Exp.CB}}}{L_{\text{CB}}} \qquad \text{(AISC Design Guide 37 Section 2.2.3)}$$

Where, $M_{p.Exp.CB}$ is expected flexural capacity of composite coupling beam. $V_{n.exp.CB}$ is expected shear strength of composite coupling beam. L_{CB} is the clear length of composite coupling beam.

5.5.5.2 EXPECTED FLEXURAL CAPACITY ($M_{P.EXP.CB}$)

The expected flexural capacity ($M_{p.Exp.CB}$) of coupling beam is calculated assuming the steel plate reaches a yield stress of R_yF_y (in both compression and tension) and infill concrete reaches a yield stress of $R_cf'_c$ (in compression). Plastic stress distribution method is used to calculate expected flexural capacity ($M_{p.Exp.CB}$). The expected flexural capacity of the composite coupling beams is calculated as follows:

Width of concrete in composite coupling beam:

$$t_{\text{c.CB}} = b_{\text{CB}} - 2t_{\text{CB.w}} = 16 - 2(0.375) = 15.25 \text{ in.}$$

Plastic neutral axis of composite coupling beam:

$$C_{\text{CB.exp}} = \frac{2\, t_{CB.w}\, b_{CB}\, R_y\, F_y + R_c\, 0.85\, f'_c\, t_{c.CB}\, t_{CB.f}}{4\, t_{CB.w}\, R_y\, F_y + R_c\, 0.85\, f'_c\, t_{c.CB}} = 5.26 \text{ in.}$$

Compression (C) and tension (T) forces in coupling beam parts:

$$C_{1.exp} = (b_{CB} - 2t_{CB.w})t_{CB.f} R_y\, F_y = 419 \text{ kips} \qquad \text{(Flange plate)}$$

$$C_{2.exp} = 2t_{CB.w}\, C_{CB.exp}\, R_y\, F_y = 217 \text{ kips} \qquad \text{(Web plates)}$$

$$C_{3.exp} = R_c\, 0.85\, f'_c\, t_{c.CB}\, \left(C_{CB.exp} - t_{CB.f}\right) = 556 \text{ kips} \qquad \text{(Concrete)}$$

$$T_{1.exp} = (b_{CB} - 2t_{CB.w})t_{CB.f} R_y\, F_y = 419 \text{ kips} \qquad \text{(Flange plate)}$$

$$T_{2.exp} = 2t_{CB.w}\left(h_{CB} - C_{CB.exp}\right) R_y\, F_y = 773 \text{ kips} \qquad \text{(Web plates)}$$

Expected flexural capacity of the composite coupling beams:

$$M_{p.Exp.CB} = C_{1.exp}\left(C_{CB.exp} - \frac{t_{CB.f}}{2}\right) + C_{2.exp}\left(\frac{C_{CB.exp}}{2}\right) + C_{3.exp}\left(\frac{C_{CB.exp} - 2t_{CB.f}}{2}\right) + T_{1.exp}\left(h_{CB} - C_{CB.exp} - \frac{2t_{CB.f}}{2}\right) + T_{2.exp}\left(\frac{h_{CB} - C_{CB.exp}}{2}\right) = 1{,}582.6 \text{ kip-ft}$$

$$M_{p.Exp.CB} = 1{,}582.6 \text{ kip-ft}$$

5.5.5.3 MINIMUM AREA OF STEEL

In accordance AISC 360 Section I2.2a, steel plates should comprise at least 1% of the total cross section area of composite coupling beam. Minimum area of steel in the composite coupling beam is checked as follows:

$$A_{s.CB.min} = 0.01\, h_{CB}\, b_{CB} = (0.01)(24)(16) = 3.8 \text{ in.}^2 \qquad \text{(AISC Spec. I2.2a)}$$

$$A_{s.CB} = (2)(24)(0.375) + (2)(15.25)(0.5) = 33.25 \text{ in.}^2$$

$$A_{s.CB} = 33.25 \text{ in.}^2 > A_{s.CB.min} = 3.8 \text{ in.}^2$$

5.5.5.4 STEEL PLATE SLENDERNESS REQUIREMENT FOR COUPLING BEAMS

In seismic design of the coupled C-PSW/CF system, composite coupling beams are designed to be compact sections. The slenderness requirements of flange and web plates are checked in accordance with AISC 360-22 Section I1.4. Web plate slenderness requirement is established to develop the shear yielding of web plate before elastic shear buckling. The flange plate slenderness requirement is established to develop the compression yielding of the flange plate before elastic buckling.

Clear unsupported width and height:

$$b_{c.CB} = b_{CB} - 2t_{CB.w} = 16 - 2(0.375) = 15.25 \text{ in.}$$

$$h_{c.CB} = h_{CB} - 2t_{CB.\mathrm{f}} = 24 - 2(0.5) = 23 \text{ in.}$$

Slenderness requirement for flange plates of coupling beam:

$$\frac{b_{c.CB}}{t_{CB.f}} = 30.5 < 2.37\sqrt{\frac{E_s}{R_y F_y}} = 2.37\sqrt{\frac{29000}{(1.1)(50)}} = 54.4 \quad \text{(AISC 360-22 Table I1.1b)}$$

Slenderness requirement for web plates of coupling beam:

$$\frac{h_{c.CB}}{t_{CB.w}} = 61.3 \geq 2.66\sqrt{\frac{E_s}{R_y F_y}} = 2.66\sqrt{\frac{29000}{(1.1)(50)}} = 61.1 \quad \text{(AISC 360-22 Table I1.1b)}$$

Although the ratio of $\frac{h_{c.CB}}{t_{CB.w}}$ is slightly higher than the slenderness requirement for web plates of coupling beam, in this design example, it is assumed the web plates of coupling beams meet the requirement.

5.5.5.5 FLEXURAL STRENGTH ($M_{P,CB}$)

The plastic stress distribution method is used to calculate flexural capacity ($M_{p.CB}$). The flexural capacity ($M_{p.CB}$) of coupling beam is calculated assuming the steel plate reaches a yield stress of F_y (in both compression and tension) and the infill concrete reaches a stress of $0.85f'_c$ (in compression). The flexural capacity of the composite coupling beam is calculated as follows:

Plastic neutral axis of composite coupling beam:

$$C_{CB} = \frac{2\, t_{CB.w}\, b_{CB}\, F_y + 0.85\, f'_c\, t_{c.CB}\, t_{CB.f}}{4\, t_{CB.w}\, F_y + 0.85\, f'_c\, t_{c.CB}} = 6.15 \text{ in.}$$

Compression (C) and tension (T) forces in coupling beam parts:

$$C_1 = (b_{CB} - 2t_{CB.w})t_{CB.f}\, F_y = 381 \text{ kips} \quad \text{(Flange plate)}$$

$$C_2 = 2t_{CB.w}\, t_{CB.f}\, C_{CB}\, F_y = 230 \text{ kips} \quad \text{(Web plates)}$$

$$C_3 = 0.85\, f'_c\, t_{c.CB}\, \left(C_{CB} - t_{CB.f}\right) = 439 \text{ kips} \quad \text{(Concrete)}$$

$$T_1 = (b_{CB} - 2t_{CB.w})t_{CB.f}\, F_y = 381 \text{ kips} \quad \text{(Flange plate)}$$

$$T_2 = 2t_{CB.w}(h_{CB} - C_{CB})\, F_y = 670 \text{ kips} \quad \text{(Web plates)}$$

Design flexural capacity of the composite coupling beams:

$$M_{p.CB} = C_1\, \left(C_{CB} - \frac{t_{CB.f}}{2}\right) + C_2\, \left(\frac{C_{CB}}{2}\right) + C_3\, \left(\frac{C_{CB} - 2t_{CB.f}}{2}\right) + T_1\, \left(h_{CB} - C_{CB} - \frac{2t_{CB.f}}{2}\right) + T_2\, \left(\frac{h_{CB} - C_{CB}}{2}\right) = 1{,}407 \text{ kip-ft}$$

$$M_{n.CB} = M_{p.CB} = 1{,}407 \text{ kip-ft}$$

$$\phi_b = 0.9$$

$$\phi_b M_{n.CB} = 1{,}266 \text{ kip-ft} \quad > \quad M_{U.CB} = 835 \text{ kip-ft}$$

Ratio of demand to capacity:

$$\frac{M_{r.CB}}{\phi_b M_{n.CB}} = \frac{835 \text{ kip-ft}}{1{,}266 \text{ kip-ft}} = 0.66$$

$$\frac{M_{U.CB}}{\phi_b M_{n.CB}} = \frac{1{,}117 \text{ kip-ft}}{1{,}266 \text{ kip-ft}} = 0.88$$

5.5.5.6 NOMINAL SHEAR STRENGTH ($V_{N.CB}$)

Nominal shear strength, $V_{n.CB}$, of composite coupling beam is calculated in accordance with AISC 360 Section I4.2. The nominal shear strength is the summation of shear strengths of steel web plates (V_s) and infill concrete (V_c).

Area of steel web plates

$$A_{w.CB} = 2h_{CB}t_{CB.w} = 2(24)(0.375) = 18 \text{ in.}^2$$

$$K_c = 1 \qquad \text{(Compact cross section)}$$

Nominal shear strength:

$$V_{n.CB} = 0.6\,F_y A_{w.CB} + 0.06\,K_c\sqrt{f_c'}A_{c.CB} = (0.6)(50)(18) + (0.06)(1)\left(\sqrt{6}\right)(15.25)(23)$$

$$V_{n.CB} = 592 \text{ kips}$$

$$\phi_v = 0.9$$

$$\phi_v V_{n.CB} = 532 \text{ kips} > V_{U.CB} = 167 \text{ kips}$$

Ratio of demand to capacity:

$$\frac{V_{r.CB}}{\phi_v V_{n.CB}} = \frac{167\ kips}{532 \text{ kips}} = 0.31$$

$$\frac{V_{U.CB}}{\phi_v V_{n.CB}} = \frac{223.5\ kips}{532 \text{ kips}} = 0.42$$

5.5.5.7 FLEXURE-CRITICAL COUPLING BEAMS (REVISITED)

The selected composite coupling beams are flexure critical members, as shown below.

$$V_{n.exp.CB} = 0.6\,R_y\,F_y A_{w.CB} + 0.06\,K_c\sqrt{R_c\,f_c'}A_{c.CB}$$
$$= (0.6)(1.1)(50)(18) + (0.06)(1)\left(\sqrt{(1.5)(6)}\right)(15.25)(23) = 657 \text{ kips}$$

$$V_{n.exp.CB} = 657\ kips > \frac{2.4\,M_{P.exp.CB}}{L_{CB}} = \frac{2.4\,(1{,}582.6)}{10} = 380 \text{ kip}$$

5.5.6 Design of C-PSW/CF

L-shaped C-PSW/CFs are sized and designed based on the design philosophy of a strong wall-weak coupling beam approach. In accordance with this design approach, the formations of plastic hinges in most coupling beams take place along the height of the structure before significant yielding at the base of C-PSW/CFs. This section presents design checks for L-shaped C-PSW/CFs.

5.5.6.1 STEP 4-1: MINIMUM AND MAXIMUM AREA OF STEEL

In accordance with ANSI/AISC 360-22 Section I1.6, the steel plates in C-PSW/CFs should comprise at least 1% but no more than 10% of the total composite cross-section area. The selected cross section for L-shaped C-PSW/CF pair (compression or tension wall pair) meets the requirements for minimum and maximum steel plate areas, as shown below:

$$A_{gross.wall} = (2)[(L_w\, t_{sc}) + (L_w - t_{sc})t_{sc}\,] = 8{,}704 \text{ in.}^2$$

$$A_{s.min} = 0.01\, A_{gross.wall} = (0.01)(8{,}704) = 87 \text{ in.}^2 \qquad \text{(ANSI/AISC 360-22 I2.2a)}$$

$$A_{s.max} = 0.1\, A_{gross.wall} = (0.1)(8{,}704) = 870 \text{ in.}^2 \qquad \text{(ANSI/AISC 360-22 I2.2a)}$$

$$A_s = (t_p)\left[8L_w + 4t_{sc} - 16t_p\,\right] = 604 \text{ in.}^2$$

$$A_{s.min} = 87 \text{ in.}^2 < A_s = 604 \text{ in.}^2 < A_{s.max} = 870 \text{ in.}^2$$

5.5.6.2 STEEL PLATE SLENDERNESS REQUIREMENTS FOR COMPOSITE WALLS

In this design example, steel tie bars are only used in L-shaped C-PSW/CFs (no shear studs); therefore, the largest unsupported length between tie bars is considered for the slenderness requirements check. Tie bar spacings are selected 12 and 14 in. for the bottom (the bottom two stories) and top (remaining stories) of the L-shaped C-PSW/CFs. In accordance with ANSI/AISC 341-22 Chapter H8 Section 4b, steel plate slenderness ratio, *b/t*, at the base of C-PSW/CFs (protected zones) should be limited as follows:

$$S_{tie} = 12 \text{ in.} \qquad \text{(The bottom two stories)}$$

$$\frac{S_{tie}}{t_p} = 24 < 1.05\sqrt{\frac{E_s}{R_y\, F_y}} = 1.05\sqrt{\frac{29{,}000}{(1.1)(50)}} = 24.1 \qquad \text{(ANSI/AISC 341-22 H8 Section 4b)}$$

The steel plate slenderness ratio, *b/t*, at regions which are not protected zones should be limited as follows:

$$S_{tie.top} = 14 \text{ in.}$$

$$\frac{S_{tie.top}}{t_p} = 28 < 1.2\sqrt{\frac{E_s}{F_y}} = 1.2\sqrt{\frac{29{,}000}{(50)}} = 28.9 \qquad \text{(ANSI/AISC 360-22)}$$

It should be noted that the first slenderness check equation has R_y because it is the slenderness check for critical plastic zones (at the base of C-PSW/CFs), which is from AISC 341-22. In the seismic

design of the coupled C-PSW/CF system, the critical plastic zones shall be highly ductile. The second slenderness check equation does not have R_y because it is the slenderness check for a portion of C-PSW/CFs that does not undergo plastic response (as shown in Figure 5-3), which is from AISC 360-22.

5.5.6.3 TIE SPACING REQUIREMENTS FOR COMPOSITE WALLS

The stability of empty steel module of C-PSW/CF during the construction and concrete casting depends on tie bar spacing to plate thickness ratio (AISC Design Guide 37). Tie bars with ¾ diameters are selected for the L-shaped C-PSW/CFs, and the tie bar spacing to plate thickness ratio is checked. In accordance with AISC 360 Section I1.6b, the tie bar spacing to plate thickness ratio, S/t_p, should be limited as follows:

$$d_{tie} = 3/4 \text{ in.}$$

$$\propto = 1.7\left(\frac{t_{sc}}{t_p} - 2\right)\left(\frac{t_p}{d_{tie}}\right)^4 = 1.7\left(\frac{16}{0.5} - 2\right)\left(\frac{0.5}{0.75}\right)^4 = 10.07$$

$$\frac{S_{tie}}{t_p} = 24 \;<\; 1.0\sqrt{\frac{E_s}{2\propto + 1}} = 1.0\sqrt{\frac{29{,}000}{2(10.07)+1}} = 37.0$$

$$\frac{S_{tie}}{t_p} = 32 \;<\; 1.0\sqrt{\frac{E_s}{2\propto + 1}} = 1.0\sqrt{\frac{29{,}000}{2(10.07)+1}} = 37.0$$

5.5.6.4 REQUIRED WALL SHEAR STRENGTH

The base shear (V_{base}) associated with the seismic forces was calculated in Section 0. A shear amplification factor of 4 is used to amplify the base shear. The amplified shear force for the core walls is calculated as 4,952 kips. The required shear strength for tension or compression C-PSW/CFs ($V_{r.wall}$) is determined to be 2,476 kips, as the base shear are resisted by two wall pairs.

$$V_{Amplified} = 4{,}952 \text{ kips}$$

$$V_{r.wall} = \frac{4{,}952}{2} = 2{,}476 \text{ kips}$$

5.5.6.5 REQUIRED FLEXURAL STRENGTH OF COUPLED C-PSW/CF

In accordance with ASCE/SEI 7-22 and ANSI/AISC 341-22 Section H8.3d, in the coupled C-PSW/CF system, walls are designed for an amplified overturning moment (OTM). The overturning moment (OTM) is amplified by an amplification factor, γ_1, which considers all coupling beams developing plastic hinges at both ends. The required amplified overturning moment (OTM) for designing the coupled C-PSW/CF system is calculated as follows:

Expected flexural capacity of coupling beam:

$$M_{p.exp.CB} = 1{,}583 \text{ kip-ft}$$

Expected shear strength of coupling beam:

$$V_{n.Mp.exp.CB} = \frac{(1.1)(1.1)(2)\ M_{P.exp.CB}}{L_{CB}} = \frac{2.4\ M_{P.exp.CB}}{L_{CB}} = 380 \text{ kips} \qquad \text{(AISC Design Guide 37)}$$

In the above equation, the first factor (1.1) is considered due to strain hardening and the second factor (1.1) is considered due to additional flexural capacity of composite coupling beam. The additional flexural capacity of composite coupling beam is because of biaxial stress state of tension flange.

In accordance with AISC Design Guide 37, overstrength amplification factor for designing of C-PSW/CF is calculated as follows:

$$\gamma_1 = \frac{\sum_n (1.1)(1.1)\ M_{p.exp.CB}}{\sum_n\ M_{U.CB}} = \frac{\sum_n 1.2\ M_{p.exp.CB}}{\sum_n\ M_{U.CB}} = \frac{(18)(1.2)(1{,}583)}{(18)(835)} = 2.27 \qquad \text{(AISC Design Guide 37)}$$

Axial force to C-PSW/CFs due to coupling action due to the seismic loads:

$$P_{CB} = 2\ \sum_n\ V_{n.Mp.exp.CB} = 13{,}673 \text{ kips}$$

In accordance with AISC Design Guide 37, required amplified overturning moment (OTM) for designing coupled C-PSW/CFs is calculated as follows:

$$M_{r.wall} = \gamma_1\ OTM - \ P_{CB}\ L_{eff} = (2.27)(217{,}217) - (13{,}673)(27) = 125{,}077 \text{ kip-ft}$$

The effect of axial compression or tension force on C-PSW/CFs should be considered in the calculation of the flexural capacity of the wall. Maximum axial compression and tension forces on the compression and tension L-shaped C-PSW/CFs are calculated as follows:

Maximum axial compression force to compression C-PSW/CFs considering the load combination of 1.2*D*+0.5*L*±*E:*

$$P = -2\ \sum_n\ V_{n.Mp.Exp.CB} - (1.2\ \sum_n\ F_{Tri.DL}) - (0.5\ \sum_n\ F_{Tri.LL}) = -20{,}644 \text{ kips}$$

Maximum axial tension force to tension C-PSW/CFs considering the load combination of 0.9D±E:

$$T = 2\ \sum_n\ V_{n.Mp.exp.CB} - (0.9\ \sum_n\ F_{Tri.DL}) = 9{,}219 \text{ kips}$$

"P" and "T" are calculated based on the design philosophy shown in Figure 5-3, and$F_{Tri.LL}$ and $F_{Tri.DL}$ were calculated in Section 5.5.4.2. In the seismic design of coupled C-PSW/CFs, maximum axial compression and maximum axial tension forces are "P" and "T" of the coupled C-PSW/CF system, as shown in Figure 5-1.

5.5.6.6 COMPOSITE WALL RESISTANCE FACTOR

Shear, flexure, compression, and tension resistance factors for composite wall are as follows:

$\phi_v = 0.9$ (ANSI/AISC 360-22 I4.1.a)

$\phi_b = 0.9$ (ANSI/AISC 360-22 I3.4b)

$\phi_c = 0.9$ (AISC Design Guide 37 Section 2.2.3)

$\phi_t = 0.9$ (AISC Design Guide 37 Section 2.2.3)

5.5.6.7 WALL TENSILE STRENGTH

Nominal tensile strength of two L-shaped C-PSW/CFs (tension walls) is calculated as follows:

$A_s = 604\ in^2$ (From Section 5.5.6.1)

$P_{n.T} = A_s\ F_y = (604)(50) = 30{,}200\ \text{kips}$

$\phi_t\ P_{n.T} = 27{,}180\ \text{kips} > T = 9{,}219\ \text{kips}$

$\frac{T}{\phi_t\ P_{n.T}} = 0.35$

5.5.6.8 WALL COMPRESSION STRENGTH

A simplified unit width method is considered to calculate nominal compression strength. This is a conservative approach to calculate the nominal compression strength, as the effect of end plates on the compression capacity is not considered. However, this simplified unit width method can be used for C-PSW/CFs with different configurations, for example, L-shaped, C-shaped, I-shaped walls. The selected unit width cross-section of the L-shaped C-PSW/CF is shown in Figure 5-10. The nominal compression strength of the L-shaped C-PSW/CF pair (compression walls) is calculated as follows:

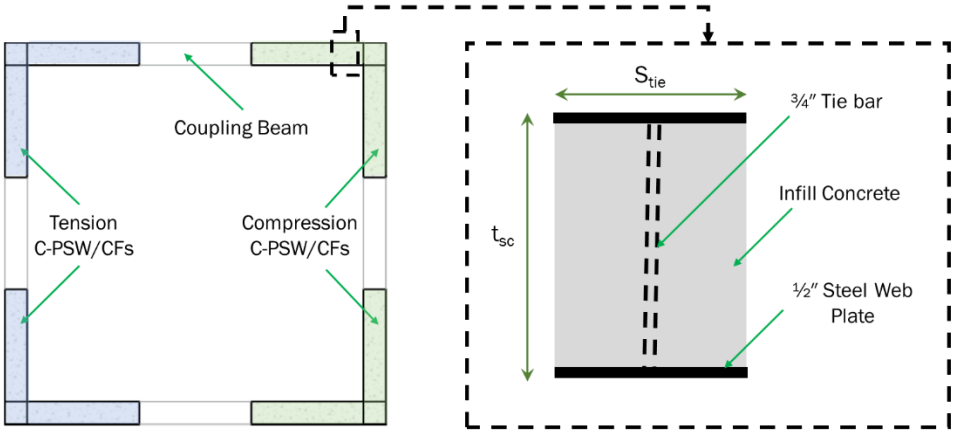

Figure 5-10. Unit Width Cross-section of L-shaped C-PSW/CF

$S_{tie} = 12 \text{ in} = 1 \text{ ft}$ (Length of selected unit width)
$L_{wall.\text{total}} = 48 \text{ ft}$ (Total length of two L-shaped C-PSW/CFs)
$P_{no} = 2t_p \, S_{tie} \, F_y + 0.85 \, f_c' \, (t_{sc} - 2t_p) \, S_{tie} = 1{,}518 \text{ kips}$ (ANSI/AISC 360-22)
$I_{min.steel} = 144 \text{ in}^4$
$I_{min.concrete} = 2{,}160 \text{ in}^4$
$EI_{eff.min} = E_s \, I_{min.steel} + 0.35 \, E_c \, I_{min.concrete} = 7{,}578{,}000 \text{ kip-in}^2$
$L_{cr} = 17 \text{ ft}$ (Critical unsupported length for buckling of wall)
$P_e = \frac{\pi^2 \, EI_{eff.min}}{{L_{cr}}^2} = 1797 \text{ kips}$
$\frac{P_{no}}{P_e} = 0.84 \quad < \quad 2.25$ (ANSI/AISC 360-22)
$P_{n.C} = P_{no} \left(0.685^{\frac{P_{no}}{P_e}}\right) = 1{,}066 \text{ kips}$
$n_{unit-width} = \frac{L_{wall.\text{total}}}{S_{tie}} = \frac{48}{1} = 48$
$P_{n.C.total} = P_{n.C} \, n_{unit-width} = (1{,}066 \text{ kips})(48) = 51{,}168 \text{ kips}$
$\phi_C \, P_{n.C.total} = (0.9)(51{,}168 \text{ kips}) = 46{,}051 \text{ kips} > P = 20{,}644 \text{ kips}$
$\frac{P}{\phi_C \, P_{n.C.total}} = 0.45$

For the wall subjected to axial compression force, a better estimate of minimum effective flexural stiffness ($EI_{eff.min}$) to calculate compression capacity is $EI_{eff.min} = E_s \, I_{min.steel} + 0.7 \, E_c \, I_{min.concrete}$. Using this estimate, the ratio of $\frac{P}{\phi_C \, P_{n.C.total}}$ becomes equal to 0.40. Even this calculation is quite conservative, as the (2L-shaped or C-shaped) wall section stiffness was not fully considered. Typically using $0.35 \, E_c \, I_{min.concrete}$ is corresponding to and for a member with zero axial compression force; however, $0.7 \, E_c \, I_{min.concrete}$ is approximately for a member with axial compression force, which results in less concrete cracking.

5.5.6.9 WALL FLEXURAL STRENGTH

Flexural capacity of the L-shaped C-PSW/CFs can be calculated using plastic stress distribution method or fiber section modeling, while the effect of axial force is considered (Shafaei et al., 2021b). When the core system is subjected to lateral seismic forces, two L-shaped C-PSW/CFs are subjected in tension force and the other two L-shaped C-PSW/CFs are in compression, as shown in Figure 5-11. The flexural capacities of tension and compression L-shaped C-PSW/CFs are calculated using plastic stress distribution method when they are subjected to -20,644 kips compression and 9,219 kips tension forces. In accordance with AISC Design Guide 37, the flexural capacities of compression and tension L-shaped C-PSW/CFs are calculated using the plastic stress distribution method as follows:

$M_{P.T.wall} = M_{n.T.wall} = 1{,}598{,}236 \text{ kip-in.} = 133{,}186 \text{ kip-ft}$

$\phi_t \, M_{n.T.wall} = 1{,}438{,}412 \text{ kip-in.} = 119{,}868 \text{ kip-ft}$

$$M_{P.C.wall} = M_{n.C.wall} = 1{,}761{,}166 \text{ kip-in.} = 146{,}764 \text{ kip-ft}$$

$$\phi_t \, M_{n.C.wall} = 1{,}585{,}050 \text{ kip-in.} = 132{,}088 \text{ kip-ft}$$

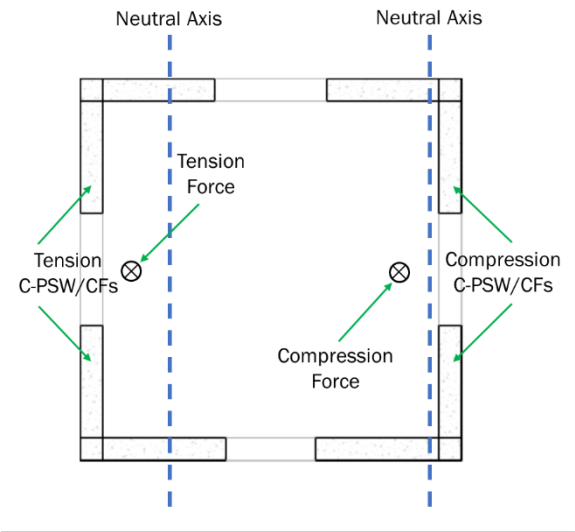

Figure 5-11. Cross-Section of Coupled L-shaped C-PSW/CF for Plastic Moment Calculation

Alternatively, the fiber section modeling can be used to calculate the moment-curvature responses and flexural capacities of tension and compression C-PSW/CFs. A fiber section model of L-shaped C-PSW/CF was developed using "Section Designer" built into SAP2000 software. Figure 5-12 illustrates moment-curvature responses of tension and compression C-PSW/CFs. In addition, the flexural capacities calculated using the plastic stress distribution method are shown in the figure. The fiber section modeling and plastic stress distribution method estimate approximately the same flexural capacities. The flexural capacities of compression and tension L-shaped C-PSW/CFs are calculated using the fiber section modeling as follows:

$$M_{Max.T.wall.fiber} = 1{,}590{,}946 \text{ kip-in.} = 132{,}579 \text{ kip-ft}$$

$$M_{Max.C.wall.fiber} = 1{,}863{,}605 \text{ kip-in.} = 155{,}300 \text{ kip-ft}$$

$$\frac{M_{P.T.wall}}{M_{Max.T.wall.fiber}} = \frac{133{,}186 \text{ kip-ft}}{132{,}579 \text{ kip-ft}} = 1.00$$

$$\frac{M_{P.C.wall}}{M_{Max.C.wall.fiber}} = \frac{146{,}764 \text{ kip-ft}}{155{,}300 \text{ kip-ft}} = 0.94$$

The effective flexural stiffness (EI_{eff}) calculated in Section 5.5.4.2 did not consider the effect of tension or compression axial force. The effective flexural stiffness (EI_{eff}) of C-PSW/CFs subjected to axial force can be accurately estimated using the moment-curvature response. The effective flexural stiffness (EI_{eff}) of C-PSW/CFs was estimated as the secant stiffness corresponding to

0.6$M_{Max.wall.fiber}$ on the moment-curvature response (Shafaei et al., 2021b). The effective flexural stiffness of tension and compression L-shaped C-PSW/CFs are estimated as follows:

$$EI_{T.wall} = 5.55 \times 10^{10} \text{ kip-in}^2$$
$$EI_{C.wall} = 7.21 \times 10^{10} \text{ kip-in}^2$$

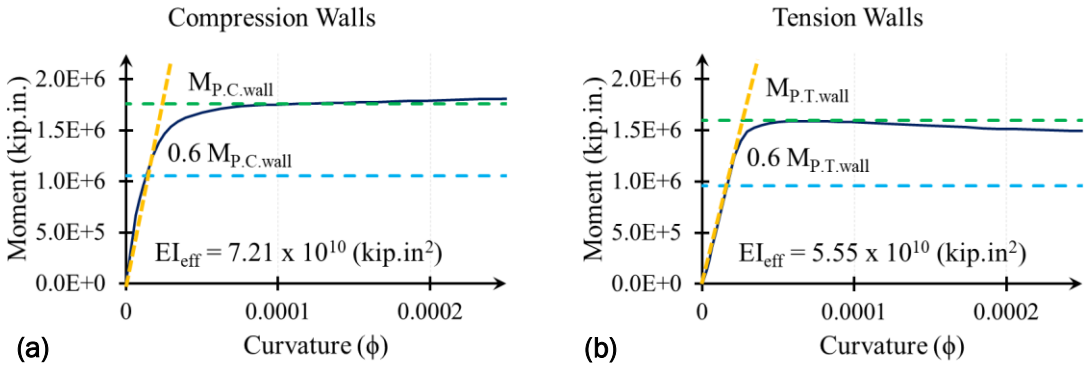

Figure 5-12. Moment-Curvature Response Developed by Fiber Section Analysis (a) Compression Walls (b) Tension Walls

The effective flexural stiffnesses of tension and compression ($EI_{T.wall}$ and $EI_{C.wall}$) L-shaped C-PSW/CFs are used to calculate required flexural strengths of tension and compression walls.

$$M_{U.T.wall} = \left[\frac{EI_{T.wall}}{(EI_{C.wall} + EI_{T.wall})}\right] M_{r.wall} = 652{,}833 \text{ kip-in.} = 54{,}403 \text{ kip-ft}$$
$$M_{U.C.wall} = \left[\frac{EI_{C.wall}}{(EI_{C.wall} + EI_{T.wall})}\right] M_{r.wall} = 848{,}094 \text{ kip-in.} = 70{,}675 \text{ kip-ft}$$

Ratio of demand to capacity:

$$\frac{M_{U.T.wall}}{\phi_t M_{n.T.wall}} = \frac{54{,}403 \text{ kip-ft}}{119{,}868 \text{ kip-ft}} = 0.45$$
$$\frac{M_{U.C.wall}}{\phi_t M_{n.C.wall}} = \frac{70{,}675 \text{ kip-ft}}{132{,}088 \text{ kip-ft}} = 0.54$$

Alternatively, P-M interaction diagrams of tension and compression L-shaped C-PSW/CFs can be developed and compared with required flexural and axial strengths. The P-M interaction diagrams of C-PSW/CFs are calculated using either hand calculations or a software program. In this design example, the P-M interaction diagrams of the considered tension and compression L-shaped C-PSW/CFs were developed using SAP2000. Figure 5-13 shows P-M interaction diagrams of tension and compression L-shaped C-PSW/CFs. As shown in the figure, L-shaped C-PSW/CFs can clearly resist the required axial (tension or compression) and flexural loads.

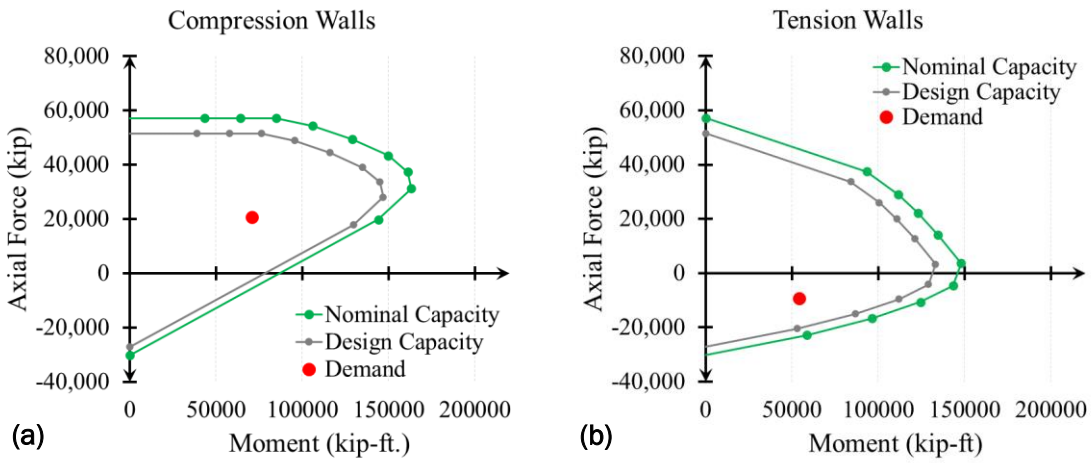

Figure 5-13. P-M Interaction of C-PSW/CFs (a) Compression Walls (b) Tension Walls

5.5.6.10 WALL SHEAR STRENGTH

In accordance with ANSI/AISC 341-22 Chapter H8 Section 6e, the nominal in-plane shear strength of L-shaped C-PSW/CFs is determined considering the steel section and infill concrete contributions as follows:

Area of steel in the direction of shear:

$$A_{s.wall} = 4\left(L_W\ t_p\right) + 2\left(t_{sc}\ t_p\right) = (4)(144)(0.5) + (2)(16)(0.5) = 304 \text{ in.}^2$$

K factor for shear strength calculation:

$$K_s = G_s\ A_{s.wall} = (11{,}200)(304) = 3.4 \times 10^6 \text{ kips}$$

$$K_{sc} = \frac{0.7\ (E_c\ A_c)\ (E_s\ A_{s.wall})}{(4E_s\ A_{s.wall}) + (E_c\ A_c)} = 3.14 \times 10^6 \text{ kips}$$

Nominal shear strength of C-PSW/CFs:

$$V_{n.wall} = \frac{K_s + K_{sc}}{\sqrt{3\ {K_s}^2 + {K_{sc}}^2}} A_{s.wall} F_y = 14{,}787 \text{ kips}$$

$$\phi_v V_{n.wall} = 13{,}308\ kips \ > \ V_{U.wall} = 2{,}476 \text{ kips}$$

Ratio of demand to capacity:

$$\frac{V_{U.wall}}{\phi_v V_{n.wall}} = 0.19$$

5.5.7 Coupling Beam Connection

There are several possible composite coupling beam-to-wall connections. In this design example, one possible coupling beam-to-wall connection is presented. Figures 5-14, 5-15, and 5-16 illustrate one possibility for coupling beam to wall connection details:

- As shown in Figure 5-14, there are slots in the C-PSW/CF web plates and coupling beam flange plates are inserted into the slots.
- Coupling beam flange plates are 1 in. wider than wall cross section from each side to provide adequate clearance for CJP welding, as shown in Figure 5-15.
- The slots of C-PSW/CF web plates are beveled and welded to the coupling beam flange plates using complete joint penetration (CJP) welding (as shown in Figure 5-15 and 5-16).
- The coupling beam web plates are overlapped the C-PSW/CF web plates and C-shaped fillet welding was done (as shown in Figures 5-15 and 5-16).
- The depth of coupling beam web plate is reduced 1 in. from top and bottom at the connection region to provide adequate clearance for fillet welding, as shown in Figures 5-14 and 5-15.

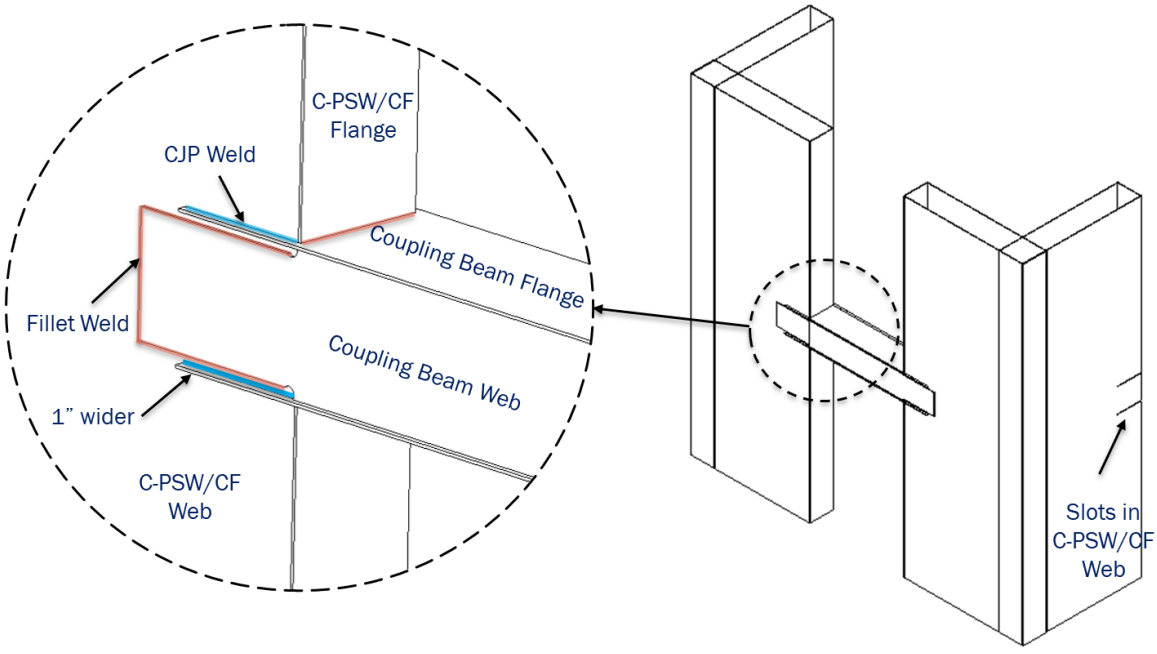

Figure 5-14. Schematic view of Coupling Beam-to-Wall Connection Details

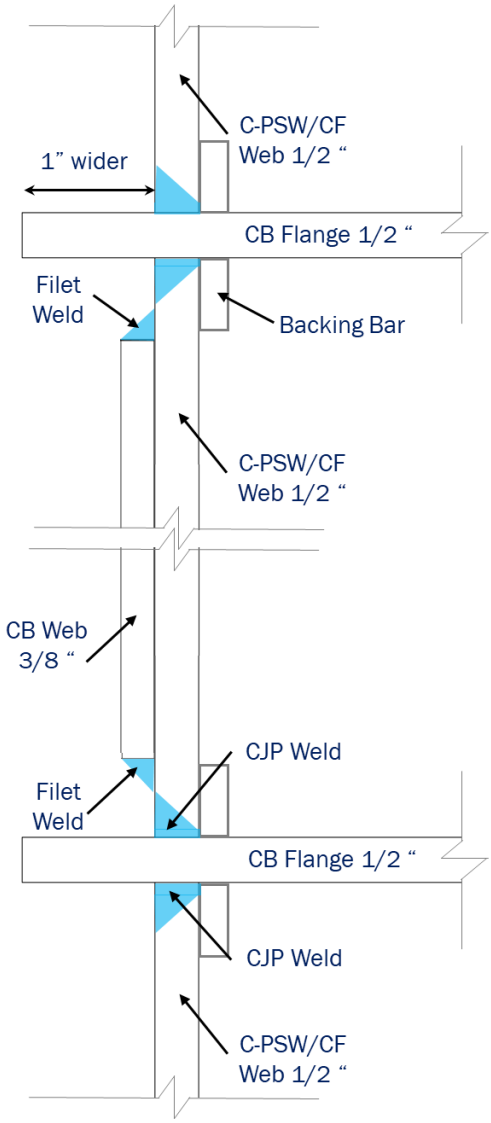

Figure 5-15. Schematic view of Coupling Beam-to-Wall Connection Details

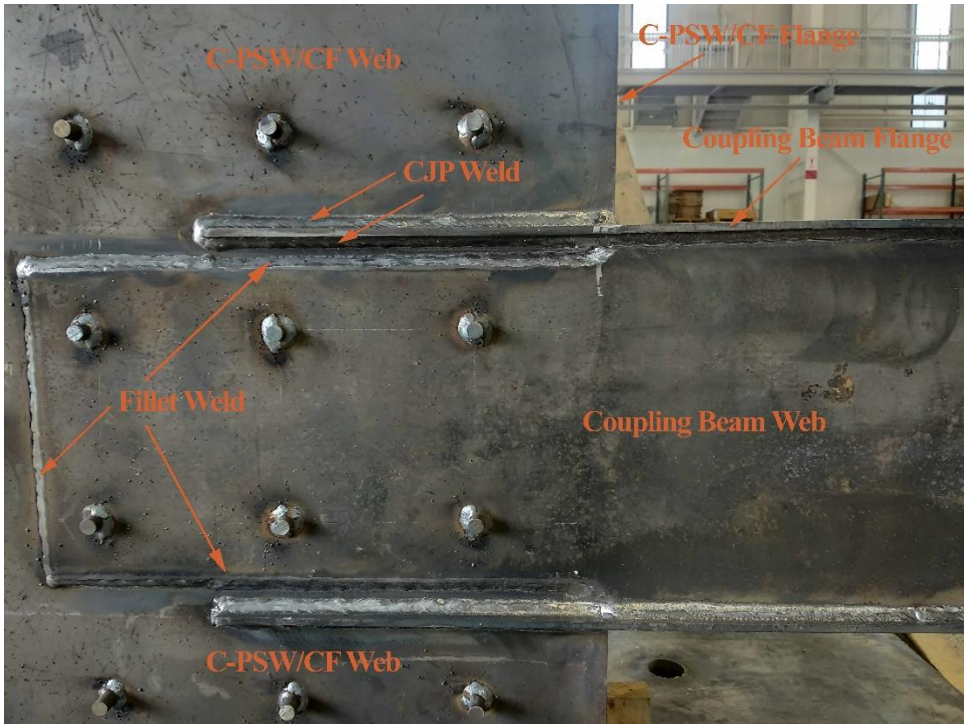

Figure 5-16. Coupling Beam-to-Wall Connection Details (Scaled Specimen Tested at Bowen Laboratory, Purdue University)

Note: The composite coupling beam cross section is changed due to the selection of this type of coupling beam-to-wall connection. The coupling beam flange plate width (b_{CB}) was previously designed to be 16 in. The coupling beam flange plate width is increased to 18 in. (b_{CB} + 2 in.) because of the connection details. In addition, the width of coupling beam is increased to 16.75 in. (16" + 3/8" + 3/8") as well. The design of the coupled C-PSW/CF should be rechecked due to this cross section change. However, this section is only provided to show a design example of a possible coupling beam-to-wall connection; therefore, the rechecking is not shown here, and the original 16" width is used in the calculations.

The coupling beam to wall connection was designed for the expected coupling beam strength. AISC *Prequalified Connections for Special and Intermediate Steel Moment Frames for Seismic Applications* (AISC, 2016) recommends a similar approach for steel connections. In the design of this connection, ductile (yielding) and non-ductile (fracture) limit state factors are 1.0 and 0.9, respectively.

$$\phi_d = 1.0$$
$$\phi_n = 0.9$$

5.5.7.1 FLANGE PLATE CONNECTION DEMAND

Required strength for designing the coupling beam flange plate to C-PSW/CF connection is calculated as the minimum of (a) 1.2 times of the expected tensile strength of flange or (b) the expected tensile rupture strength of flange.

Area of flange plate:

$$A_{CB.f} = (b_{CB} + 2in.)\, t_{CB.f} = (16 + 2)(0.5) = 9 \text{ in.}^2$$

Required strength of flange plate connection:

$R_t = 1.1$ (Expected tensile strength factor, ANSI/AISC 360-16 Table A3.1)

$$T_{flange} = \min\left(1.2\, R_y F_y A_{CB.f}, R_t F_u A_{CB.f}\right)$$

$$T_{flange} = \min[(1.2)(1.1)(50)(9)\,, (1.2)(65)(9)] = 594 \text{ kips}$$

$$\frac{T_{flange}}{2} = 297 \text{ kips}$$

5.5.7.2 CALCULATE REQUIRED LENGTH OF CJP WELDING

Required length for complete joint penetration (CJP) weld of the coupling beam flange plate to C-PSW/CF connection is governed based on the coupling beam flange capacity as follows:

$$\frac{T_{flange}}{2} \leq \phi_d\, 0.6\, F_y t_{CB.f} L_{req}$$

Required length of CJP weld:

$$L_{req.} \geq \frac{T_{flange}}{2\left(\phi_d\, 0.6\, F_y t_{CB.f}\right)} = \frac{594}{2(1.0)(0.6)(50)(0.5)} = 19.8 \text{ in.}$$

Length of CJP weld:

$$L_{weld.f} = 20 \text{ in.}$$

5.5.7.3 CHECK SHEAR STRENGTH OF COUPLING BEAM FLANGE PLATE

Shear yielding and shear rupture of coupling beam flange plate are calculated and compared with required strength of flange plate connection. Figure 5-17 shows the plane considered for the coupling beam flange plate shear yielding and shear rupture checks of this example.

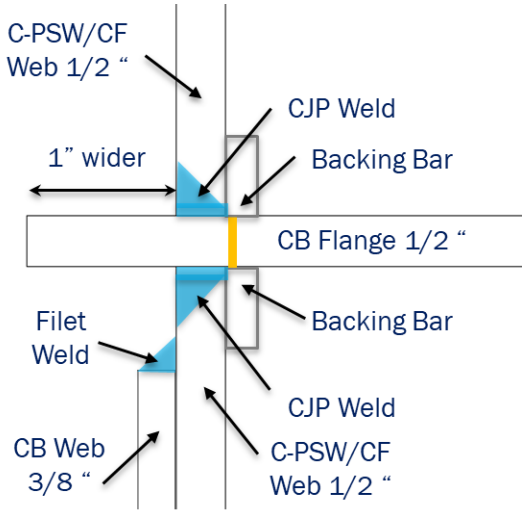

Figure 5-17. Shear Yielding and Shear Rupture of Coupling Beam Flange Plate

Gross shear area of coupling beam flange plate in shear yielding (the length along the CJP weld):

$$A_{f.SY} = t_{CB.f}\, L_{weld.f} = (0.5)(20) = 10 \text{ in.}^2$$

Shear yielding of coupling beam flange plate:

$$\phi_d\, 0.6\, F_y\, A_{f.\text{SY}} = (1.0)(0.6)(50)(10) = 300 \text{ kips} \geq \frac{T_{flange}}{2} = 297 \text{ kips}$$

Net shear area of coupling beam flange plate in shear rupture (the length along the CJP weld):

$$A_{f.SR} = t_{CB.f}\, L_{weld.f} = (0.5)(20) = 10 \text{ in.}^2$$

Shear rupture of coupling beam flange plate:

$$\phi_n\, 0.6\, F_u\, A_{f.\text{SR}} = (0.9)(0.6)(65)(10) = 351 \text{ kips} > \frac{T_{flange}}{2} = 297 \text{ kips}$$

5.5.7.4 CHECK SHEAR STRENGTH OF WALL WEB PLATES

Shear yielding and shear rupture of the C-PSW/CF web plate are calculated and compared with required strength of flange plate connection. Figure 5-18 shows planes considered for the C-PSW/CF web plate shear yielding and shear rupture checks of this example.

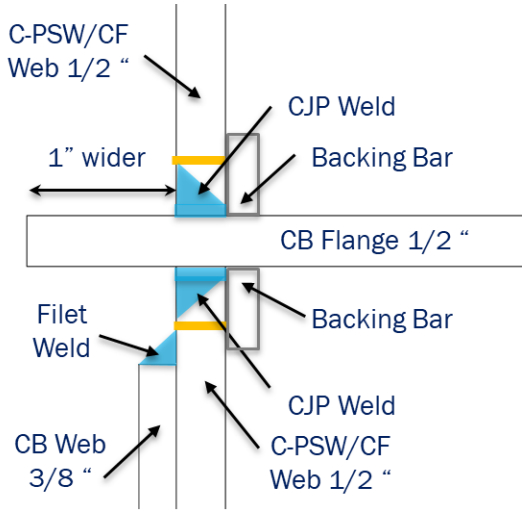

Figure 5-18. Shear Yielding and Shear Rupture of C-PSW/CF Web Plate

Gross shear area of C-PSW/CF web plate in shear yielding (the length along the CJP weld):

$$A_{w.SY} = 2\ t_p\ L_{weld.f} = 2(0.5)(20) = 20\ \text{in.}^2$$

Shear yielding of C-PSW/CF web plate:

$$\phi_d\ 0.6\ F_y\ A_{w.\text{SY}} = (1.0)(0.6)(50)(20) = \ 600\ \text{kips}\ > \frac{T_{flange}}{2} = 297\ \text{kips}$$

Net shear area of C-PSW/CF web plate in shear rupture (the length along the CJP weld):

$$A_{w.SR} = 2\ t_p\ L_{weld.f} = 2(0.5)(20) = 20\ \text{in.}^2$$

Shear rupture of C-PSW/CF web plate:

$$\phi_n\ 0.6\ F_u\ A_{w.\text{SR}} = (0.9)(0.6)(65)(20) = \ 702\ \text{kips} > \frac{T_{flange}}{2} = 297\ \text{kips}$$

5.5.7.5 CHECK DUCTILE BEHAVIOR OF FLANGE PLATES

In the coupling beam flange plate to C-PSW/CF connection design, the available tensile rupture strength should be higher than the available tensile yield strength.

Gross area of coupling beam flange plate in tension:

$$A_{CB.f.g} = (b_{CB} + 2in.)\ t_{CB.f} = (16 + 2)(0.5) = 9\ \text{in.}^2$$

Net area of coupling beam flange plate in tension:

$$A_{CB.f.n} = b_{CB}\ t_{CB.f} = (16)(0.5) = 8\ \text{in.}^2$$

Available tension yielding capacity of coupling beam flange plate:

$$R_y F_y A_{CB.f.g} = (1.1)(50)(9) = = 495 \text{ kips}$$

Available tension rupture capacity of coupling beam flange plate:

$$R_t F_u A_{CB.f.n} = (1.2)(65)(8) = 624 \text{ kips}$$

$$R_t F_u A_{CB.f.n} = 624 \text{ kips} > R_y F_y A_{CB.f.g} = 495 \text{ kips}$$

The coupling beam flange plate connection (CJP welding) designed above transfers all coupling beam flange forces to the C-PSW/CF. The following sections present all the forces and eccentricities in the coupling beam web plates, which have to be transferred to the C-PSW/CF using fillet welding.

5.5.7.6 CALCULATE FORCES IN WEB PLATES

In coupling beam web plate to C-PSW/CF connection design, axial tension, shear force, and moment of coupling beam web plates are calculated as follows:

Expected tension force of coupling beam web plate (calculated in Section 5.5.5.2):

$$T_{2.exp} = 773 \text{ kips}$$

Expected compression force of coupling beam web plate (calculated in Section 5.5.5.2):

$$C_{2.exp} = 217 \text{ kips}$$

Plastic neutral axis of coupling beam considering expected strength (calculated in Section 5.5.5.2):

$$C_{CB.exp} = 5.26 \text{ in.}$$

Coupling beam web plates tension force:

$$T_{web} = 1.2 \left(T_{2.exp} - C_{2.exp}\right) = 667 \text{ kips}$$

Coupling beam web plates moment:

$$M_{web} = 1.2 \left(T_{2.exp} \frac{C_{CB.exp}}{2} + C_{2.exp} \frac{h_{CB} - C_{CB.exp}}{2}\right) = 407 \text{ kip-ft}$$

Coupling beam web plates shear force:

$$V_{web} = 2 \left(\frac{1.2 M_{p.exp.CB}}{L_{CB}}\right) = 380 \text{ kips}$$

5.5.7.7 CALCULATE FORCE DEMAND ON C-SHAPED WELD

The C-shaped fillet weld of the coupling beam web plate to C-PSW/CF connection is designed to resist simultaneous axial tension, shear force, and moment, as shown in Figure 5-19. It should be noted that, in Figure 5-19, the details of connection, coupling flange plates, CJP welding, C-PSW/CF web plate are not shown. Required forces for the design of the C-shaped fillet weld are as follows:

C-shaped weld required tension force:

$$T_{C.weld} = \frac{T_{web}}{2} = 333 \text{ kips}$$

C-shaped weld required moment:

$$M_{C.weld} = \frac{M_{web}}{2} = 203 \text{ kip-ft}$$

C-shaped weld required shear force:

$$V_{C.weld} = \frac{V_{web}}{2} = 190 \text{ kips}$$

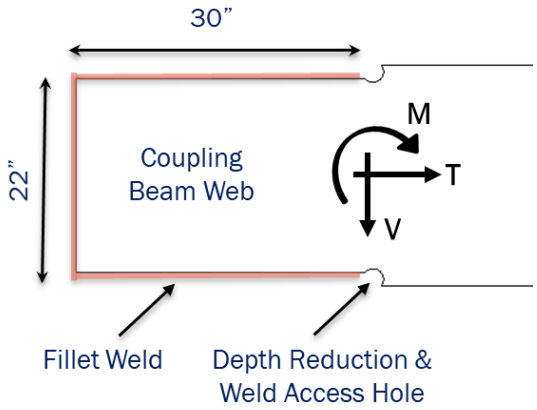

Figure 5-19. Required Forces for Designing the C-shaped Fillet Weld

5.5.7.8 SELECT WELD GEOMETRY

Vertical length of fillet weld:

$$L_{v.weld.w} = h_{CB} - 2\ in. = 22 \text{ in.}$$

Horizontal length of fillet weld:

$$L_{H.weld.w} = 30 \text{ in.}$$

Fillet weld minimum size:

$$D_{min} = 3/16\ in.$$

Fillet weld maximum size:

$$D_{max} = 5/16\ \text{in.}$$

Fillet weld maximum size is selected 5/16 in. because the coupling beam web plate thickness is 3/8 in:

Fillet weld size selected:

$$D = 5/16\ \text{in.}$$

$$D_{min} \leq D \leq D_{max}$$

5.5.7.9 CALCULATE C-SHAPED WELD SHEAR & MOMENT CAPACITIES

Instead of designing the C-shaped fillet weld of coupling beam web plate for simultaneous shear force and moment, it can be designed for an eccentric shear force, which produces an equivalent combined effect of shear force and moment. Therefore, the C-shaped fillet weld of coupling beam web plate is designed to resist simultaneous axial tension and eccentric shear force, as shown in Figure 5-20. This eccentrically loaded C-shaped fillet weld can be designed using AISC Steel Construction Manual, 15th Edition, Table 8-8 (AISC, 2017). The eccentrically loaded C-shaped fillet weld is designed as follows:

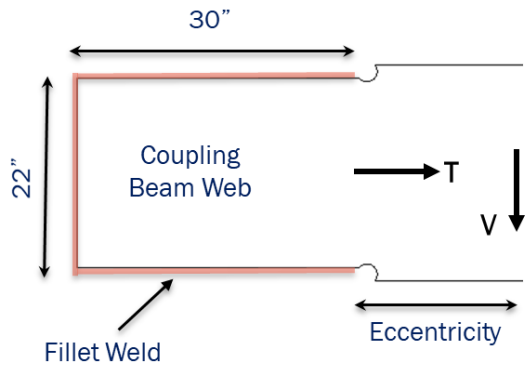

Figure 5-20. Required Tension and Eccentric Shear Forces for the Design of C-shaped Fillet Weld

$$Eccentricity = \frac{M_{C.web}}{V_{C.web}} = \frac{(203)(12)}{190} = 12.85\ \text{in.}$$

Centroid of C-shaped fillet weld (horizontal):

$$c.g. = \frac{{L_{H.weld.w}}^2}{2L_{H.weld.w}+L_{V.weld.w}} = \frac{30^2}{2(36)+(22)} = 10.98 \text{ in.}$$

Eccentricity of shear force from vertical fillet weld (horizontal):

$$e_x = Eccentricity + (L_{H.weld.w} - c.g.) = 12.9 + (30 - 11) = 31.88 \text{ in.}$$

Horizontal to vertical fillet weld length ratio:

$$k = \frac{L_{H.weld.w}}{L_{V.weld.w}} = \frac{30}{22} = 1.36$$

Eccentricity to vertical fillet weld length ratio:

$$a = \frac{e_x}{L_{V.weld.w}} = \frac{11}{22} = 1.45$$

$C_{8.8} = 3.11$ (AISC Steel Construction Manual, 15th Edition, Table 8-8)

$C_{1-8.3} = 1$ (AISC Steel Construction Manual, 15th Edition, Table 8-3)

In accordance with AISC Steel Construction Manual, 15th Edition, Table 8-8, fillet weld capacity to resist the eccentric shear force is as follows:

$$P_{V.weld} = \phi_n \, C_{8.8} \, C_{1-8.3} \, (16D) L_{V.weld.w} = (0.9)(2.99)(1)\left[16\left(\frac{5}{16}\right)\right](22) = 307 \; kips$$

$$P_{V.weld} = 334 \; kips \; > \; V_{C.weld} = 190 \text{ kips}$$

$$\frac{V_{C.weld}}{P_{V.weld}} = 0.62$$

5.5.7.10 CALCULATE C-SHAPED WELD TENSION CAPACITY

In accordance with ANSI/AISC 360-16 Section J2.4, tension (horizontal) capacity of C-shaped fillet weld is calculated as follows:

$$P_{T.weld} = \phi_n \, 0.6 \, F_{XX} \, 2 \, L_{H.weld.w} 0.7071D = (0.9)(0.6)(70)[2(30)](0.7071)(5/16)$$

$$P_{T.weld} = 501 \; kips \; > \; T_{C.weld} = 333 \text{ kips}$$

$$\frac{T_{C.weld}}{P_{T.weld}} = 0.67$$

5.5.7.11 CALCULATE THE UTILIZATION OF C-SHAPED WELD CAPACITY

Utilization ratio of the C-shaped fillet weld is calculated by taking the square root of the sum of the squared utilization of the eccentric shear capacity and tension capacity.

$$Capacity = \sqrt{\left(\frac{V_{C.weld}}{P_{V.weld}}\right)^2 + \left(\frac{T_{C.weld}}{P_{T.weld}}\right)^2} = \sqrt{(0.62)^2 + (0.67)^2} = 0.91 \leq +1$$

5.6 Acknowledgements

This design example is based on research and development of the coupled C-PSW/CF (known as SpeedCore system), which would be incomplete and inadequate without valuable input and contributions from the following:

- Mr. Ron Klemencic, Chairman and CEO, and the team of engineers from Magnusson Klemencic Associates for their significant intellectual and engineering contributions.
- AISC Engineers (Mr. Larry Kruth, Dr. Charlie Carter, Dr. Devin Huber, and Ms. Margaret Mitchell) for their technical guidance on fabrication, erection, and constructability.
- AISC Task Committee 5 (TC5) members and Committee of Specification (CoS) members for all their comments and suggestions that have significantly improved the SpeedCore design provisions in the 2022 AISC *Specification* and 2022 AISC *Seismic Provisions*.
- Members of the Building Seismic Safety Council (BSSC) and Issue Team 4 (IT-4), ASCE 7 Seismic Subcommittee (Mr. John Hooper, Chair), and the ASCE 7 Standards committee for all their comments that have significantly improved the SpeedCore seismic design provisions in the 2021 ASCE 7 Standard, Chapter 14.3.5, and NEHRP 2020.
- Prof. Michel Bruneau and his graduate students (Mr. Emre Kizilarslan) for their significant intellectual contributions and research camaraderie.
- Purdue research team (Dr. Jungil Seo, Ms. Morgan Broberg, Mr. Mubashshir Ahmad, Mr. Ataollah Taghipour Anvari, and Mr. Thomas Bradt)

5.7 References

See the “Useful Design Aid Resources” in Section 5.5 above for additional references.

ASCE (2017). *Minimum Design Loads and Associated Criteria for Buildings and Other Structures*, ASCE/SEI 7-16, American Society of Civil Engineers, Reston, VA.

ASCE (2022). *Minimum Design Loads and Associated Criteria for Buildings and Other Structures*, ASCE/SEI 7-22, public draft, American Society of Civil Engineers, Reston, VA., June 17

Anvari, A. T., Bhardwaj, S. R., Wazalwar, P., and Varma, A. H. (2020). Stability of SpeedCore walls under fire loading: summary of numerical analyses. In *Proceedings of Structural Stability Research Council (SSRC) Conference*, Atlanta, Georgia, April 21–24.

Broberg, M., Shafaei, S., Kizilarslan, E., Seo, J., Varma, A. H., Bruneau, M. and Klemencic, R. (2022). "Capacity Design of Coupled Composite Plate Shear Walls – Concrete Filled (CC-CPSW/CF)," Journal of Structural Engineering, ASCE, Accepted.

Bruneau., M., Varma, A.H., Kizilarslan, E., Broberg, M., Shafaei, S. and Seo, J. (2019). R-*Factors for Coupled Composite Plate Shear Walls—Concrete Filled (Coupled-C-PSW/CF)*, Final Report for Project CPF#05-17, Charles Pankow Foundation and American Institute of Steel Construction

FEMA (2009). *Quantification of Building Seismic Performance Factors*, FEMA P695, Federal Emergency Management Agency, Washington, D.C., June 2009.

Kizilarslan, E., Seo, J., Broberg, M., Shafaei, S., Varma, A.H., and Bruneau., M., (2018). *R-Factors for Coupled Composite Plate Shear Walls—Concrete Filled (Coupled-C-PSW/CF)*, Interim Project Report #2, Submitted to the Charles Pankow Foundation for CPF Research Grant #06-16.

Shafaei, S., Broberg, M., and Varma, A. H., (2022). "Lateral Seismic Load Behavior and Design of Coupled Composite Plate Shear Walls / Concrete-Filled (CC-PSW/CFs)" *12th National Conference on Earthquake Engineering.* Salt Lake City, Utah. June 27-July 1, 2022.

Chapter 6: Three-Story Cross-Laminated Timber (CLT) Shear Wall

Philip Line[1] and M. Omar Amini[2]

6.1 Overview

This example features the seismic design of cross-laminated timber shear walls used in a three-story, six-unit townhouse cross-laminated timber building of platform construction.

The CLT shear wall design in this example includes:

- Check of CLT shear wall shear strength
- Check of CLT shear wall hold-down size and compression zone length for overturning
- Check of CLT shear wall deflection for conformance to seismic drift limits

The following documents are used in this example.

Useful Design Aid Resources

APA (2020). *Standard for Performance-Rated Cross-Laminated Timber*, ANSI/APA PRG 320-19, APA, 2020.

ASCE (2021). *ASCE/SEI 7-22 Minimum Design Loads and Associated Criteria for Buildings and Other Structures*, public comment draft, Structural Engineering Institute of the American Society of Civil Engineers, Reston, VA, June 17.

AWC (2017). *National Design Specification (NDS) for Wood Construction*, NDS-18, American Wood Council, Leesburg, VA, 2017.

AWC (2020). *Special Design Provisions for Wind and Seismic (SDPWS)*, SDPWS-21, American Wood Council, Leesburg, VA, 2020.

FEMA (2020a). *NEHRP Recommended Seismic Provisions for New Buildings and Other Structures, Volume I: Part 1 Provisions and Part 2 Commentary*, 2020 Edition, FEMA P-2082-1,

[1] Philip Line, P.E., American Wood Council.
[2] M. Omar Amini, Ph.D, Simpson Strong-Tie.

prepared by the Building Seismic Safety Council of the National Institute of Buildings Sciences for Federal Emergency Management Agency.

6.2 Background

Design requirements for CLT shear walls as a seismic force-resisting system, including research that demonstrates adequate adjusted collapse margins ratios using the FEMA P695 methodology, can be found in General Technical Report FPL-GTR-281 (van de Lindt et al., in press). Features of the new CLT shear wall system were influenced by CLT shear wall buildings built in the U.S. and internationally that featured metal connectors attached to the CLT panel face for shear resistance and use of either conventional hold-down or rod-system for overturning. Performance observations from varied test programs, including CLT shear wall testing (FPInnovations, 2013), also influenced development of the design approach for CLT shear walls as a seismic force-resisting system.

CLT is a prefabricated engineered wood product made of at least three orthogonal layers of graded sawn lumber or structural composite lumber (SCL) that are laminated by gluing with structural adhesives. Testing, qualification, and quality assurance requirements for CLT are established by the PRG 320 product standard. The structural design of CLT as a roof, floor or wall member for resistance to tension, compression, bending, and shear, as well as the design of connections to CLT, first appeared in the 2015 *National Design Specification for Wood Construction* (AWC, 2014). Design requirements for CLT shear walls as a seismic force-resisting system appeared in SDPWS for the first time in the 2021 edition. The two defined CLT shear wall system types in SDPWS-21 are: (a) *CLT shear walls*, and (b) *CLT shear walls with shear resistance provided by high aspect ratio panels only,* and have associated seismic design factors (i.e., R, Ω_0, and C_d) provided in ASCE/SEI Standard 7-22 Table 12.2-1. The 2020 *NEHRP Provisions* contain the same seismic design factors and CLT shear wall detailing requirements very similar to those incorporated in SDPWS-21 Appendix B. The CLT shear walls in this example are based on the *CLT shear wall* system.

Individual CLT panels within the defined CLT shear wall system types designed in accordance with SDPWS-21 Appendix B are expected to exhibit rocking as shown in Figure 6-1 with strength of the system controlled by nailed connections. To ensure rocking behavior and development of the nailed connection strength, design requirements include: (1) use of CLT panels of prescribed aspect ratios; (2) use of prescribed nailed connectors at bottoms of panels, tops of panels, and adjoining vertical edge(s) of multi-panel shear walls; (3) strength requirements for overturning tension devices (e.g., hold-downs); and (4) compression zone length requirements.

This example does not address all system requirements implemented for CLT shear walls in SDPWS-21, including but not limited to requirements for CLT diaphragms and requirements for deformation compatibility of CLT walls that are not designated as part of the seismic force-resisting system. This example does not address use of CLT as part of a hybrid structural system where CLT panels are used in floors for both gravity load-carrying and diaphragm function while other structural systems are used as the vertical elements of the seismic force-resisting system such as wood-frame wood

structural panel shear walls, concrete shear walls or moment frames, or steel braced frames or moment frames.

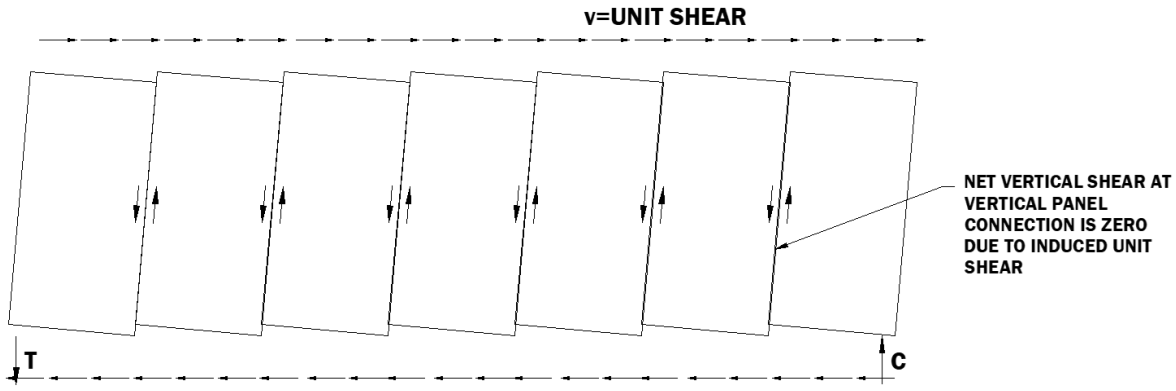

Figure 6-1. Illustration of Rocking Behavior of Seven Individual Panels in a Multi-panel CLT Shear Wall Designed in Accordance with SDPWS-21 Appendix B

6.3 Cross-laminated Timber Shear Wall Example Description

The seismic force-resisting system consists of CLT shear walls and CLT floor diaphragms in a three-story building of platform construction. Figure 6-2 shows an elevation view. Figure 6-3 shows a typical floor plan. Figure 6-4 shows the CLT shear walls of interest for this example, which are aligned with the building's transverse direction and are located along Line 4 (see Figure 6-3) in a stacked configuration. The transverse walls support CLT floor gravity loads in addition to their self-weight. Roof gravity loads are supported by the exterior walls aligned with the building's longitudinal direction. Weights are provided in Table 6-1. Tributary weights for seismic and gravity design of the CLT shear walls along Line 4 are provided in Table 6-2. Seismic loads are derived in Section 6.4.

Table 6-1. Weights of Roof/Ceiling, Floors, and Walls

Item	Description	Weight
Roof/Ceiling	Light-frame roof, gypsum board ceiling, roofing, insulation	25 psf
Floor	5-layer CLT (6.875 in. thick), gypsum board ceiling, flooring. Includes 8 psf of floor area for wall partitions.	35 psf
Interior Walls	3-layer CLT (4.125 in. thick), light-frame wall, gypsum board finish, sound insulation	20 psf

Table 6-1. Weights of Roof/Ceiling, Floors, and Walls (Continued)

Item	Description	Weight
Exterior Walls	3-layer CLT (4.125 in. thick), light-frame wall, gypsum board interior finish, stucco exterior, insulation	30 psf

Table 6-2. Seismic Weight and Gravity Load for CLT Shear Walls Along Line 4 (see Figure 6-3)

Item	Tributary Seismic Weight for Lateral Design	Tributary Dead Load for Gravity Design
	(kips)	(plf)
3rd Story Wall	26.8	190
2nd Story Wall	43.1	793
1st Story Wall	42.4	793 p

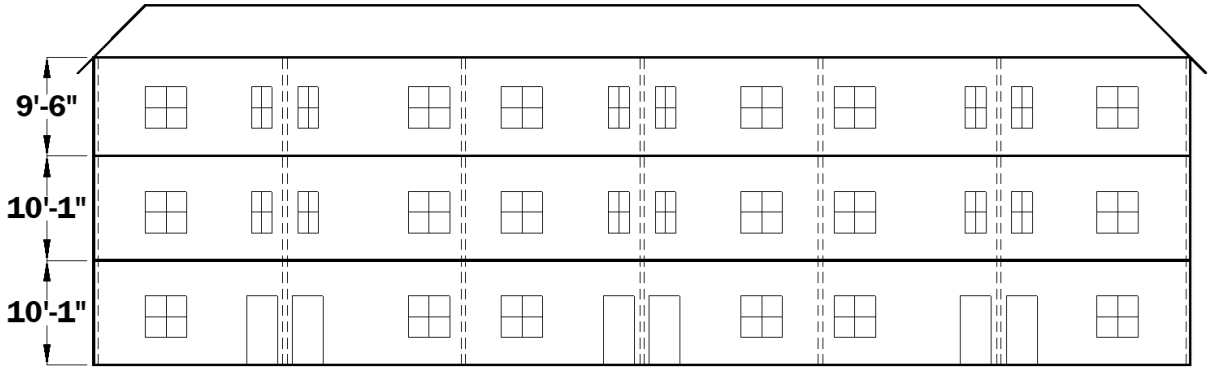

Figure 6-2. Elevation View of Three-story Cross-laminated Timber Shear Wall Building

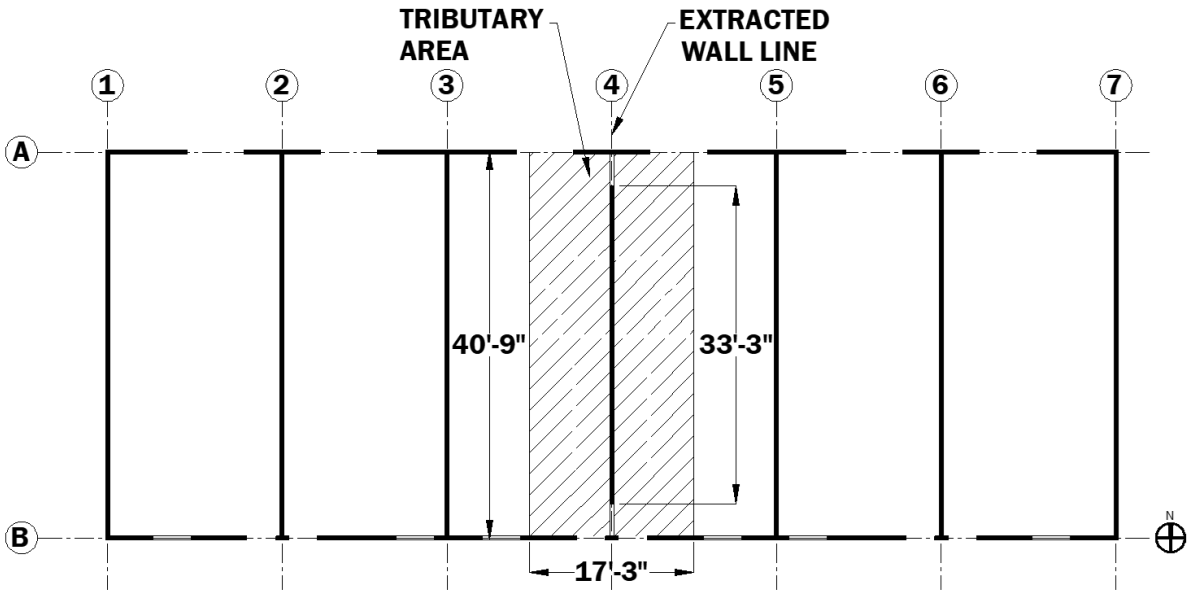

Figure 6-3. Typical Floor Plan (first story openings shown)

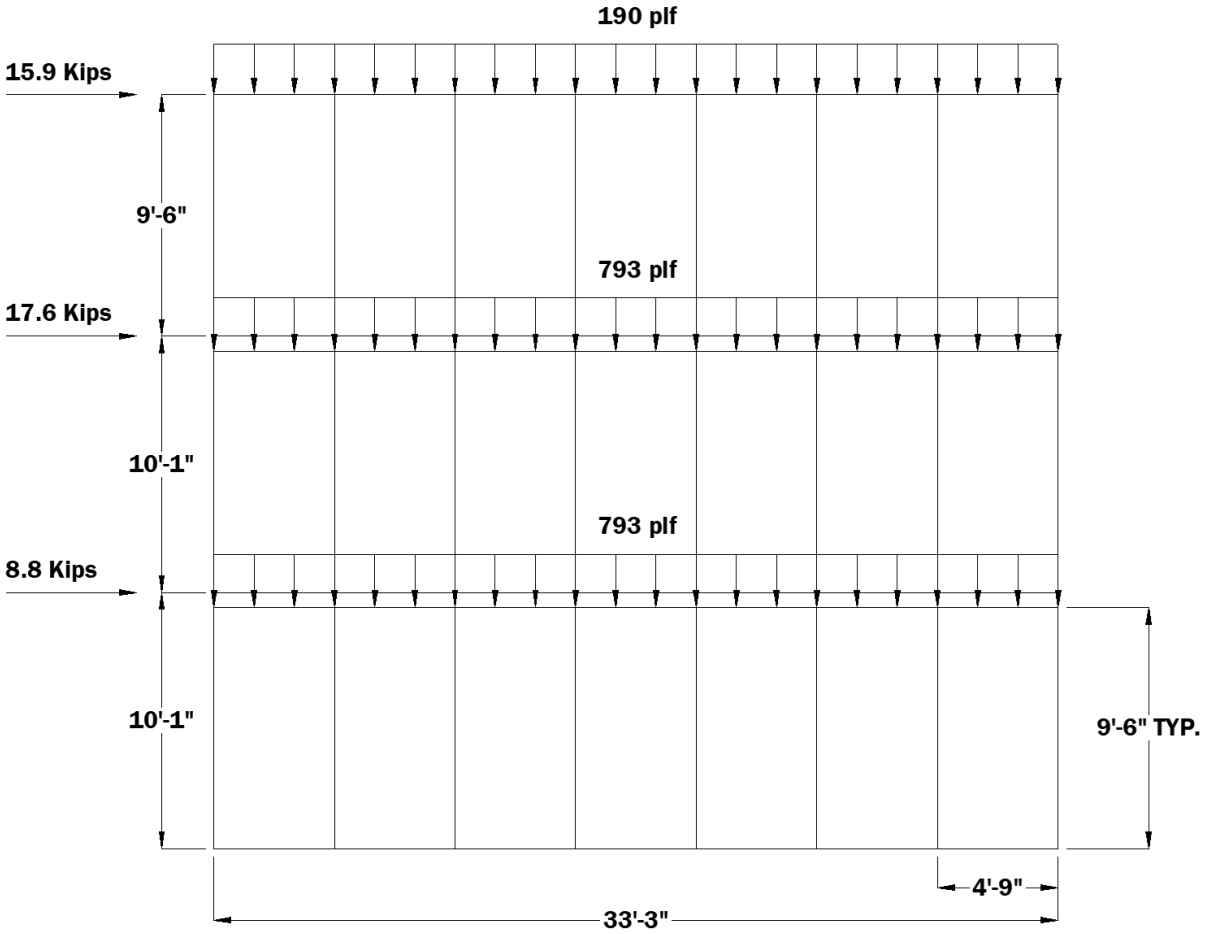

Figure 6-4. Vertical Distribution of Seismic Force and Dead Load Tributary to the CLT Shear Walls Located Along Line 4 (see Figure 6-3)

6.4 Seismic Forces

The CLT shear wall system types recognized in ASCE/SEI 7-22 Table 12.2-1 are summarized in Table 6-3. The shear wall system used in this example is *Cross-laminated timber shear walls* (i.e., R=3, Ω_0=3, C_d=3).

Table 6-3. Design Coefficients and Factors for CLT Seismic Force-Resisting Systems (appearing in ASCE/SEI 7-22 Table 12.2-1)

Seismic Force-Resisting System	Detailing Requirements, ASCE/SEI 7-22 Section	*R*	Ω_0	C_d	Structural Height, h_n, Limit Seismic Design Category B, C, D, E & F
Cross-laminated timber shear walls	14.5	3	3	3	65 feet
Cross-laminated timber shear walls with shear resistance provided by high aspect ratio panels only	14.5	4	3	4	65 feet

For the example building, the design spectral response acceleration parameter in the short period range, S_{DS}, is equal to 1.0; the seismic Importance factor, I_e, is equal to 1.0; and the response modification coefficient, *R*, is equal to 3. This CLT shear wall structure's base shear is computed using ASCE/SEI 7-22 Equation 12.8-2 (for short-period structures) as follows where *W* is seismic weight:

$$V = C_s W = \frac{S_{DS}}{(R/I)} W = \frac{1.0}{(3.0/1.0)} W = 0.333\ W\ kips$$

The portion of seismic lateral force tributary to the CLT shear walls of interest is 42.3 kips. Vertical distribution of seismic force and dead load tributary to each shear wall (including wall self-weight) are shown in Figure 6-4. Table 6-4 provides cumulative lateral shear force and associated unit shear force based on shear wall length of 33.25 feet.

Table 6-4. Summary of Cumulative Lateral Seismic Force and Unit Shear Force per Story

Story	Lateral force, V_x	Unit Shear Force per Foot of Shear Wall Length
	(kips)	(plf)
3	15.9	477
2	33.5	1,009
1	42.3	1,273

6.5 CLT Shear Wall Shear Strength

The CLT used in walls is E1 grade in accordance with PRG 320. The lumber specific gravity is G=0.42.

Each shear wall consists of seven 3-layer CLT panels with height, h, of 9'-6" and length, b_s, of 4'-9" for a panel aspect ratio, h/b_s, equal to 2. From SDPWS-21 Section B.3.1, CLT panels forming a multi-panel shear wall shall have panel aspect ratio, h/b_s, not greater than 4 nor less than 2. From SDPWS-21 Sections B.3.2 and B.3.3, the same number of connectors is provided at the top and bottom of each wall panel, and the number of connectors at adjoining vertical edges is the number of bottom of wall connectors times the CLT panel aspect ratio.

For the story unit shears given in Table 6-4, a preliminary design is depicted in Figure 6-5, showing CLT panel dimensions and the number and location of connectors and hold-downs. Associated details for wall-floor intersections are shown in Figure 6-6. The light frame roof system framing is not shown in Figure 6-6.

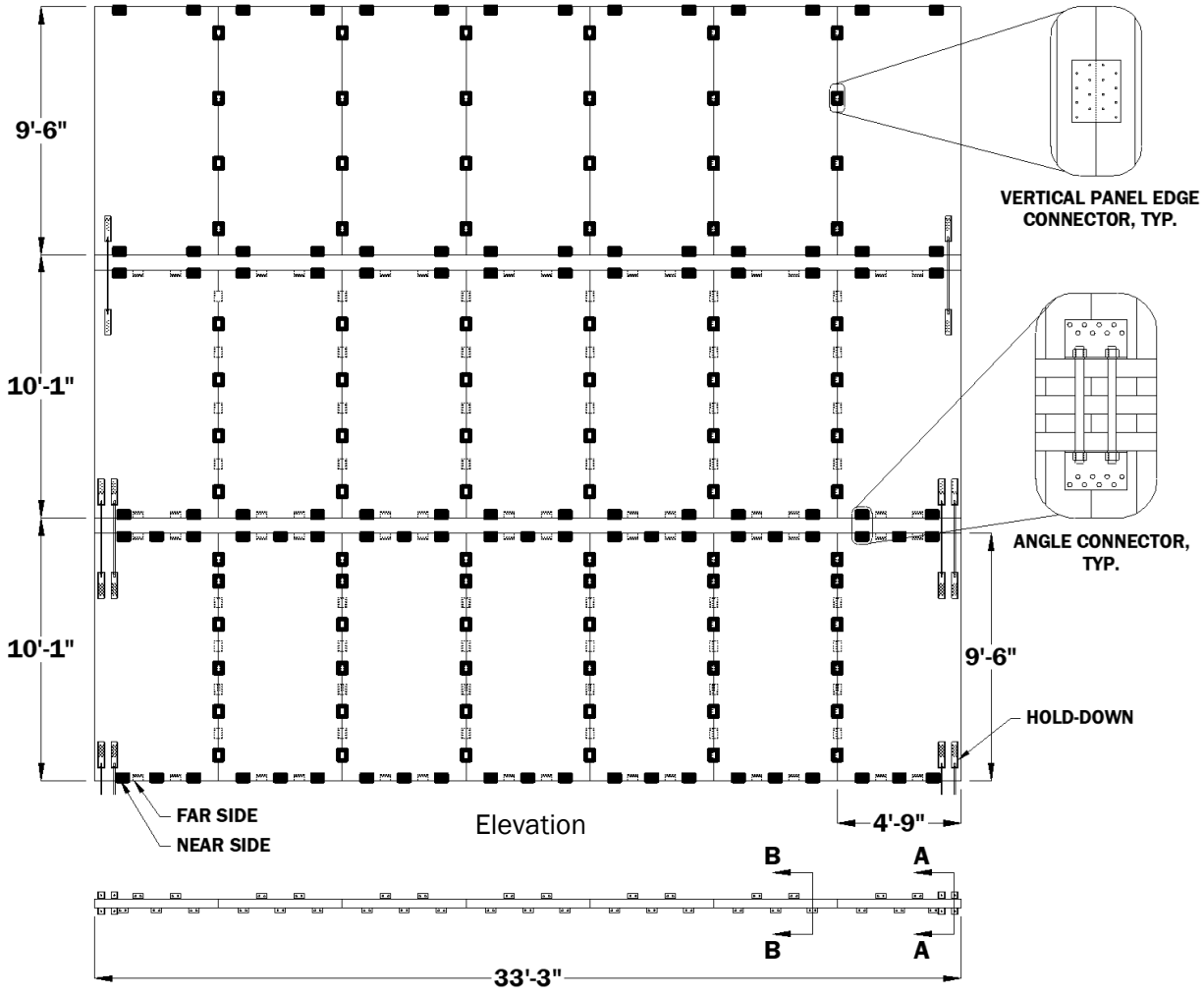

First Floor Connector Layout (5 connectors per panel)

Figure 6-5. CLT Shear Walls at 1st, 2nd, and 3rd Story with Connector and Hold-down Locations

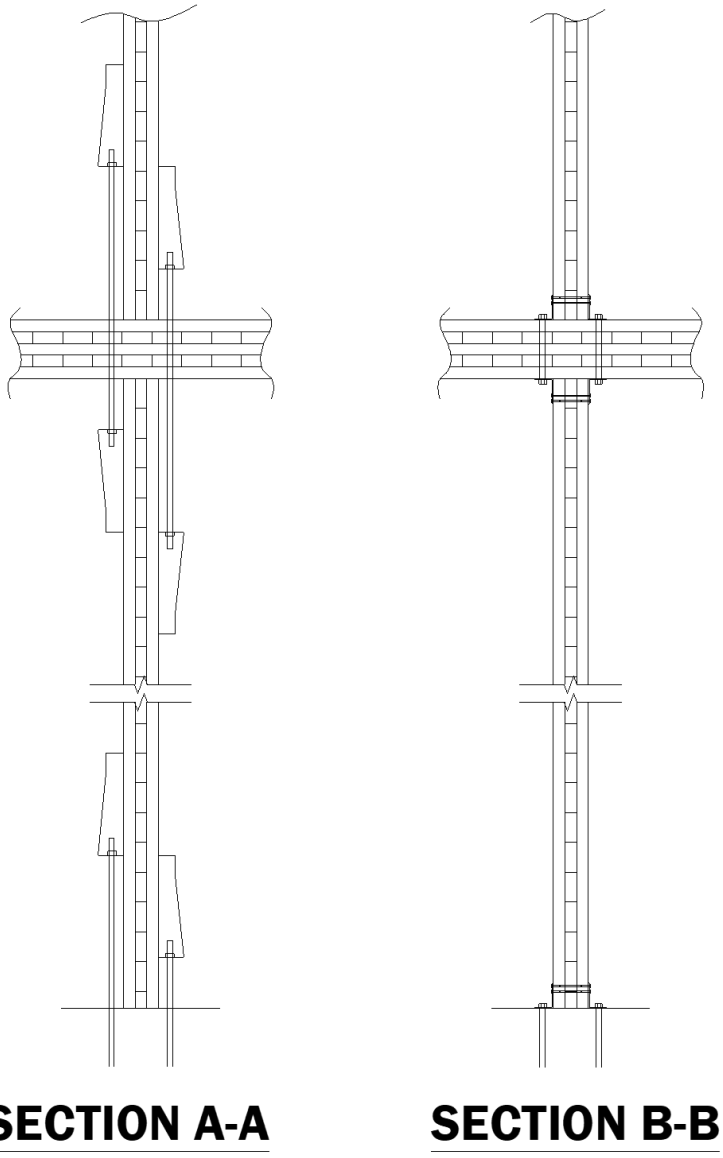

Figure 6-6. Wall-floor Intersections Showing Hold-downs (Section A-A from Figure 6-5), and Connectors (Section B-B from Figure 6-5)

6.5.1 Shear Capacity of Prescribed Connectors

From SDPWS-21 Sections B.5, the LRFD design unit shear capacity for seismic based on the number of connectors at the bottom of the wall is calculated as follows:

$$v_{s(\text{seismic})} = \phi\,(n)\left(\frac{2605}{b_s}\right)C_G$$

where:

n = number of angle connectors along bottom of panel face

2,605 = connector nominal shear capacity (lb)

b_s = individual CLT panel length (ft)

C_G = CLT panel specific gravity factor which equals 1.0 for $G \geq 0.42$ specific gravity panels used in this example, and

ϕ = resistance factor equal to 0.5 for seismic design

Table 6-5. CLT Shear Wall Connectors and LRFD Design Unit Shear Capacity

Story	Panel thick-ness	Panel length, b_s	Panel height, h	Number of connectors per panel at top and bottom panel edge	Number of connectors at each adjoining vertical panel edge	v_n, Nominal unit shear capacity, $(n \cdot 2605)/b_s$	$v_{s(seismic)}$, LRFD design unit shear capacity, (ϕ= 0.5)
	(in.)	(ft)	(ft)	(n)	(n x h/b_s)	(plf)	(plf)
3	4.125	4.75	9.5	2	4	1,096	548
2	4.125	4.75	9.5	4	8	2,193	1,097
1	4.125	4.75	9.5	5	10	2,742	1,371

Table 6-5 summarizes the number of top of wall and bottom of wall connectors, adjoining panel edge connectors, and associated design unit shear capacity. For each story, the design unit shear capacity is greater than the unit shear force per story (see Table 6-4). Therefore, CLT shear wall shear strength associated with the connector design is satisfied.

6.5.2 Shear Capacity of CLT Panel

For this 3-layer CLT panel, the in-plane unit shear capacity of the panel itself is determined using in-plane shear unit shear capacity values in the manufacturer's evaluation report and converting for use with LRFD per NDS-2018 Table 10.3.1:

$$v_r' = \phi\lambda K_F F_v(t_v) = 0.75(1.0)(2.88)(9{,}700) = 20{,}849 \text{ plf}$$

where:

ϕ = resistance factor equal 0.75 for shear

λ = time effect factor equal to 1.0 for seismic loading

K_F = Format conversion factor equal to 2.88 for shear parallel to grain, $F_v(t_v)$

$F_v(t_v)$= 9,700 plf

Note: For this example, a reference design in-plane unit shear value is obtained from the CLT panel manufacturer's evaluation report and will typically be provided separately for in-plane loading parallel to the wall face lamination and perpendicular to the wall face lamination. The smaller of the evaluation report parallel or perpendicular to the wall face lamination design value for in-plane loading is used because equal horizontal and vertical in-plane unit shear stresses are induced in the panel from in-plane shear loading.

CLT panel in-plane unit shear capacity, v_r' = 20,849 plf is significantly greater than the largest unit shear force per story demand of 1,273 plf (see Table 6-4). The nominal in-plane unit shear capacity of the CLT panel exceeds the largest nominal unit shear capacity associated with nailed connectors in the first story walls (see Table 6-5):

$$\frac{20{,}849\ plf}{0.75} > \frac{1{,}371\ plf}{0.5}$$

$$27{,}799\ plf > 2{,}742\ plf$$

The CLT panel itself satisfies the shear strength requirement. CLT panel in-plane unit shear capacity is large compared to the unit shear capacity that can be developed by the nailed connectors and will not control in a typical design that uses wall panels with limited removal of material by cutting of holes and notches.

6.6 CLT Hold-down and Compression Zone for Overturning

6.6.1 CLT Shear Wall Hold-down Design

To size the hold-down, seismic forces and gravity loads are combined in accordance with basic load combinations in ASCE/SEI 7-22.

$0.9D - E_v + E_h$ (ASCE/SEI 7-22 Section 2.3.6, Load Combination 7)

where:

$E_v = 0.2S_{DS}D$ (ASCE/SEI 7-22 Equation 12.4-4a)

$E_h = \rho Q_E$ (ASCE/SEI 7-22 Equation 12.4-3)

$0.9D - 0.2S_{DS}D \pm \rho Q_E$ (ASCE/SEI 7-22 Section 2.3.6, Load Combination 7)

$$(0.9 - 0.2S_{DS})D \pm \rho Q_E$$

For S_{DS} equal to 1.0 as used above and ρ equal to 1.0 because the number of bays requirement per ASCE/SEI 7-22 Section 12.3.4.2 for ρ equal to 1.0 is satisfied by the building configuration in this example, the load combination simplifies to:

$$0.7D - Q_E$$

A free-body diagram for the tension end panel of the CLT multi-panel shear wall is shown in Figure 6-7.

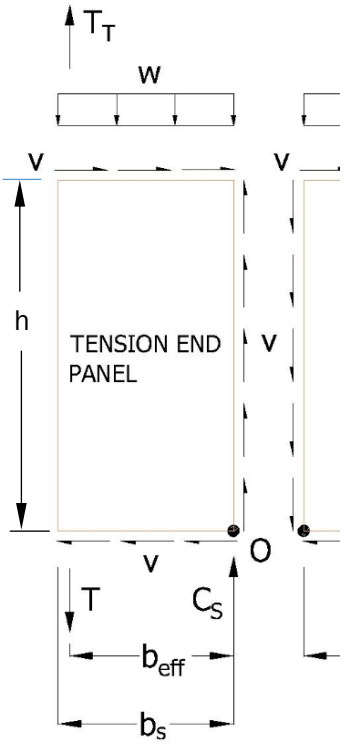

Figure 6-7. Free-body Diagram for the Tension End Panel of the CLT Multi-panel Shear Wall

The solution for tension force, *T*, is summarized in Table 6-6 based on consideration of tension end panel moment equilibrium:

$$\sum M_o = 0$$

$$T\ (b_{eff}) - vb_s h + wb_s\left(\frac{b_s}{2}\right) - T_T(b_{eff}) = 0 \qquad \text{(SDPWS-21 Equation C-B.1)}$$

$$T = \frac{vb_s h - wb_s\left(\frac{b_s}{2}\right)}{b_{eff}} + T_T$$

(SDPWS-21 Equation C-B.2)

where:

ν = unit shear, plf

Note: The unit shear force for sizing the hold-down is not less than 2.0 times the forces associated with the design unit shear capacity of the provided CLT shear wall connectors (SDPWS-21 Section B.3.4).

w = dead load including wall panel self-weight, plf

Note: Dead load used to offset overturning induced uplift is limited to that portion supported by or directly above the individual CLT panel (SDPWS-21 Section B.2). For this simple example, the 33'3" effective length of the wall is set back from the perpendicular walls, and the "T" connection at the perpendicular walls is not incorporated into the overturning resistance.

b_s = CLT panel length, ft

b_{eff} = moment arm for calculation of T force, ft

Note: Moment arm for T force calculation in a multi-panel CLT shear wall is equal to the distance from the centerline of hold-down resistance and the tension end panel compression edge. For typical multi-panel applications, rotation can be assumed to be about the tension end panel's compression edge because compression C_s is small. For single panel CLT shear walls, b_{eff}, is the distance between centerline of hold-down force and centerline of compression zone resistance.

h = CLT panel height, ft

T = tension force, lb

T_T = tension force at top of tension end panel from story above, lb

Note: For this example, per Figure 6-7 and the associated moment equilibrium equations, T and T_T are aligned and are associated with the same moment arm, b_{eff}. Accumulated tension force, T_T, is calculated using 2 times the design unit shear capacity of the provided CLT shear wall connectors.

Table 6-6. Solution for Tension Force, *T*, for Hold-down Strength Requirement

Story	Unit shear force per foot of shear wall length	$v_{s(seismic)}$, LRFD design unit shear capacity, (ϕ= 0.5)	2 x $v_{s(seismic)}$	T_T from story above	*T* for 2 x $v_{s(seismic)}$ requirement for load combination 1.0*E* - 0.7*D*
	(plf)	(plf)	(plf)	(lb)	(lb)
3	477	548	1,097	0	11,293
2	1,009	1,097	2,194	11,293	34,540
1	1,273	1,371	2,742	34,540	63,968

Required *T* force per SDPWS-21 Section B.3.4 for design of the 3rd story shear wall hold-down is calculated as follows:

$$T = \frac{vb_s h - wb_s\left(\frac{b_s}{2}\right)}{b_{eff}} + T_T \qquad \text{SDPWS-21 Equation C-B.2}$$

$$T = \frac{2(548)(4.75)(9.5) - 0.7(190)(4.75)\left(\frac{4.75}{2}\right)}{4.25} + 0 = \quad 11{,}284\ lb$$

The *T* force of 11,284 lb for the design of the 3rd story shear wall hold-down is based on 2.0 times the forces associated with the design unit shear capacity of the provided CLT shear wall connectors requirement of SDPWS-21 Section B.3.4 and matches the value in Table 6-6 with a slight difference due to rounding. In the above calculation, b_{eff} = 4.25 ft is associated with hold-down location 6" from the tension edge of the tension end panel (i.e., b_{eff} = 4.75 ft – 0.5 ft = 4.25 ft) and T_T = 0 is associated with zero tension force from the story above.

For magnitude of *T* forces in Table 6-6, conventional hold-downs can be used to provide overturning restraint. As a simplification, the same screw attached hold-down is used for all locations, with each having an LRFD design tension capacity of 17,687 lb and associated deflection of 0.253 in. Hold-downs are specified as follows and satisfy the SDPWS-21 strength requirement:

- four hold-downs at each end between bottom of 1st story walls and the foundation, total hold-down capacity = 4 x 17,687 lb = 70,748 lb which exceeds 63,968 lb;
- four hold-downs at each end between bottom of 2nd story and top of 1st story walls, total hold-down capacity = 4 x 17,687 lb = 70,748 lb which exceeds 35,540 lb; and

- two hold-downs at each end between bottom of 3rd story and top of 2nd story walls, total hold-down capacity = 2 x 17,687 lb = 37,374 lb which exceeds 11,293 lb.

From SDPWS-21 Section B.3.4, hold-down device deformation for each story shall not exceed 0.185 in. for T forces from strength design load combinations (see Table 6-7), not T forces associated with 2 times shear wall design unit shear capacity. Assuming linearly varying hold-down deflection with tension load, the four hold-downs in the first story walls, which are the most highly loaded relative to their LRFD design tension load (see Table 6-7), have deflection equal to:

$$\Delta_{hold-down} = \frac{27{,}472\ lb}{4(17{,}678\ lb)}(0.253\ in.) = 0.098\ in.$$

The hold-down deflection is less than 0.185 in., and the SDPWS-21 deflection limit is satisfied.

Table 6-7. Solution for Tension Force, *T*, for Hold-down Deflection Requirement

Story	Unit shear force per foot of shear wall length	*T* for load combination 1.0E - 0.7D
	(plf)	(lb)
3	477	4,714
2	1,009	14,604
1	1,273	27,472

The most highly loaded hold-downs at the first story CLT shear walls are associated with a required *T* force of 63,968 lb. The hold-downs are spaced to develop the end 1-ft length of CLT wall panel in tension. The LRFD design tension capacity of the panel per foot of length is based on strength contributed by the layers oriented parallel to grain and calculated as follows (see NDS-2018 Table 10.3.1):

$$T'_r = \phi\lambda K_F F_t (A_{parallel}) = 0.80(1.0)(2.70)(1{,}375\ psi)[2(1.375\ in.)(12\ in.)] = 98{,}010\ \text{lb}$$

The CLT wall panel axial strength in tension over an effective length of 1-ft is 98,010 lb, which exceeds the required *T* force equal to 63,968 lb for hold-down system design. For the screw-attached hold-downs used in this example, manufacturer design values based on Spruce-pine fir (*G*=0.42) sawn lumber posts are used for CLT panels of equivalent specie, specific gravity, *G*, and dimension.

As part of a complete design, CLT panel axial capacity in net section tension rupture including wood strength limit states at connections for the specific details of the design must also be evaluated in accordance with NDS-2018 and NDS-2018 Appendix E. Specific details of the design to be

addressed include panel modifications (holes or cuts) and effect on panel strength as well as wood strength limit states associated with multiple adjacent hold-downs and potential for row and group tear out. NDS-2018 Appendix E provisions can be conservatively applied for evaluation of row and group tear-out design capacity in CLT by utilizing only parallel oriented layers in the calculation.

6.6.2 CLT Shear Wall Compression Zone

To evaluate adequacy of the CLT shear wall compression end panel for bearing, seismic forces and gravity loads are combined in accordance with basic load combinations in ASCE/SEI 7-22.

$1.2D + E_v + E_h + L + 0.2S$ (ASCE/SEI 7-22 Section 2.3.6, Load Combination 6)

where:

$E_v = 0.2S_{DS}D$ (ASCE/SEI 7-22 Equation 12.4-4a)

$E_h = \rho Q_E$ (ASCE/SEI 7-22 Equation 12.4-3)

$1.2D + 0.2S_{DS}D \pm \rho Q_E + L + 0.2S$ (ASCE/SEI 7-22 Section 2.3.6, Load Combination 7)

For S equal to zero and residential live load used in this example where a load factor of 0.5 is permitted, the load combination simplifies to:

$$(1.2 + 0.2S_{DS})D \pm \rho Q_E + 0.5L$$

For S_{DS} equal to 1.0 and ρ equal to 1.0 for this example, the load combination further simplifies to:

$$1.4D + Q_E + 0.5L$$

A free-body diagram for the compression end panel of the CLT multi-panel shear wall is shown in Figure 6-8.

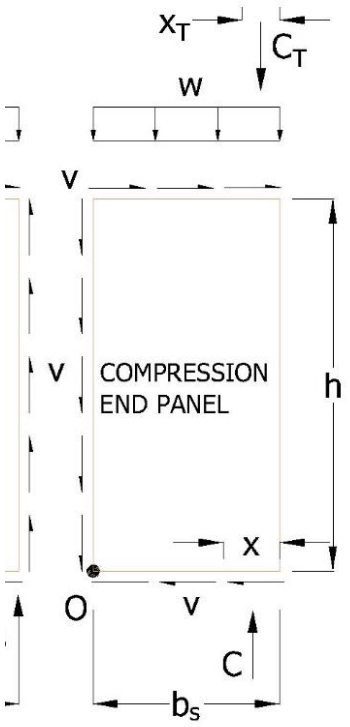

Figure 6-8. Free-body Diagram for the Compression End Panel of the CLT Multi-panel Shear Wall

The solution for compression force, *C*, and length of compression zone, *x*, is summarized in Table 6-8 based on consideration of compression end panel moment equilibrium:

$$\sum M_o = 0$$

(SDPWS-21 Equation C-B.3)

$$C\left(b_s - \frac{\mathrm{x}}{2}\right) - \nu b_s h - w b_s \left(\frac{b_s}{2}\right) - C_T\left(b_s - \frac{x_T}{2}\right) = 0$$

where:

ν = unit shear, plf

w = dead load including wall panel self-weight, plf

b_s = CLT panel length, ft

h = CLT panel height, ft

C = compression force, lb

x = length of compression zone, ft

C_T = compression force at top of compression end panel from story above, lb

x_T = length of compression zone at top of compression end panel from story above, ft

Equations for compression force, *C*, assume a uniform stress distribution (i.e., rectangular stress distribution) in the compression zone (e.g., at the compression toe of the panel). Unlike solution for *T* where b_{eff} is associated with the hold-down location prescribed as part of the design, solution for the compression zone is based on determination of required compression zone length, *x*. Once *x* is determined, b_{eff} for the compression zone (i.e., moment arm for *C* force) can be calculated as $b_s - x/2$.

For CLT walls bearing on CLT floor panels or wood plates (i.e., 3rd and 2nd story CLT walls in this example), the limiting value for compression bearing force is based on compression perpendicular to grain stress in the CLT floor panel:

$$C = F_{C\perp}{}'(t)(x)\left(\frac{12\text{in.}}{\text{ft}}\right) \qquad \text{(SDPWS-21 Equation C-B.4)}$$

And, for CLT walls bearing on steel parts or concrete foundation (i.e., 1st story CLT walls in this example), the limiting value for compression bearing force is based on bearing strength of CLT wall panel parallel to grain layers in end grain bearing. The contribution to bearing strength from the less stiff perpendicular to grain layers is ignored in the calculation:

$$C = Fc'\left(t_{parallel}\right)(x)\left(\frac{12\text{in.}}{\text{ft}}\right) \qquad \text{(SDPWS-21 Equation C-B.5)}$$

where:

x = length of compression zone, ft

C = compression force, lb

$F_{c\perp}{}'$ = bearing stress perpendicular to grain, psi

Note: For Spruce Pine-Fir floor panels in this example with *G*=0.42, LRFD $F_{c\perp}{}'$ = 638 psi and is calculated from NDS-2018 and Table 10.3.1 as follows:

$\phi\, K_F\, F_{c\perp} = 0.9(1.67)(425\text{ psi}) = 638\text{ psi}$.

$F_c{}'$ = design axial stress parallel to grain, psi

Note: For Spruce Pine-Fir wall panels in this example with *G*=0.42, LRFD $F_c{}'$ = 2,916 psi and is calculated for design axial stress parallel to grain from NDS-2018 Table 10.3.1 and 3.10.1.3 as follows where 0.75 factor accounts for high stress in end grain bearing without stiff metal bearing:

$\phi\lambda K_F\, F_c(0.75) = 0.9(1.0)(2.4)(1{,}800\text{ psi})(0.75) = 2{,}916\text{ psi}$.

t = CLT wall panel thickness, in.

$t_{parallel}$ = thickness of CLT wall panel layers oriented parallel to grain for determination of wall axial capacity, in.

12in./ft = conversion of compression zone length in feet to inches

The solution for lengths of uniform stress compression zone, *x*, to satisfy static equilibrium and the associated compression force, *C*, are summarized in Table 6-8. 2nd and 3rd story walls are supported by CLT floors where bearing stress is limited by floor panel compression perpendicular to grain stress (i.e., 638 psi for this example assuming Spruce pine-fir floor panels). The 1st story wall bears on steel and concrete foundation and is limited by axial stress in the wall panel parallel layers (i.e., 2,916 psi for the two panel layers oriented parallel to grain).

Minimum compression zone length, *x*, and associated compression force *C* for 3rd story shear walls is calculated by use of SDPWS-21 Equation C-B.3 and Equation C-B.4, which simplifies to:

$$-6F'_{C\perp}(t)\,x^2 + 12\,F'_{C\perp}(t)(b_s)\,x - \nu b_s h - w b_s\left(\frac{b_s}{2}\right) - C_T\left(b_s - \frac{x_T}{2}\right) = 0$$

Substituting known values and solving for x:

$$-6(638)(4.125)x^2 + 12(638)(4.125)(4.75)x - 477(4.75)(9.5) - 1.4(190)\left(\frac{4.75^2}{2}\right) - 0 = 0$$

x= 0.166 ft or 2.00 in.

For the 3rd story wall, compression zone length, *x*, is equal to 2.00 in., which matches the value shown in Table 6-8.

From SDPWS-21 B.3.5, the compression end zone must be contained within the outermost wall panel. Compression zone length, *x*, is less than the compression end panel length of 4.75 feet. Therefore, the compression zone length is contained within the compression end panel length, and the requirement is satisfied

For compression zone length that is contained within the compression end panel, adequate bearing capacity is automatically satisfied in accordance with the foregoing calculations, which solve for the minimum compression zone length to meet the design demand. From Table 6-8, a compression zone length, *x*, equal to 2.00 in. for the 3rd story shear wall is associated with a bearing capacity equal to 5,263 lb (i.e., 2.00 in. x 4.125 in. x 638 psi = 5,263 lb), which matches the design demand, C, equal 5,257 lb with slight difference due to rounding.

Table 6-8. Solution for Compression Zone Length, *x*, and Force *C*

Story	Unit shear force per foot of shear wall length	Dead load, w_{DL}	Live load, w_{LL}	C_T, Compression from top	Compression zone length, *x*	*C*, for load combination 1.0*E* + 1.4*D* +0.5*L*,
	(plf)	(plf)	(plf)	(lb)	(in.)	(lb)
3	477	190	0	0	2.00	5,257
2	1,009	793	690	5,257	7.64	20,144
1	1,273	793	690	20,144	4.56	36,545

As part of a complete design, CLT panel axial capacity in compression must also be evaluated in accordance with column stability provisions of NDS-2018 considering any reduction in cross-section net section subject to buckling and design specific loading and restraint conditions.

6.7 CLT Shear Wall Deflection

CLT shear wall deflection is calculated using SDPWS-21 Equation B-1 as follows:

$$\delta_{SW} = \frac{576 v b_s h^3}{EI_{eff(in-plane)}} + \frac{vh}{GA_{eff(in-plane)}} + 3\Delta_{nail\ slip,h} + 2\Delta_{nail\ slip,v}\left(\frac{h}{b_s}\right) + \Delta_a \frac{h}{\sum b_s}$$

where:

v = induced unit shear, plf

$EI_{eff\ (in\text{-}plane)}$ = Effective in-plane bending stiffness of the of CLT panel, lb-in.^{2}

$GA_{eff\ (in\text{-}plane)}$ = Effective in-plane shear stiffness of the CLT panel, lb/in. of panel length

h = CLT panel height, ft

b_s = individual CLT panel length, ft

$\sum b_s$ = sum of individual CLT panel lengths, ft

$\Delta_{nail\ slip,h} = \frac{V_{nail\ load}}{6{,}700}$, in. (Note: the equation for $\Delta_{nail\ slip,h}$ is limited to the prescribed connectors and associated fasteners prescribed for CLT shear walls in SDPWS-21)

$\Delta_{nail\ slip,v} = \Delta_{nail\ slip,h}$, in. (= 0 for a single panel shear wall)

$V_{nail\ load}$ = load per nail, lb (calculated as total shear load at base of wall divided by total number of nails in base connectors)

Δ_a = vertical deformation of the wall hold-down system (including but not limited to fastener slip, device elongation, rod elongation, and uncompensated shrinkage plus the vertical compression deformation), the effects of which are measured at the ends of the shear wall and associated with induced unit shear in the shear wall, in.

CLT shear wall deflections calculated using strength level forces are summarized in Table 6-9 showing deflections from the five terms, with nail slip terms grouped, and total top of wall deflection. For deflection calculations in Table 6-9, $EI_{eff\ (in\text{-}plane)}$ = 6.026E+10 lb-in^2, and $GA_{eff\ (in\text{-}plane)}$ = 118,300 lb/in. for the 3-layer E1 grade CLT wall panel (see SDPWS-21 Commentary C-B.4). Load per nail, V_n, is calculated as follows:

$$V_n = \frac{\text{Lateral force in wall}}{(\text{number of bottom of wall connectors})(8 \text{ nails per connector})}$$

3rd story shear wall deflections appearing in Table 6-9 are calculated using SDPWS-21 Equation B-1 as follows:

$$\delta_{SW} = \frac{576 v b_s h^3}{EI_{eff(in-plane)}} + \frac{vh}{GA_{eff(in-plane)}} + 3\Delta_{nail\ slip,h} + 2\Delta_{nail\ slip,v}\left(\frac{h}{b_s}\right) + \Delta_a \frac{h}{\sum b_s}$$

$$\delta_{SW} = \frac{576(477)(4.75)(9.5)^3}{6.026 \times 10^{10}} + \frac{477(9.5)}{118{,}300} + 3(0.02) + 2(0.02)\left(\frac{9.5}{4.75}\right) + 0.13\frac{9.5}{33.25}$$

$$\delta_{SW} = 0.02 + 0.04 + 0.06 + 0.08 + 0.04 = 0.24 \text{ in.}$$

Load per nail, V_n, and $\Delta_{nail\ slip,h}$ for the 3rd story shear wall are:

$$V_n = \frac{15{,}870 \text{ lb}}{(14 \text{ connectors})(8 \text{ nails per connector})} = 142 \text{ lb}$$

$$\Delta_{nail\ slip,h} = \frac{142 \text{ lb}}{6{,}700} = 0.02 \text{ in.}$$

For the example, Δ_a for the 3rd story shear wall is determined by the sum of hold-down device deformation and compression bearing deformation, and deformation due to uncompensated shrinkage is taken as zero.

The component of Δ_a associated with hold-down device deformation is calculated using load and deformation information provided previously (i.e., 2 hold-downs at each end of 3rd story shear wall with design capacity of 17,678 lb and associated deformation of 0.253 in. and subject to T load of 4,714 lb (see Table 6-7)):

$$\Delta_{hold-down} = \frac{4{,}714 \text{ lb}}{2(17{,}678 \text{ lb})}(0.253 \text{ in.}) = 0.034 \text{ in.}$$

The compression bearing deformation in the floor panel at the bottom of the 3rd story wall (and 2nd story wall) in this example are calculated as follows:

$$\Delta_{wood\ crush} = \frac{PL}{AE} = \frac{(\text{Compression zone length})(t_{wall})(Fc_{perp})(t_{floor})}{(\text{Compression zone length})(t_{wall})(\text{floor panel } E_{transverse},)}$$

For bearing deformation in the floor under the 3rd story wall:

$$\Delta_{wood\ crush} = \frac{(2.00 \text{ in.})(4.125 \text{ in.})(638 \text{ psi})(6.875 \text{ in.})}{(2.00 \text{ in.})(4.125 \text{ in.})(1{,}400{,}000/30 \text{ psi})} = 0.094 \text{ in.}$$

Total vertical deformation, Δ_a, for the 3rd story shear walls is: 0.034 in. + 0.094 in. = 0.13 in.

The 5th term of the deflection equation assumes a rigid body overturing behavior, which has the most applicability for single panel CLT shear walls; however, it is also applied to multi-panel walls to account for reduced stiffness associated with hold-down elongation and compression bearing deformations where bearing is on wood.

For development of Table 6-9 summarized deflection results, the bearing deformation of the wall panel itself is not included in the calculation of the wood bearing deformation term (i.e., $\Delta_{wood\ crush}$) because it is small (i.e., modulus of elasticity, *E*, of the CLT wall panel parallel to grain layers is approximately 30 times greater than $E_{transverse}$ associated with bearing on a CLT floor panel). Wood bearing deformation is taken as zero for the 1st story walls because bearing is on steel or concrete elements (not a CLT floor panel).

The allowable story drift limit is 2.5%*h* from ASCE/SEI 7-22 Table 12.12-1 (i.e., Risk Category II structures, four stories or less above the base, and with interior walls, partitions, ceilings, and exterior walls systems that have been design do accommodate the story drifts). Corresponding allowable deflection is calculated considering deflection amplification factor, C_d, equal to 3 for cross-laminated timber shear walls and wall height of 9'-6" (or, 114 in.):

$$\delta_e = \frac{0.025(h)}{C_d} = \frac{0.025(114 \text{ in.})}{3.0} = 0.95 \text{ in.}$$

Using strength level forces, CLT shear wall deflections at each story (see Table 6-9) is less than the allowable deflection limit, and therefore, the drift limit is satisfied.

Table 6-9. CLT Shear Wall Deflection Components and Total Shear Wall Deflection, δ_{SW}

Story	$\frac{576vb_s h^3}{EI_{eff(in-plane)}}$	$\frac{vh}{GA_{eff(in-plane)}}$	$3\Delta_{nail\ slip,h} + 2\Delta_{nail\ slip,v}\left(\frac{h}{b_s}\right)$	$\Delta_a \frac{h}{\sum b_s}$	δ_{SW}, shear wall deflection
	(in.)	(in.)	(in.)	(in.)	(in.)
3	0.02	0.04	0.15	0.04	0.24
2	0.04	0.09	0.16	0.04	0.33
1	0.05	0.11	0.16	0.03	0.35

6.8 References

See "Useful Design Aid Resources" in Section 6.1 above for additional references.

AWC (2014). *National Design Specification for Wood Construction*, 2015 Edition, NDS-15, American Wood Council.

van de Lindt, J., Rammer, D., Amini, M. O., Line, P., Pei, S., and Popovski, M. (2021). "Determination of Seismic Performance Factors for Cross-Laminated Timber Shear Walls Based on the FEMA P695 Methodology," General Technical Report FPL-GTR-281, Madison, WI: U.S. Department of Agriculture, Forest Service, Forest Products Laboratory, (In press).

FPInnovations (2013). *US CLT Handbook*, Special Publication SP-529E. Pointe-Claire, QC, Canada.

Chapter 7: Horizontal Diaphragm Design

Kelly Cobeen[1]

7.1 Overview

The 2020 Edition of the *NEHRP Recommended Seismic Provisions for New Buildings and Other Structures* (FEMA, 2020), referred to herein as the *Provisions*, includes three significant items related to the design of diaphragms that represent changes between the 2015 *Provisions* (FEMA, 2016), and 2020 *Provisions*. These have resulted in matching changes between ASCE/SEI 7-16 (ASCE, 2017) and ASCE/SEI 7-22 (ASCE, 2021). First, ASCE/SEI 7-16 Section 12.10.3 (Alternative Design Provisions for Diaphragms including Chords and Collectors) was expanded to permit use of bare steel deck diaphragms. Second, new Section 12.10.4 has been added, containing alternative diaphragm seismic design provisions for one-story structures with flexible diaphragms and rigid vertical elements (commonly designated as rigid-wall flexible-diaphragm (RWFD) buildings). Third, the ASCE/SEI 7-16 Section 12.10.3 alternative design provisions have been further expanded to permit use of concrete filled steel deck diaphragms. This is based in part on Resource Paper 6 in Part 3 of the 2020 *NEHRP Provisions (FEMA P-1082-2)*.

This chapter addresses use of the ASCE/SEI 7-22 diaphragm design provisions, including these three significant changes. The primary focus of this chapter is the determination of diaphragm seismic design forces. The horizontal distribution of these forces and design for shear and flexure are not addressed as this can vary depending on the classification of the diaphragm (flexible, semi-rigid or rigid), the approach taken to analytical modeling of the structure, and the diaphragm system. In accordance with Section 12.3.4.1, *rho* (ρ) is assumed to be 1.0 for diaphragm design and therefore not included in this discussion. Similarly, effects that might be triggered by plan irregularities are not discussed. While these effects are ignored for the purposes of these example problems, such effects are required to be appropriately considered in design of structures. Further information on seismic design of diaphragms can be found in the NEHRP Seismic Design Technical Brief Series, as included in the other resources section that follows; while these briefs do not address the ASCE/SEI 7-22 revisions, they provide a wealth of information on other aspects of diaphragm design.

[1] Kelly Cobeen, S.E., Wiss, Janney, Elstner Associates, Inc.

Other Changes Between ASCE/SEI 7-16 and 7-22

A number of other changes between ASCE/SEI 7-16 and 7-22 could potentially affect the design of diaphragms. Two in particular are worth mentioning in conjunction with diaphragm design:

- First, significant changes have occurred to ASCE/SEI 7-22 Section 11.4, Seismic Ground Motion Values, including the inclusion of a multi-period response spectrum in Section 11.4.5. For purposes of diaphragm design, it is intended, however, that the design spectral acceleration parameters of ASCE/SEI 7-22 Section 11.4.4 be used where S_{DS} and S_{D1} values are needed; for this reason, the change to Section 11.4.5 is not intended to affect diaphragm design.
- Second, significant changes have been made to ASCE/SEI 7-22 Sections 12.8.6 and 12.12, addressing deflection and drift. These changes do potentially affect diaphragm design and are discussed in this chapter.

For further discussion of diaphragm deflections, the reader is referred to Section 7.2, FEMA P-1026 (FEMA, 2021), Resource Paper 8 from FEMA P-2082-2, and the previously mentioned NEHRP Tech Brief series.

The following are included in this chapter:

- Section 7.2 introduces the three diaphragm seismic design methods included in ASCE/SEI 7-22.
- Section 7.3 provides step-by-step descriptions of the implementation of the three available diaphragm design methods.
- Section 7.4 provides example calculations for a one-story wood assembly hall, using the ASCE/SEI 7-22 Section 12.10.1 and 12.10.2 traditional design method and repeated using the Section 12.10.3 alternative design provisions.
- Section 7.5 provides example calculations for a multi-story steel building with concrete filled metal deck floor diaphragms and a bare steel deck roof diaphragm using the ASCE/SEI 7-22 Section 12.10.1 and 12.10.2 traditional design method and repeated using the Section 12.10.3 alternative design provisions.
- Finally, Section 7.6 provides example calculations for a one-story concrete tilt-up building with a bare steel deck diaphragm using the ASCE/SEI 7-22 Section 12.10.1 and 12.10.2 traditional design method and repeated using the Section 12.10.4 alternative RWFD provisions. The Section 12.10.4 calculations include two designs, one in which the diaphragm meets AISI S400 requirements for special seismic detailing and a second in which the diaphragm does not.

In addition to the 2020 *Provisions* and ASCE/SEI 7-22, the following documents are either referred to directly or may serve as useful design aids.

Useful Design Resources Resources

ACI (2019). *Building Code Requirements for Structural Concrete*, ACI 318-19, American Concrete Institute, Farmington Hills, MI.

AISC (2022a). *Seismic Provisions for Structural Steel Buildings*, ANSI/AISC 341-22, American Institute of Steel Construction, Chicago, IL, in press.

AISC (2022b). *Specification for Structural Steel Buildings*, ANSI/AISC 360-22, American Institute of Steel Construction, Chicago, IL, in press.

AISI (2020a). *North American Standard for Seismic Design of Cold-Formed Steel Structural Systems*, ANSI/AISI S400-20, American Iron and Steel Institute, Washington, DC.

AISI (2020b). *North American Standard for the Design of Profiled Steel Diaphragm Panels*, ANSI/AISI S310-20, American Iron and Steel Institute, Washington, DC.

APA (2007). *Diaphragms and Shear Walls, Design/Construction Guide*, Form L350A, APA The Engineered Wood Association, Tacoma, WA.

APA (1966). 1966 *Horizontal Plywood Diaphragm Tests*, American Plywood Association Laboratory Report 106, American Plywood Association, Tacoma, WA.

ASTM (2017). *Standard Specification for Driven Fasteners: Nails, Spikes, and Staples*, ASTM F1667, West Conshohocken, PA.

AWC (2021). *Special Design Provisions for Wind and Seismic*, SDPWS-21, American Wood Council, America Wood Council, Leesburg, VA.

FEMA (2009). *Quantification of Building Seismic Performance Factors*, FEMA P695 Report, Federal Emergency Management Agency, Washington, DC.

FEMA (2021). *Seismic Design of Rigid Wall-Flexible Diaphragm Buildings: An Alternate Procedure*, FEMA P-1026 Report, Federal Emergency Management Agency, Washington, DC.

Fleischman R.B., Restrepo J.I, Naito C.J., Sause R., Zhang D. and Schoettler M., (2013). "Integrated Analytical and Experimental Research to Develop a New Seismic Design Methodology for Precast Concrete Diaphragms," ASCE J. Struct. Engr., 139(7), 1192-1204.

Koliou, M., Filiatrault, A., Kelly, D., and Lawson, J., (2015a). "Buildings with Rigid Walls and Flexible Diaphragms I: Evaluation of Current U.S. Seismic Provisions," *Journal of Structural Engineering*, American Society of Civil Engineers, Reston, VA.

Koliou, M., Filiatrault, A., Kelly, D., and Lawson, J., (2015b). "Buildings with Rigid Walls and Flexible Diaphragms II: Evaluation of a New Seismic Design Approach Based on Distributed Diaphragm Yielding," *Journal of Structural Engineering*, American Society of Civil Engineers, Reston, VA.

NIST (2011). *NEHRP Seismic Design Technical Brief No. 5, Seismic Design of Composite Steel Deck and Concrete-filled Diaphragms*, NIST GRC 11-917-10 Report, National Institute of Standards and Technology, Gaithersburg, MD.

NIST (2014). *NEHRP Seismic Design Technical Brief No. 10, Seismic Design of Wood Light-Frame Structural Diaphragm Systems*, NIST GRC 14-917-32 Report, National Institute of Standards and Technology, Gaithersburg, MD.

NIST (2016a). *NEHRP Seismic Design Technical Brief No. 12, Seismic Design of Cold-Formed Steel Lateral Load-Resisting Systems*, NIST GRC 16-917-38 Report, National Institute of Standards and Technology, Gaithersburg, MD.

NIST (2016b). *NEHRP Seismic Design Technical Brief No. 3, Seismic Design of Cast-in-Place Concrete Diaphragms, Chords and Collectors, Second Edition*, NIST GRC 16-917-42 Report, National Institute of Standards and Technology, Gaithersburg, MD.

NIST (2017). *NEHRP Seismic Design Technical Brief No. 12, Seismic Design of Precast Concrete Diaphragms*, NIST GRC 17-917-47 Report, National Institute of Standards and Technology, Gaithersburg, MD.

Schafer (2019). *Research on the Seismic Performance of Rigid Wall Flexible Diaphragm Buildings with Bare Steel Deck Diaphragms*, CFSRC Report 2019-2, Cold-Form Steel Research Consortium.

7.2 Introduction to Diaphragm Seismic Design Methods

ASCE/SEI 7-22 Section 12.10, Diaphragms, Chords and Collectors, includes three separate methods for seismic design of diaphragms and their chords and collectors. Included is the traditional diaphragm design method in accordance with the provisions of Sections 12.10.1 and 12.10.2, the alternative provisions of Section 12.10.3, and the new alternative RWFD provisions of Section 12.10.4. For a given diaphragm, one of these three methods will need to be selected by the designer and implemented. Where a group of diaphragms is similar enough in elevation that they would be anticipated to interact, the use of one diaphragm design method for the group of diaphragms is recommended.

ASCE/SEI 7-22 Section 12.10.1 and 12.10.2 traditional provisions were the only diaphragm design method available until the Section 12.10.3 provisions were added in the 2015 *NEHRP Provisions* and ASCE/SEI 7-16. When using Sections 12.10.1 and 12.10.2, diaphragm design forces are determined based on the seismic design parameters of the vertical elements of the seismic force-resisting system without consideration of the effect of the diaphragm system on the response of the structure. Use of this method is permitted for all structures, with the exception of precast concrete diaphragms in Seismic Design Categories (SDC) C through F.

ASCE/SEI 7-22 Section 12.10.3 provides alternative diaphragm seismic design provisions that explicitly recognize and account for the effect of diaphragm ductility and displacement capacity on the diaphragm design forces. This is accomplished with the introduction of a diaphragm design force

reduction factor, R_S. Neither the number of stories nor the building configuration is restricted by the Section 12.10.3 provisions; however, diaphragm construction is limited to the diaphragm systems specifically noted within those provisions.

ASCE/SEI 7-22 Section 12.10.3 is mandatory for precast concrete diaphragms in structures assigned to SDC C, D, E and F. It is optional for all other diaphragm types and SDCs for which the alternative design method is applicable. The mandate for use of Section 12.10.3 for precast diaphragm systems in SDC C through F is based on recent research (Fleischman et al., 2012) that indicates that improved earthquake performance can be attained through recognition of the ductility and deformation capacity based on diaphragm detailing used. Without use of the Section 12.10.3 provisions for precast diaphragms, the seismic performance might be less than that targeted by the *NEHRP Provisions* and ASCE/SEI 7. At the same time, many conventional diaphragm systems designed in accordance with ASCE/SEI 7-22 Sections 12.10.1 and 12.10.2 have performed adequately; continued use of Sections 12.10.1 and 12.10.2 is therefore considered reasonable for diaphragm systems other than those for which Section 12.10.3 is mandated.

Design of Cast-in-Place Concrete Equivalent Precast Diaphragms

It is worth noting that ASCE/SEI 7-22 Section 14.2.2.1 defines a category of precast concrete diaphragms designated as “cast-in-place concrete equivalent precast diaphragms.” This diaphragm type uses either a noncomposite cast-in-place diaphragm over precast sections or a precast diaphragm with cast-in-place closure strips. For this type of diaphragm, use of ASCE/SEI 7-22 Section 12.10.3 is not mandated, allowing the traditional design method of Sections 12.10.1 and 12.10.2 to be used.

ASCE/SEI 7-22 Section 12.10.4 introduces diaphragm seismic design provisions that are permitted to be used for one-story structures combining flexible diaphragms with rigid vertical elements. This alternative RWFD seismic design methodology specifically recognizes the seismic response of these structures as being dominated by dynamic response of and inelastic behavior in the diaphragm. While the most common occurrences of this structure type are the concrete tilt-up and masonry “big-box” buildings, the rigid vertical element terminology of this section recognizes a wider range of vertical elements for which this methodology is permitted to be used. The primary use of Section 12.10.4 provisions is intended to be for structures where one or more spans of the diaphragm exceeds 100 feet; however, use for structures in which diaphragm spans are less than 100 feet is not precluded. Table 7-1 provides an overview of the three available diaphragm design methods.

Changes have been made to the displacement and drift provisions of ASCE/SEI 7-22 Sections 12.8.6 and 12.12 that potentially affect the design of diaphragms. Per ASCE/SEI 7-22 Sections 12.8.6.3 and 12.8.6.4, the design earthquake displacement and maximum considered earthquake displacement are to be calculated, including the diaphragm defection. When computing the design story drift, however, the diaphragm deflection is permitted to be neglected; as a result, the ASCE/SEI 7-22 Section 12.12.1 check against the allowable story drift does not need to consider diaphragm deflection. For further discussion of diaphragm deflections, the reader is referred to FEMA P-1026 (FEMA, 2021),

Resource Paper 8 from FEMA P-2082-2, and the previously mentioned NEHRP Tech Brief series. The provisions of ASCE/SEI 7-22 Section 12.12.2, structural separation; 12.12.3, members spanning between structures; and 12.12.4, deformation compatibility, use deflections and drifts that incorporate diaphragm deflection. ASCE/SEI 7-22 Section 12.12.4 criteria are particularly important for long-span diaphragms where calculated deflections can be large, thereby imposing significant drifts on the gravity system.

Table 7-1. Overview of the Three Available Diaphragm Seismic Design Methods

Method and ASCE/SEI 7-22 Section	Number of Stories Permitted	Diaphragm Systems Included	Comments
Traditional Sections 12.10.1 and 12.10.2	Any	All	▪ Not permitted for precast concrete diaphragms in SDC C through F ▪ Diaphragm design forces are determined using seismic design parameters (R, Ω_0, and C_d) for the vertical elements of the SFRS
Alternative Design Procedure Section 12.10.3	Any	▪ Cast-in-place concrete ▪ Precast concrete ▪ Wood structural panel ▪ Bare steel deck ▪ Concrete-filled steel deck	▪ Required for precast concrete diaphragms in SDC C through F, providing improved seismic performance ▪ Optional for other diaphragm types ▪ Better reflects vertical distribution of diaphragm forces ▪ R_s diaphragm design force reduction factor better reflects effect of diaphragm ductility and displacement capacity on diaphragm seismic forces ▪ Forces in collectors and their connections to vertical elements are amplified by 1.5 in place of Ω_0
Alternative RWFD Design Procedure Section 12.10.4	One Story	▪ Wood structural panel ▪ Bare steel deck ▪ When meeting the scoping limitations of ASCE/SEI 7-22 Section 12.10.4.1	▪ Primarily intended for buildings with diaphragm spans of 100 feet or greater ▪ New T_{diaph}, R_{diaph}, $\Omega_{0\text{-diaph}}$ and $C_{d\text{-diaph}}$, better reflect response of RWFD building type ▪ Provides better performance with the same or reduced construction cost

7.3 Step-By-Step Determination of Diaphragm Design Forces

The step-by-step descriptions in Section 7.3 are intended to provide a high-level overview of implementation of the three diaphragm design methods. See the examples that follow and ASCE/SEI 7-22 and commentary for more detail. The step-by-step descriptions focus on use of the ASCE/SEI 7-22 equivalent lateral force (ELF) procedure; some modifications are needed when using linear dynamic analysis procedures. This step-by-step description also focuses primarily on diaphragm inertial forces due to the mass tributary to each diaphragm level. Where diaphragm transfer forces as defined in ASCE/SEI Section 11.2 occur, they are required to be addressed in accordance with ASCE/SEI 7-22 Section 12.10.1.1 or 12.10.3.3, as applicable.

In order to perform seismic analysis of the SFRS and diaphragms, it is necessary to define the diaphragm flexibility in accordance with ASCE/SEI 7-22 Section 12.3. This section sets criteria by which diaphragms can be idealized as flexible, idealized as rigid, or calculated as flexible. Where these do not apply, the diaphragm is required to be modeled as semi-rigid. Where diaphragms are designated as rigid or semi-rigid for modeling and design, the process of seismic design will start with overall modeling of the building and then proceed to diaphragm design. Regardless of diaphragm designation, the seismic design of the diaphragm and vertical elements usually proceed in parallel.

7.3.1 Step-By-Step Determination of Diaphragm Design Forces Using the Section 12.10.1 and 12.10.2 Traditional Method

The following describes in a step-by-step fashion the determination of diaphragm seismic design forces using ASCE/SEI 7-22 Sections 12.10.1 and 12.10.2. The procedure in these sections has been in use since before the first edition of the IBC and has, in the past, been applicable to diaphragms of all materials. ASCE/SEI 7-22 Sections 12.10.1 and 12.10.2 can no longer be used for design of precast concrete diaphragms in structures assigned to SDC C through F, as noted in Exception 1 to ASCE/SEI 7-22 Section 12.10.

Step 1: Determine w_i, W and w_{px}. ASCE/SEI 7-22 Section 12.7.2 defines effective seismic weight, W. w_i is the portion of W that is tributary to level i (Figure 7-1). w_{px} is different from w_i only in that the weights of the walls parallel to the earthquake forces are permitted to be excluded from w_{px}. It is common practice to exclude the weights of these parallel walls in low-rise buildings with concrete or masonry walls; including or excluding this weight (i.e., using a value of w_{px} less than w_i) is at the discretion of the design engineer.

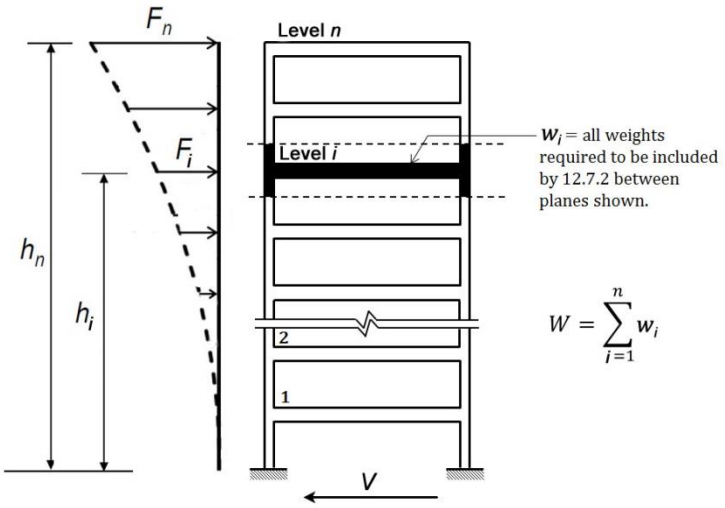

Figure 7-1. Seismic Weights and Lateral Forces Obtained from Vertical Distribution of Design Base Shear at Various Floor Levels (from FEMA, 2015)

Step 2: Determine seismic design base shear, *V*, from ASCE/SEI 7-22 Section 12.8.1. This will be determined based on the seismic response modification factor, *R*, of the vertical elements of the seismic force-resisting system (SFRS). It is most often determined using the approximate fundamental period equations of ASCE/SEI 7-22 Section 12.8.2.1.

Step 3: Determine the vertical distribution of base shear, V, and the portion of V induced at level i, Fi, for all levels from *x* to *n*, from ASCE/SEI 7-22 Section 12.8.3.

Step 4: Determine inertial diaphragm design force at level *x*, F_{px}, in accordance with ASCE/SEI 7-22 Section 12.10.1.1. The inertial forces are those due to the seismic mass tributary to level *x* and are a function of acceleration levels anticipated at level *x*; these are different from diaphragm transfer forces, discussed in Step 5. The F_{px} forces are determined as:

$$F_{px} = \frac{\sum_{i=x}^{n} F_i}{\sum_{i=x}^{n} w_i} w_{px} \qquad \text{(ASCE/SEI 7-22 Eq. 12.10-1)}$$

where

F_{px} = Diaphragm design force at level *x*,

F_i = Design force applied to level *i*,

w_i = Weight tributary to level *i*, and

w_{px} = Weight tributary to the diaphragm at level *x*.

Check F_{px} against maximum and minimum values.

F_{px} shall not be less than F_x or $0.2S_{DS}I_e w_{px}$ (ASCE-SEI 7-22 Eq. 12.10-2)

F_{px} need not be greater than $0.4S_{DS}I_e w_{px}$ (ASCE/SEI 7-22 Eq. 12.10-3)

where

S_{DS} = Design, 5% damped, spectral response acceleration parameter at short periods as defined in ASCE/SEI 7-22 Section 11.4.4, and

I_e = Importance Factor as prescribed in ASCE/SEI 7-22 Section 11.5.1.

Determine F_{px} forces to be used for design based on the results of ASCE/SEI 7-22 Equations 12.10-1 to 12.10-3.

Step 5: Determine diaphragm transfer forces, as defined in ASCE/SEI 7-22 Section 11.2, where applicable. These occur where vertical elements of the SFRS are offset or discontinued at lower levels; this also occurs due to changes in the stiffness of the SFRS vertical elements between levels. Amplify transfer forces by Ω_0 where required by ASCE/SEI 7-22 Section 12.10.1.1. Determine total diaphragm design forces as the total of F_{px} inertial forces and diaphragm transfer forces.

Step 6: Use F_{px} seismic forces and any applicable diaphragm transfer forces (amplified as required) at each diaphragm level to design the diaphragms for shear and flexure.

Step 7: Use F_{px} seismic forces and any applicable diaphragm transfer forces to design collectors and their connections to vertical elements. In SDC B, the diaphragm transfer forces are required to be amplified by Ω_0 (ASCE/SEI 7-22 Section 12.10.1.1), while the F_{px} forces are not. In SDC C through F, all diaphragm forces are required to be amplified by Ω_0 to design collectors and their connections to vertical elements (ASCE/SEI 7-22 Section 12.10.2.1). The resulting forces are not required to exceed the capacity-limited horizontal seismic load effect, E_{ci}, as defined in ASCE/SEI 7-22 Section 11.3. Note that ASCE/SEI 7-22 Section 12.10.2.1 also identifies conditions where amplification by Ω_0 is not required for the design of collectors and their connections to vertical elements.

Step 8: Check applicable ASCE/SEI 7-22 deflection and drift limitations for the overall structure in accordance with Section 12.12. See Section 7.2 for further discussion.

7.3.2 Step-By-Step Determination of Diaphragm Design Forces Using the Section 12.10.3 Alternative Provisions

The following describes in a step-by-step fashion the determination of diaphragm seismic design forces in accordance with the alternative design procedure of ASCE/SEI 7-22 Section 12.10.3. There are two primary aspects in which the Section 12.10.3 alternative provisions differ from the traditional method of ASCE/SEI 7-22 Sections 12.10.1 and 12.10.2. The first aspect is the vertical distribution of seismic forces; based on collected testing and analysis data, ASCE/SEI 7-22 Section 12.10.3.2 provides a revised vertical distribution that reflects the contributions of first mode and

higher mode effects. The second aspect is the recognition of the ductility and deformation capacity of the diaphragm system, as captured in the R_S diaphragm design force reduction factor. Diaphragm forces are calculated using the overstrength factor associated with the vertical SFRS, providing an indication of force levels anticipated considering near-elastic diaphragm response. The forces are then divided by the R_s factor. The R_s factors, provided in ASCE/SEI 7-22 Table 12.10-1 range from a low of 0.7 providing near-elastic forces to a high of three, providing significant reduction from the near-elastic forces. The studies used in the development of the alternative design method are described in the commentary to the 2015 and 2020 *NEHRP Provisions* and in the commentary to ASCE/SEI 7-22. Use of the alternative design procedure is required for precast concrete diaphragms in SDC C through F. Use of the alternative design procedure is recommended for all diaphragm systems included in ASCE/SEI 7-22 Table 12.10-1 because the procedure is believed to better capture anticipated seismic demands and should therefore lead to better seismic performance.

Step 1: Determine w_i, W, and w_{px} (ASCE 7 Section 12.10.3.2). ASCE/SEI 7-22 Section 12.7.2 defines effective seismic weight, W. w_i is the portion of W that is tributary to level i. w_{px} is different from w_i only in that the weights of the walls parallel to the earthquake forces may be excluded from w_{px}. It is common practice to exclude the weights of these parallel walls in low-rise buildings with concrete or masonry walls; including or excluding this weight (i.e., using a value of w_{px} less than w_i) is at the discretion of the design engineer.

Step 2: Determine R_s, Diaphragm Design Force Reduction Factor (ASCE/SEI 7-22 Table 12.10-1, reproduced here as Table 7-2). R_s accounts for diaphragm overstrength and/or the inelastic displacement capacity of the diaphragm. For diaphragm systems with inelastic deformation capacity sufficient to permit inelastic response under the design earthquake, R_s is typically greater than 1.0, so that F_{px} is reduced relative to the design force demand for a diaphragm that remains near elastic under the design earthquake. For diaphragm systems that do not have sufficient inelastic deformation capacity, R_s should be less than 1.0 (or in some cases as low as 0.7), so that near elastic force-deformation response can be expected under the maximum considered earthquake.

For diaphragm systems where ASCE/SEI 7-22 Table 12.10-1 includes R_s values for both shear-controlled and flexure-controlled diaphragm systems, the definitions from ASCE/SEI 7-22 Section 11.2 are used to determine which of these is applicable:

- **Flexure-Controlled Diaphragm:** Diaphragm with a flexural yielding mechanism, which limits the maximum forces that develop in the diaphragm, and a design shear strength or factored nominal shear capacity greater than the shear corresponding to the nominal flexural strength.

- **Shear-Controlled Diaphragm:** Diaphragm that does not meet the requirements of a flexure-controlled diaphragm.

For precast concrete diaphragms, the determination of EDO, BDO, and RDO are made in accordance with the provisions of ACI 318-19. As introduced in the 2015 *NEHRP Provisions* and ASCE/SEI 7-16, use of the Section 12.10.3 alternative provisions for design of precast concrete diaphragms involved not only use of the Section 12.10.3 provisions, but also further provisions for design, detailing, and

connector qualification. These additional provisions were located in ASCE/SEI 7-16, Section 14.2.4. These additional provisions have since been relocated to ACI 318-19, ACI 550.4-18 (ACI, 2018a), and ACI 550.5-18 (ACI 2018b). As a result, they have been dropped from ASCE/SEI 7-22 Chapter 14. As these additional provisions were moved from ASCE/SEI 7 to ACI standards, the basic concepts remained the same, with some limited revisions occurring.

Table 7-2. ASCE/SEI 7-22 Table 12.10-1 Diaphragm Design Force Reduction factor, R_s *(with edition numbers and notes added in italics)*

Diaphragm System		Shear-Controlled[a]	*Flexure-Controlled*[a]
Cast-in-place concrete designed in with ACI 318 *[ACI 318-19]*	-	1.5	2
Precast concrete designed in accordance with ACI 318 *[ACI 318-19]*	Elastic design option[b]	0.7	0.7
	Basic design option[b]	1.0	1.0
	Reduced design option[b]	1.4	1.4
Wood sheathed designed in accordance with *[ASCE/SEI 7-22]* Section 14.5 and AWC SDPWS *[Special Design Provisions for Wind and Seismic (SDPWS-21)]*	-	3.0	Not applicable
Bare steel deck designed in accordance with *[ASCE/SEI 7-22]* Section 14.1.5	With special seismic detailing	2.5	Not applicable
	Other	1.0	Not applicable
Concrete-filled steel deck diaphragm designed in accordance with *[ASCE/SEI 7-22]* Section 14.1.6	-	2.0	Not applicable

[a] *Flexure-controlled and Shear-controlled diaphragms are defined in ASCE/SEI 7-22 Section 11.2.*

[b] *Elastic, basic, and reduced design options are defined in ASCE/SEI 7-22 Section 11.2.*

Step 3: Determine C_{px}, Diaphragm Design Acceleration (Force) Coefficient at Level x (ASCE/SEI 7-22 Section 12.10.3.2.1 and Figure 12.10-2). In order to determine C_{px}, first C_{p0}, C_{pi}, and C_{pn} need to be determined.

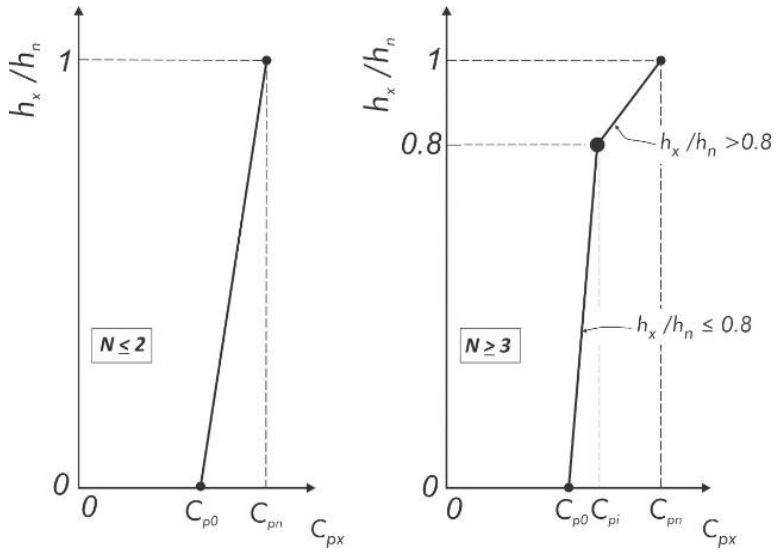

Figure 7-2. ASCE/SEI 7-22 Figure 12.10-2 Calculating the Design Acceleration Coefficient C_{px} in Buildings Two Stories or Less in Height and in Buildings Three Stories or More in Height (from Figure C12.10-7 in the 2020 *NEHRP Provisions*)

Step 3A: Determine C_{p0}, Diaphragm Design Acceleration (Force) Coefficient at the Structure Base (ASCE/SEI 7-22 Section 12.10.3.2.1). C_{p0} reflects the peak ground acceleration without amplification.

$$C_{p0} = 0.4S_{DS}I_e \qquad \text{(ASCE/SEI 7-22 Eq. 12.10-6)}$$

where

S_{DS} = Design, 5% damped, spectral response acceleration parameter at short periods as defined in ASCE/SEI 7-22 Section 11.4.4, and

I_e = Importance Factor as prescribed in ASCE/SEI 7-22 Section 11.5.1.

Step 3B: Determine C_{pi}, Diaphragm Design Acceleration (Force) Coefficient at 80 percent of h_n (ASCE/SEI 7-22 Section 12.10.3.2.1). Derived from testing and analysis data, C_{pi} reflects that at 80% of the structure height, floor accelerations are largely but not solely contributed by the first mode of response. The value $0.8C_{p0}$ serves to provide a minimum coefficient for floor accelerations.

C_{pi} is the greater of values given by:

$$C_{pi} = 0.8C_{p0} \qquad \text{(ASCE/SEI 7-22 Eq. 12.10-8)}$$

$$C_{pi} = 0.9\Gamma_{m1}\Omega_0 C_s \qquad \text{(ASCE/SEI 7-22 Eq.12.10-9)}$$

where:

C_s = Seismic response coefficient determined in ASCE/SEI 7-22 Section 12.8.1.1 or 19.3.1,

Ω_0 = Overstrength factor as defined in ASCE/SEI 7-22 Tables 12.2-1, 15.4.-1, and 15.4-2,

Γ_{m1} is first mode contribution factor

$$\Gamma_{m1} = 1 + 0.5 z_s \left(1 - \frac{1}{N}\right) \qquad \text{(ASCE/SEI 7-22 Eq. 12.10-13)}$$

z_s = modal contribution coefficient modifier dependent on seismic force-resisting system (see Table 7-3 below). This was also derived from testing and analysis data.

N = Number of stories above base of structure.

Table 7-3. Modal Contribution Coefficient Modifier, z_s

Description	z_s value
Buildings designed with Buckling-Restrained Braced Frame systems defined in ASCE/SEI 7-22 Table 12.2-1	0.30
Buildings designed with Moment-Resisting Frame systems defined in ASCE/SEI 7-22 Table 12.2-1	0.70
Buildings designed with Dual Systems defined in ASCE/SEI 7-22 Table 12.2-1 with Special or Intermediate Moment Frames capable of resisting at least 25% of the prescribed seismic forces	0.85
Buildings designed with all other seismic force-resisting systems	1.00

Step 3C: Determine C_{pn}, Diaphragm Design Acceleration (Force) Coefficient at h_n (ASCE/SEI 7-22 Section 12.10.3.2.1). C_{pn}, again derived from testing and analysis data, reflects the influence of the first mode, amplified by system overstrength, and of the higher modes without amplification.

$$C_{pn} = \sqrt{(\Gamma_{m1}\Omega_0 C_s)^2 + (\Gamma_{m2} C_{s2})^2} \qquad \text{(ASCE/SEI 7-22 Eq. 12.10-7)}$$

where:

Γ_{m2} is higher mode contribution factor.

$$\Gamma_{m2} = 0.9 z_s \left(1 - \frac{1}{N}\right)^2 \qquad \text{(ASCE/SEI 7-22 Eq. 12.10-14)}$$

C_{s2} is the higher mode seismic response coefficient. C_{s2} is the smallest of values given by ASCE/SEI 7-22 Equations 12.10-10 through 12.10-12b. These four equations consider that the periods of the higher modes contributing to the floor acceleration can lie on the ascending, constant, or first descending branch of the design response spectrum.

$$C_{s2} = (0.15N + 0.25) I_e S_{DS} \qquad \text{(ASCE/SEI 7-22 Eq. 12.10-10)}$$

$$C_{s2} = I_e S_{DS} \qquad \text{(ASCE/SEI 7-22 Eq. 12.10-11)}$$

$$C_{s2} = \frac{I_e S_{D1}}{0.03(N-1)} \qquad \text{For N} \geq 2 \qquad \text{(ASCE/SEI 7-22 Eq. 12.10-12a)}$$

$$C_{s2} = 0 \qquad \text{For N = 1} \qquad \text{(ASCE/SEI 7-22 Eq. 12.10-12b)}$$

Step 3D: Use Figure 7-2 to determine C_{px} (ASCE/SEI 7-22 Section 12.10.3.2).

Step 4: Determine F_{px}, Diaphragm Design Force at Level x (ASCE/SEI 7-22 Section 12.10.3.2):

$$F_{px} = \frac{\overbrace{C_{px}}^{\text{Step 3}}}{\underbrace{R_S}_{\text{Step 2}}} \overbrace{W_{px}}^{\text{Step 1}} \qquad \text{(ASCE/SEI 7-22 Eq. 12.10-4)}$$

$$\geq 0.2 S_{DS} I_e w_{px} \qquad \text{(ASCE/SEI 7-22 Eq. 12.10-5)}$$

Determine F_{px} forces to be used for design based on the results of ASCE/SEI 7-22 Equations 12.10-4 and 12.10-5.

Step 5: Determine diaphragm transfer forces, as defined in ASCE/SEI 7-22 Section 11.2, where applicable. These occur where vertical elements of the SFRS are offset or discontinued at lower levels; this also occurs due to changes in the stiffness of the SFRS vertical elements between levels. Amplify transfer forces by Ω_0, as determined for the vertical elements of the SFRS where required by ASCE/SEI 7-22 Section 12.10.3.3. Determine total diaphragm design forces as the total of F_{px} inertial forces and diaphragm transfer forces.

Step 6: Use the sum of F_{px} seismic forces and any applicable diaphragm transfer forces (amplified by Ω_0 as required by ASCE/SEI 7-22 Section 12.10.3.3) at each diaphragm level to design diaphragm for shear and flexure.

Step 7: Use F_{px} seismic forces and any applicable diaphragm transfer forces to design collectors and their connections to vertical elements. In SDC B, the diaphragm transfer forces are required to be amplified by Ω_0 (ASCE/SEI 7-22 Section 12.10.1.1), while the F_{px} forces are not. In SDC C through F, all diaphragm forces are required to be amplified by 1.5 to design collectors and their connections to vertical elements, as specified in ASCE/SEI 7-22 Section 12.10.3.4. The resulting forces are not required to exceed the capacity-limited horizontal seismic load effect, E_{ci}, as defined in ASCE/SEI 7-22 Section 11.3. Note that ASCE/SEI 7-22 Section 12.10.3.3 identifies conditions where amplification by 1.5 is not required for the design of collectors and their connections to vertical elements.

Step 8: Check applicable ASCE/SEI 7-22 deflection and drift limitations for the overall structure. See Section 7.2 for further discussion. When using the alternative diaphragm design procedure, 2020 NEHRP Resource Paper 8 in FEMA (2020) provides recommendations for diaphragm deflection amplification.

7.3.3. Step-By-Step Determination of Diaphragm Design Forces Using the Section 12.10.4 Alternative Diaphragm Design Provisions for One-Story Structures with Flexible Diaphragms and Rigid Vertical Elements (Alternative RWFD Provisions)

The following describes in a step-by-step approach the determination of diaphragm seismic design forces using the new provisions of ASCE/SEI 7-22 Section 12.10.4, applicable only to one-story rigid-wall, flexible diaphragm (RWFD) structures. There are two primary aspects in which ASCE/SEI 7-22 Section 12.10.4 alternative RWFD provisions differ from the traditional method of ASCE/SEI 7-22 Sections 12.10.1 and 12.10.2. The first aspect is that the seismic design forces for the diaphragm are recognized to be a function of the diaphragm period rather than the period of the vertical elements of the SFRS; this reflects the long-recognized understanding that the dynamic response of this building type is controlled by the diaphragm response. The second aspect is that for diaphragm spans greater than 100 feet, the perimeter of the diaphragm is strengthened based on amplified shear demands, while the capacity in the diaphragm interior is reduced; this was identified in studies to lead to distributed yielding at the diaphragm interior and better seismic performance overall. Use of the alternative RWFD design procedure is recommended for diaphragms with spans greater than 100 feet because it is believed to lead to better seismic performance.

This methodology can be used with wood structural panels and bare steel deck diaphragms. Permitted vertical elements include concrete shear walls, precast concrete shear walls, masonry shear walls, steel concentrically braced frames, steel and concrete composite braced frames, or steel and concrete composite shear walls. With these combinations of vertical and diaphragm systems, the diaphragms are intended to be idealized as flexible for purposes of force distribution.

Along with the ASCE/SEI 7-22 Section 12.10.4 provisions, a companion change can be found in ASCE/SEI Section 12.2.3.4, permitting the use of a two-stage analysis procedure for the vertical SFRS elements in buildings with diaphragms designed in accordance with ASCE/SEI Section 12.10.4. This two-stage procedure is not addressed in this chapter. See the ASCE/SEI 7-22 and NEHRP provisions and commentaries for information.

Step 1: Verify that the structure conforms to all of the scoping provisions of ASCE/SEI 7-22 Section 12.10.4.1. Structures that do not comply with all of the scoping provisions are not permitted to use the methodology.

Table 7-4. Limitations for Use of ASCE/SEI 7-22 Section 12.10.4 Alternative RWFD Provisions

Item	*Limitation*
1	All portions of the diaphragm shall be designed using the provisions of this section in both orthogonal directions.
2	The diaphragm shall consist of either: (a) a wood structural panel diaphragm designed in accordance with AWC SDPWS and fastened to wood framing members or wood nailers with sheathing nailing in accordance with the AWC SDPWS Section 4.2 nominal shear capacity tables, or (b) a bare (untopped) steel deck diaphragm meeting the requirements of AISI S400 and AISI S310.
3	Toppings of concrete or similar materials that affect diaphragm strength or stiffness shall not be placed over the wood structural panel or bare steel deck diaphragm.
4	The diaphragm shall not contain horizontal structural irregularities, as specified in ASCE/SEI 7-22 Table 12.3-1, except that Horizontal Structural Irregularity Type 2 is permitted.
5	The diaphragm shall be rectangular in shape or shall be divisible into rectangular segments for the purpose of seismic design, with vertical elements of the seismic force-resisting system or collectors provided at each end of each rectangular segment span.
6	The vertical elements of the seismic force-resisting system shall be limited to one or more of the following: concrete shear walls, precast concrete shear walls, masonry shear walls, steel concentrically braced frames, steel and concrete composite braced frames, or steel and concrete composite shear walls.
7	The vertical elements of the seismic force-resisting system shall be designed in accordance with ASCE/SEI 7-22 Section 12.8, except that they shall be permitted to be designed using the two-stage analysis procedure of ASCE/SEI 7-22 Section 12.2.3.4, where applicable.

Step 2: Divide roof diaphragm into a series of rectangular segments for purposes of design, with each segment spanning to vertical elements, collectors, or a combination of the two (ASCE/SEI 7-22 Section 12.10.4.2). This is one of the ASCE/SEI Section 12.10.4.1 limitations. If this cannot be met, use of the alternative RWFD provisions is not permitted. Figure 7-3 shows a diaphragm divided into two rectangles (Segments 1 and 2) for seismic forces in the direction parallel to Lines 1, 2, and 3.

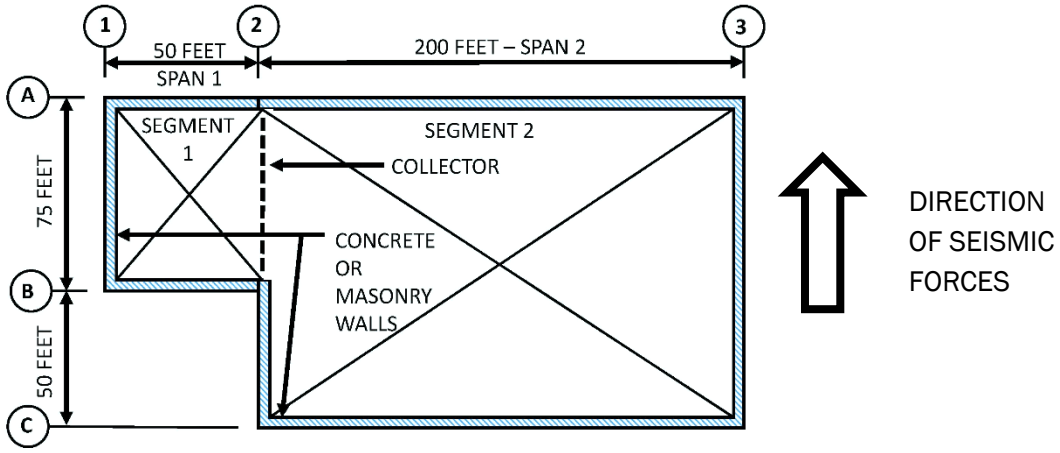

Figure 7-3. Roof Diaphragm Divided into Two Segments for Purposes of Diaphragm Design in the Direction Shown

Step 3: Determine w_i, W and w_{px}. ASCE/SEI 7-22 Section 12.7.2 defines effective seismic weight, W. w_i is the portion of W that is tributary to level i. w_{px} is different from w_i only in that the weights of the walls parallel to the earthquake forces are permitted to be excluded from w_{px}. It is common practice to exclude the weights of these parallel walls in low-rise buildings with concrete or masonry walls; including or excluding this weight (i.e., using a value of w_{px} less than w_i) is at the discretion of the design engineer.

Step 4: Determine R_{diaph}, based on ASCE/SEI 7-22 Section 12.10.4.2.1. For wood structural panel diaphragms, a value of 4.5 is assigned. For a bare steel deck diaphragm, assigning R_{diaph} will require making a determination of whether the diaphragm meets the special seismic detailing requirements of AISI S400. This determination is of significance because diaphragm design forces will vary by a factor of three as a result. The AISI S400 requirements can be met either through prescriptive methods, as summarized in Table 7-5, or by meeting comprehensive qualification requirements detailed in AISI S400.

R_{diaph} = 4.5 for wood structural panel diaphragms,
R_{diaph} = 4.5 for bare steel deck diaphragms that meet the special seismic detailing requirements for AISI S400,
R_{diaph} = 1.5 for all other bare steel deck diaphragms.

Table 7-5. Prescriptive Special Seismic Detailing Requirements for Steel Deck Diaphragms (from AISI S400 Section F3.5.1)

Item	Prescriptive Requirements
1	The steel deck panel type shall be 36 in. (914 mm) wide, 1.5 in. (38.1 mm) deep wide rib, 6 in. (152 mm) pitch (WR) deck.
2	The steel deck base steel thickness shall be greater than or equal to 0.0295 in. (0.749 mm) and less than or equal to 0.0598 in. (1.52 mm).
3	The steel deck material shall conform to Section A.3.1.1 of AISI S100 [CSA S136].
4	The structural connection between the steel deck and the supporting steel member (with minimum thickness of 1/8 in. (3.18 mm)) shall be limited to mechanical connectors qualified in accordance with AISI S400 Section F3.5.1.1.
5	The structural connection perpendicular to the steel deck ribs shall be no less than a 36/4 pattern (12 in. (305 mm) on center) and no more than a 36/9 pattern (6 in. (152mm) on center) with double fasteners in the last panel rib.
6	The structural connection parallel to the steel deck ribs shall be no less than 3 in. (76.2 mm) and no more than 24 in. (610 mm) and shall not be greater than the sidelap connection spacing.
7	The sidelap connection between steel deck shall be limited to #10, #12, or #14 screws sized such that shear in the screws is not the controlling limit state, or connectors qualified in accordance with AISI S400 Section F3.5.1.2.
8	The sidelap connection shall be spaced no less than 6 in. 9152 mm) and no more than 24 in. (610 mm).

Step 5: Determine T_{diaph} based on ASCE/SEI 7-22 Section 12.10.4.2.1. Different formulas are given for wood structural panel diaphragms and bare steel deck diaphragms.

$T_{diaph} = 0.002L_{diaph}$ for wood structural panel diaphragms,

$T_{diaph} = 0.001L_{diaph}$ for bare steel deck diaphragms,

where

T_{diaph} = Period of diaphragm for design of diaphragm using the alternative diaphragm design method of Section 12.10.4 (seconds), and

L_{diaph} = Span in feet of the horizontal diaphragm or diaphragm segment being considered, measured between vertical elements or collectors that provide support to the diaphragm or diaphragm segment.

Note that the substitution of diaphragm periods derived from analytical modeling or other sources is not permitted. The ASCE/SEI 7-22 Section 12.10.4.2 diaphragm period equations must be used.

Step 6: Determine $C_{s\text{-}diaph}$ using ASCE/SEI 7-22 Equation 12.10-16a, but not greater than equation 12.10-16b

$$C_{s-diaph} = \frac{S_{DS}}{R_{diaph}/I_e} \qquad \text{(ASCE/SEI 7-22 Eq. 12.10-16a)}$$

$$C_{s-diaph} = \frac{S_{D1}}{(R_{diaph}T_{diaph})/I_e} \qquad \text{(ASCE/SEI 7-22 Eq. 12.10-16b)}$$

Step 7: Determine diaphragm design force, F_{px}, at each diaphragm level in accordance with Equation 12.10-15:

$$F_{px} = C_{s\text{-}diaph}\,(w_{px}) \qquad \text{(ASCE/SEI 7-22 Eq. 12.10-15)}$$

Note that there are no upper or lower bounds on the F_{px} forces. With longer span diaphragms the force levels are intentionally anticipated to be lower in some cases than the lower bounds in the other diaphragm design methods.

Step 8: Determine amplified shear and extent of amplified shear boundary zone in accordance with ASCE/SEI 7-22 Section 12.10.4.2.2. For diaphragm spans less than 100 ft, the shear will be amplified by 1.5 through the entire diaphragm span. For diaphragms with spans greater or equal to 100 ft., an amplified shear zone will be located at each end of the diaphragm span and extend for ten percent of the diaphragm span. This strengthening of ten percent of the span was identified in analytical studies to move diaphragm yielding from the edge of the diaphragm to the diaphragm interior. Figure 7-4 illustrates two diaphragm segments, one of which spans less than 100 feet and uses amplified shear throughout, and the other of which spans more than 100 feet and has amplified shear zones at each end of the span (illustrated by shaded zones).

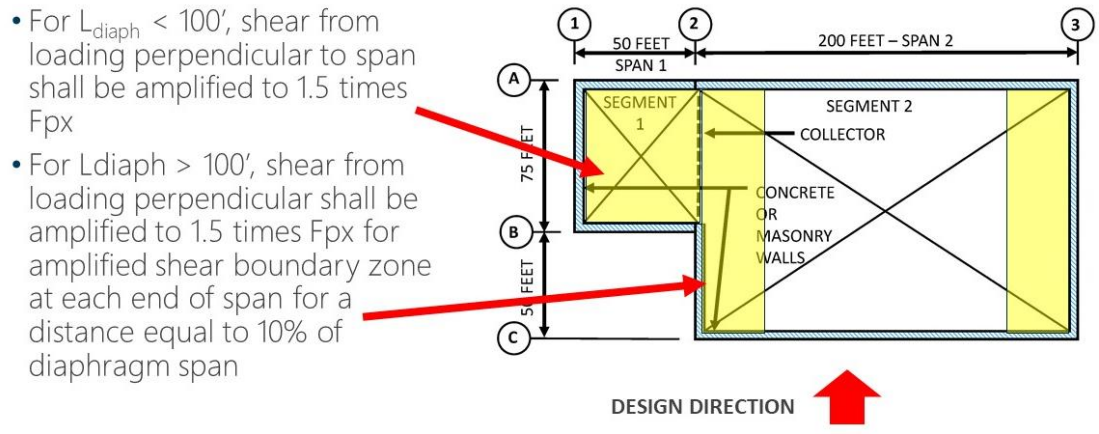

Figure 7-4. ASCE/SEI 7-22 Roof Diaphragm Illustrating Amplified Shear Zone for the Full Extent of Segment 1 and for 10 Percent of the Diaphragm for Segment 2

Step 9: Use F_{px} forces and, where applicable, amplified F_{px} forces to design for shear. Use F_{px} forces without amplification to design for flexure. Because these provisions are limited to one-story buildings, no diaphragm transfer forces are anticipated.

Step 10: Determine collector forces in accordance with ASCE/SEI 7-22 Section 12.10.4.2.4. Collector forces are to be based on F_{px} forces without the 1.5 shear amplification factor and are to be multiplied by an $\Omega_{0\text{-diaph}}$ value of 2.0.

Step 11: Where required by ASCE/SEI 7-22, determine $C_{d\text{-diaph}}$ and diaphragm deflections in accordance with Section 12.10.4.2.5.

Step 12: Check applicable ASCE/SEI 7-22 deflection and drift limitations for the overall structure. See Section 7.3 for further discussion.

7.4 Example: One-Story Wood Assembly Hall

7.4.1 Example Using the ASCE/SEI 7-22 Section 12.10.1 and 12.10.2 Traditional Diaphragm Design Method

Building Configuration

One story
Risk Category III, I_e = 1.25 (assembly use)
Mean roof height = 25 feet
Length = 90 feet
Width = 40 feet
S_{DS} = 1.0, S_{D1} = 0.60 - from ASCE/SEI 7-22 Section 11.4.4
Wood structural panel diaphragm
Wood structural panel shear walls - R=6.5, Ω_0=3, C_d=4

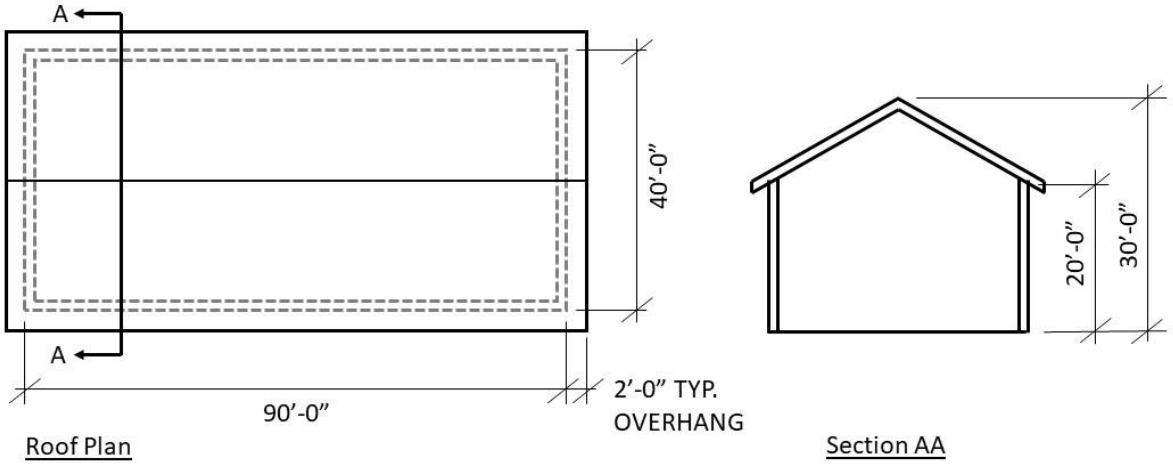

Figure 7-5. Plan and Elevation of One-story Assembly Hall

Step 1 - Determine w_i, W and w_{px}

Weight for Seismic Analysis

Roof + ceiling	= 15 psf
Roof only	= 8 psf
Wall	= 10 psf

Seismic weight –	Roof:	15 psf (40 ft) (90 ft)	= 54,000 lb
	Overhang:	8 psf (2 ft)(42 ft + 92 ft)(2 sides)	= 4,288 lb
	Side walls:	10 psf (10 ft)(90 ft.)(2 sides)	= 18,000 lb
	End walls:	10 psf (25 ft/2)(40 ft.)(2 sides)	= 10,000 lbs
	TOTAL		= 86,288 lb acting at roof

Diaphragm Weight, w_{px}, at the Roof

Diaphragm weight = Total seismic weight – weight of the walls resisting seismic forces

W_{pr} = 86,288 – 10,000 = 76,288 lb (for seismic forces in transverse direction)

W_{pr} = 86,288 – 18,000 = 68,288 lb (for seismic forces in longitudinal direction)

Step 2 - Base Shear

$$T_a = C_t h_n^x = 0.020(25)^{0.75} = 0.22 \text{ sec} \qquad \text{(ASCE/SEI 7-22 Eq. 12.8-8)}$$

Where

h_n = structural height as defined in ASCE/SEI 7-22 Section 11.2, and the coefficients

C_t and x are determined from ASCE/SEI 7-22 Table 12.8-2.

$$C_s = \frac{S_{DS}}{R/I_e} = \frac{1.00}{6.5/1.25} = 0.192 \qquad \text{(ASCE/SEI 7-22 Eq. 12.8-3)}$$

Where

S_{DS} = Design spectral response acceleration parameter in the short period range as determined from ASCE/SEI 7-22 Section 11.4.4,

R = Response modification factor in ASCE/SEI 7-22 Table 12.2-1, and

I_e = seismic importance factor determined in accordance with ASCE/SEI 7-22 Section 11.5.1.

C_s need not exceed:

$$C_s = \frac{S_{D1}}{T(R)/I_e} = \frac{0.60}{0.22(6.5)/1.25} = 0.524 \qquad \text{(ASCE/SEI 7-22 Eq. 12.8-4)}$$

$V = C_s W = 0.192\ (86{,}288) = 16{,}567$ lb (ASCE/SEI 7-22 Eq. 12.8-1)

Step 3 - Vertical Distribution of Forces

Not applicable for one-story building.

Step 4 - Determine F_{px} Forces

Strength Level diaphragm design force:

$$F_{px} = \frac{\sum_{i=x}^{n} F_i}{\sum_{i=x}^{n} w_i} w_{px} \qquad \text{(ASCE/SEI 7-22 Eq. 12.10-1)}$$

Where

F_{px} = Diaphragm design force at level x,

F_i = Design force applied to level i,

w_i = Weight tributary to level i, and

w_{px} = Weight tributary to the diaphragm at level x.

For a single-story building, $F_{px} = C_s\ (w_{px})$

The calculated diaphragm seismic forces are:

F_{px} = 0.192 (76,288 lb) = 14,647 lb (transverse direction)

F_{px} = 0.192 (68,288 lb) = 13,111 lb (longitudinal direction)

The minimum value is:

$F_{px} = 0.2 S_{DS} I_e w_{px}$ (ASCE/SEI 7-22 Eq. 12.10-2)

= 0.2(1.0)(1.25)(76,288 lb) = 19,072 lb (transverse direction)

= 0.2(1.0)(1.25)(68,288 lb) = 17,072 lb (longitudinal direction)

The maximum value is:

$F_{px} = 0.4S_{DS}I_e w_{px}$ (ASCE/SEI 7-22 Eq. 12.10-3)

= 0.4(1.0) (1.25)(76,288 lb) = 38,144 lb (transverse direction)

= 0.4(1.0) (1.25)(68,288 lb) = 34,144 lb (longitudinal direction)

Governing diaphragm design forces are:

F_{pr} = 19,072 lb (transverse direction, strength level)

F_{pr} = 17,072 lb (longitudinal direction, strength level)

ASD Level diaphragm design forces are:

F_{pr} = 0.7(19,072) = 13,350 lb (transverse direction)

F_{pr} = 0.7(17,072) = 11,950 lb (longitudinal direction)

Steps 1 through 4 have completed calculation of the F_{px} forces. From this point, Steps 5 through 8, as outlined in Section 7.3.1, complete the diaphragm design process, including consideration of transfer forces (not applicable for this one-story building), diaphragm design for shear and flexure, design of collectors, and checking of applicable ASCE/SEI 7-22 deflection and drift requirements. See Section 7.2 for further discussion.

7.4.2 Example: One-Story Wood Assembly Hall – ASCE/SEI 7-22 Section 12.10.3 Alternative Diaphragm Design Method

Step 1 - Determine w_i, W and w_{px}. From Section 7.4.1:

W = 86,288 lb

W_{pr} = 76,288 lb transverse

W_{pr} = 68,288 lb longitudinal

Step 2 - Determine R_s:

R_s = 3.0 (from Table 12.10-1) for wood sheathed (wood structural panel) diaphragm

Step 3 - Determine C_{px}, Diaphragm Design Acceleration Coefficient:

For a building two stories or less, the determination of diaphragm design forces in accordance with ASCE/SEI 7-22 Section 12.10.3 is illustrated below.

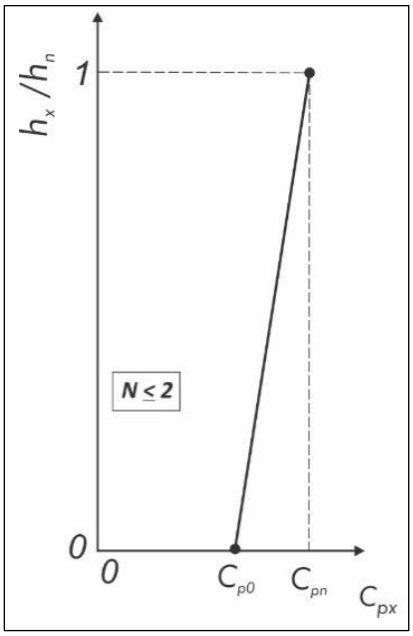

Figure 7-6. Calculating the Design Acceleration Coefficient, C_{px}, in Buildings with $N \leq 2$ (from Figure C12.10-7 in the 2020 *NEHRP Provisions*)

N =1

z_s = 1.0 (all other SFRS, ASCE/SEI 7-22 Section 12.10.3.2)

$$\Gamma_{m1} = 1 + 0.5 z_s \left(1 - \frac{1}{N}\right) = 1 + 0.5 \times 1.00 \times \left(1 - \frac{1}{1}\right) = 1.0 \qquad \text{(ASCE/SEI 7-22 Eq. 12.10-13)}$$

$$\Gamma_{m2} = 0.9 z_s \left(1 - \frac{1}{N}\right)^2 = 0.9 \times 1.00 \times \left(1 - \frac{1}{1}\right)^2 = 0 \qquad \text{(ASCE/SEI 7-22 Eq. 12.10-14)}$$

The calculated values of one for the first mode and zero for the higher modes are consistent with first mode response as would be anticipated for a single-story building.

Step 3A - Determine C_{p0}

$C_{p0} = 0.4 S_{DS} I_e = 0.4(1.0)(1.25) = 0.50$ (ASCE/SEI 7-22 Eq. 12.10-6)

Step 3B - Determine C_{pi}

C_{pi} is not used for $N \leq 2$

Step 3C - Determine C_{pn}

C_{s2} = 0 for N = 1

$$C_{pn} = \sqrt{\left(\Gamma_{m1}\Omega_0 C_s\right)^2 + \left(\Gamma_{m2} C_{s2}\right)^2} = \left(\Gamma_{m1}\Omega_0 C_s\right) = 1.0(3.0)(0.192) = 0.576 \quad \text{(ASCE/SEI 7-22 Eq. 12.10-7)}$$

Step 3D - Determine C_{px}

$C_{pr} = C_{pn} = 0.576$

Step 4 - Determine F_{px}

The strength level diaphragm design force:

$$F_{pr} = \frac{C_{pr}}{R_s} w_{px} \quad \text{(ASCE/SEI 7-22 Eq. 12.10-4)}$$

$$= \frac{0.576}{3.0} 76,288 = 14,647 \text{ lbs} \quad \text{(transverse direction)}$$

$$= \frac{0.576}{3.0} 68,288 = 13,111 \text{ lbs} \quad \text{(longitudinal direction)}$$

But not less than:

$F_{pr} = 0.2 S_{DS} I_e w_{px}$ (ASCE/SEI 7-22 Eq. 12.10-5)

= 0.2(1.0)(1.25)(76,288) = 19,072 lb (transverse direction)

= 0.2(1.0)(1.25)(68,288) = 17,072 lb (longitudinal direction)

These lower bound seismic forces control.

ASD Level diaphragm design forces:

F_{pr} = 0.7(19,072) = 13,350 lb (transverse direction)

F_{pr} = 0.7(17,072) = 11,950 lb (longitudinal direction)

Steps 1 through 4 have completed calculation of the F_{px} forces. From this point, Steps 5 through 8, as outlined in Section 7.3.1, complete the diaphragm design process, including consideration of transfer forces (not applicable for this one-story building), diaphragm design for shear and flexure, design of collectors, and checking of applicable ASCE/SEI 7-22 deflection and drift requirements. See Section 7.2 for further discussion.

7.5 Example: Multi-Story Steel Building with Steel Deck Diaphragms

7.5.1 Example: Multi-Story Steel Building - Section 12.10.1 and 12.10.2 Traditional Diaphragm Design Method

Building Configuration

Six stories
Risk Category II, I_e = 1.0
Mean roof height = 72 feet - six stories at 12 feet each
Length = 150 feet
Width = 120 feet
S_{DS} = 1.2, S_{D1} = 0.70 - from ASCE/SEI 7-22 Section 11.4.4
Concrete-filled steel deck floor diaphragms
Bare steel deck roof diaphragm
Steel special concentrically braced frame system – R = 6, Ω_0 = 2

All seismic forces are at strength level.

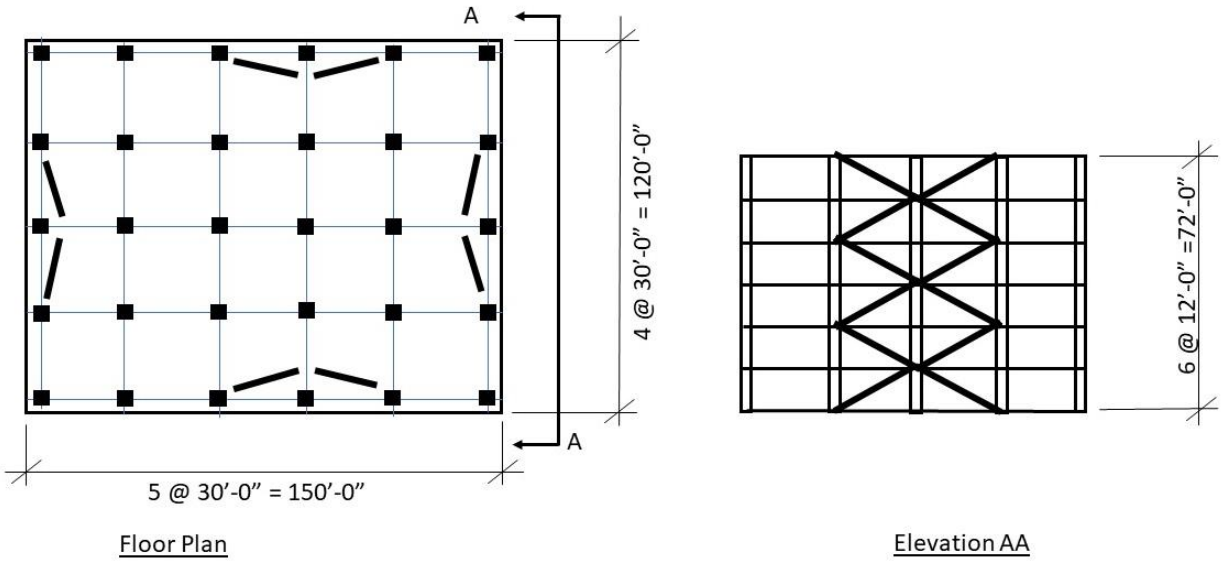

Figure 7-7. Plan and Elevation of Example Six-Story Building

Step 1 - Determine w_i, W and w_{px}

Weight for Seismic Analysis

Roof + ceiling	= 40 psf
Floor + ceiling	= 80
Exterior wall	= 20

Interior partitions are included as 10 psf in floor + ceiling weight of 80 psf

Seismic weight at roof

Roof: 40 psf (150 ft)(120 ft) = 720 kips
Longitudinal exterior walls: 20 psf (150 ft)(12/2 + 4 ft)(2 sides) = 60 kips
Transverse exterior walls: 20 psf (120 ft)(12/2 + 4 ft)(2 sides) = 48 kips

TOTAL = 720 + 60 + 48 = 828 kips acting at roof

Seismic weight at 2nd through 6th floors

Floor: 80 psf (150 ft)(120 ft) = 1440 kips
Longitudinal exterior wall: 20 psf (150 ft)(12 ft)(2 sides) = 72 kips
Transverse exterior wall: 20 psf (120 ft)(12 ft)(2 sides) = 58 kips

TOTAL = 1440 = 72 = 58 = 1,570 kips acting at floors

Seismic weight TOTAL, W = 828 + 5 (1,570) = 8,678 kips

Diaphragm Weights

Diaphragm seismic weight, w_{px}, at the roof:

= 828 kips (transverse and longitudinal directions)

Diaphragm seismic weight, w_{px}, at the 2nd through 6th floors:

= 1,570 kips (transverse and longitudinal direction)

Diaphragm seismic weights with exterior wall weight parallel to the direction of seismic forces neglected are between 4 and 8 percent lower than total seismic weight. These forces are not carried by the diaphragm but instead act directly at the vertical elements. For simplicity, however, use total seismic weights of 828 and 1,570 kips to determine diaphragm design forces.

Step 2 - Determine Base Shear

$$T_a = C_t h_n^x = 0.020(72)^{0.75} = 0.49 \text{ sec}$$ (ASCE/SEI 7-22 Eq. 12.8-8)

Where

h_n = structural height as defined in Section 11.2, and the coefficients, and

C_t and x are determined from ASCE/SEI 7-22 Table 12.8-2.

$$C_s = \frac{S_{DS}}{\frac{R}{I_e}} = \frac{1.20}{\frac{6}{1}} = 0.200 \text{ (governs)}$$ (ASCE/SEI 7-22 Eq. 12.8-3)

Where

S_{DS} = Design spectral response acceleration parameter in the short period range as determined from Section 11.4.5 or 11.4.8,

R = Response modification factor in Table 12.2-1, and

I_e = Importance Factor determined in accordance with Section 11.5.1.

C_s need not exceed:

$$C_s = \frac{S_{D1}}{T\left(\frac{R}{I_e}\right)} = \frac{0.70}{0.49\left(\frac{6}{1}\right)} = 0.238$$ (ASCE/SEI 7-22 Eq. 12.8-4)

$V = C_s W = 0.20\ (8{,}678) = 1{,}736$ kips (ASCE/SEI 7-22 Eq. 12.8-1)

Step 3 - Vertical Distribution of Seismic Base Shear

The lateral seismic force at any level is determined as

$$F_x = C_{vx} V$$ (ASCE/SEI 7-22 Eq. 12.8-11)

Where

$$C_{vx} = \frac{w_x h_x^k}{\sum_{i=1}^{n} w_i h_i^k}$$ (ASCE/SEI 7-22 Eq. 12.8-12)

w_i, w_x = Portion of the total effective seismic weight of the structure (W) located or assigned to level i or x,

h_i, h_x = Height [ft (m)] from the base to level i or x, and

k = Exponent related to the structure period as follows:

For structures that have a period of 0.5 s or less, k = 1;

for structures that have a period of 2.5 s or more, k = 2, and

for structures that have a period between 0.5 and 2.5 s, k shall be 2 or shall be determined by linear interpolation between 1 and 2.

For $T \leq 0.5$ sec., k = 1.0

Force distribution along the height of the building is shown in the table below.

Table 7-6. Vertical Distribution of Base Shear

Level x	w_x (kips)	h_x (ft)	$w_x h_x^k$ (ft-kips)	C_{vx}	F_x (kips)
Roof	828	72	59,616	0.174	302
6	1,570	60	94,200	0.275	478
5	1,570	48	75,360	0.220	382
4	1,570	36	56,520	0.165	287
3	1,570	24	37,680	0.110	191
2	1,570	12	18,840	0.055	96
Sum	8,678		342,216	0.999	1,736

Step 4 - Determine F_{px} Forces

Diaphragm design force is given by the larger of F_x determined above and F_{px} determined below.

$$F_{px} = \frac{\sum_{i=x}^{n} F_i}{\sum_{i=x}^{n} w_i} w_{px} \qquad \text{(ASCE/SEI 7-22 Eq. 12.10-1)}$$

Where

F_{px} = Diaphragm design force at level x,

F_i = Design force applied to level i,

w_i = Weight tributary to level i, and

w_{px} = Weight tributary to the diaphragm at level x.

Strength level diaphragm forces are determined in the table below. Note that for purposes of determining diaphragm design forces, ρ is set to 1.0, whether or not ρ is 1.0 for design of the vertical elements.

Table 7-7. Diaphragm Seismic Forces

Level	w_i (kips)	$\sum_{i=x}^{n} w_i$ (kips)	F_i (kips)	$\sum_{i=x}^{n} F_i = V_i$ (kips)	w_{px} (kips)	F_{px} (kips)
Roof	828	828	302	302	828	302
6	1,570	2,398	478	780	1,570	510
5	1,570	3,968	382	1,162	1,570	460
4	1,570	5,538	287	1,449	1,570	411
3	1,570	7,108	191	1,640	1,570	362
2	1,570	8,678	96	1,736	1,570	314
Sum	8,678		1,736		8,678	

F_{px} at the roof cannot be less than:

$$F_{pr} = 0.2S_{DS}I_e w_{pr}$$ (ASCE/SEI 7-22 Eq. 12.10-2)

$$= 0.2(1.2)(1.0)(828) = 199 \text{ kips}$$

F_{px} at the floor levels cannot be less than:

$$F_{px} = 0.2S_{DS}I_e w_{px}$$ (ASCE/SEI 7-22 Eq. 12.10-2)

$$= 0.2(1.2)(1.0)(1,570) = 377 \text{ kips}$$

F_{px} at roof need not exceed:

$$F_{pr} = 0.4S_{DS}I_e w_{pr}$$ (ASCE/SEI 7-22 Eq. 12.10-3)

$$= 0.4(1.2)(1.0)(828) = 397 \text{ kips}$$

F_{px} at the floor levels need not exceed:

$$F_{px} = 0.4S_{DS}I_e w_{px}$$ (ASCE/SEI 7-22 Eq. 12.10-3)

$$= 0.4(1.2)(1.0)(1,570) = 754 \text{ kips}$$

The resulting traditional method seismic design forces for the diaphragms are summarized in Table 7-8.

Table 7-8. Summary of Diaphragm Design Forces (kips)

Level	F_{px} *From Vertical Distribution* (kips)	F_{px} *Minimum* (kips)	F_{px} *Maximum* (kips)	F_{px} *Design* (kips)
Roof	302	199	397	302
6	510	377	754	510
5	460	377	754	460
4	411	377	754	411
3	362	377	754	377
2	314	377	754	377

Step 5 - Diaphragm Transfer Forces

Diaphragm transfer forces, as defined in ASCE/SEI 7-22 Section 11.2, occur where vertical elements of the SFRS are offset or discontinued at lower levels; they also occur due to changes in the stiffness of the SFRS vertical elements between levels. The occurrence of diaphragm transfer forces is determined by examining the distribution of forces from the analysis model. For simplicity, the building used in this example does not have transfer forces.

Step 6 - Design for Shear and Flexure

Diaphragms at each level are designed for shear and flexure using the tabulated F_{px} design forces. Where a computer analysis model is used, this generally involves taking the shear and flexure forces at the F_x level from the model and amplifying them to the F_{px} level.

The concrete-filled steel deck diaphragm is commonly idealized as rigid for building modeling and horizontal distribution of forces. As a result, inherent torsion, accidental torsion, and transfer forces (should they occur) will need to be addressed in the building model.

Step 7 - Collector Seismic Design Forces

Collectors in the example building are, per ASCE/SEI 7-22 Section 12.10.2.1, required to be designed for the seismic load effect, including overstrength. This involves the seismic load effect with overstrength provisions of ASCE/SEI 7-22 Section 12.4.3, used in the appropriate load combinations from ASCE/SEI 7-22 Chapter 2. The following demonstrates the calculation of the collector seismic design force due to horizontal seismic forces. This will need to the combined with applicable gravity loads and vertical seismic forces.

The locations of roof and 5th floor collectors for which forces will be calculated are shown in Figure 7-8.

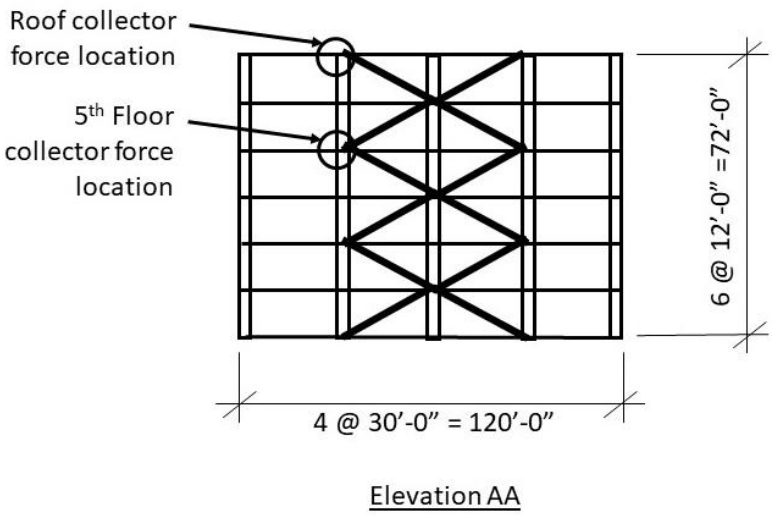

Figure 7-8. Example Building Elevation Showing Locations of Calculated Collector Forces Due to Horizontal Seismic Forces

Diaphragm Transverse Force Reactions and Units Shears

Because the bare steel deck roof diaphragm can be idealized as flexible, the unit shear in the diaphragm can be calculated as:

Roof Diaphragm V = 302 kips /2 = 151 kips

v = 151 kips / 120 ft = 1.26 klf

Because the concrete-filled steel deck floor diaphragms are idealized as rigid and designed considering inherent and accidental torsion, the shear reactions at the diaphragm perimeter (based on a structural analysis model) is determined to be 10% greater than would be determined by tributary area. The unit shear in the diaphragm can be calculated as:

5th Floor diaphragm V = 460 kips (1.1)/ 2 = 253 kips

v = 253 kips / 120 ft = 2.11 klf

Collector Force at Location shown in Figure 7-8, amplified by Ω_0

Roof Diaphragm T/C = 1.26 klf (30 ft) (2.0) = 76 kips

5th Floor Diaphragm T/C = 2.11 klf (30 ft) (2.0) = 127 kips

The resulting forces are not required to exceed the capacity-limited horizontal seismic load effect, E_{ci}, as defined in ASCE/SEI 7-22 Section 11.3. Note that ASCE/SEI 7-22 Section 12.10.2.1 also identifies conditions where amplification by Ω_0 is not required for design of collectors and their connections to vertical elements.

Step 8 addresses checking of applicable ASCE/SEI 7-22 deflection and drift limitations. See Section 7.2 for further discussion.

7.5.2 Example: Multi-story Steel Building – ASCE/SEI 7-22 Section 12.10.3 Alternative Diaphragm Design Method

Step 1 - Determine w_i, W and w_{px}. From Section 7.5.1:

W_{pr} = 828 kips roof

W_{px} = 1,570 kips floors

Step 2 - Determine R_s:

R_s = 2.0 for concrete-filled steel deck floor diaphragm (ASCE/SEI 7-22 Table 12.10-1)

R_s = 1.0 bare steel deck roof diaphragm w/ welded conn. (ASCE/SEI 7-22 Table 12.10-1)

Step 3 - Determine C_{px}, Diaphragm Design Acceleration Coefficient:

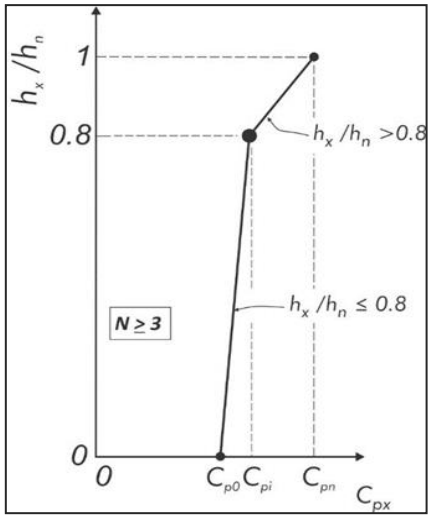

Figure 7-9. Calculating the Design Acceleration Coefficient, C_{px}, in Buildings with $N \geq 3$ (from Figure C12.10-7 in the 2020 *NEHRP Provisions*)

N =6

z_s = 1.0 (all other SFRS, ASCE/SEI 7-22 Section 12.10.3.2.1)

C_s = 0.200 (Example Section 7.5.1)

$$\Gamma_{m1} = 1 + 0.5 z_s \left(1 - \frac{1}{N}\right) \quad \text{(ASCE/SEI 7-22 Eq. 12.10-13)}$$

$$= 1 + 0.5 \times 1.00 \times \left(1 - \frac{1}{6}\right) = 1.42$$

$$\Gamma_{m2} = 0.9 z_s \left(1 - \frac{1}{N}\right)^2 = 0.9 \times 1.00 \times \left(1 - \frac{1}{6}\right)^2 = 0.625 \quad \text{(ASCE/SEI 7-22 Eq. 12.10-14)}$$

Step 3A - Determine C_{p0}

$C_{p0} = 0.4 S_{DS} I_e = 0.4(1.2)(1.00) = 0.48$ (ASCE/SEI 7-22 Eq. 12.10-6)

Step 3B - Determine C_{pi}

C_{pi} is taken as the greater of the following:

$C_{pi} = C_{p0} = 0.48$ (ASCE/SEI 7-22 Eq. 12.10-8)

$C_{pi} = 0.9 \Gamma_{m1} \Omega_0 C_s = 0.9(1.42)(2.0)(0.200) = 0.51$ (ASCE/SEI 7-22 Eq. 12.10-9)

Use C_{pi} = 0.51

Step 3C - Determine C_{pn}

C_{s2} is taken as the lesser of the following:

$$C_{s2} = (0.15N + 0.25) I_e S_{DS} \quad \text{(ASCE/SEI 7-22 Eq. 12.10-10)}$$

$$= (0.15 \times 6 + 0.25) \times 1.0 \times 1.2 = 1.38$$

$$C_{s2} = I_e S_{DS} = 1.0 \times 1.2 = 1.2 \quad \text{(ASCE/SEI 7-22 Eq. 12.10-11)}$$

$$C_{s2} = \frac{I_e S_{D1}}{0.03(N-1)} = \frac{1.0 \times 0.7}{0.03\,(6-1)} = 4.7 \quad \text{(ASCE/SEI 7-22 Eq. 12.10-12a)}$$

Use C_{s2} = 1.2

$$C_{pn} = \sqrt{(\Gamma_{m1} \Omega_0 C_s)^2 + (\Gamma_{m2} C_{s2})^2} \quad \text{(ASCE/SEI 7-22 Eq. 12.10-7)}$$

$C_{pn} = \sqrt{(1.42 \times 2 \times 0.200)^2 + (0.625 \times 1.2)^2}$ = 0.94

Step 3D - Determine C_{px}

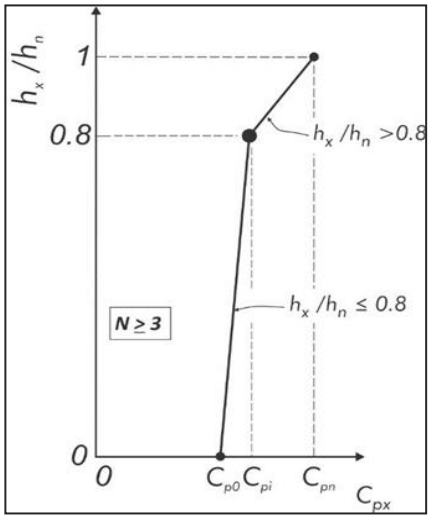

C_{p0} = 0.48

C_{pi} = 0.51

C_{pn} = 0.94

0.8h_n= 57.6 ft

Figure 7-10. Calculating the Design Acceleration Coefficient, C_{px}, in buildings with $N \geq 3$ (from Figure C12.10-7 in the 2020 *NEHRP Provisions*)

0.8h_n = 0.8 (72) = 57.6 ft (transition point in Example Figure 7-10)

h_6 = 5 (12) = 60 ft

C_{p6} = 0.51 + (0.94-0.51) (60-57.6)/12 = 0.60

Table 7-9. Summary of C_{px} Coefficients

Level	C_{px}
Roof	0.94
6	0.60
5	0.51
4	0.50
3	0.49
2	0.49

Step 4 - Determine F_{px} Forces

Force at roof using bare steel deck with welded connections, R_s = 1.0

$$F_{pr} = \frac{C_{pn}}{R_s} w_{pr}$$
$$= \frac{0.94}{1.0} 828 = 778 \text{ kips}$$

(ASCE/SEI 7-22 Eq. 12.10-4)

But not less than:

$F_{px} = 0.2 S_{DS} I_e w_{px}$ (ASCE/SEI 7-22 Eq. 12.10-5)

= 0.2(1.2)(1.0)(828) = 199 kips (roof)

Force at 6th floor using concrete-filled steel deck diaphragm:

$$F_{p6} = \frac{C_{p6}}{R_s} w_{p6}$$
$$= \frac{0.60}{2.0} 1{,}570 = 471 \text{ kips}$$

(ASCE/SEI 7-22 Eq. 12.10-4)

But not less than:

$F_{px} = 0.2 S_{DS} I_e w_{px}$ (ASCE/SEI 7-22 Eq. 12.10-5)

= 0.2(1.2)(1.0)(1,570) = 377 kips (floor)

Table 7-10. Summary of Section 12.10.3 Alternative Diaphragm Design Forces (kips)

Level	C_{px}	F_{px} *Eq. 12.10-4 Force* (kips)	F_{px} *Minimum* (kips)	F_{px} *Design* (kips)
Roof	0.94	778	199	778
6	0.60	471	377	471
5	0.51	400	377	400
4	0.50	392	377	392
3	0.49	385	377	385
2	0.49	385	377	385

Step 5 - Diaphragm Transfer Forces

Diaphragm transfer forces, as defined in ASCE/SEI 7-22 Section 11.2, occur where vertical elements of the SFRS are offset or discontinued at lower levels; this also occurs due to changes in the stiffness of the SFRS vertical elements between levels. For purposes of simplicity in this example problem, diaphragm transfer forces are assumed to not occur.

Step 6 - Design for Shear and Flexure

Diaphragms at each level are designed for shear and flexure using the tabulated F_{px} design forces. Where a computer analysis model is used, this generally involves taking the shear and flexure forces at the F_x level from the model and amplifying them to the F_{px} level.

The concrete-filled steel deck diaphragm is commonly idealized as rigid for building modeling and horizontal distribution of forces. As a result, inherent torsion, accidental torsion and transfer forces all need to be addressed in the building model.

Step 7 - Collector Seismic Design Forces

Collectors in the example building are, per ASCE/SEI 7-22 Section 12.10.3.4, required to be designed for amplified seismic forces. In lieu of the overstrength requirements of ASCE/SEI 7-22 Section 12.10.2.1, the collectors are required to be amplified by a factor of 1.5. Just like the seismic load effect with overstrength provisions of ASCE/SEI 7-22 Section 12.4.3, the amplified forces are required to be used in the appropriate load combinations from ASCE/SEI 7-22 Chapter 2. The following demonstrates the calculation of the collector seismic design forces due to horizontal seismic loads. This will need to be combined with applicable gravity loads and vertical seismic forces.

The locations of roof and 5th Floor collectors for which forces will be calculated are shown in Figure 7-8.

Diaphragm Transverse Force Reactions and Units Shears

Because the bare steel deck roof diaphragm can be idealized as flexible, the unit shear in the diaphragm can be calculated as:

Roof Diaphragm V = 778 kips /2 = 389 kips

v = 389 kips / 120 ft = 3.24 klf

Because the concrete-filled steel deck floor diaphragms are idealized as rigid and designed considering inherent and accidental torsion, the shear reactions at the diaphragm perimeter (based on a structural analysis model) is determined to be 10% greater than would be determined by tributary area. The unit shear in the diaphragm can be calculated as:

5th Floor diaphragm V = 400 kips (1.1)/ 2 = 220 kips

v= 220 kips / 120 ft = 1.83 klf

Collector Force at Location shown in Figure 7-8, amplified by 1.5 (in lieu of Ω_0)

Roof Diaphragm T/C = 3.24 klf (30 ft) (1.5) = 146 kips

5th Floor Diaphragm T/C = 1.83 klf (30 ft) (1.5) = 82 kips

Note that these collector forces may be further limited by the capacity-limited horizontal seismic load effect, E_{ci}, as defined in ASCE/SEI 7-22 Section 11.3. The collector forces may also be limited by the strength of the corresponding frame line below the collector per ASCE/SEI 7-22 Section 12.10.3.4 Exception 1. Such limits are not reflected in this example.

Step 8 addresses checking of applicable ASCE/SEI 7-22 deflection and drift limitations. See Section 7.2 for further discussion.

7.5.3 Comparison of Traditional and Alternative Procedure Diaphragm Design Forces

A comparison of the traditional design method and the alternative design method diaphragm seismic forces is provided in Table 7-11.

Table 7-11. Comparison of Traditional and Alternative F_{px} Diaphragm Design Forces (kips)

Level	*F_{PX} Traditional ASCE/SEI 7-22 Section 12.10.1 and 12.10.2* (kips)	*F_{px} Alternative ASCE/SEI 7-22 Section 12.10.3* (kips)
Roof	302	778
6	510	471
5	460	400
4	411	392
3	377	385
2	377	385

For this structure and the diaphragm systems used, the alternative method force is higher than the traditional method at some diaphragm levels (particularly at the roof) and lower at others. The much higher diaphragm design force at the roof comes from the combination of using the alternative method and the very low value of R_s = 1.0 for the welded bare steel deck diaphragm that is recognized in the ASCE/SEI 7-22 to have low ductility. If the roof diaphragm were instead changed to conform to the special seismic detailing requirements, the roof diaphragm design forces would essentially match the traditional method forces.

A comparison of the traditional design method and the alternative design method collector forces is provided in Table 7-12. As noted in Section 7.5.2 Step 7, other provisions may limit the collector forces required for design.

Table 7-12. Comparison of Traditional and Alternative Diaphragm Collector Forces (kips)

Level	*Traditional ASCE/SEI 7-22 Section 12.10.1 and 12.10.2*, (kips)	*Alternative ASCE/SEI 7-22 Section 12.10.3,* (kips)
Roof	76	146
5	127	82

7.6 Example: One-Story RWFD Bare Steel Deck Diaphragm Building

7.6.1 Example: One-Story Bare Steel Deck Diaphragm Building Diaphragm Design – ASCE/SEI 7-22 Section 12.10.1 and 12.10.2 Traditional Design method

Building Configuration

One story
Risk Category II, I_e = 1.0
Mean roof height = 30 feet
Length = 600 feet
Width = 360 feet
S_{DS} = 1.0, S_{D1} = 0.50 - from ASCE/SEI 7-22 Section 11.4.4
Bare steel deck diaphragm
Intermediate precast concrete shear walls - R=4, Ω_0=2.5, C_d=4

The system includes a bare steel deck diaphragm supported on open-web steel joists and girders. The perimeter walls are 9-1/4-inch thick tilt-up concrete walls, with a mean roof height of 30 feet, and a parapet above the roof of 3 feet.

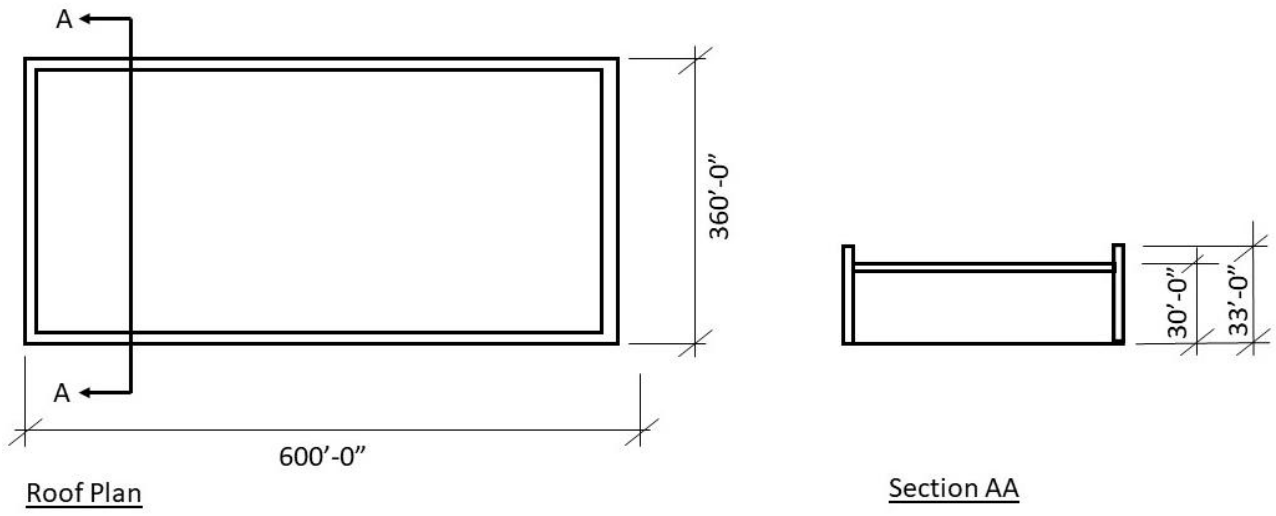

Figure 7-11. Example Building Roof Plan and Section

Step 1 - Weight for Seismic Analysis

Roof = 20 psf
Wall = 116 psf

Wall seismic weight tributary to roof:

w = 116 (33)(33/2)/30 = 2,105 plf

Seismic weight –	Roof: 0.02 ksf (600 ft) (360 ft)	= 4,320 kips
	Longitudinal walls: (2.105 klf)(600 ft)(2 sides)	= 2,526 kips
	Transverse walls: (2.105 klf)(360 ft)(2 sides)	= 1,516 kips
	TOTAL	= 8,362 kips acting at roof

Diaphragm Weight, w_{px}, at the Roof

w_{px} = Total seismic weight – weight of the walls resisting seismic forces

= 8,362 – 1,516 = 6,846 kips (for seismic forces in transverse direction)

= 8,362 – 2,526 = 5,836 kips (for seismic forces in longitudinal direction)

Step 2 - Base Shear

$T_a = C_t h_n^x = 0.020(30)^{0.75}$ =0.26 sec (ASCE/SEI 7-22 Eq. 12.8-7)

$$C_s = \frac{S_{DS}}{R/I_e} = \frac{1.0}{4/1.0} = 0.250$$ (ASCE/SEI 7-22 Eq. 12.8-2)

C_s need not exceed:

$$C_s = \frac{S_{D1}}{T(R)/I_e} = \frac{0.50}{0.26(4)/1.0} = 0.481 \qquad \text{(ASCE/SEI 7-22 Eq. 12.8-3)}$$

Base Shear V = $C_s W$ = (0.250)(8,362) = 2,090 kips (ASCE/SEI 7-22 Eq. 12.8-1)

Step 3 - Vertical Distribution of Base Shear

Not applicable to one-story example building.

Step 4 - Determination of F_{px} Forces

Strength Level diaphragm design force:

$$F_{px} = \frac{\sum_{i=x}^{n} F_i}{\sum_{i=x}^{n} w_i} w_{px} \qquad \text{(ASCE/SEI 7-22 Eq. 12.10-1)}$$

For a single-story building:

$F_{px} = C_s\ (w_{px})$

= 0.25 (6,846) = 1,712 kips (transverse direction)

= 0.25 (5,836) = 1,459 kips (longitudinal direction)

The minimum value of F_{px} is:

$F_{px} = 0.2 S_{DS} I_e w_{px}$ (ASCE/SEI 7-22 Eq. 12.10-2)

= 0.2(1.0)(1.0)(6,846) = 1,369 kips (transverse direction)

= 0.2(1.0)(1.0)(5,836) = 1,167 kips (longitudinal direction)

The maximum value of F_{px} is:

$F_{px} = 0.4 S_{DS} I_e w_{px}$ (ASCE/SEI 7-22 Eq. 12.10-3)

= 0.4(1.0) (1.0)(6,846) = 2,738 kips (transverse direction)

= 0.4(1.0) (1.0)(5,836) = 2,334 kips (longitudinal direction)

Governing diaphragm design force = 1,712 kips (transverse direction)

= 1,459 kips (longitudinal direction)

Step 5 - Diaphragm Transfer Forces

Not applicable to this example.

Step 6 - Diaphragm Design for Shear and Flexure

Diaphragm Design for Shear

The diaphragm is designed for shear using F_{px} forces. The following illustrates shear calculations for the transverse direction.

For transverse roof diaphragm forces:

w = 1,712 kips / 600 ft = 2.85 klf

V = 2.85 klf (600 ft / 2) = 856 kips

v = 856 kips / 360 ft = 2.37 klf maximum at end of diaphragm span

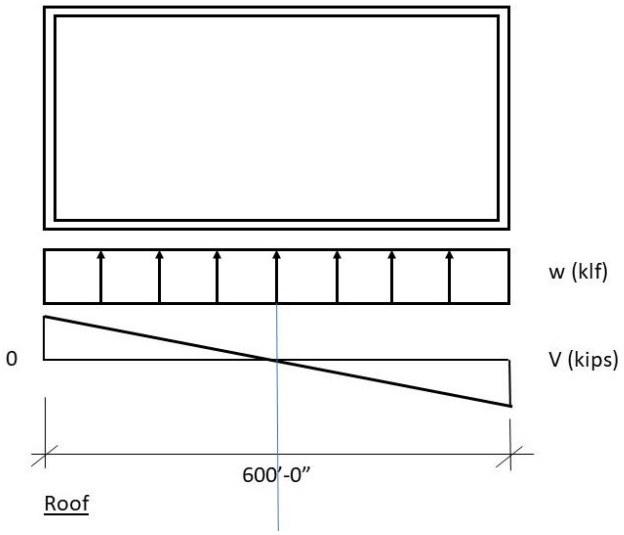

Figure 7-12. Plan Showing Uniform Seismic Forces and Diaphragm Shears in the Transverse Direction

Diaphragm Design for Flexure

For transverse roof diaphragm forces:

w = 1,712 kips / 600 ft = 2.85 klf

M = 2.85 klf (600 ft)^2 / 8 = 128,250 kip-ft

Chord T/C = 128,250 kip-ft / 360 ft = 356 kips maximum at diaphragm mid-span

Step 7 - Diaphragm Collector Design with Seismic Forces Amplified by Ω_0

The following illustrates calculation of collector seismic forces.

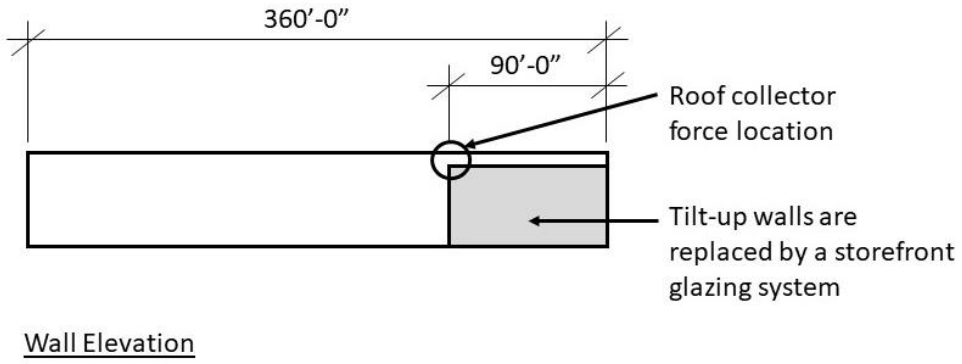

Figure 7-13. Example Building Elevation Showing Collector Force Location

The collector force is calculated based on the maximum transverse diaphragm shear, amplified by Ω_0:

T/C = 2.37 klf (90 ft) (2.5) = 533 kips

Step 8 applicable ASCE/SEI 7-22 deflection and drift limitations.

All applicable ASCE/SEI 7-22 deflection and drift checks are to be completed. It is important that this includes a check that the gravity system can accommodate the mid-span deflection of the roof diaphragm and the P-Δ stability of the tilt-up wall panels when subject to the diaphragm deflection. See Section 7.2 for further discussion.

7.6.2 Example: One-Story Bare Steel Deck Diaphragm Building Diaphragm Design - Section 12.10.4 Alternative Design Method with Diaphragm Meeting AISI S400 Special Seismic Detailing Provisions

Step 1 - Check ASCE/SEI 7-22 Section 12.10.4.1 Scoping Limitations

The following are application limits of the method that must be checked. If the building conforms to all scoping limitations, it is eligible to use the ASCE/SEI 7-22 Section 12.10.4 procedure.

Table 7-13. Limitations For Use of ASCE/SEI 7-22 Section 12.10.4 Alternative RWFD Provisions

Item	*Limitation*
1	All portions of the diaphragm shall be designed using the provisions of this section in both orthogonal directions.
2	The diaphragm shall consist of either: (a) a wood structural panel diaphragm designed in accordance with AWC SDPWS and fastened to wood framing members or wood nailers with sheathing nailing in accordance with the AWC SDPWS Section 4.2 nominal shear capacity tables, or (b) a bare (untopped) steel deck diaphragm meeting the requirements of AISI S400 and AISI S310.
3	Toppings of concrete or similar materials that affect diaphragm strength or stiffness shall not be placed over the wood structural panel or bare steel deck diaphragm.
4	The diaphragm shall not contain horizontal structural irregularities, as specified in ASCE/SEI 7-22 Table 12.3-1, except that Horizontal Structural Irregularity Type 2 is permitted.
5	The diaphragm shall be rectangular in shape or shall be divisible into rectangular segments for purpose of seismic design, with vertical elements of the seismic force-resisting system or collectors provided at each end of each rectangular segment span.
6	The vertical elements of the seismic force-resisting system shall be limited to one or more of the following: concrete shear walls, precast concrete shear walls, masonry shear walls, steel concentrically braced frames, steel and concrete composite braced frames, or steel and concrete composite shear walls.
7	The vertical elements of the seismic force-resisting system shall be designed in accordance with ASCE/SEI 7-22 Section 12.8, except that they shall be permitted to be designed using the two-stage analysis procedure of ASCE/SEI 7-22 Section 12.2.3.4, where applicable.

The example building conforms to all of these limitations and can be designed in accordance with ASCE/SEI 7-22 Section 12.10.4.

Step 2 - Divide Diaphragms into Rectangles

Break roof diaphragm into a series of rectangular segments for purposes of design, with each segment spanning to vertical elements or a collector (see Figure 7-3).

Because the example building is rectangular in plan and shear walls are located at the building perimeter, a single rectangular segment extending for the full building plan (600 ft by 360 ft) will be used.

Step 3 - Determine W_{px}

W_{px} was determined in Section 7.7.1 to be:

6,846 kips (transverse forces)

5,836 kips (longitudinal forces)

Step 4 - Determine R_{diaph}

R_{diaph} = 4.5 for bare steel deck diaphragms that meet the special seismic detailing requirements of AISI S400

This example building has a bare steel deck diaphragm that meets the prescriptive requirements of AISI S400 Section F3.5.1, qualifying it as meeting special seismic detailing requirements. The AISI S400 requirements are provided in Table 7-14. These requirements have been identified through testing to provide a good hysteretic response, including retaining post-peak cyclic load capacity. Of note in these AISI prescriptive requirements is Item 4, requiring qualified mechanical connectors between the decking and supporting steel members, and Item 7 requiring screws for sidelap connections. At the time of writing, welded bare steel deck diaphragms are not able to meet the special seismic detailing requirements and are therefore required to be designed using R_{diaph} = 1.5.

Table 7-14. Prescriptive Special Seismic Detailing Requirements for Steel Deck Diaphragms (From AISI S400 Section F3.5.1)

Item	Prescriptive Requirements
1	The steel deck panel type shall be 36 in. (914 mm) wide, 1.5 in. (38.1 mm) deep wide rib, 6 in. (152 mm) pitch (WR) deck.
2	The steel deck base steel thickness shall be greater than or equal to 0.0295 in. (0.749 mm) and less than or equal to 0.0598 in. (1.52 mm).
3	The steel deck material shall conform to Section A.3.1.1 of AISI S100 [CSA S136].
4	The structural connection between the steel deck and the supporting steel member (with minimum thickness of 1/8 in. (3.18 mm)) shall be limited to mechanical connectors qualified in accordance with AISI S400 Section F3.5.1.1.
5	The structural connection perpendicular to the steel deck ribs shall be no less than a 36/4 pattern (12 in. (305 mm) on center) and no more than a 36/9 pattern (6 in. (152 mm) on center) with double fasteners in the last panel rib.
6	The structural connection parallel to the steel deck ribs shall be no less than 3 in. (76.2 mm) and no more than 24 in. (610 mm) and shall not be greater than the sidelap connection spacing.
7	The sidelap connection between steel deck shall be limited to #10, #12, or #14 screws sized such that shear in the screws is not the controlling limit state, or connectors qualified in accordance with AISI S400 Section F3.5.1.2.
8	The sidelap connection shall be spaced no less than 6 in. 9152 mm) and no more than 24 in. (610 mm).

Step 5 - Determine T_{diaph}

T_{diaph} = 0.001L_{diaph} for bare steel deck diaphragms (ASCE/SEI 7-22 Section 12.10.4.2.1)

where

T_{diaph} = Period of diaphragm for design of diaphragm using the alternative diaphragm design method of Section 12.10.4 (seconds), and

L_{diaph} = Span in feet of the horizontal diaphragm or diaphragm segment being considered, measured between vertical elements or collectors that provide support to the diaphragm or diaphragm segment.

T_{diaph} = 0.001 (600) = 0.60 s (transverse forces)

T_{diaph}= 0.001 (360) = 0.36 s (longitudinal forces)

Step 6 - Determine $C_{s\text{-}diaph}$

For transverse forces:

$$C_{s-diaph} = \frac{S_{DS}}{R_{diaph}/I_e} = \frac{1.0}{4.5/1.0} = 0.222 \qquad \text{(ASCE/SEI 7-22 Eq. 12.10-16a)}$$

But need not exceed

$$C_{s-diaph} = \frac{S_{D1}}{T_{diaph}(R_{diaph})/I_e} = \frac{0.50}{0.60(4.5)/1.0} = 0.185 \qquad \text{(ASCE/SEI 7-22 Eq. 12.10-16b)}$$

Use $C_{s\text{-}diaph}$ = 0.185 transverse

For longitudinal forces:

$$C_{s-diaph} = \frac{S_{DS}}{R_{diaph}/I_e} = \frac{1.0}{4.5/1.0} = 0.222 \qquad \text{(ASCE/SEI 7-22 Eq. 12.10-16a)}$$

But need not exceed:

$$C_{s-diaph} = \frac{S_{D1}}{T_{diaph}(R_{diaph})/I_e} = \frac{0.50}{0.36(4.5)/1.0} = 0.309 \qquad \text{(ASCE/SEI 7-22Eq. 12.10-16b)}$$

Use $C_{s\text{-}diaph}$ = 0.222 longitudinal

Step 7 - Determine diaphragm design force, F_{px}

$F_{px} = C_{s\text{-}diaph}\,(w_{px})$ (ASCE/SEI 7-22 Eq.12.10-15)

F_{px} = 0.185 (6,846) = 1,266 kips transverse

F_{px} = 0.222 (5,836) = 1,296 kips longitudinal

Note that unlike the ASCE/SEI 7-22 Section 12.10.1 and 12.10.2 traditional method and the Section 12.10.3 alternative method, for the Section 12.10.4 alternative RWFD method there is no lower bound for diaphragm seismic design forces.

Step 8 - Determine amplified shear and extent of amplified shear boundary zone

Because the diaphragm span in both directions is greater than 100 ft., an amplified shear zone will be located at each end of the diaphragm span and extend for ten percent of the diaphragm span. The extent of the amplified shear zones are:

0.10 (600) = 60 ft each end for transverse forces

0.10 (360) = 36 ft each end for longitudinal forces.

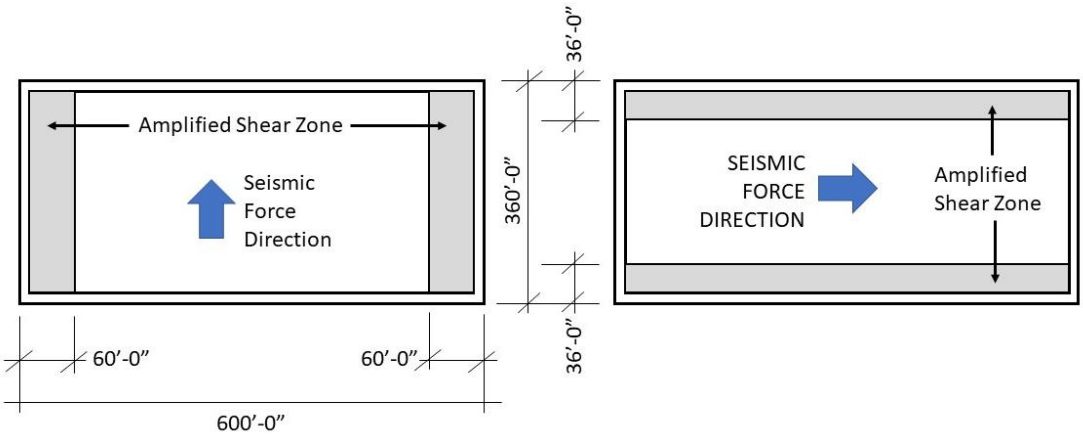

Figure 7-14. Roof Plans Showing Amplified Shear Zones for Seismic Forces in the Transverse and Longitudinal Directions

Step 9 - Design for Shear and Flexure

Diaphragm Design for Shear

The diaphragm is designed for shear using F_{px} forces. The following illustrates shear calculations for the transverse direction.

For transverse roof diaphragm forces:

w = 1,266 kips / 600 ft = 2.11 klf

V = 2.11 klf (600 ft / 2) = 633 kips

v = 633 kips / 360 ft = 1.76 klf maximum at end of diaphragm span WITHOUT shear amplification

v = 1.76 klf (1.5) = 2.64 klf maximum at end of diaphragm span WITH shear amplification

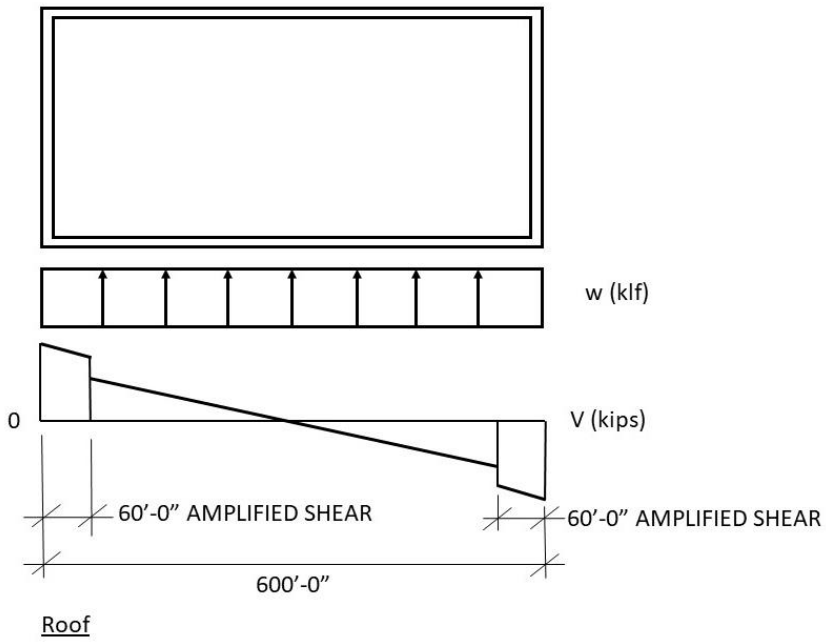

Figure 7-15. Plan Showing Uniform Seismic Forces and Diaphragm Shears in the Transverse Direction, Including Amplified Shear Zone

Diaphragm Design for Flexure

For transverse roof diaphragm forces the chord force is calculated using F_{px} forces WITHOUT amplification:

w = 1,266 kips / 600 ft = 2.11 klf

M = 2.11 klf (600 ft)^2 / 8 = 94,950 kip-ft

Chord *T*/*C* = 94,950 kip-ft / 360 ft = 264 kips maximum at diaphragm mid-span

Step 10 - Design Collectors and Their Connections to Vertical Elements

Determine collector forces in accordance with ASCE/SEI 7-22 Section 12.10.4.2.4. Collector forces are to be based on F_{px} forces WITHOUT the 1.5 shear amplification factor, multiplied by $\Omega_{0\text{-diaph}}$.

The following illustrates the calculation of collector seismic forces.

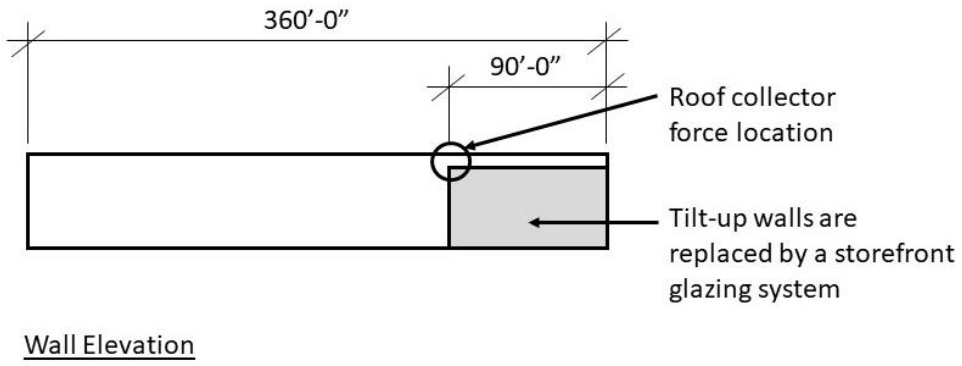

Figure 7-16. Example Building Elevation Showing Collector Force Location

Per ASCE/SEI 7-22 Section 12.10.4.2.4, the collector force is calculated based on the maximum transverse diaphragm shear WITHOUT amplification, multiplied by $\Omega_{o\text{-}diaph}$:

T/C = 1.76 klf (90 ft) (2.0) = 317 kips

Steps 11 and 12 - Check applicable ASCE/SEI 7-22 deflection and drift limitations.

Where required by ASCE/SEI 7-22, determine $C_{d\text{-}diaph}$ and diaphragm deflections in accordance with ASCE/SEI 7-22 Section 12.10.4.2.5. All applicable ASCE/SEI 7-22 deflection and drift checks are to be completed. It is important that this includes a check that the gravity system can accommodate the mid-span deflection of the roof diaphragm and the P-Δ stability of the tilt-up wall panels when subject to the diaphragm deflection.

With respect to drift, it is noted that per ASCE/SEI 7-22 Section 12.12.1, the design story drift will need to be checked against the allowable story drift unless the building can be exempted under Table 12.12.-1 Footnote c. Further, per ASCE/SEI 7-22 Section 12.8.6.3, the deflection of the diaphragm will need to be included in the design story drift. See Section 7.1 and 7.2.1 discussion. Note that for the alternative RWFD diaphragm design method, $C_{s\text{-}diaph}$ is be used in place of C_d for amplification of design diaphragm deflections.

7.6.3 Example: One-Story Bare Steel Deck Diaphragm Building Diaphragm Design – ASCE/SEI 7-22 Section 12.10.4 Alternative Design Method with Diaphragm NOT Meeting AISI S400 Special Seismic Detailing Provisions

This example building has a bare steel deck diaphragm that is welded instead of using mechanical fasteners. Because of this, the diaphragm does not meet the requirements of AISI S400 Section F3.5.1, and so it does not qualify as meeting special seismic detailing requirements.

Step 1 - Check ASCE/SEI 7-22 Section 12.10.4.1 Scoping Limitations

These scoping limitations were checked in Section 7.6.2. The building conforms with all scoping limitations and is eligible to use the ASCE/SEI 7-22 Section 12.10.4 procedure.

Step 2 - Divide Diaphragm Into Rectangular Sections

Break roof diaphragm into a series of rectangular segments for purposes of design, with each segment spanning to vertical elements or a collector.

Because the example building is rectangular in plan and shear walls are located at the building perimeter, one rectangular segment extending for the full building plan will be used.

Step 3 - Determine w_{px}.

W_{px} was determined in Example Section 7.7.1 to be:

6,846 kips (transverse forces)

5,836 kips (longitudinal forces)

Step 4 - Determine R_{diaph}

R_{diaph} = 1.5 for bare steel deck diaphragms not meeting the special seismic detailing requirements for AISI S400

Step 5 - Determine T_{diaph}

$T_{diaph} = 0.001L_f$ for bare steel deck diaphragms (ASCE/SEI 7-22 Section 12.10.4.2.1)

where

T_{diaph} = Period of diaphragm for design of diaphragm using the alternative diaphragm design method of Section 12.10.4 (seconds), and

L_{diaph} = Span in feet of the horizontal diaphragm or diaphragm segment being considered, measured between vertical elements or collectors that provide support to the diaphragm or diaphragm segment.

T_{diaph} = 0.001 s/ft (600 ft) = 0.60 s (transverse forces)

T_{diaph}= 0.001 s/ft (360 ft) = 0.36 s (longitudinal forces)

Step 6 - Determine $C_{s\text{-}diaph}$

For transverse forces:

$$C_{s-diaph} = \frac{S_{DS}}{R_{diaph}/I_e} = \frac{1.0}{1.5/1.0} = 0.667$$ (ASCE/SEI 7-22Eq. 12.10-16a)

But need not exceed

$$C_{s-diaph} = \frac{S_{D1}}{T_{diaph}(R_{diaph})/I_e} = \frac{0.50}{0.60(1.5)/1.0} = 0.555$$ (ASCE/SEI 7-22 Eq. 12.10-16b)

Use $C_{s\text{-}diaph}$ = 0.555 transverse

For longitudinal forces:

$$C_{s-diaph} = \frac{S_{DS}}{R_{diaph}/I_e} = \frac{1.0}{1.5/1.0} = 0.667$$ (ASCE/SEI 7-22 Eq. 12.10-16a)

But need not exceed:

$$C_{s-diaph} = \frac{S_{D1}}{T_{diaph}(R_{diaph})/I_e} = \frac{0.50}{0.36(1.5)/1.0} = 0.926$$ (ASCE/SEI 7-22 Eq. 12.10-16b)

Use $C_{s\text{-}diaph}$ = 0.667 longitudinal

Step 7 - Determine Diaphragm Design Force, F_{px}

$F_{px} = C_{s\text{-}diaph}\,(w_{px})$ (ASCE/SEI 7-22 Eq. 12.10-15)

F_{px} = 0.555 (6,846) = 3,800 kips transverse

F_{px} = 0.667 (5,836) = 3,893 kips longitudinal

Step 8 - Determine Amplified Shear and Extent of Amplified Shear Boundary Zone

Because the diaphragm span in both directions is greater than 100 ft., an amplified shear zone will be located at each end of the diaphragm span and extend for ten percent of the diaphragm span. The extent of the amplified shear zones are:

0.10 (600 ft) = 60 ft each end for transverse forces

0.10 (360 ft) = 36 ft each end for longitudinal forces.

See Figure 7-14 for illustration of the amplified shear zones.

Step 9 - Diaphragm Design for Shear and Flexure

Diaphragm Design for Shear

The diaphragm is designed for shear using F_{px} Forces. The following illustrates shear calculations for the transverse direction.

For transverse roof diaphragm forces:

w = 3,800 kips / 600 ft = 6.33 klf

V = 6.33 klf (600 ft / 2) = 1,899 kips

v = 1,899 kips / 360 ft = 5.28 klf maximum at end of diaphragm span WITHOUT shear amplification

v = 5.28 klf (1.5) = 7.92 klf maximum at end of diaphragm span WITH shear amplification

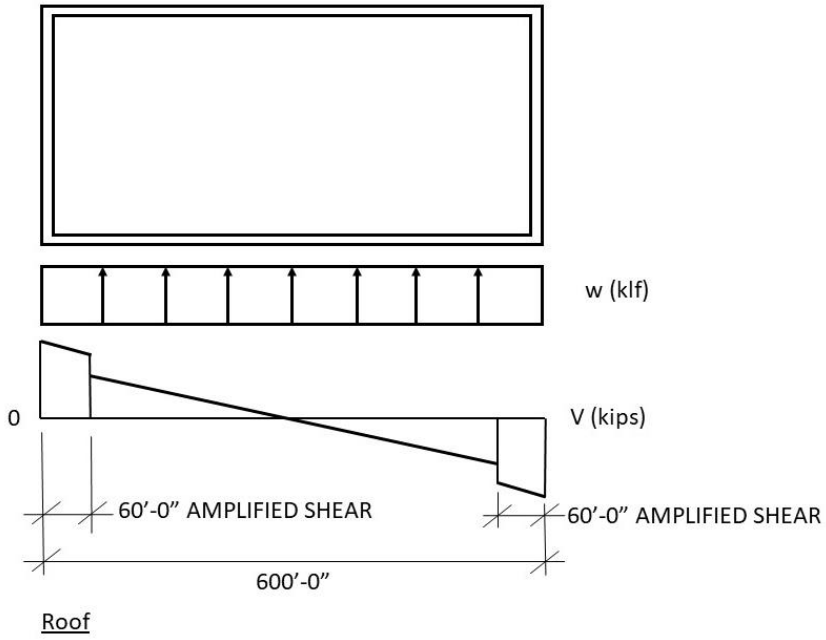

Figure 7-17. Plan Showing Uniform Seismic Forces and Diaphragm Shears in the Transverse Direction, Including Amplified Shear Zone

Diaphragm Design for Flexure

For transverse roof diaphragm forces the chord force is calculated using F_{px} forces WITHOUT amplification:

w = 3,800 kips / 600 ft = 6.33 klf

M = 6.33 klf $(600 \text{ ft})^2$ / 8 = 284,850 kip-ft

Chord T/C = 284,850 kip-ft / 360 ft = 791 kips maximum at diaphragm mid-span

Step 10 - Collectors and Their Connections to Vertical Elements

Determine collector forces in accordance with ASCE/SEI 7-22 Section 12.10.4.2.4. Collector forces are to be based on F_{px} forces WITHOUT the 1.5 shear amplification factor, multiplied by $\Omega_{0\text{-diaph}}$., however $\Omega_{0\text{-diaph}}$ need not be taken as greater than R_{diaph}.

The following illustrates a calculation of collector seismic forces.

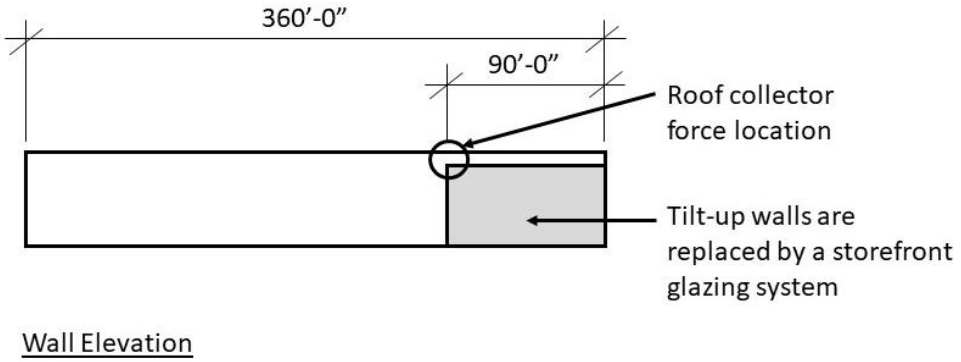

Figure 7-18. Example Building Elevation Showing Collector Force Location

Per ASCE/SEI 7-22 Section 12.10.4.2.4, the collector force is calculated based on the maximum transverse diaphragm shear WITHOUT amplification, multiplied by $\Omega_{0\text{-diaph}}$, however $\Omega_{0\text{-diaph}}$ need not be taken as greater than R_{diaph} = 1.5.

T/C = 5.28 klf (90 ft) (1.5) = 713 kips

Steps 11 and 12 - Check applicable ASCE/SEI 7-22 deflection and drift limitations.

Where required by ASCE/SEI 7-22, determine $C_{d\text{-}diaph}$ and diaphragm deflections in accordance with ASCE/SEI 7-22 Section 12.10.4.2.5. All applicable ASCE/SEI 7-22 deflection and drift checks are to be completed. It is important that this include a check that the gravity system can accommodate the mid-span deflection of the roof diaphragm and the P-Δ stability of the tilt-up wall panels when subject to the diaphragm deflection.

With respect to drift, it is noted that per ASCE/SEI 7-22 Section 12.12.1, the design story drift will need to be checked against the allowable story drift unless the building can be exempted under Table 12.12.-1 Footnote c. Further, per ASCE/SEI 7-22 Section 12.8.6.3, the deflection of the diaphragm will need to be included in the design story drift. See Section 7.1 and 7.2.1 discussion. Note that for the alternative RWFD diaphragm design method, $C_{s\text{-}diaph}$ is be used in place of C_d for amplification of design diaphragm deflections.

7.6.4 Comparison of Diaphragm Design Forces for Traditional and Alternative RWFD Provisions

Table 7-15 provides a comparison of Fpx diaphragm design forces and design shears for the traditional and alternative RWFD diaphragm design procedures.

Table 7-15. One-Story RWFD Building Comparison of F_{px} Forces and Diaphragm Shears for Traditional and Alternative RWFD Design Provisions

Diaphragm Design Method	*Transverse*			*Longitudinal*		
	F_{px} (kips)	v_{px} (plf)	v_{px} *amplified shear zone* (plf)	F_{px} (kips)	v_{px} (plf)	v_{px} *amplified shear zone* (plf)
Traditional ASCE/SEI 7-22 Section 12.10.1 and 12.10.2	1,712	2,370	NA	1,459	1,220	NA
Alternative RWFD ASCE/SEI 7-22 Section 12.10.4 with Special Seismic Detailing	1,266	1,760	2,640	1,296	1,080	1,620
Alternative RWFD ASCE/SEI 7-22 Section 12.10.4 without Special Seismic Detailing	3,800	5,280	7,920	3,893	3,240	4,870

Table 7-16 provides a comparison of diaphragm chord and collector forces for the traditional and alternative RWFD diaphragm design procedures.

Table 7-16. One-Story RWFD Building Comparison of Collector Forces for Traditional and Alternative RWFD Design Provisions

Diaphragm Design Method	*Chord Force T/C (kips)*	*Collector Force T/C (kips)*
Traditional ASCE/SEI 7-22 Section 12.10.1 and 12.10.2	356	533
Alternative RWFD ASCE/SEI 7-22 Section 12.10.4 with Special Seismic Detailing	264	317
Alternative RWFD ASCE/SEI 7-22 Section 12.10.4 without Special Seismic Detailing	791	713

From the tabulated values, it can be observed that using the alternative RWFD procedure in combination with bare steel deck diaphragms meeting special seismic detailing requirements results in a reduction of diaphragm design forces.

7.7 References

See "Useful Design Aid Resources" in Section 7.1 above for additional references.

ACI (2018a). *Qualification of Precast Concrete Diaphragm Connections and Reinforcement at Joints for Earthquake Loading and Commentary,* ACI 550.4-18, American Concrete Institute, Farmington Hills, MI.

ACI (2018b). *Code Requirements for the Design of Precast Concrete Diaphragms for Earthquake Motions and Commentary*, ACI 550.5-18 and ACI 550.5R, American Concrete Institute, Farmington Hills, MI.

ASCE (2017). *Minimum Design Loads and Associated Criteria for Buildings and Other Structures,* ASCE/SEI 7-16, Structural Engineering Institute of the American Society of Civil Engineers, Reston, VA.

ASCE (2021). ASCE 7-22: *Minimum Design Loads and Associated Criteria for Buildings and Other Structures,* public comment draft, Structural Engineering Institute of the American Society of Civil Engineers, Reston, VA, June 17.

FEMA (2015). *NEHRP Recommended Seismic Provisions for New Buildings and Other Structures*, Volume I: Part 1 Provisions, Part 2 Commentary, FEMA P-1050-1 Report, 2015 Edition, prepared by the Building Seismic Safety Council for the Federal Emergency Management Agency, Washington, D.C., September.

FEMA (2016). 2015 *NEHRP Recommended Seismic Provisions: Training and Educational Materials*, FEMA P-1052 Report, prepared by the Building Seismic Safety Council for the Federal Emergency Management Agency, Washington, D.C.

FEMA (2020). *NEHRP Recommended Seismic Provisions for New Buildings and Other Structures*, Volume I: Part 1 Provisions, Part 2 Commentary, FEMA P-2082-1 Report, prepared by the Building Seismic Safety Council for the Federal Emergency Management Agency, Washington, D.C., September.

Chapter 8: Nonstructural Components

Bret Lizundia[1] and Jorge Moreno[2]

8.1 Overview

Chapter 13 of ASCE/SEI 7-22 (ASCE, 2021) addresses seismic design of the architectural, mechanical, and electrical components in buildings. Chapter 13 was significantly revised for ASCE/SEI 7-22, with new equations governing the forces that are used for nonstructural design. This chapter contains a series of design examples to illustrate many of the requirements and procedures.

- Section 8.2 reviews the development and basis of the revised equations.
- Section 8.3 covers component design and anchorage for exterior precast concrete cladding, including spandrel and column cover design and their attachment to the primary structure, and how seismic interstory drift is accommodated.
- Section 8.4 addresses seismic design and anchorage of egress stairs, including requirements for design forces and for seismic interstory drift.
- Section 8.5 illustrates anchorage for seismic forces for a roof-mounted HVAC unit. The rooftop unit is examined for two common installations: directly attached to the structure and a vibration-isolated component installed with snubbers.
- Section 8.6 shows how to treat non-ASME piping, and its associated distribution system supports located within a healthcare facility.
- Section 8.7 covers a platform-supported vessel located on an upper floor within a building.

The variety of materials and industries involved with nonstructural components is large, and numerous documents define and describe methods of design, construction, manufacture, installation, attachment, etc. Some of the documents address seismic issues, but many do not. ASCE/SEI 7-22 Chapter 23 contains a listing of approved standards for various nonstructural components.

In addition to the 2020 *NEHRP Provisions* (FEMA, 2020) and ASCE/SEI 7-22, the following documents are either referred to directly in the design examples or may serve as useful design aids.

[1] Bret Lizundia, S.E., Rutherford + Chekene
[2] Jorge Moreno, P.E., Rutherford + Chekene

Useful Design Aid Resources

ACI (2019). *Building Code Requirements for Structural Concrete and Commentary*, ACI 318-19, American Concrete Institute, Farmington Hills, Michigan.

ACI (2019). *Qualification of Post-Installed Mechanical Anchors in Concrete and Commentary*, ACI 355.2-19, American Concrete Institute.

ANSI/AISC (2016a). *Seismic Provisions for Structural Steel Buildings,* ANSI/AISC 341-16 American Institute of Steel Construction.

ANSI/AISC (2016b). *Specification for Structural Steel Buildings*, ANSI/AISC 360-16, American Institute of Steel Construction.

ANSI/AISC (2022a). *Seismic Provisions for Structural Steel Buildings,* ANSI/AISC 341-22 American Institute of Steel Construction, in press.

ANSI/AISC (2022b). *Specification for Structural Steel Buildings*, ANSI/AISC 360-22, American Institute of Steel Construction, in press.

ASHRAE (2019). *2019 ASHRAE Handbook - HVAC Applications,* "Chapter 56 Seismic and Wind Restraint Design," ASHRAE A56, American Society of Heating, Refrigeration and Air-Conditioning Engineers.

ASME (2018). *Power Piping*, ASME B31.1, American Society of Mechanical Engineers.

ASME (2018). *Process Piping*, ASME B31.3, American Society of Mechanical Engineers.

ASME (2010). *Transportation Systems for Liquid Hydrocarbons and Other Liquids, Pipeline*, ASME B31.4, American Society of Mechanical Engineers.

ASME (2019). *Refrigeration Piping and Heat Transfer Components*, ASME B31.5, American Society of Mechanical Engineers.

PCI (2007). *Architectural Precast Concrete Manual*, Report MNL-122, Precast/Prestressed Concrete Institute, Chicago, IL.

TMS (2016). *Building Code Requirements for Masonry Structures*, TMS 402, The Masonry Society.

8.2 Development and Background of the Requirements for Nonstructural Components

8.2.1 Approach to and Performance Objectives for Seismic Design of Nonstructural Components

Nonstructural components include architectural components, mechanical, and electrical equipment, and distribution systems such as piping, ducts, and electrical raceways. These items make up the majority of the replacement value of most buildings. ASCE/SEI 7-22 requires that nonstructural components be checked for two fundamentally different demands placed upon them by the response of the structure to earthquake ground motion:

- Resistance to inertial forces, referred to as seismic forces, and
- Accommodation of imposed displacements due to interstory drift of the structure or differential displacements for components spanning between structures.

For seismic design, nonstructural components are grouped in broad categories based on their function and behavior under seismic loading. Requirements vary with the ground motion intensity. Components serving essential functions are subject to more stringent requirements.

Specific performance goals for nonstructural components are not explicitly defined, although the ASCE/SEI 7-22 Commentary Section C13.1.3 provides expectations of the anticipated behavior of noncritical components in three levels of earthquake shaking intensity:

1. *Minor earthquake ground motions—minimal damage; not likely to affect functionality;*
2. *Moderate earthquake ground motions—some damage that may affect functionality; and*
3. *Design Earthquake ground motions—major damage but significant falling hazards are avoided; likely loss of functionality.*

While the nonstructural design provisions focus on reducing the risk to life safety, in some cases, the provisions protect functionality and limit economic losses. For example, noncritical equipment units in mechanical rooms that are unlikely to topple in an earthquake still require anchorage, although they pose minimal risk to life safety. The flexible connections between unbraced piping and noncritical equipment are required but serve mainly to reduce the likelihood of leakage.

Seismic forces for design are computed, considering variation of acceleration with relative height within the structure, the influence of the seismic force-resisting system of the supporting structure, and reduction in design force based upon estimated ductility of the component or its attachment. ASCE/SEI 7-22 also includes procedures for evaluating nonstructural components subject to imposed deformations, such as story drift. The seismic force demands tend to control the design for vibration-isolated or heavy components, while the imposed deformations are important for the seismic design of elements that are continuous through multiple levels of a structure or across expansion joints between adjacent structures, such as cladding or piping.

Chapter 13 of ASCE/SEI 7-22 is organized into six major sections.

- Section 13.1 provides information on the applicability of the nonstructural design provisions.
- Section 13.2 includes general information, with guidance on determining the importance of the component or system, methods for establishing the adequacy of the component for seismic forces, and certification requirements for items identified as critical to life safety or, in essential facilities, items critical to continued function following an earthquake.
- Section 13.3 contains the procedures for determining the acceleration and displacement demands on nonstructural components.
- Section 13.4 covers design considerations for attachment of nonstructural components to the structure.
- Section 13.5 provides detailed design considerations for architectural components.
- Section 13.6 provides detailed design considerations for mechanical and electrical components.

The remaining portions of this section describe the equations used for nonstructural design and their development. Significant changes were made to equations in ASCE/SEI 7-22. The equations are first summarized in Section 8.2.2; then, their development is described in Section 8.2.3.

8.2.2 Force Equations

The following seismic force equations are prescribed for nonstructural components:

$$F_p = 0.4 S_{DS} I_p W_p \left[\frac{H_f}{R_\mu}\right] \left[\frac{C_{AR}}{R_{po}}\right] \qquad \text{(ASCE/SEI 7-22 Eq. 13.3-1)}$$

$$F_{p,max} = 1.6 S_{DS} I_p W_p \qquad \text{(ASCE/SEI 7-22 Eq. 13.3-2)}$$

$$F_{p,min} = 0.3 S_{DS} I_p W_p \qquad \text{(ASCE/SEI 7-22 Eq. 13.3-3)}$$

where:

F_p = horizontal equivalent static seismic design force centered at the component's center of gravity and distributed relative to the component's mass distribution

S_{DS} = five percent damped spectral response acceleration parameter at short period as defined in ASCE/SEI 7-22 Section 11.4.4

I_p = Component Importance Factor (either 1.0 or 1.5) as indicated in ASCE/SEI 7-22 Section 13.1.3

W_p = component operating weight

H_f = factor for force amplification as a function of height in the structure as determined by ASCE/SEI 7-22 Section 13.3.1.1

R_μ = structure ductility reduction factor as determined by ASCE/SEI 7-22 Section 13.3.1.2

C_{AR} = component resonance ductility factor that converts peak floor or ground acceleration into the peak component acceleration as determined by ASCE/SEI 7-22 Section 13.3.1.3

R_{po} = component strength factor as determined by ASCE/SEI 7-22 Section 13.3.1.4

The seismic design force, F_p, is to be applied independently in the longitudinal and transverse directions. F_p should be applied in both the positive and negative directions if higher demands will result. Per ASCE/SEI 7-22 Section 13.3.1, the directions of F_p used shall be those that produce the most critical load effects on the component, the component supports, and attachments. Alternatively, it is permitted to use the more severe of the following two load cases:

- Case 1: A combination of 100% of F_p in any one horizontal direction and 30% of F_p in a perpendicular horizontal direction applied simultaneously.
- Case 2: The combination from Case 1 rotated 90 degrees.

ASCE/SEI 7-22 Equations 13.3-2 and 13.3-3 provide maximum and minimum limits for the seismic design. The effects of seismic loads on the component are combined with the effects of dead, live, and operating loads.

Many nonstructural components are attached to the structure at different heights in the structure, such as pipe risers and many curtain wall systems. When this condition occurs, a force, F_p, should be determined based on ASCE/SEI 7-22 Equation 13.3-1 for each point of attachment. The minima and maxima determined from ASCE/SEI 7-22 Equations 13.3-2 and 13.3-3 must be considered in determining each F_p. The weight, W_p, used to determine each F_p should be based on the tributary weight of the component associated with the point of attachment. When designing the component, the attachment force, F_p, should be distributed relative to the component's mass distribution over the area used to establish the tributary weight. With the exception of structural walls and anchorage of concrete or masonry structural walls, which are covered by ASCE/SEI 7-22 Chapter 12, each anchorage force should be based on simple statics determined by using all the distributed loads applied to the complete component. Cantilever parapets that are part of a continuous element should be checked separately for parapet forces.

8.2.3 Development of Nonstructural Seismic Design Force Equations in ASCE/SEI 7-22

In ASCE/SEI 7-22, significant revisions have been made to the nonstructural seismic design force equations. They are based on the proposed equations and underlying research in the Applied Technology Council ATC-120 project that resulted in NIST GCR 18-917-43 *Recommendations for*

Improved Seismic Performance of Nonstructural Components (NIST, 2018). Lizundia (2019) summarizes the initial development in NIST (2018) and the revisions in the 2020 *NEHRP Provisions*. Section C13.3.1 commentary on ASCE/SEI 7-22 also provides a comprehensive summary of the issues and resulting ASCE/SEI 7-22 provisions. The following discussion is taken from or paraphrased from these sources.

8.2.3.1 NIST GCR 18-917 43

The ATC-120 effort took a broad but detailed look at nonstructural design and developed many recommendations. One of the key goals of the ATC-120 effort was to develop nonstructural seismic design force equations that have a more rigorous scientific basis and capture the key parameters that can affect nonstructural component response and yet remain appropriate for use in design by practicing engineers.

The ATC-120 project team reviewed the available literature, identified key parameters of interest, assessed the influence of these parameters individually on component response, focused on parameters shown to strongly affect response, and then tested a set of equations combining all the selected parameters of interest using an extensive set of nonlinear analyses of archetype buildings and components as well as analysis of strong motion records from instrumented buildings. Chapter 4 and Appendices B and C of NIST (2018) summarize the literature review, analysis approach and findings, and resulting equations.

The parameters that were investigated include ground shaking intensity, seismic force-resisting system of the building, building modal period, building ductility, inherent building damping, building configuration, floor diaphragm rigidity, vertical location of the component within the building, component period, component and/or anchorage ductility, inherent component damping, and component overstrength. Parameters selected for inclusion in the final set of equations include all of the above except inherent building damping, building configuration, and floor diaphragm rigidity. Inherent building damping was found to have a relatively small effect on component response. Building configuration and floor diaphragm rigidity can have a significant effect on component response, but, given the complexity of the issues involved and desire to keep code equations practical, building configuration and diaphragm rigidity were not included in final set of equations.

Using the above selected parameters, the proposed equations in NIST (2018) and in ASCE/SEI 7-22 Section 13.3.1 include a set of key features. These include:

- Ratio of Peak Floor Acceleration (PFA) to Peak Ground Acceleration (PGA): Based on a detailed review of instrumented building strong motion records, a more refined equation was developed to relate PFA to PGA at different heights in the building. The equation incorporates building period. This is accounted for in the variable H_f of Equation 13.3-1. It replaces the [1 + 2 (z/h)] portion of the F_p equation in ASCE/SEI 7-16.

- Building ductility: Increased building ductility has been shown to generally reduce nonstructural component response. This is captured by the variable R_u. The equation for determining R_u is based on a series of archetype case studies using different seismic force-resisting systems,

numbers of stories, and overstrength assumptions. Building ductility was not included in the F_p equation in ASCE/SEI 7-16.

- Ratio of Peak Component Acceleration (PCA) to Peak Floor Acceleration (PFA): In ASCE/SEI 7-16, the effect of PCA amplification over PFA was coarsely addressed in a binary fashion in the a_p factor where components either have no amplification with a_p =1.0 or significant dynamic amplification of a_p =2.5. A more refined approach to PCA/PFA amplification has been incorporated into ASCE/SEI 7-22.

- The relationship between PCA and PFA, defined as C_{AR} in Equation 13.3-1, is affected by several parameters including the ratio of component period to building period and component ductility. When component and building periods are close, component response is increased due to resonance; when component ductility is larger, component response decreases. These effects are captured by two concepts in the equation framework. The first is whether component response is likely or unlikely to be in resonance with the building response. When the ratio of component period to building period is relatively small or relatively large, resonance is unlikely, and C_{AR} is set to 1.0. When the ratio is closer to unity, resonance is likely, and C_{AR} is amplified to account for resonance. The second concept is to create low, moderate, or high component ductility categories for situations with likely resonance. C_{AR} values for low ductility are higher than those for high ductility. The selected C_{AR} values are based on archetype studies and account for some level of reduction from the theoretical peak value to address the probability of overlap between component and building periods.

- Ground vs. Superstructure: The amplification of PCA/PFA as the ratio of component to building period approaches unity comes from narrow band filtering of response by the dynamic properties of the building. Components that are ground supported can see dynamic amplification due to component flexibility, based on structural dynamics, but this amplification is typically less than what occurs in the building. Given that there are both theoretical and numerical differences between the ground and superstructure cases, it was decided to distinguish the two.

- Component Strength: Like building structural systems, the component and its attachments to the structure typically have some inherent overstrength. This is captured by the variable R_{po}. Since it is in the denominator of the F_p equation, it serves to reduce the design force needed.

- Architectural component categories: Revisions were proposed to the ASCE/SEI 7-16 Table 13.5-1 architectural component categories. These included:

    - “Plain (unreinforced) masonry walls” were removed as a category for interior nonstructural walls and partitions to disincentivize their use due to obvious concerns regarding life-safety protection. The revision does not expressly prohibit the unreinforced masonry walls, as they fall under the “all other wall and partitions” category. However, the reader should be aware that TMS 402-16 requires reinforcement for partition walls (called “nonparticipating elements” by TMS) in Seismic Design Categories (SDC) C, D, E, and F. Minimum detailing requirements are more stringent with the higher SDC. Also, as seismic requirements

increase, partition wall design will likely be controlled by seismic demands on nonstructural components rather than the minimum partition 5 psf (at allowable stress design levels) that is required by the International Building Code (ICC, 2020).

- Interior nonstructural walls and partitions were subdivided into shorter light frame (less than or equal to 9 ft in height), taller light frame (over 9 ft in height), reinforced masonry, and all other walls and partitions. Taller light frame partitions were considered to have the potential for PCA/PFA amplification, but shorter light frame and reinforced masonry partitions are stiffer and were assigned a C_{AR} value of 1.0.

- Cabinets were separated into out-of-plane in their narrow direction where amplified response is more likely and in-plane in their longer direction where amplified response is less likely. This recommended change did not get incorporated in subsequent developments.

- Equipment support structures and platforms: A two-stage analysis was developed, where the component is designed based on parameters associated with its properties, and the supporting structure or platform similarly is designed with parameters associated with the properties of the supporting structure or platform. The distinction addresses the dissimilarities between the components and the equipment support structures. In ASCE/SEI 7-16, there were no restrictions on the nature of the equipment support structure. As an example, a nonstructural component governed by the minimum lateral force could be supported on a brittle support also designed for minimum lateral forces.

8.2.3.2 REVISIONS MADE IN THE 2020 *NEHRP PROVISIONS*

The NIST (2018) recommendations were used to develop code proposals for the 2020 *NEHRP Provisions*. During the code development process, revisions were made that include the following key issues.

- Terminology revision: The terminology used for the variables in NIST (2018) was shortened. For example, PGA was replaced with $0.4S_{DS}$, PFA/PGA became H_f, PCA/PFA was replaced with C_{AR}, R_{ubldg} became R_u, and R_{pocomp} was replaced with R_{po}.

- R_u clarification: For ground supported components, there is no building superstructure involved to modify response, so R_u was set to unity.

- Values for C_{AR}, R_{po}, and Ω_{0p}: Values of these parameters for different classes of components (resonance unlikely, and low-ductility, moderate-ductility, and high-ductility components with resonance likely) were determined using the principles from NIST (2018).

- Assignment of components to ductility and likelihood of resonance categories: Engineering judgment was used (1) to assign components in ASCE/SEI 7-22 Table 13.5-1 and Table 13.6-1 as to whether the components are likely or unlikely to be in resonance and, (2) if the components are likely to be in resonance, to assign the appropriate ductility category and the resulting C_{AR}

value. The component properties in ASCE/SEI 7-16 were used as the starting basis for assignment of components to ductility and likelihood of resonance categories.

- Revisions in the Table 13.6-1 categories: Elevators and escalators were separated into two categories due to differences in component dynamic response, detailing, and ductility.

- R_{po} refinement: NIST (2018) has a placeholder value of R_{po} = 1.3 for all components. The consensus of code writers for the 2020 *NEHRP Provisions* was that a value of R_{po} = 1.5 was reasonable for most components. However, components deemed to have somewhat higher than typical overstrength were assigned higher R_{po} values in Table 13.5-1 and Table 13.6-1.

- Maximum (cap) value: In the NIST (2018) report, a default component strength factor of R_{po} =1.3 was used together with a cap of $2.0S_{DS}I_pW$. With the typical value of the component strength factor increased to R_{po} =1.5 noted above, the ASCE/SEI 7-16 cap of $1.6S_{DS}I_pW_p$ was found to be generally compatible with the analytical results, and it was thus the consensus of code writers to retain the cap of $1.6S_{DS}I_pW_p$ from ASCE/SEI 7-16 in the 2020 *NEHRP Provisions*.

- The overstrength factors for anchors in concrete and masonry, Ω_{0p}, were slightly revised for compatibility with the F_p equation. The revision provides a consistent basis for the factors – components presumed unlikely to be in resonance or posing high ductility are assigned larger Ω_{0p} values to provide higher anchor strength should some resonance occur.

- Equipment support: Equipment support conditions can have a significant impact on the response of the component itself. Furthermore, the structural properties of the equipment and equipment support structure may be completely different, making the design of the supports using coefficients of the equipment itself unconservative. Detailed provisions were added to address different types of support, including support structures and platforms, distribution system supports, and integral equipment supports. These are discussed in Section 8.2.11 of this chapter.

- Penthouses and rooftop structures: Provisions were added to clarify and improve requirements for the seismic design of penthouses and rooftop structures.

8.2.3.3 REVISIONS MADE FOR ASCE/SEI 7-22

The 2020 *NEHRP Provisions* were used to develop code proposals for ASCE/SEI 7-22. During the code development process, revisions were made that include the following key issues. Minor word changes are not listed here.

- Structure ductility reduction factor: The Seismic Importance Factor, I_e, was added to the denominator of ASCE/SEI 7-22 Equation 13.3-6. The Seismic Importance Factor, I_e, is prescribed in Section 11.5.1. The Seismic Importance Factor, I_e, accounts for the higher lateral strength required for Risk Category III and IV structures, which results in lower ductility demands in the Design Earthquake. Lower ductility demands increase the building response and associated component response.

- Direction of F_p: ASCE/SEI 7-22 Section 13.3.1 was revised to specify the directions of loading using F_p. It requires use of the direction that produces the most critical effects on the component, support, and attachments. Alternatively, it is permitted to use a combination of 100% of F_p in a horizontal direction and 30% of F_p in the perpendicular direction, and then flip the orientation.

- Values for architectural components in Table 13.5-1: Revisions were made to raise the values of Ω_{0p} from 1.5 to 2.0 for selected components including cantilever elements, exterior wall elements, veneer, ceilings, cabinets, and laboratory equipment. This increases the demands used in design and the level of conservatism for anchorage in concrete and masonry.

- Values for mechanical and electrical components in Table 13.6-1: Revisions were made to raise the values of Ω_{0p} from 1.5 and 1.75 to 2.0 for selected components. This increases the demands used in design and the level of conservatism for anchorage in concrete and masonry. The components include:

    - Wet-side HVACR, boilers, furnaces, atmospheric tanks and bins, chillers, water heaters, heat exchangers, evaporators, air separators, manufacturing or process equipment, and other mechanical components constructed of high-deformability materials

    - Engines, turbines, pumps, compressors, and pressure vessels not supported on skirts

    - Elevators and escalators

    - Generators, batteries, inverters, motors, transformers, and other electrical components constructed of sheet metal framing

    - Communication equipment, computers, instrumentation, and controls

    - Roof-mounted stacks, cooling and electrical towers laterally braced above their center of mass

    - Lighting fixtures

    - Other mechanical and electrical components

    - Support structures and platforms where $T_p/T_a<0.2$ or $T_p<0.6$

    - Several types of distribution system supports, including tension-only and cable bracing, cold-formed steel rigid bracing, hot-rolled steel bracing, and other rigid bracing

    - Duct systems, including in-line components, constructed of high- or limited-deformability materials with joints made by means other than welding or brazing

    - Electrical conduit, cable trays, and raceways

- Bus ducts
- Plumbing
- Pneumatic tube transport systems

- Values for piping systems in Table 13.6-1: Revisions were also made to raise both the value of R_{po} from 1.5 up to 3.0 and the value Ω_{0p} from 1.5 up to 2.0 for selected piping components. The values for R_{po} were raised for piping systems with proven performance, Higher over strengths are warranted for components that due to operational design considerations have substantial strength, such as brazed or welded piping systems and components whose required structural strength is not governed by seismic design requirements. In NIST (2018), demands on piping with R_p=4.5 and higher were increasing by a factor of 2 or more. For nonbuilding structures, demands were increasing by factors of 5. No new information was available to justify such increases. The increase in R_{po} reduces the design values substantially, but the increase in Ω_{0p} recovers some of the forces used for anchorage into concrete and masonry. These components include:
  - Piping in accordance with ASME B31 (2001, 2002, 2008, and 2010), including in-line components, with joints made by welding or brazing
  - Piping in accordance with ASME B31, including in-line components, constructed of high- or limited-deformability materials, with joints made by threading, bonding, compression couplings, or grooved couplings
  - Piping in accordance not in accordance with ASME B31, including in-line components, constructed of high-deformability materials, with joints made by welding or brazing
- Values for duct systems in Table 13.6-1: Similar to piping systems, revisions were made to raise the value of R_{po} from 1.5 to 2.0 for duct systems, including in-line components, constructed of high-deformability materials, with joints made by welding or brazing.

Ω_{0p} Revisions in ASCE/SEI 7 22

The overstrength component factor, Ω_{0p}, values were revised to be consistent for components likely and unlikely to be in resonance.

For components likely to be in resonance, Ω_{0p} increases as the assumed ductility of the component increases. This provides more ductile components higher levels of safety for component anchors in case the anticipated level of component ductility fails to materialize. The higher the level of expected ductility, the larger the value of Ω_{0p} is assigned. Low ductility components are assigned an Ω_{0p} = 1.5 since the increase in demands due to missing the expected level of ductility is limited.

For components unlikely to be in resonance, they were previously assigned the minimum Ω_{0p} = 1.5, even though resonance could occur, and the component response could be potentially higher. However, the ASCE/SEI 7-22 revision makes the Ω_{0p} consistent, as all components unlikely to be in resonance were assigned Ω_{0p} = 2.0.

- An additional consideration for the overstrength component factor is that higher values were warranted for components that have substantial strength due to operational design considerations, such as brazed or welded piping systems, and components whose required structural strength is not governed by seismic design considerations. Design forces for elements in the load path with limited ductility: The ATC-120 project explored the viability of requiring ductile design for nonstructural components. While a noble goal, many practical challenges were found. However, concern remained about brittle elements being permitted in the load path from the nonstructural component to the primary structure. The following sentence based on the ATC-120 recommendations was placed in the ASCE/SEI 7-22 Commentary Section C13.3.1.

  Anchors in concrete or masonry that cannot develop a ductile yield mechanism are required to use design forces increased by the Ω_{0p} factor. Designers should consider amplifying design forces by an overstrength factor for elements in the load path between the component and the anchor that have limited ductility.

8.2.4 Load Combinations and Acceptance Criteria

The load combinations applicable to the nonstructural components chapter are now explicitly referenced in ASCE/SEI 7-22 Section 13.2.2:

> *Nonstructural components, including their supports and attachments, covered by this Chapter and not otherwise exempt by Section 13.1.8 shall comply with Section 1.3, including consideration of load combinations of either Section 2.3 or 2.4, as appropriate. For the purposes of combining load effects, F_p shall be used per Section 12.4.2.1 and horizontal seismic design forces including overstrength shall be used per Section 12.4.3.1.*

Earthquakes cause loads on structures and nonstructural components in both the horizontal and vertical directions. When these loads are applied to structural and nonstructural systems, the results (forces, stresses, displacements, etc.) are called “effects.” In ASCE/SEI 7-22 Section 12.4.2, seismic load effects are defined. The effects resulting from horizontally applied seismic loads are termed horizontal load effects, E_h, and the effects resulting from vertically applied seismic loads are termed vertical load effects, E_v. The E_v term is simply a constant $0.2S_{DS}$ multiplied by the dead load.

Strength design load combinations for use in determining the overall demand on an item are defined in ASCE/SEI 7-22 Section 2.3. Because the load combinations defined in ASCE/SEI 7-22 Section 2.3 provide a single term, E, to define the earthquake, ASCE/SEI 7-22 Section 12.4.2 separates the horizontal and vertical components of the seismic load. Unless otherwise noted in ASCE/SEI 7-22, the load combinations provided in ASCE/SEI 7-22 Section 12.4 are used for the seismic design of all structures and nonstructural components.

The horizontal seismic load effect, E_h, and vertical seismic load effect, E_v, are determined by applying the horizontal component load, F_p, and the vertical dead load, D, respectively, in the structural analysis as indicated below.

$E_h = \rho Q_E$ (ASCE/SEI 7-22 Eq. 12.4-3)

$E_v = 0.2 S_{DS} D$ (ASCE/SEI 7-22 Eq. 12.4-4a)

where:

Q_E = effect of horizontal seismic forces (due to application of F_p for nonstructural components) (ASCE/SEI 7-22 Sec. 12.4.2.1)

ρ = redundancy factor = 1.0 for nonstructural components (ASCE/SEI 7-22 Sec 13.3.1)

D = dead load effect (due to vertical load application)

Where the effects of vertical gravity loads and horizontal earthquake loads are additive:

$E = \rho Q_E + 0.2 S_{DS} D$

where:

E = effect of horizontal and vertical earthquake-induced forces

And where the effects of vertical gravity load counteract those of horizontal earthquake loads:

$E = \rho Q_E - 0.2 S_{DS} D$

Strength load combinations in ASCE/SEI 7-22 Sections 2.3 and 2.4 provide load combinations to determine design member forces, stresses, and displacements. In ASCE/SEI 7-22 Section 2.3, load combinations are provided for Strength Design, and in ASCE/SEI 7-22 Section 2.4, load combinations are provided for Allowable Stress Design. For purposes of the examples in this chapter, only the Strength Load Combinations are used.

The terms defined above are substituted for E in the Basic Load Combinations for Strength Design of ASCE/SEI 7-22 Section 2.3.6 to determine the design seismic loads. Once the substitutions have been made, the strength load combinations are presented in ASCE/SEI 7-22 Section 2.3.6:

$1.2D + E_v + E_h + L + 0.2S$ (ASCE/SEI 7-22 Basic Load Combination 6)

$0.9D - E_v + E_h$ (ASCE/SEI 7-22 Basic Load Combination 7)

For nonstructural components, the terms L and S are typically zero. For nonstructural components, load combinations with the overstrength factor are applicable only to the design of attachments to concrete and masonry and are discussed in Section 8.2.15 of this chapter – Component Anchorage Factors and Acceptance Criteria.

8.2.5 Component Importance Factor, I_p

The Component Importance Factor, I_p, is determined per ASCE/SEI 7-22 Section 13.1.3. It has a value of either 1.0 or 1.5, and it is applied to the force and displacement demands on the component. A Component Importance Factor of 1.5 is applied to components with greater life safety or hazard exposure importance. The Component Importance Factor of 1.5 is intended to improve the functionality of the component or structure by requiring design for a lesser amount of inelastic behavior and providing a larger capacity to accommodate seismically induced displacements. It is assumed that reducing the amount of inelastic behavior will result in a component that will have a higher likelihood of functioning after a major earthquake.

In accordance with ASCE/SEI 7-22, in Seismic Design Categories B and C, a Component Importance Factor, I_p, greater than 1.0 triggers seismic design for nonstructural components that are exempt when I_p =1.0.

8.2.6 Seismic Coefficient at Grade, $0.4S_{DS}$

The short-period design spectral acceleration, S_{DS}, considers the site seismicity and local soil conditions. S_{DS} is determined in accordance with ASCE/SEI 7-22 Section 11.4.4. The coefficient S_{DS} is used to design the structure. ASCE/SEI 7-22 approximates the effective peak ground acceleration as $0.4S_{DS}$, which is why 0.4 appears in ASCE/SEI 7-22 Equation 13.3-1.

8.2.7 Amplification with Height, H_f

The H_f term scales the seismic coefficient at grade to the peak floor acceleration, resulting in values varying from 1.0 at grade to up to 3.5 at the roof level. This factor approximates the dynamic amplification of ground acceleration by the supporting structure. As noted in Section 8.2.13, dynamic analysis procedures are provided that permit alternate methods for considering the effects of dynamic amplification of ground accelerations.

For nonstructural components supported at or below the grade plane, H_f = 1.0. For components supported above the grade plane by a building or nonbuilding structure, H_f is permitted to be determined by ASCE/SEI 7-22 Equation 13.3-4 or 13.3-5. Where the approximate fundamental period of the supporting building or nonbuilding structure is unknown, H_f *is* permitted to be determined by ASCE/SEI 7-22 Equation 13.3-5.

$$H_f = 1 + a_1\left(\frac{z}{h}\right) + a_2\left(\frac{z}{h}\right)^{10} \qquad \text{(ASCE/SEI 7-22 Eq. 13.3-4)}$$

$$H_f = 1 + 2.5\left(\frac{z}{h}\right) \qquad \text{(ASCE/SEI 7-22 Eq. 13.3-5)}$$

where:

$$a_1 = \frac{1}{T_a} \leq 2.5 \qquad \text{(ASCE/SEI 7-22 Sec. 13.3.1.1)}$$

$$a_2 = [1 - (0.4/T_a)^2] \geq 0 \qquad \text{(ASCE/SEI 7-22 Sec. 13.3.1.1)}$$

where:

z = height above the base of the structure to the point of attachment of the component. For items at or below the base, z shall be taken as 0. The value of $\frac{z}{h}$ need not exceed 1.0;

h = average roof height of structure with respect to the base; and

T_a = the lowest approximate fundamental period of the supporting building or nonbuilding structure in either orthogonal direction. For structures with combinations of seismic force-resisting systems, the seismic force-resisting system that produces the lowest value of T_a shall be used.

In ASCE/SEI 7-16, the variation with height was linear, using the relationship [1 + 2(z/h)]. The dynamic characteristics of the building, as reflected by building fundamental period, were not incorporated. Figure 8-1 shows the relationship between (z/h) and T_a on the amplification factor as a function of height in the structure, H_f. Shorter building periods have higher and more linear amplification. Longer building periods have lower amplification that is also more nonlinear. The H_f equation is based on both the recorded variation in PFA normalized by PGA in instrumented buildings and the mean (average) variation computed in simplified continuous models consisting of a flexural beam laterally coupled with a shear beam as adapted from Taghavi and Miranda (2006) and from Alonso-Rodríguez and Miranda (2016). Although the maximum value at the roof has increased from [1 + 2(z/h)] = [1+2(h/h)] = 3 in ASCE/SEI 7-16 to 3.5 in ASCE/SEI 7-22 for short period buildings, the values are lower in ASCE/SEI 7-22 in many other cases and other locations below the roof.

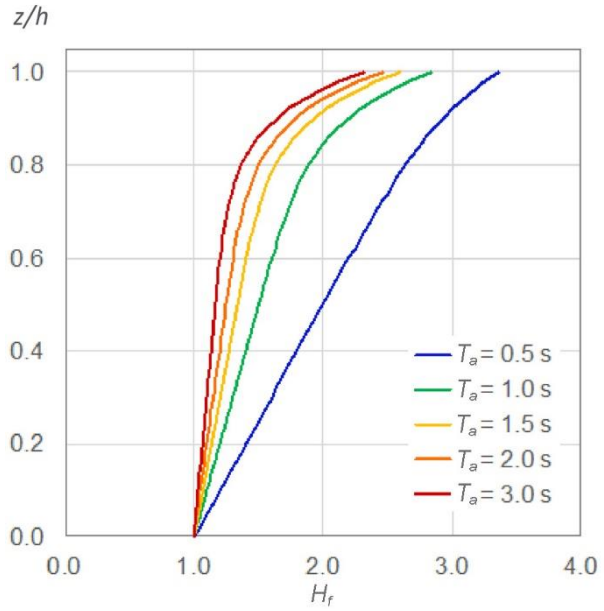

Figure 8-1. Five-story Building Elevation Showing Panel Location (adapted from NIST, 2018)

For buildings, for the purposes of computing H_f, T_a is determined using ASCE/SEI 7-22 Equation 12.8-7. Where the seismic force-resisting system is unknown, T_a *is* permitted to be determined by Equation 12.8-7 using the approximate period parameters for "All other structures."

For nonbuilding structures, T_a *is* permitted to be taken as any one of the following:

a. The period of the nonbuilding structure, T, determined using the structural properties and deformation characteristics of the resisting elements in a properly substantiated analysis as indicated in ASCE/SEI Section 12.8.2, or

b. The period of the nonbuilding structure, T, determined using ASCE/SEI Equation 15.4-6, or

c. The period T_a determined by ASCE/SEI Equation 12.8-7, using the approximate period parameters for "All other structures."

Rationale of Using T_a for Buildings as a Parameter to Calculate H_f

Based on the FEMA P-58/BD-3.7.17 report (FEMA, 2016), it was observed that the code estimated period, T_a, may underestimate the fundamental period of a structure, whereas the bare frame period, T tends to overestimate it.

In building structures, T_a was recommended by the ATC-120 project team to provide a reasonable estimate of the building fundamental period for the purposes of computing forces on nonstructural components. The gravity system, partitions, and cladding all act to reduce the fundamental period, which will increase the lateral force on nonstructural components.

For nonbuilding structures, the bare frame period T is permitted, as they generally lack partitions and cladding, and the gravity system is less extensive than that found in buildings. The bare frame period T is close to the actual period of the structure suitable for component lateral force calculations.

8.2.8 Structure Ductility Reduction Factor, R_μ

Building ductility has been shown to affect component response. Typically, PCA/PGA is larger when the building is elastic and lower when there is nonlinearity of the building. Studies show significant reduction in PCA/PFA with increasing levels of shaking, though PCA itself still increases with increasing levels of shaking. It can be difficult to separate building ductility from ground shaking intensity. The effect of building ductility is not only to reduce the PFA/PGA and PCA/PFA ratios. If an earthquake ground motion induces an inelastic response in the supporting structure, the floor spectral accelerations will saturate over a wider nonstructural period range because of the lengthening of the effective period of the supporting structure.

Determination of the structure ductility reduction factor, R_μ, relies on the R and Ω_0 values in ASCE/SEI 7-22 Table 12.2-1, Table 15.4-1, and Table 15.4-2, and the Seismic Importance Factor, I_e, as prescribed in ASCE/SEI Section 11.5.1. While these variables were not originally intended to be

used in the determination of lateral forces on nonstructural components, they provide a reasonable basis for estimating ductility and strength of building lateral force-resisting systems commonly used in Seismic Design Category D and higher. For nonbuilding structures, the tabulated values of R and Ω_0 were assigned on both technical considerations and to facilitate inclusion of low ductility systems into the building codes. In regions of high seismicity, the low values of R that are used, especially for nonbuilding structures not similar to buildings, do not reflect behaviors such as sliding and rocking that reduce floor accelerations in these structures. To reflect this, a lower limit of 1.3 is placed on the value of R_μ.

When determining the value of R_μ, several alternative situations can arise, including the following.

- If a seismic force-resisting system is not listed in these tables or the seismic force-resisting system does not conform to the associated requirements for the system, then use $R_\mu = 1.3$. This situation can apply to existing buildings with detailing provisions that do not meet current requirements and have less available ductility.

- If the seismic force-resisting system in which the component will be placed is not known, but it is known that it will be a system that complies with ASCE/SEI 7-22 Table 12.2-1, Table 15.4-1, or Table 15.4-2, then use the lowest value of R_u in the applicable table for the applicable Seismic Design Category. This situation can arise when the component anchorage and bracing are designed to be able to be installed in a range of potential code conforming buildings. It can also apply when the engineer responsible for anchorage and bracing of the component is told the component will be placed in a new building, but information about the building's seismic force-resisting system is not provided.

- If an alternative system has been developed with associated R and Ω_o values and approved by the Authority Having Jurisdiction, then use those values to determine R_μ.

- If the seismic force-resisting system category is known, but the details are unknown, such as it is known that the system for an office building is a braced frame but which type of braced frame system is not known, then use the braced frame system with the lowest value of R_u, which is the steel ordinary concentrically braced frame with $R_\mu=(1.1R/(I_e\Omega_o))^{1/2} = [(1.1)(3.25)/((1.0)(2.0)]^{1/2} = 1.3$.

- If nonlinear response history analysis is performed, then the procedure in Section 13.1.3.1.5 can be used, and R_u need not be calculated.

Increasing building ductility generally reduces nonstructural component seismic demands, and reduced ductility generally increases component demands. Buildings with higher design forces (such as those using a Seismic Importance Factor $I_e > 1.0$) and/or higher levels of overstrength will have less ductility demand for the same level of seismic shaking than those designed to code minimums and with limited overstrength. The ATC-120 project analyses included building archetypes with both limited overstrength and with substantial overstrength. Calibration studies were done to reasonably bound results from the archetypes with substantial overstrength.

8.2.9 Component Resonance Ductility Factor, C_{AR}

The component resonance ductility factor, C_{AR}, is the ratio of Peak Component Acceleration (PCA) to Peak Floor Acceleration (PFA). It is influenced by the relationship of the component period, T_{comp}, and the building period, T_{bldg}, and the component ductility.

8.2.9.1 COMPONENT PERIOD AND BUILDING PERIOD

Component period has been shown to have a significant effect on PCA/PFA response. Floor spectra are characterized by ordinates equal or approximately equal to the peak floor acceleration for frequencies larger than about 30 Hz and with large amplifications at frequencies near or equal to modal frequencies of the building. Nonstructural components with components periods longer than about two times the fundamental period of the building (although this rarely occurs) typically undergo accelerations smaller than the peak floor acceleration. Figure 8-2 shows some example spectra that illustrate the general shape and some of the variations of instrumentally recorded floor spectra.

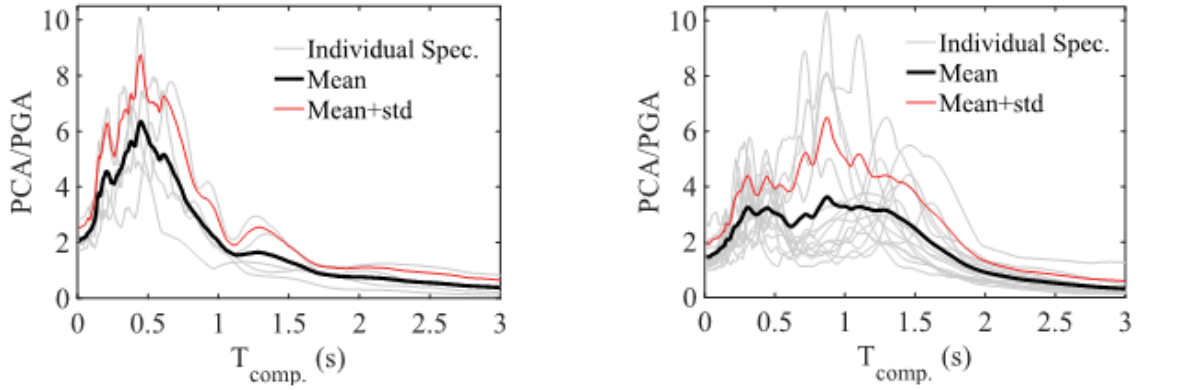

(a) normalized roof spectra for relatively stiff five-to-seven story buildings (a sample size of seven)

(b) normalized roof spectra for relatively flexible five-to-seven story buildings (a sample size of 24)

Figure 8-2. The Effect of Building Stiffness on PCA/PGA for Instrumental Recordings. An elastic component is assumed with inherent component damping, β_{comp} = 5%. The dataset includes 19 recordings with PGA > 0.15g. From NIST (2018) and Lizundia (2019).

In ASCE/SEI 7-16, the a_p factor was used, in part, to represent PCA/PFA. ASCE/SEI 7-16 Equation 13.3-1 simplified the a_p factor, such that it was equal to 1 for up to T_{comp} = 0.06 seconds and then jumps to 2.5 for T_{comp} > 0.06 seconds. Figure 8-3 compares the ASCE/SEI 7-16 formula with the maximum, mean plus one standard deviation, and mean for 3,743 floor acceleration histories (for an elastic component with 5% inherent component damping).

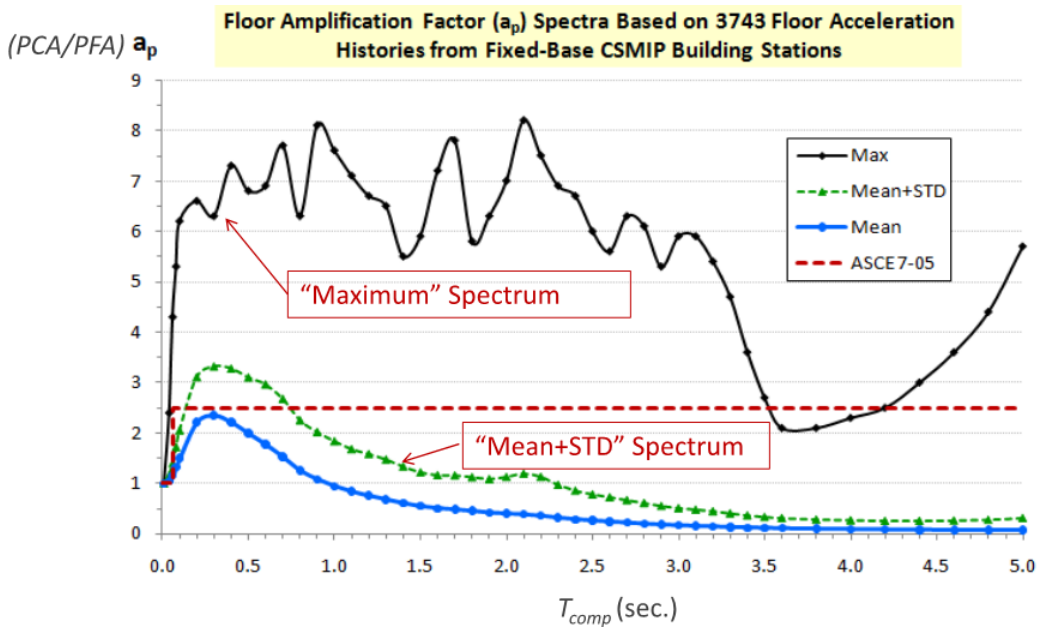

Figure 8-3. PCA/PFA Versus T_{comp} in Fathali and Lizundia (2011). An elastic component is assumed with inherent component damping, β_{comp} = 5%

It has also been shown that PCA/PFA rises significantly as T_{comp} and T_{bldg} approach resonance. Figure 8-4 illustrates the PCA/PFA amplification factor with the spectral ordinates of the average of eight different recorded motions based on T_{comp} and the same motions with the x-axis normalized to T_{comp}/T_{bldg}. These records come from eight different buildings and five different earthquakes and were selected from a suite of 86 records with 5% PCA values over 0.9g. The significant amplification of demand when the component period matches one of the building periods, typically referred to as resonance, was an important subject of investigation since the peak component accelerations can greatly exceed those typically used for design.

ASCE/SEI 7-16 Equation 13.3-1 did not explicitly include a factor for T_{comp}/T_{bldg}. In the ATC-120 project, it was decided to include the effect of resonance and the presentation approach of normalizing response against T_{comp}/T_{bldg} as the basis of the new nonstructural design equation.

For most nonstructural components, the component fundamental period, T_{comp}, can be obtained accurately only by expensive shake-table or pullback tests. As a result, the determination of a component's fundamental period by dynamic analysis, considering T_{comp}/T_{bldg} ratios, is not always practicable. Engineering judgment is needed.

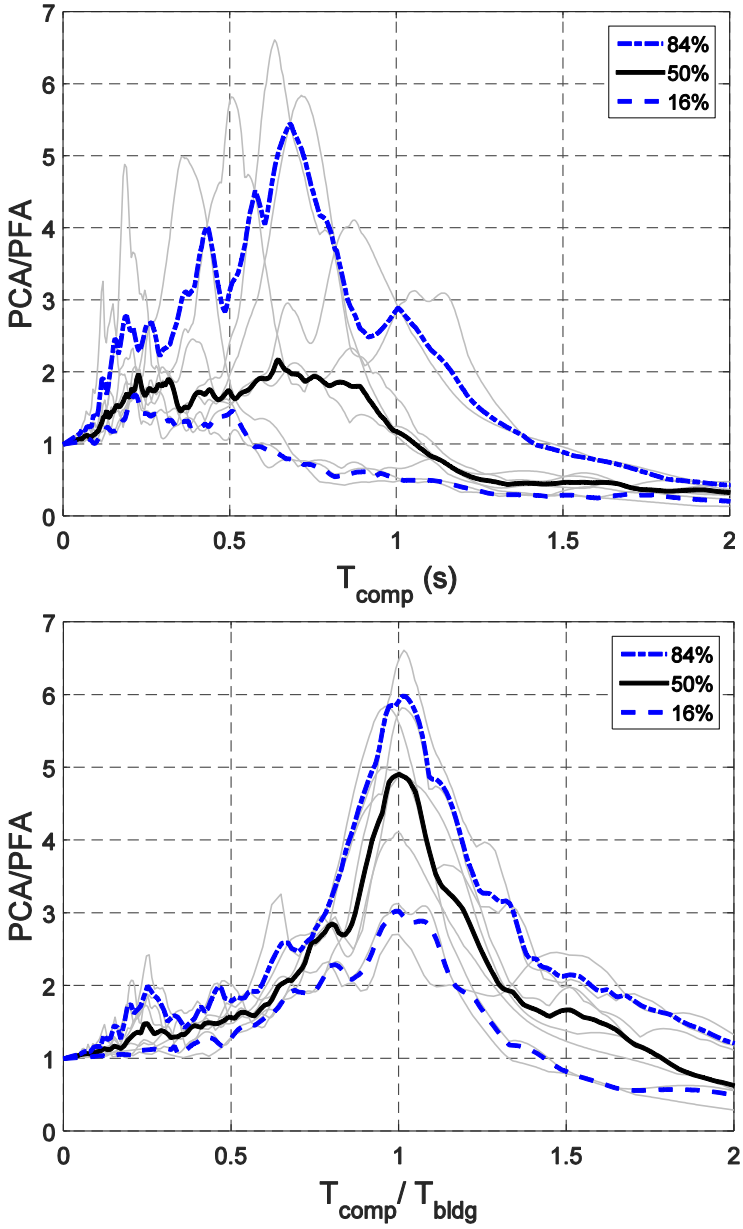

Figure 8-4. Relationship Between PCA/PFA Comparing Spectra Without (Top) and With (Bottom) Normalization by T_{bldg}. An elastic component is assumed with inherent component damping = 5%. The dataset includes eight recordings with PCA > 0.9g. From Kazantzi et al. (2018)

8.2.9.2 COMPONENT AND/OR ANCHORAGE DUCTILITY

ASCE/SEI 7-16 Equation 13.3-1 included the R_p factor, which indirectly accounted for reductions in response that component ductility can provide, but there was not an explicit link in the code between the R_p factor and component ductility, μ_{comp}.

There can be ductility in the component, the attachment of the component to the anchor, the anchor itself, or a combination of any of the items. Anchorage ductility is often difficult or impossible to achieve given practical considerations of available substrate depth for anchor. Project studies

lumped these three potential sources of component and anchorage ductility together into one simple model where the single-degree-of-freedom (SDOF) oscillator representing a component yields and then continues to deform, providing a measure of component ductility. Component ductility was found to have a significant effect.

Figure 8-5 overlays the mean response for each component ductility level for β_{comp} = 5%. For β_{comp} = 5% at T_{comp}/T_{bldg} = 1 resonance, PCA/PFA drops from about 4.6 for an elastic component, to about 2.8 for a component with a ductility, μ_{comp}, of 1.25, to about 2.0 for μ_{comp} = 1.5, then to about 1.4 for μ_{comp} = 2. Note that for these "constant component ductility" PCA/PFA spectra, the strength of the component is different for each level of μ_{comp} at each value of T_{comp}.

Given the significant effect of component and/or anchorage ductility on component response, it was decided in the ATC-120 project to explicitly incorporate this effect into the new nonstructural component design equation.

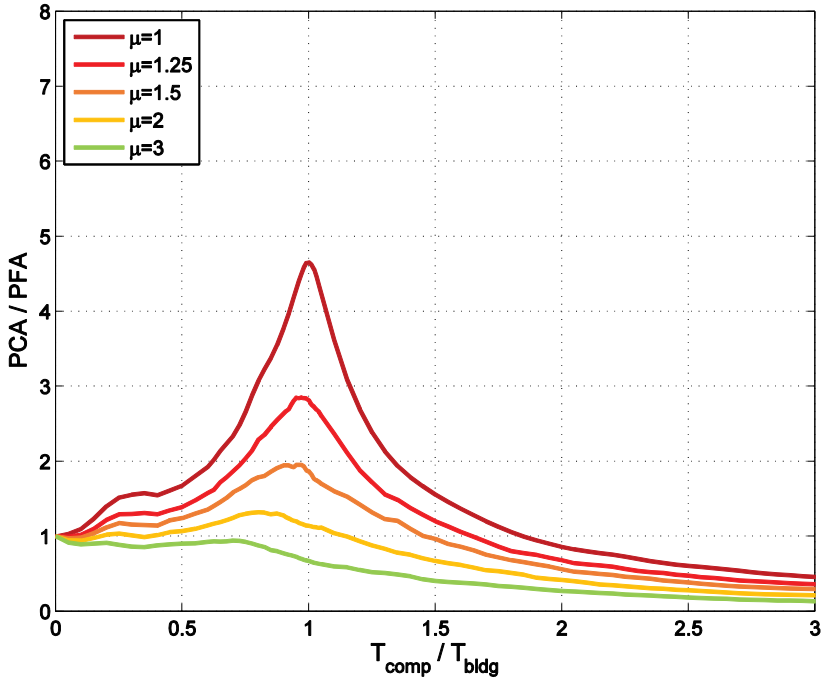

Figure 8-5. Comparison of Mean Response of PCA/PFA Versus T_{comp}/T_{bldg} for Different Levels of Component Ductility for β_{comp} = 5%. The dataset includes 86 recordings with PCA > 0.9g. From NIST (2018) and Lizundia (2019)

8.2.9.3 C_{AR} CATEGORIES

Table 8-1, taken from NIST (2018), shows the underlying relationships used in the ATC-120 project between the location of the component (at or below grade or in the superstructure), the likelihood of a component being in resonance (more likely or less likely), and the component ductility category (elastic, low, moderate, and high), and the PCA/PFA (or C_{AR}) categories.

Table 8-1. PCA/PFA Values

		Component Ductility		
Location of Component	**Possibility of Being in Resonance with Building**	**Category**	**Assumed Ductility**	$\left(\frac{PCA}{PFA}\right)$ (1)
Ground	More Likely	Elastic Low Moderate High	μ_{comp}=1 μ_{comp}=1.25 μ_{comp}=1.5 $\mu_{comp}\geq$2	2.5 2.0 1.8 1.4
	Less Likely	Any	-	1.0
Roof or Elevated Floor	More Likely	Elastic Low Moderate High	μ_{comp}=1 μ_{comp}=1.25 μ_{comp}=1.5 $\mu_{comp}\geq$2	4.0 2.8 2.2 1.4
	Less Likely	Any	-	1.0

(1) Inherent component damping of 5% is assumed.

Determination of Ground vs. Superstructure Category

Nonstructural components supported by slabs or foundation elements at grade that are not part of a building use the ground category. Similarly, nonstructural components supported by slabs or foundations, or other elements of the superstructure located at or below grade use the ground category. For the definition of grade, including sloping sites, see the definition of "Grade Plane" in ASCE/SEI 7-22 Section 11.2.

Determination of Likelihood of Being in Resonance

Nonstructural components have been categorized as likely or unlikely to be in resonance by engineering judgment. An underlying concept is that if the component period, T_p, is less than 0.06 seconds, then resonance is unlikely regardless of building period since the building period will typically be well above that level. In the 2016 and earlier editions of ASCE/SEI 7, components with $T_p \leq 0.06$ seconds were termed "rigid" and did not receive any amplification of PFA (while those with $T_p > 0.06$ were termed "flexible" and received an increase of 2.5 times PFA). A second underlying concept is that, when the ratio of component period to building period is relatively low or relatively large, then resonance is also unlikely. A criterion of $T_p / T_a < 0.5$ or $T_p / T_a > 1.5$ can be used, as suggested by NIST (2018), as well as extrapolation of results from Hadjian and Ellison (1986). Distribution systems may experience resonance, but its effect is judged to be minimized due to reduced mass participation caused by multiple points of support.

Ductility Categories

As discussed in NIST (2018), the elastic category is used for reference only. It is assumed that typical nonstructural components and their attachments to the structure systems used in practice have at least the low levels of component ductility. Thus, nonstructural components have been assigned to one of three categories of component ductility: low, moderate, and high. Engineering judgment has been used in the development of the tables.

Alternative C_{AR} values can be developed for components that are not in the table or when substantiating data is available. Such data can be derived from instrumented shake table component tests that compare the acceleration experienced by the component (PCA) at its effective center of mass versus the acceleration of the shake table (PFA). Such tests need to include realistic attachments between the component and the anchors and realistic anchorage.

8.2.10 Component Strength Factor, R_{po}

For *building* design, there is an inherent reserve strength margin between the design value and the eventual peak strength. This comes in part from capacity reduction factors, ϕ, but also as a result of other design factors, design simplifications, redundancy, and design decisions. This inherent reserve strength margin is a substantial part of the response modification coefficient, R, that is used to reduce elastic response levels down to design levels. See the discussion on R_o in the *SEAOC Recommended Lateral Force Requirements and Commentary* (SEAOC, 1999).

It is assumed that *component*s also have some inherent reserve strength margin that occurs as part of the design process. This inherent reserve strength margin has traditionally been considered by code writers in the development of nonstructural design equations. While a component's inherent reserve strength margin factor has not been explicitly identified, effects have been considered as part of the R_p factor in previous versions of ASCE/SEI 7.

It was decided to explicitly incorporate a value for the effect of component reserve strength in the nonstructural component design equation. The ATC-120 project team decided to assume a placeholder value of 1.3 for the inherent component reserve strength margin in NIST (2018). This was termed R_{pocomp}. In the development of the code change that eventually was approved for ASCE/SEI 7-22, the term was changed to the component strength factor, R_{po}. values selected vary from 1.5 for most components to 3.0 for components possessing exceptional strength, such as welded steel piping conforming to ASME B31. The component strength is related to the component itself and should not be confused with the component *anchorage* overstrength design force increase factor, Ω_{0p}, provided in Tables 13.5-1 and 13.6-1 of ASCE/SEI 7-22. The component anchorage overstrength design force is discussed in Section 8.2.15 of this chapter.

8.2.11 Equipment Support Structures and Platforms and Distribution System Supports

Previous editions of ASCE/SEI 7 have not made a distinction in design forces between the component and the supporting structure. They required the nonstructural components and

supporting structure to be designed with the same seismic design forces, F_p, regardless of their potential dynamic interaction, and the force was based on the component properties. For example, a platform supporting a pressure vessel would be designed for pressure vessel forces regardless of whether the platform structure was made of concrete, steel braced frames or steel moment frames. Or the trapeze assembly bracing a piping run would be designed for the pipe force, regardless of the type of trapeze assembly. In some cases, this could produce comparatively weak component supports, especially for distribution systems that had relatively low design forces for certain types of piping.

In ASCE/SEI 7-22, a significant refinement has been made to distinguish the requirements for design of the component from the supporting structure. This permits a more accurate determination of forces that more realistically reflect the differences in dynamic properties and ductilities between the component and the support structure or platform. Definitions are given in ASCE/SEI 7-12 Section 11.2 for three different types of support. ASCE/SEI 7-22 Commentary Section C13.6.4 provides figures for each type.

- Integral equipment supports: This is where the supports, such as short legs, are directly connected to both the component and the attachment to the structure. Integral equipment supports are designed for the seismic design force computed for the component itself. Integral equipment supports include legs less than or equal to 24 inches in length, lugs, skirts, and saddles. The 24-inch length limit for legs was determined by judgement and experience to be a reasonable length, above which the leg will no longer likely respond in a manner similar to the component.

- Equipment support structures and platforms: These are assemblies of members or manufactured elements, other than integral equipment supports, including moment frames, braced frames, skids, legs longer than 24 inches, or walls. An equipment support structure supports one piece of equipment; an equipment support platform supports multiple pieces of equipment.

- Distribution system supports: These are members that provides vertical or lateral resistance for distribution systems, including hangers, braces, pipe racks, and trapeze assemblies.

Required Familiarity with Nonstructural Components

Prior to performing any nonstructural component seismic design, the engineer should be familiar with the nature of the components, their support condition, and their associated terminology. The nonstructural component nomenclature is not always straightforward. Even though there may be parallel concepts in structural design, it takes a certain effort to understand.

For an adequate seismic design, it is the engineer's responsibility to determine an adequate load path to transfer forces from the nonstructural components and supports to the structure. For this purpose, the engineer should understand the different pieces conforming to the component and the attachments that are used to connect it to the supports and the supports to the structure.

Nonstructural component terminology is seldom taught in engineering programs. However, several resources are available to help designers understand the nature of the nonstructural components, such as specification sheets provided by the manufacturer, technical websites, and guidelines on nonstructural components.

Due to the complexity of nonstructural component design, engineers are also encouraged to consult experienced practitioners in this discipline.

ASCE/SEI 7-22 Table 13.6-1 has been modified to include C_{AR}, R_{po}, and Ω_{0p} design values for different types of equipment support structures and platforms and for distribution system supports. For example, a rigid concrete shear wall equipment support structure would fall under the category of "support structures and platforms where $T_p/T_a < 0.2$ or $T_p < 0.06$ seconds." It would thus be unlikely to be in resonance with the building fundamental period, and it is assigned a low C_{AR} value of 1.0, per Table 8-1. As a second example, an ordinary moment frame or steel special moment frame equipment support platform would fall under the category of "Seismic Force-Resisting Systems with $R > 3$" since the R values for these systems in ASCE/SEI 7-22 Table 12.2-1 are 3-1/2 (ordinary moment frame) and 8 (steel special moment frame). They are potentially in resonance with the building fundamental period resulting in amplification of component accelerations over floor accelerations, but they are considered to have a relatively high degree of ductility, so a C_{AR} value of 1.4 is assigned, per Table 8-1.

Section 13.6.4.6 has been added to ASCE/SEI 7-22 to require that the equipment support structures and platforms be designed using the design values in Table 13.6-1 and to also require that the seismic force-resisting systems be designed and detailed to one of the systems in ASCE/SEI 7-22 Table 12.2-1 or Table 15.4-1 and the additional requirements of ASCE/SEI 7-22 Chapter 14. An exception is provided in Table 13.5-1 under "Equipment Support Structures and Platforms" for "Other Systems." They are not required to be one of the systems in Table 12.2-1 or Table 15.4-1, but they must be designed using the highest value of C_{AR}. Finally, the component resonance ductility factor for mechanical and electrical equipment mounted on equipment support structures or

platforms shall not be less than the component resonance ductility factor used for the equipment support structure or platform itself.

Similarly, Section 13.6.4.7 has been added to ASCE/SEI 7-22 to require that distribution system supports be designed using the design values in Table 13.6-1.

8.2.12 Upper and Lower Bound Seismic Design Forces

ASCE/SEI 7-22 Equation 13.3-3 establishes a minimum seismic design force, F_p, which is unchanged from ASCE/SEI 7-16. ASCE/SEI 7-22 Equation 13.3-2 provides a simple maximum value of F_p that prevents multiplication of the individual factors from producing a design force that would be unreasonably high, considering the expected nonlinear response of support and component. It is also unchanged from ASCE/SEI 7-16. ASCE/SEI 7-22 Figure C13.3-1 illustrates the distribution of the specified lateral design forces and the relationship between the minimum of Equation 13.3-3, the maximum of Equation 13.3-2 and basic varying Equation 13.3-1. Note that depending upon the nature of the supporting structure, the value of F_p calculated using Eq. 13.3-1 may not vary linearly with height.

8.2.13 Nonlinear Response History Analysis

ASCE/SEI 7-22 Section 13.3.1.5 describes an alternative procedure where, in lieu of the forces determined per ASCE/SEI Equation 13.3-1, nonlinear response history analyses procedures of Chapters 16, 17, and 18 may be used to determine the seismic design force for nonstructural components. It replaces a procedure that was in ASCE/SEI 7-16. The seismic design force, F_p, shall be determined in accordance with ASCE/SEI 7-22 Equation 13.3-7.

$$F_p = 0.4 S_{DS} I_p W_p a_i \left[\frac{C_{AR}}{R_{po}}\right] \qquad \text{(ASCE/SEI 7-22 Eq. 13.3-7)}$$

In this equation, a_i, replaces the ratio H_f/R_μ in ASCE/SEI 7-22 Equation 13.3-1. It represents the maximum acceleration at level *i* at the center of mass obtained from the nonlinear response history analysis at the Design Earthquake seismic hazard level. The nonlinear analysis can account for the variation of acceleration up the height of the building that is specific to the building dynamic properties (the H_f factor) as well as the reduction in PFA due to building ductility (the R_μ factor). The upper and lower limits for F_p from ASCE/SEI 7-22 Equations 13.3-2 and 13.3-3 still apply.

8.2.14 Accommodation of Seismic Relative Displacements

In addition to the seismic design force, nonstructural components must be capable of accommodating the effects of seismic relative displacements, both within the structure in the form of interstory drifts and between structures when nonstructural components are supported on separate adjacent structures. The seismic relative displacement demands, D_{pI}, are determined using Equation 13.3-8 of ASCE/SEI 7-22:

$$D_{pI} = D_p I_e$$

where:

D_p = displacements within or between structures

I_e = the Seismic Importance Factor for the structure (ASCE/SEI 7-22 Section 11.5.1)

ASCE/SEI 7-22 requires that displacements, D_p, be determined in accordance with several equations. For two connection points on Structure A (or on the same structural system), one at Level *x* and the other at Level *y*, D_p is determined from ASCE/SEI 7-22 Equation 13.3-9:

$$D_p = \delta_{xA} - \delta_{yA}$$

where:

δ_{xA} = deflection at building Level x of Structure A, determined in accordance with ASCE/SEI 7-22 Equation 12.8-15

δ_{yA} = deflection at building Level y of Structure A, determined in accordance with ASCE/SEI 7-22 Equation 12.8-15

Because the computed displacements frequently are not available to the designer of nonstructural components, one may use the maximum permissible structural displacements per ASCE/SEI 7-22 Equation 13.3-10:

$$D_p = \frac{(h_x - h_y)\Delta_{aA}}{h_{sx}}$$

where:

h_x = height of upper support attachment at Level *x* as measured from the base.

h_y = height of lower support attachment at Level *y* as measured from the base.

Δ_{aA} = allowable story drift for Structure A as defined in ASCE/SEI 7-22 Table 12.2-1.

h_{sx} = story height used in the definition of the allowable drift, Δ_a, in ASCE/SEI 7-22 Table 12.2-1.

For two connection points on separate Structures A and B (or on two separate structural systems), one at Level *x* and the other at Level *y*, D_p is determined from ASCE/SEI 7-22 Equations 13.3-11 and 13.3-12:

$$D_p = |\delta_{xA}| + |\delta_{yB}|$$

For structures in which the story drifts associated with the Design Earthquake Displacement does not exceed the allowable story drift, as defined in ASCE/SEI 7-22 Table 12.12-1, D_p is not required to be taken as greater than

$$D_p = \frac{h_x \Delta_{aA}}{h_{sx}} + \frac{h_y \Delta_{aB}}{h_{sx}}$$

where:

D_p = seismic displacement that the component must be designed to accommodate.

δ_{xA} = deflection of building Level *x* of Structure A, determined by an elastic analysis as defined in ASCE/SEI 7-22 Section 12.8.6 including being multiplied by the C_d factor.

δ_{yA} = deflection of building Level y of Structure A, determined in the same fashion as δ_{xA}.

δ_{yB} = deflection of building Level *y* of Structure B, determined in the same fashion as δ_{xA}.

h_x = height of upper support attachment at Level *x* as measured from the base.

h_y = height of lower support attachment at Level *y* as measured from the base.

Δ_{aA} = allowable story drift for Structure A as defined in ASCE/SEI 7-22 Table 12.2-1.

Δ_{aB} = allowable story drift for Structure B as defined in ASCE/SEI 7-22 Table 12.2-1.

h_{sx} = story height used in the definition of the allowable drift, Δ_a, in ASCE/SEI 7-22 Table 12.2-1. Note that Δ_{aA}/h_{sx} = the drift index.

The effects of seismic relative displacements must be considered in combination with displacements caused by other loads as appropriate. Specific methods for evaluating seismic relative displacement effects on components and associated acceptance criteria are not specified in ASCE/SEI 7-22. However, the intention is to satisfy the purpose of ASCE/SEI 7-22. Therefore, for nonessential facilities, nonstructural components can experience serious damage during the design-level earthquake provided they do not constitute a serious life-safety hazard. For essential facilities, nonstructural components can experience some damage or inelastic deformation during the design-level earthquake provided they do not significantly impair the function of the facility.

8.2.15 Component Anchorage Factors and Acceptance Criteria

Design seismic forces in the connected parts, F_p, are prescribed in ASCE/SEI 7-22 Section 13.4. The requirements for anchorage to concrete and masonry were revised in the 2010 and 2016 editions of ASCE/SEI 7.

Design capacity for anchors in concrete is determined in accordance with Chapter 17 of ACI 318-19. Design capacity for anchors in masonry is determined in accordance with TMS 402. Anchors are designed to either have ductile behavior, or they must have a specified degree of excess strength. Anchors whose nominal strength is controlled by breakout, crushing, or anchor pryout are considered to exhibit nonductile behavior. The specific criteria for nonductile behavior are in the design standard for the particular anchor instead of ASCE/SEI 7-22. The determination is made during the anchor

design process. This can be an iterative procedure, although with experience, the probable need to apply the overstrength factor, Ω_{0p}, can be judged prior to the anchor capacity calculation. For example, the "shallow anchor" definition used in ASCE/SEI 7-02 (embedment depth to diameter ratio less than 8) is still often a useful predictor of whether the overstrength factor, Ω_{0p}, factor will need to be applied. When required to apply the seismic load effects including overstrength in ASCE/SEI 7-22 Section 12.4.3, Ω_0 shall be taken as the anchorage overstrength factor, Ω_{0p}, given in ASCE/SEI 7-22 Tables 13.5-1 and 13.6-1.

The revisions to the force equations in ASCE/SEI 7-22 produce more accurate estimates of seismic demands on nonstructural components. The revised force equations allow correlation between the component resonance ductility factor, C_{AR}, and the anchorage overstrength factor, Ω_{0p}. In general, components unlikely to be in resonance and high ductility components likely to be in resonance are assigned the highest anchorage overstrength factor. These components are designed for lower lateral forces, and an extra margin of strength in anchorage to concrete and masonry is warranted in the event that some resonance does occur or the component ductility is lower than anticipated. Low ductility components that are likely to be in resonance are designed for high seismic design force levels. Since minimal reductions in response due to ductile behavior are expected, the seismic design force is less likely to be exceeded in a design earthquake, warranting a lower anchorage overstrength factor. The typical correlations between C_{AR} and Ω_{0p} in ASCE/SEI 7-22 Tables 13.5-1 and 13.6-1 are shown in Table 8-2.

Table 8-2. Typical Correlations Between C_{AR} and Ω_{0p}

Component Resonance Ductility Factor, C_{AR}	Anchorage Overstrength Factor, Ω_{0p}
1	2
1.4	2
1.8	1.75
2.2	1.75
2.8	1

Post-installed anchors in concrete must be prequalified for seismic applications in accordance with the procedures of ACI 355.2 or other approved standards. Post-installed anchors in masonry must be prequalified for seismic applications in accordance with approved qualification procedures. Use of power actuated fasteners in concrete, masonry, or steel is not permitted for sustained tension or bracing applications in Seismic Design Categories D, E and F unless approved for such loading.

Exceptions in ASCE/SEI 7-22 Section 13.4.5 permit the use of power actuated fasteners in certain conditions when the applied loads are low.

Per ASCE/SEI 7-22 Section 13.4.6, friction clips may be used to resist seismic loads, but they are not permitted to resist sustained gravity loads in Seismic Design Categories D, E and F.

Determination of design seismic forces in anchors must consider installation eccentricities, prying effects, multiple anchor effects, and the stiffness of the connected system. When there are multiple attachments in one location, such as a base plate with multiple anchors, the stiffness and ductility of all parts of the seismic load path, including the component itself, component supports, attachments, and the supporting structure must be evaluated for their ability to redistribute loads to the attachments in the group.

8.2.16 Construction Documents

Construction documents must be prepared by a registered design professional and must include sufficient detail for use by the owner, building officials, contractors and special inspectors. ASCE/SEI 7-22 Section 13.2.7 includes specific requirements.

8.2.17 Exempt Items

The requirements in Chapter 13 of ASCE/SEI 7-22 are intended to apply only to permanently attached components, not to furniture, temporary items, or mobile units. Permanently attached nonstructural components may be exempt, provided that due to their inherent strength and stability, they can meet the nonstructural performance objectives without explicitly meeting all the requirements of Chapter 13.

The 2022 edition substitutes the list of nonstructural components that are exempt from the seismic design requirements with the ASCE/SEI 7-22 Table 13.1-1, replicated in Table 8-3 of this chapter. This table includes changes to the exceptions for distribution systems.

Table 8-3. Nonstructural Components Exempt Items per ASCE/SEI 7-22 Table 13.3-1.

Seismic Design Category (SDC)	Nonstructural Components Exempt from the Requirements of this Chapter
All Categories	▪ Furniture (except storage cabinets, as noted in Table 13.5-1) ▪ Temporary or movable equipment
A	▪ All components
B	▪ Architectural Components, other than parapets, provided that the component Importance Factor, I_p, is equal to 1.0 ▪ Mechanical and Electrical Components
C	▪ Mechanical and Electrical Components, provided that either ○ the component Importance Factor, I_p, is equal to 1.0 and the component is positively attached to the structure; or ○ the component weighs 20 lb (89 N) or less
D, E, F	▪ Mechanical and electrical components positively attached to the structure, provided that ○ For discrete mechanical and electrical components, the component weighs 400 lb (1,779 N) or less, the center of mass is located 4 ft (1.22 m) or less above the adjacent floor level, flexible connections are provided between the component and associated ductwork, piping, and conduit, and the Component Importance Factor, I_p, is equal to 1.0; or ○ For discrete mechanical and electrical components, the component weighs 20 lb (89 N) or less; or ○ For distribution systems, the Component Importance Factor, Ip, is equal to 1.0 and the operating weight of the system is 5 lb/ft (73 N/m) or less. ▪ Distribution systems included in the exceptions for conduit, cable tray, and raceways in Section 13.6.5, duct systems in 13.6.6, and piping and tubing systems in 13.6.7.3. Where in-line components, such as valves, in-line suspended pumps, and mixing boxes, require independent support, they shall be addressed as discrete components and shall be braced considering the tributary contribution of the attached distribution system.

8.2.18 Pre-Manufactured Modular Mechanical and Electrical Systems

ASCE/SEI 7-22 includes guidance on the design of pre-manufactured modular mechanical and electrical systems. These factory-built units are transported to the site and assembled together. Section 13.1.5 of ASCE/SEI 7-22 directs the user to ASCE/SEI 7-22 Chapter 15, Nonbuilding Structures, for the design of the modular unit itself. Nonstructural components installed or supported by the modular unit are designed in accordance with ASCE/SEI 7-22 Chapter 13.

8.3 Architectural Concrete Wall Panel

8.3.1 Example Description

Example Summary

- **Nonstructural component:** Architectural – exterior nonstructural wall elements and connections
- **Building seismic force-resisting system:** Steel special moment frames
- **Equipment support:** Not applicable
- **Occupancy:** Office
- **Risk Category:** II
- **Component Importance Factor:** $I_p = 1.0$
- **Number of stories:** 5
- $\boldsymbol{S_{DS}} = 1.487$

In this example, the architectural components are a 4.5-inch-thick precast normal-weight concrete spandrel panel and a column cover supported by the structural steel frame of a five-story office building, as shown in Figures 8-6 and 8-7. The cladding components do not meet any of the requirements in ASCE/SEI 7-22 Section 13.1.3 for increasing the Component Importance Factor to $I_p = 1.5$: they are not required for life-safety purposes after an earthquake; they do not convey or support toxic, explosive, or hazardous materials; and the building is not classified as Risk Category IV or as a hazardous occupancy. Thus, the Component Importance Factor is $I_p = 1.0$.

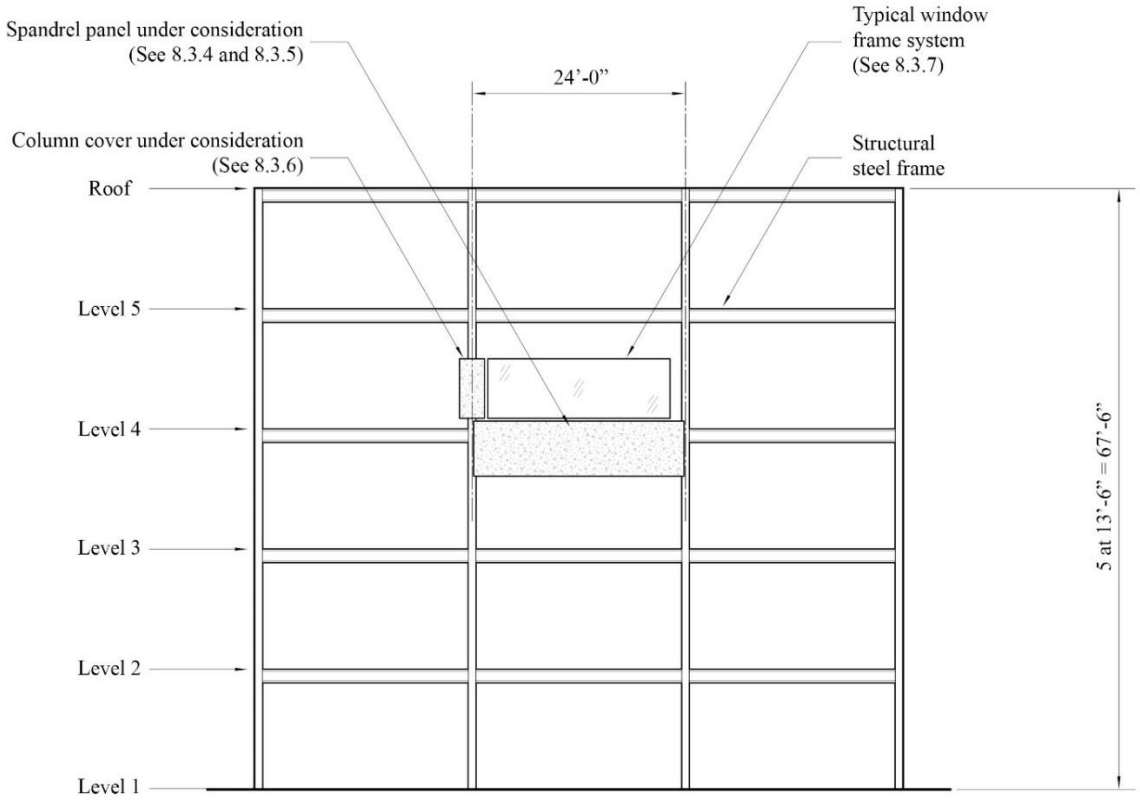

Figure 8-6. Five-story Building Elevation Showing Panel Location

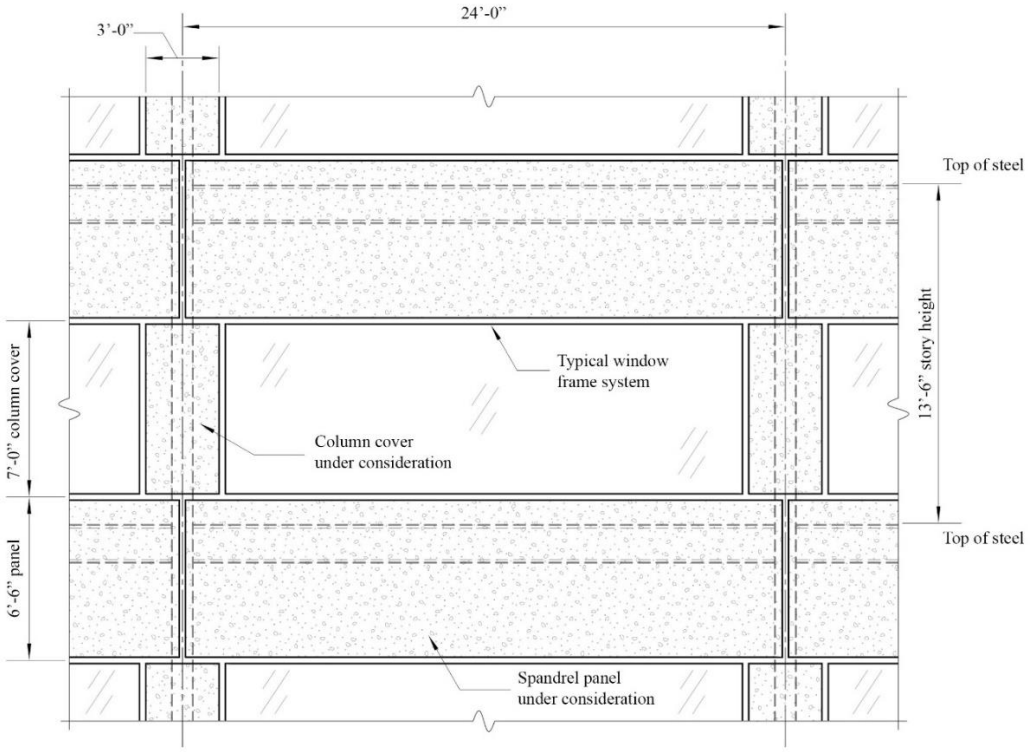

Figure 8-7. Detailed Building Elevation

The seismic force-resisting system for the building consists of steel special moment frames in the two orthogonal directions. The girders at Level 3 of the five-story office building support the spandrel panel under consideration. The columns between the Level 3 and Level 4 of the building support the column cover under consideration. The office building is assigned to Risk Category II per Table 1.5-1 of ASCE/SEI 7-22. The spandrel panel supports glass windows weighing 10 psf.

Section 8.3.2 discusses general strategies for providing gravity support and accommodating interstory drift for cladding. Then, this example illustrates the following calculation procedures:

- Prescribed seismic forces, proportioning, and design forces for spandrel panel (see Section 8.3.3 in this example).
- Prescribed seismic forces, proportioning, and design forces for spandrel panel connection fasteners (see Section 8.3.4 in this example).
- Prescribed seismic displacements for column cover (see Section 8.3.5 in this example).
- Additional design considerations, such as window frame system, and detailing (see Section 8.3.6 in this example).

Details of precast connections vary according to the preferences and local practices of the precast panel supplier. In addition, some connections may involve patented designs. This example concentrates on quantifying the prescribed seismic forces and displacements. After the prescribed seismic forces and displacements are determined, the connections can be detailed and designed according to the appropriate AISC and ACI codes, and the recommendations of the Precast/Prestressed Concrete Institute (PCI). ASCE/SEI 7-22 requirements for connections that accommodate story drift through sliding or bending of steel rods are discussed.

8.3.2 Providing Gravity Support and Accommodating Story Drift in Cladding

Understanding the cladding system components is the first step for the concrete precast panel seismic design. Then two crucial items should be determined:

- Gravity support approach for the precast panel components
- Mechanism to accommodate story drift,

The gravity support dictates the location and type of the bearing connections (see Section 8.3.4.1 of this chapter), whereas the mechanism to accommodate the story drift determines how the cladding will deform or displace without compromising the integrity of concrete panels and windows based on the connection types and layout.

Two common approaches to accommodating interstory drift are rocking and sliding. See Figure 8-8 for a schematic representation of the mechanisms associated with these two approaches.

- Rocking: This approach relies on the rotation of the precast panels that are connected at different floor elevations, and racking of the window framing system, which can also cause the glass to rotate. The geometry and discretization of the panels and window units often determines which components will rock. For example, in some systems with spandrels and piers or column covers, the spandrels are designed to be supported independently by each floor and move with each floor. It is only the column covers that rock and window framing that racks.

- Sliding: In this approach, there is a horizontal slip plane, typically under the precast spandrel. The spandrel above the slip plane is supported by the floor above and moves in-plane with the floor above. The glazing, spandrel, and column cover below the slip plane are supported by the floor below and move in-plane with the floor above. The precast and glazing elements do not rotate or rack; instead, they stay in their original geometric form. In the out-of-plane direction, the panels and glazing tilt as the floor above moves with respect to the floor below. The slip plane usually has out-of-plane support for the top of the glazing and column cover. It also is the location of a vertical gap to accommodate differential live load deflection between the floors.

A more detailed discussion specific to the performance intent of ASCE/SEI 7-22 for glazing and how drift is accommodated is in Section 8.3.7 of this chapter.

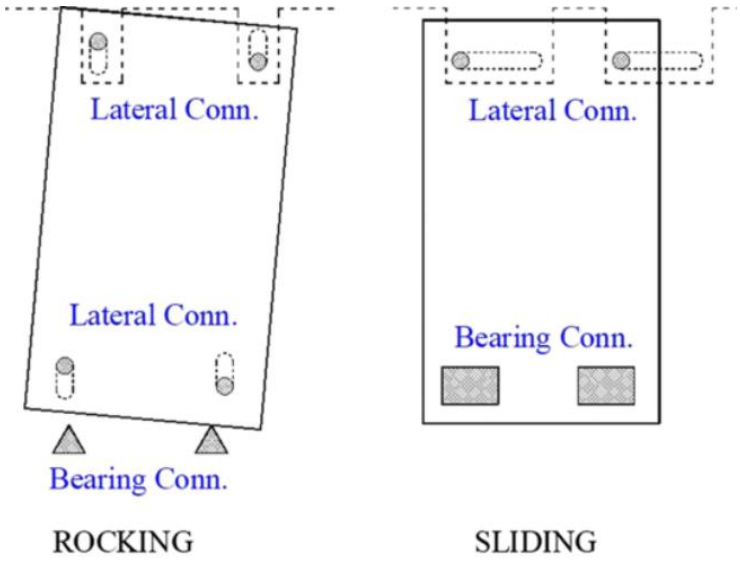

Figure 8-8. Rocking Mechanism and Sliding Mechanism in Panels

For this example, a rocking cladding connection system is selected. Refer to Figures 8-9 and 8-10 that illustrate the condition of precast panels and window glazing at rest and the deformed configuration to accommodate the relative lateral movement due to story drift.

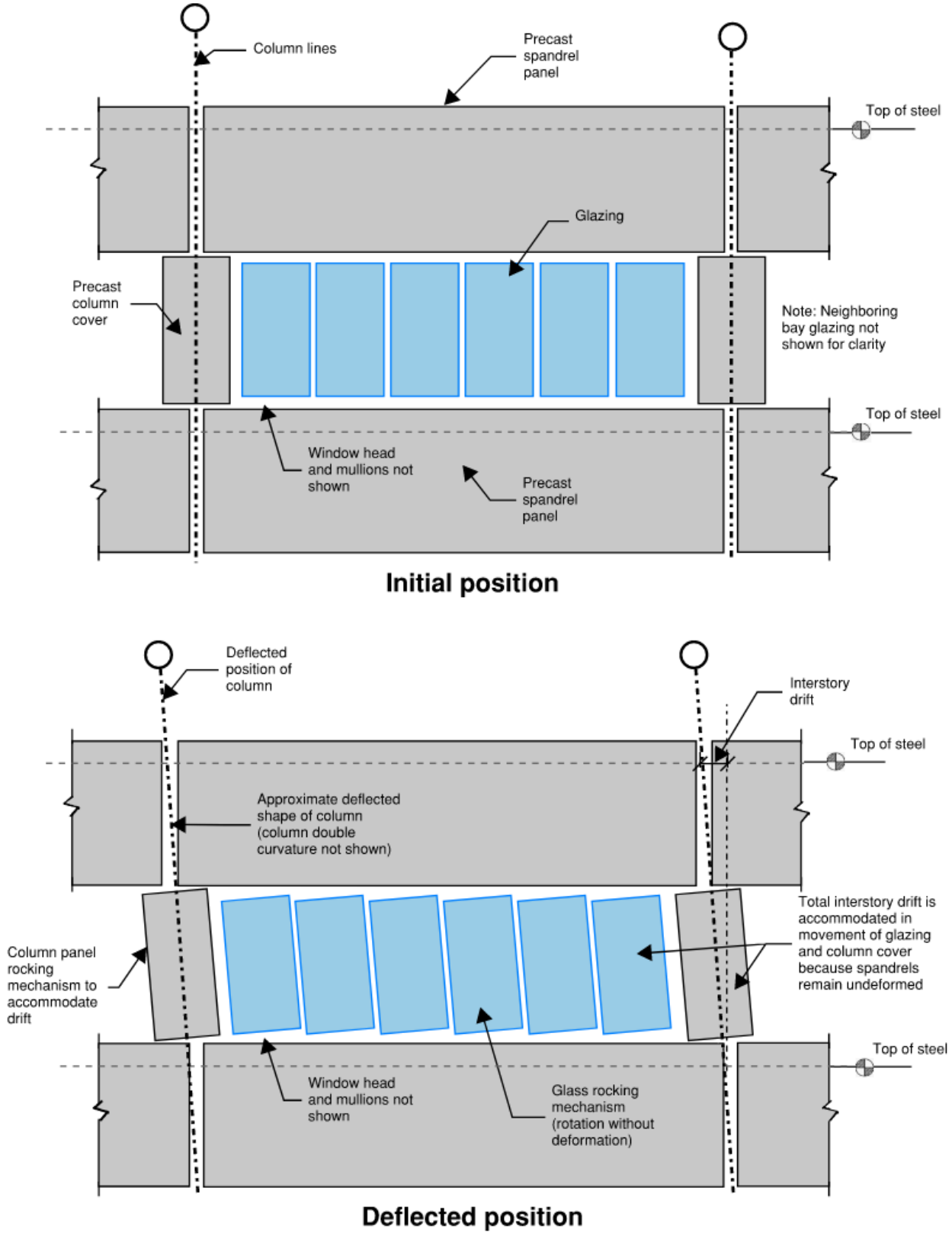

Figure 8-9. Precast Panel Mechanism to Accommodate Story Drift

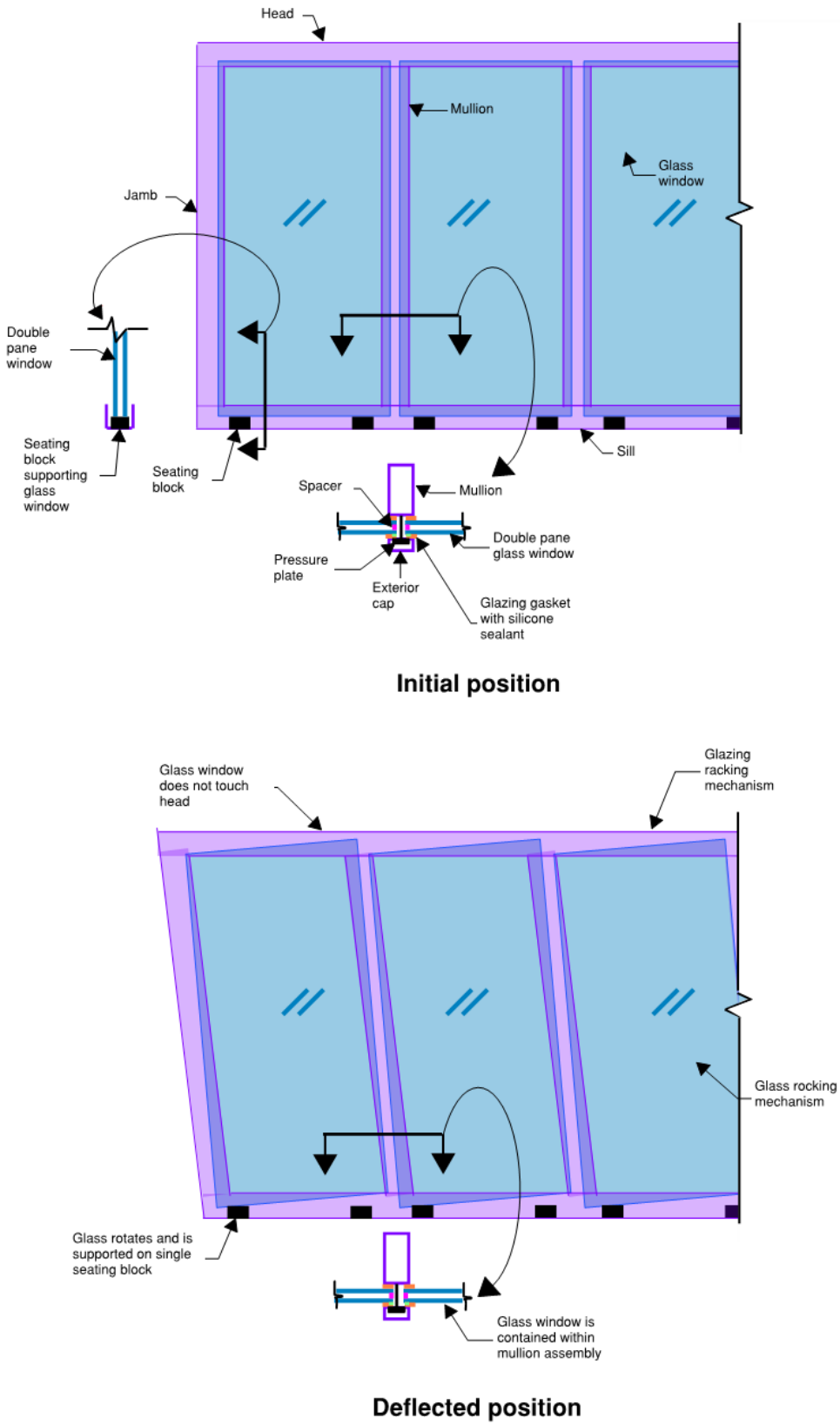

Figure 8-10. Window Framing System Racking Mechanism

8.3.3 Design Requirements

8.3.3.1 ASCE/SEI 7-22 PARAMETERS AND COEFFICIENTS

The following parameters and coefficients are derived from the example description, or it is known information based on the structure, selected location, and site class.

Coefficients for architectural components

Exterior nonstructural wall elements and connections – wall element, and body of wall panel connections:

$C_{AR} = 1.0$ (ASCE/SEI 7-22 Table 13.5-1)

$R_{po} = 1.5$ (ASCE/SEI 7-22 Table 13.5-1)

$\Omega_{0p} = 2.0$ (ASCE/SEI 7-22 Table 13.5-1)

Exterior nonstructural wall elements and connections – fasteners of the connecting system:

$C_{AR} = 2.8$ (ASCE/SEI 7-22 Table 13.5-1)

$R_{po} = 1.5$ (ASCE/SEI 7-22 Table 13.5-1)

$\Omega_{0p} = 1.0$ (ASCE/SEI 7-22 Table 13.5-1)

Design coefficients and factors for seismic force-resisting system

Moment-resisting frame systems – special steel moment frames:

$R = 8.0$ (ASCE/SEI 7-22 Table 12.2-1)

$\Omega_0 = 3.0$ (ASCE/SEI 7-22 Table 12.2-1)

Nonstructural Design Forces are Now Influenced by the Seismic Force Resisting System of the Building

The seismic design requirements for nonstructural components in Chapter 13 require the engineer to know more information regarding the seismic force-resisting system for the primary structure in the new edition of ASCE/SEI 7.

The seismic design forces, F_p, can still be calculated without knowing the seismic force-resisting system. However, this should be avoided, as the seismic design forces can increase significantly.

Short period design spectral acceleration, $S_{DS} = 1.487$ (given)

Seismic Design Category: D (ASCE/SEI 7-22 Sec. 11.6)

Seismic Importance Factor, $I_e = 1.0$ (ASCE/SEI 7-22 Table 1.5-2)

Component Importance Factor, $I_p = 1.0$ (ASCE/SEI 7-22 Sec. 13.1.3)

Redundancy factor for nonstructural components, $\rho = 1.0$ (ASCE/SEI 7-22 Sec. 13.3.1)

Height of attachment at Level 3, $z = 40.5$ ft (given)

Average roof height with respect to the base, $h = 67.5$ ft (given)

Story height, $h_{sx} = 13.5$ ft (given)

Spandrel panel weight:

$$W_p = (150 \text{ lb/ft}^3)(24 \text{ ft long})(6.5 \text{ ft high})(4.5 \text{ in. thick}/12 \text{ ft/in.})$$

$$W_p = 8{,}775 \text{ lb}$$

The glass dead load is assumed to be supported by spandrel panel below. As shown in Figure 8-11, the seismic load of the glass tributary to the spandrel, both in-plane and out-of-plane, comes from half of the glass panel above and half of the glass panel below, so the dead load and tributary weight for seismic loading is the same.

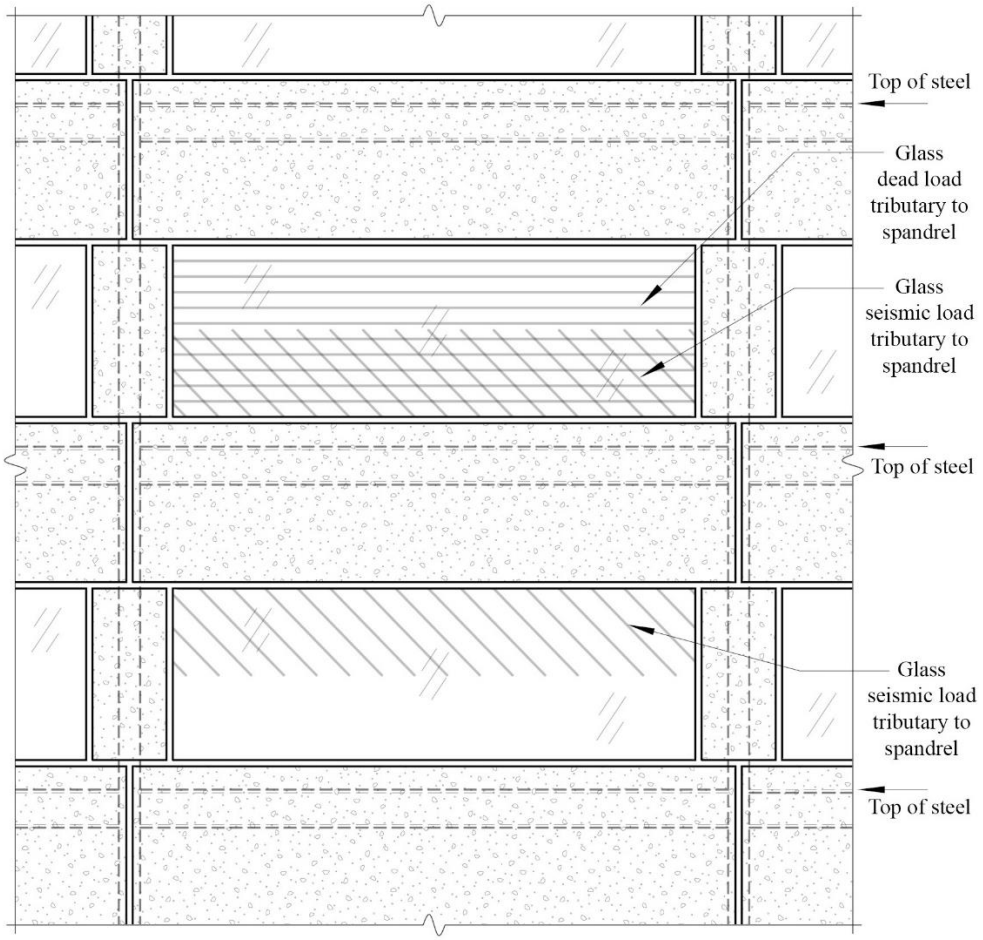

Figure 8-11. Detailed Building Elevation with Tributary Dead Load and Seismic Load

Glass weight:

$$W_p = (10 \text{ lb/ft}^2)(21 \text{ ft long})(7 \text{ ft high})$$

$$W_p = 1{,}470 \text{ lb}$$

Column cover weight:

$$W_p = (150 \text{ lb/ft}^3)(3 \text{ ft wide})(7 \text{ ft high})(4.5 \text{ in. thick}/12 \text{ ft/in.})$$

$$W_p = 1{,}181 \text{ lb}$$

Approximate fundamental period of the supporting structure, T_a – steel moment-resisting frame

$h_n = h = 67.5$ ft (structural height)

$C_t = 0.028$ (ASCE/SEI 7-22 Table 12.8-2)

$x = 0.8$ (ASCE/SEI 7-22 Table 12.8-2)

$T_a = C_t {h_n}^x = (0.028)(67.5 \text{ ft})^{0.8} = 0.81\ s$ (ASCE/SEI 7-22 Eq. 12.8-7)

Force amplification factor as a function of height in the structure, H_f

$a_1 = \frac{1}{T_a} \leq 2.5$ (ASCE/SEI 7-22 Sec. 13.3.1.1)

$a_1 = \frac{1}{0.81 \text{ s}} = 1.23 \leq 2.5$

$a_2 = [1 - (0.4/T_a)^2] \geq 0$ (ASCE/SEI 7-22 Sec. 13.3.1.1)

$a_2 = [1 - (0.4/0.81 \text{ s})^2] = 0.76 > 0$

$H_f = 1 + a_1 \left(\frac{z}{h}\right) + a_2 \left(\frac{z}{h}\right)^{10}$ (ASCE/SEI 7-22 Eq. 13.3-4)

$H_f = 1 + 1.23 \left(\frac{40.5 \text{ ft}}{67.5 \text{ ft}}\right) + 0.76 \left(\frac{40.5 \text{ ft}}{67.5 \text{ ft}}\right)^{10} = 1.74$

Force Amplification Factor, H_f, where the Approximate Fundamental Period is Unknown

Where the approximate fundamental period of the supporting building or nonbuilding structure is unknown, H_f is permitted to be determined by the following equation:

$H_f = 1 + 2.5 \left(\frac{z}{h}\right)$ (ASCE/SEI 7-22 Eq. 13.3-5)

When computing the force amplification factor, H_f, using Eq. 13.3-5:

$H_f = 1 + 2.5 \left(\frac{40.5 \text{ ft}}{67.5 \text{ ft}}\right) = 2.50$

For this example, by considering the approximate fundamental period of the structure, the force amplification factor, H_f, and consequently, the seismic design force, F_p, are reduced by 30%.

Structure ductility reduction factor, R_μ

$R_\mu = (1.1\, R/(\, I_e\, \Omega_0))^{1/2} \geq 1.3$ (ASCE/SEI 7-22 Eq. 13.3-6)

$R_\mu = (1.1(8/((1)(3)))^{1/2} = 1.71 \geq 1.3$

Change Between the 2020 *NEHRP Provisions* and ASCE/SEI 7 22

Equation 13.3-6 in the 2020 *NEHRP Provisions* was modified for ASCE/SEI 7-22 by adding I_e into the denominator to better estimate the structure ductility.

8.3.3.2 APPLICABLE REQUIREMENTS

The architectural, mechanical, and electrical components, supports, and attachments shall comply with the sections referenced in ASCE/SEI 7-22 Table 13.2-1. Thus, the nonstructural components of this example are designed in accordance with the following considerations:

- Component failure shall not cause failure of an essential architectural, mechanical, or electrical component (ASCE/SEI 7-22 Section 13.2.4).
- Component seismic attachments shall be bolted, welded, or otherwise positively fastened without considering the frictional resistance produced by the effects of gravity (ASCE/SEI 7-22 Section 13.4).
- The horizontal seismic design force, F_p, shall be applied at the component's center of gravity and distributed relative to the component's mass distribution (ASCE/SEI 7-22 Section 13.3.1).
- The effects of seismic relative displacements shall be considered in combination with displacements caused by other loads as appropriate (ASCE/SEI 7-22 Section 13.3.2).
- Exterior nonstructural wall panels or elements that are attached to or enclose the structure shall be designed to accommodate the seismic relative displacements and movements caused by temperature changes (ASCE/SEI 7-22 Section 13.5.3).

8.3.4 Spandrel Panel – Wall Element and Body of Wall Panel Connections

8.3.4.1 CONNECTION LAYOUT

Figure 8-12 shows the types and locations of connections that support a single spandrel panel.

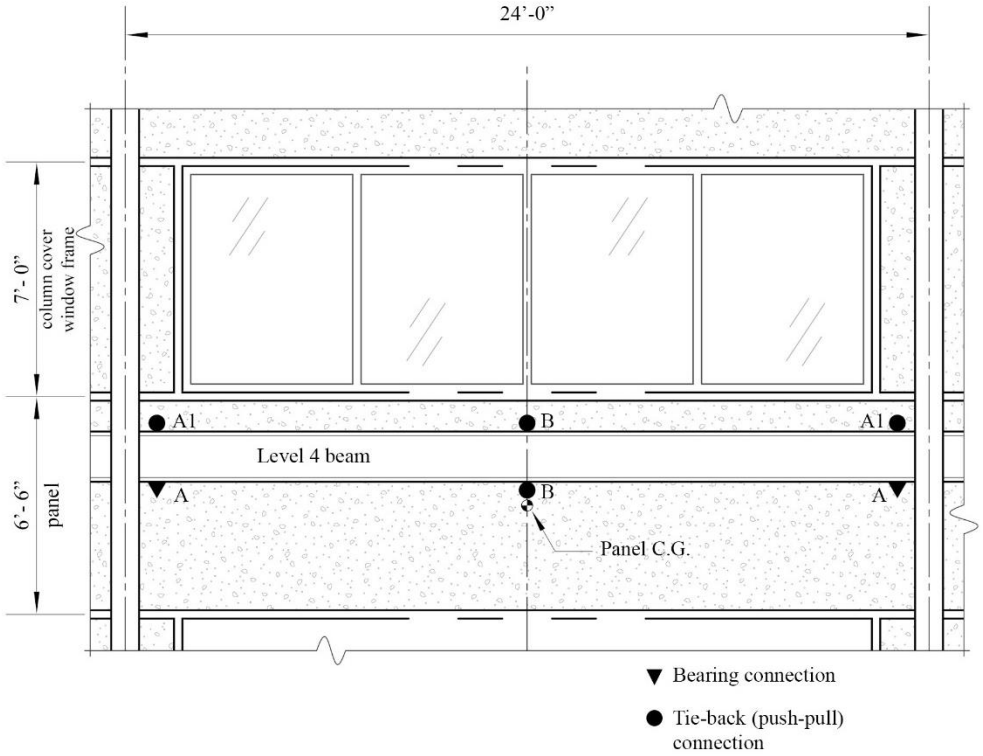

Figure 8-12. Spandrel Panel Connection Layout from Interior

The connection system must resist the weight of the panel and supported construction, the additional demand due to the eccentricity between the loads and the supports, and the forces generated by response to the seismic motions. Furthermore, the connection system must not create undue interaction between the structural frame and the panel, such as restraint of thermal movements of the panel or the transfer of floor live load from the floor beam to the panel. The panels are usually very stiff compared to the frame, and this requires careful release of potential constraints at connections. The Architectural Precast Concrete Manual (PCI, 2007) provides an extended discussion of important design concepts for such panels.

For this example, the panel dead load and vertical seismic accelerations are resisted at the two connections identified as 'A', which provide the recommended simple and statically determinant system for supporting the gravity load of the panel. These connections are often referred to as bearing connections. As shown in Figure 8-15, there is an eccentricity between the center of mass of the panel and the reaction at the vertical support, which generates a moment that is resisted by a force couple at the pairs of 'A1' and 'A' connections. Horizontal loads parallel to the panel are resisted by the 'A' connections. Horizontal loads perpendicular to the panel are resisted by the 'A' and 'A1' connections at the ends of the panel and the pair of 'B' connections midspan. These connections intended to resist lateral loads perpendicular to the precast panel are referred to as tie-back or push-pull connections. In summary, the 'A' bearing connections resist forces in the vertical, longitudinal (in-plane), and transverse (out-of-plane) directions, while the 'A1' and 'B' connections resist forces in only the out-of-plane direction.

The practice of resisting the horizontal in-plane force at two points varies with seismic demand and local industry practice. An alternative option is to resist all of the in-plane horizontal force at one connection in order to avoid restraint of panel shrinkage and thermal movements. The decision to use one or several in-plane horizontal connections is made based on seismic demands, and local experience with restraint issues in precast panels of similar length.

The 'A' and 'A1' connections are often designed to take the loads directly to the columns, particularly on steel moment frames where attachments to the flexural hinging regions of beams are difficult to accomplish. To provide sufficient stiffness and strength to resist the out-of-plane loads, the lower 'B' connection often requires bracing the bottom flange of the exterior beam to the floor or roof deck in order to control torsional behavior of the exterior beam, unless the connection can be placed near an intersecting beam that will prevent twisting of the exterior beam.

Typical Connection Layouts in Precast Panels

Precast panels typically include two bearing connections and two tie-back connections. The weight of the panel should be supported on not more than two points and only at one level. Otherwise, the deflections of the frame members may cause a different weight distribution than the calculations and could compromise the structural performance.

A typical connection layout for spandrel panels that is different from this design example consists of bearing connections at the upper ends of the panel, tie-back connections at the lower ends of the panel, and optional tie-back connections at midspan to minimize flexural stresses and deflection in longer panels. The selection of the connection layout is contingent upon the cladding system. Refer to Section 8.3.2 of this chapter for a discussion regarding the selection of cladding system interstory drift method.

The detail at midspan of the precast spandrel panel of this example is represented in Figure 8-13. Bolted tie-back connections permit in-plane movement, as the steel rods flex relatively easily in this direction. A steel angle functions as bracing for the bottom flange of the exterior beam to control torsional effects in the members.

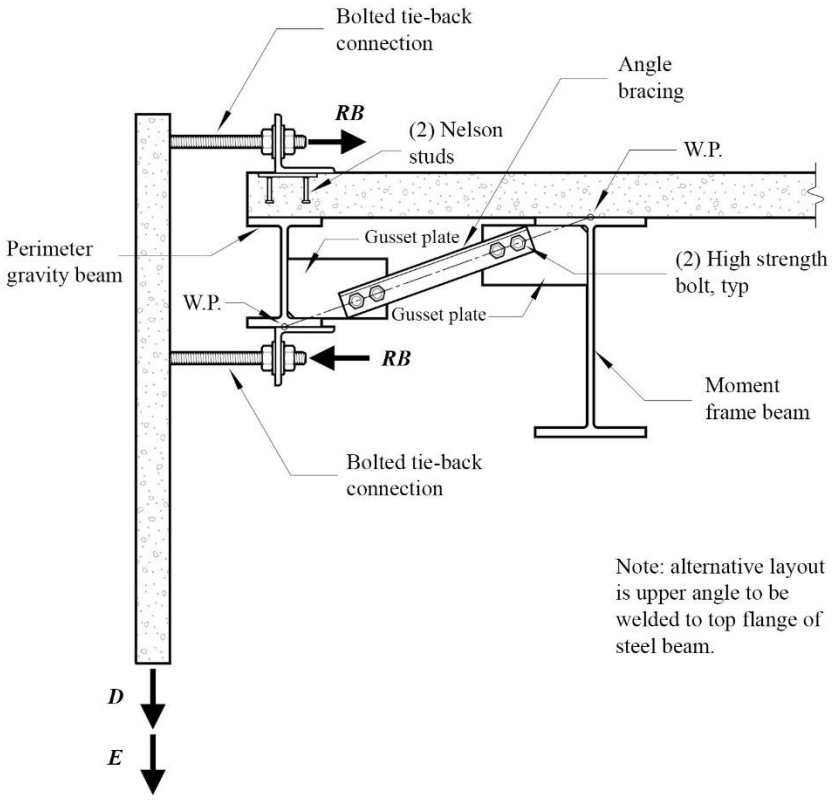

Figure 8-13. Spandrel Panel Connection at Midspan

The column cover is supported both vertically and horizontally by the column, transfers no loads to the spandrel panel and provides no support for the window frame.

The window frame is supported both vertically and horizontally along the length of the spandrel panel and transfers no loads to the column covers.

8.3.4.2 PRESCRIBED SEISMIC FORCES

Lateral forces on the wall panels and connection fasteners include seismic loads and wind loads. Design for wind forces is not presented in this example.

Spandrel panel and glass weight, W_p

$$D = 8{,}775 \text{ lb} + 1{,}470 \text{ lb} = 10{,}245 \text{ lb} \qquad \text{(dead load)}$$

$$W_p = D = 10{,}245 \text{ lb} \qquad \text{(component weight)}$$

Seismic design force, F_p

$$F_p = 0.4 S_{DS} I_p W_p \left[\frac{H_f}{R_\mu}\right] \left|\frac{C_{AR}}{R_{po}}\right| \qquad \text{(ASCE/SEI 7-22 Eq. 13.3-1)}$$

$$F_p = 0.4(1.487)(1.0)\left(W_p\right)\left[\frac{1.74}{1.71}\right]\left|\frac{1.0}{1.5}\right| = 0.403W_p$$

$F_{p,max} = 1.6S_{DS}I_pW_p$ (ASCE/SEI 7-22 Eq. 13.3-2)

$$F_{p,max} = 1.6(1.487)(1.0)\left(W_p\right) = 2.379W_p$$

$F_{p,min} = 0.3S_{DS}I_pW_p$ (ASCE/SEI 7-22 Eq. 13.3-3)

$F_{p,min} = 0.3(1.487)(1.0)\left(W_p\right) = 0.446W_p$ (controlling equation)

$F_p = 0.446W_p = 0.446(10{,}245\text{ lb}) = 4{,}570\text{ lb}$ (controlling seismic design force)

Horizontal seismic load effect, E_h

$Q_E = F_p = 4{,}570\text{ lb}$ (effect from F_p)

$E_h = \rho Q_E$ (ASCE/SEI 7-22 Eq. 12.4-3)

$E_h = (1.0)(4{,}570\text{ lb}) = 4{,}570\text{ lb}$

Vertical seismic load effect, E_v

$E_v = 0.2S_{DS}D$ (ASCE/SEI 7-22 Eq. 12.4-4a)

$E_v = (0.2)(1.487\text{g})(10{,}245\text{ lb}) = 3{,}047\text{ lb}$

The above terms are then substituted into the following Basic Load Combinations for Strength Design from ASCE/SEI 7-22 Sections 2.3.6 and 12.4.2 to determine the design member and connection forces to be used in conjunction with seismic loads.

$1.2D + E_v + E_h + L + 0.2S$ (ASCE/SEI 7-22 Load Combination 6)

$0.9D - E_v + E_h$ (ASCE/SEI 7-22 Load Combination 7)

For nonstructural components, the terms *L* and *S* are typically zero.

8.3.4.3 PROPORTIONING AND DESIGN

The wall panels shall be designed for the following loads in accordance with ACI 318-19. The design of the precast concrete panel is standard and is not illustrated in this example. The spandrel panel moments are shown in Figure 8-14. The vertical forces, V_u, horizontal forces, H_u, and moments, M_u, are calculated using the applicable strength load combinations.

For this example, the values of *L* and *S* are assumed to be zero.

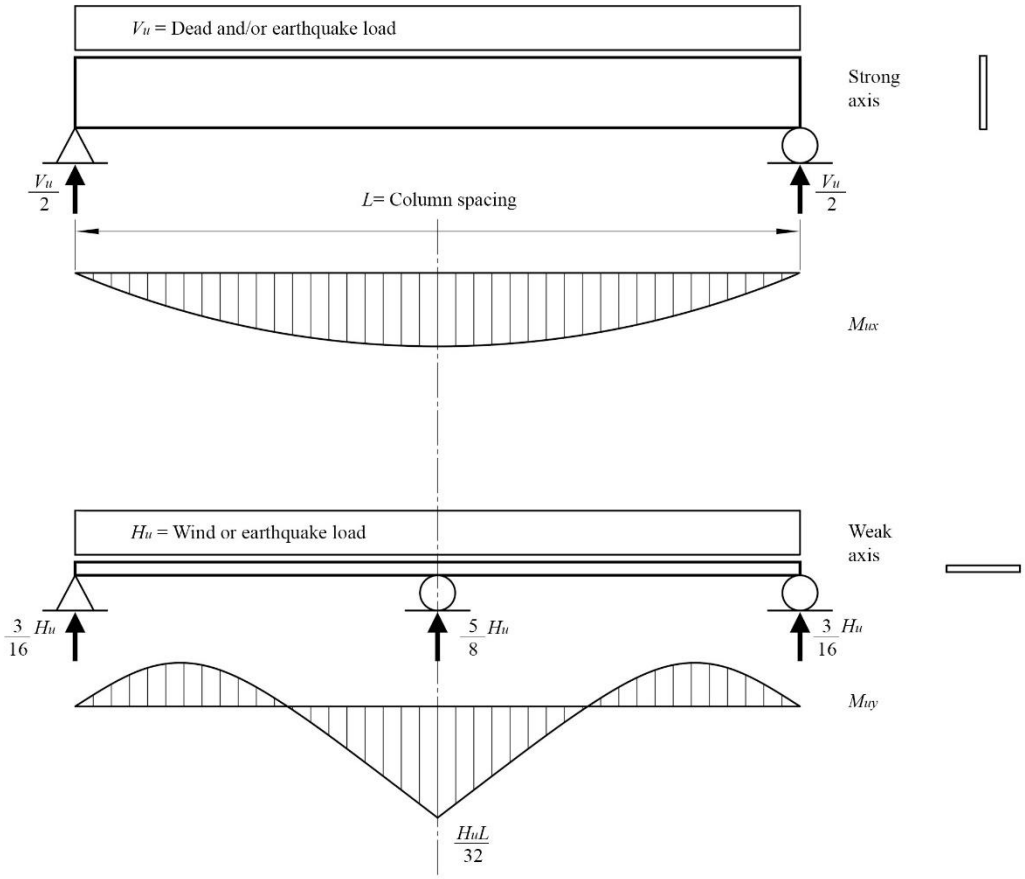

Figure 8-14. Spandrel Panel Bending Moments

Basic Load Combination 1: $1.4D$ (ASCE/SEI 7-22 Sec. 2.3.1)

$V_u = 1.4D$ (vertical downward force)

$V_u = 1.4(10{,}245 \text{ lb}) = 14{,}343 \text{ lb}$

$M_{ux} = \frac{V_u L}{8} = \frac{(14{,}343 \text{ lb})(24 \text{ ft})}{8} = 43{,}029 \text{ lb-ft}$ (strong axis bending moment)

Basic Load Combination 6: $1.2D + E_v + E_h + L + 0.2S$ (ASCE/SEI 7-22 Sec. 2.3.1)

$V_{u,max} = 1.2D + E_v$ (vertical downward force)

$V_{u,max} = 1.2(10{,}245 \text{ lb}) + 3{,}047 \text{ lb} = 15{,}341 \text{ lb}$

$\parallel H_u = E_h = 4{,}570$ lb (horizontal load parallel to panel)

$\perp H_u = E_h = 4{,}570$ lb (horizontal load perp. to panel)

$M_{ux,max} = \frac{V_{u,max}L}{8} = \frac{(15{,}341 \text{ lb})(24 \text{ ft})}{8} = 46{,}023$ lb-ft (strong axis bending moment)

$M_{uy} = \frac{H_u L}{32} = \frac{(4{,}570 \text{ lb})(24 \text{ ft})}{32} = 3{,}428$ lb-ft (weak axis bending moment)

Basic Load Combination 7: $0.9D - E_v + E_h$ (ASCE/SEI 7-22 Sec. 2.3.1)

$V_{u,min} = 0.9D - E_v$ (vertical downward force)

$V_{u,min} = 0.9(10{,}245 \text{ lb}) - 3{,}047 \text{ lb} = 6{,}174$ lb (gravity exceeds earthquake uplift)

$\parallel H_u = E_h = 4{,}570$ lb (horizontal load parallel to panel)

$\perp H_u = E_h = 4{,}570$ lb (horizontal load perp. to panel)

$M_{ux,min} = \frac{V_{u,min}L}{8} = \frac{(6{,}174 \text{ lb})(24 \text{ ft})}{8} = 18{,}521$ lb-ft (strong axis bending moment)

$M_{uy} = \frac{H_u L}{32} = \frac{(4{,}570 \text{ lb})(24 \text{ ft})}{32} = 3{,}428$ lb-ft (weak axis bending moment)

8.3.4.4 PRESCRIBED SEISMIC DISPLACEMENTS

The prescribed seismic displacements are not applicable to the spandrel panel wall element because all connections are virtually at the same elevation. Refer to Section 8.3.2 of these Design Examples for a description of the precast panel mechanism to accommodate drift.

8.3.5 Spandrel Panel – Fasteners of the Connecting System

8.3.5.1 PRESCRIBED SEISMIC FORCES

ASCE/SEI 7-22 specifies an increased C_{AR} for "fasteners of the connecting system" with the intention of preventing premature failure in those elements of connections that are inherently brittle, such as embedded items that depend on concrete breakout strength, or connection elements that are simply too small to adequately dissipate energy inelastically, such as welds, bolts, inserts, and dowels.

Spandrel panel and glass weight, W_p

$D = 8{,}775 \text{ lb} + 1{,}470 \text{ lb} = 10{,}245$ lb (dead load)

$W_p = D = 10{,}245$ lb (component weight)

Seismic design force, F_p

$$F_p = 0.4 S_{DS} I_p W_p \left[\frac{H_f}{R_\mu}\right] \left|\frac{C_{AR}}{R_{po}}\right| \quad \text{(ASCE/SEI 7-22 Eq. 13.3-1)}$$

$$F_p = 0.4(1.487)(1.0)\left(W_p\right) \left[\frac{1.74}{1.71}\right] \left|\frac{2.8}{1.5}\right| = 1.129 W_p \quad \text{(controlling equation)}$$

$$F_{p,max} = 1.6 S_{DS} I_p W_p \quad \text{(ASCE/SEI 7-22 Eq. 13.3-2)}$$

$$F_{p,max} = 1.6(1.487)(1.0)\left(W_p\right) = 2.379 W_p$$

$$F_{p,min} = 0.3 S_{DS} I_p W_p \quad \text{(ASCE/SEI 7-22 Eq. 13.3-3)}$$

$$F_{p,min} = 0.3(1.487)(1.0)\left(W_p\right) = 0.446 W_p$$

$$F_p = 1.1291 W_p = 1.129(10{,}245 \text{ lb}) = 11{,}568 \text{ lb} \quad \text{(controlling seismic design force)}$$

Horizontal seismic load effect, E_h

$$Q_E = F_p = 11{,}568 \text{ lb} \quad \text{(effect from } F_p\text{)}$$

$$E_h = \rho Q_E \quad \text{(ASCE/SEI 7-22 Eq. 12.4-3)}$$

$$E_h = (1.0)(11{,}568 \text{ lb}) = 11{,}568 \text{ lb}$$

Vertical seismic load effect, E_v

$$E_v = 0.2 S_{DS} D \quad \text{(ASCE/SEI 7-22 Eq. 12.4-4a)}$$

$$E_v = (0.2)(1.487\text{g})(10{,}245 \text{ lb}) = 3{,}047 \text{ lb}$$

The above terms are then substituted into the following Basic Load Combinations for Strength Design from ASCE/SEI 7-22 Sections 2.3.6 and 12.4.2 to determine the design member and connection forces to be used in conjunction with seismic loads.

$$1.2D + E_v + E_h + L + 0.2S \quad \text{(ASCE/SEI 7-22 Load Combination 6)}$$

$$0.9D - E_v + E_h \quad \text{(ASCE/SEI 7-22 Load Combination 7)}$$

For nonstructural components, the terms L and S are typically zero.

For this example, the seismic design force, F_p, determined with Eq. 13.3-1 almost triples when compared to the spandrel panel wall element calculations.

Where required for nonductile anchorage to concrete and masonry, the nonstructural component overstrength factor, Ω_{0p}, given in Table 13.5-1 for "fasteners of the connecting system" is set as 1.0.

8.3.5.2 PROPORTIONING AND DESIGN

"Fasteners of the Connecting System" Definition

Requirement 4 in ASCE/SEI 7-22 Section 13.5.3 defines bolts, inserts, welds, and dowels as "fasteners of the connecting system." Nonetheless, for other connecting elements in concrete wall panels such as steel rods, tubes, angles, and kickers, the transition between "wall element," "body of wall panel connections," and "fasteners of the connecting system" per Table 13.5-1 is not explicitly defined in ASCE/SEI 7-22.

The "fasteners of the connecting system" category is intended to apply to the connections with limited ductility that can have a brittle failure mechanism. Engineering judgement is required to identify these elements, as higher seismic design forces are applied for their design.

The bolted tie-back connections shown in Figure 8-13, in addition to the welds and bolts, are recommended to be designed using the higher "fastener" seismic design forces, F_p. The angle bracing and connecting plates, if designed adequately, behave in a ductile manner and can be sized using the lower seismic forces for "body of wall panel connections."

The design of the connection fasteners is not illustrated in this example. They should be designed for the loads calculated below, in accordance with ACI 318-19 Chapter 17 and ANSI/AISC 360-22. There are special reduction factors for anchorage in high seismic demand locations, such as factors for anchors in cracked concrete, and those reduction factors would apply to this example. The spandrel panel connection forces are shown in Figure 8-15. The vertical forces, V_u, horizontal forces, H_u, and moments, M_u, are calculated using the applicable strength load combinations. In Figure 8-15, the top push-pull connection is attached directly to the top of the beam. When the perimeter beam is part of a moment frame, the connection cannot be made in the protected zone of the moment frame beam, and an attached such as the one shown in Figure 8-13 could be used, where the push-pull connection is attached to the concrete slab.

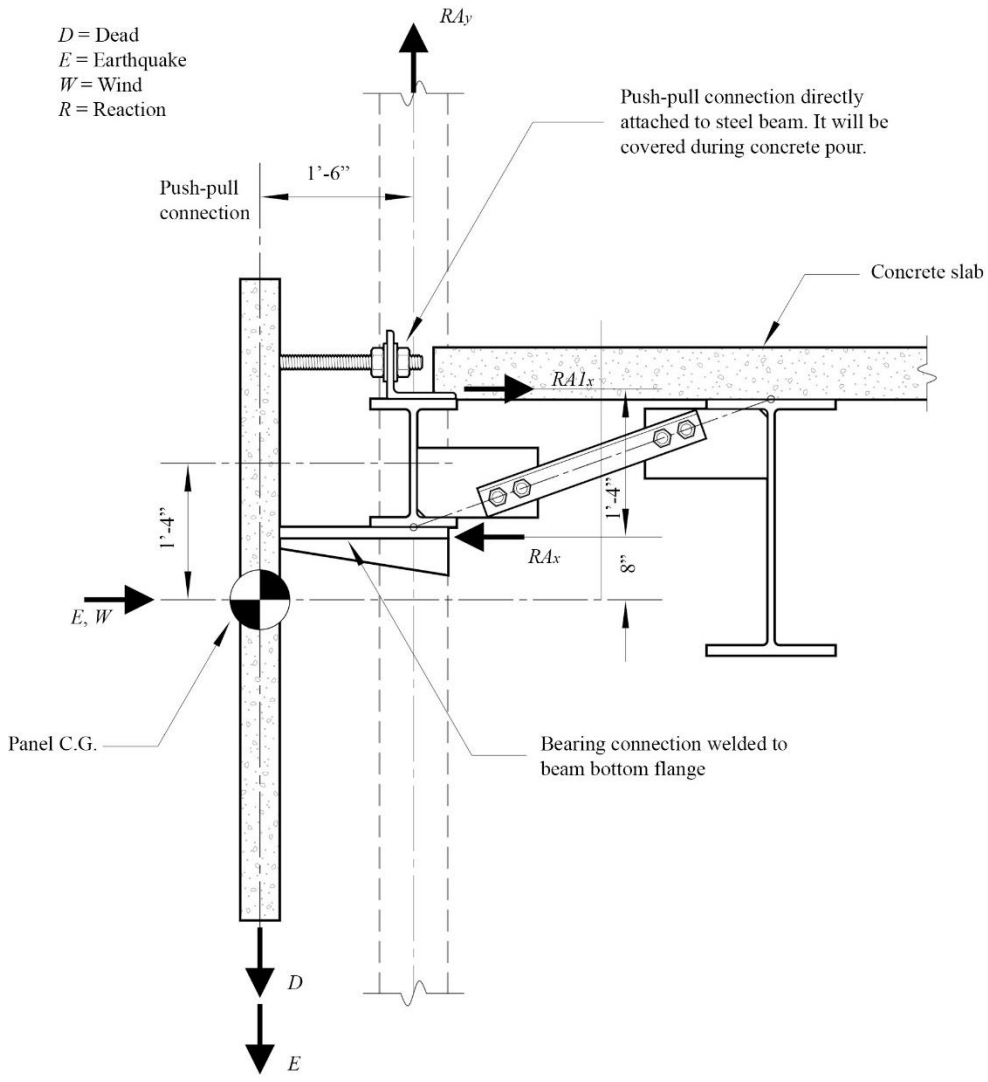

Figure 8-15. Spandrel Panel Connection and Design Forces

Basic Load Combination 1: $1.4D$ (ASCE/SEI 7-22 Sec. 2.3.1)

$V_{uA} = \left(\frac{1}{2}\right) 1.4D$ (vertical force at each Point A)

$V_{uA} = \left(\frac{1}{2}\right)(1.4)(10{,}245 \text{ lb}) = 7{,}172 \text{ lb}$

$M_{uA} = V_{uA}(1.5 \text{ ft plan eccentricity})$ (moment resisted by Points A and A1)

$M_{uA} = (7{,}172 \text{ lb})(1.5 \text{ ft plan eccentricity}) = 10{,}757 \text{ lb-ft}$

$H_{uA} = H_{uA1} = \frac{M_{uA}}{1.333 \text{ ft}}$ (horizontal couple from moment at Points A and A1 which are

separated vertically by 1.333 ft, noted as *RA1x* and *RAx* in Figure 8-15)

$$H_{uA} = H_{uA1} = \frac{10{,}757 \text{ lb-ft}}{1.333 \text{ ft}} = 8{,}068 \text{ lb}$$

Basic Load Combination 6: $1.2D + E_v + E_h + L + 0.2S$ (ASCE/SEI 7-22 Sec. 2.3.1)

$V_{uA,max} = \left(\frac{1}{2}\right)(1.2D + E_v)$ (vertical downward force)

$$V_{uA,max} = \left(\frac{1}{2}\right)(1.2(10{,}245 \text{ lb}) + 3{,}047 \text{ lb}) = 7{,}670 \text{ lb}$$

$\| H_{uA} = \left(\frac{1}{2}\right) E_h = \left(\frac{1}{2}\right)(11{,}568 \text{ lb}) = 5{,}784 \text{ lb}$ (horizontal load parallel to panel at Point A)

$M_{uA} = \| H_{uA}(1.5 \text{ ft})$ (flexural moment at Points A and A1)

$$M_{uA} = (5{,}784 \text{ lb})(1.5 \text{ ft plan eccentricity}) = 8{,}676 \text{ lb-ft}$$

$\perp H_{uA} = \left(\frac{3}{16}\right) E_h$ (horizontal load perpendicular to panel at Points A and A1)

$$\perp H_{uA} = \left(\frac{3}{16}\right)(11{,}568 \text{ lb}) = 2{,}169 \text{ lb}$$

$H_{uA,in} = V_{uA,max}\left(\frac{1.5 \text{ ft}}{1.333 \text{ ft}}\right) + \perp H_{uA}\left(\frac{2.0 \text{ ft}}{1.333 \text{ ft}}\right)$ (inward force at Point A, noted as *RA1x* and *RAx* in Figure 8-15)

$$H_{uA,in} = (7{,}670 \text{ lb})\left(\frac{1.5 \text{ ft}}{1.333 \text{ ft}}\right) + (2{,}169 \text{ lb})\left(\frac{2.0 \text{ ft}}{1.333 \text{ ft}}\right) = 11{,}883 \text{ lb}$$

$H_{uA1,out} = V_{uA,max}\left(\frac{1.5 \text{ ft}}{1.333 \text{ ft}}\right) + \perp H_{uA}\left(\frac{0.667 \text{ ft}}{1.333 \text{ ft}}\right)$ (outward force at Point A1, noted as *RA1x* and *RAx* in Figure 8-15)

$$H_{uA1,out} = (7{,}670 \text{ lb})\left(\frac{1.5 \text{ ft}}{1.333 \text{ ft}}\right) + (2{,}169 \text{ lb})\left(\frac{0.667 \text{ ft}}{1.333 \text{ ft}}\right) = 9{,}714 \text{ lb}$$

$\perp H_{uB} = \left(\frac{5}{8}\right) E_h$ (horizontal load perpendicular to panel at Points B and B1)

$$\perp H_{uB} = \left(\frac{5}{8}\right)(11{,}568 \text{ lb}) = 7{,}230 \text{ lb}$$

$H_{B,in/out} = \perp H_{uB}\left(\frac{2.0 \text{ ft}}{1.333 \text{ ft}}\right)$ (inward or outward force at Point B)

$$H_{B,in/out} = (7{,}230 \text{ lb})\left(\frac{2.0 \text{ ft}}{1.333 \text{ ft}}\right) = 10{,}845 \text{ lb}$$

$$H_{B1,in/out} = \perp H_{uB}\left(\frac{0.667 \text{ ft}}{1.333 \text{ ft}}\right) \quad \text{(inward or outward force at Point B1)}$$

$$H_{B1,in/out} = (7{,}230 \text{ lb})\left(\frac{0.667 \text{ ft}}{1.333 \text{ ft}}\right) = 3{,}615 \text{ lb}$$

Basic Load Combination 7: $0.9D - E_v + E_h$ (ASCE/SEI 7-22 Sec. 2.3.1)

$$V_{uA,min} = \left(\frac{1}{2}\right)(0.9D - E_v) \quad \text{(vertical downward force)}$$

$$V_{uA,min} = \left(\frac{1}{2}\right)(0.9(10{,}245 \text{ lb}) - 3{,}047 \text{ lb}) = 3{,}087 \text{ lb}$$

The minimum vertical reaction at Point A, $V_{uA,min}$, is positive, thus, no uplift occurs in the bearing connections, as the net reaction at Point A is downward. The horizontal seismic load effect, E_h, is the same for the Basic Load Combinations 6 and 7; however, the combination with the other loads using the Basic Load Combination 6 provides the controlling maximum forces for design.

As depicted in this example, the direction of the horizontal forces, i.e., inward or outward, leads to different demands, depending on the eccentricity between the connections and the element center of mass. Only the maximum reactions are computed.

8.3.5.3 PRESCRIBED SEISMIC DISPLACEMENTS

The interstory drift is accommodated in the spandrel panels and window glazing. The spandrel panels move with the floors. The glazing deforms as a parallelogram. Typically, this is accommodated by rotation of the glazing units within the mullions, head, and sill that bound the glazing. The prescribed seismic displacements are not applicable to the spandrel panel because all connections are virtually at the same elevation. Refer to Section 8.3.2 of this design example for a description of the precast panel mechanism to accommodate drift.

8.3.6 Column Cover

8.3.6.1 CONNECTION LAYOUT

The precast column cover is supported by the steel column. Figure 8-16 shows the key to the connection types at each column cover connection. Figure 8-17 shows details of how the forces are resisted.

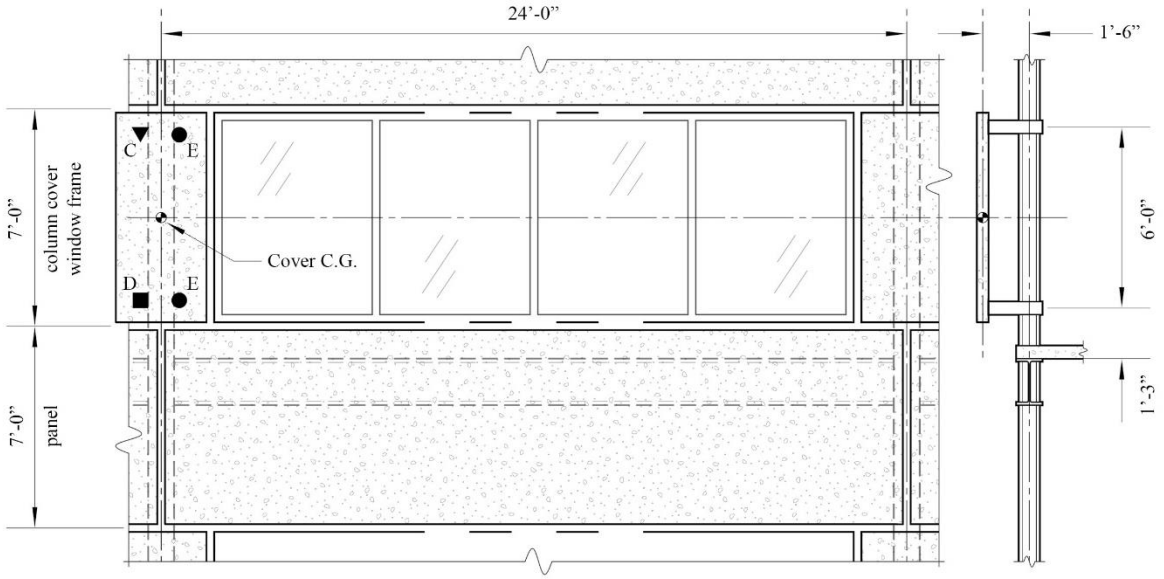

Figure 8-16. Column Cover Connection Layout

Vertical loads, horizontal loads parallel to the panel (the "in-plane" direction) and horizontal loads perpendicular to the panel (the "out-of-plane" direction) are resisted at Point C. The 1'-6" plan eccentricity of vertical loads is resisted by a horizontal force couple at Points 'C and D. The horizontal load parallel to the panel eccentricity between the panel and the support is resisted in flexure of the connection at Point 'C'. This connection is designed to take the loads directly to the column.

In-plane horizontal loads parallel to the panel are resisted at Point D. The eccentricity between center of mass of the panel and the reaction at the vertical support generates a moment that is resisted by a force couple of Points C and D. The eccentricity of horizontal loads parallel to the panel is resisted by flexure at the connection at Point D. The connection is designed so as not to restrict vertical movement of the panel due to thermal effects or seismic input. The connection is designed to take the loads directly to the columns.

Out-of-plane horizontal loads perpendicular to the panel are resisted equally at Points C and D and the two points identified as Points E. The connections are designed to take the loads directly to the columns. There is no load eccentricity associated with the horizontal loads perpendicular to the panel.

This connection scheme at the column cover accommodates story drift by a rocking mechanism, which is more compatible with glazed curtain wall displacement behavior (racking) than one that relies on sliding.

In this example, all connections are made to the sides of the column because usually there is not enough room between the outside face of the column and the inside face of the cover to allow a feasible load-carrying connection.

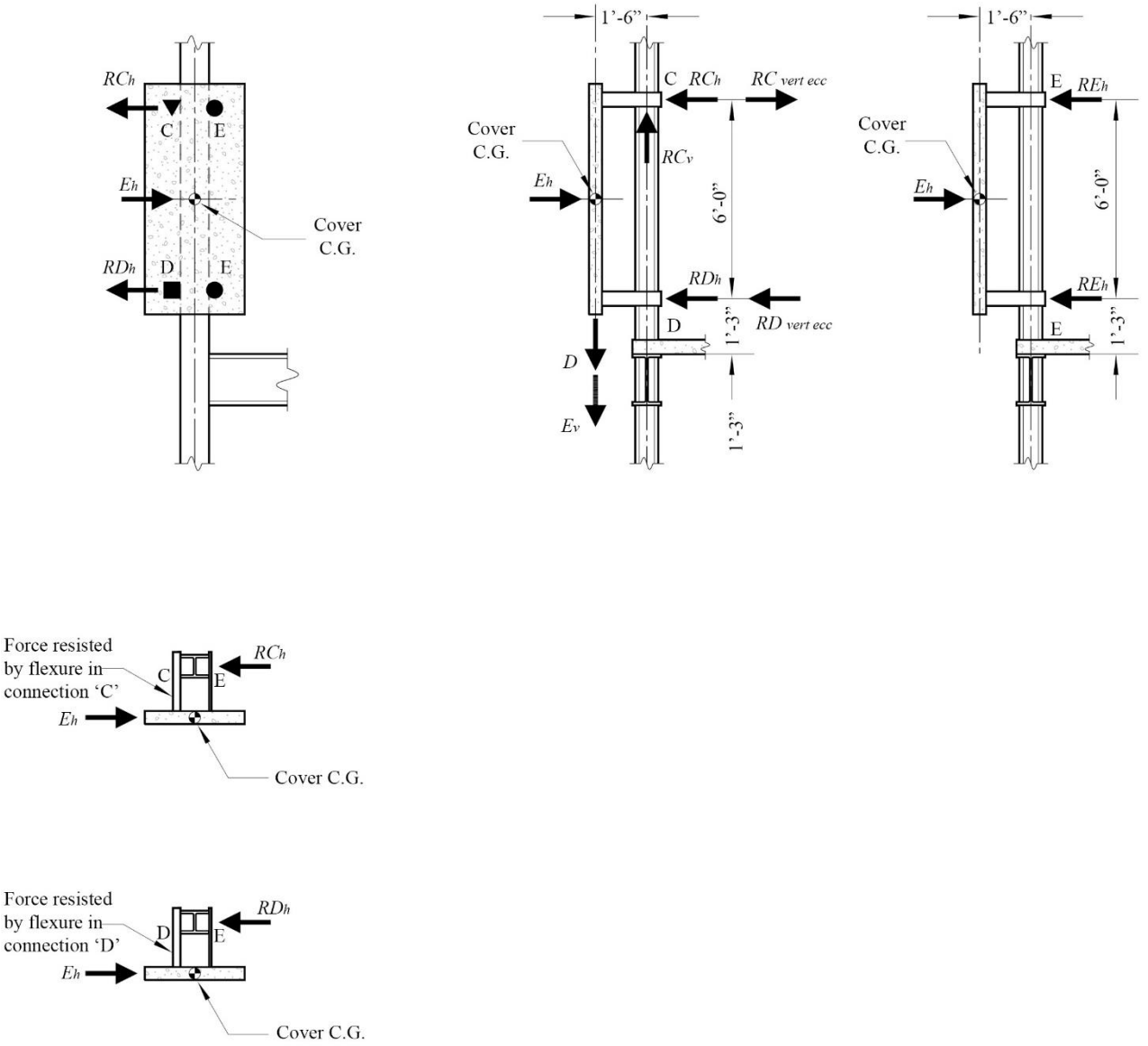

Figure 8-17. Column Cover Panel Connection Forces

8.3.6.2 PRESCRIBED SEISMIC FORCES

The calculation of prescribed seismic forces for the column cover is not shown in this example. They should be determined in the same manner as illustrated for the spandrel panels.

8.3.6.3 PRESCRIBED SEISMIC DISPLACEMENTS

The results of an elastic analysis of the building structure are not always available in time for use in the design of the precast cladding system. As a result, prescribed seismic displacements are usually calculated based on allowable story drift requirements. The allowable story drift is in Table 12.12-1 of ASCE/SEI 7-22. Since this is a five-story building, does not use masonry in the primary seismic

force-resisting system, and it is in Risk Category II, then the allowable story drift is $0.020h_{sx}$. Refer to Section 8.3.2 of this design example for a description of the precast panel mechanism to accommodate drift.

Seismic relative displacements, D_{pI}

$h_{sx} = 13.5\mathrm{ft}$ (story height)

$h_x = 47.75\mathrm{ft}$ (height of upper support attachment)

$h_y = 41.75\mathrm{ft}$ (height of lower support attachment)

$\Delta_{aA} = 0.020h_{sx}$ (ASCE/SEI 7-22 Table 12.12-1)

$D_p = \frac{(h_x - h_y)\Delta_{aA}}{h_{sx}}$ (ASCE/SEI 7-22 Eq.13.3-10)

$D_p = \frac{(47.75\mathrm{ft} - 41.75\mathrm{ft})(12\ \mathrm{in./ft})(0.020h_{sx})}{h_{sx}} = 1.44\ \mathrm{in.}$

$D_{pI} = D_p I_e = (1.44\ \mathrm{in.})(1.0) = 1.44\ \mathrm{in.}$ (ASCE/SEI 7-22 Eq. 13.3-8)

The joints at the top and bottom of the column cover must be designed to accommodate an in-plane relative displacement of 1.44 inches. The column cover will rotate somewhat as these displacements occur, depending on the nature of the connections to the column. If the supports at one level are “fixed” to the columns while the other level is designed to “float”, that is, free to allow vertical movement, then the rotation will be that of the column at the point of attachment.

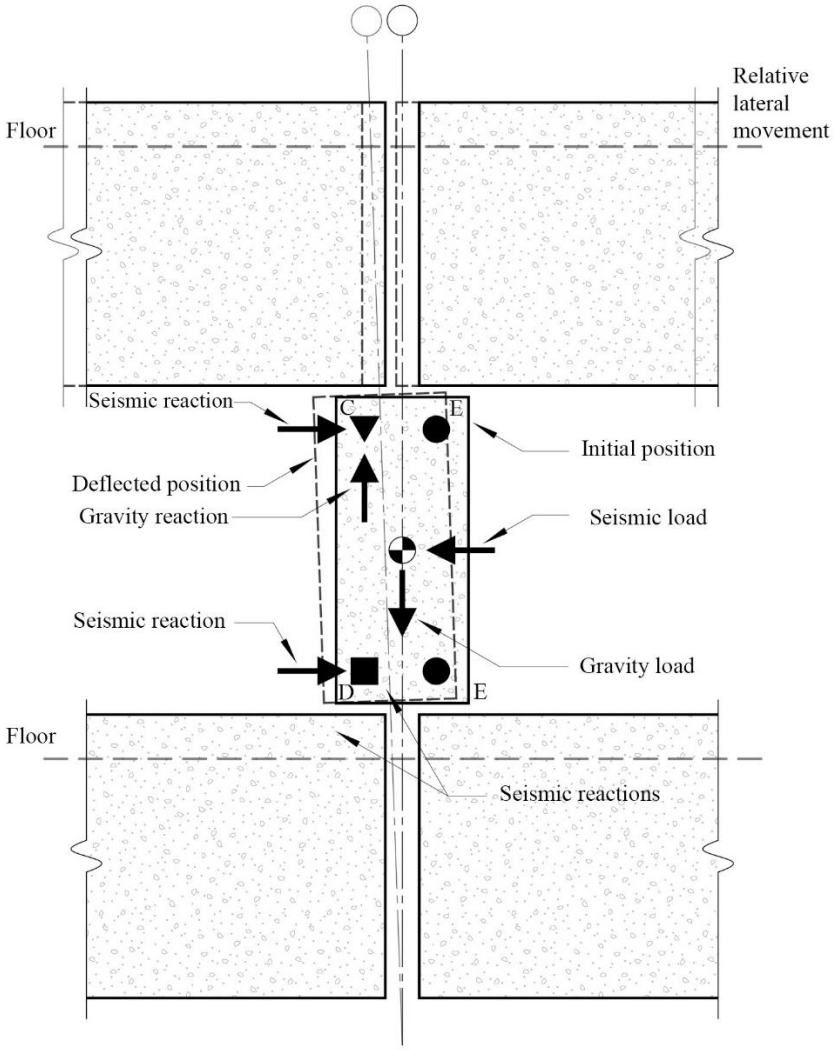

Figure 8-18. Column Panel Deformation

The connections accommodating story drift through sliding mechanism or bending of threaded steel rods shall satisfy several requirements, per ASCE/SEI 7-22 Section 13.5.3. For instance, threaded rods or bolts in these applications should be fabricated of low-carbon or stainless steel. Where cold-worked carbon steel threaded rod is used, the rods as fabricated shall meet or exceed the reduction of area, elongation, and specified tensile strength requirements. For sliding connections utilizing slotted or oversized holes, the rods shall have length to diameter ratios of 4 or less, where the length is the clear distance between the nuts or threaded plates. The slots or oversized holes shall be proportioned to accommodate the full in-plane design story drift in each direction.

In connections that accommodate story drift by bending of the threaded rod, the following equation shall be satisfied in order to provide a sufficient level of flexibility:

$$(L/d)/D_{pI} \geq 6.0[1/\text{in.}] \qquad \text{(ASCE/SEI 7-22 Eq.13.5-1)}$$

where:

L = clear length of rod between nuts or threaded plates [in.]

d = rod diameter [in.]

Consider a ½ inch diameter threaded rod with a clear length of the rod of 10 inches is selected:

$$(10 \text{ in.}/0.5 \text{ in.})/(1.44 \text{ in.}) = 13.9 \text{ in.}^{-1} \geq 6.0 \text{ in.}^{-1} \qquad \text{(ASCE/SEI 7-22 Eq.13.5-1)}$$

The threaded rod geometry complies with this requirement.

8.3.7 Additional Design Considerations

8.3.7.1 PERFORMANCE INTENT FOR GLAZING IN EARTHQUAKES

ASCE/SEI 7-22 Commentary Section C13.5.9, "Glass in Glazed Curtain Walls, Glazed Storefronts, and Glazed Partitions," provides a helpful statement of the performance intent for glass in earthquakes in response to interstory drift, which is quoted here:

The performance of glass in earthquakes falls into one of four categories:

1. *The glass remains unbroken in its frame or anchorage.*
2. *The glass cracks but remains in its frame or anchorage while continuing to provide a weather barrier and be otherwise serviceable.*
3. *The glass shatters but remains in its frame or anchorage in a precarious condition, likely to fall out at any time.*
4. *The glass falls out of its frame or anchorage, either in fragments, shards, or whole panels.*

Categories 1 and 2 provide both Immediate Occupancy and Life Safety Performance Objectives. Although the glass is cracked in Category 2, immediate replacement is not required. Categories 3 and 4 cannot provide for immediate occupancy, and their provision of life safety depends on the post-breakage characteristic of the glass and the height from which it can fall. Tempered class shatters into multiple, pebble-size fragments that fall from the frame or anchorage in clusters. These broken glass clusters are relatively harmless to humans when they fall from limited heights, but they could be harmful when the fall from greater heights.

The window frame system typically accommodates in-plane relative displacement by clearance between the glass and the frame. ASCE/SEI 7-22 Section 13.5.9.1 prescribes a method for checking this clearance. It requires that the clearance be large enough so that the glass panel will not fall out of the frame as required by the Equation 13.5-2 or 0.5", whichever is larger.

$$\Delta_{fallout} \geq 1.25 D_{pl} \qquad \text{(ASCE/SEI 7-22 Equation 13.5-2)}$$

where:

$\Delta_{fallout}$ = the relative seismic displacement (drift) at which glass fallout from the curtain wall, storefront, or partition occurs.

D_{pl} = the relative seismic displacement that the component must be designed to accommodate. And which shall be applied over the height of the glass component.

I_e = the building Importance Factor.

There are four ways to show this:

1. By test per ASCE/SEI 7-22 Section 13.5.9.2 or engineering analysis. The test is AAMA 501.6, *Recommended Dynamic Test Method for determining the Seismic Drift Causing Glass Fallout from a Wall System* (AAMA, 2018).

2. Use the prescriptive formula in ASCE/SEI 7-22 Section 13.5.9.1 Exception 1, as discussed below.

3. Use the prescriptive requirements of ASCE/SEI 7-22 Section 13.5.9.1 Exception 2 (fully tempered monolithic glass in Risk Category I, II, or III and less than 10 feet above a walking surface).

4. Use the prescriptive requirements of ASCE/SEI 7-22 Section 13.5.9.1 Exception 3 (annealed or heat-strengthened laminated glass in single thickness with interlayer no less than 0.030 in. that is captured mechanically in a wall system glazing pocket, and whose perimeter is secured to the frame by a wet glazed gunable curing elastomeric sealant perimeter bead of ½ in. (13 mm) minimum glass contact width, or other approved anchorage system).

For the prescriptive formula in ASCE/SEI 722 Section 13.5.9.1 Exception 1, the equations are based on the principle that a rectangular window frame anchored mechanically to adjacent stories of the primary structural system of the building becomes a parallelogram as a result of interstory drift and that glass-to-frame contact occurs when the length of the shorter diagonal of the parallelogram is equal to the diagonal of the glass panel itself. A formula is provided as follows.

$$D_{clear} = 2c_1\left(1 + \frac{h_p c_2}{b_p c_1}\right)$$ (ASCE/SEI 7-22 Sec. 13.5.9.1, Exception 1)

where:

h_p = height of the rectangular glass panel

b_p = width of the rectangular glass panel

c_1 = average of clearances on both sides between the vertical glass edges and the frame

c_2 = average of clearances at the top and bottom between the horizontal glass edges and the frame

Figures 8-19 and 8-20 illustrate the basis of this equation, showing four "scenarios." For these figures, c_1 is assumed to be the same on each side, and c_2 is the same at the top and bottom (except in Scenario 4). The common simplifications for small angle geometry are made so that the height differences between h_p and $c_2 + h_p$ are ignored.

Scenario 1 is when the glass does not move at all and the frame racks as a parallelogram and the top of the right side of the frame comes in contact with the glass. This permits a drift of up to c_1.

Scenario 2 occurs after Scenario 1 and is when the glass translates as the frame pushes it to the left until there is contact between the bottom left corner of the glass and the bottom of the left side of the frame. This permits a drift of up to $2c_1$.

Scenario 3 is where the translation of Scenario 2 is combined with counterclockwise rotation of the glass. In Scenario 3, the glass is assumed to be able to rotate such that the bottom left corner moves down (such as in a flexible sealant) in the c_2 clearance at the base, and the top right moves up into the c_2 clearance at the top. Combining the Scenario 2 drift with the rotation leads to the ASCE/SEI 7-22 Section 13.5.9.1 Exception 1 equation such that the permitted drift is up to $D_{clear} = 2\ c_1\ (1 + (h_p c_2 / b_p c_1))$. As part of the small angle geometry assumption, the shortening of the height of the parallelogram as it racks is ignored.

Scenario 4 is similar to Scenario 3, except that there is no effective clearance at the base because the glass rests on two seating blocks or shims that have negligible ability to compress. This is a common approach used by cladding subcontractors, and it is what is illustrated in the figures of Section 8.3.2 of this chapter. There is no downward movement on the toe shim as the glass rotates. However, since the definition of c_2 is that it is the average of the top and the bottom (zero), then the top clearance has to be equal to $2c_2$ to get the average to be c_2. So the same equation applies. In Figure 8-20, the seating blocks are conservatively assumed to be located at the ends of the glass. In actual practice, they are often located inboard from the ends, such as at the quarter point and three-quarter point along the base of the glass. In such a situation, some rotation about the seating block nearest the toe will occur and downward movement of the glass into the bottom of the frame is possible. This will increase the lateral drift to a value between that shown in Scenario 3 and Scenario 4.

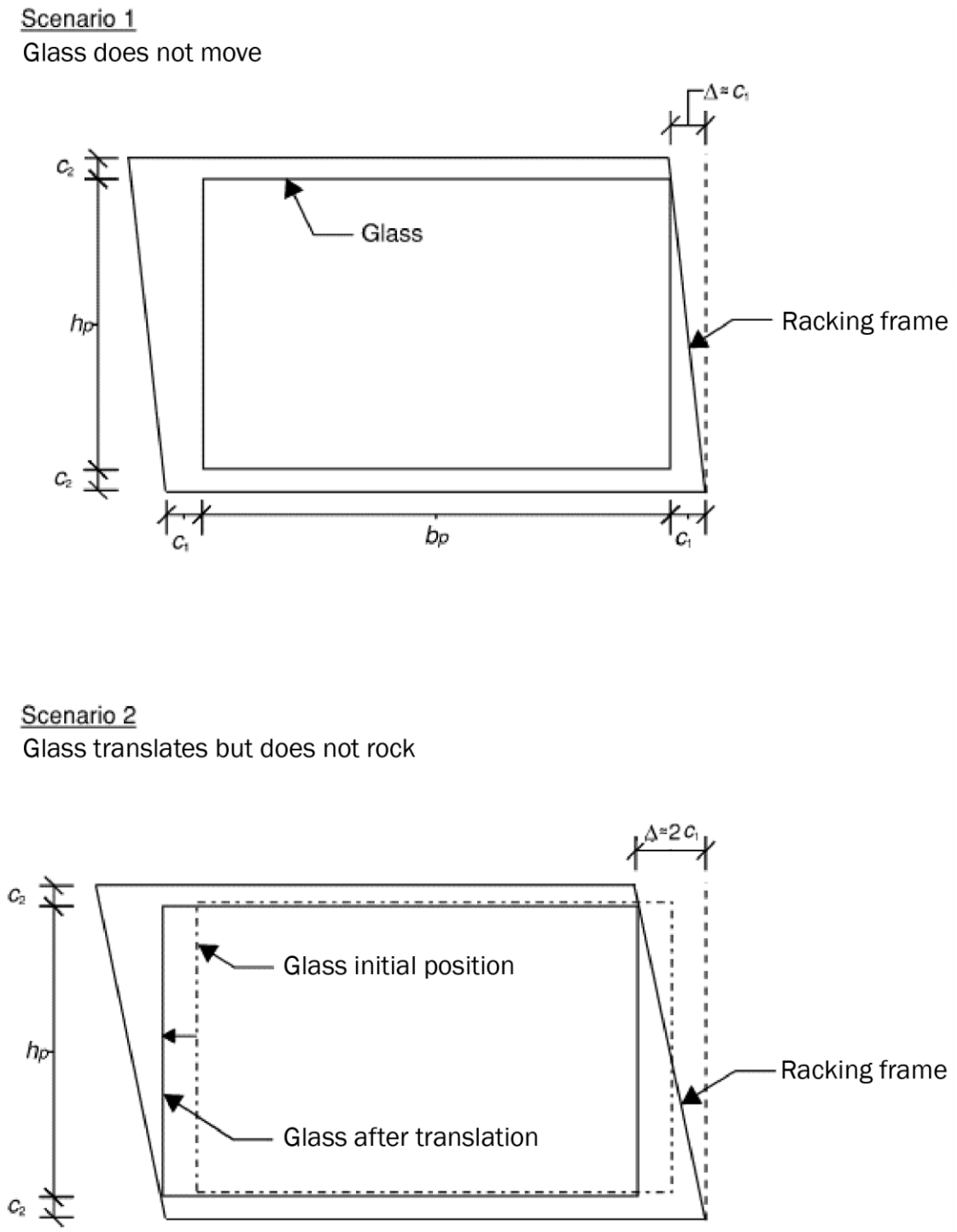

Figure 8-19. Glazing Drift – Scenarios 1 and 2

Scenario 3

Glass translates and rocks with vertical movement at both sill and head

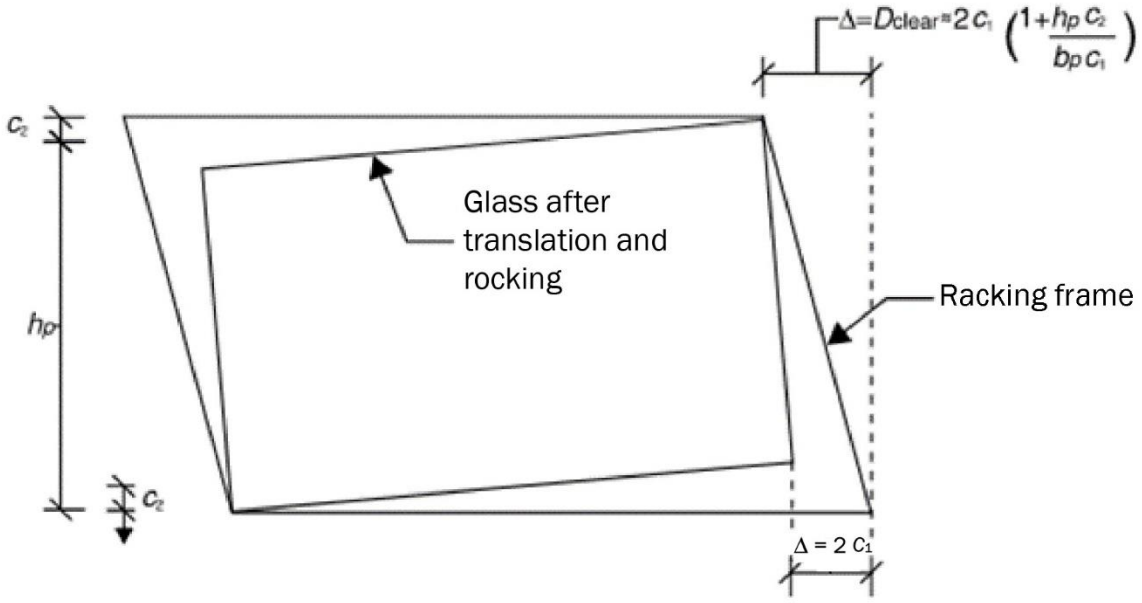

Scenario 4

Glass translates and rocks on seating block

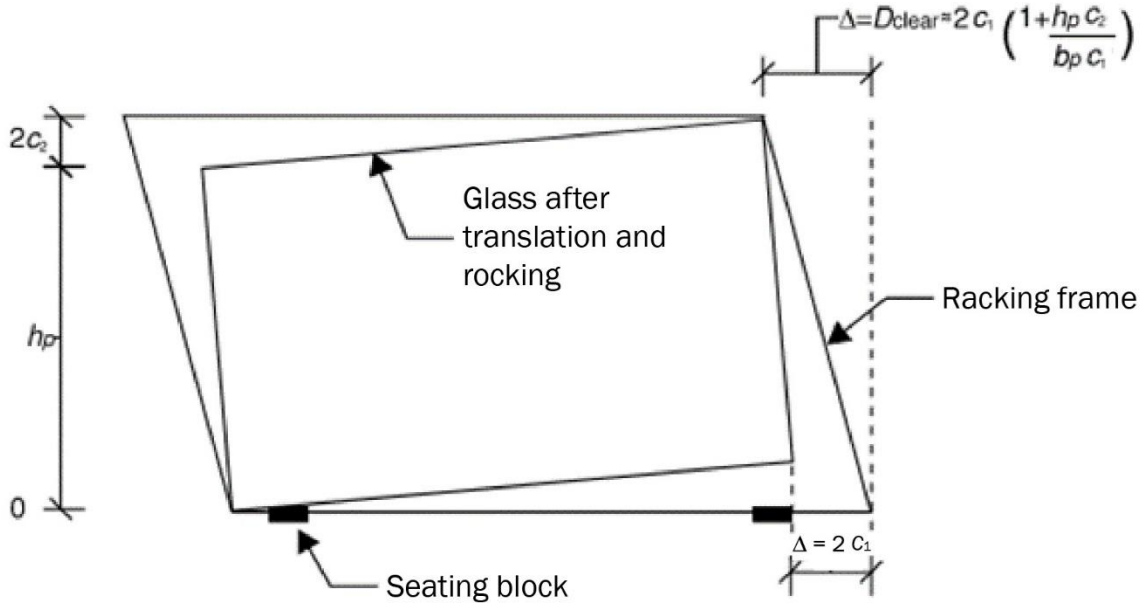

Figure 8-20. Glazing Drift – Scenarios 3 and 4

8.3.7.2 WINDOW FRAME SYSTEM

The window frame system is supported by the spandrel panels above and below. Assuming that the spandrel panels move in-plane with each floor level and are rigid when subject to in-plane forces, the window frame system shall accommodate the entire prescribed seismic displacement based on the full story height.

$h_{sx} = h_x - h_y = 13.5 \text{ ft}$ (story height)

$\Delta_{aA} = 0.020 h_{sx}$ (ASCE/SEI 7-22 Table 12.12-1)

$D_p = \frac{(h_x - h_y)\Delta_{aA}}{h_{sx}}$ (ASCE/SEI 7-22 Eq 13.3-10)

$D_p = \frac{(13.5 \text{ ft})(12 \text{ in./ft})(0.020 h_{sx})}{h_{sx}} = 3.24 \text{ in.}$

$D_{pI} = D_p I_e = (3.24 \text{ in.})(1.0) = 3.24 \text{ in.}$ (ASCE/SEI 7-22 Eq. 13.3-8)

The window frame system must be designed to accommodate an in-plane relative displacement of 3.24 inches between the top and bottom spandrels. This is accommodated by a clearance between the glass and the frame.

Based on the glass panel geometry, and the previous calculations: $h_p = 7$ ft, $b_p = 5$ ft, and $D_{pI} = 3.24$ in.

Setting $c_1 = c_2$, the minimum required clearance is:

$D_{clear} \geq 1.25 D_{pI}$ (ASCE/SEI 7-22 Eq. 13.5-3)

$D_{clear} = 1.25(3.24 \text{ in.}) = 4.05 \text{ in.}$

Solving D_{clear} equation for c_1:

$D_{clear} = 2c_1 \left(1 + \frac{h_p c_2}{b_p c_1}\right)$ (ASCE/SEI 7-22 Sec. 13.5.9.1, Exception 1)

$4.05 \text{ in.} = 2c_1 \left(1 + \frac{(7 \text{ ft})c_1}{(5 \text{ ft})c_1}\right) = 4.80 c_1$

The required clearance is $c_1 = c_2 = 0.84$ in.

8.3.7.3 BUILDING CORNERS

Some thought needs to be given to seismic behavior at external building corners. The preferred approach is to detail the corners with two separate panel pieces, mitered at a 45-degree angle, with high grade sealant between the sections. An alternative choice of detailing L-shaped corner pieces introduces more seismic mass and load eccentricity into connections on both sides of the corner

column, and it may also trigger the need for wider joints between the column cover and adjacent glazing and curtain wall units to prevent interaction under story drift. This is often the case if panels that accommodate story drift by rocking or rotation are adjacent to panels that do not rock or rotate, such as the spandrel in this example.

8.3.7.4 DIMENSIONAL COORDINATION

It is important to coordinate dimensions with the architect and structural engineer. Precast concrete panels must be located a sufficient distance from the building structural frame to allow room for the design of efficient load transfer connection pieces. However, distances must not be so large as to increase unnecessarily the load eccentricities between the panels and the frame.

8.4 Seismic Analysis of Egress Stairs

8.4.1 Example Description

Example Summary

- **Nonstructural components**
  Architectural – egress stairways not part of the building seismic force-resisting system
  Architectural – egress stair and ramp fasteners and attachments
- **Building seismic force-resisting systems**
  East–west direction: steel special concentrically braced frames
  North–south direction: steel special moment frames
- **Equipment support:** Not applicable
- **Occupancy:** Emergency medical facility
- **Risk Category:** IV
- **Component Importance Factor:** $I_p = 1.5$
- **Number of stories:** 5
- $\boldsymbol{S_{DS}} = 1.00$

Egress stairs are an essential part of the system used to evacuate building occupants following an earthquake. Failure of the stairs may trap building occupants on the upper levels of the structure. Ladders on emergency vehicles can usually only reach the lower floors in mid- and high-rise structures. This was especially prevalent in the 2011 Christchurch Earthquake. In recognition of their importance, egress stairs are assigned a Component Importance Factor, $I_p = 1.5$.

The ASCE/SEI 7-22 includes specific requirements intended to limit damage and improve functionality after an earthquake for egress stairs not part of the building seismic force-resisting system. These requirements do not apply to egress stair systems and ramps that are integral with

the building structure, since it is assumed that the seismic resistance of these systems is addressed in the overall building design. Examples include stairs and ramps integral with monolithic concrete construction, light-frame wood and cold-formed metal stair systems in multiunit residential construction, and integrally constructed masonry stairs.

In this example, egress stairs of prefabricated steel construction are installed in a five-story steel frame building, which serves as an emergency medical facility. The seismic force-resisting system consists of special concentrically braced frames in the east-west direction and special moment frames in the north-south direction. The example focuses on the flight of stairs and landing running between Level 3 and Level 4 of the building. The elevation, plan, and isometric views of the stairs are shown in Figures 8-21, 8-22, and 8-23, respectively.

The treads and landings are fabricated from 1/8 inch-thick steel checkered plate. The stringers are fabricated from 1/4 inch-thick steel plates, and other members and supports are fabricated from steel channels, angles, and tubes. The effective dead load is computed as 20 psf for both stair runs and landings, and the design live load is 100 psf, per ASCE/SEI 7-22. This example calculates the prescribed seismic forces and displacements. The design of the stairs themselves and their connections for dead, live, and seismic loads are not covered. While this example focuses on stairs required for egress, the principles can be applied to all types of stairs.

This example illustrates the following calculation procedures:

- Prescribed seismic forces for a flight of stairs and landing between Level 3 and Level 4. (see Section 8.4.3 in this example).
- Prescribed seismic displacements for egress stairs between Level 3 and Level 4 (see Section 8.4.4 in this example).

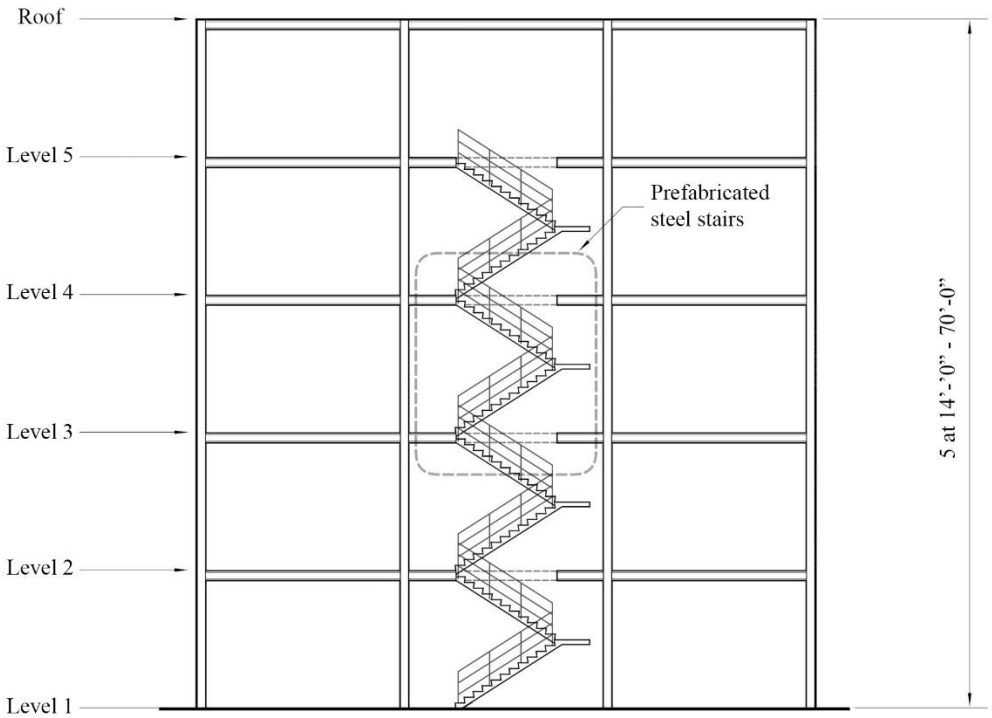

Figure 8-21. Elevation of Egress Stairs

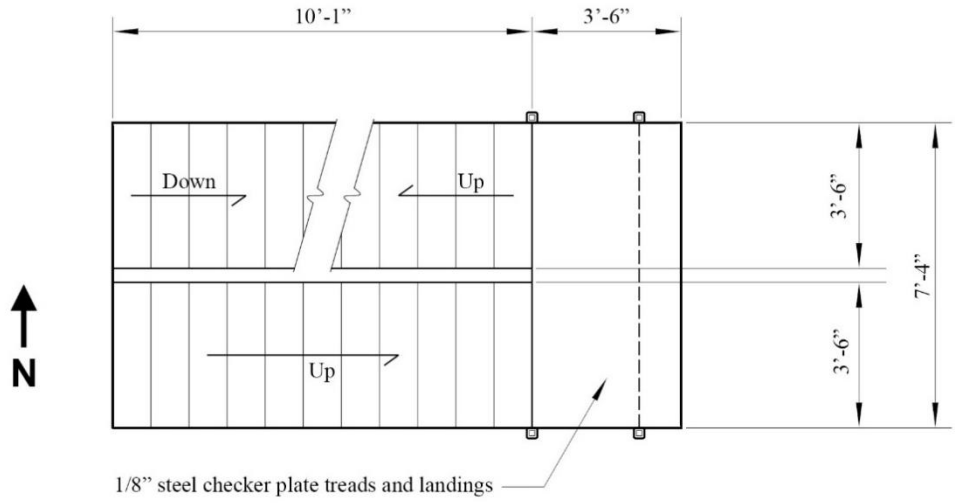

Figure 8-22. Plan of Egress Stairs

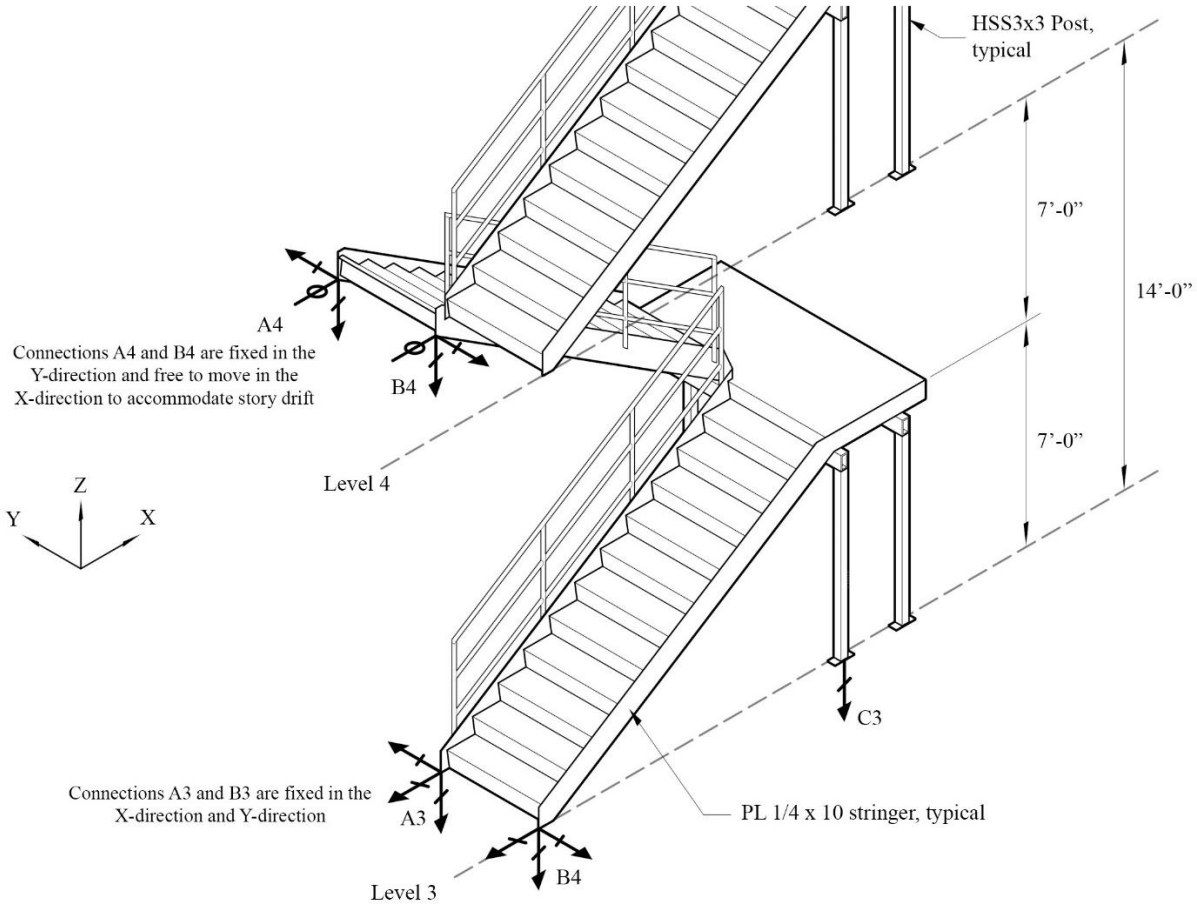

Figure 8-23. Isometric View of Egress Stairs

8.4.2 Design Requirements

8.4.2.1 ASCE/SEI 7-22 PARAMETERS AND COEFFICIENTS

The following parameters and coefficients are derived from the example description, or it is known information based on the structure, selected location, and site class.

Coefficients for architectural components

Egress stairways not part of the building seismic force-resisting system:

$C_{AR} = 1.0$ (ASCE/SEI 7-22 Table 13.5-1)

$R_{po} = 1.5$ (ASCE/SEI 7-22 Table 13.5-1)

$\Omega_{0p} = 2.0$ (ASCE/SEI 7-22 Table 13.5-1)

Egress stairs and ramp fasteners and attachments:

$C_{AR} = 2.2$ (ASCE/SEI 7-22 Table 13.5-1)

$R_{po} = 1.5$ (ASCE/SEI 7-22 Table 13.5-1)

$\Omega_{0p} = 1.75$ (ASCE/SEI 7-22 Table 13.5-1)

Design coefficients and factors for seismic force-resisting systems

East-west direction: building frame systems – steel special concentrically braced frames:

$R = 6.0$ (ASCE/SEI 7-22 Table 12.2-1)

$\Omega_0 = 2.0$ (ASCE/SEI 7-22 Table 12.2-1)

North-south direction: moment-resisting frame systems – steel special moment frames:

$R = 8.0$ (ASCE/SEI 7-22 Table 12.2-1)

$\Omega_0 = 3.0$ (ASCE/SEI 7-22 Table 12.2-1)

Short period design spectral acceleration, $S_{DS} = 1.00$ (given)

Seismic Design Category: D

Seismic Importance Factor, $I_e = 1.5$ (ASCE/SEI 7-22 Table 1.5-2)

Component Importance Factor, $I_p = 1.5$ (ASCE/SEI 7-22 Sec. 13.1.3)

Redundancy factor for nonstructural components, $\rho = 1.0$ (ASCE/SEI 7-22 Sec. 13.3.1)

Height of attachment at Level 3, $z = 28$ ft (given)

Height of attachment at Level 4, $z = 42$ ft (given)

Average height of attachments, $z = 35$ ft (given)

Average roof height with respect to the base, $h = 70$ ft (given)

Stair flight weight

$$W_p = (20 \text{ lb/ft}^2)(10.083 \text{ ft long})(3.5 \text{ ft wide})$$

$$W_p = 706 \text{ lb}$$

Stair landing weight

$$W_p = (20\text{lb/ft}^2)(7.333\text{ ft long})(3.5\text{ ft wide})$$

$$W_p = 513\text{ lb}$$

Approximate fundamental period of the supporting structure, T_a

- East-west direction: steel special concentrically braced frames (all other structural systems, per ASCE/SEI 7-22 Table 12.8-2)

$h_n = h = 70$ ft (structural height)

$C_t = 0.02$ (ASCE/SEI 7-22 Table 12.8-2)

$x = 0.75$ (ASCE/SEI 7-22 Table 12.8-2)

$T_a = C_t {h_n}^x = (0.02)(70\text{ ft})^{0.75} = 0.484\text{ s}$ (ASCE/SEI 7-22 Eq. 12.8-7)

- North-south direction: steel moment-resisting frames

$h_n = h = 70$ ft (structural height)

$C_t = 0.028$ (ASCE/SEI 7-22 Table 12.8-2)

$x = 0.8$ (ASCE/SEI 7-22 Table 12.8-2)

$T_a = C_t {h_n}^x = (0.028)(70\text{ ft})^{0.8} = 0.838\text{ s}$ (ASCE/SEI 7-22 Eq. 12.8-7)

ASCE/SEI 7-22 Section 13.3.1.1 indicates that for structures with combinations of seismic force-resisting systems, the lowest value of T_a shall be used. For this example, the steel special concentrically braced frame in the east-west direction controls.

$T_a = 0.484\text{ s}$ (controlling T_a)

Force amplification factor as a function of height in the structure, H_f

$a_1 = \frac{1}{T_a} \leq 2.5$ (ASCE/SEI 7-22 Sec. 13.3.1.1)

$a_1 = \frac{1}{0.484\text{ s}} = 2.07 \leq 2.5$

$a_2 = [1 - (0.4/T_a)^2] \geq 0$ (ASCE/SEI 7-22 Sec. 13.3.1.1)

$a_2 = [1 - (0.4/0.484\text{ s})^2] = 0.32 > 0$

$H_f = 1 + a_1\left(\frac{z}{h}\right) + a_2\left(\frac{z}{h}\right)^{10}$ (ASCE/SEI 7-22 Eq. 13.3-4)

$$H_f = 1 + 2.07\left(\frac{35\text{ ft}}{70\text{ ft}}\right) + 0.32\left(\frac{35\text{ ft}}{70\text{ ft}}\right)^{10} = 2.03$$

Structure ductility reduction factor, R_μ

East-west direction: steel special concentrically braced frames

$$R_\mu = (1.1\,R/(I_e\Omega_0))^{1/2} \geq 1.3 \qquad \text{(ASCE/SEI 7-22 Eq. 13.3-6)}$$

$$R_\mu = (1.1(6/((1.5)(2)))^{1/2} = 1.48 \geq 1.3$$

North-south direction: steel moment-resisting frames

$$R_\mu = (1.1\,R/(I_e\Omega_0))^{1/2} \geq 1.3 \qquad \text{(ASCE/SEI 7-22 Eq. 13.3-6)}$$

$$R_\mu = (1.1(8/((1.5)(3)))^{1/2} = 1.40 \geq 1.3$$

ASCE/SEI 7-22 Section 13.3.1.2 states that if the structure supporting the component contains combinations of seismic force-resisting systems in different directions, the structure ductility reduction factor shall be based on the seismic force-resisting system that results in the lowest value of R_μ. For this example, the steel moment-resisting frames in the north-south direction controls.

$$R_\mu = 1.40 \qquad \text{(controlling } R_\mu\text{)}$$

8.4.2.2 APPLICABLE REQUIREMENTS

The architectural, mechanical, and electrical components, supports, and attachments shall comply with the sections referenced in ASCE/SEI 7-22 Table 13.2-1. Thus, the nonstructural components of this example are designed in accordance with the following considerations:

- Supports, attachments, and the egress stairs themselves shall be designed to meet the seismic requirements of the ASCE/SEI 7-22, Chapter 13 (ASCE/SEI 7-22 Section 13.2.1).
- Component failure shall not cause failure of an essential architectural, mechanical, or electrical component (ASCE/SEI 7-22 Section 13.2.4).
- Component seismic attachments shall be bolted, welded, or otherwise positively fastened without considering the frictional resistance produced by the effects of gravity (ASCE/SEI 7-22 Section 13.4).
- The horizontal seismic design force, F_p, shall be applied at the component's center of gravity and distributed relative to the component's mass distribution (ASCE/SEI 7-22 Section 13.3.1).
- The effects of seismic relative displacements shall be considered in combination with displacements caused by other loads as appropriate (ASCE/SEI 7-22 Section 13.3.2).

- The net relative displacement shall be assumed to occur in any horizontal direction, and it shall be accommodated through slotted or sliding connections or metal supports designed with rotation capacity to accommodate seismic relative displacements (ASCE/SEI 7-22 Section 13.5.10).

- Sliding connections with slotted or oversize holes, sliding bearing supports with restraints that engage after the displacement, D_{pI}, is exceeded (e.g., keeper assemblies or end stops), and connections that permit movement by deformation of metal attachments shall accommodate a displacement D_{pI}, but not less than 0.5 in. (13 mm), without loss of vertical support or inducement of displacement-related compression forces in the stair (ASCE/SEI 7-22 Section 13.5.10).

- Sliding bearing supports without keeper assemblies or end stops shall be designed to accommodate a displacement $1.5D_{pI}$, but not less than 1.0 in. (25 mm) without loss of vertical support. Break-away restraints are permitted if their failure does not lead to loss of vertical support (ASCE/SEI 7-22 Section 13.5.10).

- The strength of the supports shall not be limited by bolt shear, weld fracture, or other limit states with lesser ductility (ASCE/SEI 7-22 Section 13.5.10).

- If sliding or ductile connections are not provided to accommodate seismic relative displacements, the stiffness and strength of the stair or ramp structure shall be included in the building structural model of ASCE/SEI 7-22 Section 12.7.3, and the stair shall be designed with Ω_0 corresponding to the seismic force-resisting system but not less than 2.5 (ASCE/SEI 7-22 Section 13.5.10).

8.4.3 Prescribed Seismic Forces

Stairs are generally displacement-controlled. Unless the stairs are included in the design of the structure's lateral force-resisting system, they must be either isolated from the lateral displacement of the building or provided with ductile connections capable of accepting the lateral displacements without loss of vertical load-carrying capacity. Sufficient ductility shall be provided in these connections to accommodate multiple cycles at anticipated maximum drift levels.

There are different approaches for dealing with seismic displacement demand on egress stairs. In this example for the stair assembly, Connections A3 and B3 at Level 3 are fixed in the X-direction (longitudinal direction) and Y-direction (transverse direction). Connections A4 and B4 at Level 4 are detailed to accommodate lateral displacements in the X-direction (longitudinal direction) and fixed in the Y-direction (transverse direction) to provide horizontal support in the upper floor. See Figure 8-23 for the stair isometric view with the connection conditions. This approach is repeated in each story for the stair design. This stair configuration induces warping of the stairs due to the eccentricity between the center of gravity of the stairs and the center of resistance of the connections. This eccentricity must be accounted for in the design.

When designing the stairs themselves, the seismic forces should be distributed relative to the component mass distribution. Since the mass of the stairway assembly is distributed between Level 3 and Level 4, the lateral forces are calculated using the average elevation between levels, $z = 35$ ft, which coincides with the landing elevation for this example.

Point of Attachment of Component in the Structure

The force amplification factor, H_f, is a function of height above the base of the structure to the point of attachment of the component, z. The higher the point of attachment, the greater the seismic design forces, F_p, that are required for the design of the nonstructural component.

For this example, Level 3 and Level 4 are located at Elevations 28 ft and 42 ft with respect to the base, respectively. Based on the connections, the egress stair is attached at both levels in the Y-direction (transverse direction) but only attached to Level 3 in the X-direction (longitudinal direction).

Using the average elevation between Level 3 and Level 4, $z = 35$ ft, for both orthogonal directions to calculate the prescribed seismic forces is conservative, and it simplifies the analysis. An even more conservative approach would be to use the Level 4 elevation, $z = 42$ ft, as the force amplification factor would be calculated at the highest point of attachment.

Theoretically, a more refined analysis could consider the point of attachment at the average elevation between Level 3 and Level 4 for transverse loads and at the Level 3 elevation for longitudinal loads.

Lateral forces on the egress stairs and attachments include seismic loads and can include wind loads, depending on their location. Design for wind forces is not presented in this example.

8.4.3.1 EGRESS STAIRWAYS NOT PART OF THE BUILDING SEISMIC FORCE-RESISTING SYSTEM

Flight of stairs

Gravity loads and component weight, W_p

$$D = 706 \text{ lb} \quad \text{(dead load)}$$

$$L = \left(100 \frac{\text{lb}}{\text{ft}^2}\right)(10.083 \text{ ft long})(3.5 \text{ ft wide}) = 3{,}528 \text{ lb} \quad \text{(live load)}$$

$$W_p = D = 706 \text{ lb} \quad \text{(component weight)}$$

Height at point of analysis

$$z = 35 \text{ ft} \quad \text{(average height of attachments)}$$

Seismic design force, F_p

$$F_p = 0.4 S_{DS} I_p W_p \left[\frac{H_f}{R_\mu}\right] \left[\frac{C_{AR}}{R_{po}}\right] \quad \text{(ASCE/SEI 7-22 Eq. 13.3-1)}$$

$$F_p = 0.4(1.0)(1.5)\left(W_p\right) \left[\frac{2.03}{1.40}\right] \left[\frac{1.0}{1.5}\right] = 0.582 W_p \quad \text{(controlling equation)}$$

$$F_{p,max} = 1.6 S_{DS} I_p W_p \quad \text{(ASCE/SEI 7-22 Eq. 13.3-2)}$$

$$F_{p,max} = 1.6(1.0)(1.5)\left(W_p\right) = 2.4 W_p$$

$$F_{p,min} = 0.3 S_{DS} I_p W_p \quad \text{(ASCE/SEI 7-22 Eq. 13.3-3)}$$

$$F_{p,min} = 0.3(1.0)(1.5)\left(W_p\right) = 0.45 W_p$$

$$F_p = 0.582 W_p = 0.582(706 \text{ lb}) = 410 \text{ lb} \quad \text{(controlling seismic design force)}$$

Horizontal seismic load effect, E_h

$$Q_E = F_p = 410 \text{ lb} \quad \text{(effect from } F_p\text{)}$$

$$E_h = \rho Q_E \quad \text{(ASCE/SEI 7-22 Eq. 12.4-3)}$$

$$E_h = (1.0)(335 \text{ lb}) = 410 \text{ lb}$$

Vertical seismic load effect, E_v

$$E_v = 0.2 S_{DS} D \quad \text{(ASCE/SEI 7-22 Eq. 12.4-4a)}$$

$$E_v = (0.2)(1.0\text{g})(706 \text{ lb}) = 141 \text{ lb}$$

The above terms are then substituted into the following Basic Load Combinations for Strength Design from ASCE/SEI 7-22 Sections 2.3.6 and 12.4.2 to determine the design member and connection forces to be used in conjunction with seismic and gravity loads.

$$1.2D + E_v + E_h + L + 0.2S \quad \text{(ASCE/SEI 7-22 Load Combination 6)}$$

$$0.9D - E_v + E_h \quad \text{(ASCE/SEI 7-22 Load Combination 7)}$$

Landing

Gravity loads and component weight, W_p

$$D = 513 \text{ lb} \quad \text{(dead load)}$$

$L = \left(100\frac{\text{lb}}{\text{ft}^2}\right)(7.333\text{ ft long})(3.5\text{ ft wide}) = 2{,}566\text{ lb}$ (live load)

$W_p = D = 513\text{ lb}$ (component weight)

Height at point of analysis

$z = 35\text{ ft}$ (average height of attachments)

Seismic design force, F_p

$F_p = 0.4S_{DS}I_pW_p\left[\frac{H_f}{R_\mu}\right]\left[\frac{C_{AR}}{R_{po}}\right]$ (ASCE/SEI 7-22 Eq. 13.3-1)

$F_p = 0.4(1.0)(1.5)\left(W_p\right)\left[\frac{2.03}{1.40}\right]\left[\frac{1.0}{1.5}\right] = 0.582W_p$ (controlling equation)

$F_{p,max} = 1.6S_{DS}I_pW_p$ (ASCE/SEI 7-22 Eq. 13.3-2)

$F_{p,max} = 1.6(1.0)(1.5)\left(W_p\right) = 2.4W_p$

$F_{p,min} = 0.3S_{DS}I_pW_p$ (ASCE/SEI 7-22 Eq. 13.3-3)

$F_{p,min} = 0.3(1.0)(1.5)\left(W_p\right) = 0.45W_p$

$F_p = 0.582W_p = 0.582(513\text{ lb}) = 298\text{ lb}$ (controlling seismic design force)

Horizontal seismic load effect, E_h

$Q_E = F_p = 298\text{ lb}$ (effect from F_p)

$E_h = \rho Q_E$ (ASCE/SEI 7-22 Eq. 12.4-3)

$E_h = (1.0)(298\text{ lb}) = 298\text{ lb}$

Vertical seismic load effect, E_v

$E_v = 0.2S_{DS}D$ (ASCE/SEI 7-22 Eq. 12.4-4a)

$E_v = (0.2)(1.0\text{g})(513\text{ lb}) = 103\text{ lb}$

The above terms are then substituted into the following Basic Load Combinations for Strength Design from ASCE/SEI 7-22 Sections 2.3.6 and 12.4.2 to determine the design member and connection forces to be used in conjunction with seismic and gravity loads.

$1.2D + E_v + E_h + L + 0.2S$ (ASCE/SEI 7-22 Load Combination 6)

$$0.9D - E_v + E_h$$ (ASCE/SEI 7-22 Load Combination 7)

After the prescribed seismic forces and displacements are determined, the stairs members are designed to carry the dead, live, and seismic loads and the connections can be detailed and designed according to the appropriate standards.

8.4.3.2 EGRESS STAIRS AND RAMP FASTENERS AND ATTACHMENTS

The ASCE/SEI 7-22 specifies an increased C_{AR} for egress stair and ramp fasteners and attachments with the intention of preventing premature failure in those elements connecting to the primary structure, which could cause loss of vertical support. The change in C_{AR} only effects the force calculated using the ASCE/SEI 7-22 Equation 13.3-1.

Fasteners and Attachments

"Attachments" are defined in ASCE/SEI 7-22 Section 11.2 as the "means by which nonstructural components or supports of nonstructural components are secured or connected to the seismic force-resisting system of the structure." Fasteners are a subset of attachments, per the definition.

Following the ASCE/SEI 7-22 definition and Table 13.5-1, the stringer connection attached to the primary structure is required to be designed for the increased design forces corresponding to the "egress stair and ramp fasteners and attachments." The rest of the egress stairway connections can be sized using the same design forces as the "egress stairways not part of the building seismic force-resisting system."

As the attachment to the primary structure is not well delimited to the rest of the egress stairway connections, it is recommended to apply the increased design forces in attachments with a nonductile failure mechanism. Refer to Figure 8-24 for a typical stringer at floor connection.

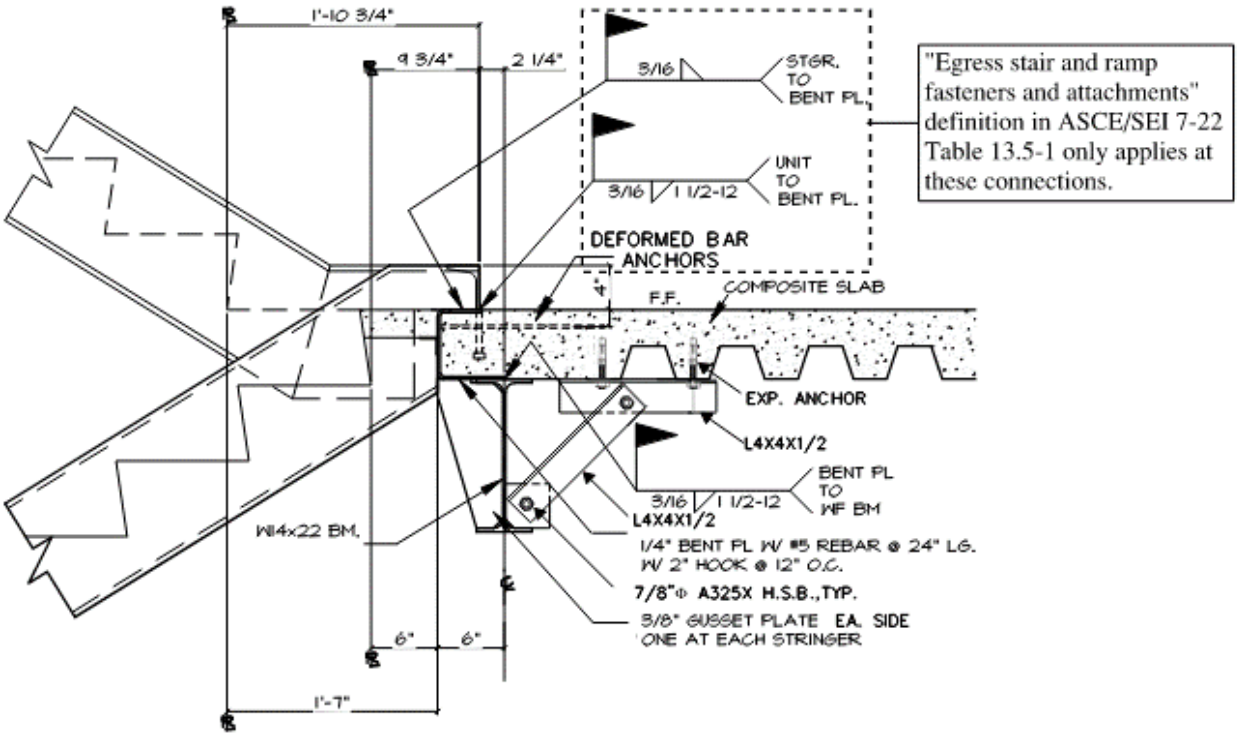

Figure 8-24. Typical Stringer at Floor Connection

The loads tributary to the connection of the stair to the primary structure come from both the flights of the stairs and the landing.

Flight of stairs

Seismic design force, F_p

$$F_p = 0.4 S_{DS} I_p W_p \left[\frac{H_f}{R_\mu}\right] \left|\frac{C_{AR}}{R_{po}}\right| \qquad \text{(ASCE/SEI 7-22 Eq. 13.3-1)}$$

$$F_p = 0.4(1.0)(1.5)\left(W_p\right) \left[\frac{2.03}{1.40}\right] \left|\frac{2.2}{1.5}\right| = 1.280 W_p \qquad \text{(controlling equation)}$$

$$F_{p,max} = 1.6 S_{DS} I_p W_p = 2.4 W_p \qquad \text{(ASCE/SEI 7-22 Eq. 13.3-2)}$$

$$F_{p,min} = 0.3 S_{DS} I_p W_p = 0.45 W_p \qquad \text{(ASCE/SEI 7-22 Eq. 13.3-3)}$$

$$F_p = 1.280 W_p = 1.280(706 \text{ lb}) = 903 \text{ lb} \qquad \text{(controlling seismic design force)}$$

ASCE/SEI 7-22 Eq. 13.3-1 governs, and $F_p = 903$ lb.

Landing

Seismic design force, F_p

$$F_p = 0.4 S_{DS} I_p W_p \left[\frac{H_f}{R_\mu}\right] \left|\frac{C_{AR}}{R_{po}}\right| \qquad \text{(ASCE/SEI 7-22 Eq. 13.3-1)}$$

$$F_p = 0.4(1.0)(1.5)\left(W_p\right) \left[\frac{2.03}{1.40}\right] \left|\frac{2.2}{1.5}\right| = 1.280 W_p \qquad \text{(controlling equation)}$$

$$F_{p,max} = 1.6 S_{DS} I_p W_p = 2.4 W_p \qquad \text{(ASCE/SEI 7-22 Eq. 13.3-2)}$$

$$F_{p,min} = 0.3 S_{DS} I_p W_p = 0.45 W_p \qquad \text{(ASCE/SEI 7-22 Eq. 13.3-3)}$$

$$F_p = 1.280 W_p = 1.280(513 \text{ lb}) = 657 \text{ lb} \qquad \text{(controlling seismic design force)}$$

Again, ASCE/SEI 7-22 Eq. 13.3-1 governs, and $F_p = 657$ lb.

8.4.4 Prescribed Seismic Displacements

Assuming the results of an elastic analysis of the building structure are not available for use in the design of the egress stairs, prescribed seismic displacements are calculated based on allowable story drift requirements. The allowable story drift is in Table 12.12-1 of ASCE/SEI 7-22. Since this is a five-story building, does not use masonry in the primary seismic force-resisting system, and it is in Risk Category IV, then the allowable story drift is $0.010h_{sx}$.

Seismic relative displacements, D_{pI}

$$h_{sx} = 14 \text{ ft} \qquad \text{(story height)}$$

$h_x = 42$ ft (height of upper support attachment)

$h_y = 28$ ft (height of lower support attachment)

$\Delta_{aA} = 0.010 h_{sx}$ (ASCE/SEI 7-22 Table 12.12-1)

$D_p = \frac{(h_x - h_y)\Delta_{aA}}{h_{sx}}$ (ASCE/SEI 7-22 Eq.13.3-10)

$D_p = \frac{(42\text{ft} - 28\text{ft})(12\text{ in./ft})(0.010 h_{sx})}{h_{sx}} = 1.68\text{ in.}$

$D_{pI} = D_p I_e = (1.68\text{ in.})(1.5) = 2.52\text{ in.}$ (ASCE/SEI 7-22 Eq.13.3-8)

Assuming that the connections of the egress stairs to the structure at Level 4 are sliding connections with slotted or oversize holes, sliding bearing supports must be provided with restraints that engage after the displacement D_{pI}, is exceeded (e.g., keeper assemblies or end stops). The connections must be designed to accommodate D_{pI}, without loss of vertical support or inducement of displacement-related compression forces in the stair. The displacement can act in any direction, so the connection must be able to accommodate a total range of movement of two times D_{pI}, or 2.52 in. times 2 = 5.04 inches in all directions. If a keeper assemblies or end stops are not provided, the connection must be designed to accommodate 1.5 $D_p I_e$, or 3.78 inches, or a total range of movement of 7.56 inches.

Accommodating displacements of these magnitudes may be problematic from a practical design perspective, and connection options that rely on yielding of ductile steel elements may produce a more efficient design.

Stairway Design Load Combinations

The horizontal displacements due to story drifts and seismic relative displacements, D_{pI}, lead to additional demands that are required to be accounted for in the calculations for stairways and corresponding attachments.

The egress stairways and connections should be designed for the linear combination of the prescribed seismic forces, i.e., inertial forces, and the induced forces associated with the building or nonbuilding structure displacements, as shown in the following equation.

Design Load Combination = Inertial Force Demand + Displacement-Induced Demand

For this egress stair example, the following load combinations would be required in the analysis:

Egress stairs not part of the building seismic force-resisting system:

$$EQX = \pm F_{pX}$$

$$EQY = \pm F_{pY} \pm EQY_{drift}$$

Where: F_{pX} = prescribed seismic forces in the X-direction (longitudinal direction)

F_{pY} = prescribed seismic forces in the Y-direction (transverse direction)

EQY_{drift} = displacement-induced demand in the Y-direction (transverse direction)

The unrestrained connection in the X-direction (longitudinal direction) and the induced demand at the fixed connection in the Y-direction (transverse direction) at Level 4 shall be able to accommodate the story drift and the seismic relative displacements, per ASCE/SEI 7-22 Section 13.5.10.

8.5 HVAC Fan Unit Support

8.5.1 Example Description

Example Summary

- **Nonstructural components**
  Case 1: mechanical and electrical – HVAC fan unit
  Case 2: mechanical and electrical – spring-isolated component
- **Building seismic force-resisting system:** Ordinary reinforced masonry shear wall (bearing wall system)
- **Equipment support:** Integral
- **Occupancy:** Office
- **Risk Category:** II
- **Component Importance Factor:** $I_p = 1.0$
- **Number of stories:** 3
- $\boldsymbol{S_{DS}} = 0.474$

In this example, the mechanical component is a 4-foot-high, 5-foot-wide, 8-foot-long, 3,000-pound HVAC fan unit that is supported on the two long sides near each corner, as shown in Figure 8-25. The component is located at the roof level of a three-story office building. All the stories are 12 feet tall. The building is assigned to Risk Category II. The fan unit does not meet any of the requirements in ASCE/SEI 7-22 Section 13.1.3 for increasing the Component Importance Factor to I_p = 1.5: the fan is not required for life-safety purposes after an earthquake; the fan does not convey or support toxic, explosive or hazardous materials; and the building is not classified as Risk Category IV or as a hazardous occupancy. Thus, the Component Importance Factor is I_p = 1.0.

Depending on the type of component, manufacturer's manual, the component supplier, and recommendations from the vibration or acoustic consultant, nonstructural components either have fixed supports or vibration-isolated supports. For this example, both potential cases of attaching the component to the 4,000 psi, normal weight concrete roof slab are considered, as follows:

- **Case 1:** Direct attachment to the structure using 36 ksi, carbon steel, cast-in-place anchors (see Section 8.5.3 in this example).
- **Case 2:** Support on vibration isolation springs that are attached to the slab with 36 ksi, carbon steel, post-installed expansion anchors. The nominal gap between the vibration spring seismic restraints and the base frame of the fan unit is presumed to be greater than 0.25 in. (see Section 8.5.4 in this example).

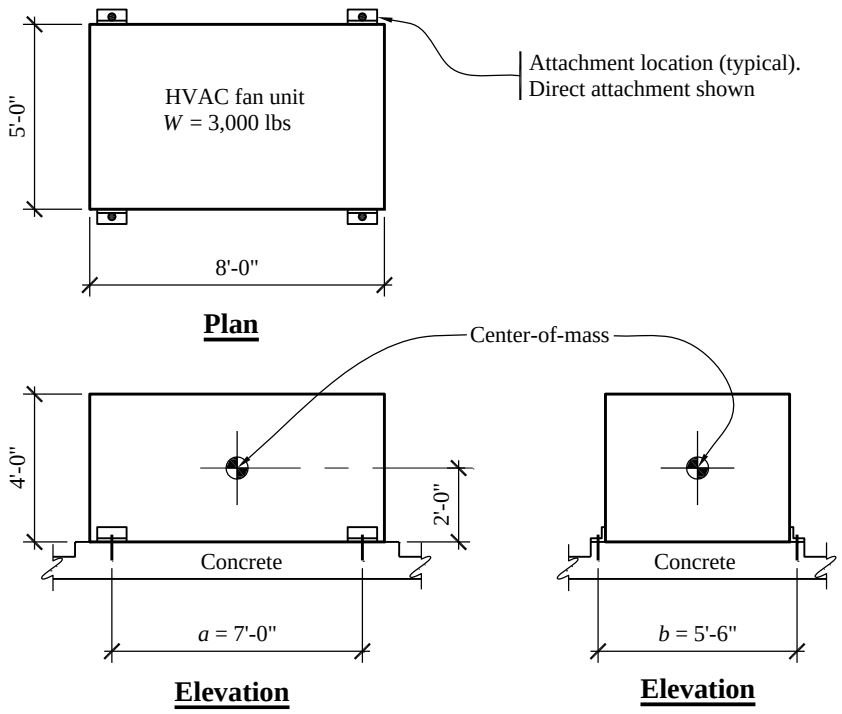

Figure 8-25. HVAC Fan Unit

8.5.2 Design Requirements

8.5.2.1 ASCE/SEI 7-22 PARAMETERS AND COEFFICIENTS

The following parameters and coefficients are derived from the example description, or it is known information based on the structure, selected location, and site class.

Coefficients for mechanical and electrical components

Case 1

Mechanical and electrical components – air-side HVACR, fans, air handlers, air conditioning units, cabinet heaters, air distribution boxes, and other mechanical components constructed of sheet metal framing:

$C_{AR} = 1.4$ (ASCE/SEI 7-22 Table 13.6-1)

$R_{po} = 2.0$ (ASCE/SEI 7-22 Table 13.6-1)

$\Omega_{0p} = 2.0$ (ASCE/SEI 7-22 Table 13.6-1)

Case 2

Vibration-isolated components and systems – spring-isolated components and systems and vibration-isolated floors closely restrained using built-in or separate elastomeric snubbing devices or resilient perimeter stops:

$C_{AR} = 2.2$ (ASCE/SEI 7-22 Table 13.6-1)

$R_{po} = 1.3$ (ASCE/SEI 7-22 Table 13.6-1)

$\Omega_{0p} = 1.75$ (ASCE/SEI 7-22 Table 13.6-1)

Design coefficients and factors for seismic force-resisting system

Bearing wall systems – ordinary reinforced masonry shear walls:

$R = 2.0$ (ASCE/SEI 7-22 Table 12.2-1)

$\Omega_0 = 2.5$ (ASCE/SEI 7-22 Table 12.2-1)

Seismic Design Category: C (ASCE/SEI 7-22 Sec. 11.6)

Short period design spectral acceleration, $S_{DS} = 0.474$ (given)

Seismic Importance Factor, $I_e = 1.0$ (ASCE/SEI 7-22 Table 1.5-2)

Component Importance Factor, $I_p = 1.0$ (ASCE/SEI 7-22 Sec. 13.1.3)

Redundancy factor for nonstructural components, $\rho = 1.0$ (ASCE/SEI 7-22 Sec. 13.3.1)

Height of attachment at roof, $z = 36$ ft (given)

Average roof height with respect to the base, $h = 36$ ft (given)

Story height, $h_{sx} = 12$ ft (given)

HVAC fan unit weight, $W_p = 3{,}000$ lb (given)

Approximate fundamental period of the supporting structure, T_a – ordinary reinforced masonry shear walls (all other structural systems, per ASCE/SEI 7-22 Table 12.8-2)

$h_n = h = 36$ ft (structural height)

$C_t = 0.02$ (ASCE/SEI 7-22 Table 12.8-2)

$x = 0.75$ (ASCE/SEI 7-22 Table 12.8-2)

$T_a = C_t {h_n}^x = (0.02)(36 \text{ ft})^{0.75} = 0.29$ s (ASCE/SEI 7-22 Eq. 12.8-7)

Force amplification factor as a function of height in the structure, H_f

$$a_1 = \frac{1}{T_a} \leq 2.5 \qquad \text{(ASCE/SEI 7-22 Sec. 13.3.1.1)}$$

$$a_1 = \frac{1}{0.29\ \text{s}} = 3.45 > 2.5, \text{ use } a_1 = 2.5$$

$$a_2 = [1 - (0.4/T_a)^2] \geq 0 \qquad \text{(ASCE/SEI 7-22 Sec. 13.3.1.1)}$$

$$a_2 = [1 - (0.4/0.29\ s)^2] = -0.90 < 0, \text{ use } a_2 = 0$$

$$H_f = 1 + a_1\left(\frac{z}{h}\right) + a_2\left(\frac{z}{h}\right)^{10} \qquad \text{(ASCE/SEI 7-22 Eq. 13.3-4)}$$

$$H_f = 1 + 2.5\left(\frac{36\ \text{ft}}{36\ \text{ft}}\right) + 0\left(\frac{36\ \text{ft}}{36\ \text{ft}}\right)^{10} = 3.5$$

Force Amplification Factor as a Function of Height, H_f, for Structures with $T_a \leq 0.4\ s$

For supporting building or nonbuilding structures with approximate fundamental periods equal or less than 0.4 seconds, the parameters a_1 and a_2 are controlled by their limits, i.e., $a_1 = 2.5$ and $a_2 = 0$, as shown in this example.

For these short-period structures, the ASCE/SEI 7-22 Equation 13.3-4 leads to the same results as the ASCE/SEI 7-22 Equation 13.3-5, where the approximate fundamental period of the supporting building or nonbuilding structure is unknown:

$$H_f = 1 + 2.5\left(\frac{z}{h}\right) \qquad \text{(ASCE/SEI 7-22 Eq. 13.3-5)}$$

Structure ductility reduction factor, R_μ

$$R_\mu = (1.1\,R/(I_e\Omega_0))^{1/2} \geq 1.3 \qquad \text{(ASCE/SEI 7-22 Eq. 13.3-6)}$$

$$R_\mu = (1.1(2/((1.0)(2.5)))^{1/2} = 0.94 < 1.3, \text{ use } R_\mu = 1.3$$

Changes in the ASCE/SEI 7 22

For the 2022 edition of ASCE/SEI-7, the seismic design force, F_p, is dependent on the building or nonbuilding structure seismic force-resisting system. The force amplification factor as a function of height, H_f, and the structure ductility reduction factor, R_μ, are functions of the following parameters of the supporting building or nonbuilding structure:

- Approximate fundamental period, T_a
- Response modification factor, R
- Seismic importance factor, I_e
- Overstrength factor, Ω_0

Consider the following comparison between different bearing wall systems in this example to illustrate the importance of the seismic force-resisting system for the seismic design forces:

- Ordinary reinforced masonry shear walls ($R = 2$ and $\Omega_0 = 2.5$):

  $R_\mu = 1.3$

- Ordinary reinforced concrete shear walls ($R = 4$ and $\Omega_0 = 2.5$):

  $R_\mu = 1.33$

  Seismic design forces, F_p, are reduced by 2.3% with respect to the original system.

- Special reinforced concrete shear walls ($R = 5$ and $\Omega_0 = 2.5$):

  $R_\mu = 1.48$

  Seismic design forces, F_p, are reduced by 12.2% with respect to the original system.

8.5.2.2 APPLICABLE REQUIREMENTS

Architectural, mechanical, and electrical components, supports, and attachments shall comply with the sections referenced in ASCE/SEI 7-22 Table 13.2-1. Thus, the nonstructural components of this example are designed in accordance with the following considerations:

- Component failure shall not cause failure of an essential architectural, mechanical, or electrical component (ASCE/SEI 7-22 Section 13.2.4).
- Component seismic attachments shall be bolted, welded, or otherwise positively fastened without consideration of frictional resistance produced by the effects of gravity (ASCE/SEI 7-22 Section 13.4).

- The horizontal seismic design force, F_p, shall be applied at the component's center of gravity and distributed relative to the component's mass distribution (ASCE/SEI 7-22 Section 13.3.1).
- Per ASCE/SEI 7-22 Section 13.4.2, attachments to concrete or masonry shall be designed to resist the seismic load effects, including overstrength, in accordance with ASCE/SEI 7-22 Section 12.4.3, and Ω_0 shall be taken as Ω_{0p} (ASCE/SEI 7-22 Section 13.4.2).
- Attachments and supports transferring seismic loads shall be constructed of materials suitable for the application and must be designed and constructed in accordance with a nationally recognized structural standard (ASCE/SEI 7-22 Section 13.6.4.4).
- Components mounted on vibration isolation systems shall have a bumper restraint or snubber in each horizontal direction. Vertical restraints must be provided where required to resist overturning. Isolator housings and restraints must also be constructed of ductile materials. A viscoelastic pad, or similar material of appropriate thickness, must be used between the bumper and equipment item to limit the impact load. Such components also must resist doubled seismic design forces if the nominal clearance (air gap) between the equipment support frame and restraints is greater than 0.25 in. (ASCE/SEI 7-22 Section 13.6.4.5 and Table 13.6-1, Footnote a).

8.5.3 Case 1: Direct Attachment to Structure

This section illustrates determination of forces for cast-in-place concrete anchors, where the design anchor strength is greater than the strength capacity of the ductile steel anchorage element. Therefore, the load combinations considering the anchorage overstrength factor, Ω_{0p}, are not used for the component anchorage design. As noted in Section 8.2.15 of this chapter, there are also requirements in the masonry design standards for post-installed anchors.

Figure 8-26 shows a free-body diagram for seismic force analysis.

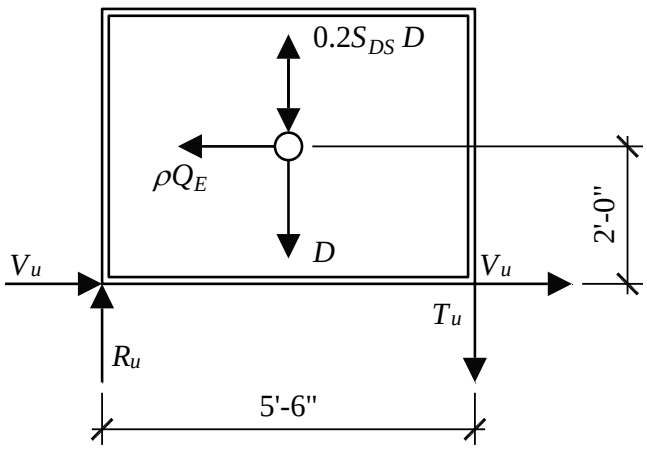

Figure 8-26. Free-Body Diagram for Seismic Force Analysis

8.5.3.1 PRESCRIBED SEISMIC FORCES

HVAC fan unit weight, W_p

$$W_p = D = 3{,}000 \text{ lb} \qquad \text{(component weight)}$$

Seismic design force, F_p

$$F_p = 0.4 S_{DS} I_p W_p \left[\frac{H_f}{R_\mu}\right] \left|\frac{C_{AR}}{R_{po}}\right| \qquad \text{(ASCE/SEI 7-22 Eq. 13.3-1)}$$

$$F_p = 0.4(0.474)(1.0)\left(W_p\right)\left[\frac{3.5}{1.3}\right]\left|\frac{1.4}{2.0}\right| = 0.357 W_p \qquad \text{(controlling equation)}$$

$$F_{p,max} = 1.6 S_{DS} I_p W_p \qquad \text{(ASCE/SEI 7-22 Eq. 13.3-2)}$$

$$F_{p,max} = 1.6(0.474)(1.0)\left(W_p\right) = 0.758 W_p$$

$$F_{p,min} = 0.3 S_{DS} I_p W_p \qquad \text{(ASCE/SEI 7-22 Eq. 13.3-3)}$$

$$F_{p,min} = 0.3(0.474)(1.0)\left(W_p\right) = 0.142 W_p$$

$$F_p = 0.357 W_p = 0.357(3{,}000 \text{ lb}) = 1{,}072 \text{ lb} \qquad \text{(controlling seismic design force)}$$

Horizontal seismic load effect, E_h

$$Q_E = F_p = 1{,}072 \text{ lb} \qquad \text{(effect from } F_p\text{)}$$

$$E_h = \rho Q_E \qquad \text{(ASCE/SEI 7-22 Eq. 12.4-3)}$$

$$E_h = (1.0)(1{,}072 \text{ lb}) = 1{,}072 \text{ lb}$$

Vertical seismic load effect, E_v

$$E_v = 0.2 S_{DS} D \qquad \text{(ASCE/SEI 7-22 Eq. 12.4-4a)}$$

$$E_v = (0.2)(0.474\text{g})(3{,}000 \text{ lb}) = 284 \text{ lb}$$

The above terms are then substituted into the following Basic Load Combinations for Strength Design from ASCE/SEI 7-22 Sections 2.3.6 and 12.4.2 to determine the design member and connection forces to be used in conjunction with seismic loads.

$$1.2D + E_v + E_h + L + 0.2S \qquad \text{(ASCE/SEI 7-22 Load Combination 6)}$$

$$0.9D - E_v + E_h \qquad \text{(ASCE/SEI 7-22 Load Combination 7)}$$

For nonstructural components, the terms *L* and S are typically zero.

8.5.3.2 PROPORTIONING AND DESIGN

Based on the free-body diagram, the seismic load effects can be used to determine bolt shear, V_u, and tension, T_u (where a negative value indicates tension). In the calculations below, the signs of E_v and E_h have been selected to result in the largest value of T_u.

ASCE/SEI 7-22 Basic Load Combination 6:

$$1.2D - E_v + E_h + L + 0.2S \qquad \text{(ASCE/SEI 7-22 Load Combination 6)}$$

$$V_u = \frac{E_h}{4 \text{ bolts}}$$

$$V_u = \frac{1{,}072 \text{ lb}}{4 \text{ bolts}} = 268 \text{ lb/bolt}$$

$$T_u = \frac{(1.2D - E_v)(5.5/2 \text{ ft}) - (E_h)(2 \text{ ft})}{(5.5 \text{ ft})(2 \text{ bolts})}$$

$$T_u = \frac{(1.2(3{,}000 \text{ lb}) - 284 \text{ lb})(5.5/2 \text{ ft}) - (1{,}072 \text{ lb})(2 \text{ ft})}{(5.5 \text{ ft})(2 \text{ bolts})} = 634 \text{ lb/bolt (no tension)}$$

ASCE/SEI 7-22 Basic Load Combination 7:

$$0.9D - E_v + E_h \qquad \text{(ASCE/SEI 7-22 Load Combination 7)}$$

$$V_u = \frac{E_h}{4 \text{ bolts}}$$

$$V_u = \frac{1{,}072 \text{ lb}}{4 \text{ bolts}} = 268 \text{ lb/bolt}$$

$$T_u = \frac{(0.9D - E_v)(5.5/2 \text{ ft}) - (E_h)(2 \text{ ft})}{(5.5 \text{ ft})(2 \text{ bolts})}$$

$$T_u = \frac{(0.9(3{,}000 \text{ lb}) - 284 \text{ lb})(5.5/2 \text{ ft}) - (1{,}072 \text{ lb})(2 \text{ ft})}{(5.5 \text{ ft})(2 \text{ bolts})} = 409 \text{ lb/bolt (no tension)}$$

Anchors with design capacities exceeding the calculated demands would be selected using the procedures in ACI 318 Chapter 17.

8.5.4 Case 2: Support on Vibration Isolation Springs

This portion of the example illustrates the design of the same HVAC unit when the component is supported on vibration isolators and determination of anchor design forces when the attachment to the structure is made with anchors controlled by concrete breakout. The nominal clearance (air gap) between the equipment support frame and the seismic restraint is presumed to be greater than 0.25 in., so the design value of F_p is doubled, per ASCE/SEI 7-22 Table 13.6-1, Footnote a. If a limit of gap clearance to 0.25 in. was specified (which would require special inspection during construction), it would reduce design seismic forces on seismic restraints and associated anchorage. For anchors to

concrete, the load combinations considering overstrength, Ω_{0p}, are used for the component anchorage design.

ASCE/SEI 7-22 requirement of doubling the seismic design forces, F_p, for components mounted on vibration isolators with an air gap greater than 0.25 in. between the support frame and restraint is based on experimental research. Studies showed that air gaps having more space for the component to displace can develop higher accelerations, leading to higher seismic forces in the nonstructural component. This requirement is associated with the lessons learned from previous earthquakes, especially the 1971 San Fernando earthquake, where nonstructural components exhibited severe damage.

Equipment that contains rotating or reciprocating components may be internally isolated. Externally, the equipment is directly attached to the structure, but vibration isolators are installed on some of the internal components. Internally isolated components are subject to higher seismic design forces, and the appropriate design coefficients from ASCE/SEI 7-22 Table 13.6-1 should be used. Any mechanical component that normally would contain rotating or reciprocating items and is directly attached to the structure should be investigated to determine if it is internally isolated. Any component which contains one or more internal items that are mounted on vibration isolators, such as fans or motors inside air handler units, is considered an internally isolated component and should be designed for higher loads as specified in ASCE/SEI 7-22.

Design forces applied to the top of the vibration isolators are determined by an analysis of earthquake forces applied in a diagonal horizontal direction, as shown in Figure 8-27. Terminology and concept are derived from ASHRAE A56. In the equations below, $F_{pv} = E_v = 0.2S_{DS}W_p$:

Angle of diagonal loading:

$$\theta = \tan^{-1}\left(\frac{b}{a}\right) \qquad \text{(ASHRAE A56)}$$

Tension per isolator:

$$T_u = \frac{W_p - F_{pv}}{4} - \frac{F_p h}{2}\left(\frac{\cos\theta}{b} + \frac{\sin\theta}{a}\right) \qquad \text{(ASHRAE A56)}$$

Compression per isolator:

$$C_u = \frac{W_p + F_{pv}}{4} + \frac{F_p h}{2}\left(\frac{\cos\theta}{b} + \frac{\sin\theta}{a}\right) \qquad \text{(ASHRAE A56)}$$

Shear per isolator:

$$V_u = \frac{F_p}{4} \qquad \text{(ASHRAE A56)}$$

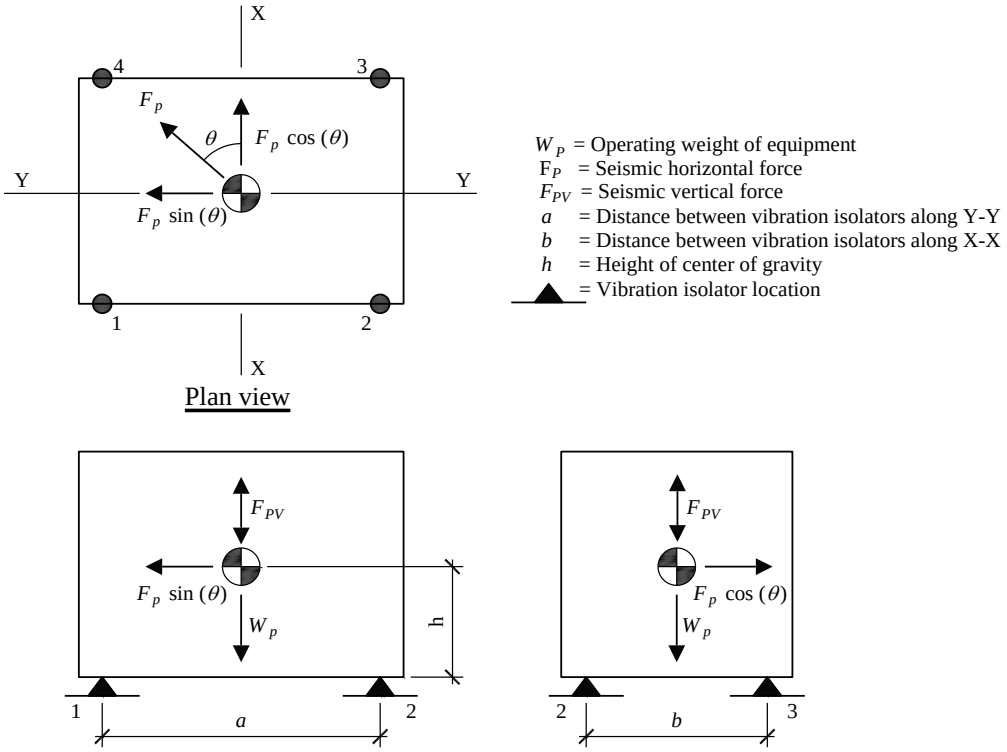

Figure 8-27. ASHRAE Diagonal Seismic Force Analysis for Vibration Isolation Springs

8.5.4.1 PRESCRIBED SEISMIC FORCES

HVAC fan unit weight, W_p

$W_p = D = 3{,}000$ lb (component weight)

Seismic design force, F_p

$$F_p = 0.4 S_{DS} I_p W_p \left[\frac{H_f}{R_\mu}\right]\left[\frac{C_{AR}}{R_{po}}\right] \quad \text{(ASCE/SEI 7-22 Eq. 13.3-1)}$$

$$F_p = 0.4(0.474)(1.0)\left(W_p\right)\left[\frac{3.5}{1.3}\right]\left[\frac{2.2}{1.3}\right] = 0.864 W_p$$

$$F_{p,max} = 1.6 S_{DS} I_p W_p \quad \text{(ASCE/SEI 7-22 Eq. 13.3-2)}$$

$$F_{p,max} = 1.6(0.474)(1.0)\left(W_p\right) = 0.758 W_p \quad \text{(controlling equation)}$$

$$F_{p,min} = 0.3 S_{DS} I_p W_p \quad \text{(ASCE/SEI 7-22 Eq. 13.3-3)}$$

$$F_{p,min} = 0.3(0.474)(1.0)\left(W_p\right) = 0.142 W_p$$

$F_p = 0.758W_p = 0.758(3{,}000 \text{ lb}) = 2{,}275 \text{ lb}$ (controlling seismic design force)

Components mounted on vibration isolation systems shall have a bumper restraint or snubber in each horizontal direction. Per ASCE/SEI 7-22 Table 13.6-1, Footnote a, the design force must be taken as $2F_p$ if nominal clearance (air gap) between equipment and seismic restraint is greater than 0.25 in.

Horizontal seismic load effect, E_h

$Q_E = 2F_p = 2(2{,}275 \text{ lb}) = 4{,}550 \text{ lb}$ (ASCE/SEI 7-22 Table 13.6-1)

$E_h = \rho Q_E$ (ASCE/SEI 7-22 Eq. 12.4-3)

$E_h = (1.0)(4{,}550 \text{ lb}) = 4{,}550 \text{ lb}$

Vertical seismic load effect, E_v

$E_v = 0.2S_{DS}D$ (ASCE/SEI 7-22 Eq. 12.4-4a)

$E_v = (0.2)(0.474\text{g})(3{,}000 \text{ lb}) = 284 \text{ lb}$

The above terms are then substituted into the following Basic Load Combinations for Strength Design from ASCE/SEI 7-22 Sections 2.3.6 and 12.4.2 to determine the design member and connection forces to be used in conjunction with seismic loads.

$1.2D + E_v + E_h + L + 0.2S$ (ASCE/SEI 7-22 Load Combination 6)

$0.9D - E_v + E_h$ (ASCE/SEI 7-22 Load Combination 7)

For nonstructural components, the terms L and S are typically zero.

8.5.4.2 PROPORTIONING AND DESIGN

The seismic load effects are used to determine the bolt shear, V_u, and tension, T_u (where a negative value indicates tension). The ASHRAE A56 equations are used to estimate these demands acting on the nonstructural component attachment. These formulas are modified to account for the ASCE/SEI 7-22 Basic Load Combinations for W_p, the horizontal seismic load effect E_h instead of F_p, and the vertical load effect E_v as F_{pv}.

In the calculations below, the signs of E_v and E_h have been selected to result in the largest value of T_u. Similar calculations are performed to determine the maximum compressive force, C_u.

$\theta = tan^{-1}\left(\frac{b}{a}\right)$ (ASHRAE A56)

$\theta = tan^{-1}\left(\frac{5.5 \text{ ft}}{7.0 \text{ ft}}\right) = 38.16°$

ASCE/SEI 7-22 Basic Load Combination 6:

$$1.2D + E_v + E_h + L + 0.2S \qquad \text{(ASCE/SEI 7-22 Load Combination 6)}$$

$$T_u = \frac{1.2D - E_v}{4} - \frac{E_h h}{2}\left(\frac{\cos\theta}{b} + \frac{\sin\theta}{a}\right) \qquad \text{(Modified from ASHRAE A56)}$$

$$T_u = \frac{1.2(3{,}000\text{ lb}) - 284\text{ lb}}{4} - \frac{(4{,}550\text{ lb})(2\text{ ft})}{2}\left(\frac{\cos(38.16°)}{5.5\text{ ft}} + \frac{\sin(38.16°)}{7\text{ ft}}\right) = -223\text{ lb}$$

$$C_u = \frac{1.2D + E_v}{4} + \frac{E_h h}{2}\left(\frac{\cos\theta}{b} + \frac{\sin\theta}{a}\right) \qquad \text{(Modified from ASHRAE A56)}$$

$$C_u = \frac{1.2(3{,}000\text{ lb}) + 284\text{ lb}}{4} + \frac{(4{,}550\text{ lb})(2\text{ ft})}{2}\left(\frac{\cos(38.16°)}{5.5\text{ ft}} + \frac{\sin(38.16°)}{7\text{ ft}}\right) = 2{,}023\text{ lb}$$

$$V_u = \frac{E_h}{4} \qquad \text{(Modified from ASHRAE A56)}$$

$$V_u = \frac{4{,}550\text{ lb}}{4} = 1{,}138\text{ lb}$$

ASCE/SEI 7-22 Basic Load Combination 7:

$$0.9D - E_v + E_h \qquad \text{(ASCE/SEI 7-22 Load Combination 7)}$$

$$T_u = \frac{0.9D - E_v}{4} - \frac{E_h h}{2}\left(\frac{\cos\theta}{b} + \frac{\sin\theta}{a}\right) \qquad \text{(Modified from ASHRAE A56)}$$

$$T_u = \frac{0.9(3{,}000\text{ lb}) - 284\text{ lb}}{4} - \frac{(4{,}550\text{ lb})(2\text{ ft})}{2}\left(\frac{\cos(38.16°)}{5.5\text{ ft}} + \frac{\sin(38.16°)}{7\text{ ft}}\right) = -448\text{ lb}$$

$$C_u = \frac{0.9D + E_v}{4} + \frac{E_h h}{2}\left(\frac{\cos\theta}{b} + \frac{\sin\theta}{a}\right) \qquad \text{(Modified from ASHRAE A56)}$$

$$C_u = \frac{0.9(3{,}000\text{ lb}) + 284\text{ lb}}{4} + \frac{(4{,}550\text{ lb})(2\text{ ft})}{2}\left(\frac{\cos(38.16°)}{5.5\text{ ft}} + \frac{\sin(38.16°)}{7\text{ ft}}\right) = 1{,}798\text{ lb}$$

$$V_u = \frac{E_h}{4} \qquad \text{(Modified from ASHRAE A56)}$$

$$V_u = \frac{4{,}550\text{ lb}}{4} = 1{,}138\text{ lb}$$

The vibration isolator would be designed to resist these forces.

In this example, there is no component or a support in the load path leading to the structure that undergoes ductile yielding at a load level less than the design strength of the corresponding anchor. The anchors are designed to resist the load combinations with overstrength, Ω_{0p}, in accordance with ASCE/SEI 7-22 Sections 2.3.6, 12.4.3, and 13.4.2. In the calculations below, the signs of E_v and E_h have been selected to result in the largest value of T_u. The geometry of the vibration isolators is shown in Figure 8-28. By inspection, the load combination that results in net tension on the anchors

governs. Thus, the ASCE/SEI 7-22 Basic Load Combination 7, including overstrength, is applied to obtain the controlling vertical design tension force:

$$0.9D - E_v + E_{mh} \qquad \text{(ASCE/SEI 7-22 Load Combination 7)}$$

Where: $E_{mh} = \Omega_{0p} Q_E$ (ASCE/SEI 7-22 Eq. 12.4-7 and Sec 13.4.2)

Tension per isolator:

$$T_u = \frac{0.9D - E_v}{4} - \frac{\Omega_{0p} E_h h}{2}\left(\frac{\cos\theta}{b} + \frac{\sin\theta}{a}\right)$$

$$T_u = \frac{0.9(3{,}000\text{ lb}) - 284\text{ lb}}{4} - \frac{(1.75)(4{,}550\text{ lb})(2\text{ ft})}{2}\left(\frac{\cos(38.16°)}{5.5\text{ ft}} + \frac{\sin(38.16°)}{7\text{ ft}}\right) = -1{,}237\text{ lb}$$

Acting concurrently with tension, the horizontal design shear force is:

$$V_u = \frac{\Omega_{0p} E_h}{4}$$

$$V_u = \frac{(1.75)(4{,}550\text{ lb})}{4} = 1{,}991\text{ lb}$$

Changes in the ASCE/SEI 7 22

The 2022 edition of ASCE/SEI 7 makes a clear distinction between two different overstrength factors in Chapter 13 for nonstructural components:

- Ω_0 is the overstrength factor for the building or nonbuilding structure supporting the component from ASCE/SEI 7-22 Table 12.2-1, Table 15.4-1, and Table 15.4-2. This factor is required to calculate the structure ductility reduction factor in ASCE/SEI 7-22 Equation 13.3-6.
- Ω_{0p} is the anchorage overstrength factor from ASCE/SEI 7-22 Table 13.5-1 and Table 13.6-1. This factor is necessary to calculate nonstructural component anchorage forces. Per ASCE/SEI 7-22 Section 13.4.2, for anchors in concrete or masonry, where required to apply the seismic load effects including overstrength, Ω_0 shall be taken as Ω_{0p}.

These parameters were prone to ambiguity in the previous editions of ASCE/SEI 7, as they used the same symbol, Ω_0.

Since the horizontal shear force is applied at the top of the isolator, it generates a moment that induces prying action, which will increase the tension on the anchor. Other local prying effects are assumed to be negligible, although in some cases these effects will be significant and would further increase the design anchor force. Assuming that each isolator is attached to the concrete slab with two anchors, the design tension force per anchor including the effects of prying, T_b, is:

$$T_b = \frac{T_u}{2 \text{ anchors}} - \left(\frac{5 \text{ in.}}{2 \text{ in.}}\right)\left(\frac{V_u}{2 \text{ anchors}}\right)$$

$$T_b = \frac{-1{,}237 \text{ lb}}{2 \text{ anchors}} - \left(\frac{5 \text{ in.}}{2 \text{ in.}}\right)\left(\frac{1{,}991 \text{ lb}}{2 \text{ anchors}}\right) = -3{,}107 \text{ lb}$$

The design shear force per bolt, is:

$$V_b = \frac{V_u}{2 \text{ anchors}}$$

$$V_b = \frac{1{,}991 \text{ lb}}{2 \text{ anchors}} = 995 \text{ lb}$$

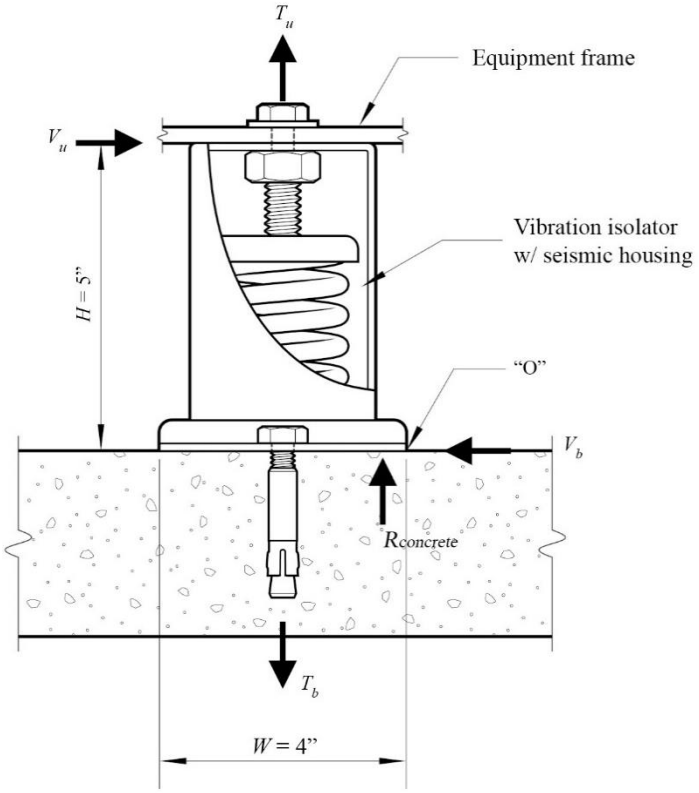

Figure 8-28. Anchor and Snubber Loads for Support on Vibration Isolation Springs

8.5.5 Additional Considerations for Support on Vibration Isolators

Vibration isolation springs are provided for equipment to prevent vibration from being transmitted to the building structure. However, they provide virtually no resistance to horizontal seismic forces. In such cases, some type of restraint is required to resist the seismic forces. Figure 8-29 illustrates one concept where a bolt attached to the equipment base is allowed to displace a controlled distance (gap) in either direction along its longitudinal axis before it contacts resilient impact material.

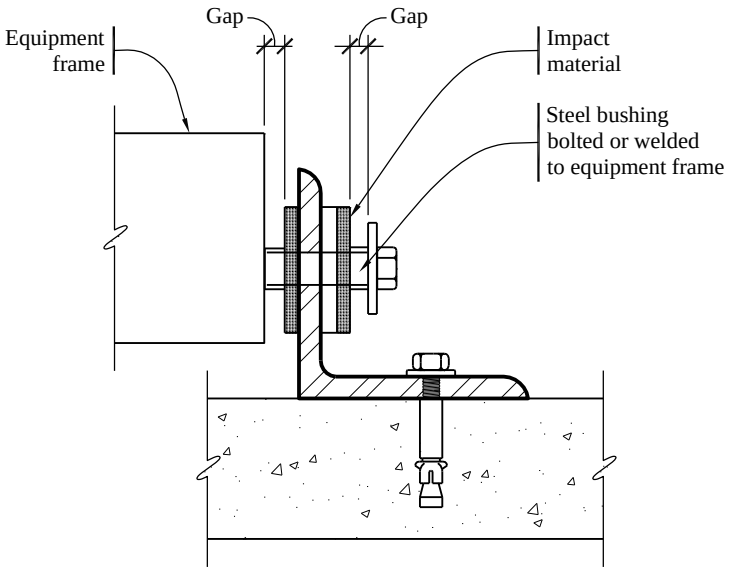

Figure 8-29. Lateral Restraint Required to Resist Seismic Forces

Design of restraints for vibration-isolated equipment varies for different applications and for different manufacturers. In most cases, restraint design incorporates all directional capability with an air gap, a soft impact material, and a ductile restraint or housing.

Restraints should have all-directional restraint capability to resist both horizontal and vertical motion. Vibration isolators have little or no resistance to overturning forces. Therefore, if there is a difference in height between the equipment's center of gravity and the support points of the springs, rocking is inevitable and vertical restraint is required.

An air gap between the restraint device and the equipment prevents vibration from transmitting to the structure during normal operation of the equipment. Air gaps generally are no greater than 1/4 in. Dynamic tests indicate a significant increase in acceleration for air gaps larger than 1/4 in., and this is reflected in the requirement in ASCE/SEI 7-22 Table 13.6-1, Footnote a, where F_p is doubled if the air gap exceeds 1/4 in.

A soft impact material, often an elastomer such as bridge bearing neoprene, reduces accelerations and impact loads by preventing steel-to-steel contact. The thickness of the elastomer can significantly reduce accelerations to both the equipment and the restraint device and should be addressed specifically for life-safety applications.

In Section 8.5.3, the example was for a housed isolator, where the vibration isolator and seismic restraints are combined into a single unit. A ductile restraint or housing is critical to prevent catastrophic failure. Unfortunately, housed isolators made of brittle materials such as cast iron often are assumed to be capable of resisting seismic loads and continue to be installed in seismic zones.

Overturning calculations for vibration-isolated equipment must consider a worst-case scenario, as illustrated in Section 8.5.4. However, important variations in calculation procedures merit further

discussion. For equipment that is usually directly attached to the structure or mounted on housed vibration isolators, the weight can be used as a restoring force since the equipment will not transfer a tension load to the anchors until the entire equipment weight is overcome at any corner. For equipment installed on any other vibration-isolated system (such as the separate spring and snubber arrangement shown in Figure 8-29), the weight of the unit cannot be used to provide a restoring force in the overturning calculations.

As the foregoing illustrates, design of restraints for resiliently mounted equipment is a specialized topic. ASCE/SEI 7-22 sets out only a few of the governing criteria. Some suppliers of vibration isolators in the highest seismic zones are familiar with the appropriate criteria and procedures. Consultation with these suppliers may be beneficial.

8.6 Piping System Seismic Design

8.6.1 Example Description

Example Summary

- **Nonstructural components**: Mechanical and electrical – piping not in accordance with ASME B31 with threaded joints
- **Building seismic force-resisting system:** Steel buckling-restrained braced frames
- **Equipment support:** Distribution system supports – distribution system supports using hot-rolled steel bracing
- **Occupancy:** Acute care hospital
- **Risk Category:** IV
- **Component Importance Factor:** $I_p = 1.5$
- **Number of stories:** 2
- $\boldsymbol{S_{DS}} = 1.00$

The 2022 edition of the ASCE/SEI 7 makes the distinction between “distribution systems” and “distribution system supports” for seismic design forces. The seismic demands are different, as they have different seismic coefficients, per ASCE/SEI 7-22 Table 13.6-1.

Piping and tubing systems requirements are contained in ASCE/SEI 7-22 Section 13.6.7. Suspended components that are installed in-line and rigidly connected to and supported by the piping system, such as valves, strainers, traps, pumps, air separators and tanks, are permitted to be considered part of the piping system for the purposes of determining the need for and sizing of lateral bracing. Where components are braced independently due to their weight, but the associated piping is not braced, flexibility must be provided to accommodate relative movement between the components.

This example focuses on the seismic design for a portion of a piping system and associated supports and bracing. The piping system is housed in a two-story acute care hospital. The stories have a typical story height of 15 feet. The seismic force-resisting system consists of steel buckling-restrained braced frames in the two orthogonal directions. The piping system is illustrated in Figure 8-30 and Figure 8-31. The typical trapeze-type support assembly is shown in Figure 8-32 and Figure 8-33. One run of the piping system crosses a seismic separation joint to enter an adjacent structure. The building is located in an area of high ground shaking potential. Given the assigned Risk Category IV for emergency facilities, the components are assigned $I_p = 1.5$, unless it can be shown that the component is not needed for continued operation of the facility and failure of the component would not impair operations. Since failure of the piping system will result in flooding of the hospital, $I_p = 1.5$.

This example considers three piping runs of a chilled water piping system supported from the roof of a two-story structure. The system is not intended to meet the ASME B31 requirements.

This example illustrates the following calculation procedures:

- Prescribed seismic forces, proportioning, and design forces for the piping system (see Section 8.6.3 in this example).
- Prescribed seismic forces, proportioning, and design forces for the pipe supports and bracing (see Section 8.6.4 in this example).
- Prescribed seismic displacements and displacement-induced demand in piping system (see Section 8.6.5 in this example).

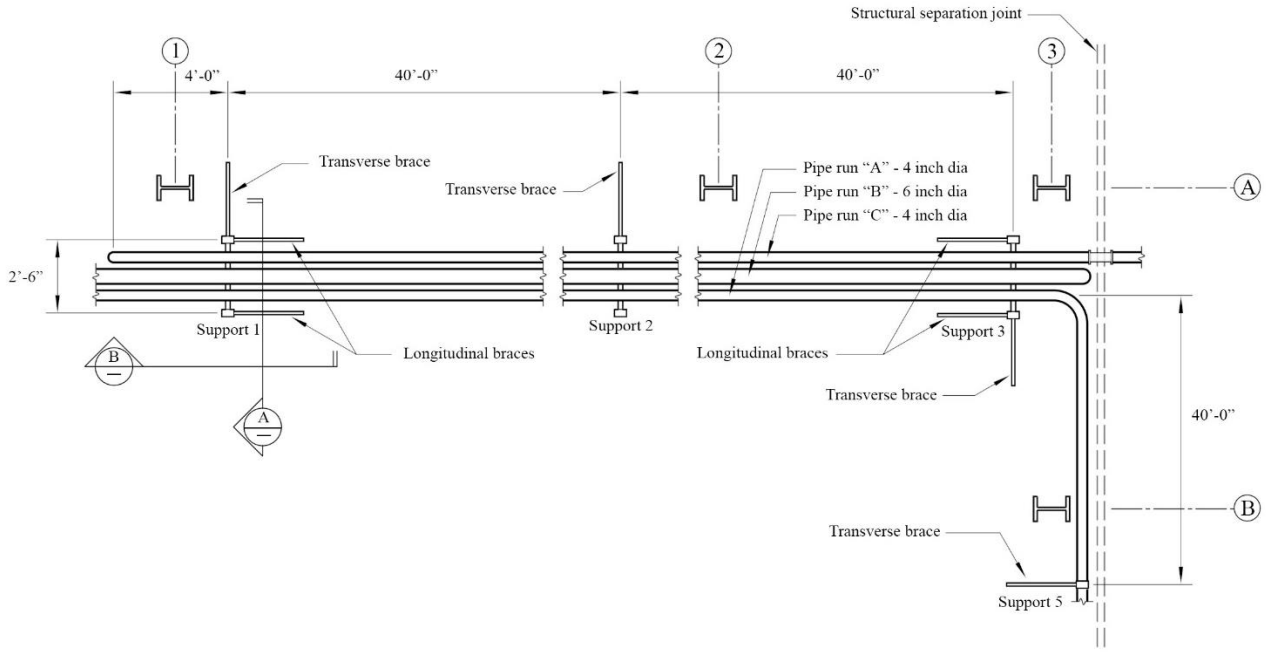

Figure 8-30. Plan of Piping System

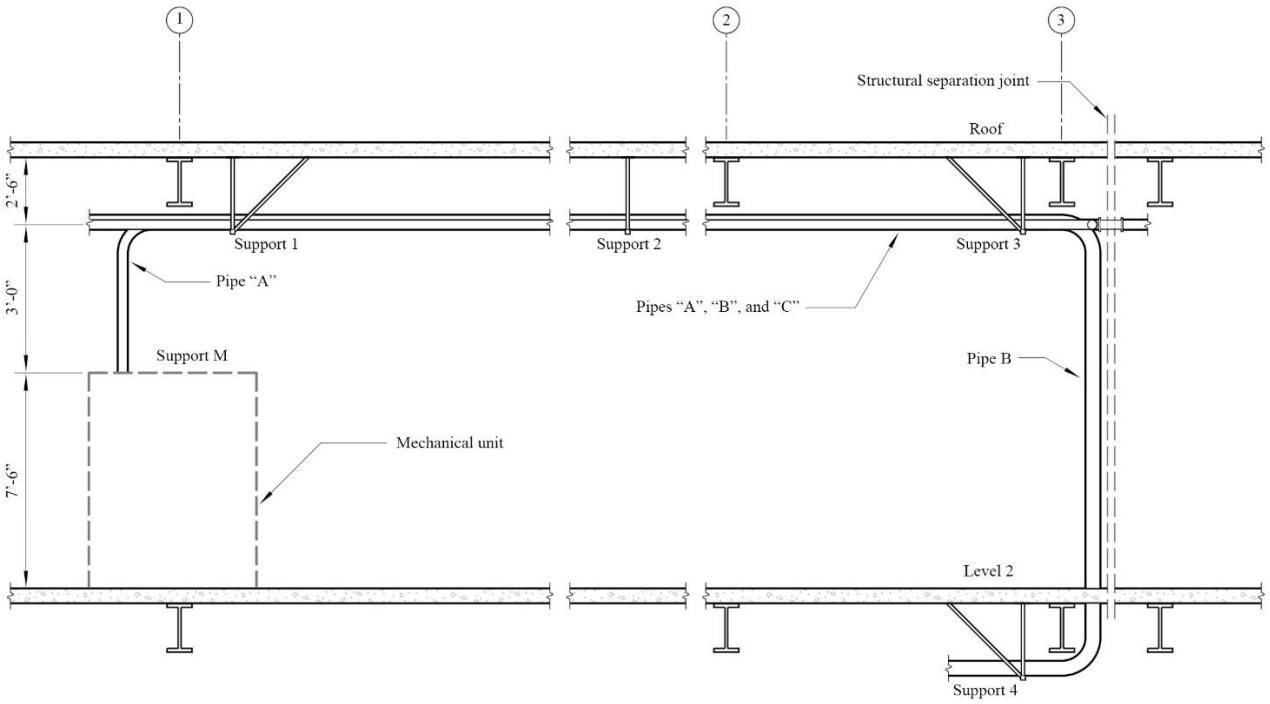

Figure 8-31. Piping System Near Column Line A

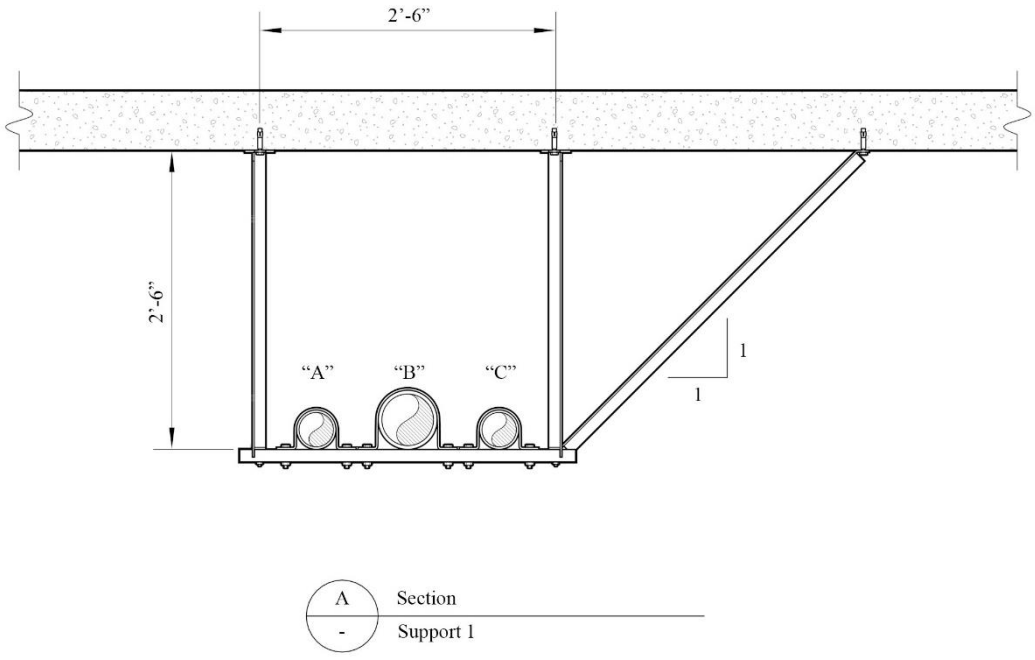

Figure 8-32. Typical Trapeze-Type Support Assembly with Transverse Bracing

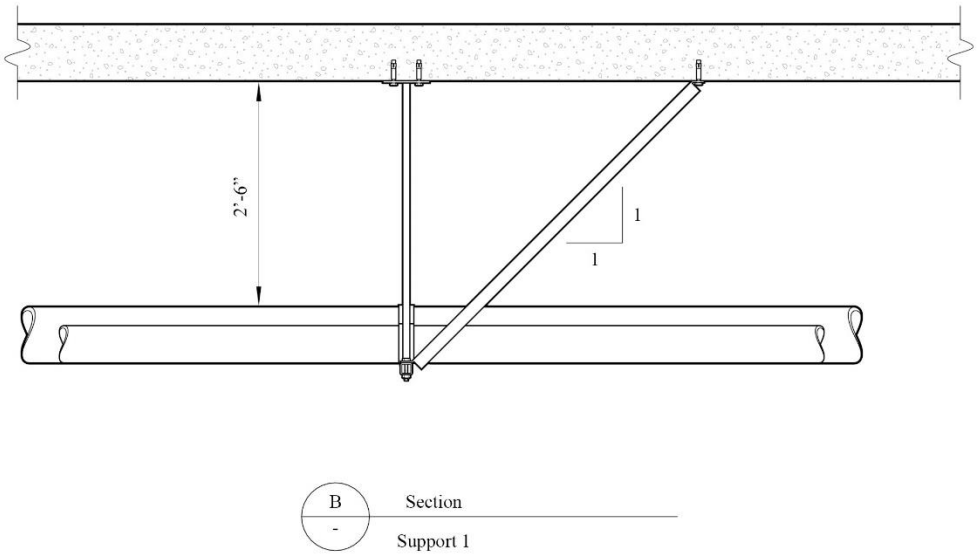

Figure 8-33. Typical Trapeze-Type Support Assembly with Longitudinal Bracing

System Configuration

The portion of the piping system under consideration consists of three piping runs:

- Piping Run “A,” a 4-inch-diameter pipe, which connects to a large mechanical unit at Line 1 supported at Level 2. It crosses a seismic separation between adjacent structures at Line 3.
- Piping Run "B," a 6-inch-diameter pipe, which has a vertical riser to Level 2 at Line 3.
- Piping Run "C," a 4-inch-diameter pipe, which turns 90 degrees to parallel Line 3 at Column Line 3-A.

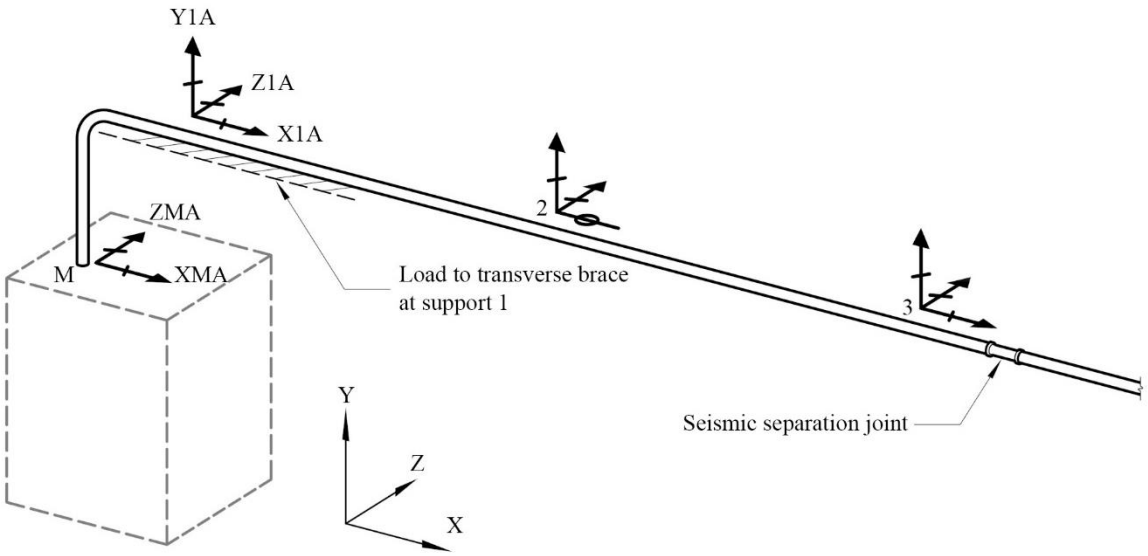

Figure 8-34. Piping Run “A”

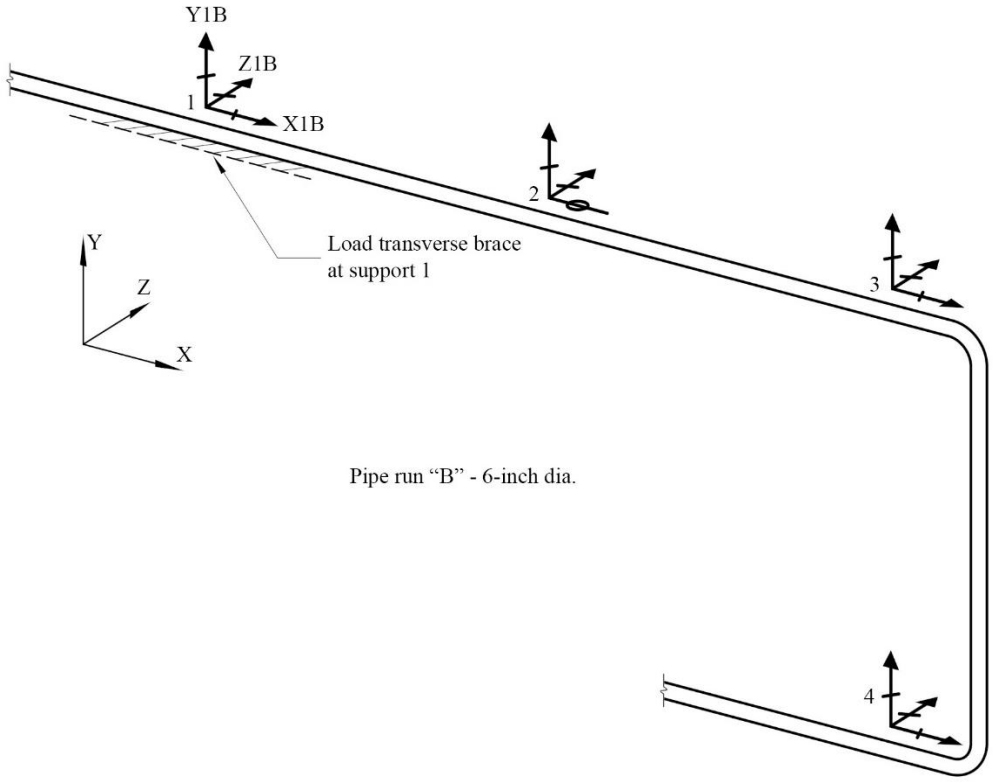

Figure 8-35. Piping Run "B"

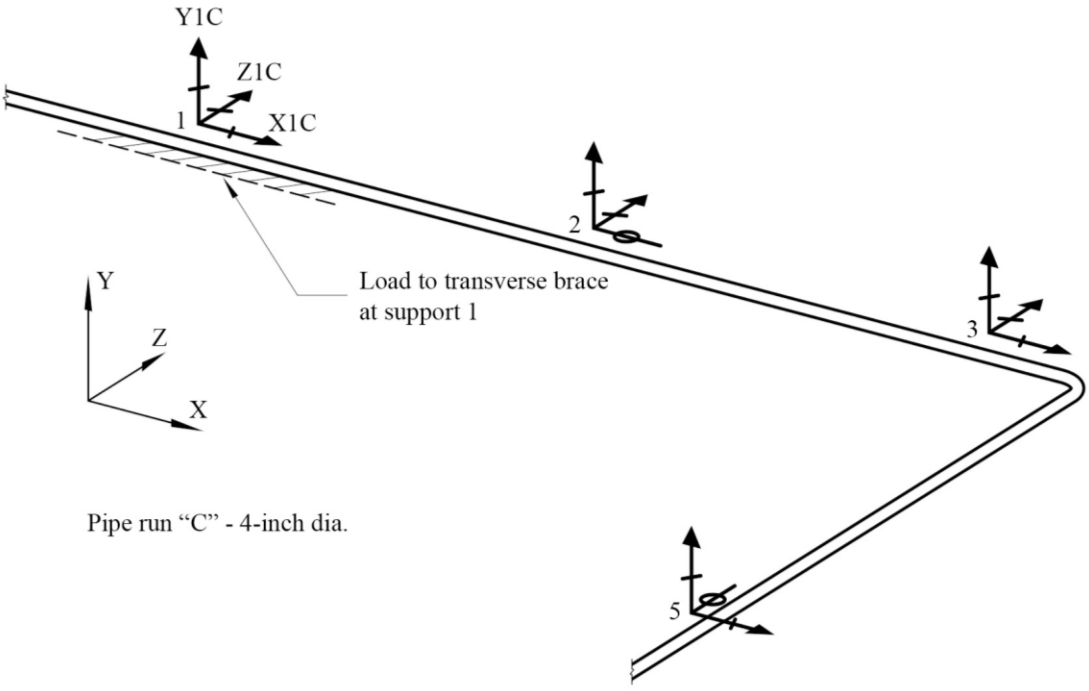

Figure 8-36. Piping Run "C"

ASCE/SEI 7-22 provides requirements for three types of piping systems:

- ASME B31 pressure piping systems in Section 13.6.7.1.
- Fire protection piping systems in accordance with NFPA 13 in Section 13.6.7.2.
- Piping and tubing systems that are not compliant with the ASME B31 and NFPA 13 in Section 13.6.7.

The third type corresponds to the appropriate classification for this example, and ASCE/SEI 7-22 Section 13.6.7 is followed in the design.

Earthquake design requirements for piping systems in the ASCE/SEI 7-22 depend on the Component Importance Factor, I_p, the pipe diameter, and the installation geometry. The exemptions in Section 13.1.4 have been revised in the 2022 edition of ASCE/SEI 7. Refer to Section 8.2.17 of this chapter. For the piping system of the example, the exceptions are not applicable because the pipe size exceeds the conduit trade size limit. Thus, it shall be provided with flexible connections or designed for seismic forces and seismic relative displacements.

Piping systems may be exempt from the seismic design requirements if they meet the requirements in ASCE/SEI 7-22 Section 13.6.5. Per that section, piping systems may be exempt if flexible connections, expansion loops, or other assemblies are provided to accommodate the relative displacement between component and piping, the piping system is positively attached to the structure, and where one of the following applies:

1. Trapeze assemblies are supported by 3/8 in. (10 mm) diameter rod hangers not exceeding 12 in. (305 mm) in length from the pipe support point to the connection at the supporting structure, do not support piping with I_p greater than 1.0, no single pipe exceeds the limits set forth in Items 4a, 4b, or 4c below, and the total weight supported by any single trapeze is 100 lb (445 N) or less; or
2. Trapeze assemblies are supported by 1/2 in. (13 mm) diameter rod hangers not exceeding 12 in. (305 mm) in length from the pipe support point to the connection at the supporting structure, do not support piping with I_p greater than 1.0, no single pipe exceeds the diameter limits set forth in Items 4a, 4b, or 4c below, and the total weight supported by any single trapeze is 200 lb (890 N) or less; or
3. Trapeze assemblies are supported by 1/2 in. (13 mm) diameter rod hangers not exceeding 24 in. (610 mm) in length from the pipe support point to the connection at the supporting structure, do not support piping with I_p greater than 1.0, no single pipe exceeds the diameter limits set forth in Items 4a, 4b, or 4c below, and the total weight supported by any single trapeze is 100 lb (445 N) or less; or
4. Piping is supported by rod hangers and provisions are made to avoid impact with other structural or nonstructural components or to protect the piping in the event of such impact, or pipes are supported by individual rod hangers 3/8 in. (10 mm) or 1/2 in. (13 mm) in diameter, where each

hanger in the pipe run is 12 in. (305 mm) or less in length from the pipe support point to the connection at the supporting structure, and the total weight supported by any single hanger is 50 lb (220 N) or less. In addition, the following limitations on the size of piping shall be observed:

- In structures assigned to Seismic Design Category C where I_p is greater than 1.0, the nominal pipe size shall be 2 in. (50 mm) or less.
- In structures assigned to Seismic Design Category D, E, or F where I_p is greater than 1.0, the nominal pipe size shall be 1 in. (25 mm) or less.
- In structures assigned to Seismic Design Category D, E, or F where $I_p = 1.0$, the nominal pipe size shall be 3 in. (80 mm) or less.

None of these exceptions is applicable to our example piping system, as the Component Importance Factor, $I_p = 1.5$, and the pipe exceeds the size limits for the exception. ASCE/SEI 7-22 13.6.5 Item 4 waives seismic support requirements for piping with I_p greater than 1.0 if the pipe is 1 in. or less in diameter in Seismic Design Categories D, E, and F. The piping system in our example includes 4-in. diameter and 6-in. diameter pipes; thus, seismic design and lateral supports are required.

It should be noted that details of pipe bracing systems vary according to the local preferences and practices of mechanical and plumbing contractors. In addition, the use of proprietary pipe hanging and bracing systems is relatively common. As a result, this example concentrates on quantifying the prescribed seismic forces and displacements and on simplified stress checks of the piping system itself. After the seismic forces and displacements are determined, the bracing and anchorage connections can be designed and detailed according to the appropriate AISC and ACI codes. The sizing of the elements is not covered in this example.

8.6.2 Design Requirements

8.6.2.1 ASCE/SEI 7-22 PARAMETERS AND COEFFICIENTS

The following parameters and coefficients are derived from the example description, or it is known information based on the structure, selected location, and site class.

Coefficients for mechanical and electrical components

Distribution systems – Piping and tubing not in accordance with ASME B31, including in-line components, constructed of high- or limited-deformability materials, with joints made by threading, bonding, compression couplings, or grooved couplings:

$C_{AR} = 2.2$ (ASCE/SEI 7-22 Table 13.6-1)

$R_{po} = 2.0$ (ASCE/SEI 7-22 Table 13.6-1)

$\Omega_{0p} = 1.75$ (ASCE/SEI 7-22 Table 13.6-1)

Distribution system supports – hot-rolled steel bracing:

$C_{AR} = 1.0$ (ASCE/SEI 7-22 Table 13.6-1)

$R_{po} = 1.5$ (ASCE/SEI 7-22 Table 13.6-1)

$\Omega_{0p} = 2.0$ (ASCE/SEI 7-22 Table 13.6-1)

Changes in the ASCE/SEI 7 22

The ASCE/SEI 7-22, Table 13.6-1 includes four bracing types for distribution system supports in mechanical and electrical components: "tension-only and cable bracing," "cold-formed steel rigid bracing," "hot-rolled steel bracing," and "other rigid bracing." The latter refers to bracing constructed of materials other than steel.

For this edition of ASCE/SEI 7, the seismic coefficients C_{AR}, R_{po}, and Ω_{0p} are identical for all bracing options. However, it is expected that research indicates variations in the performance of these systems, which will be captured in future editions.

Design coefficients and factors for seismic force-resisting systems

Building frame systems – steel buckling-restrained braced frames:

$R = 8.0$ (ASCE/SEI 7-22 Table 12.2-1)

$\Omega_0 = 2.5$ (ASCE/SEI 7-22 Table 12.2-1)

Short period design spectral acceleration, $S_{DS} = 1.00$ (given)

Seismic Design Category: D (ASCE/SEI 7-22 Sec. 11.6

Seismic Importance Factor, $I_e = 1.5$ (ASCE/SEI 7-22 Table 1.5-2)

Component Importance Factor, $I_p = 1.5$ (ASCE/SEI 7-22 Sec. 13.1.3)

Redundancy factor for nonstructural components, $\rho = 1.0$ (ASCE/SEI 7-22 Sec. 13.3.1)

Height of attachment at roof, $z = 30$ ft (given)

Story height, $h_{sx} = 15$ ft (given)

Gravity (non-seismic) support spacing, $L_{grav\ sup} = 10$ ft (given)

Lateral brace spacing, $L_{lat\ brace} = 40$ ft (given)

Longitudinal brace spacing, $L_{long\ brace} = 80$ ft (given)

Length from Support 1 to mechanical unit, $L_{1M} = 9$ ft (given)

ASTM A53 Pipe with threaded connections, $F_y = 35{,}000$ psi (given)

System working pressure, $P = 200$ psi (given)

4-inch diam. water-filled pipe weight, $D = W_p = 16.4$ plf (given)

6-inch diam. water-filled pipe weight, $D = W_p = 31.7$ plf (given)

Approximate fundamental period of the supporting structure, T_a – steel buckling-restrained braced frames

$h_n = h = 30$ ft (structural height)

$C_t = 0.03$ (ASCE/SEI 7-22 Table 12.8-2)

$x = 0.75$ (ASCE/SEI 7-22 Table 12.8-2)

$T_a = C_t {h_n}^x = (0.03)(30\text{ ft})^{0.75} = 0.38$ s (ASCE/SEI 7-22 Eq. 12.8-7)

Force amplification factor as a function of height in the structure, H_f

$a_1 = \frac{1}{T_a} \leq 2.5$ (ASCE/SEI 7-22 Sec. 13.3.1.1)

$a_1 = \frac{1}{0.38\ s} = 2.63 \leq 2.5$, use $a_1 = 2.5$

$a_2 = [1 - (0.4/T_a)^2] \geq 0$ (ASCE/SEI 7-22 Sec. 13.3.1.1)

$a_2 = [1 - (0.4/0.38\ s)^2] = -0.11 > 0$, use $a_2 = 0$

$H_f = 1 + a_1\left(\frac{z}{h}\right) + a_2\left(\frac{z}{h}\right)^{10}$ (ASCE/SEI 7-22 Eq. 13.3-4)

$H_f = 1 + 2.5\left(\frac{30\text{ ft}}{30\text{ ft}}\right) + 0\left(\frac{30\text{ ft}}{30\text{ ft}}\right)^{10} = 3.5$

Structure ductility reduction factor, R_μ

$R_\mu = (1.1\,R/(\,I_e\Omega_0))^{1/2} \geq 1.3$ (ASCE/SEI 7-22 Eq. 13.3-6)

$R_\mu = (1.1(8/((1.5)(2.5)))^{1/2} = 1.53 \geq 1.3$

8.6.2.2 APPLICABLE REQUIREMENTS

The architectural, mechanical, and electrical components, supports, and attachments shall comply with the sections referenced in ASCE/SEI 7-22 Table 13.2-1. Thus, the nonstructural components of this example are designed in accordance with the following considerations:

- System failure shall not cause failure of an essential architectural, mechanical, or electrical component (ASCE/SEI 7-22 Section 13.2.4).
- Component seismic attachments shall be bolted, welded, or otherwise positively fastened without considering the frictional resistance produced by the effects of gravity (ASCE/SEI 7-22 Section 13.4).
- The horizontal seismic design force, F_p, shall be applied at the component's center of gravity and distributed relative to the component's mass distribution (ASCE/SEI 7-22 Section 13.3.1).
- The effects of seismic relative displacements shall be considered in combination with displacements caused by other loads as appropriate (ASCE/SEI 7-22 Section 13.3.2).
- The piping system shall be designed for the seismic forces and seismic relative displacements of Section 13.3 (ASCE/SEI 7-22 Section 13.6.7).
- The distribution system supports shall be designed for seismic forces and seismic relative displacements, as required in Section 13.3.1. Distribution systems shall be braced to resist vertical, transverse, and longitudinal seismic loads (ASCE/SEI 7-22 Section 13.6.4.7).

8.6.3 Piping System Design

The piping system consists of non-ASME B31 piping fabricated from steel Schedule 40 pipe with threaded connections. This example covers determination of the seismic forces acting on the system and checking of the seismically induced stresses in the pipes using simplifying assumptions.

8.6.3.1 PRESCRIBED SEISMIC FORCES

Seismic design force, F_p

$$F_p = 0.4 S_{DS} I_p W_p \left[\frac{H_f}{R_\mu}\right] \left|\frac{C_{AR}}{R_{po}}\right| \qquad \text{(ASCE/SEI 7-22 Eq. 13.3-1)}$$

$$F_p = 0.4(1.0)(1.5)\left(W_p\right) \left[\frac{3.5}{1.53}\right] \left|\frac{2.2}{2.0}\right| = 1.508 W_p \qquad \text{(controlling equation)}$$

$$F_{p,max} = 1.6 S_{DS} I_p W_p \qquad \text{(ASCE/SEI 7-22 Eq. 13.3-2)}$$

$$F_{p,max} = 1.6(1.0)(1.5)\left(W_p\right) = 2.40 W_p$$

$$F_{p,min} = 0.3 S_{DS} I_p W_p \qquad \text{(ASCE/SEI 7-22 Eq. 13.3-3)}$$

$$F_{p,min} = 0.3(1.0)(1.5)\left(W_p\right) = 0.45W_p$$

$F_p = 1.508W_p$ (controlling seismic design force)

Horizontal seismic load effect, E_h

$Q_E = F_p = 1.508W_p$ (effect from F_p)

$E_h = \rho Q_E$ (ASCE/SEI 7-22 Eq. 12.4-3)

$$E_h = (1.0)\left(1.508W_p\right) = 1.508W_p$$

Vertical seismic load effect, E_v

$E_v = 0.2S_{DS}D$ (ASCE/SEI 7-22 Eq. 12.4-4a)

The above terms are then substituted into the following Basic Load Combinations for Strength Design from ASCE/SEI 7-22 Sections 2.3.6 and 12.4.2 to determine the design member and connection forces to be used in conjunction with seismic loads.

$1.2D + E_v + E_h + L + 0.2S$ (ASCE/SEI 7-22 Load Combination 6)

$0.9D - E_v + E_h$ (ASCE/SEI 7-22 Load Combination 7)

For nonstructural components, the terms *L* and *S* are typically zero.

8.6.3.2 PROPORTIONING AND DESIGN

Where $I_p > 1.0$, the component itself, in this case, the pipe, shall also meet the seismic loading and stress limit requirements.

The spacing of seismic supports is often determined by the need to limit stresses in the pipe. Therefore, the piping stress check is often performed first in order to confirm the assumptions on brace spacing. For non-ASME B31 piping that is not subject to high operating temperatures or pressures, the stress check assumptions may be simplified. The pipes can be idealized as continuous beams spanning between lateral braces, while longitudinal forces can be determined using the length of pipe tributary to the longitudinal brace.

The permissible stresses in the pipe are given in ASCE/SEI 7-22 Section 13.6.7, Item c. For piping with threaded connections, the permissible stresses are limited to 70 percent of the minimum specified yield strength.

The section properties of the Schedule 40 pipes are as follows:

4-inch diameter pipe:

Inner diameter, $d_1 = 4.026$ in.

Outer diameter, $d = 4.5$ in.

Wall thickness, $t = 0.237$ in.

Plastic modulus, $Z = \frac{d^3}{6} - \frac{d1^3}{6} = \frac{(4.5 \text{ in.})^3}{6} - \frac{(4.026 \text{ in.})^3}{6} = 4.31 \text{ in.}^3$

Moment of inertia, $I = \frac{\pi}{64}(d^4 - d_1^4) = \frac{\pi}{64}((4.5 \text{ in.})^4 - (4.026 \text{ in.})^4) = 7.23 \text{ in.}^4$

6-inch diameter pipe:

Inner diameter, $d_1 = 6.065$ in.

Outer diameter, $d = 6.625$ in.

Wall thickness, $t = 0.28$ in.

Plastic modulus, $Z = \frac{d^3}{6} - \frac{d1^3}{6} = \frac{(6.625 \text{ in.})^3}{6} - \frac{(6.065 \text{ in.})^3}{6} = 11.28 \text{ in.}^3$

Moment of inertia, $I = \frac{\pi}{64}(d^4 - d_1^4) = \frac{\pi}{64}((6.625 \text{ in.})^4 - (6.065 \text{ in.})^4) = 28.14 \text{ in.}^4$

Gravity and Pressure Loads

The longitudinal stresses in piping due to pressure and weight may be estimated using the following equation:

$$f_L = \frac{Pd}{4t} + \frac{M_g}{Z}$$

where:

f_L = sum of the longitudinal stresses due to pressure and weight

P = internal design pressure, psig

d = outside diameter of pipe, in.

t = pipe wall thickness, in.

M_g = resultant moment loading in cross-section due to weight and sustained loads, lb-in.

Z = section modulus, in.^{3}

The resultant moment due to forces in the gravity direction, M_g, may be conservatively estimated as follows:

$$M_g = \frac{(D)\left(L_{grav\,sup}\right)^2}{8}$$

For a 4-inch-diameter pipe:

Resultant moment, M_g

$$M_g = \frac{(16.4\text{ plf})(10\text{ ft})^2}{8} = 205\text{ lb-ft} = 2{,}460\text{ lb-in.}$$

Longitudinal stresses due to dead load, $f_{L,Dead}$

$$f_{L,Dead} = \frac{M_g}{Z} = \frac{2{,}460\text{ lb-in.}}{4.31\text{ in.}^3} = 571\text{ psi}$$

Longitudinal stresses due to system working pressure, $f_{L,Pressure}$

$$f_{L,Pressure} = \frac{Pd}{4t} = \frac{(200\text{ psi})(4.5\text{ in.})}{4(0.237\text{ in.})} = 949\text{ psi}$$

For a 6-inch-diameter pipe:

Resultant moment, M_g

$$M_g = \frac{(31.7\text{ plf})(10\text{ ft})^2}{8} = 396\text{ lb-ft} = 4{,}755\text{ lb-in.}$$

Longitudinal stresses due to dead load, $f_{L,Dead}$

$$f_{L,Dead} = \frac{M_g}{Z} = \frac{4{,}755\text{ lb-in.}}{11.28\text{ in.}^3} = 422\text{ psi}$$

Longitudinal stresses due to system working pressure, $f_{L,Pressure}$

$$f_{L,Pressure} = \frac{Pd}{4t} = \frac{(200\text{ psi})(6.625\text{ in.})}{4(0.28\text{ in.})} = 1{,}183\text{ psi}$$

Seismic Loads on Piping Runs "A" and "C"

By idealizing the piping runs as continuous beams, the maximum bending moments and reactions can be readily estimated.

Piping Runs "A" and "C" are 4-inch-diameter pipes, shown schematically in Figure 8-34 and Figure 8-36. They are idealized as a two-span continuous beam. The horizontal seismic load effect, $E_{h,}$ and vertical seismic load effect, E_v, are calculated as follows:

$$F_p = 1.508W_p = 1.508(16.4 \text{ plf}) = 24.7 \text{ lb/ft}$$

$$E_h = \rho Q_E = \rho F_p = (1.0)(24.7 \text{ lb/ft}) = 24.7 \text{ lb/ft}$$

$$E_v = 0.2S_{DS}D = 0.2(1.0)(16.4 \text{ plf}) = 3.28 \text{ lb/ft}$$

Maximum moment due to horizontal seismic load, M_{Eh}

$$M_{Eh} = \frac{(E_h)(L_{lat\ brace})^2}{8} = \frac{(24.7 \text{ lb/ft})(40 \text{ ft})^2}{8} = 4{,}946 \text{ lb-ft} = 59{,}353 \text{ lb-in.}$$

The flexural stress associated with this moment is:

$$f_{bh} = \frac{M_{Eh}}{Z} = \frac{59{,}353 \text{ lb-in.}}{4.31 \text{ in.}^3} = 13{,}766 \text{ psi}$$

Moment due to vertical seismic load, M_{Ev}

$$M_{Ev} = \frac{(E_v)(L_{grav\ sup})^2}{8} = \frac{(3.28 \text{ plf})(10 \text{ ft})^2}{8} = 41 \text{ lb-ft} = 492 \text{ lb-in.}$$

The flexural stress associated with this moment is:

$$f_{bv} = \frac{M_{Ev}}{Z} = \frac{492 \text{lb-in.}}{4.31 \text{ in.}^3} = 114 \text{ psi}$$

Note that for vertical seismic effects, the span of the pipe is taken as the distance between vertical supports, not the distance between lateral bracing.

The Basic Load Combination for Strength Design including earthquake effects from ASCE/SEI 7-22 Sections 2.3.6 and 12.4.2 that will govern is Load Combination 6:

$$1.2D + E_v + E_h + L + 0.2S \qquad \text{(ASCE/SEI 7-22 Load Combination 6)}$$

In this example, the terms L and S are equal to zero. The dead load, *D*, includes bending stress due to dead load. The load factor for internal pressure is the same as that for dead load. The design stress in the pipe is therefore:

$$f_u = 1.2(f_{L,Dead} + f_{L,Pressure}) + f_{bv} + f_{bh}$$

$$f_u = 1.2(571 \text{ psi} + 949 \text{ psi}) + 114 \text{ psi} + 13{,}766 \text{ psi} = 15{,}704 \text{ psi}$$

The permissible stress from ASCE/SEI 7-22 Section 13.6.7, Item c, is $0.7F_y = 0.7(35{,}000 \text{ psi}) = 24{,}500$ psi. Comparing the demand to capacity:

$$f_u < 0.7F_y$$

$$15{,}704 \text{ psi} < 24{,}500 \text{ psi} \qquad \textbf{OK}$$

Note that a number of conservative assumptions were made for the sake of simplicity. A more precise analysis can be performed, where the piping is modeled to achieve more accurate bending moments and the effects of biaxial bending in the pipe are considered separately. Also note that at any point in the pipe wall, the stresses caused by dead (and vertical seismic) load and by horizontal seismic load occur in different physical locations in the pipe. The peak stresses due to vertically applied load occur at the top and bottom of the pipe, while the peak stress for horizontally applied load occurs at mid-height of the pipe. Assuming that they are both occurring in the same location and are summed algebraically is quite conservative.

Seismic Loads on Piping Run "B"

Piping Run "B," a 6-inch-diameter pipe, is shown schematically in Figure 8-35. It is idealized as a two-span continuous beam. Note that the effects of the 15-foot-high riser between Level 2 and the roof are considered separately. The horizontal seismic load effect, E_h, and vertical seismic load effect, E_v, are calculated as follows:

$$F_p = 1.508W_p = 1.508(31.7 \text{ plf}) = 47.8 \text{ lb/ft}$$

$$E_h = \rho Q_E = \rho F_p = (1)(47.8 \text{ lb/ft}) = 47.8 \text{ lb/ft}$$

$$E_v = 0.2S_{DS}D = 0.2(1.0)(31.7 \text{ plf}) = 6.34 \text{ lb/ft}$$

Maximum moment due to horizontal seismic load, M_{Eh}

$$M_{Eh} = \frac{(E_h)(L_{lat\ brace})^2}{8} = \frac{(47.8 \text{ lb/ft})(40 \text{ ft})^2}{8} = 9{,}560 \text{ lb-ft} = 114{,}725 \text{ lb-in.}$$

The flexural stress associated with this moment is:

$$f_{bh} = \frac{M_{Eh}}{Z} = \frac{114{,}725 \text{ lb–in.}}{11.28 \text{ in.}^3} = 10{,}171 \text{ psi}$$

Moment due to vertical seismic load, M_{Ev}

$$M_{Ev} = \frac{(E_v)(L_{grav\ sup})^2}{8} = \frac{(6.34 \text{ plf})(10 \text{ ft})^2}{8} = 79 \text{ lb-ft} = 951 \text{ lb-in.}$$

The flexural stress associated with this moment is:

$$f_{bv} = \frac{M_{Ev}}{Z} = \frac{951 \text{ lb–in.}}{11.28 \text{ in.}^3} = 84 \text{ psi}$$

Note that for vertical seismic effects, the span of the pipe is taken as the distance between vertical supports, not the distance between lateral bracing.

The Basic Load Combination for Strength Design including earthquake effects from ASCE/SEI 7-22 Sections 2.3.6 and 12.4.2 that will govern is the Basic Load Combination 6:

$$1.2D + E_v + E_h + L + 0.2S \qquad \text{(ASCE/SEI 7-22 Load Combination 6)}$$

In this example, the terms L and S are equal to zero. The dead load, D, includes bending stress due to dead load. The load factor for internal pressure is the same as that for dead load. The design stress in the pipe is therefore:

$$f_u = 1.2(f_{L,Dead} + f_{L,Pressure}) + f_{bv} + f_{bh}$$

$$f_u = 1.2(421 \text{ psi} + 1{,}183 \text{ psi}) + 84 \text{ psi} + 10{,}171 \text{ psi} = 12{,}181 \text{ psi}$$

The permissible stress from ASCE/SEI 7-22 Section 13.6.7, Item c, is $0.7F_y = 0.7(35{,}000 \text{ psi}) = 24{,}500 \text{ psi}$. Comparing the demand to capacity:

$$f_u < 0.7F_y$$

$$12{,}181 \text{ psi} < 24{,}500 \text{ psi} \qquad \textbf{OK}$$

8.6.4 Pipe Supports and Bracing

In this section, design demands are calculated for vertical supports, lateral supports, and anchorage at the piping Support 1. The support geometry and configuration are presented in Figure 8-37. As with the design of the piping system, design of the support is simplified by considering conservative assumptions.

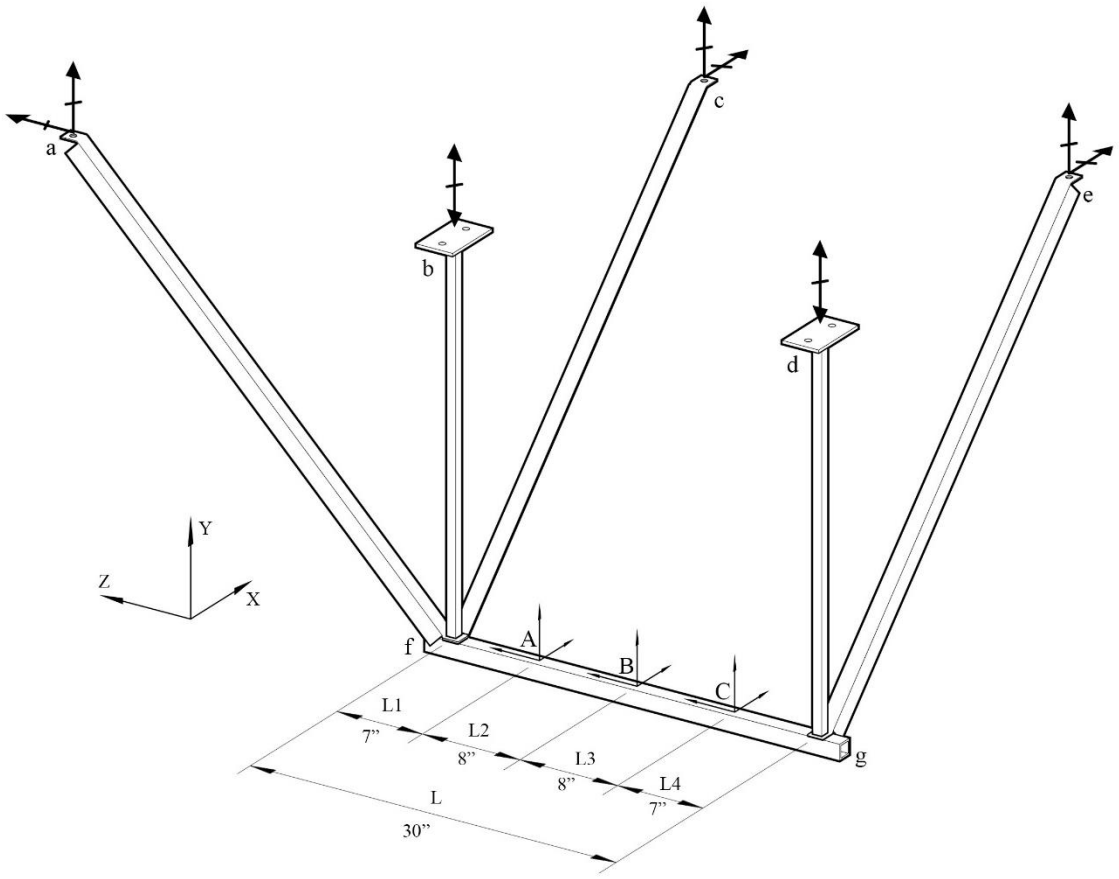

Figure 8-37. Design Demands on Piping Support Assembly

8.6.4.1 PRESCRIBED SEISMIC FORCES

Seismic design force, F_p

$$F_p = 0.4 S_{DS} I_p W_p \left[\frac{H_f}{R_\mu}\right] \left|\frac{C_{AR}}{R_{po}}\right| \qquad \text{(ASCE/SEI 7-22 Eq. 13.3-1)}$$

$$F_p = 0.4(1.0)(1.5)\left(W_p\right) \left[\frac{3.5}{1.53}\right] \left|\frac{1.0}{1.5}\right| = 0.914 W_p \qquad \text{(controlling equation)}$$

$$F_{p,max} = 1.6 S_{DS} I_p W_p \qquad \text{(ASCE/SEI 7-22 Eq. 13.3-2)}$$

$$F_{p,max} = 1.6(1.0)(1.5)\left(W_p\right) = 2.40 W_p$$

$$F_{p,min} = 0.3 S_{DS} I_p W_p \qquad \text{(ASCE/SEI 7-22 Eq. 13.3-3)}$$

$$F_{p,min} = 0.3(1.0)(1.5)\left(W_p\right) = 0.45 W_p$$

$$F_p = 0.914 W_p \qquad \text{(controlling seismic design force)}$$

Horizontal seismic load effect, E_h

$$Q_E = F_p = 0.914W_p \qquad \text{(effect from } F_p\text{)}$$

$$E_h = \rho Q_E \qquad \text{(ASCE/SEI 7-22 Eq. 12.4-3)}$$

$$E_h = (1.0)\left(0.914W_p\right) = 0.914W_p$$

Vertical seismic load effect, E_v

$$E_v = 0.2S_{DS}D \qquad \text{(ASCE/SEI 7-22 Eq. 12.4-4a)}$$

The above terms are then substituted into the following Basic Load Combinations for Strength Design from ASCE/SEI 7-22 Sections 2.3.6 and 12.4.2 to determine the design member and connection forces to be used in conjunction with seismic loads.

$$1.2D + E_v + E_h + L + 0.2S \qquad \text{(ASCE/SEI 7-22 Load Combination 6)}$$

$$0.9D - E_v + E_h \qquad \text{(ASCE/SEI 7-22 Load Combination 7)}$$

For nonstructural components, the terms *L* and *S* are typically zero.

Changes in the ASCE/SEI 7 22

For the 2022 edition of ASCE/SEI-7, Table 13.6-1 is modified to incorporate two new categories: “equipment support structures and platforms” and “distribution system supports.” As indicated in the commentary to Chapter 13 in ASCE/SEI 7-22:

In the 2016 and earlier editions of ASCE/SEI 7, a single seismic design force was used for both the mechanical or electrical component and for their supports and attachments, no matter how dissimilar the components and supports were. This could produce weak component supports, especially for distribution systems which tended to have high values of the component response coefficient, R_p, which was in use at that time.

The ASCE/SEI 7-22 provisions require a separate design for more complex equipment supports (equipment support structures and platforms) and for distribution system supports. The design coefficients for these equipment supports are selected based on the nature of the support lateral force-resisting system, rather than the type of equipment or system being supported.

8.6.4.2 PROPORTIONING AND DESIGN

Vertical Loads

Vertical pipe supports are often considered separately from lateral bracing. Configuration and spacing of vertical supports may be governed by plumbing codes or other standards and guidelines. Given that the vertical component of seismic force, E_v, is often low relative to other vertical loads, vertical supports proportioned for gravity and operational loads generally are adequate to resist the vertical seismic forces. However, where a support resists the vertical component of a lateral or longitudinal brace force, it should be designed explicitly to resist all applied forces. This example focuses on vertical supports associated with the lateral bracing system.

Due to the repetitious nature of the pipe gravity support system, the vertical load at the brace assembly due to gravity or vertical seismic load can be estimated based on the tributary length of pipe, a 10-foot spacing on center of vertical supports.

For 4-inch diameter pipes:

Dead load, $P_{v4} = (D)(L_{grav\ sup}) = (16.4\ \text{plf})(10\ \text{ft}) = 164\ \text{lb}$

Vertical seismic load, $P_{Ev4} = 0.2S_{DS}D\left(L_{grav\ sup}\right) = 0.2(1.0)(16.4\ \text{plf})(10\ \text{ft}) = 33\ \text{lb}$

For 6-inch diameter pipe:

Dead load, $P_{v6} = (D)\left(L_{grav\ sup}\right) = (31.7\ \text{plf})(10\ \text{ft}) = 317\ \text{lb}$

Vertical seismic load, $P_{Ev6} = 0.2S_{DS}D\left(L_{grav\ sup}\right) = 0.2(1.0)(31.7\ \text{plf})(10\ \text{ft}) = 63\ \text{lb}$

Longitudinal Lateral Loads

Spacing of longitudinal bracing may be dictated by the system geometry, thermal demands on the pipe, anchorage and brace capacities, or prescriptive limitations in standards and guidelines. In this example, we assume longitudinal braces are provided every 80 feet, which is twice the transverse brace spacing.

For Piping Run “A,” the total length of pipe tributary to Support 1 is approximately 40 feet (half the distance between longitudinal braces at Supports 1 and 3) plus 9 feet (length of pipe from Support 1 to Support M, the mechanical unit), or 49 feet.

Longitudinal seismic load, P_{X1A}, for the 4-inch-diameter Piping Run “A”

$$P_{X1A} = \rho F_p = \rho(0.914W_p) = (1)(0.914)(16.4\ \text{lb/ft})(49\ \text{ft}) = 734\ \text{lb}$$

For Piping Runs “B” and “C,” the total length of pipe tributary to Support 1 is approximately 80 feet.

Longitudinal seismic load, P_{X1B}, for the 6-inch-diameter Piping Run “B”

$$P_{X1B} = \rho F_p = \rho(0.914W_p) = (1)(0.914)(31.7 \text{ lb/ft})(80 \text{ ft}) = 2{,}318 \text{ lb}$$

Longitudinal seismic load, P_{X1C}, for the 4-inch-diameter Piping Run "C"

$$P_{X1C} = \rho F_p = \rho(0.914W_p) = (1)(0.914)(16.4 \text{ lb/ft})(80 \text{ ft}) = 1{,}199 \text{ lb}$$

Transverse Lateral Loads

To determine the transverse loads at support points, the pipes are idealized as continuous beams spanning between pinned connections, representing the transverse braces. The reactions are conservatively calculated assuming a continuous beam (representing the pipe) with two uniformly loaded spans. The reaction at the beam's midspan is calculated as:

$$P_Z = \frac{5}{8} W(L_{left} + L_{right})$$

Where W is the distributed lateral load, and L represents the span length to the left and to the right of the support. For Piping Run "B" and "C," L corresponds to the spacing between transverse braces.

For Piping Run "A," we analyze the transverse Support 1, which is adjacent to the mechanical unit (see Figure 8-34). L_{left} is the total length between the mechanical unit, i.e. 5 ft of riser plus 4 ft of horizontal pipe section, per Figure 8-30 and Figure 8-31.

The maximum transverse reaction due to Piping Run "A" at Support 1 is calculated as:

$$P_{Z1A} = \left(\frac{5}{8}\right) W(L_{left} + L_{right}) = \left(\frac{5}{8}\right) (\rho F_p)(L_{1M} + L_{lat\ brace})$$

$$P_{Z1A} = \left(\frac{5}{8}\right) (1)(0.914)\left(16.4 \frac{\text{lb}}{\text{ft}}\right)(9 \text{ ft} + 40 \text{ ft}) = 459 \text{ lb}$$

For Piping Runs "B" and "C," we assume that 5/8 of the total length of pipe on each side of Support 1 is laterally braced at Support 1 (see Figure 8-35 and Figure 8-36).

The maximum transverse reaction due to Piping Run "B" at Support 1 is calculated as:

$$P_{Z1B} = \left(\frac{5}{8}\right) W(L_{left} + L_{right}) = \left(\frac{5}{8}\right) (\rho F_p)((2)(L_{lat\ brace}))$$

$$P_{Z1B} = \left(\frac{5}{8}\right) (1)(0.914)\left(31.7 \frac{\text{lb}}{\text{ft}}\right)((2)(40 \text{ ft})) = 1{,}449 \text{ lb}$$

The maximum transverse reaction due to Piping Run "C" at Support 1 is calculated as:

$$P_{Z1C} = \left(\frac{5}{8}\right) W(L_{left} + L_{right}) = \left(\frac{5}{8}\right) (\rho F_p)((2)(L_{lat\ brace}))$$

$$P_{Z1C} = \left(\frac{5}{8}\right) (1)(0.914)\left(16.4 \frac{\text{lb}}{\text{ft}}\right)((2)(40 \text{ ft})) = 749 \text{ lb}$$

Support Design

The bracing system at Support 1 is shown in Figure 8-37. The analysis considers the design of the following bracing elements:

- Beam f-g
- Hangers f-b and g-d
- transverse Brace a-f
- longitudinal Braces f-c and g-e

The connections at a, b, c, d, and e must also be designed and are subject to special requirements.

Beam f-g

Beam f-g is subject to biaxial bending under vertical (Y-direction) and longitudinal (X-direction) forces. The maximum moment, which occurs at the center, is equal to:

$$M = \frac{P_A L_1}{2} + \frac{P_B L}{4} + \frac{P_C L_4}{2}$$

Vertical direction:

The maximum factored vertical loads for the piping runs using the Basic Load Combination 6 are:

$1.2D + E_v + E_h + L + 0.2S$ (ASCE/SEI 7-22 Load Combination 6)

Piping Run A: $P_A = 1.2(P_{v4}) + (P_{Ev4}) = 1.2(164\text{ lb}) + 33\text{ lb} = 230\text{ lb}$

Piping Run B: $P_B = 1.2(P_{v6}) + (P_{Ev6}) = 1.2(317\text{ lb}) + 63\text{ lb} = 443\text{ lb}$

Piping Run C: $P_C = 1.2(P_{v4}) + (P_{Ev4}) = 1.2(164\text{ lb}) + 33\text{ lb} = 230\text{ lb}$

The maximum moment about the x-axis, M_x, of the beam due to vertical loads is:

$$M_x = \frac{(230\text{ lb})(7\text{ in.})}{2} + \frac{(443\text{ lb})(30\text{ in.})}{4} + \frac{(230\text{ lb})(7\text{ in.})}{2} = 4{,}936\text{ lb–in.}$$

The vertical reactions at f and g are:

$$R_{vf} = R_{vg} = \frac{P_A + P_B + P_C}{2} = \frac{230\text{ lb} + 443\text{ lb} + 230\text{ lb}}{2} = 451\text{ lb}$$

Figure 8-38 illustrates a free-body diagram for beam f-g with the forces acting in the vertical direction at Support 1.

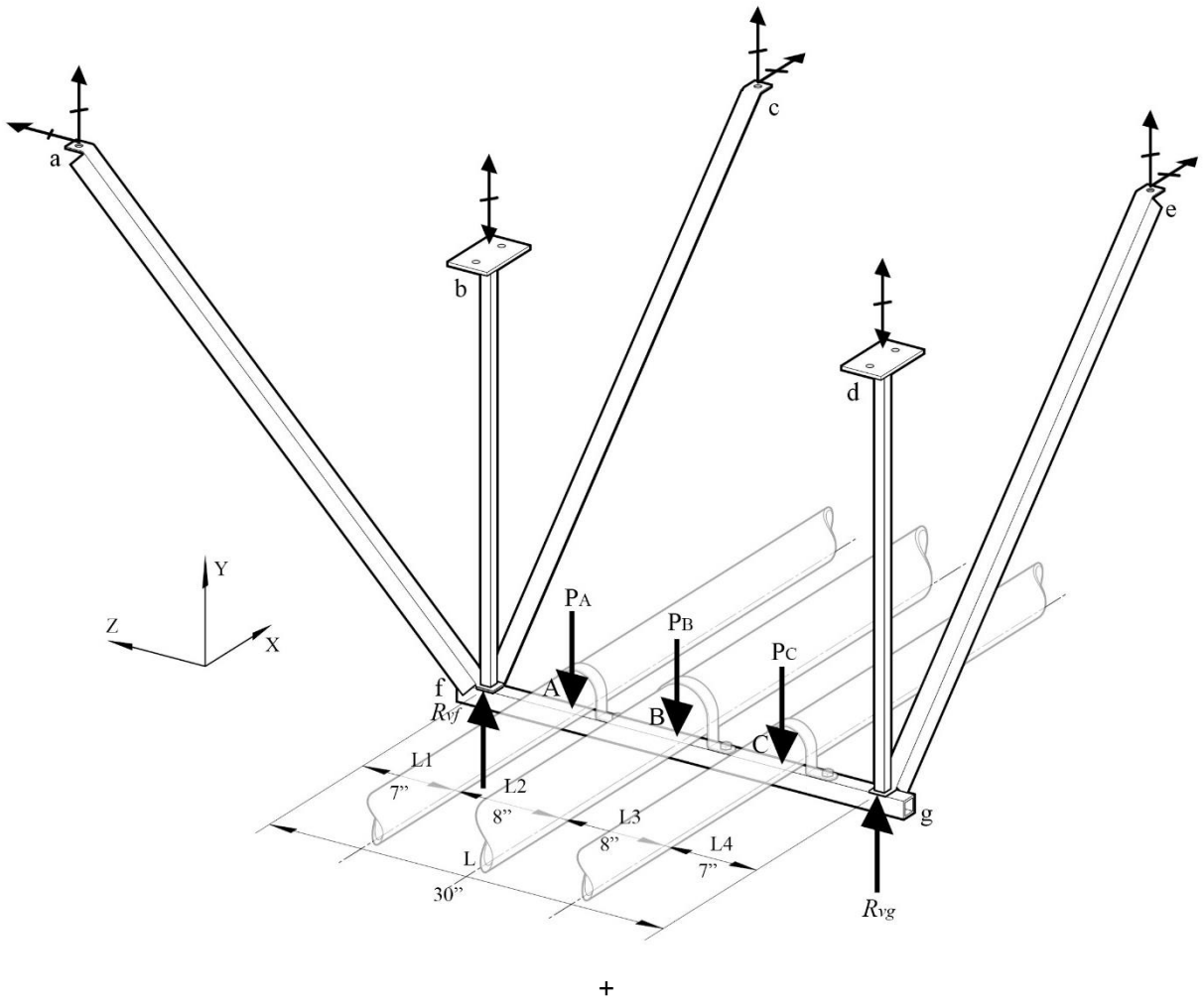

Figure 8-38. Vertical Loads Acting on Beam f-g

Longitudinal direction:

According to previous calculations, the factored lateral loads in the longitudinal direction are:

Piping Run A: $P_A = P_{X1A} = 734$ lb

Piping Run B: $P_B = P_{X1B} = 2{,}318$ lb

Piping Run C: $P_C = P_{X1C} = 1{,}199$ lb

The maximum moment about the y-axis, M_y, of the beam due to lateral loads is:

$$M_y = \frac{(734 \text{ lb})(7 \text{ in.})}{2} + \frac{(2{,}318 \text{ lb})(30 \text{ in.})}{4} + \frac{(1{,}199 \text{ lb})(7 \text{ in.})}{2} = 24{,}150 \text{ lb-in.}$$

The horizontal reactions at f and g are:

$$R_{hf} = \frac{P_A(L_2+L_3+L_4)}{L} + \frac{P_B}{2} + \frac{P_C L_4}{L} = \frac{(734\text{ lb})(8\text{ ft}+8\text{ ft}+7\text{ ft})}{30\text{ ft}} + \frac{2{,}318\text{ lb}}{2} + \frac{(1{,}199\text{lb})(7\text{ ft})}{30\text{ ft}} = 2{,}002\text{ lb}$$

$$R_{hg} = \frac{P_A L_1}{L} + \frac{P_B}{2} + \frac{P_C(L_1+L_2+L_3)}{L} = \frac{(734\text{ lb})(7\text{ ft})}{30\text{ ft}} + \frac{2{,}318\text{ lb}}{2} + \frac{(1{,}199\text{lb})(7\text{ ft}+8\text{ ft}+8\text{ ft})}{30\text{ ft}} = 2{,}249\text{ lb}$$

Beam f-g must be designed for moments M_x and M_y acting simultaneously.

Brace Design

By inspection, Brace g-e will govern the longitudinal brace design since the horizontal reaction at g ($R_{hg} = 2{,}249$ lb) is larger than that at f ($R_{hf} = 2{,}002$ lb).

The horizontal load that must be resisted by the transverse Brace a-f is the sum of the loads from the three pipes calculated previously:

$$R_Z = P_{Z1A} + P_{Z1B} + P_{Z1C}$$

$$R_Z = 459\text{ lb} + 1{,}449\text{ lb} + 749\text{ lb} = 2{,}657\text{ lb}$$

Assuming the same member will be used for all braces, Brace a-f governs the design. Since the brace is installed at a 1:1 slope (45 degrees), the maximum tension or compression in the brace would be:

$$T_{max} = C_{max} = \sqrt{2}R_Z = \sqrt{2}(2{,}657\text{ lb}) = 3{,}758\text{ lb}$$

The brace selected must be capable of carrying C_{max} with an unbraced length of $\sqrt{2}(30\text{ in.}) = 42\text{ in.}$ Bracing elements subject to compression should meet the slenderness ratio requirements of the appropriate material design standards.

Hangers

By inspection, Hanger f-b will govern the vertical element design since the brace force in Brace f-a governs the brace design. Since the brace is installed at a 1:1 slope (45 degrees), the maximum tension or compression due to seismic forces in the hanger is the same as the horizontal force resisted by the brace: 2,169 lb. The vertical component of the brace force must be combined with gravity loads and the vertical seismic component.

$$R_{YD} = \frac{P_{v4}+P_{v6}+P_{v4}}{2} = \frac{164\text{ lb}+317\text{ lb}+164\text{ lb}}{2} = 323\text{ lb}$$

$$R_{YEv} = \frac{P_{Ev4}+P_{Ev6}+P_{Ev4}}{2} = \frac{33\text{ lb}+63\text{ lb}+33\text{ lb}}{2} = 65\text{ lb}$$

The maximum tension force in the hanger is determined using the Basic Load Combination 6:

$$1.2D + E_v + E_h + L + 0.2S \qquad \text{(ASCE/SEI 7-22 Load Combination 6)}$$

In this example, the terms *L* and S are equal to zero. The unfactored reaction at Point f due to dead load of the water-filled pipes is $323\ lb$. Substituting the values from above:

$$F_U = 1.2(R_{YD}) + R_{YEv} + R_Z$$

$$F_U = 1.2(323\ \text{lb}) + 65\ \text{lb} + 2{,}657\ \text{lb} = 3{,}108\ \text{lb} \qquad \text{(tension)}$$

The maximum compression force in the hanger is determined using the Basic Load Combination 7:

$$0.9D - E_v + E_h \qquad \text{(ASCE/SEI 7-22 Load Combination 7)}$$

Substituting the values from above:

$$F_U = 0.9(R_{YD}) - R_{YEv} - R_Z$$

$$F_U = 0.9(323\ \text{lb}) - 65\ \text{lb} - 2{,}657\ \text{lb} = -2{,}431\ \text{lb} \qquad \text{(compression)}$$

E_h should be applied in the direction which creates the largest value for the item being checked. According to direction of loads, a negative sign indicates compression. The hanger selected shall be capable of carrying the maximum compression with an unbraced length of 30 inches. Again, bracing elements subject to compression should meet the slenderness ratio requirements of the appropriate material design standards. It is also important to note that the length of pipe that contributes dead load to counteract the vertical component of brace force is based on the spacing of the vertical hangers, not the spacing between lateral braces.

Anchorage Design

ASCE/SEI 7-22 Section 13.4 covers the attachment of the hangers and braces to the structure. Component forces and displacements are those determined in ASCE/SEI 7-22 Sections 13.3.1 and 13.3.2, with important exceptions. Anchors in concrete and masonry are proportioned so that either the component or support that the anchor is connecting to the structure undergoes ductile yielding at a load level corresponding to anchor forces not greater than their design strength, or the anchors shall be designed to resist the load combinations considering overstrength, Ω_{0p}, in accordance with ASCE/SEI 7-22 Section 2.3.6 and 13.4.2.

To illustrate the effects of these provisions, consider the design of the attachment to the structure at Point a in Figure 8-37.

The horizontal and vertical components of the seismic brace force at Point a are $2{,}657\ \text{lb}$ each. Assuming the brace capacity limits the force to the anchor and that the brace does not resist vertical loads due to gravity or the vertical seismic component, the minimum design forces for the anchor are $2{,}657\ lb$ in tension acting currently with $2{,}657\ \text{lb}$ in shear.

The maximum design force for the anchor, assuming that a ductile element does not govern the anchorage capacity is determined using the load combinations considering Ω_{0p} in accordance with ASCE/SEI 7-22 Section 2.3.6 and 13.4.2.

By inspection, the load combination that results in net tension on the anchor will govern the design of the anchor. Thus, the ASCE/SEI 7-22 Basic Load Combination 7, including overstrength, is applied to obtain the controlling vertical design tension force:

$$0.9D - E_v + E_{mh} \qquad \text{(ASCE/SEI 7-22 Load Combination 7)}$$

Where: $E_{mh} = \Omega_{0p} Q_E$ (ASCE/SEI 7-22 Eq. 12.4-7 and Sec 13.4.2)

Vertical design tension force, T_u

$$T_u = \Omega_{0p} Q_E = (2.0)(2{,}657 \text{ lb}) = 5{,}314 \text{ lb}$$

Acting concurrently with tension, the horizontal design shear force, V_u

$$V_u = \Omega_{0p} Q_E = (2.0)(2{,}657 \text{ lb}) = 5{,}314 \text{ lb}$$

8.6.5 Prescribed Seismic Displacements

In addition to design for seismic forces, the piping system must accommodate seismic relative displacements. For the purposes of this example, we assume that the building has a 15 foot story height and has been designed for a maximum allowable story drift of 1.5% per floor (Risk Category IV, non-masonry, four stories or less):

$$\Delta_a = 0.015 h_{sx} \qquad \text{(ASCE/SEI 7-22 Table 12.12-1)}$$

$$\Delta_a = 0.015(15 \text{ ft})(12 \text{ in./ft}) = 2.7 \text{ in.}$$

Design for Displacements within Structures

Piping Run "A," a 4-inch-diameter pipe, connects to a large mechanical unit at Line 1 supported at the Level 2. For a nonstructural component subject to displacements within a structure, the relative displacement, D_p, is given in ASCE/SEI 7-22 Equation 13.3-7 as the difference between lateral story drifts at the points of attachment. Because the mechanical unit can be assumed to behave as a rigid body and the piping system is rigidly braced to the roof structure, the entire story drift must be accommodated in the 5 feet piping drop (see Figure 8-31).

Seismic relative displacement demands, D_{pI}

$$D_{pI} = D_p I_e \qquad \text{(ASCE/SEI 7-22 Eq.13.3-8)}$$

$$D_{pI} = (2.7 \text{ in.})(1.5) = 4.05 \text{ in.}$$

Seismic Importance Factor, I_e, and Component Importance Factor, I_p

Chapter 13 of ASCE/SEI 7-22 uses two different importance factors in their calculations for the seismic design requirements for nonstructural components:

- Seismic Importance Factor, I_e, defined in Section 1.5.1 based upon the risk categorization.
- Component Importance Factor, I_p, according to Section 13.1.3.

The Seismic Importance Factor, I_e, is used to calculate the structure ductility reduction factor, R_μ in Equation 13.3-6, and the seismic relative displacements, D_{pI}, in Equation 13.3-8.

The Component Importance Factor, I_p, is required to calculate the horizontal seismic force, F_p, in Equations 13.3-1 through 13.3-3 and Equation 13.3-7.

There are several approaches to accommodate the drift. The first is to provide a flexible coupling (articulated connections or braided couplings, for example). A second approach is to accommodate the drift through bending in the pipe. Loops are often used to make the pipe more flexible for thermal expansion and contraction and this approach also works for seismic loads.

In this example, a straight length of a pipe is assumed. For a 4-inch-diameter Schedule 40 pipe, the moment of inertia, $I = 7.23\ \text{in.}^4$, and the plastic modulus, $Z = 4.31\ \text{in.}^3$ Assuming the pipe is fixed against rotation at both ends, the shear and moments required to deflect the pipe 4.05 in. are:

$$V = \frac{12EID_{pI}}{L^3}$$

$$V = \frac{12(29{,}000{,}000\ \text{psi})(7.23\ \text{in}^4)(4.05\ \text{in.})}{((5\ \text{ft})(12\ \text{in./ft}))^3} = 47{,}193\ \text{lb}$$

$$M = VL = (47{,}176\ \text{lb})(5\ \text{ft})(12\ \text{in./ft}) = 2{,}831{,}563\ \text{lb-in.}$$

The stress in the pipe displaced D_{pI} is:

$$f_b = \frac{M}{Z} = \frac{2{,}831{,}563\ \text{lb–in.}}{4.31\ \text{in}^3} = 656{,}750\ \text{psi}$$

The permissible stress from ASCE/SEI 7-22 Section 13.6.7, Item c, is $0.7F_y = 0.7(35{,}000\ \text{psi}) = 24{,}500\ \text{psi}$. These demands far exceed the capacity of the pipe and would overload the nozzle on the mechanical unit as well. Therefore, either a flexible coupling or a loop piping layout is required to accommodate the story drift.

Piping Run "B," a 6-inch-diameter pipe, drops from the roof level to Level 2 at Line 3. Again, the drift demand is the same, but in this case, it may be accommodated over the full story height of 15 feet. A simplified analysis assumes that the pipe is fixed at the roof and Level 2. This assumption is conservative since, in reality, the horizontal runs of the pipe at the roof and Level 2 provide restraint

but not fixity. For a 6-inch-diameter Schedule 40 pipe, the moment of inertia, $I = 28.14 \text{ in}^4$ and the plastic modulus, $Z = 11.28 \text{ in.}^3$ The shear and moments required to deflect the pipe 4.05 in. are:

$$V = \frac{12EID_{pI}}{L^3}$$

$$V = \frac{12(29{,}000{,}000 \text{ psi})(28.14 \text{ in}^4)(4.05 \text{ in.})}{((15 \text{ ft})(12 \text{ in./ft}))^3} = 6{,}801 \text{ lb}$$

$$M = VL = (6{,}800 \text{ lb})(15 \text{ ft})(12 \text{ in./ft})/2 = 612{,}092 \text{ lb-in.}$$

The stress in the pipe displaced D_{pI} is:

$$f_b = \frac{M}{Z} = \frac{612{,}092 \text{ lb–in.}}{11.28 \text{ in}^3} = 54{,}264 \text{ psi}$$

The permissible stress from ASCE/SEI 7-22 Section 13.6.7, Item c, is $0.7F_y = 0.7(35{,}000 \text{ psi}) = 24{,}500 \text{ psi}$. This demand exceeds the permissible stress in the pipe, but not by a wide margin. Refining the analysis to more accurately consider the effects of the rotational restraint provided by the horizontal piping runs (which will tend to reduce the rigidity of the pipe and therefore reduce the bending stress), providing loops in the piping layout, or providing flexible couplings will produce more favorable results. It is critical that the capacity of the nozzle on the equipment where the pipe is attached is sufficient to resist the shears and moments applied by the pipe.

In practice, the risers are often overlooked in the distribution systems design. The seismic relative displacements induce demands in these vertical pipes, causing additional loads in the piping system and the distribution support system. Typically, the steel pipes have enough capacity and ductility to accommodate the displacements; however, the pipe joints and the supports are potential weak links in the system. For example, using Figure 8-31 as a reference, the displacement-induced demand transferred from Pipe B to Support 3 leads to large elastic stresses in the pipes, pipe connections, supports, and bracing elements until a plastic hinge forms. The plastic hinge triggers a load redistribution in the system, which is different from the initial assumptions in the elastic analysis. Thus, further analysis for these cases might be required to address these potential mechanisms and refined models may be necessary.

Design for Displacements Between Structures

As this is a Risk Category IV two-story hospital building, per ASCE/SEI 7-22 Table 12.12-1, the allowable story drift is $0.015h_{sx}$. At the roof level, Piping Run "A" crosses a seismic separation between adjacent two-story structures at Line 3. Assuming story heights of 15 feet and design for a maximum allowable story drift for both buildings, the deflections of the buildings are:

$$\delta_{XA} = \delta_{XB} = (2)(0.015)h_{sx}$$

$$\delta_{XA} = \delta_{XB} = (2)(0.015)(15 \text{ ft})(12 \text{ in./ft}) = 5.4 \text{ in.}$$

The displacement demand, D_P

is determined from ASCE/SEI 7-22 Equation 13.3-11, as follows:

$$D_{pmax} = |\delta_{XA}| + |\delta_{XB}| = |5.4 \text{ in.}| + |5.4 \text{ in.}| = 10.8 \text{ in.}$$

Seismic relative displacement demands, D_{pI}

$$D_{pI} = D_p I_e \qquad \text{(ASCE/SEI 7-22 Eq.13.3-8)}$$

$$D_{pI} = (10.8 \text{ in.})(1.5) = 16.2 \text{ in.}$$

In addition to motions perpendicular to the pipe, the seismic isolation joint must accommodate movement parallel to the pipe. Assuming an 18-inch seismic separation joint is provided, during an earthquake, the joint could vary from 8.1 inches (if the structures move towards each other) to 32.4 inches (if the structures move away from each other). The flexible coupling, which could include articulated connections, braided couplings, or pipe loops, must be capable of accommodating this range of movements.

8.7 Elevated Vessel Seismic Design

8.7.1 Example Description

Example Summary

- **Nonstructural components:**
  Mechanical and electrical – pressure vessel not supported on skirts
- **Building seismic force-resisting system:** Special reinforced concrete shear walls
- **Equipment support:** Equipment support structures and platforms – Seismic Force-Resisting Systems with $R > 3$
- **Occupancy**: Storage
- **Risk Category:** II
- **Component Importance Factor:** $I_p = 1.0$
- **Number of stories:** 3
- $\boldsymbol{S_{DS}} = 1.20$
- $\boldsymbol{S_1} = 0.65$

This example considers a vessel supported by an ordinary braced-frame platform with tension-only rods as braces. The contents of the vessel, a compressed non-flammable gas, are not hazardous. The nonstructural component platform is attached at the Level 3 of a three-story building structure. As the vessel does not contain toxic or explosive substances, nor is required to function for life-safety

purposes after an earthquake, the component Importance Factor, $I_p = 1.0$, per ASCE/SEI 7-22 Section 13.1.3. Special reinforced concrete shear walls in the two orthogonal directions are used as the seismic force-resisting system for the building. The building serves as a storage facility and is assigned a Risk Category II.

The design approach for vessels depends on the weight and location of the component. ASCE/SEI 7-22 provides requirements for nonstructural components in Chapter 13 and nonbuilding structures in Chapter 15. According to ASCE/SEI 7-22 Section 15.3, where the vessel weight is less than 20% of the combined effective seismic weights of the vessel and supporting structure, the design seismic forces shall be determined in accordance with Chapter 13. There is a parallel provision in ASCE/SEI 7-22 Section 13.1.1. For this example, the weight of the vessel is less than 5% the total weight of the building structure, and ASCE/SEI 7-22 Chapter 13 is used to determine the prescribed seismic forces.

This example illustrates the following calculation procedures:

- Prescribed seismic forces, proportioning, and design forces for vessel support and attachment. These include legs supporting the vessel, connection between the legs and vessel shell, base plates, welds, and bolts (see Section 8.7.3 in this example).
- Prescribed seismic forces, proportioning, and design forces for supporting frame. These include the beams supporting the vessel legs, braces, columns, base plates, and anchors (see Section 8.7.4 in this example).
- Design considerations for the gravity load-carrying system, illustrating the contribution of the vessel load to the concrete slab at Level 3 (see Section 8.7.5 in this example).

After the seismic demands are determined, the bracing and anchorage connections shall be designed and detailed according to the appropriate AISC and ACI codes. The sizing of the various elements (beams, columns, braces, connections, anchor bolts, etc.) are not covered in detail.

The vessel is of steel construction and supported on four legs, which are bolted to a steel frame support. A section through the structure showing the location of the vessel is presented in Figure 8-39. A plan of Level 3 showing the location of the vessel is shown in Figure 8-40. An elevation of the vessel and supporting frame is shown in Figure 8-41.

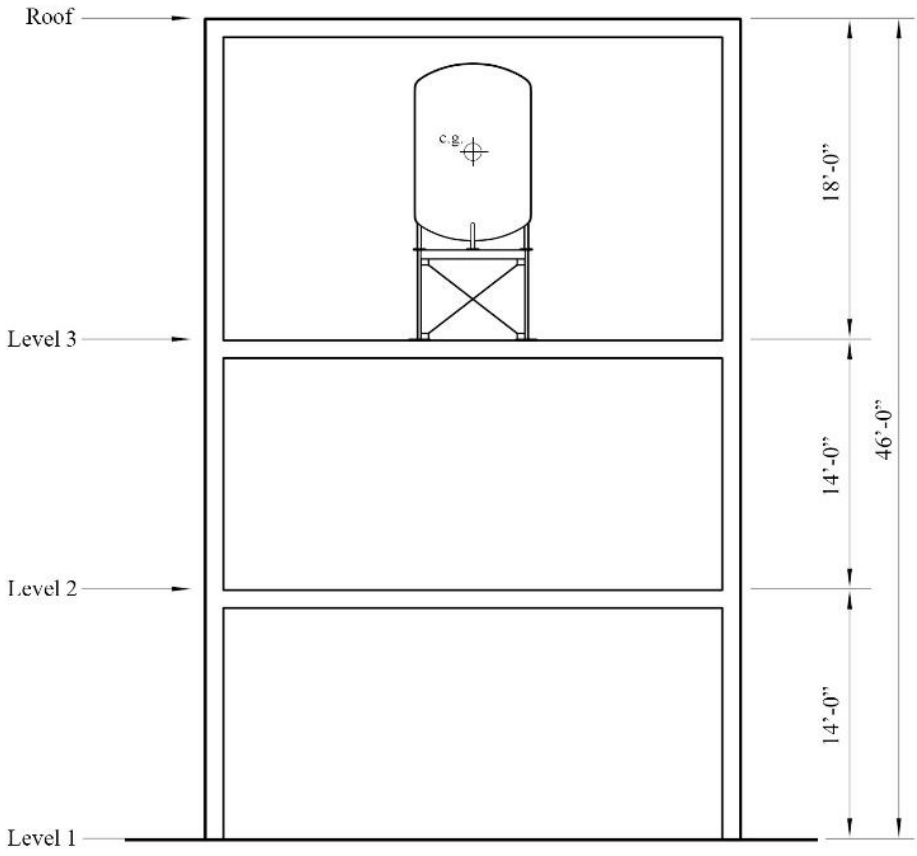

Figure 8-39. Elevated Vessel – Section

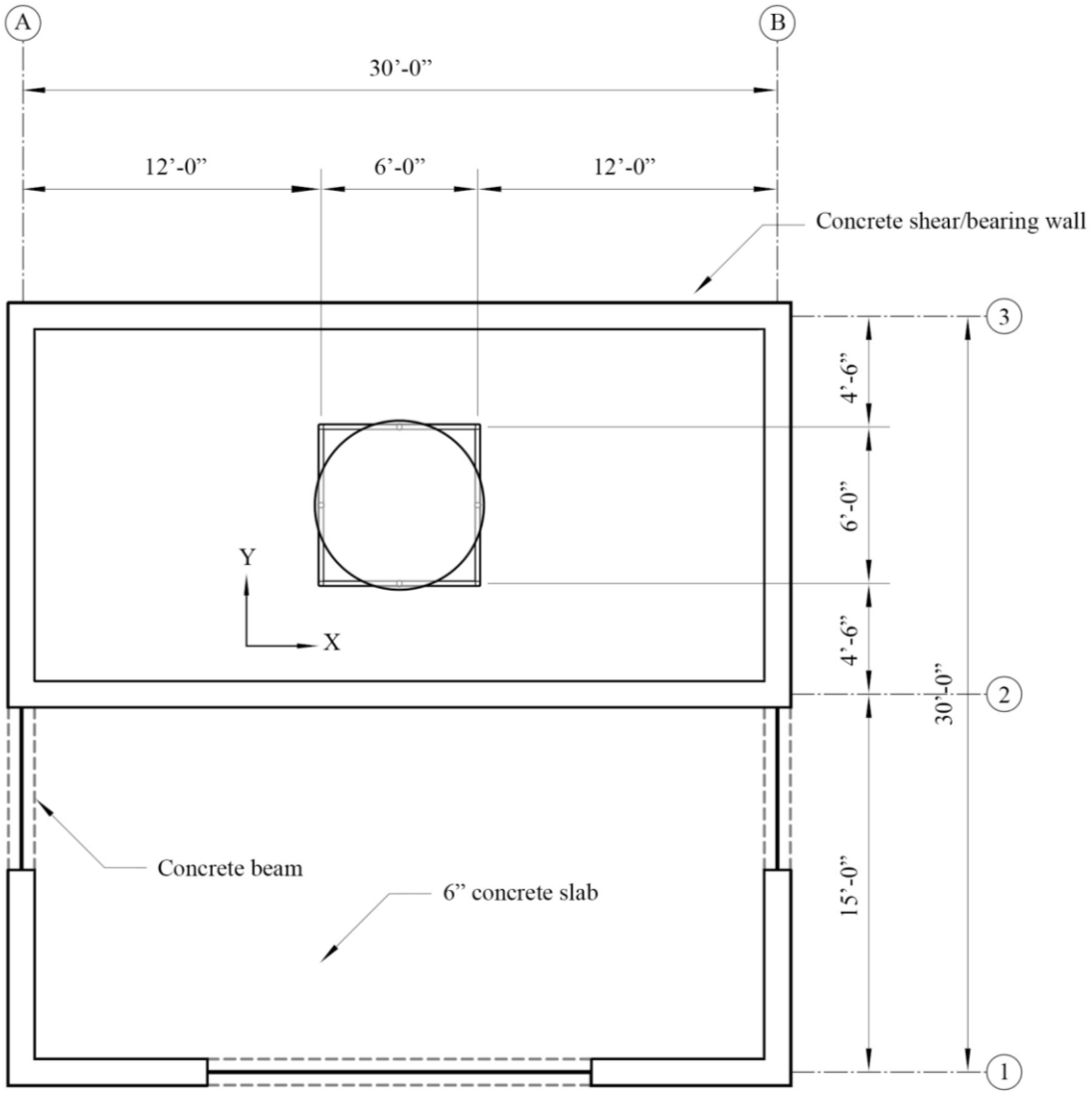

Figure 8-40. Elevated Vessel – Level 3 Plan

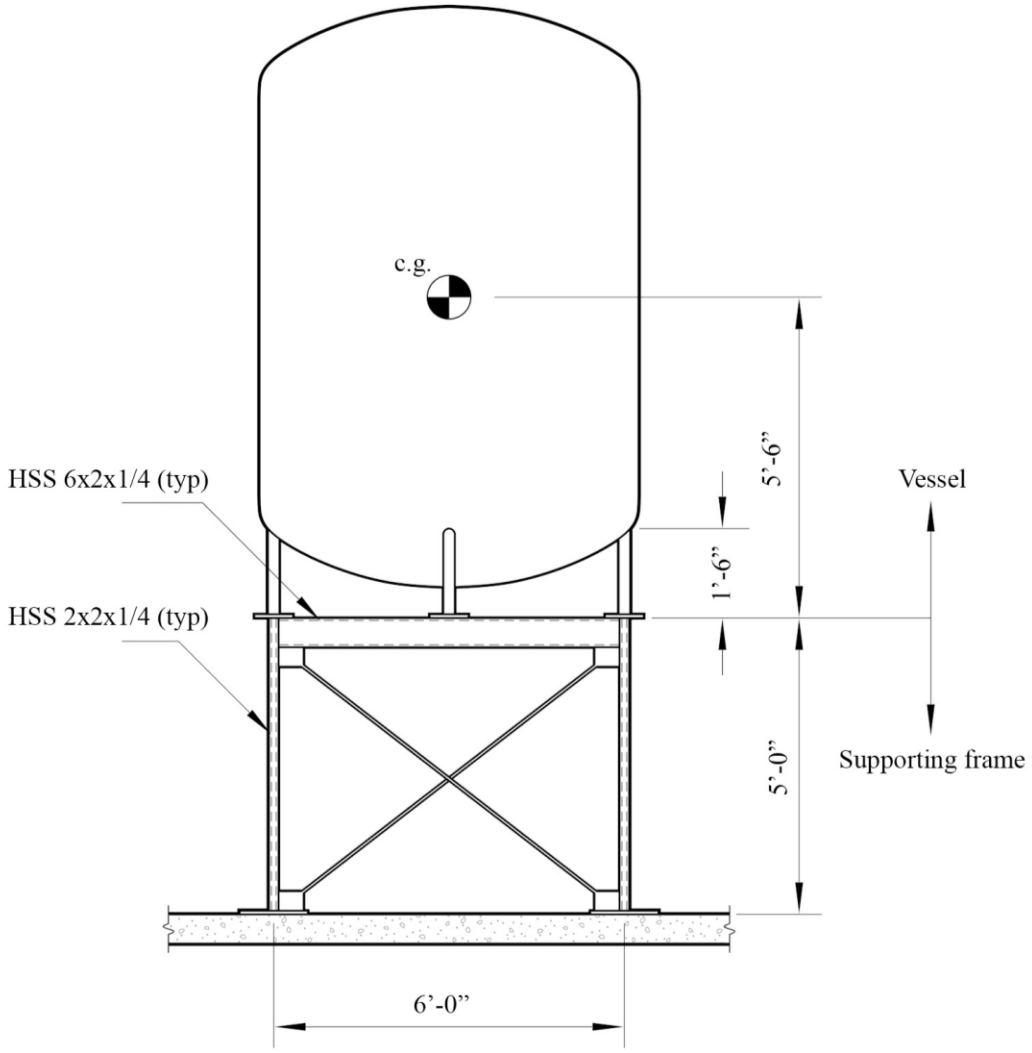

Figure 8-41. Elevated Vessel – Supporting Frame System

8.7.2 Design Requirements

8.7.2.1 ASCE/SEI 7-22 PARAMETERS AND COEFFICIENTS

The following parameters and coefficients are derived from the example description, or it is known information based on the structure, selected location, and site class.

Coefficients for mechanical and electrical components

Mechanical and electrical components – Engines, turbines, pumps, compressors, and pressure vessels not supported on skirts and not within the scope of (ASCE/SEI 7-22) Chapter 15:

$C_{AR} = 1.4$ (ASCE/SEI 7-22 Table 13.6-1 and Section 13.3.1.3)

$R_{po} = 1.5$ (ASCE/SEI 7-22 Table 13.6-1)

$\Omega_{0p} = 2.0$ (ASCE/SEI 7-22 Table 13.6-1)

Equipment support structures and platforms – Seismic Force-Resisting Systems with $R > 3$: Per ASCE/SEI 7-22 Section 13.6.4.6, the seismic force-resisting system for the equipment support structure shall conform one of the types indicated in ASCE/SEI 7-22 Table 12.2-1 or Table 15.4-1. For this example, it is classified as a building frame system – steel ordinary concentrically braced frame, per Table 12.2-1, which has an *R*=6. It thus uses the *R* > 3 category in ASCE/SEI 7-22 Table 13.6.1.

$C_{AR} = 1.4$ (ASCE/SEI 7-22 Table 13.6-1)

$R_{po} = 1.5$ (ASCE/SEI 7-22 Table 13.6-1)

$\Omega_{0p} = 2.0$ (ASCE/SEI 7-22 Table 13.6-1)

Per ASCE/SEI 7-22 Section 13.6.4.6, detailing requirements for the selected system must be followed. In this case, this includes the ASCE/SEI 7-22 Table 12.2-1 height limits. These depend on the Seismic Design Category. Since the building is assigned to Risk Category II, S_{DS} = 1.20 > 0.50, and S_1 =0.65 <0.75, then per ASCE/SEI 7-22 Section 11.6, the building is assigned to Seismic Design Category D. In Table 12.2-1, for Seismic Design Category D, the height limit for a steel ordinary concentrically braced frame in a building frame 35 feet. In this circumstance, the height limit applies to the equipment support structure, not the building. The equipment support structure is 5 ft tall, so it is well below the 35 ft limit. Footnote "j" of Table 12.2-1 could be applied as well, which would permit an even higher equipment support structure.

Skirt Supports in Pressure Vessels

The "skirt" is a cylindrical shell with a diameter equal to or greater than the outer diameter of the vessel. It is welded at the bottom of the vessel and rests over a bearing plate. From a designer's perspective, skirt-supported pressure vessels are a convenient option because they produce low local stresses due to mechanical loads at the joints. Table 13.6-1 in ASCE/SEI 7-22 provides different seismic coefficients depending on the presence of skirt supports in the pressure vessels.

The engineer needs to understand and counterbalance the advantages and disadvantages of the different support systems for the nonstructural components. As an example, skirt-supported pressure vessels are designed with higher seismic design forces, but there is a better stress distribution at the vessel-to-support connection.

Refer to Section 8.2.11 of this chapter for a discussion about the importance of nonstructural component support structures and their terminology.

When the design coefficients of the equipment and the equipment support structure differ, a two-stage analysis approach may be needed. In the first stage, the design of the equipment and its supports (in this case, legs) and attachments are designed using the design coefficients of the component. In the second stage, the equipment support structure is designed, using the design coefficients for the equipment support structure.

However, ASCE/SEI 7-22 Section 13.3.1.3 states in part, "The component resonance ductility factor for mechanical and electrical equipment mounted on the equipment support structures or platforms shall not be less than the component resonance ductility factor used for the equipment support structure or platform itself." In this case, the tabulated value of C_{AR}=1.0, per ASCE/SEI 7-22 Table 13.6-1 for the vessel is less than that of the equipment support structure. C_{AR} must be increased to 1.4, the value of C_{AR} for the selected equipment support structure lateral system.

The weight of supported mechanical and electrical components is included when calculating the component operating weight, W_p, of the equipment support structure. In some cases, the supported component may be designed for a higher lateral force, as a percentage of W_p, than the component equipment support structure. This can be beneficial, such as when a moderate-ductility or low-ductility component is mounted on a support structure or platform with high ductility. In this case, the support structure or platform will limit the shaking demands on supported components by providing a structure with ductile behavior in the load path.

Changes in ASCE/SEI 7 22

Section 13.6.4.6 is added in ASCE/SEI 7-22. This section requires the engineers to select the seismic force-resisting system listed in ASCE/SEI 7-22 Table 12.1-1 or Table 15.4-1 for equipment support structures and platforms. Based on their selection, the support structure and platforms shall be designed and detailed according to the system using the applicable requirements and reference documents.

By allowing a seismic force-resisting systems specified in ASCE/SEI 7-22 Table 15.4-1, the low ductility systems that are commonly used for equipment support structures are permitted. Nonetheless, the equipment support shall meet the requirements of this table. As stated in ASCE/SEI 7-22 Section C13.6.4:

"Force-resisting systems for equipment support structures and platforms may be selected from Chapter 12 or Chapter 15, and are subject to the system limitations and detailing requirements for the system selected."

Design coefficients and factors for seismic force-resisting system

Bearing wall systems – special reinforced concrete shear walls:

$R = 5.0$ (ASCE/SEI 7-22 Table 12.2-1)

$\Omega_0 = 2.5$ (ASCE/SEI 7-22 Table 12.2-1)

Short period design spectral acceleration, $S_{DS} = 1.20$ (given)

Seismic Design Category: D (ASCE/SEI 7-22 Sec. 11.6)

Seismic Importance Factor, $I_e = 1.0$ (ASCE/SEI 7-22 Table 1.5-2)

Component Importance Factor, $I_p = 1.0$ (ASCE/SEI 7-22 Sec. 13.1.3)

Redundancy factor for nonstructural components, $\rho = 1.0$ (ASCE/SEI 7-22 Sec. 13.3.1)

Height of attachment at Level 3, $z = 28$ ft (given)

Average roof height with respect to the base, $h = 46$ ft (given)

Vessel and legs weight, $D_{ves} = W_{p,ves} = 5{,}000$ lb (given)

Supporting frame weight, $D_{sup} = W_{p,sup} = 1{,}000$ lb (given)

Vessel leg length, $L_{leg} = 18$ in. (given)

Steel material properties

HSS sections: ASTM A500 Grade B, $F_y = 46$ ksi, $F_u = 58$ ksi (given)

Bars and plates: ASTM A36, $F_y = 36$ ksi, $F_u = 58$ ksi (given)

Pipes: ASTM A53 Grade B, $F_y = 35$ ksi, $F_u = 60$ ksi (given)

Bolts and threaded rods: ASTM A307 (given)

Approximate fundamental period of the supporting structure, T_a – special reinforced concrete shear walls (all other structural systems, per ASCE/SEI 7-22 Table 12.8-2)

$h_n = h = 46$ ft (structural height)

$C_t = 0.02$ (ASCE/SEI 7-22 Table 12.8-2)

$x = 0.75$ (ASCE/SEI 7-22 Table 12.8-2)

$T_a = C_t {h_n}^x = (0.02)(46 \text{ ft})^{0.75} = 0.353$ s (ASCE/SEI 7-22 Eq. 12.8-7)

Force amplification factor as a function of height in the structure, H_f

$a_1 = \frac{1}{T_a} \leq 2.5$ (ASCE/SEI 7-22 Sec. 13.3.1.1)

$a_1 = \frac{1}{0.353 \text{ s}} = 2.83 > 2.5$, use $a_1 = 2.5$

$a_2 = [1 - (0.4/T_a)^2] \geq 0$ (ASCE/SEI 7-22 Sec. 13.3.1.1)

$a_2 = [1 - (0.4/0.353 \text{ s})^2] = -0.28 < 0$, use $a_2 = 0$

$H_f = 1 + a_1 \left(\frac{z}{h}\right) + a_2 \left(\frac{z}{h}\right)^{10}$ (ASCE/SEI 7-22 Eq. 13.3-4)

$H_f = 1 + 2.5 \left(\frac{28 \text{ ft}}{46 \text{ ft}}\right) + 0 \left(\frac{28 \text{ ft}}{46 \text{ ft}}\right)^{10} = 2.52$

Structure ductility reduction factor, R_μ

$R_\mu = (1.1 \, R/(\, I_e \, \Omega_0))^{1/2} \geq 1.3$ (ASCE/SEI 7-22 Eq. 13.3-6)

$R_\mu = (1.1(5/((1)(2.5)))^{1/2} = 1.48 \geq 1.3$

8.7.2.2 APPLICABLE REQUIREMENTS

The architectural, mechanical, and electrical components, supports, and attachments shall comply with the sections referenced in ASCE/SEI 7-22 Table 13.2-1. Thus, the nonstructural components of this example are designed in accordance with the following considerations:

- Component failure shall not cause failure of an essential architectural, mechanical, or electrical component (ASCE/SEI 7-22 Section 13.2.4).
- Component seismic attachments shall be bolted, welded, or otherwise positively fastened without considering the frictional resistance produced by the effects of gravity (ASCE/SEI 7-22 Section 13.4).
- The horizontal seismic design force, F_p, shall be applied at the component's center of gravity and distributed relative to the component's mass distribution (ASCE/SEI 7-22 Section 13.3.1). For this example, the seismic design force is split into one force $F_{p,ves}$ for the vessel at its center of gravity and a second $F_{p,sup}$ for the supporting platform.
- The effects of seismic relative displacements shall be considered in combination with displacements caused by other loads as appropriate (ASCE/SEI 7-22 Section 13.3.2).
- Local elements of the structure, including connections, shall be designed and constructed for the component forces where they control the design of the elements or their connections (ASCE/SEI 7-22 Section 13.4).
- Per ASCE/SEI 7-22 Section 13.4.2, attachments to concrete or masonry shall be designed to resist the seismic load effects including overstrength, in accordance with ASCE/SEI 7-22 Section 12.4.3, and Ω_0 shall be taken as Ω_{0p} (ASCE/SEI 7-22 Section 13.4.2).
- The equipment support structures and platforms shall be designed for horizontal seismic design force, F_p, in accordance with Section 13.3.1, using the design coefficients listed in Table 13.6-1. The seismic force-resisting system for the equipment support structures and platforms shall conform to one of the types indicated in Table 12.2-1 or Table 15.4-1 and abide by the system limitations noted in the tables (ASCE/SEI 7-22 Section 13.6.4.6).

8.7.3 Vessel Support and Attachments

8.7.3.1 PRESCRIBED SEISMIC FORCES

Vessel and legs weight, $W_{p,ves}$

$$W_{p,ves} = D_{ves} = 5{,}000\ lb \qquad \text{(component weight)}$$

Seismic design force, $F_{p,ves}$

$F_p = 0.4 S_{DS} I_p W_p \left[\frac{H_f}{R_\mu}\right] \left|\frac{C_{AR}}{R_{po}}\right|$ (ASCE/SEI 7-22 Eq. 13.3-1)

$F_p = 0.4(1.2)(1.0)\left(W_p\right) \left[\frac{2.52}{1.48}\right] \left|\frac{1.4}{1.5}\right| = 0.762 W_p$ (controlling equation)

$F_{p,max} = 1.6 S_{DS} I_p W_p$ (ASCE/SEI 7-22 Eq. 13.3-2)

$F_{p,max} = 1.6(1.2)(1.0)\left(W_p\right) = 1.92 W_p$

$F_{p,min} = 0.3 S_{DS} I_p W_p$ (ASCE/SEI 7-22 Eq. 13.3-3)

$F_{p,min} = 0.3(1.2)(1.0)\left(W_p\right) = 0.360 W_p$

$F_{p,ves} = 0.762 W_p = 0.762(5{,}000 \text{ lb}) = 3{,}808 \text{ lb}$ (controlling seismic design force)

Horizontal seismic load effect, $E_{h,ves}$

$Q_E = F_p = 3{,}808 \text{ lb}$ (effect from F_p)

$E_h = \rho Q_E$ (ASCE/SEI 7-22 Eq. 12.4-3)

$E_{h,ves} = (1.0)(3{,}808\ l\text{b}) = 3{,}808 \text{ lb}$

Vertical seismic load effect, $E_{v,ves}$

$E_v = 0.2 S_{DS} D$ (ASCE/SEI 7-22 Eq. 12.4-4a)

$E_{v,ves} = (0.2)(1.2\text{g})(5{,}000 \text{ lb}) = 1{,}200 \text{ lb}$

The above terms are then substituted into the following Basic Load Combinations for Strength Design from ASCE/SEI 7-22 Sections 2.3.6 and 12.4.2 to determine the design member and connection forces to be used in conjunction with seismic loads.

$1.2D + E_v + E_h + L + 0.2S$ (ASCE/SEI 7-22 Load Combination 6)

$0.9D - E_v + E_h$ (ASCE/SEI 7-22 Load Combination 7)

For nonstructural components, the terms *L* and *S* are typically zero.

8.7.3.2 PROPORTIONING AND DESIGN

The supports and attachments for the vessel shall meet the requirements listed in ASCE/SEI 7-22 Table 13.2-1. Seismic design of the vessel itself is not required, since $I_p = 1.0$. While the vessel itself need not be checked for seismic loading, the component supports listed in ASCE/SEI 7-22 Section

13.6.4 shall be designed to resist the prescribed seismic forces. The affected components include the following:

- The legs supporting the vessel.
- Connection between the legs and the vessel shell.
- Base plates and the welds attaching them to the legs.
- Bolts connecting the base plates to the supporting frame.

Seismic Design of Integral Equipment Supports

Integral equipment supports are defined in ASCE/SEI 7-22 Section 11.2 and are required to be designed for seismic demands. For nonstructural components with integral supports, it is a common practice to have assembly delivered to the site with the supports already attached by the manufacturer.

Based on previous earthquake observations, many nonstructural component failures were caused by the failure of integral support or attachments because their design was overlooked. Hence, information regarding the integral supports and attachments of the component should be requested from the manufacturer to confirm their adequacy.

Figure 8-42 shows the free-body diagram of the vessel support and attachments with the applicable forces to be used for design.

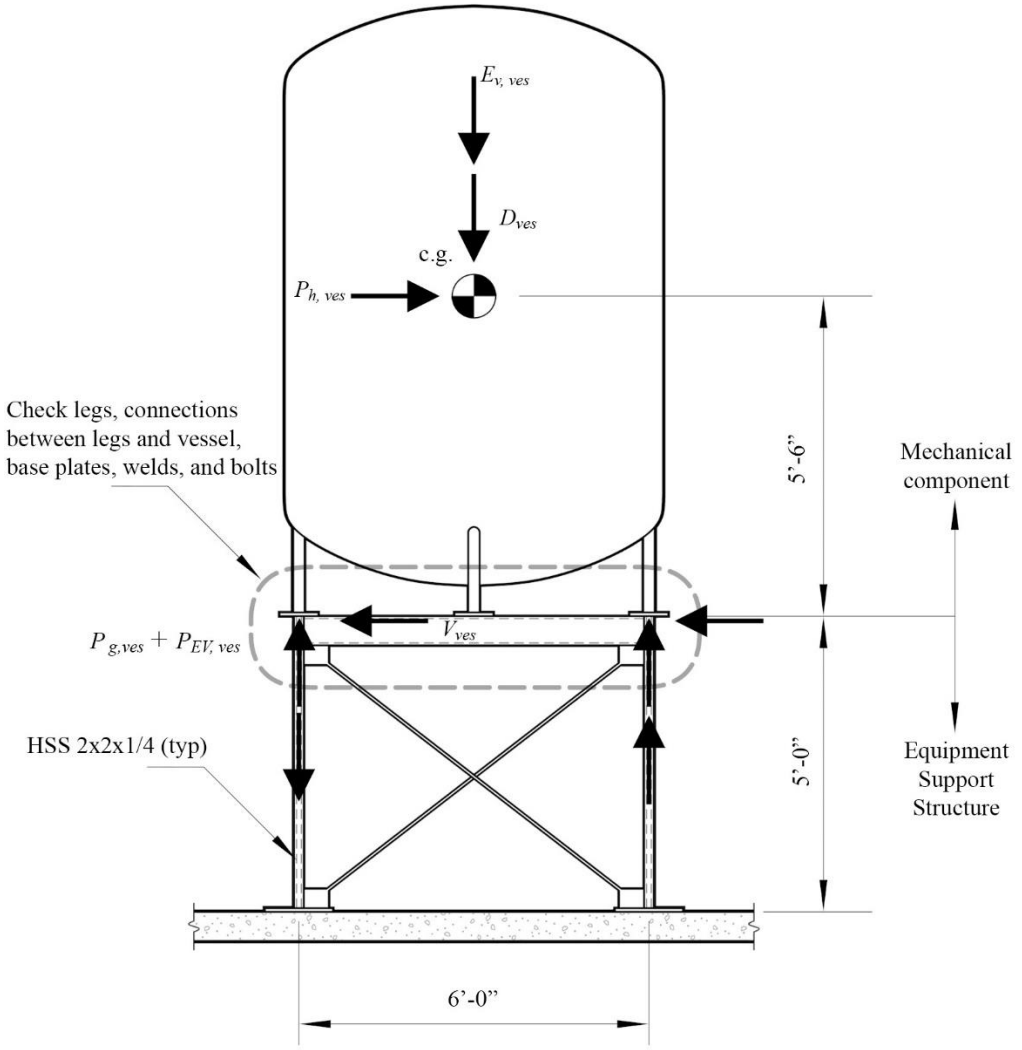

Figure 8-42. Free-body Diagram for Vessel Support and Attachments Design

Based on the vessel support geometry, the vertical loads and shear forces are equally distributed in the four vessel legs, as follows:

Vessel vertical load in each leg due to dead load, $P_{g,ves}$

$$P_{g,ves} = \frac{D_{ves}}{4\text{ legs}} = \frac{5{,}000\text{ lb}}{4\text{ legs}} = 1{,}250\text{ lb/leg}$$

Vessel vertical load in each leg due to vertical seismic load effect, $P_{Ev,ves}$

$$P_{Ev,ves} = \frac{E_{v,ves}}{4\text{ legs}} = \frac{1{,}200\text{ lb}}{4\text{ legs}} = 300\text{ lb/leg}$$

Vessel shear force in each leg due to the horizontal seismic load effect, V_{ves}

$$V_{ves} = \frac{E_{h,ves}}{4 \text{ legs}} = \frac{3{,}808 \text{ lb}}{4 \text{ legs}} = 952 \text{ lb/leg}$$

The height between the vessel's center-of-gravity and the bottom of the leg base plates is 5.5 feet. The overturning moment at the bottom of leg base plates due to the horizontal seismic forces is calculated as:

$$M = (5.5 \text{ ft})(E_{h,ves}) = (5.5 \text{ ft})(3{,}808 \text{ lb}) = 20{,}946 \text{ lb-ft}$$

ASCE/SEI 7-22 Section 13.3.1 states that the lateral force, F_p, shall be applied independently in at least two orthogonal horizontal directions. For vertically cantilevered systems, the lateral force also shall be assumed to act in any horizontal direction. In this example, the layout of the vessel legs is symmetric, and there are two horizontal directions of interest, separated by 45 degrees. These two load cases are illustrated in Figure 8-43.

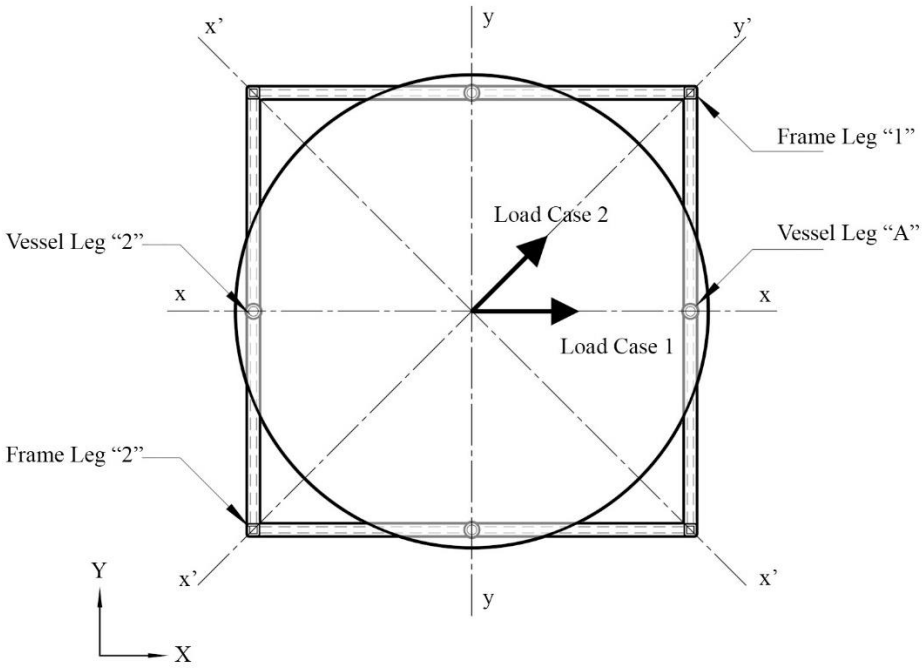

Figure 8-43. Elevated Vessel Support Load Cases

Load Case 1 – Overturning Moment About the y-y Axis

Assuming the vessel acts as a rigid body, in Load Case 1 the overturning moment is resisted by the two legs along the x-x axis – one leg in tension and the opposite leg in compression. The vessel is assumed to rotate about the legs on the y-y axis. The maximum tension and compression loads in each leg are estimated as:

$$P_{Eh_{y-y}} = \frac{M}{d}$$

where the distance between Legs A and C is $d = 6$ ft. Therefore:

$$P_{Eh_{y-y}} = \frac{M}{d} = \frac{20{,}946 \text{ lb-ft}}{6 \text{ ft}} = 3{,}491 \text{ lb}$$

Load Case 2 – Overturning Moment About the x'-x' Axis

In Load Case 2, the overturning moments are resisted by all four legs – two legs in compression and two legs in tension. Under seismic load, the vessel is assumed to rotate about the x'-x' axis. The maximum tension and compression loads in each leg are estimated as:

$$P_{Eh_{x'-x'}} = \frac{M}{2(d/\sqrt{2})}$$

where the distance between Legs A and C is $d/\sqrt{2}$=4.24 ft. Therefore:

$$P_{Eh_{x'-x'}} = \frac{M}{2(d/\sqrt{2})} = \frac{20{,}946 \text{ lb-ft}}{2(4.24 \text{ ft})} = 2{,}469 \text{ lb}$$

The axial loads in the vessel legs due to seismic overturning about the y-y axis (Load Case 1) are substantially larger than those obtained for overturning about the x'-x' axis (Load Case 2). Therefore, Load Case 1 governs the vessel leg design.

$$P_{Eh,ves} = 3{,}491 \text{ lb}$$

The axial load in the vessel legs using Load Cases 1 and 2 are derived using a conservative and simplified approach, in which it is assumed that there are the same number of legs in compression and tension resisting the overturning moment. A more accurate analysis would consider a model whereby the overturning moment can be resisted by a single leg in compression and the rest in tension, and vice versa. This refined analysis is out of the scope of this example, as it is intended to illustrate the rationale for seismic demand calculations using the 2022 edition of ASCE/SEI 7.

The design compression loads on the vessel legs is controlled by the ASCE/SEI 7-22 Basic Load Combination 6:

$$1.2D + E_v + E_h + L + 0.2S \qquad \text{(ASCE/SEI 7-22 Load Combination 6)}$$

$$C_u = 1.2\left(P_{g,ves}\right) + P_{Ev,ves} + P_{Eh,ves}$$

$$C_u = 1.2(1{,}250 \text{ lb}) + 300 \text{ lb} + 3{,}491 \text{ lb} = 5{,}291 \text{ lb}$$

The design tension load on the vessel legs is controlled by the ASCE/SEI 7-22 Basic Load Combination 7:

$$0.9D - E_v + E_h \qquad \text{(ASCE/SEI 7-22 Load Combination 7)}$$

$$T_u = 0.9\left(P_{g,ves}\right) - P_{Ev,ves} + P_{Eh,ves}$$

$$T_u = 0.9(1{,}250 \text{ lb}) - 300 \text{ lb} - 3{,}491 \text{ lb} = -2{,}666 \text{ lb (tension)}$$

The vessel legs shall be designed for the following shear force:

$$V_u = V_{ves} = 952 \text{ lb}$$

Vessel Leg Design

The design of the vessel legs involves checking the connection between the vessel and the leg, and the induced stress of the leg itself. The length of the leg is $L = 18$ in., and the legs are fabricated from 2-inch-diameter standard pipes.

Section properties of the vessel leg:

$$A = 1.02 \text{ in.}^2$$

$$Z = 0.713 \text{ in.}^3$$

Maximum axial compressive stress in the leg:

$$f_a = \frac{C_u}{A} = \frac{5{,}291 \text{ lb}}{1.02 \text{ in.}^2} = 5{,}291 \text{ psi}$$

Assuming the leg is pinned at the connection to the supporting frame and fixed at the connection to the vessel, the moment and bending stress in the leg are calculated as follows:

$$M_u = (V_u)(L_{leg}) = (952 \text{ lb})(18 \text{ in.}) = 17{,}138 \text{ lb-in.}$$

$$f_b = \frac{M_u}{Z} = \frac{17{,}138 \text{ lb-in.}}{0.713 \text{ in.}^3} = 24{,}036 \text{ psi}$$

The capacities of the leg and the connection to the vessel are determined using the *Specifications for Structural Steel Buildings*, ANSI/AISC 360-22. The permissible compressive strength, and bending strength are:

$$F_a = 31{,}500 \text{ psi}$$

$$F_{bw} = 31{,}500 \text{ psi}$$

For combined loading:

$$\left|\frac{f_a}{F_a} + \frac{f_b}{F_{bw}}\right| \leq 1.0$$

$$\left|\frac{5{,}291 \text{ psi}}{31{,}500 \text{ psi}} + \frac{24{,}036 \text{ psi}}{31{,}500 \text{ psi}}\right| = 0.93 \leq 1.0$$

Thus, the vessel legs are adequate.

Connections of the Vessel Leg

The connection between the bottom of the vessel leg and the supporting frame is shown in Figure 8-44. The design of this connection involves checking the weld between the pipe leg and the base plate, the base plate, and the bolts to the supporting frame.

The design load on the vessel legs using the ASCE/SEI 7-22 Basic Load Combination 7 results in tension forces, which govern the design of the base plates and the bolts to the supporting frame. The design of the base plate and bolts shall consider the effects of prying on the tension demand in the bolts.

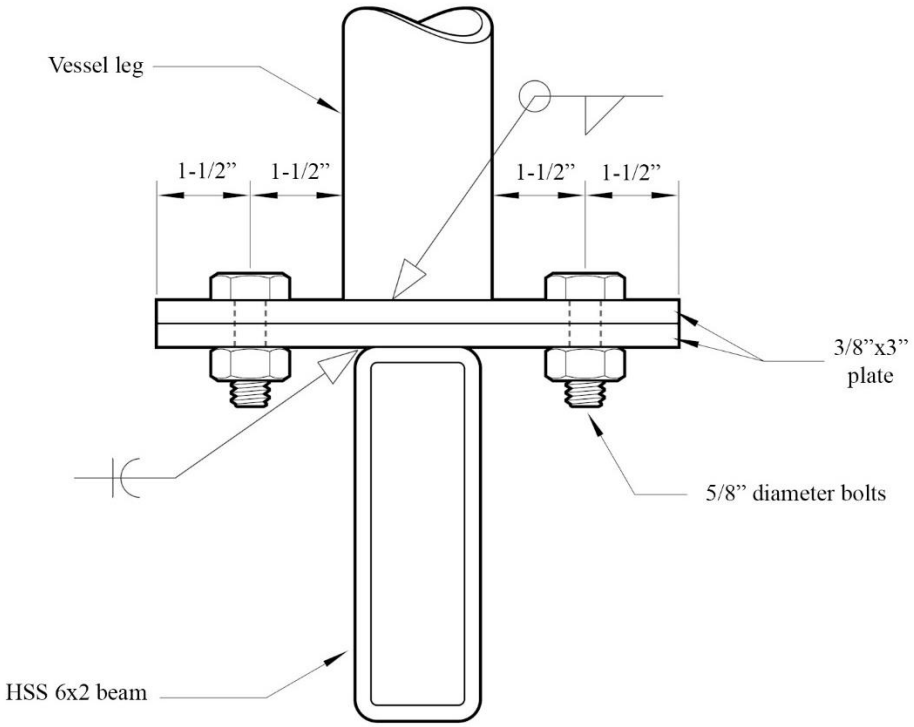

Figure 8-44. Elevated Vessel Leg Connection

Each vessel leg is connected to the supporting frame by a pair of 5/8-inch-diameter bolts. The load path for this connection consists of the following elements: the weld of the leg to the connecting plate, the connecting plate acting in bending considering the effects of prying as appropriate, the bolts, the connection plate welded to the supporting frame beam, and the welding of the connection plate to the supporting frame beam. Again, by inspection, Load Case 1 for direction of overturning moment governs.

As previously determined, the maximum compression per the ASCE/SEI 7-22 Basic Load Combination 6 and maximum tension per the ASCE/SEI 7-22 Basic Load Combination 7 in the connection are:

$C_u = 5{,}291$ lb

$T_u = -2{,}666$ lb (tension)

The design shear in each leg is:

$V_u = V = 952$ lb

The design forces for the vessel leg base plates and the connection plates at the supporting frame beams are the same.

Since each vessel leg connection has two bolts, the connection demand is divided by two to calculate the demand for each bolt.

The maximum tension in each bolt is:

$$T_{u,bolt} = \frac{T_u}{2 \text{ bolts}} = \frac{-2{,}666 \text{ lb}}{2 \text{ bolts}} = -1{,}333 \text{ lb/bolt}$$

The maximum shear per bolt is:

$$V_{u,bolt} = \frac{V_u}{2 \text{ bolts}} = \frac{952 \text{ lb}}{2 \text{ bolts}} = 476 \text{ lb/bolt}$$

The available tensile and shear strengths of the of 5/8-inch-diameter ASTM A307 bolts are:

$\phi r_n = 10{,}400$ lb (tension)

$\phi_v r_n = 5{,}520$ lb (shear)

Therefore, the bolts are adequate.

The connection plates are 3/8 inch thick and 3 inches wide.

$$Z = \frac{bd^2}{4} = \frac{(3 \text{ in.})(0.375 \text{ in.})^2}{4} = 0.1055 \text{ in.}^3$$

The maximum moment in the plate based on the 1.5 in. edge distance to the bolt centerline is:

$$M_{u,plate} = T_{u,bolt}(1.5 \text{ in.}) = (1{,}333 \text{ lb/bolt})(1.5 \text{ in.}) = 1{,}999 \text{ lb-in.}$$

The bending stress in the plate is:

$$f_b = \frac{M_u}{Z} = \frac{1{,}999 \text{ lb-in.}}{0.1055 \text{ in}^3} = 18{,}958 \text{ psi}$$

The bending stress capacity of the ASTM A36 plate is:

$$F_b = \Phi F_y = 0.9(36{,}000 \text{ psi}) = 32{,}400 \text{ psi}$$

$$F_b > f_b$$

Thus, the connection plate is adequate.

Prying action can have the effect of increasing the tensile forces in the bolts. The AISC Steel Construction Manual, 15th Edition, Equation 9-20 permits prying action to be neglected if the plate meets minimum thickness requirements, given by:

$$t_{min} = \sqrt{\frac{4.44Tb'}{pF_u}} \qquad \text{(AISC Steel Construction Manual, 15th Edition, Eq. 9-20)}$$

where $p = 3\ in.$ is the tributary length per pair of bolts.

$$b' = (b - db/2) = (1.5\ in. - 0.625\ \text{in.}/2) = 1.188\ \text{in.}$$

$$t_{min} = \sqrt{\frac{4.44Tb'}{pF_u}} = \sqrt{\frac{(4.44)(1{,}333\ \text{lb/bolt})(1.188\ \text{in.})}{(3\ \text{in.})(58{,}000\ \text{psi})}} = 0.201\ \text{in.}$$

$t_{min} = 0.201$ in. is less than the 0.375 inch thickness provided for the connection plates. Thus, prying action need not be considered further.

The vessel legs have two welds at each end: the welds to the vessel body, and the welds to the upper connection plate. These connections are proportioned in a similar manner. The calculation can be simplified by assuming the weld is of unit thickness. This entails a demand per inch of weld, which facilitates the selection of an appropriate weld thickness.

The outer diameter of the vessel leg is $d = 2.38$ in. The weld properties for a weld of unit thickness are shown below. The area, A, and the plastic section modulus of the weld, Z_w, are conservatively calculated at the face of the pipe, and not at the centerline of the weld.

$$Z_w = \frac{\pi d^2}{4} = \frac{\pi(2.38\ \text{in.})^2}{4} = 4.45\ \text{in.}^2$$

$$A = \pi d = \pi(2.38\ \text{in.}) = 7.48\ \text{in.}$$

The shear force in the weld of unit thickness is:

$$v = \frac{V_u}{A} = \frac{952\ lb}{7.48\ \text{in.}} = 127\ \text{lb/in.}$$

The tension force due to axial load in a weld of unit thickness is:

$$T_a = \frac{T_u}{A} = \frac{2{,}666\ \text{lb}}{7.48\ \text{in.}} = 356\ \text{lb/in.}$$

The tension force due to bending in a weld of unit thickness (at the connection to the vessel) is:

$$T_b = \frac{M}{Z_w} = \frac{17{,}138 \text{ lb-in.}}{4.45 \text{ in.}^2} = 3{,}852 \text{ lb/in.}$$

For E70 electrodes, the capacity of a fillet weld is given by:

$$\phi R_n = 1.392\, DL \text{ (kips/in.)}$$

where D is the size of the weld in sixteenths of an inch, and L is the weld length.

For a unit length, a 3/16-inch fillet weld has a capacity of:

$$\phi R_n = 1.392\,(3)(1) = 4.18 \text{ kip/in.}$$

Thus, the 3/16-inch fillet weld is adequate.

The same weld size is used for the leg-to-vessel body joint, and for the leg-to-upper connection plate joint. A similar design approach is used to proportion the weld of the lower connection plate to the HSS 6x2 beam.

Design of Nonstructural Component Connection

The proportioning and design calculations for the elevated vessel connection is intended to illustrate a rational distribution of forces to estimate the demand in the attachments. In a project, the nonstructural component's manufacturer typically provides the required capacity for the connections based on the specific component and anticipated demand. Hence, it is possible that a significant amount of these calculations is not required, as they were already performed by the fabricator.

8.7.4 Supporting Frame

8.7.4.1 PRESCRIBED SEISMIC FORCES

Supporting frame weight, $W_{p,sup}$

$$W_{p,sup} = D_{sup} = 1{,}000 \text{ lb} \qquad \text{(component weight)}$$

Seismic design force, $F_{p,sup}$

$$F_p = 0.4 S_{DS} I_p W_p \left[\frac{H_f}{R_\mu}\right] \left|\frac{C_{AR}}{R_{po}}\right| \qquad \text{(ASCE/SEI 7-22 Eq. 13.3-1)}$$

$$F_p = 0.4(1.2)(1.0)\left(W_p\right) \left[\frac{2.52}{1.48}\right] \left|\frac{1.4}{1.5}\right| = 0.762 W_p \qquad \text{(controlling equation)}$$

$$F_{p,max} = 1.6 S_{DS} I_p W_p \qquad \text{(ASCE/SEI 7-22 Eq. 13.3-2)}$$

$$F_{p,max} = 1.6(1.2)(1.0)\left(W_p\right) = 1.92W_p$$

$$F_{p,min} = 0.3S_{DS}I_pW_p \qquad \text{(ASCE/SEI 7-22 Eq. 13.3-3)}$$

$$F_{p,min} = 0.3(1.2)(1.0)\left(W_p\right) = 0.360W_p$$

$$F_{p,sup} = 0.762W_p = 0.762(1{,}000\text{ lb}) = 762\text{ lb} \qquad \text{(controlling seismic design force)}$$

Horizontal seismic load effect, $E_{h,sup}$

$$Q_E = F_p \qquad \text{(effect from } F_p\text{)}$$

$$E_h = \rho Q_E \qquad \text{(ASCE/SEI 7-22 Eq. 12.4-3)}$$

$$E_{h,sup} = \rho Q_E = (1.0)(762\text{ lb}) = 762\text{ lb}$$

Vertical seismic load effect, $E_{v,sup}$

$$E_v = 0.2S_{DS}D \qquad \text{(ASCE/SEI 7-22 Eq. 12.4-4a)}$$

$$E_{v,sup} = 0.2S_{DS}D = (0.2)(1.2\text{g})(1{,}000\text{ lb}) = 240\text{ lb}$$

Changes in ASCE/SEI 7 22

ASCE/SEI 7-16 required the nonstructural components and supporting structure to be designed with the same seismic design forces, F_p, regardless of their interaction, and the force was based on the component properties. A platform supporting a pressure vessel would be designed for pressure vessel forces regardless of whether the platform structure was made of concrete, steel braced frames, or steel moment frames.

In ASCE/SEI 7-22, the concept of an equipment support structure or platform has been introduced and defined. Definitions are given in Section 11.2 and properties have been added to Table 13.6-1. Section 13.6.4.6 has been added to ASCE/SEI 7-22 to require that the support structures and platforms be designed in accordance with those properties. This permits a more accurate determination of forces that more realistically reflect the differences in dynamic properties and ductilities between the component and the support structure or platform.

The support structure design requires the gravity and seismic forces associated with the inertial mass of the support itself and the attached nonstructural component. In this case, the prescribed seismic forces for the vessel and legs calculated in Section 8.7.3 of this chapter are repeated below.

Prescribed seismic forces for vessel and legs

$W_{p,ves} = D_{ves} = 5{,}000$ lb (component weight)

$F_{p,ves} = 0.762W_p = 3{,}808$ lb (controlling seismic design force)

$E_{h,ves} = \rho Q_E = 3{,}808$ lb (horizontal seismic load effect, E_h)

$E_{v,ves} = 0.2S_{DS}D = 1{,}200$ lb (vertical seismic load effect, E_v)

The above terms are then substituted into the following Basic Load Combinations for Strength Design from ASCE/SEI 7-22 Sections 2.3.6 and 12.4.2 to determine the design member and connection forces to be used in conjunction with seismic loads.

$1.2D + E_v + E_h + L + 0.2S$ (ASCE/SEI 7-22 Load Combination 6)

$0.9D - E_v + E_h$ (ASCE/SEI 7-22 Load Combination 7)

For nonstructural components, the terms *L* and S are typically zero.

8.7.4.2 PROPORTIONING AND DESIGN

The 2022 edition of ASCE/SEI 7 considers different prescribed seismic forces for the equipment support design. Refer to ASCE/SEI 7-22 Section 11.2 for the equipment support structure and platform definition and classifications. The design of the supporting frame shall be performed separately from that of the vessel, as the seismic design force factors may be different. The reactions from the vessel are applied to the frame and combined with the seismic loads resulting from the supporting frame itself. The configuration of the supporting frame is shown in Figure 8-45.

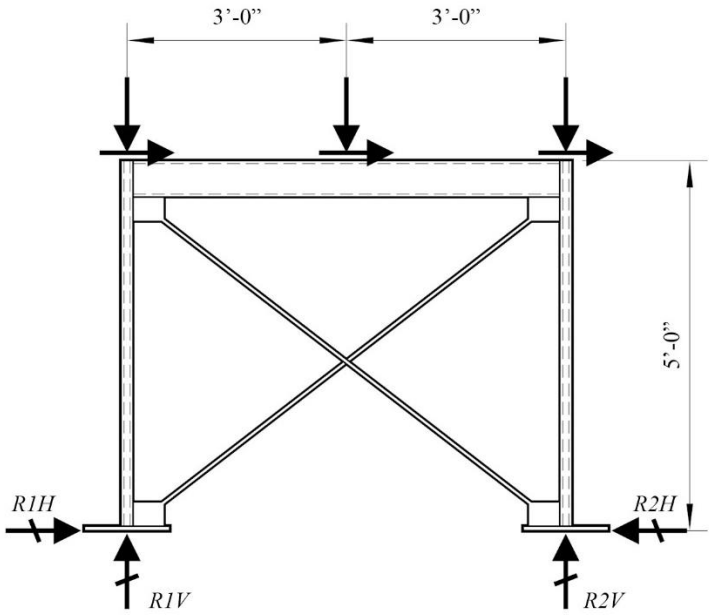

Figure 8-45. Elevated Vessel Supporting Frame

The supporting frame uses steel ordinary braced frames (OBF) with rods as tension-only braces. While the supporting frame is designed for seismic forces determined in ASCE/SEI 7-22 Section 13.3, the design process for the frame itself is similar to that used for building frames or nonbuilding structures similar to buildings. In this example, seismic loads are developed for the following elements:

- Beams supporting the vessel legs.
- Braces.
- Columns supporting the platform and vessel.
- Base plates and anchor bolts.

To simplify the analysis, the self-weight of the supporting frame is lumped at the vessel leg connection locations.

Figure 8-46 shows the free-body diagram for the vessel and supporting frame with the applicable forces to be used for design.

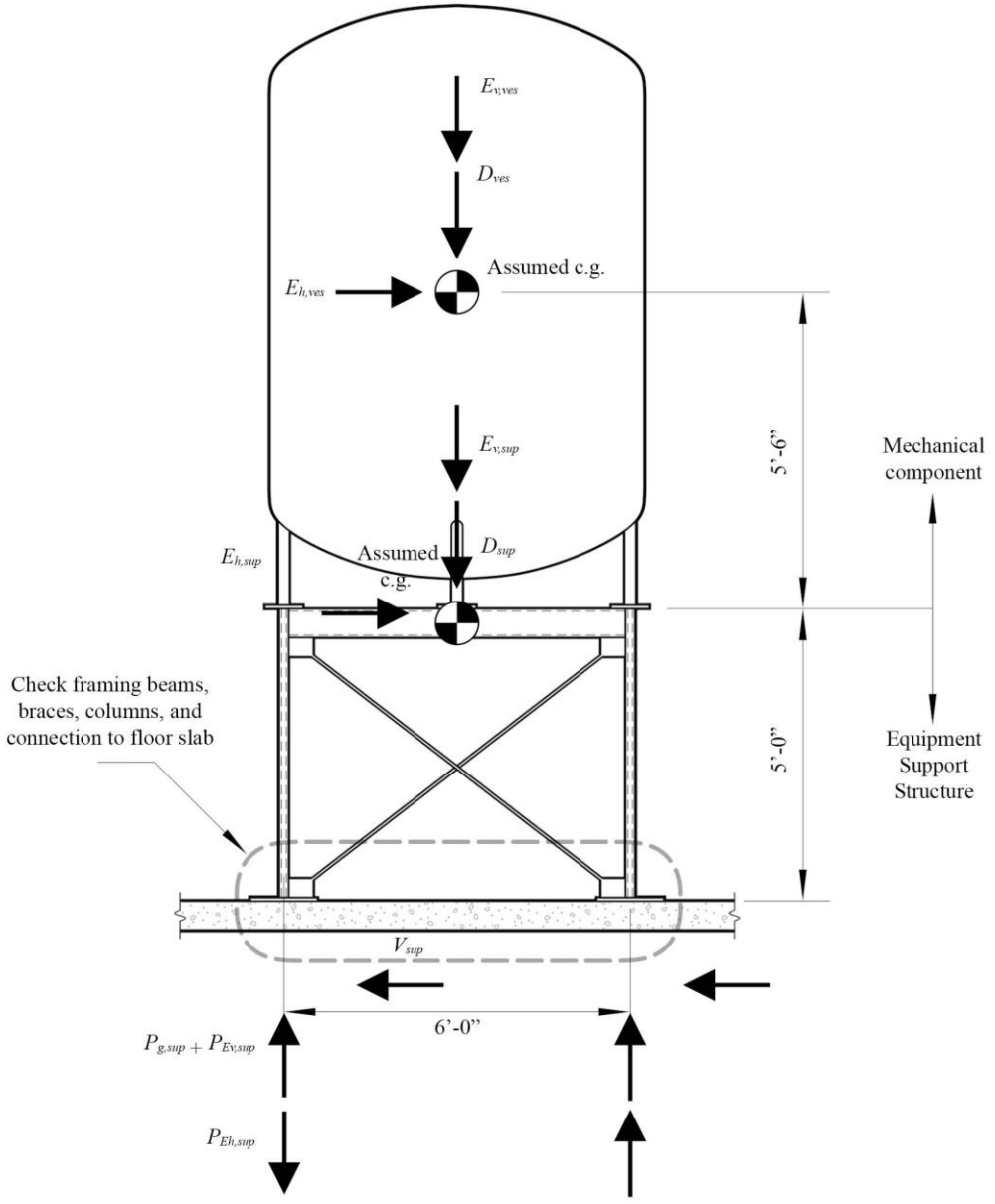

Figure 8-46. Free-body Diagram for Supporting Frame Design

Support Frame Beams

The beams transfer vertical and horizontal loads from the vessel to the brace frames. The beams, fabricated from HSS6x2x1/4 members, are idealized as simply supported with a span of 6 feet. The reactions from the vessel legs are idealized as point loads applied at midspan.

Beam vertical load at midspan due to dead load, $P_{g,sup}$

$$P_{g,sup} = \frac{D_{ves}+D_{sup}}{4 \text{ supports}} = \frac{5{,}000 \text{ lb}+1{,}000 \text{ lb}}{4 \text{ supports}} = 1{,}500 \text{ lb/support}$$

Beam vertical load at midspan due to vertical seismic load effect, $P_{Ev,sup}$

$$P_{Ev,sup} = \frac{E_{v,ves}+E_{v,sup}}{4 \text{ supports}} = \frac{1{,}200 \text{ lb}+240 \text{ lb}}{4 \text{ supports}} = 360 \text{ lb/support}$$

Beam lateral load of the combined vessel and supporting frames, V_{sup}

$$V_{sup} = \frac{E_{h,ves}+E_{h,sup}}{4 \text{ supports}} = \frac{3{,}808 \text{ lb}+762 \text{ lb}}{4 \text{ supports}} = 1{,}143 \text{ lb/support}$$

The supporting frame resist the overturning moment of the vessel when the horizontal seismic load effect, $E_{h,ves}$, is applied. The load path consists of a tension – compression couple at the vessel legs, which is transferred to the supporting frame at the beams' midspan. Per Section 8.7.3.2 of this design example, the overturning moment about the y-y axis is identified as the controlling direction of analysis.

Beam vertical load at midspan due to horizontal seismic load effect, $P_{Eh,beam}$

$$P_{Eh,beam} = P_{Eh,ves} = 3{,}491 \text{ lb/support}$$

Potential Two Stage Analysis Approach for Component and Support Structure

The component resonance ductility factor, C_{AR}, for the supported component cannot be less than that for the equipment support structure. This is clearly stated in ASCE/SEI 7-22 Section 13.3.1.3. The intention is to design the supported component with higher seismic forces (regardless of its tabulated C_{AR}) as if it were a low ductility system when the equipment support structure is actually a low ductility system.

For the equipment support design, since the weight of the supported components is included in the calculation of W_p, and C_{AR} cannot exceed the value associated with the component, the reactions applied by the component to the support structure can either stay the same or are effectively scaled down.

When comparing the design coefficient multiplying the component weight, $W_{p,}$ for F_p, if the design coefficient for the supported component is greater than the one for the equipment support, the reactions can be scaled down. For this example, the design coefficients are the same, $F_{p,ves} = 0.762W_p$ and $F_{p,sup} = 0.762W_p$; thus, no scaling is required.

For the cases where the reactions transferred from the component to the support structure can be reduced, an approach analogous to a two-stage analysis approach can be used. In the first stage, the design of the equipment and its supports and attachments are designed using the design coefficients of the component. In the second stage, the equipment support structure is designed, using the design coefficients for the equipment support structure.

It is important to clarify that even though the approach is similar to a two-stage analysis of a building structure, the conditions are different. For buildings, the two-stage analysis entails a flexible system supported on a rigid base. For nonstructural components, the components may be stiff or flexible, high or low ductility, and are carried on support structures that may also be stiff or flexible, high or low ductility.

The maximum factored vertical load, which will generate strong axis bending in the beam, is determined using the ASCE/SEI 7-22 Basic Load Combination 6:

$$1.2D + E_v + E_h + L + 0.2S \qquad \text{(ASCE/SEI 7-22 Load Combination 6)}$$

$$C_u = 1.2\left(P_{g,sup}\right) + P_{Ev,sup} + P_{Eh,beam}$$

$$C_u = 1.2(1{,}500\ \text{lb}) + 360\ \text{lb} + 3{,}491\ \text{lb} = 5{,}651\ \text{lb}$$

Acting with the horizontal load, V_u:

$$V_u = V_{sup} = 1{,}143\ \text{lb}$$

The HSS6x2x1/4 frame beams have the following geometric and material properties:

$$Z_{x-x} = 5.84 \text{ in.}^3$$

$$Z_{y-y} = 2.61 \text{ in.}^3$$

$$F_b = \Phi F_y = 0.9(46{,}000 \text{ psi}) = 41{,}400 \text{ psi}$$

The moment and bending stress about the x-x axis in the beams, where $L = 6$ ft, is:

$$M_{x-x} = \frac{C_u L}{4} = \frac{(5{,}651 \text{ lb})(6 \text{ ft})(12 \text{ in./ft})}{4} = 101{,}718 \text{ lb-in.}$$

$$f_{bx} = \frac{M_{x-x}}{Z_{x-x}} = \frac{101{,}718 \text{ lb-in.}}{5.84 \text{ in.}^3} = 17{,}417 \text{ psi}$$

The moment and bending stress about the y-y axis in the beams, where $L = 6$ ft, is:

$$M_{y-y} = \frac{V_u L}{4} = \frac{(1{,}143 \text{ lb})(6 \text{ ft})(12 \text{ in./ft})}{4} = 20{,}565 \text{ lb-in.}$$

$$f_{by} = \frac{M_{x-x}}{Z_{y-y}} = \frac{20{,}565 \text{ lb-in.}}{2.61 \text{ in.}^3} = 7{,}879 \text{ psi}$$

The interaction of bending demand in the strong and weak axis is checked:

$$\left|\frac{f_{bx}}{F_b} + \frac{f_{by}}{F_b}\right| \leq 1.0$$

$$\left|\frac{17{,}417 \text{ psi}}{41{,}400 \text{ psi}} + \frac{7{,}879 \text{ psi}}{41{,}400 \text{ psi}}\right| = 0.611 \leq 1.0$$

Thus, the support frame beams are adequate.

Support Frame Braces

The maximum brace force occurs where loads are applied in the x-x or y-y direction and the loads are resisted by two braces. The horizontal force is:

$$V_{brace} = \frac{E_{h,ves} + E_{h,sup}}{2 \text{ braces}} = \frac{3{,}808 \text{ lb} + 762 \text{ lb}}{2 \text{ braces}} = 2{,}285 \text{ lb/brace}$$

The length of the brace is:

$$L = \sqrt{(5 \text{ ft})^2 + (6 \text{ ft})^2} = 7.81 \text{ ft}$$

The tension force in the brace then is:

$$T_u = \left(\frac{7.81 \text{ ft}}{6 \text{ ft}}\right)(2{,}285 \text{ lb}) = 2{,}974 \text{ lb (tension)}$$

The braces consist of 5/8-inch-diameter ASTM A307 threaded rod. The nominal tensile capacity is:

$\phi r_n = 10{,}400$ lb (tension)

$\phi r_n > T_u$

$10{,}400 \text{ lb} > 2{,}974 \text{ lb}$

Thus, the threaded rods are adequate.

It is good practice to design the supporting frame connections to the same level as a nonbuilding structure subject to ASCE/SEI 7-22 Chapter 15. In this example, the supporting frames would be treated as an ordinary braced frame. For this system, ANSI/AISC 341-22 requires the strength of the bracing connection to be the lesser of the expected yield strength of the brace in tension, the maximum force that can be developed by the system, or the load effect based on the amplified load.

Support Frame Columns

The columns support the vertical loads from the vessel and frame, including the vertical component of the supporting frame brace forces. The columns are fabricated from HSS2x2x1/4 members and are idealized as pinned top and bottom with a length of $L = 5$ ft. The case where the vessel rotates about the x'-x' axis governs the design of the supporting frame columns. The overturning moment is:

$$M = (10.5 \text{ ft})\left(E_{h,ves}\right) + (5.0 \text{ ft})\left(E_{h,sup}\right)$$

$$M = (10.5 \text{ ft})(3{,}808 \text{ lb}) + (5.0 \text{ ft})(762 \text{ lb}) = 43{,}796 \text{ lb-ft}$$

Assuming the vessel acts as a rigid body, in Load Case 2 the overturning moment is resisted by the two legs along the y'-y' axis. The vessel is assumed to rotate about the legs on the x'-x' axis. The maximum tension and compression loads in the columns due to overturning is computed as follows:

$$P_{Eh,col} = \frac{M}{d}$$

where the distance between the frame Legs 1 and 2, $d = (6 \text{ ft})\sqrt{2} = 8.48$ ft. Therefore:

$$P_{Eh,col} = \frac{M}{d} = \frac{43{,}796 \text{ lb-ft}}{8.48 \text{ ft}} = 5{,}161 \text{ lb}$$

The vertical load in each leg due to gravity is $P_{g,sup} = 1{,}500$ lb/support and $P_{Ev,sup} = 360$ lb/support.

The design compression load on the supporting frame columns is governed by the ASCE/SEI 7-22 Basic Load Combination 6:

$1.2D + E_v + E_h + L + 0.2S$ (ASCE/SEI 7-22 Load Combination 6)

$$C_u = 1.2\left(P_{g,sup}\right) + P_{Ev,sup} + P_{Eh,col}$$

$$C_u = 1.2(1{,}500\ \text{lb}) + 360\ \text{lb} + 5{,}161\ \text{lb} = 7{,}321\ \text{lb}$$

The design tension load on the supporting frame columns is governed by the ASCE/SEI 7-22 Basic Load Combination 7:

$$0.9D - E_v + E_h \qquad \text{(ASCE/SEI 7-22 Load Combination 7)}$$

$$T_u = 0.9\left(P_{g,sup}\right) - P_{Ev,sup} - P_{Eh,col}$$

$$T_u = 0.9(1{,}500\ \text{lb}) - 360\ \text{lb} - 5{,}161\ \text{lb} = -4{,}171\ \text{lb}$$

The capacity of the HSS2x2x1/4 column is 38,300 lb. Therefore, it is adequate.

Support Frame Connection to the Floor Slab

The connection of the support frame columns to the floor slab includes the following elements:

- Welds of the column and brace connection to the base plate.
- Base plates.
- Anchor bolts.

The design of the base plate connection and of the base plate itself follows the typical procedures used for other structures. There are special considerations for the design of the anchor bolts to the concrete slab that are unique to nonstructural components. Anchors in concrete and masonry shall be proportioned so that either the component or support that the anchor is connecting to the structure undergoes ductile yielding at a load level corresponding to anchor forces not greater than their design strength, or the anchors shall be designed to resist the load combinations with overstrength, Ω_{0p},in accordance with ASCE/SEI 7-22 Sections 2.3.6, 12.4.3, and 13.4.2. In this example, it is assumed that the anchor design strength is less than the yielding strength of the vessel or supporting frame, and so $\Omega_{0\text{p}}$ shall be applied to the anchor loads.

The horizontal and vertical reactions of the supporting frame columns calculated are used for the support frame connection to the floor slab:

Vertical load due to dead load, $P_{g,sup} = 1{,}500\ \text{lb}$.

Vertical load due to vertical seismic load effect, $P_{Ev,sup} = 360\ \text{lb}$.

Tension and Compression due to seismic overturning, $P_{Eh,col} = 5{,}161\ \text{lb}$.

Horizontal seismic force transferred from the braces, $V_{brace} = 2{,}285\ \text{lb}$

By inspection, the load combination that results in net tension on the anchors will govern. Thus, the ASCE/SEI 7-22 Basic Load Combination 7, including overstrength, is applied to obtain the controlling vertical design tension force:

$$0.9D - E_v + E_{mh} \qquad \text{(ASCE/SEI 7-22 Load Combination 7)}$$

Where: $E_{mh} = \Omega_{0p} Q_E$ (ASCE/SEI 7-22 Eq. 12.4-7 and Sec 13.4.2)

Vertical design tension force:

$$T_u = 0.9\left(P_{g,sup}\right) - P_{Ev,sup} - \Omega_{0p} P_{Eh,col}$$

$$T_u = 0.9(1{,}500 \text{ lb}) - 360 \text{ lb} - (2.0)(5{,}161 \text{ lb}) = -9{,}333 \text{ lb}$$

Acting concurrently with tension, the horizontal design shear force is:

$$V_u = \Omega_{0p} V_{Eh,col}$$

$$V_u = (2.0)(1{,}143 \text{ lb}) = 2{,}285 \text{ lb}$$

When comparing the support frame column forces to the connection to the floor slab forces, the design tension force increases by 124%, and the design shear force increases by 100%.

8.7.5 Design Considerations for the Gravity Load-Carrying System

This portion of the example illustrates design considerations for the floor slab supporting the nonstructural component. The floor system at Level 3 consists of a 6-inch-thick reinforced concrete flat-slab spanning between steel beams. To illustrate the effects of the vessel, the contribution of the vessel load to the overall slab demand is examined.

Slab Design Assumptions

Dead load, $w_D = 100$ psf

Live load, $w_L = 100$ psf (non-reducible)

Effect of Vessel Loading

During design, the slab moments and shear are checked at different points along each span. In order to simply illustrate the potential effects of the vessel, this investigation will be limited to the change in the negative moments about the x-x axis over the area bounded by Gridlines A, B, 2, and 3. In an actual design, a complete analysis of the slab for the loads imposed by the vessel would be required. At the center support, the moments due to dead load and live load are:

Maximum dead load moment, $M_D = \frac{w_D L^2}{8} = \frac{(100 \text{ psf})(15 \text{ ft})^2}{8} = 2{,}813 \frac{\text{lb-ft}}{\text{ft}}$

Maximum live load moment, $M_L = \frac{w_L L^2}{8} = \frac{(100 \text{ psf})(15 \text{ ft})^2}{8} = 2{,}813 \frac{\text{lb-ft}}{\text{ft}}$

The support frame columns are 6 feet apart. Assuming an additional 3 feet of slab on each side of the frame to resist loads generated by the vessel, the design moments for the strip of slab supporting the vessel are:

$$M_D = \left(2{,}813 \frac{\text{ft-lb}}{\text{ft}}\right)(12 \text{ ft}) = 33{,}750 \text{ ft-lb}$$

$$M_L = \left(2{,}813 \frac{\text{ft-lb}}{\text{ft}}\right)(12 \text{ ft}) = 33{,}750 \text{ ft-lb}$$

The moments at the center support due to a point load, P, in one of the spans is:

$$M = \frac{Pab}{4l^2}(l + a)$$

where:

a = distance from the end support to the point load

b = distance from the point load to the center support

l = span between supports, equal to 15 ft

The point load due to the vessel and support frame self-weight is:

$$P_{slab} = 2\left(P_{g,sup}\right) = 2(1{,}500 \text{ lb}) = 3{,}000 \text{ lb}$$

The moment in the slab due to the vessel and support frame is:

$$M_{VD} = \frac{(3{,}000 \text{ lb})(4.5 \text{ ft})(10.5 \text{ ft})}{4(15 \text{ ft})^2}(15 \text{ ft} + 4.5 \text{ ft}) + \frac{(3{,}000 \text{ lb})(10.5 \text{ ft})(4.5 \text{ ft})}{4(15 \text{ ft})^2}(15 \text{ ft} + 10.5 \text{ ft})$$

$$M_{VD} = 7{,}088 \text{ lb-ft}$$

The overturning moment at the support frame columns is:

$$M = 43{,}796 \text{ lb-ft}$$

The moment is resisted by point loads at each leg, where the distance between frame Legs 1 and 2 is $d = 6$ ft as follows:

$$P_{Eh,col} = \frac{M}{d} = \frac{43{,}796 \text{ lb-ft}}{6.0 \text{ ft}} = 7{,}299 \text{ lb}$$

The moment in the slab due to the overturning of the vessel and support frame for seismic forces in the Y-direction is:

$$M_{Eh} = \frac{(7{,}299 \text{ lb})(4.5 \text{ ft})(10.5 \text{ ft})}{4(15 \text{ ft})^2}(15 \text{ ft} + 4.5 \text{ ft}) + \frac{(-7{,}299 \text{ lb})(10.5 \text{ ft})(4.5 \text{ ft})}{4(15 \text{ ft})^2}(15 \text{ ft} + 10.5 \text{ ft})$$

$$M_{Eh} = -2{,}299 \text{ lb-ft}$$

or:

$$M_{Eh} = \frac{(-7{,}299 \text{ lb})(4.5 \text{ ft})(10.5 \text{ ft})}{4(15 \text{ ft})^2}(15 \text{ ft} + 4.5 \text{ ft}) + \frac{(7{,}299 \text{ lb})(10.5 \text{ ft})(4.5 \text{ ft})}{4(15 \text{ ft})^2}(15 \text{ ft} + 10.5 \text{ ft})$$

$$M_{Eh} = 2{,}299 \text{ lb-ft}$$

The factored moments for the slab without the vessel not including seismic overturning is calculated using the ASCE/SEI 7-22 Basic Load Combination 2:

$$1.2D + 1.6L + 0.5(L_r \text{ or } S \text{ or } R) \qquad \text{(ASCE/SEI 7-22 Load Combination 2)}$$

$$M_u = 1.2M_D + 1.6M_L$$

$$M_u = 1.2(33{,}750 \text{ ft-lb}) + 1.6(33{,}750 \text{ ft-lb}) = 94{,}500 \text{ ft-lb}$$

The factored moments for the slab, including the vessel not including seismic overturning, is calculated using the ASCE/SEI 7-22 Basic Load Combination 2:

$$1.2D + 1.6L + 0.5(L_r \text{ or } S \text{ or } R) \qquad \text{(ASCE/SEI 7-22 Load Combination 2)}$$

$$M_u = 1.2(M_D + M_{VD}) + 1.6M_L$$

$$M_u = 1.2(33{,}750 \text{ ft-lb} + 7{,}088 \text{ lb-ft}) + 1.6(33{,}750 \text{ ft-lb}) = 103{,}005 \text{ ft-lb}$$

The factored moments including seismic effects and using 50 percent of the live load per ASCE/SEI 7-22 Section 2.3.6 Exception 1 are:

ASCE/SEI 7-22 Basic Load Combination 6:

$$1.2D + E_v + E_h + L + 0.2S \qquad \text{(ASCE/SEI 7-22 Load Combination 6)}$$

$$M_u = 1.2(M_D + M_{VD}) + 0.2S_{DS}(M_D + M_{VD}) + M_{Eh} + 1.6M_L$$

$$M_u = 1.2(33{,}750 \text{ ft-lb} + 7{,}088 \text{ lb-ft}) + (0.2)(1.2)(33{,}750 \text{ ft-lb} + 7{,}088 \text{ lb-ft}) + 2{,}299 \text{ lb-ft} + 0.5(33{,}750 \text{ ft-lb})$$

$$M_u = 77{,}980 \text{ lb-ft}$$

ASCE/SEI 7-22 Basic Load Combination 7:

$$0.9D - E_v + E_h \qquad \text{(ASCE/SEI 7-22 Load Combination 7)}$$

$$M_u = 0.9(M_D + M_{VD}) - 0.2S_{DS}(M_D + M_{VD}) + M_{Eh}$$

$$M_u = 0.9(33{,}750 \text{ ft-lb} + 7{,}088 \text{ lb-ft}) - (0.2)(1.2)(33{,}750 \text{ ft-lb} + 7{,}088 \text{ lb-ft}) \\ -2{,}299 \text{ lb-ft}$$

$$M_u = 24{,}653 \text{ lb-ft}$$

In this case, the loads from the vessel do not control the design of the slab over the area bounded by Gridlines A, B, 2, and 3.

8.8 References

See the "Useful Design Aid Resources" in Section 8.1 above for additional references.

Alonso-Rodríguez, A., and Miranda, E. (2016). "Dynamic behavior of buildings with non-uniform stiffness along their height assessed through coupled flexural and shear beams," *Bulletin of Earthquake Engineering*, Vol. 14, No. 12, pp. 3463-3483.

AAMA (2018). *Recommended Dynamic Test Method for determining the Seismic Drift Causing Glass Fallout from a Wall System*, AAMA 501.6-2018, American Architectural Manufacturers Association.

FEMA (2016). *Development of Fundamental Period Adjustment Factors for Buildings in Low-to-Moderate Seismic Excitation*, FEMA P-58/BD-3.7.17 Report, Federal Emergency Management Agency.

ICC (2020). *International Building Code, 2021 Edition*, First Printing in October 2020, International Code Council, Whittier, CA.

Lizundia, B. (2019). "Proposed Nonstructural Seismic Design Force Equations," 2019 *SEAOC Convention Proceedings*, Structural Engineers Association of California, Sacramento, CA.

National Institute of Standards and Technology (2018). *Recommendations for Improved Seismic Performance of Nonstructural Components*, GCR 18-917-43 Report, 2018, Gaithersburg, MD.

SEAOC (2009). *Recommended Lateral Force Requirements and Commentary,* Structural Engineers Association of California Seismology Committee.

Taghavi, S., and Miranda, E., (2006). "Probabilistic Seismic Assessment of Floor Acceleration Demands in Multi-Story Buildings," *Technical Report 162*, the John A. Blume Earthquake Engineering Center, Stanford University, Stanford, CA.

Kazantzi, A., Vamvatsikos, D., and Miranda, E. (2018). "The effect of yielding on the seismic demands of nonstructural elements," *Proceedings of the 16th European Conference on Earthquake Engineering*, Thessaloniki, Greece.